UNCLASSIFIED

AD NUMBER

AD921137

NEW LIMITATION CHANGE

TO

Approved for public release, distribution unlimited

FROM

Distribution authorized to U.S. Gov't. agencies only; Test and Evaluation; APR 1974. Other requests shall be referred to Eustis Directorate, U.S. Army Air Mobility Research and Development Lab., Fort Eustis, VA 23604.

AUTHORITY

Eustis Directorate, U.S. Army Air Mobility Research and Development Lab. ltr dtd 18 Nov 1975

THIS PAGE IS UNCLASSIFIED

AD

USAAMRDL TECHNICAL REPORT 74-15

10:1 PRESSURE RATIO SINGLE-STAGE CENTRIFUGAL COMPRESSOR PROGRAM

AD921137

By

William J. McAnally, III

April 1974

EUSTIS DIRECTORATE
U. S. ARMY AIR MOBILITY RESEARCH AND DEVELOPMENT LABORATORY
FORT EUSTIS, VIRGINIA

CONTRACT DAAJ02-70-C-0006
PRATT & WHITNEY AIRCRAFT DIVISION
UNITED AIRCRAFT CORPORATION
FLORIDA RESEARCH AND DEVELOPMENT CENTER
WEST PALM BEACH, FLORIDA

Distribution limited to U. S. Government agencies only; test and evaluation; April 1974. Other requests for this document must be referred to the Eustis Directorate, U. S. Army Air Mobility Research and Development Laboratory, Fort Eustis, Virginia 23604

DDC
RECEIVED
AUG 2 1974
D

DISCLAIMERS

The findings in this report are not to be construed as an official Department of the Army position unless so designated by other authorized documents.

When Government drawings, specifications, or other data are used for any purpose other than in connection with a definitely related Government procurement operation, the United States Government thereby incurs no responsibility nor any obligation whatsoever; and the fact that the Government may have formulated, furnished, or in any way supplied the said drawings, specifications, or other data is not to be regarded by implication or otherwise as in any manner licensing the holder or any other person or corporation, or conveying any rights or permission, to manufacture, use, or sell any patented invention that may in any way be related thereto.

Trade names cited in this report do not constitute an official endorsement or approval of the use of such commercial hardware or software.

DISPOSITION INSTRUCTIONS

Destroy this report when no longer needed. Do not return it to the originator.

DEPARTMENT OF THE ARMY
U. S. ARMY AIR MOBILITY RESEARCH & DEVELOPMENT LABORATORY
EUSTIS DIRECTORATE
FORT EUSTIS, VIRGINIA 23604

The objective of this contractual effort was to conduct the preliminary design, detail design, fabrication, test, and evaluation of a single-stage, high-pressure-ratio centrifugal compressor. The performance targets stated herein were derived from potential performance indicated by tests of earlier compressors and are in no way felt to be the ultimate in performance for this type of compressor.

This report was prepared by Pratt & Whitney Aircraft Division of United Aircraft Corporation, Florida Research and Development Center, under the terms of Contract DAAJ02-70-C-0006. It describes the design approach, test equipment and procedures, instrumentation, and results of tests of the compressor. The details of the aerodynamic design are presented in a separate volume as Appendix II to this report.

This report has been reviewed by technical personnel of this directorate. The conclusions contained herein are concurred in by this directorate and will be considered in any future research programs. The U.S. Army project engineer for this effort was Mr. Robert A. Langworthy, Technology Applications Division.

Task 1G162203D14413
Contract DAAJ02-70-C-0006
USAAMRDL Technical Report 74-15
April 1974

10:1 PRESSURE RATIO SINGLE-STAGE CENTRIFUGAL COMPRESSOR PROGRAM

Final Report

By

William J. McAnally, III

Prepared By

Pratt & Whitney Aircraft Division
United Aircraft Corporation
Florida Research and Development Center
West Palm Beach, Florida

for

EUSTIS DIRECTORATE
U. S. ARMY AIR MOBILITY RESEARCH
AND DEVELOPMENT LABORATORY
FORT EUSTIS, VIRGINIA

DDC
RECEIVED
AUG 2 1974
D

Distribution limited to U. S. Government agencies only; test and evaluation; April 1974. Other requests for this document must be referred to the Eustis Directorate, U.S. Army Air Mobility Research and Development Laboratory, Fort Eustis, Virginia 23604.

PRECEDING PAGE BLANK-NOT FILMED

SUMMARY

The objective of this program was to design, fabricate and test a 2-to-5 lb/sec airflow single-stage centrifugal compressor that could be incorporated in a future Army advanced technology gas turbine engine. The design speed performance goals were to exceed 75% efficiency at 10:1 pressure ratio. Since gas turbine engines for Army aircraft applications operate under part-power conditions a majority of the time, an off-design performance goal of 80% efficiency at 8:1 pressure ratio was established.

In the design of the compressor, parametric studies were conducted to select an overall design consistent with optimum compressor performance at both performance goals. These studies defined the compressor inlet corrected flow rate, impeller inlet hub and tip radii, corrected impeller rotational speed, and inlet prewhirl. Airflow selection and the selection of the hub radius were influenced by the decision to design a compressor that could be used in a small turboshaft engine with a concentric shaft front drive.

The tip radius was selected after determining the effect on axial Mach number, inducer tip relative Mach number, and inlet choke flow margin. The effect of inlet guide vane losses, inlet shock losses, diffuser losses, and shroud friction heating were parametrically evaluated analytically before selecting an IGV prewhirl and rotor speed to provide optimum overall compressor performance. A remote inducer design was selected over an integral inducer-impeller configuration so that the inducer could be designed using transonic axial-flow compressor technology. The work split between the inducer and impeller was selected so that the relative Mach number into the impeller would be subsonic. A pipe diffuser was selected over vane island and cascade diffusers, because it has the lowest demonstrated losses over the largest range of Mach number and because P&WA™ has substantial experience in designing and fabricating this type of diffuser.

Demonstrated total-to-static performance was as high as 79.6% efficiency at 8.192:1 pressure ratio and 73.8% efficiency at 10.03:1 pressure ratio. Performance adjusted for increased losses from a damaged diffuser (10.15:1 pressure ratio and 75.9% efficiency) indicates that the basic compressor design would surpass the minimum 10:1 pressure ratio program goal. A composite overall performance map for the compressor is presented in Figure 1. Evaluation of component performance data revealed that excessive losses occurred in the inducer above 95% of design speed and that a redesign of this component could produce an additional performance improvement at 10:1 pressure ratio.

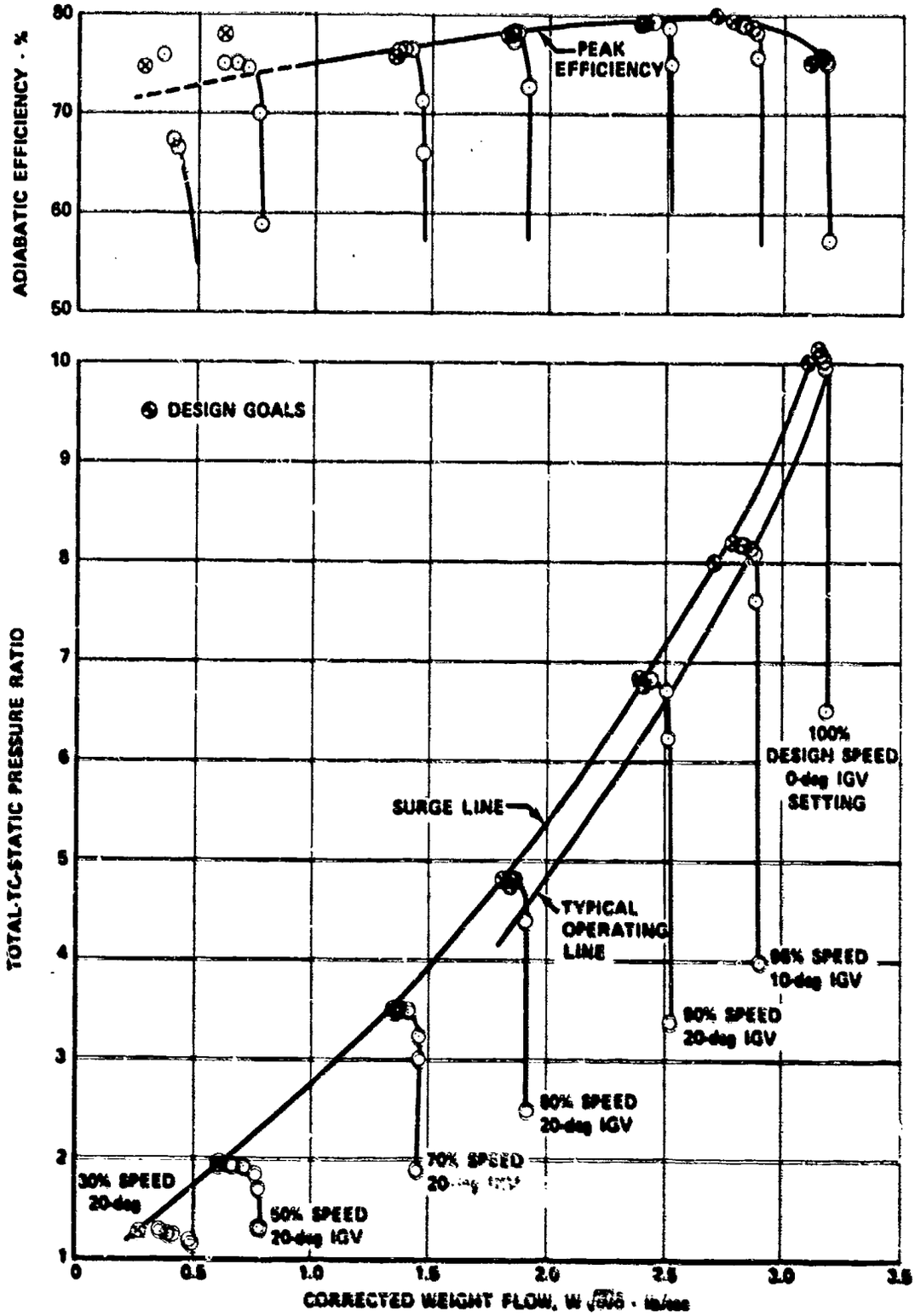

Figure 1. Composite 10:1 Overall Performance Map.

TABLE OF CONTENTS

	Page
SUMMARY	iii
LIST OF ILLUSTRATIONS	vi
LIST OF TABLES	xxv
LIST OF SYMBOLS	xxxii
INTRODUCTION	1
DESIGN APPROACH	3
Aerodynamic Design	3
Mechanical Design	6
Mechanical Redesign	16
TEST EQUIPMENT	21
Compressor Test Rig	21
Test Facilities	21
INSTRUMENTATION	28
PROCEDURES	
Test Procedures	44
Data Reduction Procedures	49
Validation of Test Data	56
RESULTS AND DISCUSSION	64
Overall Performance	64
Component Performance	73
High-Frequency Response Data	127
CONCLUSIONS	130
RECOMMENDATIONS	131
APPENDIX I - Overall Performance Tabulations	132
APPENDIX II - Aerodynamic Design (Classified Confidential - under separate cover)	
DISTRIBUTION	385

LIST OF ILLUSTRATIONS

Figure		Page
1	Composite 10:1 Overall Performance Map	iv
2	10:1 Pressure Ratio Centrifugal Compressor Stage	3
3	10:1 Pressure Ratio Centrifugal Impeller and Remote Inducer	4
4	Initial Design of 10.0:1 Pressure Ratio Centrifugal Compressor and P&WA™ Drive Turbine	7
5	Inducer Vibration Analysis	8
6	Impeller and Inducer Attachment	9
7	Tip Clearance Probe Installation	10
8	Initial Compressor Drive and Bearing Support Design	11
9	Bearing Designs	12
10	Compressor and Turbine Rotor Assembly	14
11	Initial Rotor Configuration Predicted Front Bearing Loads	14
12	Initial Rotor Configuration Predicted Rear Bearing Loads	15
13	Predicted Ball Bearing Minimum Thrust Load Requirements	15
14	Impeller Shaft Attachment Modification	16
15	Redesigned 10:1 Pressure Ratio Centrifugal Compressor and P&WA™ Drive Turbine	17
16	Redesigned Rotor Assembly	18
17	Redesigned Rotor Assembly Predicted Front Bearing Load vs Speed	19
18	Redesigned Rotor Assembly Predicted Rear Bearing Load vs Speed	20

LIST OF ILLUSTRATIONS (Continued)

Figure		Page
19	Front Bearing Compartment Carbon Face Seal	20
20	Compressor Test Rig Nonrotating Components	22
21	Impeller Spin Tooling	22
22	Impeller Installation in Diffuser Case	23
23	Redesigned Rotor Assembly Components	23
24	Assembled and Fully Instrumented Compressor Rig	24
25	P&WA™ FRDC High-Speed Compressor Test Stand	25
26	Particle Separator With Integral Fast-Acting Shutoff Valve	26
27	Compressor Rig Installed in B-2 Test Facility	27
28	Compressor Instrumentation Station Locations	28
29	Inlet Orifice Installation	29
30	Diffuser Exit Total Pressure Rakes	30
31	Location of Diffuser Exit Total Pressure Rakes	31
32	Placement of Total Pressure Probes in Diffuser Exit Plane Station	32
33	Collector Instrumentation Locations	34
34	Axial Locations of Inlet and Inducer Instrumentation	36
35	Construction of Traverse Cobra Probes	37
36	Location of Impeller Shroud Static Pressure Taps	37
37	Impeller Tip Static Pressure Passage	38
38	Impeller Exit Cobra Probe Installation	39
39	Impeller Exit Total Temperature Probe Construction	40

LIST OF ILLUSTRATIONS (Continued)

Figure		Page
40	Location of Diffuser Static Pressure Instrumentation	42
41	High-Frequency Response Kulites	43
42	Maximum Front Bearing 1E Acceleration, Build No. 6	45
43	Impeller Tip Axial Shroud Clearance, Build No. 2	46
44	Clearance Probe Measurements, Build No. 3	46
45	Shroud Clearance Measurements, Build No. 6	47
46	Inlet Guide Vane Exit Flow Correspondence, Build No. 6	61
47	Inducer Exit Integrated Flow Correspondence, Build No. 6	61
48	Impeller Exit Integrated Flow Correspondence, Build No. 6	62
49	Overall Performance, Build No. 2 Shakedown Test	65
50	High-Speed Centrifugal Compressor Flow Characteristics	65
51	Diffuser Loss Characteristic, Build No. 2 Shakedown Test	66
52	Diffuser Throat Blockage Characteristic, Build No. 2 Shakedown Test	66
53	Overall Performance, Build No. 3, 10-deg IGV	67
54	Overall Performance, Build No. 3, 0-deg IGV	68
55	Build No. 3 Overall Performance, 20-deg IGV	69
56	Build No. 6 Overall Performance	71
57	Composite Overall Performance Map	72
58	Component Efficiency Representation	74

LIST OF ILLUSTRATIONS (Continued)

Figure		Page
59	IGV Turning vs Setting, Build No. 6	75
60	IGV Exit Prewhirl Distribution, 10-deg IGV	75
61	Inlet Section Total Pressure Loss Characteristics	76
62	IGV Circumferential Traverse, Build No. 6, 100% Speed, 10-deg IGV, 50% Span	77
63	IGV Exit Radial Traverse, Build No. 6, 100% Speed, 10-deg IGV, Near Stall	78
64	Build No. 6, Inlet Guide Vane Losses at Approximately 0.46 Mach Number	79
65	Inducer Inlet Conditions, 100% Speed, 10-deg IGV	81
66	Inducer Inlet Conditions, 101% Speed, -4-deg IGV	82
67	Inducer Inlet Conditions, Build No. 3, 95% Speed, 10-deg IGV, Near Stall	83
68	Inducer Performance, Build No. 6	84
69	Inducer Exit Traverse, Build No. 6, 101% Speed, -4-deg IGV, Wide Open Discharge	85
70	Inducer Exit Traverse, Build No. 6, 100% Speed, 10-deg IGV	86
71	Inducer Exit Traverse, Build No. 6, 95% Speed, 10-deg IGV, Near Stall	88
72	Inducer Losses	89
73	Impeller Inlet Conditions, 100% Design Speed, 10-deg IGV	90
74	Inducer Exit Air Angle Profile, 100% Design Speed, 10-deg IGV	90
75	Impeller Inlet Conditions, 101% Speed, -4-deg IGV	91
76	Inducer Exit Air Angle Profile, 101% Speed, -4-deg IGV	91

LIST OF ILLUSTRATIONS (Continued)

Figure		Page
77	IGV Exit Static Pressure Profile, 100% Speed, 10-deg IGV	93
78	Inducer Exit Static Pressure Profile, 100% Speed, 10-deg IGV	93
79	Impeller Inlet Conditions, 100% Speed, 10-deg IGV	94
80	Inducer Exit Air Angle Profile, 100% Speed, 10-deg IGV	
81	Choke Point Flow as a Function of Rotor Speed, Build No. 3	95
82	Build No. 6 Choke Point Flow as a Function of Rotor Speed	95
83	Build No. 6 Impeller Performance Derived From Traverse Data	97
84	Inducer-Impeller Performance Derived From Traverse Data	98
85	Build No. 3 Impeller Performance Map Derived From Internal Flow Analysis	99
86	Build No. 6 Inducer-Impeller Performance Map Derived From Internal Analysis	100
87	Build No. 3 Impeller Efficiency-Incidence Characteristic	101
88	Build No. 6 Inducer-Impeller Efficiency-Incidence Characteristic	102
89	Effect of Prewhirl on Inducer-Impeller Performance Near 10:1 Pressure Ratio	104
90	Effect of Prewhirl on Inducer-Impeller Performance Near 8:1 Pressure Ratio	104
91	Impeller Exit Slip Factor	105
92	Impeller Exit Discharge Coefficient	105

LIST OF ILLUSTRATIONS (Continued)

Figure		Page
93	Impeller Exit Traverse, Build No. 6, 101% Speed, -4-deg IGV, Near Stall	106
94	Impeller Exit Traverse, Build No. 3, 95% Speed, 10-deg IGV, Near Stall	107
95	Impeller Exit Traverse, Build No. 6, 95% Speed, 10-deg IGV, Near Stall	108
96	Normalized Radial Velocity Distribution, Build No. 6, 101% Speed, -4-deg IGV	109
97	Normalized Radial Velocity Distribution, Build No. 3, 95% Speed, 10-deg IGV	109
98	Normalized Radial Velocity Distribution, Build No. 6, 95% $N/\sqrt{\theta}$ Design, 10-deg IGV	110
99	Discharge Velocity Ratio Comparisons	111
100	Stall Transient Data at 1 Scan/sec and Continuous Scan	112
101	Static Pressure Variation Along Impeller Shroud, 95% Speed, Near Stall, 10-deg IGV	113
102	Diffuser Static Pressure Profile: Build No. 3, 95% Speed, 10-deg IGV	114
103	Diffuser Static Pressure Profile: Build No. 3, 100% Speed, 10-deg IGV, Near Stall	115
104	Diffuser Gapwise Static Pressure Distributions Along the Tangency Radius: Build No. 3, 10-deg IGV Setting	115
105	Diffuser Shroud Static Pressure Contours: Build No. 3, 100% Speed, 10-deg IGV	116
106	Diffuser Throat Static Pressure Distribution: Build No. 3, 95% Speed, 10-deg IGV	117
107	Damaged Diffuser Pipe Leading Edges	118
108	Typical Undamaged Diffuser Pipe Leading Edge	119

LIST OF ILLUSTRATIONS (Continued)

Figure		Page
109	Post-Test Condition of Diffuser	119
110	Diffuser Static Pressure Profile: Build No. 6, 95% Speed, 10-deg IGV, Near Stall	120
111	Diffuser Static Pressure Profile: Build No. 6, 100% Speed, 10-deg IGV, Near Stall	120
112	Diffuser Static Pressure Profile: Build No. 6, 101% Speed, -4-deg IGV	121
113	Diffuser Exit Mach Number Profile: Build No. 3, 95% Speed, $N/\sqrt{\theta}$ 10-deg IGV, Near Stall	122
114	Diffuser Exit Mach Number Profile: Build No. 6, 95% Speed, 10-deg IGV, Near Stall	122
115	Diffuser Exit Mach Number Profile: Build No. 6, 100% Speed, 10-deg IGV, Near Stall	123
116	Diffuser Exit Mach Number Profile: Build No. 6, 101% Speed, -4-deg IGV, Near Stall	123
117	Diffuser Exit Mach Number Profile: Build No. 6, 101% Speed, -4-deg IGV, Wide Open Discharge	124
118	Diffuser Losses vs Corrected Weight Flow, Near Stall	125
119	Diffuser Losses vs Impelier Exit Mach Number, Near Stall	125
120	Diffuser Dump Losses Near Stall	126
121	Diffuser Static Pressure Rise Coefficient vs Corrected Weight Flow	126
122	High-Frequency Response Data at 70% Speed	128
123	High-Frequency Response Data at 78% Speed	129
124	IGV Exit Radial Traverse, Build No. 6, 101% Speed, 0-deg IGV, Near Stall	140
125	IGV Circumferential Traverse, Build No. 6, 101% Speed, 0-deg IGV, 10% Span	141

LIST OF ILLUSTRATIONS (Continued)

Figure		Page
126	IGV Circumferential Traverse, Build No. 6, 101% Speed, 0-deg IGV, 30% Span	142
127	IGV Circumferential Traverse, Build No. 6, 101% Speed, 0-deg IGV, 50% Span	143
128	IGV Circumferential Traverse, Build No. 6, 101% Speed, 0-deg IGV, 70% Span	144
129	IGV Circumferential Traverse, Build No. 6, 101% Speed, 0-deg IGV, 90% Span	145
130	IGV Exit Radial Traverse, Build No. 6, 101% Speed, -4-deg IGV	146
131	IGV Circumferential Traverse, Build No. 6, 101% Speed, -4-deg IGV, 10% Span	147
132	IGV Circumferential Traverse, Build No. 6, 101% Speed, -4-deg IGV, 30% Span	148
133	IGV Circumferential Traverse, Build No. 6, 101% Speed, -4-deg IGV, 50% Span	149
134	IGV Circumferential Traverse, Build No. 6, 101% Speed, -4-deg IGV, 70% Span	150
135	IGV Circumferential Traverse, Build No. 6, 101% Speed, -4-deg IGV, 90% Span	151
136	IGV Exit Radial Traverse, Build No. 6, 101% Speed, -5-deg IGV	152
137	IGV Exit Radial Traverse, Build No. 6, 100% Speed, 10-deg IGV, Near Stall	153
138	IGV Circumferential Traverse, Build No. 6, 100% Speed, 10-deg IGV, 10% Span	154
139	IGV Circumferential Traverse, Build No. 6, 100% Speed, 10-deg IGV, 30% Span	155
140	IGV Circumferential Traverse, Build No. 6, 100% Speed, 10-deg IGV, 50% Span	156
141	IGV Circumferential Traverse, Build No. 6, 100% Speed, 10-deg IGV, 70% Span	157

LIST OF ILLUSTRATIONS (Continued)

Figure		Page
142	IGV Circumferential Traverse, Build No. 6, 100% Speed, 10-deg IGV, 90% Span	158
143	IGV Circumferential Traverse, Build No. 3, 70% Speed, 10-deg IGV, 10% Span	159
144	IGV Circumferential Traverse, Build No. 3, 70% Speed, 10-deg IGV, 30% Span	160
145	IGV Circumferential Traverse, Build No. 3, 70% Speed, 10-deg IGV, 50% Span	161
146	IGV Circumferential Traverse, Build No. 3, 70% Speed, 10-deg IGV, 70% Span	162
147	IGV Circumferential Traverse, Build No. 3, 70% Speed, 10-deg IGV, 90% Span	163
148	IGV Exit Radial Traverse, Build No. 6, 70% Speed, 10-deg IGV, Near Stall	164
149	IGV Circumferential Traverse, Build No. 6, 70% Speed, 10-deg IGV, 10% Span	165
150	IGV Circumferential Traverse, Build No. 6, 70% Speed, 10-deg IGV, 30% Span	166
151	IGV Circumferential Traverse, Build No. 6, 70% Speed, 10-deg IGV, 50% Span	167
152	IGV Circumferential Traverse, Build No. 6, 70% Speed, 10-deg IGV, 70% Span	168
153	Inducer Exit Traverse, Build No. 6, 101% Speed, 5-deg IGV, Wide Open Discharge	169
154	Inducer Exit Traverse, Build No. 6, 101% Speed, 5-deg IGV, Near Stall	170
155	Inducer Exit Traverse, Build No. 6, 101% Speed, 0-deg IGV, Wide Open Discharge	171
156	Inducer Exit Traverse, Build No. 6, 101% Speed, 0-deg IGV, Near Stall	172
157	Inducer Exit Traverse, Build No. 6, 101% Speed, -4-deg IGV, Wide Open Discharge	173

LIST OF ILLUSTRATIONS (Continued)

Figure		Page
158	Inducer Exit Traverse, Build No. 6, 101% Speed, -4-deg IGV, Near Stall	174
159	Inducer Exit With Coolant, Build No. 6, 101% Speed, -4-deg IGV, Near Stall	175
160	Inducer Exit Traverse, Build No. 6, 101% Speed, -5-deg IGV	176
161	Inducer Exit Traverse, Build No. 6, 100% Speed, 10-deg IGV	177
162	Inducer Exit Traverse, Build No. 6, 95% Speed, 15-deg IGV, Wide Open Discharge	178
163	Inducer Exit Traverse, Build No. 6, 95% Speed, 15-deg IGV, Near Stall	179
164	Inducer Exit Traverse, Build No. 3, 95% Speed, 10-deg IGV, Wide Open Discharge	179
165	Inducer Exit Traverse, Build No. 3, 95% Speed, 10-deg IGV, Near Stall	180
166	Inducer Exit Traverse, Build No. 3, 95% Speed, 10-deg IGV, Below Near Stall	180
167	Inducer Exit Traverse, Build No. 6, 95% Speed, 10-deg IGV, Wide Open Discharge	181
168	Inducer Exit Traverse, Build No. 6, 95% Speed, 10-deg IGV, Near Stall	182
169	Inducer Exit Traverse, Build No. 6, 95% Speed, 10-deg IGV, Wide Open Discharge	183
170	Inducer Exit Traverse, Build No. 6, 95% Speed, 10-deg IGV, Near Stall	184
171	Inducer Exit Traverse, Build No. 6, 85% Speed, 30-deg IGV, Near Stall	185
172	Inducer Exit Traverse, Build No. 6, 85% Speed, 20-deg IGV, Near Stall	186
173	Inducer Exit Traverse, Build No. 6, 70% Speed, 30-deg IGV, Near Stall	187

LIST OF ILLUSTRATIONS (Continued)

Figure		Page
174	Inducer Exit Traverse, Build No. 6, 70% Speed, 20-deg IGV, Near Stall	188
175	Impeller Exit Traverse, Build No. 6, 101% Speed, 5-deg IGV, Near Stall	189
176	Impeller Exit Traverse, Build No. 6, 101% Speed, 0-deg IGV, Near Stall	190
177	Impeller Exit Traverse, Build No. 6, 101% Speed, -4-deg IGV, Near Stall	191
178	Impeller Exit Traverse With Flange Coolant, Build No. 6, 101% Speed, -4-deg IGV	192
179	Impeller Exit Traverse, Build No. 6, 101% Speed, -5-deg IGV	193
180	Impeller Exit Traverse, Build No. 6, 101% Speed, -5-deg IGV	193
181	Impeller Exit Traverse, Build No. 6, 95% Speed, 15-deg IGV	194
182	Impeller Exit Traverse, Build No. 3, 95% Speed, 10-deg IGV, Wide Open Discharge	195
183	Impeller Exit Traverse, Build No. 3, 95% Speed, 10-deg IGV, Near Stall	196
184	Impeller Exit Traverse, Build No. 3, 95% Speed, 10-deg IGV, Below Near Stall	197
185	Impeller Exit Traverse, Build No. 6, 95% Speed, 10-deg IGV, Wide Open Discharge	198
186	Impeller Exit Traverse, Build No. 6, 95% Speed, 10-deg IGV	199
187	Impeller Exit Traverse, Build No. 6, 95% Speed, 10-deg IGV, Near Stall	200
188	Impeller Exit Traverse, Build No. 6, 85% Speed, 30-deg IGV	201
189	Impeller Exit Traverse, Build No. 6, 85% Speed, 20-deg IGV, Near Stall	202

LIST OF ILLUSTRATIONS (Continued)

Figure		Page
190	Impeller Exit Traverse, Build No. 3, 70% Speed, 20-deg IGV, Wide Open Discharge	203
191	Impeller Exit Traverse, Build No. 3, 70% Speed, 20-deg IGV, Near Stall	204
192	Impeller Exit Traverse, Build No. 3, 70% Speed, 20-deg IGV, Below Near Stall.....	205
193	Impeller Exit Traverse, Build No. 3, 70% Speed, 10-deg IGV, Wide Open Discharge.....	206
194	Impeller Exit Traverse, Build No. 3, 70% Speed, 10-deg IGV, Near Stall	207
195	Impeller Exit Traverse, Build No. 3, 70% Speed, 10-deg IGV, Below Near Stall.....	208
196	Impeller Exit Traverse, Build No. 3, 70% Speed, 0-deg IGV, Wide Open Discharge	209
197	Impeller Exit Traverse, Build No. 3, 70% Speed, 0-deg IGV, Near Stall.....	210
198	Impeller Exit Traverse, Build No. 3, 70% Speed, 0-deg IGV, Below Near Stall	211
199	Impeller Exit Traverse, Build No. 6, 70% Speed, 30-deg IGV	212
200	Impeller Exit Traverse, Build No. 6, 70% Speed, 20-deg IGV	213
201	Impeller Exit Traverse, Build No. 3, 30% Speed, 20-deg IGV, Wide Open Discharge.....	214
202	Impeller Exit Traverse, Build No. 3, 30% Speed, 20-deg IGV, Near Stall	215
203	Impeller Exit Traverse, Build No. 3, 30% Speed, 20-deg IGV, Below Near Stall.....	216
204	Impeller Exit Traverse, Build No. 3, 30% Speed, 10-deg IGV, Wide Open Discharge.....	217
205	Impeller Exit Traverse, Build No. 3, 30% Speed, 10-deg IGV, Near Stall	218

LIST OF ILLUSTRATIONS (Continued)

Figure		Page
206	Impeller Exit Traverse, Build No. 3, 30% Speed, 10-deg IGV, Below Near Stall	219
207	Impeller Exit Traverse, Build No. 3, 30% Speed, 10-deg IGV, Below Near Stall	220
208	Impeller Exit Traverse, Build No. 3, 30% Speed, 0-deg IGV, Wide Open Discharge	221
209	Impeller Exit Traverse, Build No. 3, 30% Speed, 0-deg IGV, Near Stall	222
210	Impeller Exit Traverse, Build No. 3, 30% Speed, 0-deg IGV, Below Near Stall	223
211	Impeller Exit Temperature Traverse, Build No. 6, 101% Speed, 5-deg IGV	224
212	Impeller Exit Temperature Traverse, Build No. 6, 101% Speed, 0-deg IGV	225
213	Impeller Exit Traverse With Coolant, Build No. 6, 101% Speed, -4-deg IGV	226
214	Impeller Exit Traverse With Coolant, Build No. 6, 101% Speed, -4-deg IGV	227
215	Impeller Exit Temperature Traverse, Build No. 6, 101% Speed, -4-deg IGV	228
216	Impeller Exit Temperature Traverse, Build No. 6, 94.5% Speed, 15-deg IGV	229
217	Impeller Exit Temperature Traverse, Build No. 6, 94.5% Speed, 10-deg IGV	230
218	Impeller Exit Temperature Traverse, Build No. 6, 95% Speed, 10-deg IGV, Wide Open Discharge	231
219	Impeller Exit Temperature Traverse, Build No. 6, 95% Speed, 10-deg IGV	232
220	Static Pressure Profile Along Flow Path, Build No. 3, 100% Speed, 10-deg IGV, Near Stall	316

LIST OF ILLUSTRATIONS (Continued)

Figure		Page
221	Static Pressure Profile Along Flow Path, Build No. 3, 95% Speed, 20-deg IGV, Near Stall	316
222	Static Pressure Profile Along Flow Path, Build No. 3, 95% Speed, 10-deg IGV, Wide Open Discharge	317
223	Static Pressure Profile Along Flow Path, Build No. 3, 95% Speed, 10-deg IGV, Near Stall	317
224	Static Pressure Profile Along Flow Path, Build No. 3, 95% Speed, 0-deg IGV, Near Stall	318
225	Static Pressure Profile Along Flow Path, Build No. 3, 70% Speed, 10-deg IGV, Near Stall	318
226	Static Pressure Profile Along Flow Path, Build No. 6, 101% Speed, -4-deg IGV, Wide Open Discharge	319
227	Static Pressure Profile Along Flow Path, Build No. 6, 100% Speed, 10-deg IGV, Near Stall	319
228	Static Pressure Profile Along Flow Path, Build No. 6, 101% Speed, -4-deg IGV, Near Stall	320
229	Static Pressure Profile Along Flow Path, Build No. 6, 95% Speed, 10-deg IGV, Near Stall	320
230	Static Pressure Variation Along Impeller Shroud, Build No. 3, 100% Speed, 10-deg IGV, Near Stall	321
231	Static Pressure Variation Along Impeller Shroud, Build No. 3, 95% Speed, 20-deg IGV, Near Stall	321
232	Static Pressure Variation Along Impeller Shroud, Build No. 3, 95% Speed, 10-deg IGV, Wide Open Discharge	322
233	Static Pressure Variation Along Impeller Shroud, Build No. 3, 95% Speed, 10-deg IGV, Near Stall	322
234	Static Pressure Variation Along Impeller Shroud, Build No. 3, 95% Speed, 0-deg IGV, Near Stall	323
235	Static Pressure Variation Along Impeller Shroud, Build No. 3, 70% Speed, 10-deg IGV, Near Stall	323

LIST OF ILLUSTRATIONS (Continued)

Figure		Page
236	Static Pressure Variation Along Impeller Shroud, Build No. 6, 101% Speed, -4-deg IGV, Wide Open Discharge	324
237	Static Pressure Variation Along Impeller Shroud, Build No. 6, 101% Speed, -4-deg IGV, Near Stall	324
238	Static Pressure Variation Along Impeller Shroud, Build No. 6, 100% Speed, 10-deg IGV, Near Stall	325
239	Static Pressure Variation Along Impeller Shroud, Build No. 6, 95% Speed, 10-deg IGV, Near Stall	325
240	Diffuser Static Pressure Profile, Build No. 3, 95% Speed, Near Stall	326
241	Diffuser Static Pressure Profile, Build No. 3, 10-deg IGV, Near Stall	326
242	High-Frequency Response Data, 70% Speed, Steady-State, PTIDK1	328
243	High-Frequency Response Data, 70% Speed, Steady-State, PSDVK1	329
244	High-Frequency Response Data, 70% Speed, Steady-State, PSDVK2	330
245	High-Frequency Response Data, 70% Speed, Steady-State, PSDEK1	331
246	High-Frequency Response Data, 70% Speed, Stall Transient, Time 406, PTIDK1	332
247	High-Frequency Response Data, 70% Speed, Stall Transient, Time 426, PTIDK1	333
248	High-Frequency Response Data, 70% Speed, Stall Transient, Time 434 PTIDK1	334
249	High-Frequency Response Data, 70% Speed, Stall Transient, Time 436, PTIDK1	335
250	High-Frequency Response Data, 70% Speed, Time 438, PTIDK1	336

LIST OF ILLUSTRATIONS (Continued)

Figure		Page
251	High-Frequency Response Data, 70% Speed, Stalled, Time 440, PTIDK1	337
252	High-Frequency Response Data, 70% Speed, Stall Transient, Time 406, PSDVK1	338
253	High-Frequency Response Data, 70% Speed, Stall Transient, Time 426, PSDVK1	339
254	High-Frequency Response Data, 70% Speed, Stall Transient, Time 434, PSDVK1	340
255	High-Frequency Response Data, 70% Speed, Stall Transient, Time 436, PSDVK1	341
256	High-Frequency Response Data, 70% Speed, Stalled, Time 438, PSDVK1	342
257	High-Frequency Response Data, 70% Speed, Stalled, Time 440, PSDVK1	343
258	High-Frequency Response Data, 70% Speed, Stall Transient, Time 406, PSDVK2	344
259	High-Frequency Response Data, 70% Speed, Stall Transient, Time 426, PSDVK2	345
260	High-Frequency Response Data, 70% Speed, Stall Transient, Time 434, PSDVK2	346
261	High-Frequency Response Data, 70% Speed, Stall Transient, Time 436, PSDVK2	347
262	High-Frequency Response Data, 70% Speed, Stalled, Time 438, PSDVK2	348
263	High-Frequency Response Data, 70% Speed, Stalled, Time 440, PSDVK2	349
264	High-Frequency Response Data, 70% Speed, Stall Transient, Time 406, PSDEK1	350
265	High-Frequency Response Data, 70% Speed, Stall Transient, Time 426, PSDEK1	351

LIST OF ILLUSTRATIONS (Continued)

Figure		Page
266	High-Frequency Response Data, 70% Speed, Stall Transient, Time 434, PSDEK1	352
267	High-Frequency Response Data, 70% Speed, Stall Transient, Time 436, PSDEK1	353
268	High-Frequency Response Data, 70% Speed, Stalled, Time 438, PSDEK1	354
269	High-Frequency Response Data, 70% Speed, Stalled, Time 440, PSDEK1	355
270	High-Frequency Response Data, 78% Speed, Steady-State, PTIDK1	356
271	High-Frequency Response Data, 78% Speed, Steady-State, PSDVK1	357
272	High-Frequency Response Data, 78% Speed, Steady-State, PSDVK2	358
273	High-Frequency Response Data, 78% Speed, Steady-State, PSDEK1	359
274	High-Frequency Response Data, 78% Speed, Stall Transient, Time 533, PTIDK1	360
275	High-Frequency Response Data, 78% Speed, Stall Transient, Time 553, PTIDK1	361
276	High-Frequency Response Data, 78% Speed, Stall Transient, Time 561, PTIDK1	362
277	High-Frequency Response Data, 78% Speed, Stall Transient, Time 563, PTIDK1	363
278	High-Frequency Response Data, 78% Speed, Stalled, Time 565, PTIDK1	364
279	High-Frequency Response Data, 78% Speed, Stalled, Time 567, PTIDK1	365
280	High-Frequency Response Data, 78% Speed, Stall Transient, Time 533, PSDVK1	366

LIST OF ILLUSTRATIONS (Continued)

Figure		Page
281	High-Frequency Response Data, 78% Speed, Stall Transient, Time 553, PSDVK1	367
282	High-Frequency Response Data, 78% Speed, Stall Transient, Time 561, PSDVK1	368
283	High-Frequency Response Data, 78% Speed, Stall Transient, Time 563, PSDVK1	369
284	High-Frequency Response Data, 78% Speed, Stalled, Time 565, PSDVK1	370
285	High-Frequency Response Data, 78% Speed, Stalled, Time 567, PSDVK1	371
286	High-Frequency Response Data, 78% Speed, Stall Transient, Time 533, PSDVK2	372
287	High-Frequency Response Data, 78% Speed, Stall Transient, Time 553, PSDVK2	373
288	High-Frequency Response Data, 78% Speed, Stall Transient, Time 561, PSDVK2	374
289	High-Frequency Response Data, 78% Speed, Stall Transient, Time 563, PSDVK2	375
290	High-Frequency Response Data, 78% Speed, Stalled, Time 565, PSDVK2	376
291	High-Frequency Response Data, 78% Speed, Stalled, Time 567, PSDVK2	377
292	High-Frequency Response Data, 78% Speed, Stall Transient, Time 533, PSDEK1	378
293	High-Frequency Response Data, 78% Speed, Stall Transient, Time 553, PSDEK1	379
294	High-Frequency Response Data, 78% Speed, Stall Transient, Time 561, PSDEK1	380
295	High-Frequency Response Data, 78% Speed, Stall Transient, Time 563, PSDEK1	381

LIST OF ILLUSTRATIONS (Continued)

Figure		Page
296	High-Frequency Response Data, 78% Speed, Stall Transient, Time 565, PSDEK1	382
297	High-Frequency Response Data, 78% Speed, Stalled, Time 567, PSDEK1	383
298	Stall Transient Data, 101% Speed, 5-deg IGV, ISPS Rate	385
299	Stall Transient Data, 101% Speed, 5-deg IGV, Maximum Rate	386
300	Stall Transient Data, 101% Speed, 0-deg IGV, ISPS Rate	387
301	Stall Transient Data, 101% Speed, 0-deg IGV, Maximum Rate	388
302	Stall Transient Data, 101% Speed, -4-deg IGV, ISPS Rate	389
303	Stall Transient Data, 101% Speed, -4-deg IGV, Maximum Rate	390
304	Stall Transient Data, 94.5% Speed, 15-deg IGV, ISPS Rate	391
305	Stall Transient Data, 94.5% Speed, 15-deg IGV, Maximum Rate	392
306	Stall Transient Data, 95% Speed, 10-deg IGV, ISPS Rate	393
307	Stall Transient Data, 95% Speed, 10-deg IGV, Maximum Rate	394

LIST OF TABLES

Table		Page
I	Single-Stage Centrifugal Compressor Design Summary	5
II	Bearing Features	13
III	Test Facility Safety Systems	26
IV	Compressor Instrumentation Stations	28
V	Compressor Component Performance Instrumentation Summary	35
VI	High-Frequency Response Probe Locations	41
VII	Data Summary	48
VIII	Estimate of Instrumentation Accuracy	57
IX	Typical Printout for a Near-Stall, Steady-State Point at 101% Design Speed and -4-deg Inlet Guide Vane Setting	59
X	Traverse Data - Internal Flow Analysis Performance Comparison	63
XI	Inlet Guide Vane Circumferential Traverse Data - 100% Speed, 10-deg IGV Setting	80
XII	Inducer Exit Traverse Data, 101% Speed, -4-deg IGV Setting	87
XIII	Inducer Exit Traverse Data, 100% Speed, 10-deg IGV Setting	87
XIV	Overall Performance Tabulation - Build No. 3, 0-deg Prewhirl	133
XV	Overall Performance Tabulation - Build No. 3, 10-deg Prewhirl	134
XVI	Overall Performance Tabulation - Build No. 3, 20-deg Prewhirl	135
XVII	Overall Performance Tabulation - Build No. 6	137
XVIII	Inlet Guide Vane Performance Printout, 70% Speed, 10-deg IGV, Near Stall, Build No. 3	234

LIST OF TABLES (Continued)

Table		Page
XIX	Inlet Guide Vane Performance Printout, 90% Speed, 10-deg IGV, Near Stall, Build No. 3	235
XX	Inlet Guide Vane Performance Printout, 85% Speed, 20-deg IGV, Near Stall, Build No. 6	236
XXI	Inlet Guide Vane Performance Printout, 85% Speed, 30-deg IGV, Near Stall, Build No. 6	237
XXII	Inlet Guide Vane Performance Printout, 8/1 Speed, 10-deg IGV, Near Stall, Build No. 6	238
XXIII	Inlet Guide Vane Performance Printout, 8/1 Speed, 15-deg IGV, Near Stall, Build No. 6	239
XXIV	Inlet Guide Vane Performance Printout, 101% Speed, 5-deg IGV, Below Near Stall, Build No. 6	240
XXV	Inlet Guide Vane Performance Printout, 95% Speed, 10-deg IGV, Near Stall, Build No. 6	241
XXVI	Inlet Guide Vane Performance Printout, 100% Speed, 10-deg IGV, Near Stall, Build No. 6	242
XXVII	Inlet Guide Vane Performance Printout, 101% Speed, -4-deg IGV, Near Stall, Build No. 6	243
XXVIII	Inlet Guide Vane Performance Printout, 101% Speed, 0-deg IGV, Near Stall, Build No. 6	244
XXIX	Inlet Guide Vane Performance Printout, 101% Speed, 5-deg IGV, Near Stall, Build No. 6	245
XXX	10/1 Centrifugal Compressor, Impeller Traverse, 30 Percent Speed, WDCV, Run 3.06, IGV = 0 deg Flow Rate = 0.494, Speed = 19700.0	247
XXXI	10/1 Centrifugal Compressor, Impeller Traverse, 30 Percent Speed, Below Near Stall, Run 3.06, IGV Setting = 0 deg, Flow Rate = 0.302, Speed = 19420.0	248
XXXII	10/1 Centrifugal Compressor, Impeller Traverse, 30 Percent Speed, Near Stall, Run 3.06, IGV Setting = 0 deg, Flow Rate = 0.253, Speed = 19537.0.	249

LIST OF TABLES (Continued)

Table		Page
XXXIII	10/1 Centrifugal Compressor, Impeller Traverse, 30 Percent Speed, WDCV, Run 3.05, IGV Setting = 10 deg, Flow Rate = 0.432, Speed = 19798.0	250
XXXIV	10/1 Centrifugal Compressor, Impeller Traverse, 30 Percent Speed, Knee, Run 3.06, IGV Setting = 10 deg, Flow Rate = 0.337, Speed = 19877.0	251
XXXV	10/1 Centrifugal Compressor, Impeller Traverse, 30 Percent Speed, Below Near Stall, Run 3.05, IGV Setting = 10 deg, Flow Rate = 0.246, Speed = 19647.0	252
XXXVI	10/1 Centrifugal Compressor, Impeller Traverse, 30 Percent Speed, Near Stall, Run 3.05, IGV Setting = 10 deg, Flow Rate = 0.223, Speed = 19422.0	253
XXXVII	10/1 Centrifugal Compressor, Impeller Traverse, 30 Percent Speed, WDCV, Run 3.06, IGV Setting = 20 deg, Flow Rate = 0.494, Speed = 19874.0	254
XXXVIII	10/1 Centrifugal Compressor, Impeller Traverse, 30 Percent Speed, Below Near Stall, Run 3.06, IGV Setting = 20 deg, Flow Rate = 0.358, Speed = 19912.0	255
XXXIX	10/1 Centrifugal Compressor, Impeller Traverse, 30 Percent Speed, Near Stall, Run 3.06, IGV Setting = 20 deg, Flow Rate = 0.269, Speed = 19458.0	256
XL	10/1 Centrifugal Compressor, Impeller Traverse, 70 Percent Speed, Wide Open Discharge, Run 3.07, IGV Turning = 0 deg, Flow Rate = 1.454, Speed = 45557.0	257
XLI	10/1 Centrifugal Compressor, Impeller Traverse, 70 Percent Speed, Below Near Stall, Run 3.07, IGV Turning = 0 deg, Flow Rate = 1.464, Speed = 45712.0	258
XLII	10/1 Centrifugal Compressor, Impeller Traverse, 70 Percent Speed, Near Stall, Run 3.07, IGV Turning = 0 deg, Flow Rate = 1.452, Speed = 45542.0	259
XLIII	10/1 Centrifugal Compressor, Impeller Traverse, 70 Percent Speed, Wide Open Discharge, Run 3.07, IGV Turning = 10 deg, Flow Rate = 1.463, Speed = 45806.0	260

LIST OF TABLES (Continued)

Table		Page
XLIV	10/1 Centrifugal Compressor, Impeller Traverse, 70 Percent Speed, Below Near Stall, Run 3.07, IGV Turning = 10 deg, Flow Rate = 1.460, Speed = 45883.0 ...	261
XLV	10/1 Centrifugal Compressor, Impeller Traverse, 70 Percent Speed, Near Stall, Run 3.07, IGV Turning = 10 deg, Flow Rate = 1.462, Speed = 45771.0 ...	262
XLVI	10/1 Centrifugal Compressor, Impeller Traverse, 70 Percent Speed, Wide Open Discharge, Run 3.07, IGV Turning = 20 deg, Flow Rate = 1.448, Speed = 45574.0 ...	263
XLVII	10/1 Centrifugal Compressor, Impeller Traverse, 70 Percent Speed, Below Near Stall, Run 3.07, IGV Turning = 20 deg, Flow Rate = 1.459, Speed = 45699.0 ...	264
XLVIII	10/1 Centrifugal Compressor, Impeller Traverse, 70 Percent Speed, Near Stall, Run 3.07, IGV Turning = 20 deg, Flow Rate = 1.458, Speed = 45913.0 ...	265
XLIX	10/1 Centrifugal Compressor, Impeller Exit Traverse, 90 Percent Speed, Near Stall, Run 3.08, IGV Turning = 0 deg, Flow Rate = 2.604, Speed = 58529.6 ...	266
L	10/1 Centrifugal Compressor, Inducer and Impeller Traverse, 8/1 Line, Wide Open Discharge, Run 3.09, IGV Turning = 10 deg, Flow Rate = 2.898, Speed = 61877.0	268
LI	10/1 Centrifugal Compressor, Inducer Traverse, 8/1 Line, Below Near Stall, Run 3.09, IGV Turning = 10 deg, Flow Rate = 2.902, Speed = 61921.0	270
LII	10/1 Centrifugal Compressor, Impeller Traverse, 8/1 Line, Below Near Stall, Run 3.09, IGV Turning = 10 deg, Flow Rate = 2.902, Speed = 61904.0	271
LIII	10/1 Centrifugal Compressor, Inducer Traverse, 8/1 Line, Near Stall, Run 3.09, IGV Turning = 10 deg, Flow Rate = 2.818, Speed = 62035.0	272
LIV	10/1 Centrifugal Compressor, Impeller Traverse, 8/1 Line, Near Stall, Run 3.09, IGV Turning = 10 deg, Flow Rate = 2.895, Speed = 62126.0	273

LIST OF TABLES (Continued)

Table		Page
LV	10/1 Centrifugal Compressor, Inducer and Impeller Traverse, 70 Percent Speed, Near Stall, 20 deg IGV Turning, Build 6, Flow Rate = 1.279, Speed = 45548.9	274
LVI	10/1 Centrifugal Compressor, Inducer and Impeller Traverse, 70 Percent Speed, Near Stall, 30 deg IGV Turning, Build 6, Flow Rate = 1.242, Speed = 45528.7	276
LVII	10/1 Centrifugal Compressor, Inducer and Impeller Traverse, 85 Percent Speed, Near Stall, 20 deg IGV Turning, Build 6, Flow Rate = 2.125, Speed = 55663.1	278
LVIII	10/1 Centrifugal Compressor, Inducer and Impeller Traverse, 85 Percent Speed, Near Stall, 30 deg IGV Turning, Build 6, Flow Rate = 2.071, Speed 55505.1	280
LIX	10/1 Centrifugal Compressor, Inducer Traverse, 8/1 Speedline, WOD, 10 deg IGV Turning, Build 6, Flow Rate = 2.823, Speed = 61657.2	282
LX	10/1 Centrifugal Compressor, Inducer and Impeller Traverse, 8/1 Speedline, Near Stall, 10 deg IGV Turning, Build 6, Flow Rate = 2.796, Speed = 61819.2	283
LXI	10/1 Centrifugal Compressor, Inducer Traverse, 8/1 Speedline, WOD, 15 deg IGV Turning, Build 6, Flow Rate = 2.807, Speed = 61605.6	285
LXII	10/1 Centrifugal Compressor, Inducer and Impeller Traverse, 8/1 Speedline, Near Stall, 15 deg IGV Turning, Build 6, Flow Rate = 2.787, Speed = 61700.7	286
LXIII	10/1 Centrifugal Compressor, Inducer and Impeller Traverse, 95 Percent Speed, WOD, 10 deg IGV Turning, Build 6, Flow Rate = 2.885, Speed = 62114.1	288
LXIV	10/1 Centrifugal Compressor, Inducer and Impeller Traverse, 95 Percent Speed, Near Stall, 10 deg IGV Turning, Build 6, Flow Rate = 2.877, Speed = 62138.8	290
LXV	10/1 Centrifugal Compressor, Inducer Traverse, 100 Percent Speed, Near Stall, 10 deg IGV Turning, Build 6, Flow Rate = 3.058, Speed = 65238.1	292

LIST OF TABLES (Continued)

Table		Page
LXVI	10/1 Centrifugal Compressor, Inducer Traverse, 101 Percent Speed, WOD, -4 deg IGV Turning, Build 6, Flow Rate = 3.214, Speed = 65934.3	293
LXVII	10/1 Centrifugal Compressor, Inducer and Impeller Traverse, 101 Percent Speed, Near Stall, -4 deg IGV Turning, Build 6, Flow Rate = 3.209, Speed = 65987.7 . . .	294
LXVIII	10/1 Centrifugal Compressor, Inducer and Impeller Traverse, 101 Percent Speed, Near Stall, -4 deg IGV, With Coolant, Build 6, Flow Rate = 3.214, Speed = 65779.6 . . .	296
LXIX	10/1 Centrifugal Compressor, Inducer Traverse, 101 Percent Speed, WOD, 0 deg IGV Turning, Build 6, Flow Rate = 3.192, Speed = 65834.8	298
LXX	10/1 Centrifugal Compressor, Inducer and Impeller Traverse, 101 Percent Speed, Near Stall, 0 deg IGV Turning, Build 6, Flow Rate = 3.185, Speed = 65952.8 . . .	299
LXXI	10/1 Centrifugal Compressor, Inducer Traverse, 101 Percent Speed, WOD, 5 deg IGV Turning, Build 6, Flow Rate = 3.150, Speed = 65974.5	301
LXXII	10/1 Centrifugal Compressor, Inducer and Impeller Traverse, 101 Percent Speed, Near Stall, 5 deg IGV Turning, Build 6, Flow Rate = 3.142, Speed = 66122.6 . . .	302
LXXIII	10/1 Centrifugal Compressor, Inducer Traverse, 100 Percent Speed, Near Stall, 10 deg IGV Turning, Build 6, Flow Rate = 3.058, Speed = 65238.1	304
LXXIV	10/1 Centrifugal Compressor, Inducer and Impeller Traverse, 101 Percent Speed, Near Stall, -4 deg IGV Turning, Build 6, Flow Rate = 3.209, Speed = 65987.7 . . .	305
LXXV	10/1 Centrifugal Compressor, Impeller Traverse, 8/1 Speedline, Near Stall, 10 deg IGV Turning, Build 6, Flow Rate = 2.796, Speed = 61819.2	307
LXXVI	10/1 Centrifugal Compressor, Impeller Traverse, 8/1 Speedline, Near Stall, 15 deg IGV Turning, Build 6, Flow Rate = 2.787, Speed = 61700.7	308

LIST OF TABLES (Continued)

Table		Page
LXXVII	10/1 Centrifugal Compressor, Impeller Traverse, 95 Percent Speed, WOD, 10 deg IGV Turning, Build 6, Flow Rate = 2.885, Speed = 62114.1	309
LXXVIII	10/1 Centrifugal Compressor, Impeller Traverse, 95 Percent Speed, Near Stall, 10 deg IGV Turning, Build 6, Flow Rate = 2.877, Speed = 62138.8	310
LXXIX	10/1 Centrifugal Compressor, Impeller Traverse, 101 Percent Speed, Near Stall, -4 deg IGV Turning, Build 6, Flow Rate = 3.209, Speed = 65987.7	311
LXXX	10/1 Centrifugal Compressor, Impeller Traverse, 101 Percent Speed, Near Stall, -4 deg IGV, With Coolant, Build 6, Flow Rate = 3.214, Speed = 65779.6	312
LXXXI	10/1 Centrifugal Compressor, Impeller Traverse, 101 Percent Speed, Near Stall, 0 deg IGV Turning, Build 6, Flow Rate = 3.185, Speed = 65952.8	313
LXXXII	10/1 Centrifugal Compressor, Impeller Traverse, 101 Percent Speed, Near Stall, 5 deg IGV Turning, Build 6, Flow Rate = 3.142, Speed = 66122.6	314

LIST OF SYMBOLS

A	cross-sectional area, $in.^2$
A*	throat area, $in.^2$
a	speed of sound, ft/sec
B*	throat blockage
C_d	inlet flow coefficient
C_d*	diffuser discharge coefficient
C_p	pressure recovery coefficient
e	uncertainty of an individual sensor
G	gravitational constant = 32.174, lb_m-ft/lb_f-sec^2
h	enthalpy/unit mass
i	incidence, deg
K	f (Mach number) = $M\sqrt{\frac{\gamma G}{R}}\left(1+\frac{\gamma-1}{2}M^2\right)^{\frac{-\gamma+1}{2(\gamma-1)}}$
M	relative Mach number
M_o	absolute Mach number
N	rotor speed, rpm
n	Number of sensors
P	static pressure, psia
P_r	pressure ratio
P_t	total pressure, psia
R	gas constant = 53.345, ft-lb_f/lb_m-°R
T	total temperature, °R
T_r	temperature ratio
T_s	static temperature, °R

LIST OF SYMBOLS (Continued)

U	rotor speed, ft/sec
u	overall uncertainty
V	absolute velocity, ft/sec
W	relative velocity, ft/sec
w	weight flow, lb/sec
α	absolute air angle, deg
β	relative air angle, deg
β^*	leading edge metal angle, deg
γ	ratio of specific heats
δ	$P_0/14.694$
ϵ	diffuser effectiveness
η	adiabatic efficiency
θ	$T_0/518.688$

SUBSCRIPTS

act	actual
cal	calculated
cor	corrected to standard day inlet conditions
i	ideal
m	axial component
rel	relative
s	strut
t-s	total to static
u	tangential component

LIST OF SYMBOLS (Continued)

v	vane
o	plenum
1	IGV exit instrumentation station
1.5	inducer exit instrumentation station
2	impeller exit instrumentation station
3	collector

SUPERSCRIPTS

$(\bar{})$	mass averaged
$()^*$	sonic (throat) condition

INTRODUCTION

High-pressure ratio, single-stage centrifugal compressors offer the possibility of providing rugged, relatively erosion-resistant and low-cost compression systems for advanced gas turbine engines of the 2-to-5-lb/sec airflow class. If good efficiency can be obtained at high pressure ratios, this type of compressor will be more useful than the multistage axial flow compressors now used in small military aircraft engines. The objective of this five-phase program was to design, fabricate, and test a high pressure ratio centrifugal compressor with the following minimum goals:

1. Pressure ratio of 10.0:1 and corresponding adiabatic efficiency of 75% at design speed and flow.

2. Pressure ratio of 8.0:1 and corresponding adiabatic efficiency of 80% at a speed and flow condition less than that of the design point.

The five program phases are (1) initial compressor design, (2) fabrication and assembly of the test hardware, (3) test of the initial configuration, (4) evaluation of the test data, and (5) compressor modification to include fabrication and assembly of new hardware, test, and data evaluation.

This report contains information pertaining to all phases of the program. It includes two appendixes. Appendix I contains tabulated and plotted data not necessary to the general text. Appendix II (separately bound) contains the detailed aerodynamic design and is classified CONFIDENTIAL.

The two test phases of the program were completed during six test periods over a 3-year span. The progress of the contract experimental program was interrupted to permit redesign and modification of the test rig to achieve its rated rpm. The following chronological sequence of the tests conducted during this program will aid in understanding the design and data described in this report. Each successive configuration of either the test stage or rig is identified by a build number.

Build No. 1: The initial build of the rig was tested to approximately 70% of the design speed. The impeller rubbed the shroud and the run program was terminated.

Build No. 2: The second build contained modifications to prevent the impeller from contacting the shroud. This build was tested to approximately 85% of design speed, where testing was terminated due to high rig vibration levels. Performance data from this test were evaluated and permitted a minor aerodynamic redesign to be completed. As a result of the redesign, the diffuser was resized to match the inducer-impeller characteristic.

Build No. 3: The vibrations encountered in Build No. 2 were diagnosed as a critical speed problem, and the rotor system and impeller attachment were stiffened to increase the critical

speed out, hopefully, of the running range. While these modifications improved the rig operating envelope, high vibrations were again encountered at design speed. The entire test program was completed, with the exception of the design speed testing and special instrumentation tests. It was determined that the prediction of rig critical speed was relatively inaccurate for the overhung rotor configuration. It was further determined that a straddle-mounted bearing system (impeller between bearings) would be capable of running at higher speeds without failure, and the rig was redesigned accordingly, including rerouting the inlet flow path around the new front bearing compartment.

Build No. 4: This build was tested as a checkout for the redesigned rig bearing system; however, testing was terminated by an impeller-to-shroud rub, which occurred at approximately 85% speed. Silver scraped from the shroud during the rub caused damage to the diffuser entrance region during this test. Data obtained during this test indicated the presence of potential heat transfer into the inlet and also through the cases. The inlet and inlet plenum were insulated and a thermal dam was machined between the inducer and impeller shrouds to eliminate these problems.

Build No. 5: The rig was modified to include a thermal dam to limit the heat transfer between the inducer and impeller shrouds, and the clearances were modified to prevent rubbing between impeller and shroud. The rig mechanical redesign was successfully checked out to design speed.

Build No. 6: This build concluded the contract test program, as all phases of the modified test plan that concentrated on obtaining data near design speed were successfully completed. Stable rig operation was demonstrated at speeds as high as 72,000 rpm (112% of design speed).

The aerodynamic and performance data in this report primarily result from the tests of Builds No. 2, 3, and 6. The only change in aerodynamic hardware from Build No. 2 to Build No. 3 consisted of removal of 0.020 in. of the impeller exit diameter to prevent contact with the diffuser shroud during testing. The Build No. 6 impeller did not have this 0.020 in. of material removed and thus was identical to the original design. Build No. 6 did have a new inlet bellmouth and a converging inlet with two additional inlet struts due to the new rig mechanical arrangement required to achieve design speed. The inlet guide vanes and inducer were unchanged from the original design, and the diffuser was repaired as much as possible, but still contained damage in the entrance region due to the Build No. 4 impeller-to-shroud rub.

DESIGN APPROACH

AERODYNAMIC DESIGN

The aerodynamic design is completely described in a separate volume as Appendix II to this report and is classified CONFIDENTIAL. A brief summary of the design of the stage, shown in Figure 2, is presented herein. The design consists of variable inlet guide vanes, an impeller with a remote inducer, and a pipe diffuser.

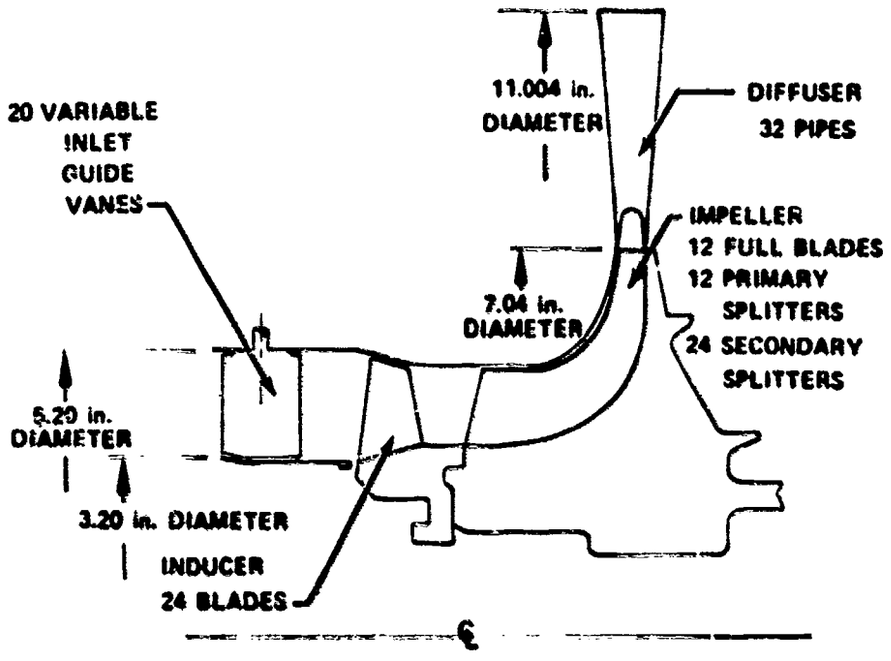

Figure 2. 10:1 Pressure Ratio Centrifugal Compressor Stage.

The objective of the program was to design a 2-to-5-lb/sec airflow single-stage centrifugal compressor that could be incorporated in a future Army advanced technology gas turbine engine. The design speed performance goals were to exceed 75% efficiency at 10:1 pressure ratio. Since gas turbine engines for Army aircraft applications operate under part-power conditions a majority of the time, an off-design performance goal of 80% efficiency at 8:1 pressure ratio was established.

In the design of the compressor, parametric studies were conducted to select an overall design consistent with optimum compressor performance at both performance goals. These studies defined the compressor inlet corrected flow rate, impeller inlet hub and tip radii, corrected impeller rotational speed, and inlet prewhirl. Airflow selection and the selection of the hub radius were influenced by the decision to design a compressor that could be used in a small turboshaft engine with a concentric shaft front drive. This configuration required a larger inlet hub radius than that normally associated with research impellers but it was felt that the loss in potential performance was not significant.

The tip radius was selected after determining the effect on axial Mach number, inducer tip relative Mach number, and inlet choke flow margin. The effect of inlet guide vane losses, inlet shock losses, diffuser losses, and shroud friction heating were parametrically evaluated before selecting IGV prewhirl and rotor speed to provide the optimum overall compressor performance.

A remote inducer design was selected over an integral inducer-impeller configuration so that the inducer could be designed using transonic axial-flow compressor technology. The work split between the inducer and impeller was selected so that the relative Mach number into the impeller would be subsonic with no more than a 1.6:1 inducer pressure ratio. The resultant 10:1 pressure ratio impeller with remote inducer is shown in Figure 3.

Figure 3. 10:1 Pressure Ratio Centrifugal Impeller and Remote Inducer.

[illegible] over configurations were evaluated with respect to their potential for application to the single-stage compressor. A pipe diffuser was selected over vaneless radial and cascade diffusers, because it has the lowest losses over the largest range of Mach number and because P&WA[FM] has had substantial experience in designing and fabricating this type of diffuser.

A tabulation of pertinent compressor design information is presented in Table I.

TABLE I. SINGLE-STAGE CENTRIFUGAL COMPRESSOR DESIGN SUMMARY

Compressor Overall	
Pressure Ratio	10:1*
Adiabatic Efficiency, %	75
Flow rate, lb/sec	3.1
Rotor Speed, rpm	65,300
Specific Speed	80
Inlet	
4 Struts	NACA 400 Series
20 Inlet Guide Vanes	NACA 63 Series
Nominal Guide Vane Setting, deg	10
Specific Flow, $lb/ft^2/sec$	34
Hub Radius, in.	1.6
Tip Radius, in.	2.6
Inducer	
Remote Arrangement	
24-Transonic Blades	
Hub-Tip Ratio	0.615
Nominal Pressure Ratio	1.57:1
Nominal Efficiency, %	87.6
Impeller	
Nominal Pressure Ratio	7.34:1
Nominal Efficiency, %	82.8
Exit Flow Angle, deg	19.5
Exit Tip Radius, in.	3.52
Exit Blade Height, in.	0.230
Nominal Operating Clearance	0.005
Diffuser	
32-Passage Conical Pipe Type	
Vaneless Space Radius Ratio, in.	1.10
Throat Radius	0.11
Straightening Section	L/d = 0.5
Cone Geometry, deg	3 to 5
Nominal Loss ($\Delta P_t/P_t$)	0.12
Pressure Recovery Coefficient	0.789

*Unless otherwise specified, pressure ratio is the ratio of discharge static (plenum) pressure to inlet stagnation pressure. Efficiency is also specified using this pressure ratio.

MECHANICAL DESIGN

Although the objectives of this program were primarily aerodynamic, the mechanical aspects of the test compressor, drive turbine, and the test facility exerted a large influence on the course of the program. As is the case with all high-speed rotating machinery, design emphasis was placed on the evaluation of blade and disk stress limits, determination of rotor critical speeds, and calculation of bearing loads. Tests using the original compressor-drive turbine configuration, described in the Introduction section, uncovered serious limitations to the safe rig operating envelope and necessitated a substantial redesign of the rig rotor system. Although the design and development of the high-speed drive turbine was not part of the scope of the work of this contract, the contract compressor stage was directly mounted on the drive turbine rotor and their system dynamics were integral. Consequently, a discussion of the drive turbine design and its subsequent redesign are included in this section. The mechanical design of the 10:1 pressure ratio centrifugal stage is discussed in the following paragraphs. A schematic drawing of the initial drive turbine and compressor test hardware design is provided in Figure 4. The design featured an axial flow inlet, variable inlet guide vanes, overhung spline drive inducer and impeller, and a double radial inflow drive turbine.

Inlet

The inlet section was required to support the inlet centerbody, house the variable inlet guide vanes, and provide lubricating oil to the front bearing and instrumentation routing channels. It was fabricated from aluminum weldments. The thickness of the four supporting struts was determined by the size of the oil supply line. An analysis indicated that the oil flow requirement could be accomplished with a 1/8-in. OD tube. Therefore, a conservative maximum thickness of 1/4-in. strut was selected.

With 4 struts and 20 inlet guide vanes, it was appropriate to place every 5th guide vane in line with a strut. All of the guide vanes were connected to a synchronizing ring, which allowed variable positioning of the vanes from zero to 30 deg of prewhirl. An actuator was used to position the vanes. The actuation linkage was designed with close tolerances wherever feasible to keep alignment errors to a minimum. The calculated maximum misalignment of an individual vane was ±1.5 deg from the nominal angle. Sealing of leakage flow around each vane was accomplished with an O-ring on each vane shaft. Contouring of the vane hub and tip provided a clearance of 0.005 to 0.015 in. at all positions of actuation.

Inducer

In the mechanical design of the inducer, a thin conical splined shaft was used to transmit torque from the drive shaft. The design of the remote inducer permitted it to be readily modified to a close-coupled inducer configuration at a later date. A stress analysis of the AISI Ti-6Al-4V inducer disk showed the maximum effective disk stress to be just under 35,000 psi, which gave a burst margin of 106%. An analysis of the 1.04 aspect ratio blade natural frequencies indicated that there were no bending or torsional modes within the intended operating range (Figure 5).

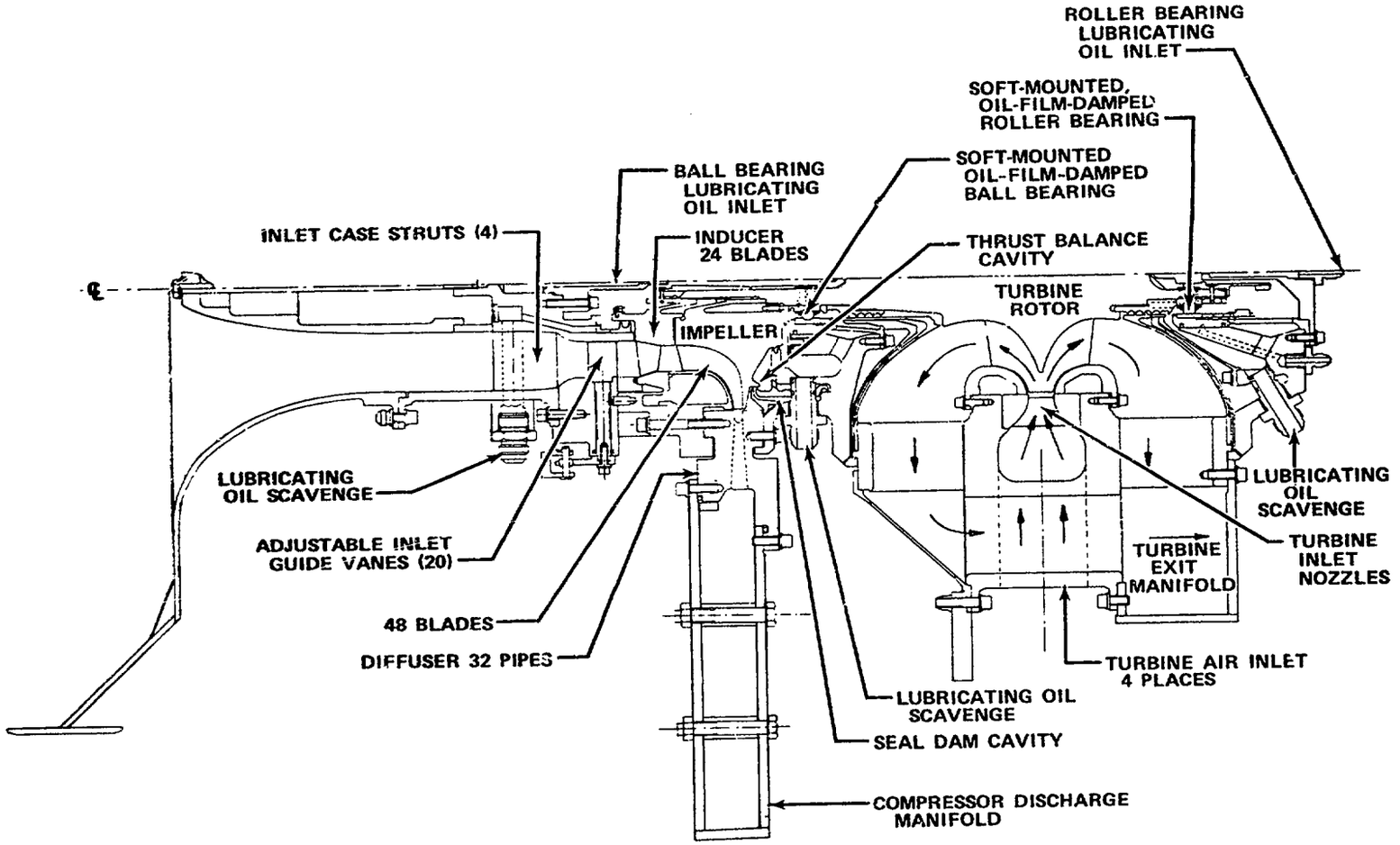

Figure 4. Initial Design of 10.0:1 Pressure Ratio Centrifugal Compressor and P&WA™ Drive Turbine.

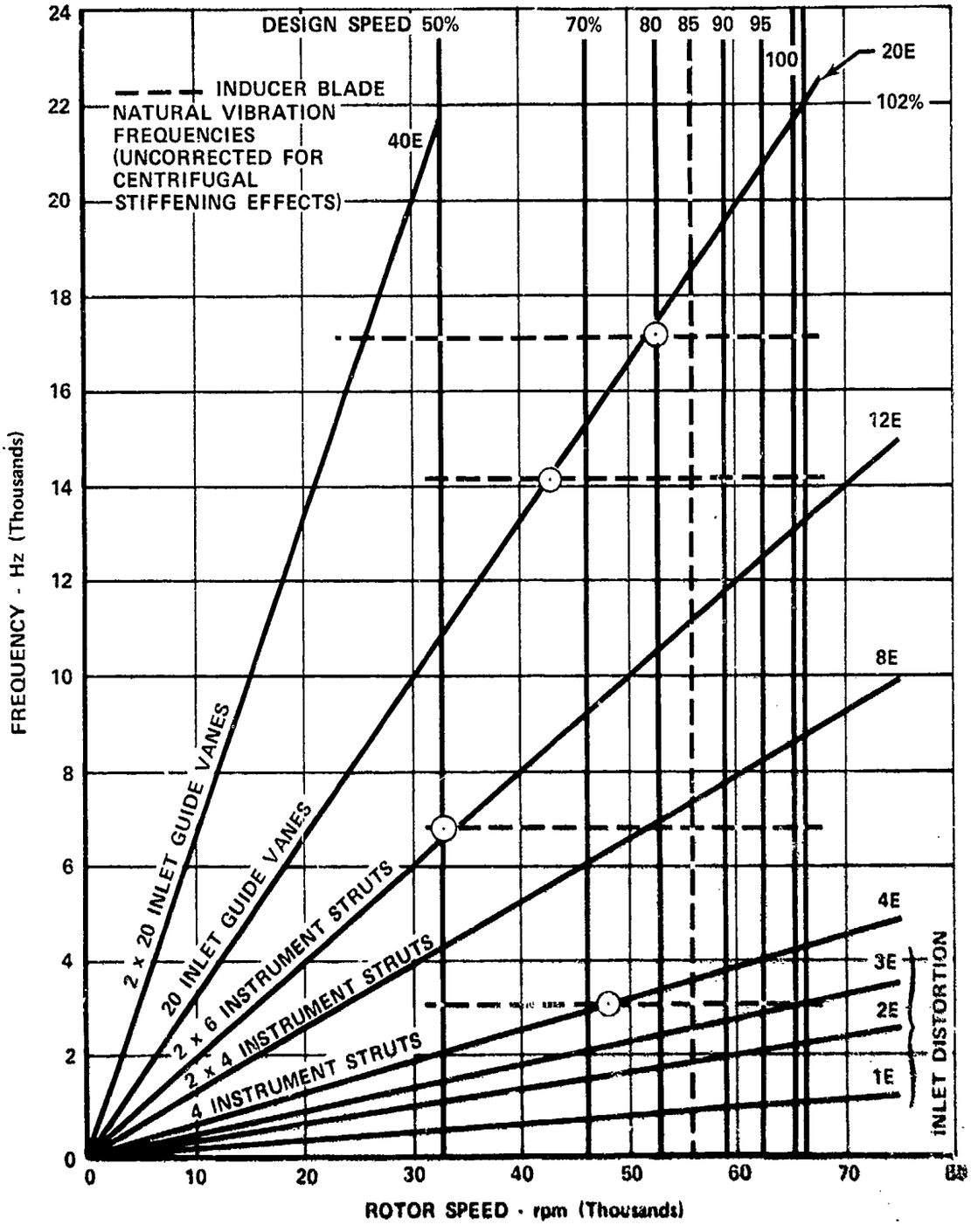

Figure 5. Inducer Vibration Analysis.

Impeller

The impeller attachment design also employed a thin conical splined shaft to transmit torque and had a press fit on the drive shaft for alignment. The impeller and inducer were mated with an interference (snap) fit, as shown in Figure 6. Stress analysis of the impeller disk at 72,000 rpm showed maximum predicted bore effective stress of 133,000 psi. Using AISI Ti-6Al-2Sn-4Zr-6Mo material, with a 0.2% yield strength of 153,000 psi, at the maximum predicted bore temperature of 220°F, the disk stresses are within acceptable limits. A calculated burst speed of 98,900 rpm results in an adequate burst margin of 37.2%. A stress analysis of the impeller blades predicted maximum blade stresses at about 75% of the local yield stress (loss of strength due to increased temperature taken into account).

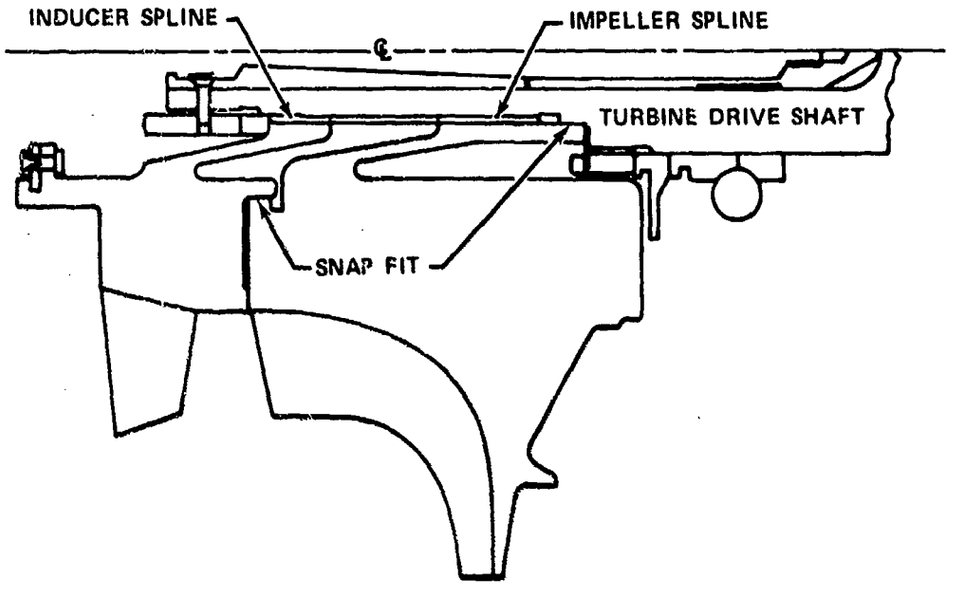

Figure 6. Impeller and Inducer Attachment.

Shrouds and Diffuser

Aerodynamic design of the inducer had the tip diameter converge from the leading to the trailing edges. This convergence resulted in a separate inducer and impeller to allow assembly. The aerodynamic design of the impeller and inducer also required operation with very small shroud clearances, on the order of 0.005 in. To minimize the consequences of rubbing a titanium blade on a stainless steel shroud, both impeller and inducer shrouds were plated with a thin layer of silver, 0.005 to 0.007 in. thick, which provided a relatively soft rub surface. Positioning of the shrouds relative to the impeller-inducer was accomplished by means of shim selection at assembly.

Stainless Steel 410 was selected for making the 32-passage pipe diffuser because its low coefficient of thermal expansion approaches that of the titanium impeller. The insides of the diffuser pipes were nickel plated to minimize corrosion. The

alignment of the diffuser inlet with respect to the impeller blade exit was designed to be adjusted at assembly with shims.

To define running clearances and diffuser-impeller alignment, mechanical clearance probes were designed to experimentally measure the running tip clearance (Figure 7). The projection of the replaceable aluminum wire into the clearance space was measured during assembly. On the test stand, rotor rpm was increased by increments, and after each increment, the probes were removed and the length of wire was measured to determine clearance as a function of rotor speed. The clearance thus determined is the net result of any impeller movement and shroud and diffuser thermal growth.

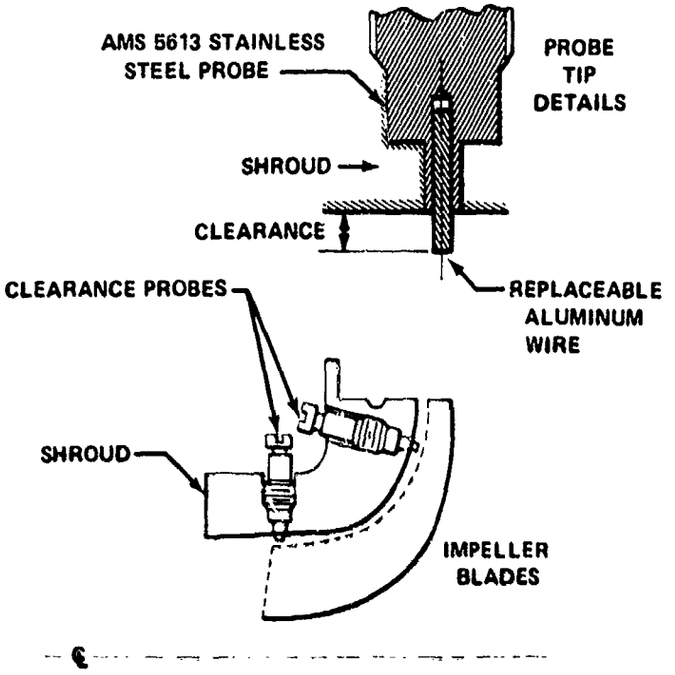

Figure 7. Tip Clearance Probe Installation.

Bearings and Seals

The bearing support for the compressor and drive turbine consisted of two 35-mm rolling element bearings straddle mounted on either side of the turbine rotor. The compressor splined drive shaft was overhung beyond the front bearing, as shown in Figure 8.

The forward bearing, which also functions as a thrust bearing and, hence, positions the impeller, is a split-inner-race ball bearing that can accommodate transient thrust reversals. The rear bearing is a straight-through-outer-ring roller bearing that can accommodate axial thermal growth. At the design speed of 63,300 rpm, the bearing DN (bore diameter in mm x rpm) is 2.28 million. Selecting a smaller bearing diameter would force more severe limitations on potential

front-drive capability in an engine application. It would also reduce the allowable thrust load range of the ball bearing (between skid and fatigue limits) to a point where precise thrust balance control would be required. The bearing material, M50 alloy steel (PWA™ 725), was selected as the best available alloy for both bearings. Bearing cross sections are shown in Figure 9, and pertinent design parameters are listed in Table II. Both bearings have one-piece, inner-land-riding cages that are machined from AMS 6414 steel and silver plated. Wide cage lands ensure adequate cage journal support area. Lubricating oil is supplied from within the shaft to ensure adequate inner race cooling and positive oil distribution within the bearings. Total oil flows are 7 and 4 lb/min, respectively, for the ball and roller bearings.

Ball bearing raceway curvatures for the compressor rig were selected to limit Hertz stress and to keep spin-to-roll ratio (heat generation) to reasonable levels. The inner race curvature was increased somewhat above the optimum fatigue life value to reduce potential cage problems and heat generation. The higher curvature tends to provide lower cage loading and wear by restricting contact angle variation due to misalignment or excessive radial load. To provide additional margin in this respect, it was desirable to restrict radial loads on the ball bearing to no more than one third of the thrust load. Within this framework, the design analysis indicated that a complement of 15 balls with 5/16 in. diameter would provide the maximum fatigue life.

The compressor rig roller bearing was designed to support radial loads (predicted from rotor dynamic analysis) up to 150 lb in excess of 150 hr with proper balance, alignment, and lubrication. This resulted in a complement of fourteen 7.5- by 7.5-mm rollers.

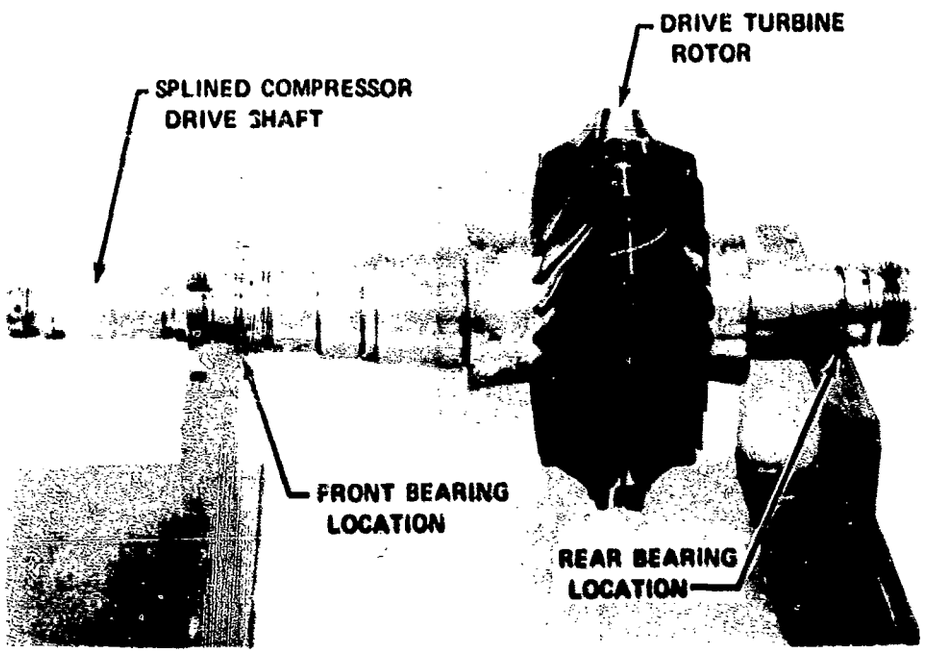

Figure 8. Initial Compressor Drive and Bearing Support Design.

BORE SIZE, mm: 35

OIL: MIL-L-23699

INLET TEMPERATURE, °F: 150

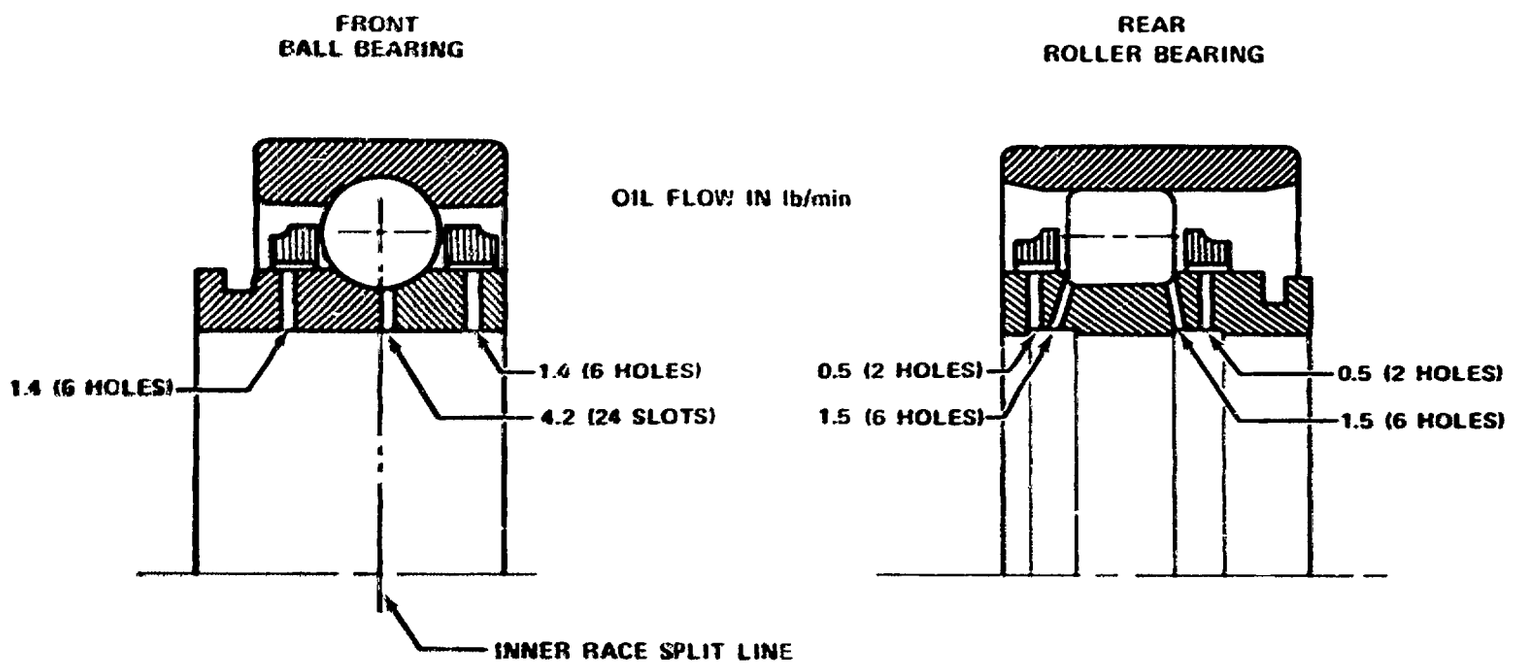

Figure 9. Bearing Designs.

TABLE II. BEARING FEATURES[1]

	Ball	Roller
Nominal bore size, mm	35	35
OD, in.	2.4408	2.4408
ID, in.	1.3779	1.3779
Number of elements	15	14
Element size	5/16 in.	7.5 x 7.5 mm[2]
Pitch circle diameter, in.	1.9095	1.9095
Outer raceway curvature, %[3]	52	-
Inner raceway curvature, %[3]	56	-
Contact angle, deg	25	-

[1] Room temperature

[2] 10-in. radius crown

[3] (radius of curvature/ball diameter) x 100

Due to the high centrifugal loading, the rollers were designed with more than normal crown drop to reduce the tendency for end loading and wear.

Rotor Dynamics

A vibrational analysis of the compressor and turbine rotor assembly, shown in Figure 10, indicated acceptable bearing loads and rotor deflections. The bounce and pitch modes (11,000 and 25,000 rpm, respectively) of the rotor were in the lower end of the operating speed range and their response would be readily damped by the oil film dampers at the ball and roller bearing supports. Calculation of the first bending mode rotor critical speed showed it was well out of the running range. Dynamic response calculations of bearing loads are shown in Figures 11 and 12 for a 0.1 oz-in. unbalance at the front and rear bearings, respectively.

Thrust Balance

An external system was incorporated to supply gaseous nitrogen on the rear face of the compressor impeller to maintain a minimum thrust load on the ball bearing. Calculated load as a function of speed required to prevent the ball bearing from skidding is shown in Figure 13. The 240 lb required at design speed was well below the maximum recommended ball bearing thrust load capacity of 400 lb. Labyrinth-type knife edge seals were used to contain the nitrogen in the thrust balance cavity. In addition, a seal dam cavity between the impeller tip backface and the thrust balance cavity was incorporated that minimized flow between the impeller tip backface and the thrust balance cavity.

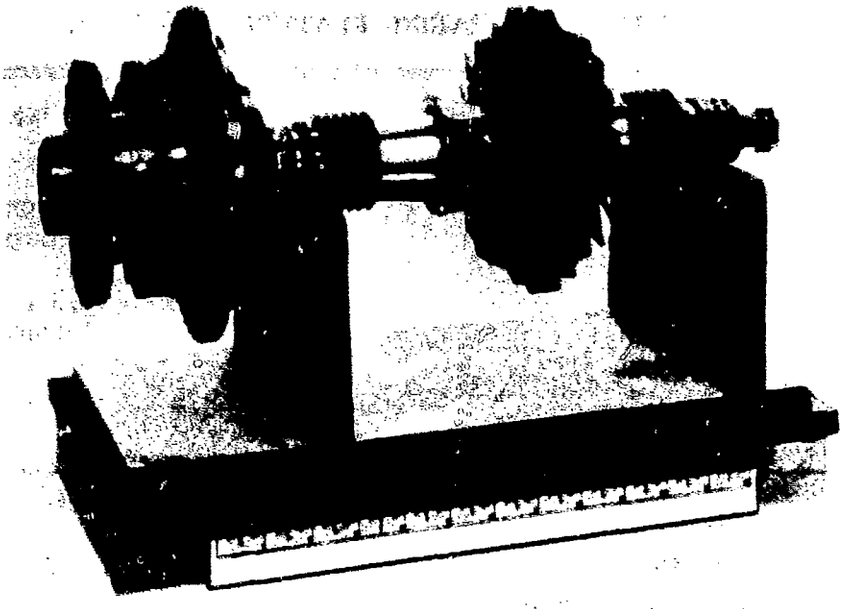

Figure 10. Compressor and Turbine Rotor Assembly.

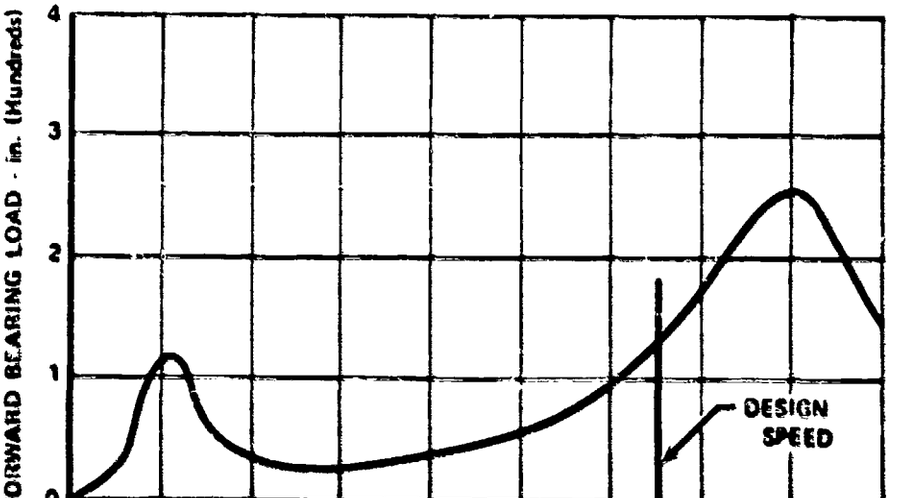

Figure 11. Initial Rotor Configuration Predicted Front Bearing Loads.

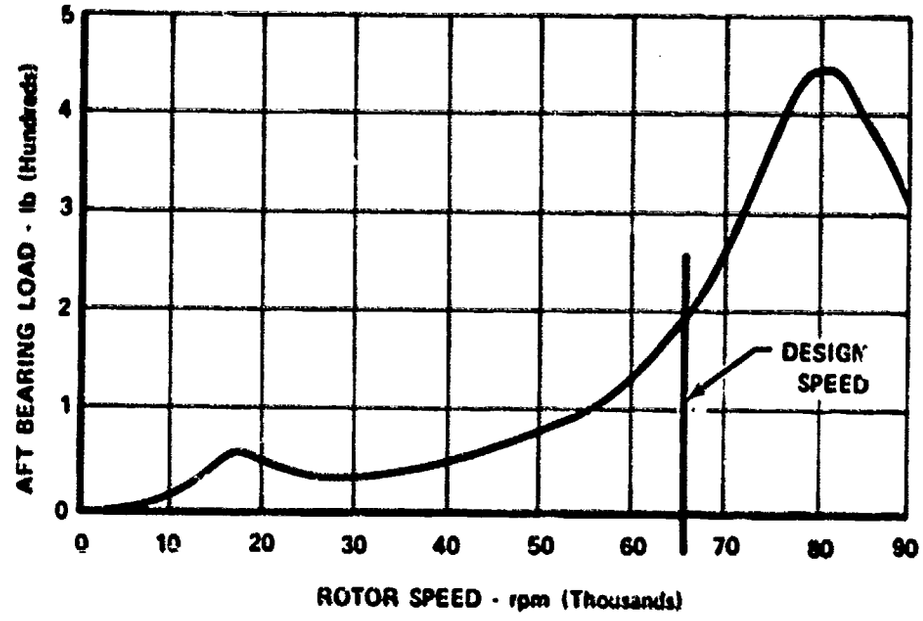

Figure 12. Initial Rotor Configuration Predicted Rear Bearing Loads.

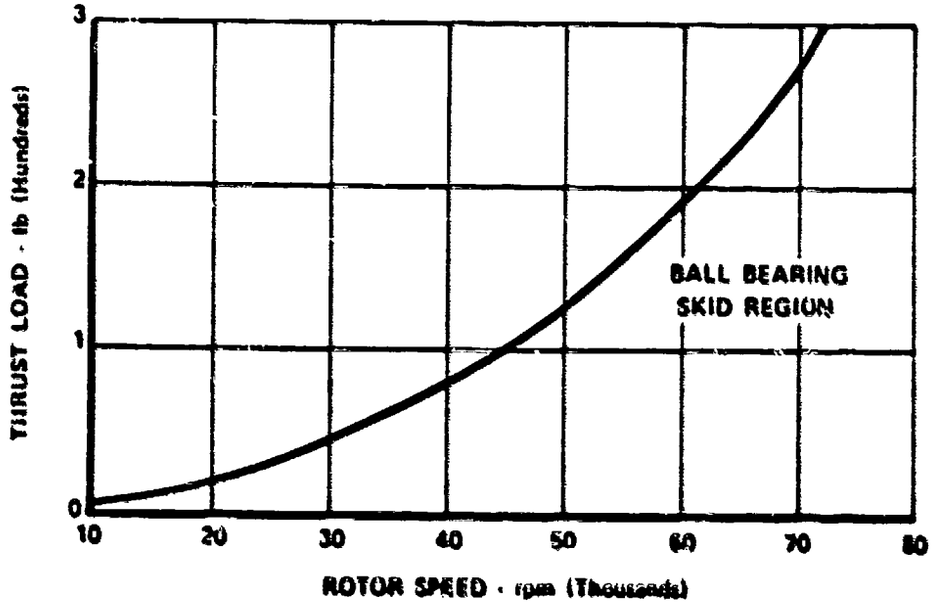

Figure 13. Predicted Ball Bearing Minimum Thrust Load Requirements.

Modifications

The impeller attachment scheme was stiffened when high rotor vibrations in Build No. 2 limited maximum speed to 58,000 rpm. The impeller bore diameter was increased to permit insertion of a cylindrical spacer, shown in Figure 14. The cylindrical spacer added stiffness at the impeller-shaft attachment point due to the larger diameter in the impeller region. A spacer was also added between the inducer and impeller. This spacer, in conjunction with the impeller cylindrical spacer, permitted the axial load to be transmitted from the front of the inducer, through the impeller, to the drive shaft in a more direct fashion. Further action was taken to prevent a rub from occurring in the event rotor vibrations were not corrected. The impeller exit diameter was reduced 0.020 in. to prevent the impeller tip from rubbing the diffuser vaneless space.

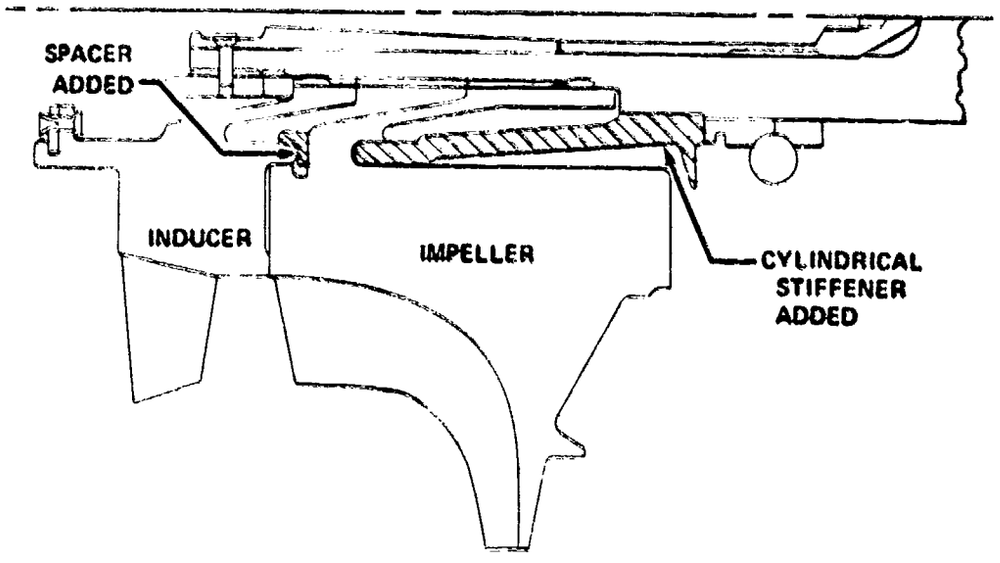

Figure 14. Impeller Shaft Attachment Modification.

The impeller attachment modifications increased the maximum allowable rotor speed to slightly in excess of design speed (63,300 rpm). However, during Build No. 3, high vibrations at or near design speed caused the front bearing to fail after 5.1 hr of operation at 95 to 100% of design speed. Rapid shutdown procedures prevented any damage to the compressor, but it was decided not to resume testing until after the rotor assembly was completely redesigned for increased dynamic stability.

MECHANICAL REDESIGN

The approach taken in the mechanical redesign of the compressor/turbine rotor assembly was to significantly increase critical speed margin and to increase the front bearing radial load capacity to ensure continuous operation at design speeds and above. The redesigned test hardware, shown in Figure 15, features tandem ball and roller bearings, a carbon face seal in front of the impeller, and a CURVIC® coupling to join the impeller and drive turbine.

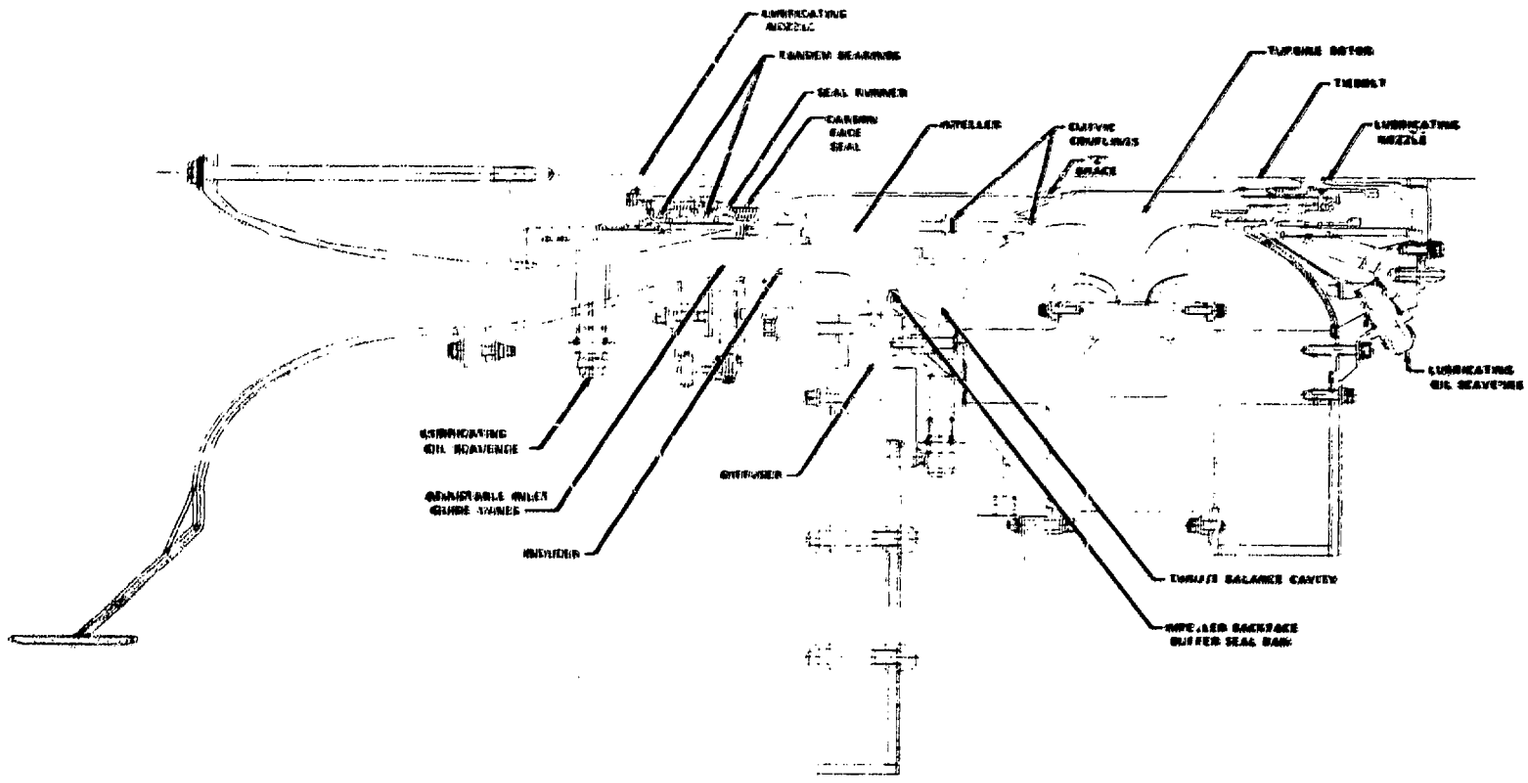

Figure 15. Redesigned 10:1 Pressure Ratio Centrifugal Compressor and P&WA™ Drive Turbine.

Inlet

Placing two bearings and a carbon seal in front of the impeller required the flow path to be changed from a parallel flow inlet to a converging configuration to provide the additional space needed for the bearing compartment and seal support. The increased supply of oil needed for lubricating the two bearings and cooling the carbon seal plate, and additional scavenge and breather requirements could not be accommodated in the four original inlet struts. Two additional struts were incorporated for a total of six equally spaced struts. By terminating the flow path convergence at the inlet guide vanes, it was possible to use the same 20 inlet guide vanes that were used in the original inlet.

Inducer

In the redesign of the rotor assembly, the attachment of the inducer was changed to eliminate the spline. Friction was used to drive the inducer and was transmitted by the tiebolt and the radial inducer-impeller interface. The axial tiebolt load at room temperature was 18,500 lb. A stress analysis of the redesigned inducer disk indicated maximum effective stress to be 96,000 psi. This was equivalent to a burst margin of 49%, which, although less than the original design, was still more than adequate. The inducer remote spacing was maintained.

Impeller

The attachment of the impeller to the drive turbine was redesigned to use a CURVIC coupling for maintaining rotor assembly concentricity and transmitting the torque from the drive turbine. The redesigned rotor assembly is shown in Figure 16. The forward end of the original drive turbine was modified for a CURVIC coupling. A CURVIC spacer was used to separate the turbine and impeller. The use of a tiebolt to hold the rotor assembly together required changing the original impeller bore geometry. A stress analysis showed the redesigned impeller maximum bore stresses to be 120,000 psi, which was nearly the same as the original impeller design and provided an adequate burst margin of 41%.

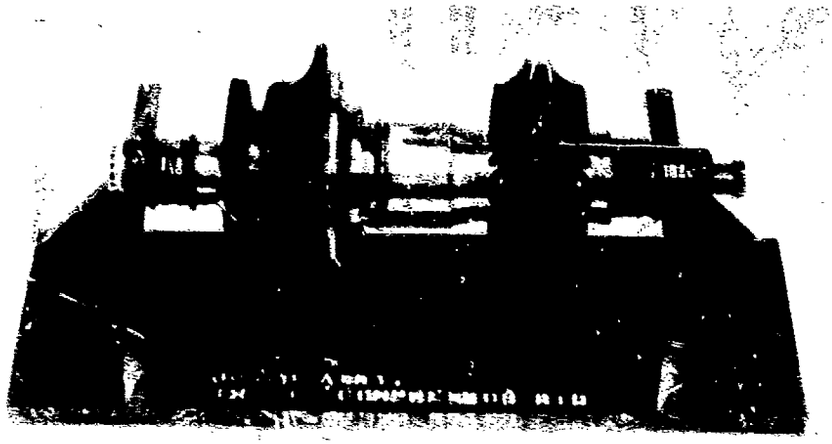

Figure 16. Redesigned Rotor Assembly.

Bearings and Seals

A dual front-bearing configuration was selected to provide a substantial increase in radial load capacity over the original design. This dual arrangement located a "floating" ball thrust bearing adjacent to a roller bearing, which allowed the roller bearing to carry all the radial load and the ball bearing all the thrust load. The rear bearing compartment (turbine end) was the same as the original design.

Both the front and rear bearings were the same as the original designs and were soft mounted on oil-film-damped supports, with lubrication provided through the inner races as before.

A vibration analysis of the redesigned rotor assembly predicted substantially lower bearing unbalance loads at design speed compared to the loads predicted for the initial design, as shown in Figures 17 and 18 for the front and rear bearings, respectively.

A carbon face seal was incorporated in the redesigned inlet case to eliminate air and oil leakage to and from the forward bearing compartment and inlet flow path. The seal nosepiece was graphitic carbon, and the seal runner was AMS 6322 alloy steel, with a flame-sprayed coating of chrome-carbide to improve wear characteristics. The seal runner was cooled by flowing oil through small radial holes. Secondary sealing was accomplished by a bellows, which was damped at the OD to reduce bellows fatigue problems. The face seal cross section is shown in Figure 19.

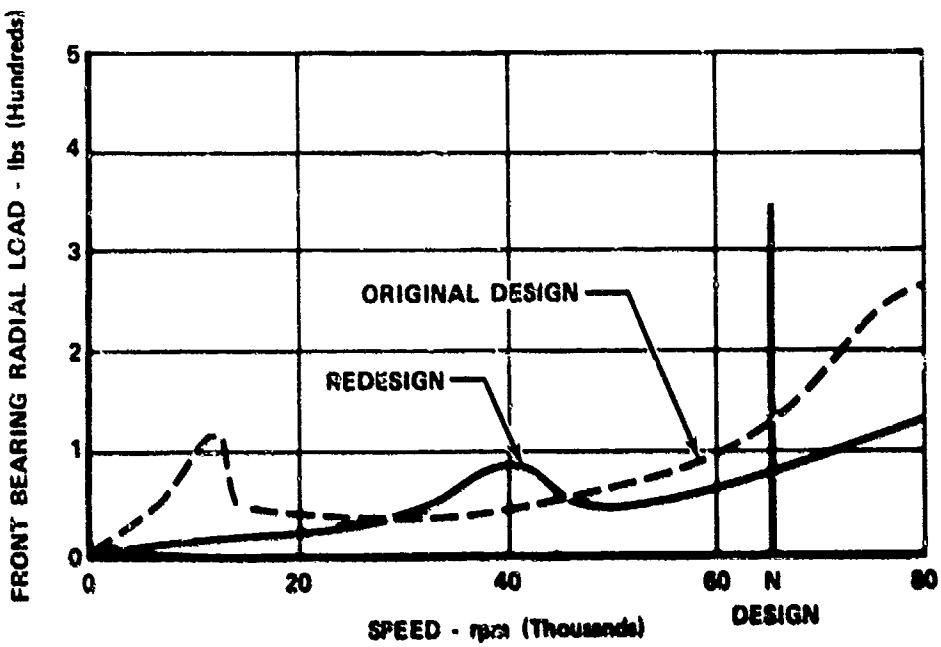

Figure 17. Redesigned Rotor Assembly Predicted Front Bearing Load vs Speed.

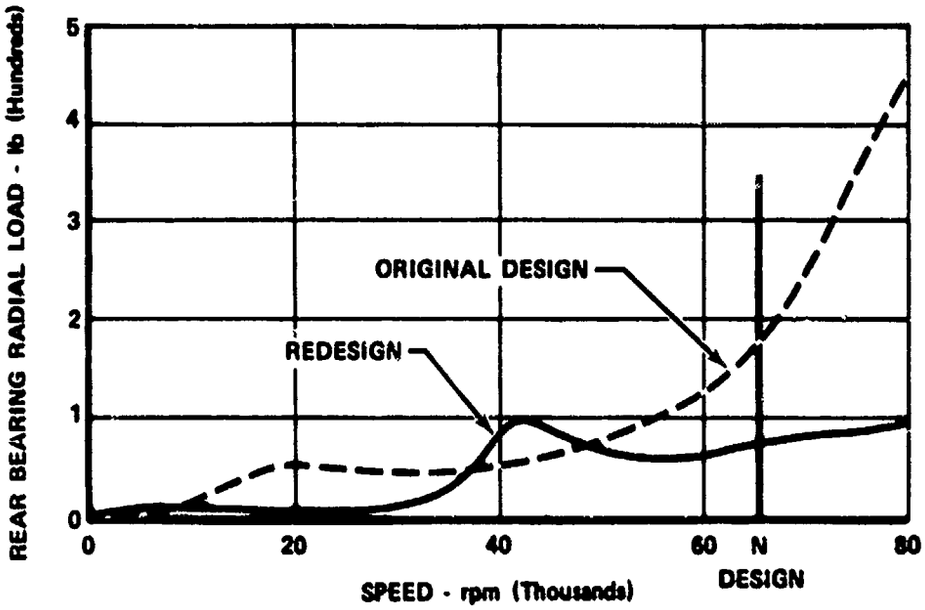

Figure 18. Redesigned Rotor Assembly Predicted Rear Bearing Load vs Speed.

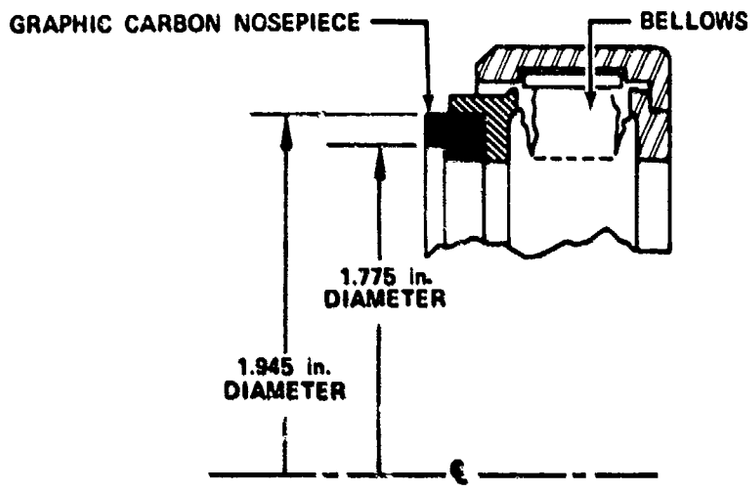

Figure 19. Front Bearing Compartment Carbon Face Seal.

Although the seal rubbing speeds (520 to 530 ft/sec) were higher than current engine experience, seal requirements in terms of differential pressure (less than 10 psi) and temperature (250°F) were relatively modest. A seal pressure balance was selected to reduce the contribution of pressure-area forces on the seal face to minimize the wear rate.

The dual ball and roller bearing arrangement and the carbon face seal performed satisfactorily in subsequent tests in the compressor rig, and provided new experience with high-speed bearing and seal designs of this type.

TEST EQUIPMENT

COMPRESSOR TEST RIG

The major nonrotating components of the compressor test rig are shown in Figure 20. They consist of the bellmouth inlet, inlet case, inlet guide vanes, inducer shroud, impeller shroud, diffuser, and diffuser collector. Prior to assembling the impeller in the cases, it was first spin tested with the tooling shown in Figure 21 to 73,000 rpm (112% of design speed) to verify its mechanical integrity.

Installation of the impeller into the diffuser in its original spline-drive configuration is shown in Figure 22. When the impeller attachment geometry was changed from the original spline-drive configuration to a CURVIC coupling, the impeller and drive turbine became an integral rotor assembly. The components used to build up the redesigned rotor assembly are shown in Figure 23. The inducer, impeller, spacer, and turbine were held together with a tiebolt. A "Z" brace was used in the assembly to support the middle of the tiebolt and increase its critical speed to well beyond the design operating range.

During the assembly of the compressor rig, particular attention was given to balancing operations. Rotor components such as the inducer, impeller, and turbine were individually balanced by material removal. Then the rotor was assembled out of the cases, concentricities were checked for less than 0.001-in. runout, and the assembly was balanced to less than 0.0003-oz-in. unbalance, again by material removal from the impeller and turbine. This method put an unbalance in the impeller and turbine as components; however, the correction plane was near the true plane of unbalance, since these two components were the heaviest in the rotor assembly. Final balance of the rotor assembly in the compressor and turbine cases was accomplished within 0.0012 oz-in. unbalance with rivets and pins on each end of the rotor assembly.

The assembled and fully instrumented compressor rig and drive turbine are shown in Figure 24. The compressor rig and drive turbine were installed in a combination shipping and mount stand for ease of installation in the test stand.

TEST FACILITIES

A schematic of the B-2 test stand high-speed compressor test facility is shown in Figure 25. The drive turbine was powered by compressor bleed air from a P&WA™ J-75 slave engine. Drive turbine supply air was controlled by two pneumatic valves, one of which was used as vernier control. Since the drive turbine was a radial inflow-type and particles in the supply air tend to erode the blade tips, a particle separator was installed downstream of the drive turbine control valves. The design of the particle separator (Figure 26) was a derivative of the semi-reverse flow separator, designed and tested under Army Contract DAAJ02-70-C-0003. The separator center body was free to move and act as an emergency shutdown valve. Safety systems built into the test facilities included a rapid shutdown and an abort system. These systems operated automatically when preset conditions were encountered. Table III summarizes the initiating actions required to activate the safety controls and the actions taken.

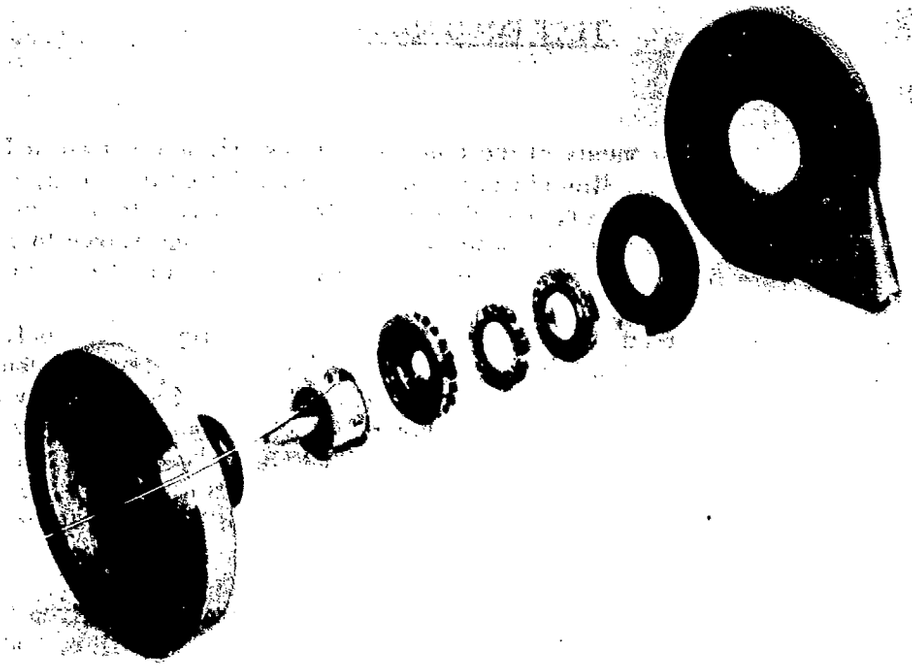

Figure 20. Compressor Test Rig Nonrotating Components.

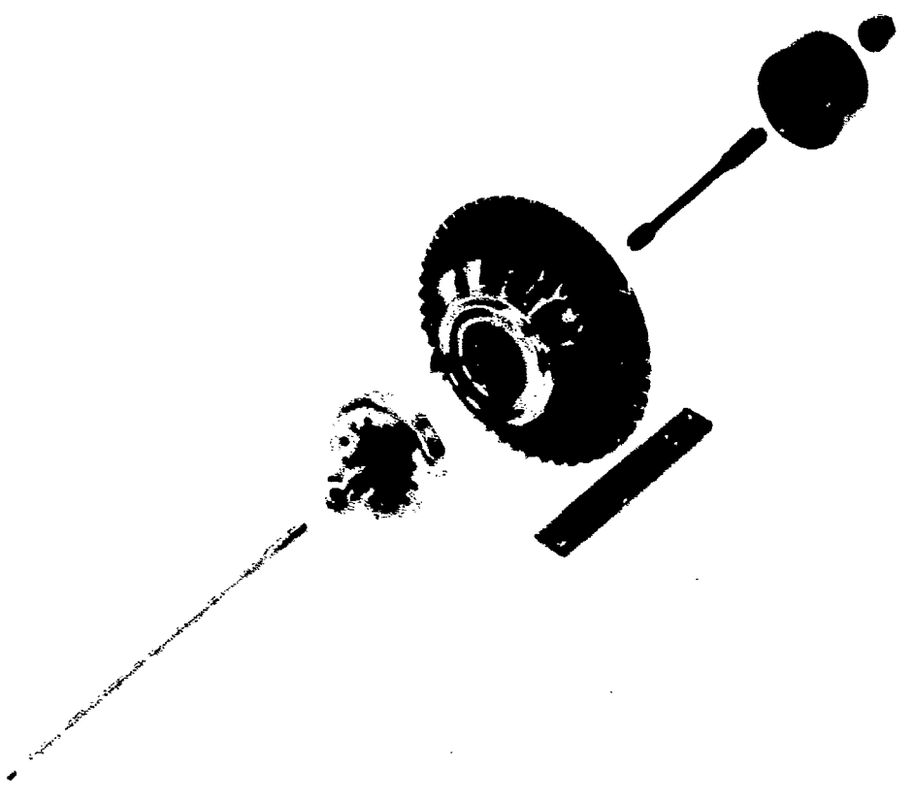

Figure 21. Impeller Spin Tooling.

Figure 22. Impeller Installation in Diffuser Case.

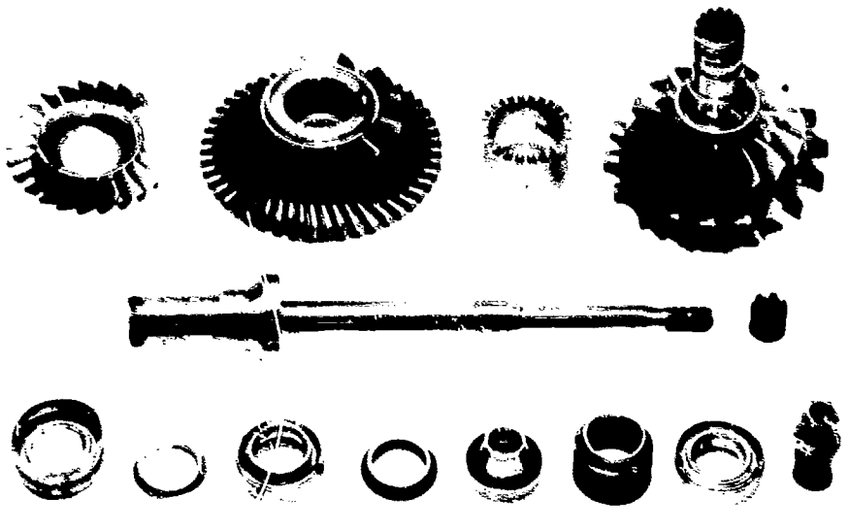

Figure 23. Redesigned Rotor Assembly Components.

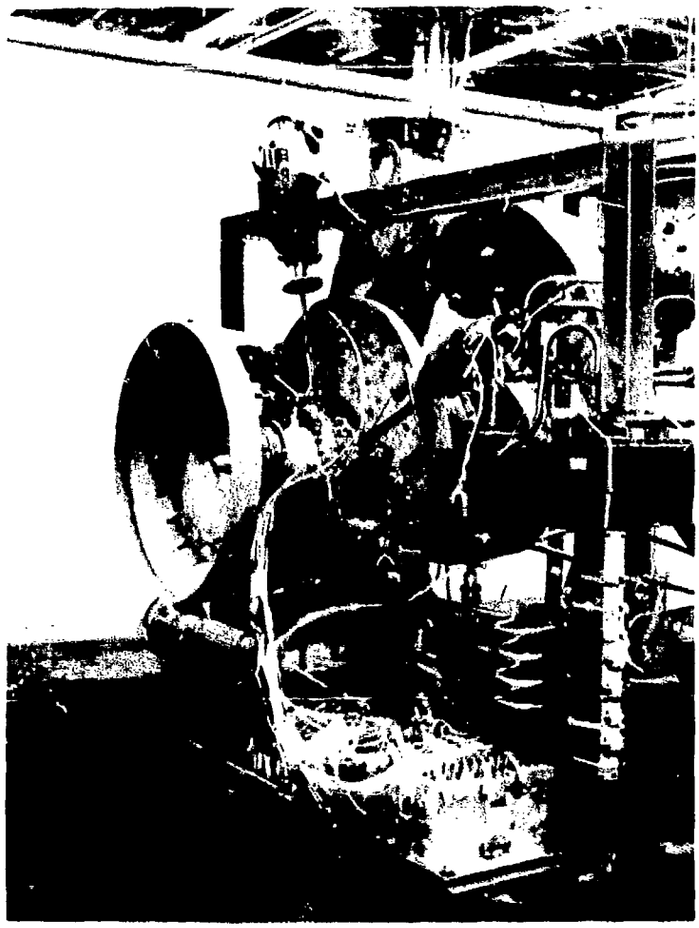

Figure 24. Assembled and Fully Instrumented Compressor Rig.

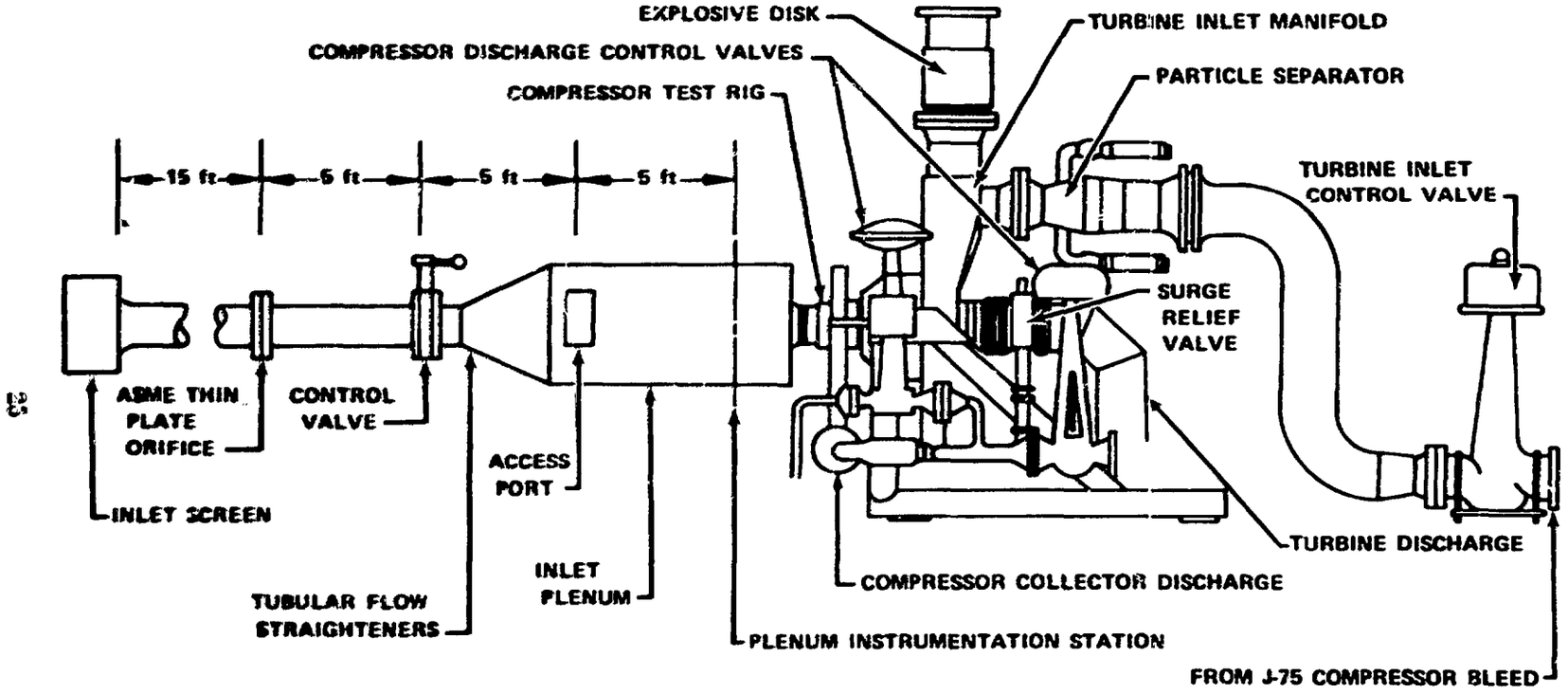

Figure 25. P&WA™ FRDC High-Speed Compressor Test Stand.

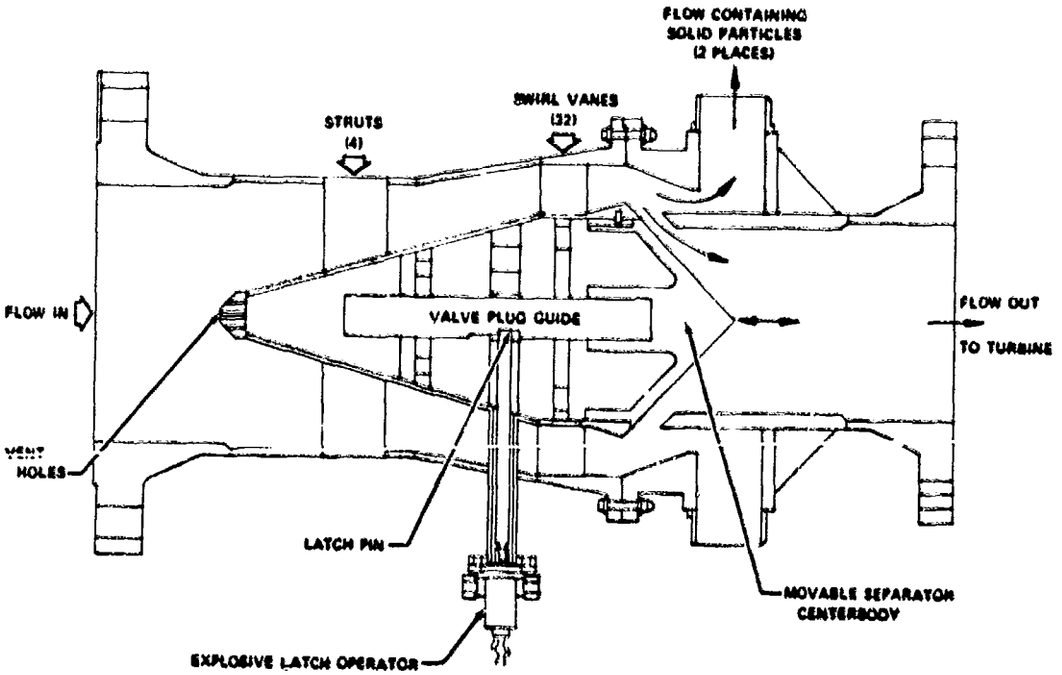

Figure 26. Particle Separator With Integral Fast-Acting Shutoff Valve.

TABLE III. TEST FACILITY SAFETY SYSTEMS

Rapid Shutdown System		
Initiating Action	1.	Low thrust balance pressure
	2.	Loss of control room A/C power
Results	1.	Turbine inlet control valves closed
	2.	Compressor discharge valve opened
	3.	Slave engine throttled to idle
Rig Abort System		
Initiating Action	1.	Low lubricating oil supply pressure
	2.	Rotor overspeed
	3.	Manual abort by test engineer
Results	1.	Explosive-actuated turbine inlet valve closed
	2.	If manual abort, turbine inlet manifold vented to ambient
	3.	Turbine inlet control valves closed
	4.	Compressor discharge valve opened
	5.	Slave engine throttled to idle

The installation of the compressor rig in the test facility is shown in Figure 27. The compressor inlet duct contains a sharp-edged flow measuring orifice, control valve, flow straightening tubes, and a plenum chamber. An inflatable rubber seal sealed the plenum to the compressor bellmouth. The control valve in the compressor inlet duct remained in a full-open position during all testing.

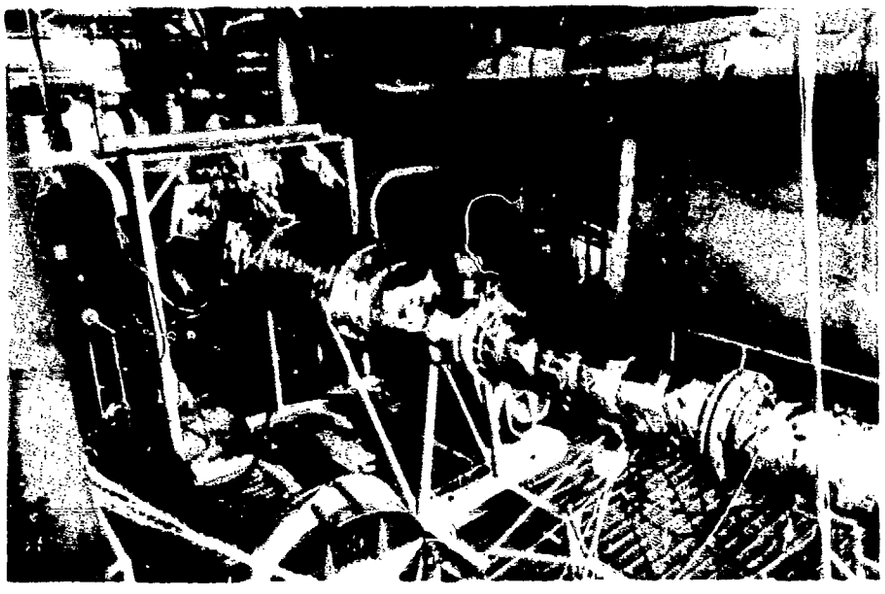

Figure 27. Compressor Rig Installed in B-2 Test Facility.

The compressor exhausted to atmosphere from the diffuser collector through two back-pressure control valves, one of which also acted as a backup control. By controlling the compressor discharge back pressure, it was possible to operate the compressor along a speedline with transients into and out of stall. A surge relief system was designed and used to detect the onset of surge. The system used a high-frequency response pressure sensing transducer in the diffuser collector. A control module allowed the selection of a rate of change of pressure that would actuate the system. If a higher rate of change of pressure was sensed, a fast-operating valve in the compressor discharge duct was opened. This reduced the compressor back pressure, thereby automatically allowing the compressor to move away from a surge condition.

A differential pressure control system was used between the impeller hub side backface and a buffer seal dam compartment (Figure 15). All performance data were taken with this delta pressure equal to zero to prevent flow out of or into the flow path at the impeller exit-diffuser entrance. This pressure differential could however, be adjusted to either side of the zero delta pressure point, if desired.

The required thrust load on the ball bearing was maintained by supplying gaseous nitrogen to the impeller thrust balance cavity (Figure 15) through an automatic control valve. This valve was adjustable to any set point and was changed while the rig was in operation.

INSTRUMENTATION

Instrumentation was provided to establish stage overall performance, stage component performance, and monitor rig operation. The instrumentation used to take these data and the instrumentation locations are described in this section. Major instrumentation stations for the test compressor are defined in Table IV, and the axial and radial locations of these stations are shown in Figure 28.

TABLE IV. COMPRESSOR INSTRUMENTATION STATIONS		
00	-	Compressor Inlet-Plenum
0	-	Compressor Inlet-Bellmouth Throat
1.0	-	Inlet Guide Vane Exit
1.5	-	Inducer Exit
2.0	-	Impeller Exit
3.0	-	Diffuser Exit
3.5	-	Compressor Discharge Collector Manifold

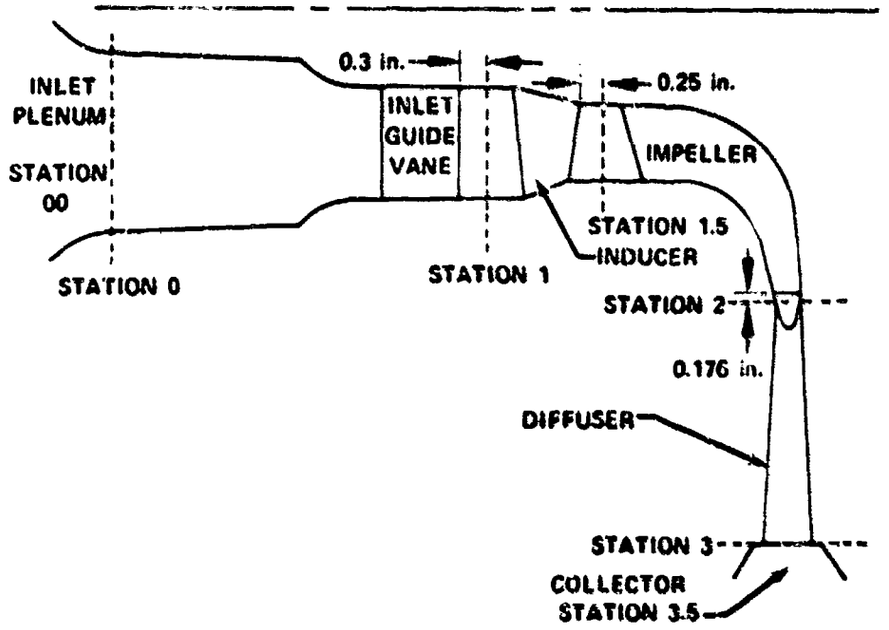

Figure 28. Compressor Instrumentation Station Locations.

Overall Performance Instrumentation

Instrumentation was provided to obtain inlet flow rate, impeller speed, compressor inlet conditions (Station 00), and compressor discharge conditions (Stations 3.0 and 3.5). These data were combined to define overall performance in terms of total-pressure-to-total-pressure conditions (Stations 00 to 3.0) and total-pressure-to-static-pressure conditions (Stations 00 to 3.5).

Compressor inlet flow rate was calculated from data obtained from a 5.270-in.-diameter thin plate orifice installed upstream of the inlet plenum in a 12.5-in.-diameter inlet duct, as shown in Figure 29. The orifice was installed in accordance with ASME standards. Orifice upstream static pressure was measured by means of three static pressure taps, each sensed by a 0- to 15-psia transducer. Three orifice differential static pressures were each sensed by a 5-psid transducer. The temperature of the orifice flow was measured in the inlet plenum.

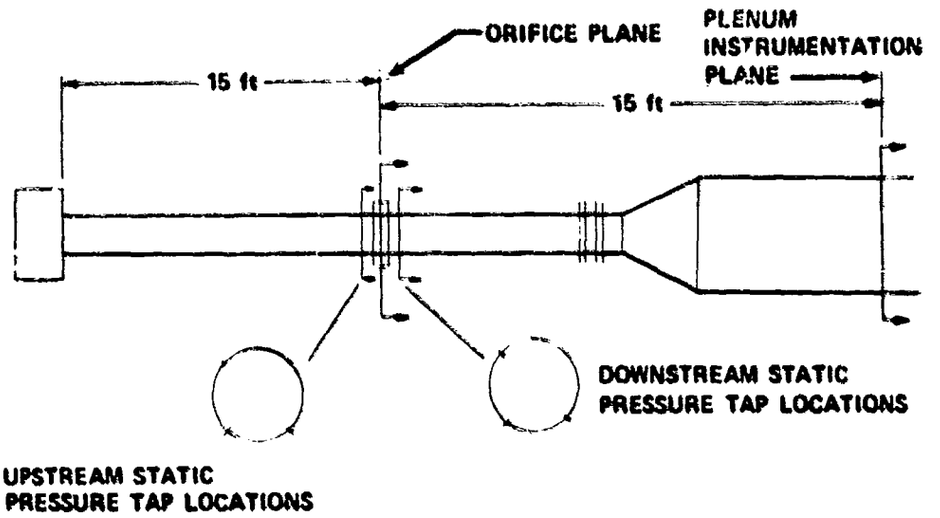

Figure 29. Inlet Orifice Installation.

Compressor inlet total pressure was measured with three Kiel-type total pressure probes, located in the inlet plenum. The probes were each sensed with a 0- to 15-psia transducer. Compressor inlet total temperature was measured with a Rosemount resistance thermometer in the inlet plenum. Redundant inlet temperature measurements were obtained with three half-shielded copper-constantan (C/C) thermocouples, also located in the inlet plenum. Beginning with Build No. 5 of the compressor, the C/C thermocouples were deleted and four additional Rosemount resistance thermometers were installed at various radial positions in the inlet plenum to accurately measure any radial variation in temperature.

Diffuser exit total pressure was measured by means of three total pressure rakes, each consisting of three elements, as shown in Figure 30. Each element was sensed by a pressure-scanning system using a 0- to 150-psia transducer. The rakes were installed at the exit of the diffuser tubes, shown in Figure 31. The locations of the nine total pressure probes superimposed onto one diffuser tube are shown in Figure 32. It was noted that the center probe of each rake was in the same relative position in each tube to provide redundant measurements at this point. Also shown in Figure 32 are the seven equal areas that were assigned to the total pressures measured by the rakes for mass-averaging purposes.

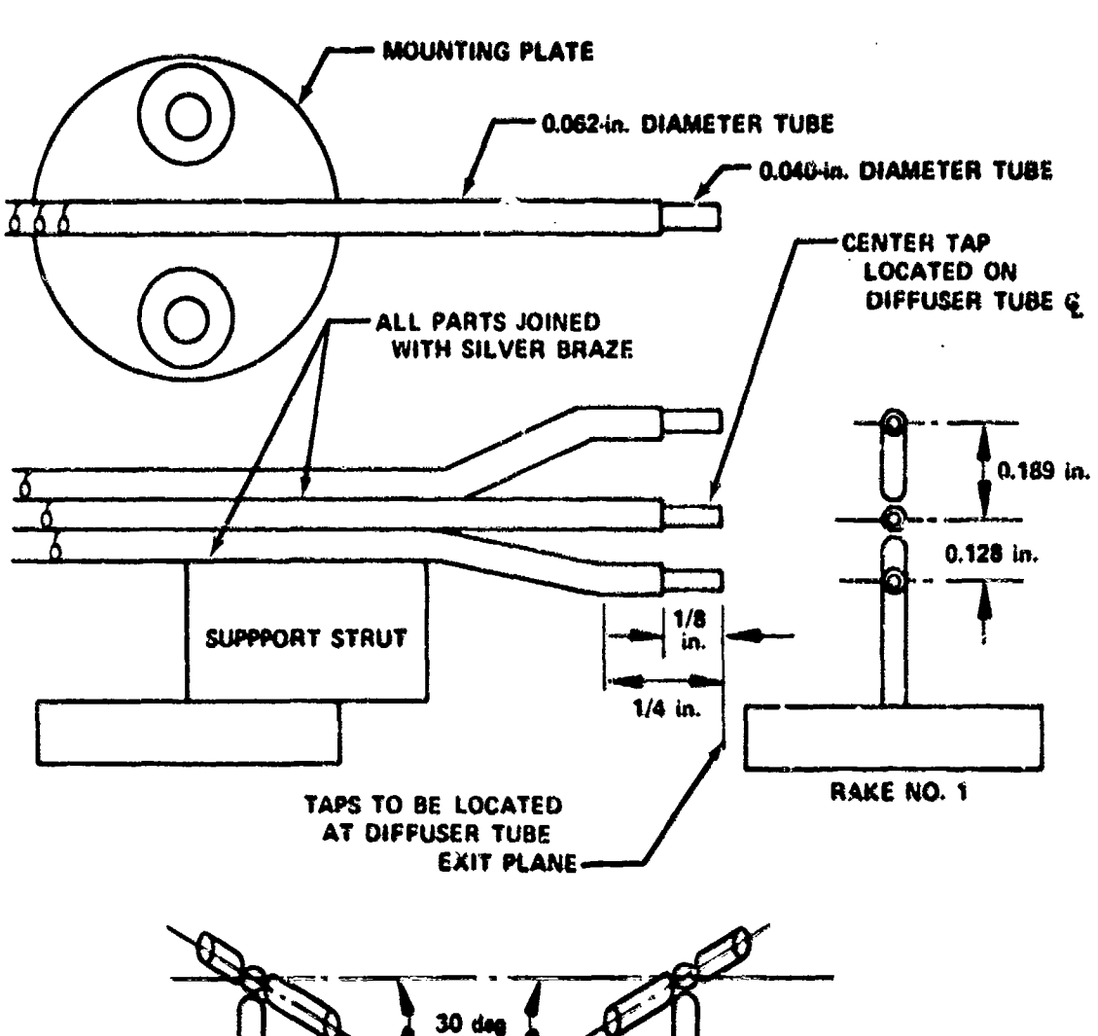

Figure 30. Diffuser Exit Total Pressure Rakes.

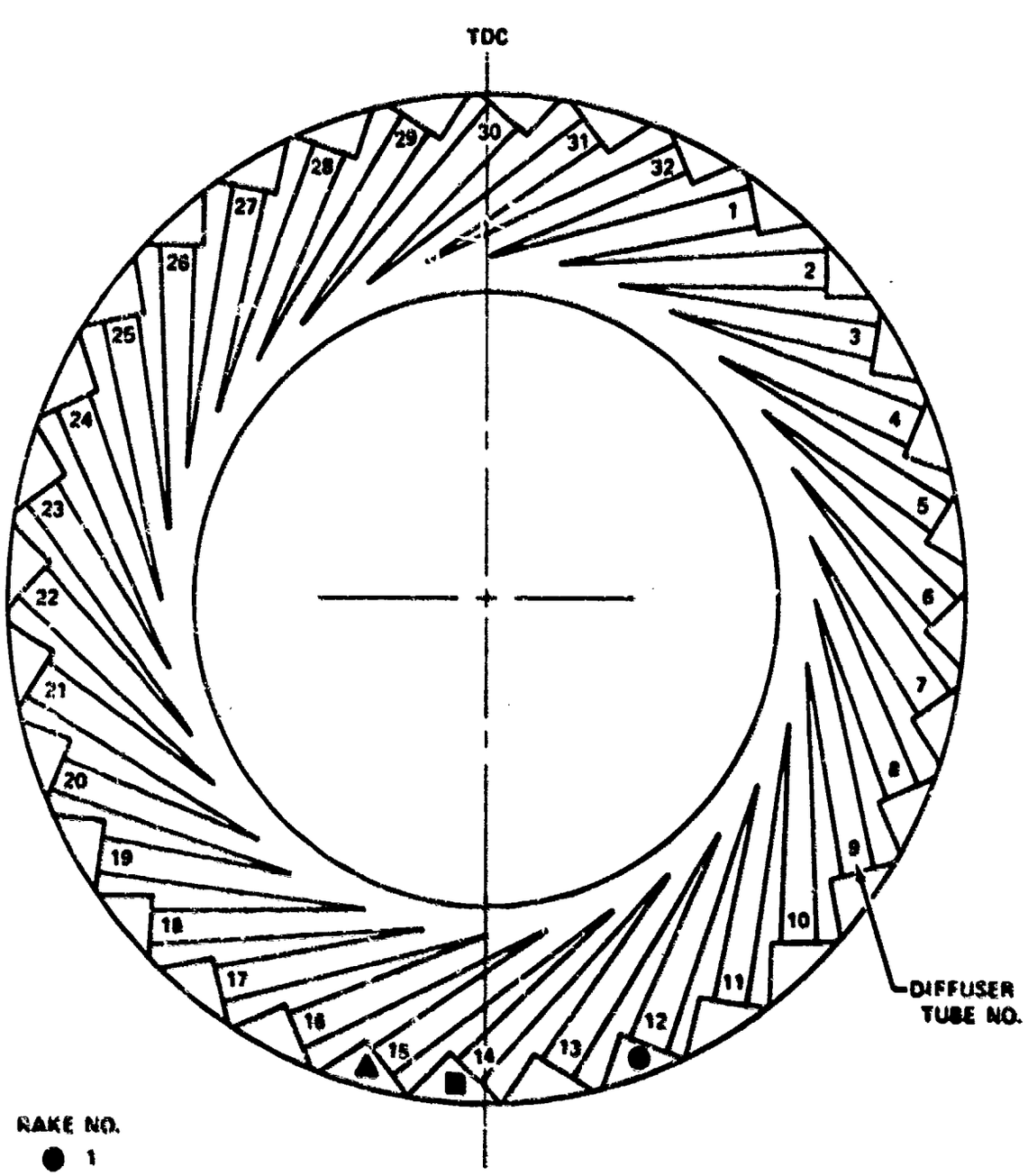

Figure 31. Location of Diffuser Exit Total Pressure Rakes.

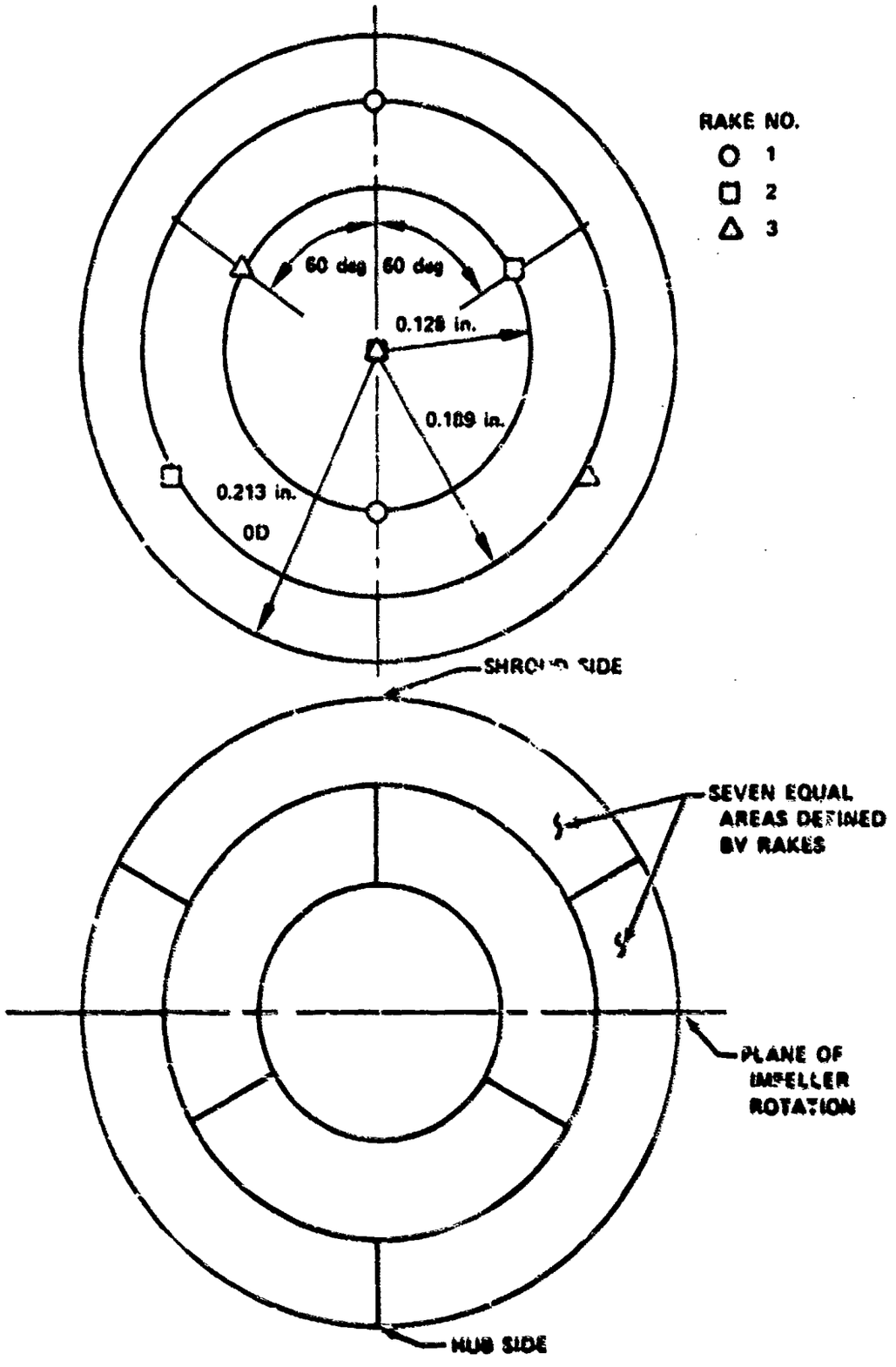

Figure 33. Placement of Total Pressure Probes in Diffuser Exit Plane Station.

Compressor exit static pressure was measured by means of eight static pressure taps in the collector, each connected to a pressure-scanning system using a 0- to 150-psia transducer. The taps were located on the shroud-side wall so that neither diffuser discharge velocity nor the collector struts interfered with the measurements. The design and location of these taps are shown in Figure 33. Compressor exit total temperature was measured with four chromel-alumel (C/A) shielded thermocouples in the exhaust collector. The thermocouple probes were axially located midway between the collector manifold walls and circumferentially located as shown in Figure 33. To increase the accuracy of the temperature measurement, the thermocouples were constructed from a single batch of calibrated special-limits-of-error wire. This wire was continuous from the thermocouple junction to the reference junction to eliminate errors caused by connectors and by the lower quality wire normally used between the connector and the reference junction. A thermocouple was attached to the shroud-side wall of the collector manifold to aid in estimation of potential radiation errors on the collector thermocouple measurements.

Component Performance Instrumentation

Instrumentation was provided to evaluate the component performance; namely, the inlet guide vane, inducer, impeller, and diffuser. The component performance instrumentation is described below and is also summarized in Table V.

Instrumentation was provided downstream of the inlet guide vane to measure wall static pressures and radial distributions of total pressure and air angle (and in Build No. 6, total temperature). Similar instrumentation downstream of the inducer was used to describe its performance, with the exception that total temperature was also measured at the exit of the inducer. The axial and circumferential locations of the inlet guide vane and inducer instrumentation are shown in Figure 34.

Static pressure at the leading and trailing edges of the inlet guide vanes was measured by one shroud wall static pressure tap at the leading-edge and single hub and shroud wall static taps at the trailing-edge plane to define the static pressure along the flow path. All three static pressure taps had to be deleted in the revised inlet case, Builds No. 4 through No. 6. Inlet guide vane exit (Station 1.0) wall static pressure data were obtained by four wall taps equally spaced about the circumference on both the hub and shroud walls. Builds No. 4 through No. 6 did not contain the hub wall taps as the revised inlet case prevented their installation. The hub wall taps were located approximately on design midchannel streamlines. It should be noted that the shroud wall taps were located on a circumferential traverse ring.

Static pressure at the leading- and trailing-edge planes of the inducer was obtained by single hub and shroud wall taps at the leading-edge plane and a shroud wall tap at the trailing-edge plane. Additionally, four static pressure taps equally spaced about the circumference on the shroud wall were installed at the inducer exit traverse station (Station 1.5).

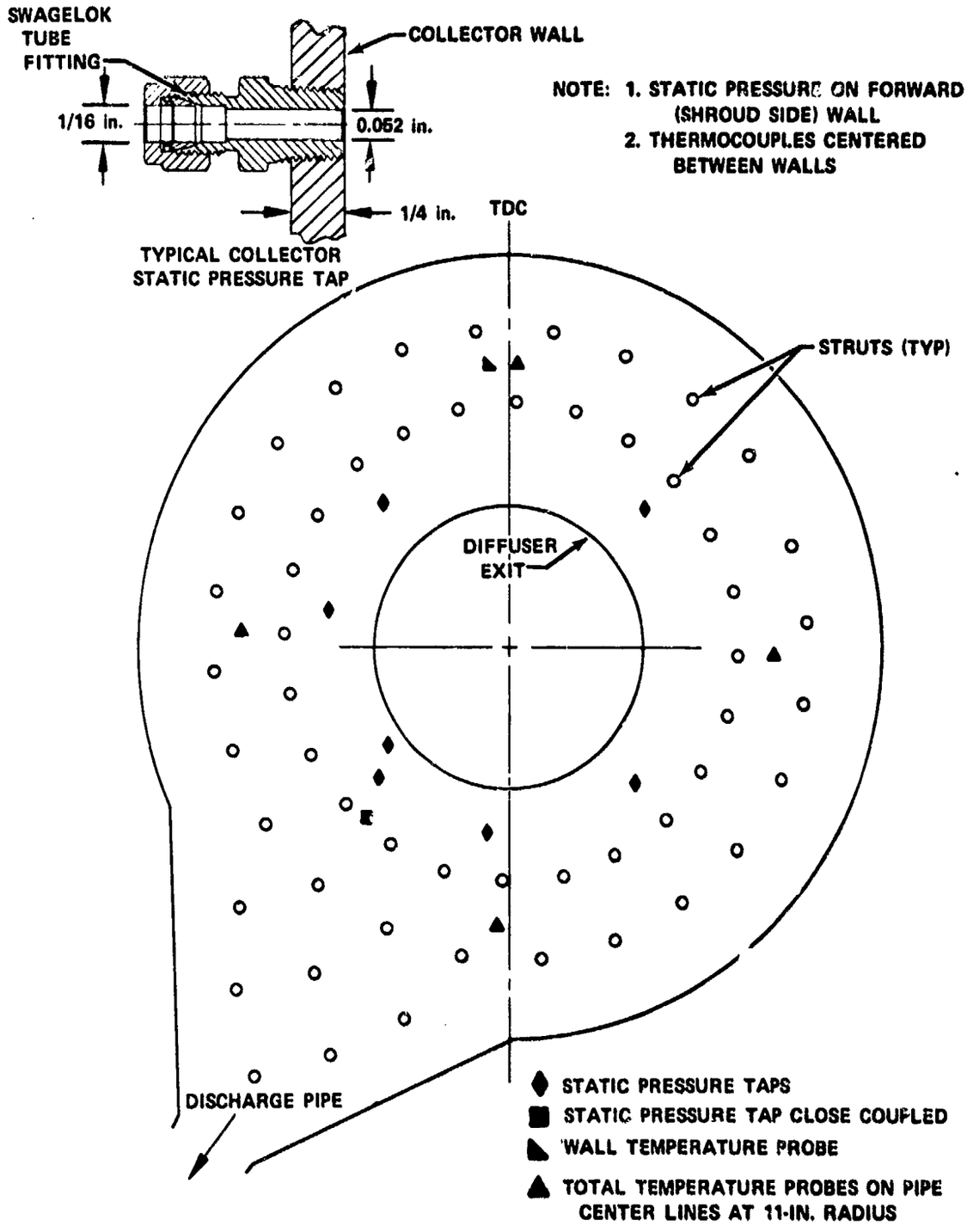

Figure 33. Collector Instrumentation Locations.

TABLE V. COMPRESSOR COMPONENT PERFORMANCE INSTRUMENTATION SUMMARY

Location	Flow Variable	Instrument Type	Quantity
Station 0	P	Wall Tap	4
Inlet Guide Vane	P	Shroud Wall Tap	2(1)
	P	Hub Wall Tap	1(1)
		Chord Angle Indicator	1
Station 1	P	Shroud Wall Tap	4
	P	Hub Wall Tap	4(1)
	P_t, T	Circumferential and Radial Traversing Cobra Probe	1(2)
Inducer	P	Hub Wall Tap	1(1)
	P	Shroud Wall Tap	2
Station 1.5	P	Shroud Wall Tap	4
	P_t, T	Radial Traversing Cobra Probe with Thermocouple	1
Impeller Shroud	P	Wall Tap	14
Impeller Tip Shroud Side	P	Communicating Groove	4
Impeller Tip Backface	P	Tube	2
Station 2	P	Shroud Wall Tap	4
	P	Hub Wall Tap	4
	P_t	Axial Traversing Cobra Probe	1
	T	Axial Traversing Thermocouple	1
Diffuser	P	Shroud Wall Tap	32
	P	Hub Wall Tap	8

(1) Deleted from Build No. 6 due to relocation of front bearing compartment.

(2) No T_t for Build No. 3.

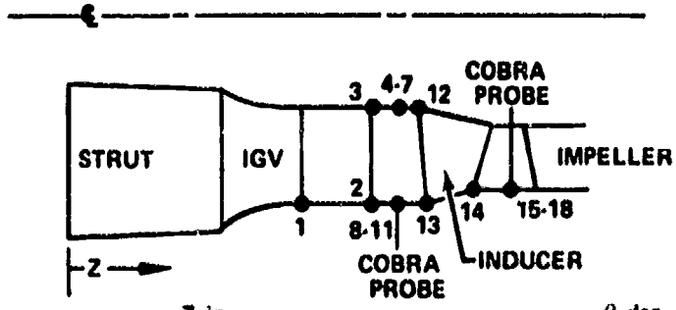

TAP NO.		Z, in.	θ, deg
1		2.5	133
2-3		3.2	210
4-7		3.55	90 deg APART FROM 47 deg
8-11		3.55	90 deg APART FROM 18 deg FROM COBRA
COBRA		3.55	330 TO 15
12		3.7	30
13	TIP	INDUCER INLET - 0.05	135
14		INDUCER EXIT +0.05	150
15-18		4.701	90 APART FROM 15
COBRA		4.701	295

θ MEASURED CLOCKWISE FROM TOP DEAD CENTER - LOOKING FORWARD
PROBES 1-13 ORIENTED CIRCUMFERENTIALLY AT NOMINAL (10 deg TURNING) IGV MIDCHANNEL.

Figure 34. Axial Locations of Inlet and Inducer Instrumentation.

Radial distributions of total pressure and air angle (and total temperature in Build No. 6) at Station 1.0 were measured by means of a cobra probe that was traversed in both the radial and circumferential directions. The cobra probe was traversed circumferentially at five radial locations corresponding to 10, 30, 50, 70, and 90% spans. At each spanwise location, the probe was traversed through a 45-deg arc, which permitted measurement of total pressure and air angle data behind two inlet guide vanes and one inlet strut in the Build No. 1 through No. 3 configuration. In the redesigned inlet configuration, the probe was rotated through an arc of 52 deg. The cobra probe used was constructed of 0.020-in.-OD tubing and is shown in Figure 35. The Build No. 3, Station 1.0 cobra probe was not constructed with a thermocouple. Radial distributions of total pressure, total temperature, and air angle at the inducer exit (Station 1.5) were obtained by means of a radially traversing cobra probe.

Impeller instrumentation was provided to measure wall static pressures along the impeller shroud, impeller tip static pressure on both the shroud side and the hub side, total pressure and air angle distributions across the flow path at the impeller exit, and total temperature distribution across the flow path at the impeller exit. The locations of the 0.040-in.-diameter wall static pressure taps along the impeller shroud are shown in Figure 36. The positions of these taps were selected so that the data obtained from them would define the static pressure distribution at the impeller entrance, the splitter regions, areas of possible flow separation, and areas of possible flow distortion due to influence of the diffuser passages. The circumferential relationship of taps were superimposed onto one diffuser tube inlet.

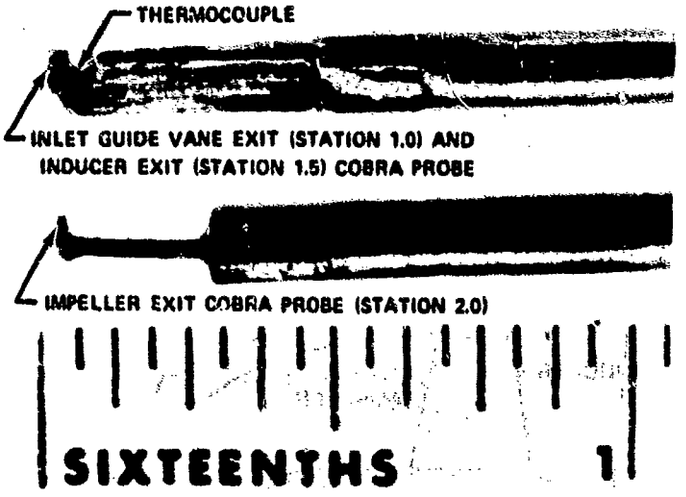

Figure 35. Construction of Traverse Cobra Probes.

SHROUD NO.	Z, in.	R, in.
1	0.0	2.4505
2	0.1522	2.4505
3	0.3613	2.4513
4	0.4163	2.4523
5	0.8812	2.5258
6	0.9721	2.5338
7	1.0837	2.6061
8	1.2271	2.7621
9	1.4043	3.1533
10	1.4512	3.3897
11	1.4512	3.3897
12	1.4512	3.3897
13	1.4512	3.3897
14	1.4512	3.3897

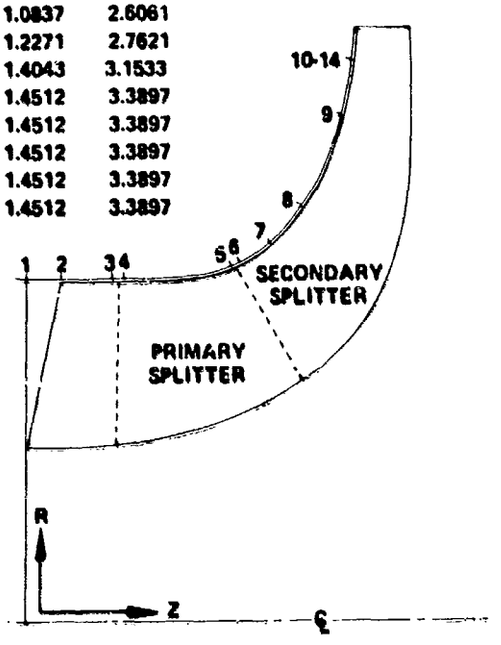

Figure 36. Location of Impeller Shroud Static Pressure Taps.

Impeller tip static pressure on the shroud side was obtained from measurements of the pressure in a circumferential passage that is connected with the flow path by a 0.015-in.-wide circumferential groove between the impeller shroud and the diffuser. Pressure was measured through four ports that were equally spaced around the circumference. This circumferential groove scheme is shown in Figure 37. Impeller tip backface pressure was measured by means of two 0.062-in.-diameter tubes installed 180 deg apart in the impeller tip backface cavity. Beginning with Build No. 5, one chromel-alumel thermocouple was located in the backface cavity to measure temperature.

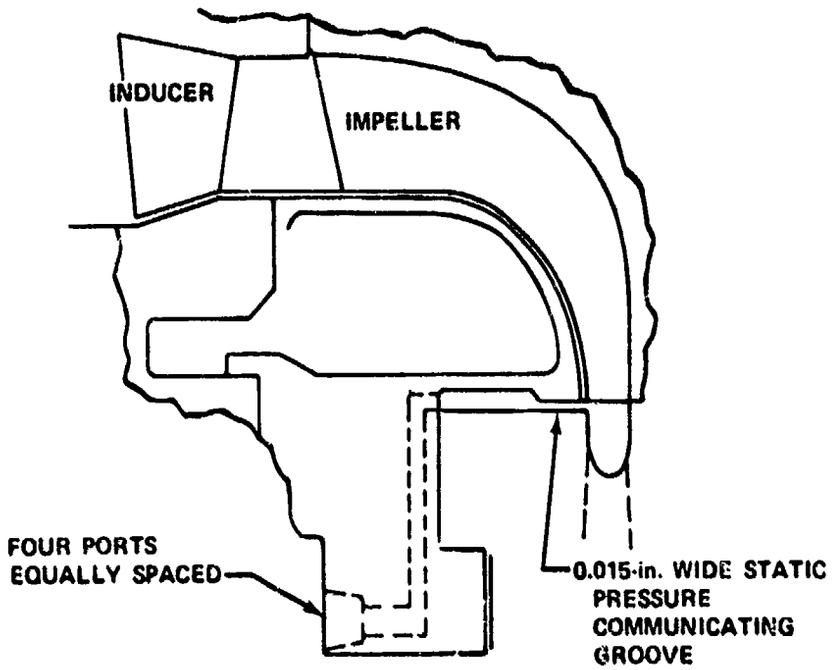

Figure 37. Impeller Tip Static Pressure Passage.

Impeller exit air angle and total pressure were measured at an impeller exit radius ratio of 1.05 by means of a cobra probe that was traversed across the impeller exit flow path in the plane of the rig centerline. The probe was installed as shown in Figure 38; the cobra probe is shown in Figure 35.

Total temperature across the flow path at the impeller exit was measured with the temperature probe shown in Figure 39. This probe was designed with an aspirated head to maximize the temperature recovery, and sheathed wire was used to minimize the conduction error. The temperature probe was installed in the same location as the cobra probe.

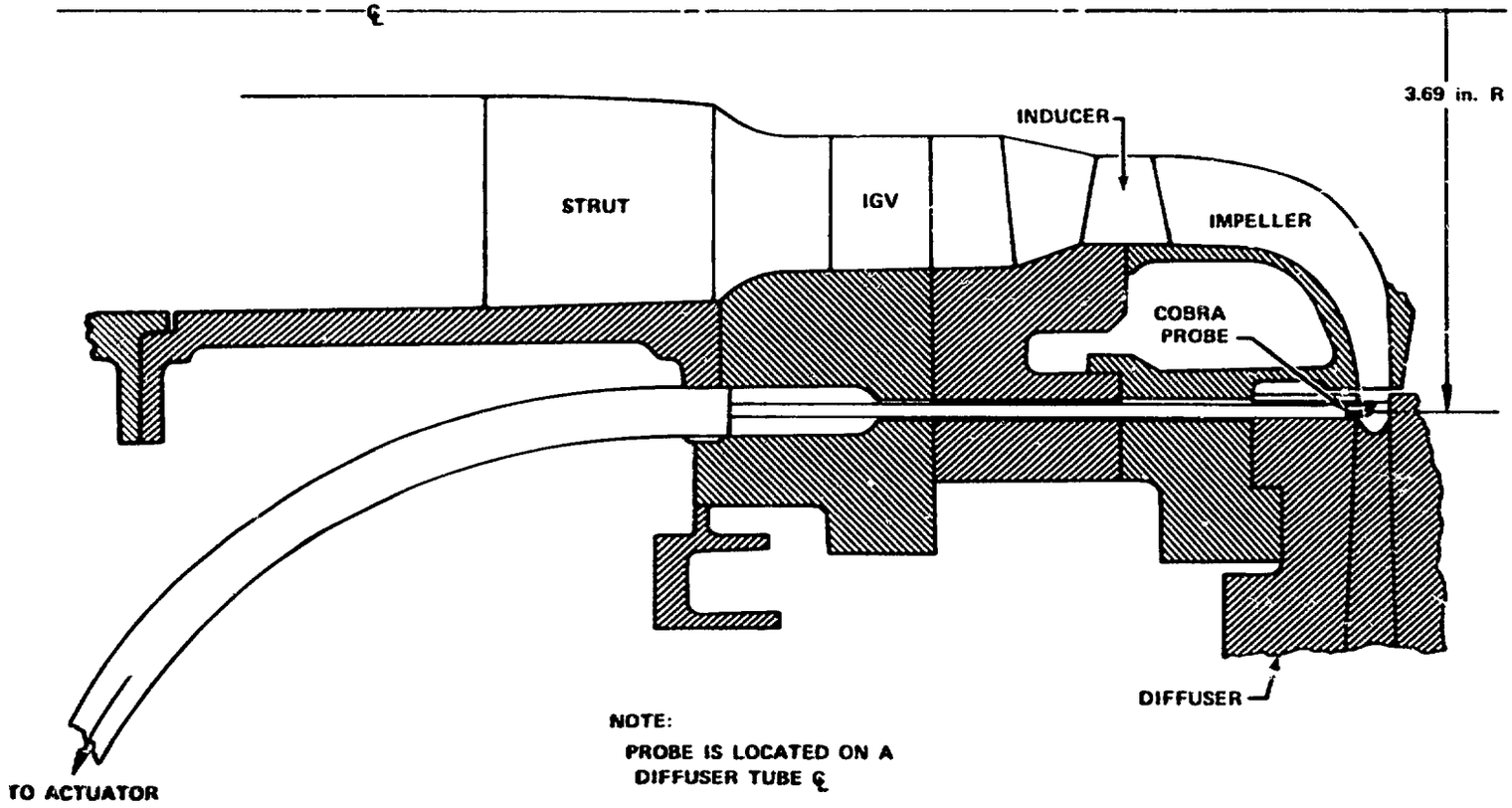

Figure 38. Impeller Exit Cobra Probe Installation.

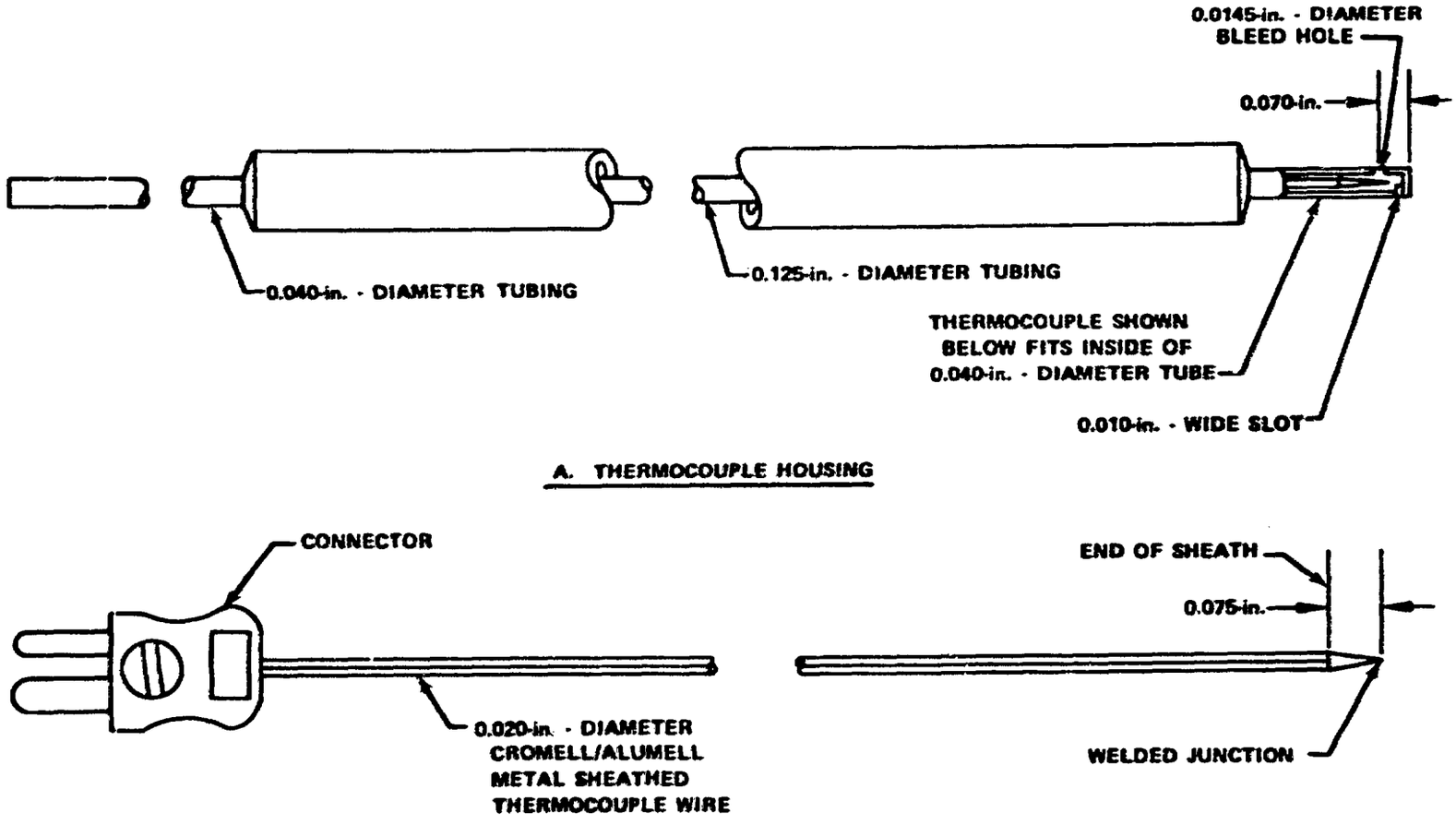

Figure 39. Impeller Exit Total Temperature Probe Construction.

The diffuser instrumentation consisted of 48 wall static pressure taps. The locations of the diffuser wall static pressure taps are shown in Figure 40. This figure also shows the location of the impeller exit cobra probe. Figure 40 shows that composite static pressure data were obtained in the vaneless space, diffuser throat, and along the diffuser length. The construction of the static pressure taps is also shown in this figure; the 0.020-in.-diameter taps were made by the electrical discharge machining process to eliminate drilling burrs and to ensure sharp edges at the intersection of the pressure port and the diffuser passage.

Special Instrumentation

Total pressure in the plenum, static pressure in the inlet bellmouth, total pressure in the diffuser exit, and static pressure in the collector manifold were measured with close-coupled transducers to achieve the fast response required to define overall performance during compressor stall. The transducers used had a frequency response of up to 100 Hz, and the data recording system could record each transducer at a maximum of 65 scans/sec. These response characteristics permitted good definition of stall characteristics.

High-frequency instrumentation, capable of response between 200 and 100,000 Hz, was installed in the compressor rig in the following locations:

1. Total pressure probe at Station 2 traversing location
2. Two static pressure probes on the Station 2 shroud walls
3. One static pressure probe at the diffuser exit.

Exact radial and circumferential locations in the diffuser are shown in Table VI.

TABLE VI. HIGH-FREQUENCY RESPONSE PROBE LOCATIONS

Probe	Circumferential Location (CCW From TDC)	Radial Location, in.
Total Pressure	66 deg 5 min	3.69
Vaneless Space Static	29 deg 30 min	3.69
Vaneless Space Static	315 deg	3.69
Diffuser Exit Static	18 deg	

The total pressure probe that was inserted in the Station 2 traversing mechanism was a flush diaphragm Kulite XCELW-200A; the three static probes were Kulite CEL-125-200A probes. These sensors were mounted in probe housings, as shown in Figure 41. The probes were temperature compensated to 450°F and had a maximum operating temperature of 325°F (which corresponds to an exit temperature reached at less than 80% of design speed).

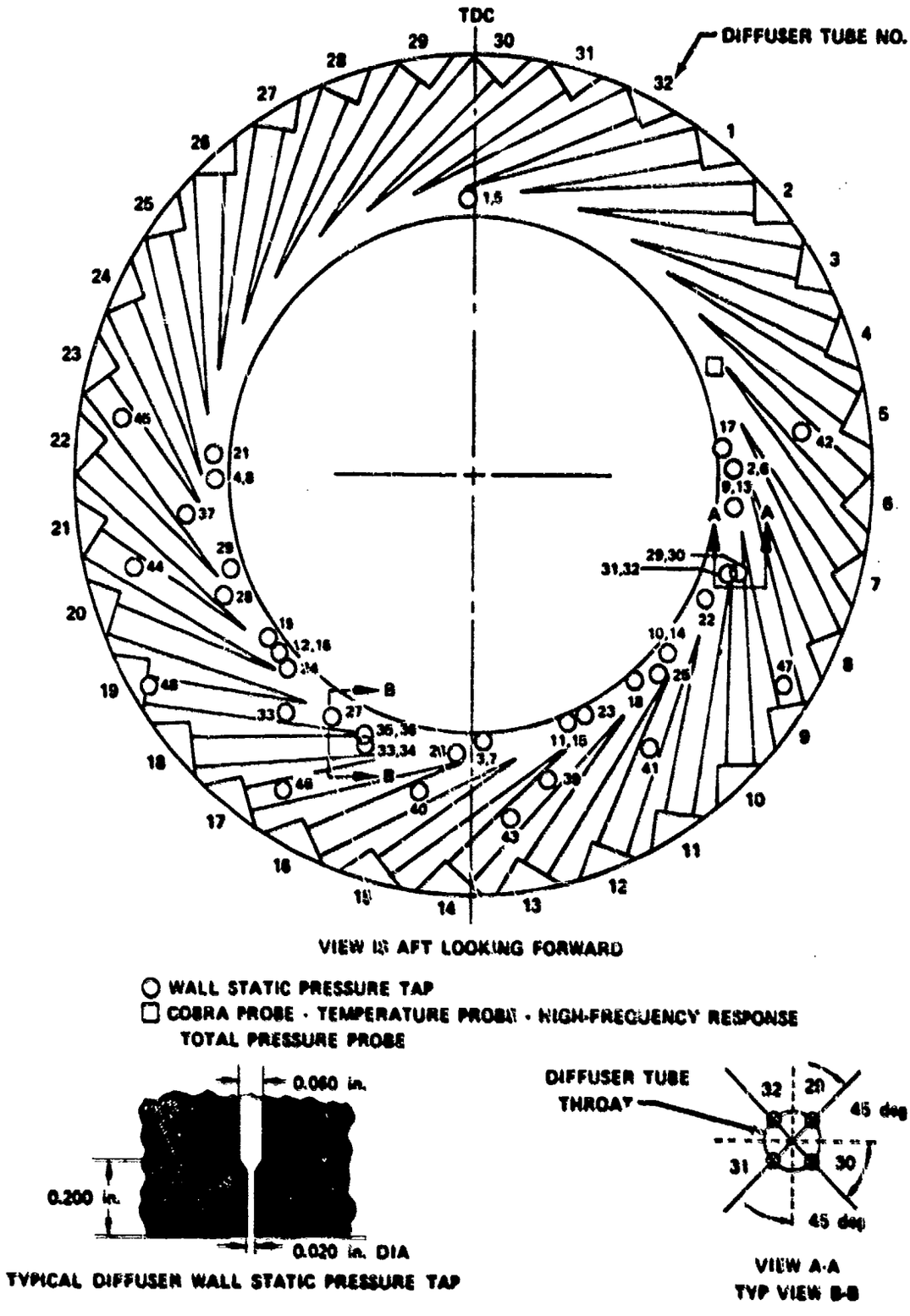

Figure 40. Location of Diffuser Static Pressure Instrumentation.

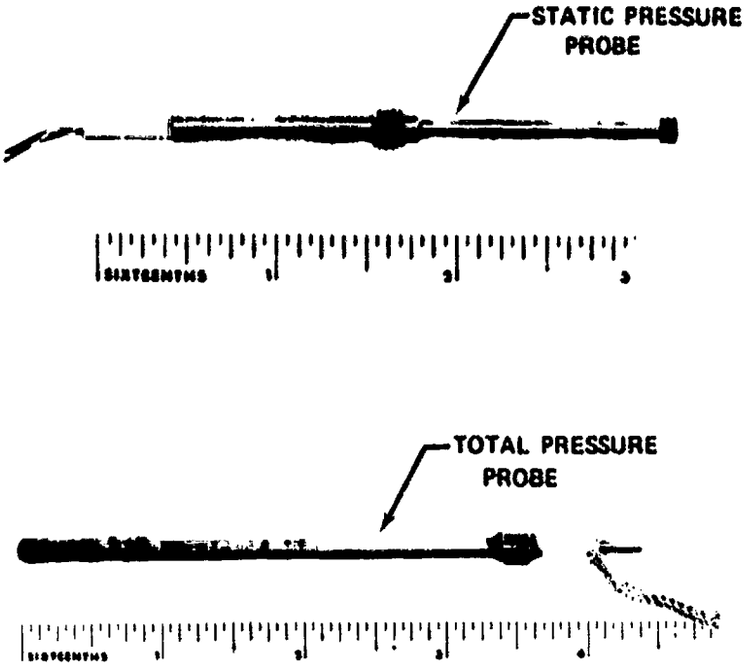

Figure 41. High-Frequency Response Kulites.

Data Readout and Recording Systems

The primary data recording system was an automatic digital magnetic tape recorder. This system recorded all compressor rig data except that from the high-frequency response transducers. The high-frequency data were recorded on analog magnetic tape.

Information needed for safe operation of the rig and for setting data points was displayed in the control room. Control room data readouts included rotor speed, rig vibration levels, bearing temperatures, oil pressures, inlet orifice differential pressure, thrust balance pressure, rig inlet pressure, and rig discharge pressure. Impeller rotational speed was obtained from two electromagnetic pickups mounted adjacent to a 6-tooth gear on the rear of the drive turbine rotor shaft.

When cobra probe data were obtained, the total pressure measured by the cobra probe was displayed on X-Y plotters, located adjacent to the traverse actuator controls. This allowed changing the speed, or, if necessary, stopping the cobra probe actuator to allow the probe to respond to changes in the air flow angle.

PROCEDURES

TEST PROCEDURES

Shakedown Test

Prior to the initiation of any performance testing, each build of the compressor test rig was subjected to a prerun (nonrotating) checkout of all rig systems and then a shakedown test. The objectives of this checkout and shakedown test were to (1) verify the mechanical integrity of the test rig and (2) check the instrumentation and the data acquisition system. Any difficulties encountered during the shakedown test, such as test equipment or instrumentation malfunction, were subsequently corrected prior to the initiation of the performance tests.

During the shakedown test, rig vibrations and bearing temperatures were monitored over the entire range of rig operation. Areas of high vibration and high temperatures were noted, and prolonged running in these areas during the performance tests was then avoided. A maximum allowable limit of 160 g's was set for extended life of the bearings; however, 220 g's were recorded during the Build No. 3 shakedown test. The extensive redesign of the rig bearing system reduced these vibrations to well within the acceptable level. Build No. 6 vibration levels are plotted as a function of speed in Figure 42. Vibration data were recorded continuously during the main portion of the test program on analog magnetic tape, too.

The thrust balance system for the test rig was checked out during each shakedown test, and the thrust load on the bearings was caluclated at several speed conditions. Adjustments were made to the automatic surge relief system, as necessary, so that it responded to stall associated pressure fluctuations and not to the gradual pressure changes caused by closing the throttle valves or random pressure fluctuations.

The inducer radial, impeller radial, and impeller axial shroud clearances were measured with mechanical rub probes. These clearance probes were withdrawn and measured after a very low-speed rotation to obtain a cold clearance and then were similarly examined after the impeller rotational speed had reached 70, 85, 95, and 100% of design speed. Figures 43 through 45 show the clearance changes measured during the Builds No. 2, 3, and 6 shakedown tests, respectively.

All instrumentation was checked for continuity from the test rig back to the data recording system. Just prior to the start of each run, all transducer and thermocouple output voltages were calibrated over their operating ranges, and a set of ambient readings was recorded for all the instrumentation for comparison to true ambient conditions. During the shakedown test, overall performance, component performance, and transient data were obtained and processed through the data reduction system to determine if all the instrumentation was recording properly and to check the data acquisition and the data reduction systems.

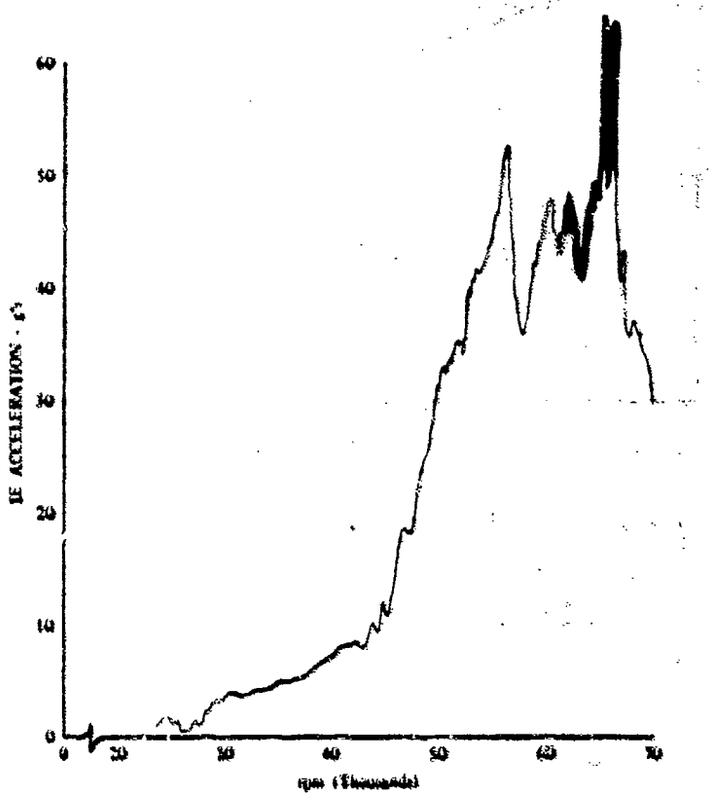

Figure 42. Maximum Front Bearing 1E Acceleration, Build No. 6.

Overall Performance Data Acquisition

Each speedline was defined by a stall transient and by steady-state points at near-stall, wide-open discharge, and at several intermediate points. Slow-stall transients were first performed by recording data at a rate of 1 scan/sec, while closing the compressor discharge valve from its wide-open position, thus increasing back pressure, until the rig surged. During the transient, adjustments to the turbine inlet control valves were made to hold the rotor rpm constant. A near-stall point was then set, based on the collector static pressure, and the compressor again operated into stall while recording data at a higher scan rate. This recording rate was 10 scans/sec during Build No. 3 testing, and the maximum recording rate of approximately 65 scans/sec was used during Build No. 6 testing.

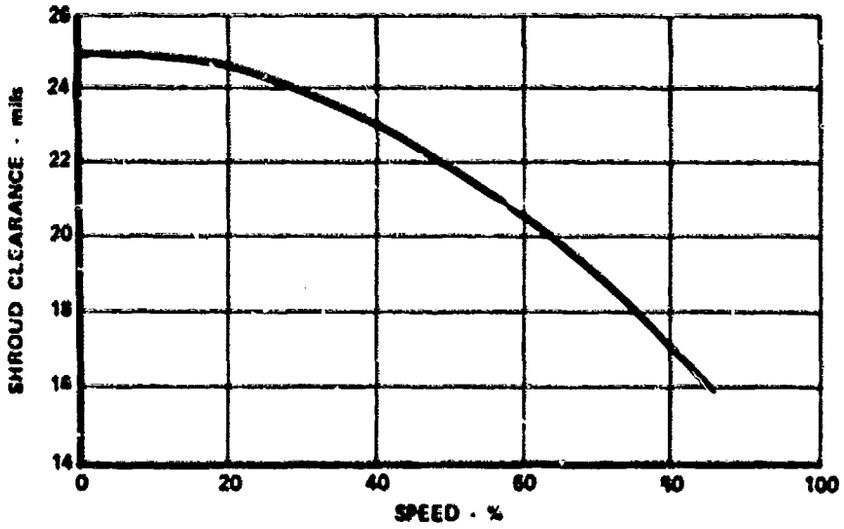

Figure 43. Impeller Tip Axial Shroud Clearance, Build No. 2.

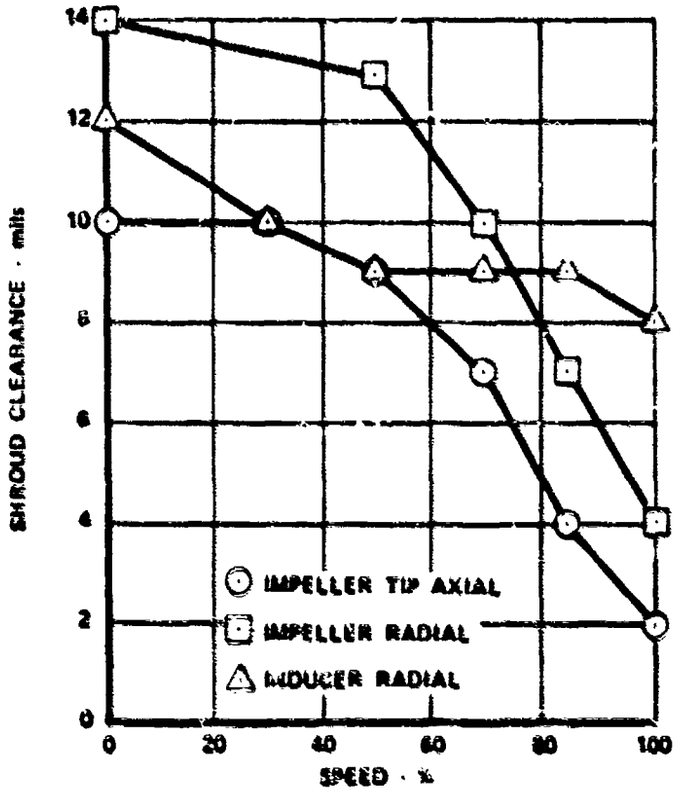

Figure 44. Clearance Probe Measurements, Build No. 3.

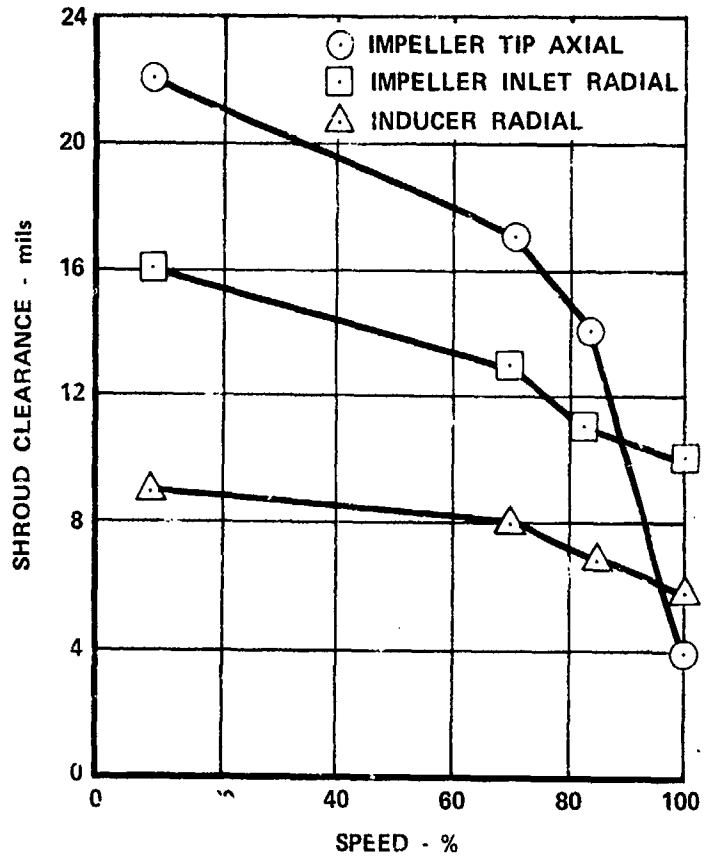

Figure 45. Shroud Clearance Measurements, Build No. 6.

Steady-state data points were distributed along a speedline, based on the collector static pressure range recorded during the first slow-stall transient. A steady-state point consisted of cycling the pressure scanning units twice at a rate of 2 ports/sec, followed by the recording of the rest of the rig instrumentation for 10 sec at a rate of 10 scans/sec. A detailed outline of all data points taken is shown in Table VII.

Component Performance Data Acquisition

Component performance data were obtained by radially traversing air angle, total pressure, and total temperature probes behind the inducer and the impeller and by both radially and circumferentially traversing behind the inlet guide vanes. The data recording rate for all traverses was 1 scan/sec. Total pressure vs radial or circumferential travel data could be monitored in the control room on an X-Y plotter and the traverse rate governed, as required, to obtain good profile definition in wakes and near the walls.

TABLE VII. DATA SUMMARY

Speed	IGV, deg	Overall Performance: Steady-State Build No. 3	Overall Performance: Steady-State Build No. 6	Overall Performance: Stall Transient Build No. 3	Overall Performance: Stall Transient Build No. 6	Component Performance: IGV Exit Radial Traverse Build No. 6	Component Performance: IGV Exit Circumferential Traverse Build No. 3	Component Performance: IGV Exit Circumferential Traverse Build No. 6	Component Performance: Inducer Exit Radial Traverse Build No. 3	Component Performance: Inducer Exit Radial Traverse Build No. 6	Component Performance: Impeller Exit Traverse Build No. 3	Component Performance: Impeller Exit Traverse Build No. 6	Remarks
30%	0	6		1			1				3		
	10	6		1							3		
	20	6		1							3		
50%	0	6		1			1						
	10	6		1			1						
	20	6		1			1						
70%	0	6		1			1				3		
	10	6	1	1		1	1	1			3		
	20	6	4	1	2	1	1	1		1	3	1	
	30		4		2	1		1		1		1	
	40				1								
80%	0	6		1									
	10	6		1									
	20	6		1									
85%	0				1								
	20		4		1	1		1		1		1	
	30		4		1	1		1		1		1	
90%	0	6		1					1		1		
	10	6		1			1						
	20	6		1									
8/1	10		6		1(1)	1		1		2		1	
	15		6		1(1)	1		1		2		1	
95%	0	6		1	1								
	5				1								
	10	6	7	1	4(1)	1		1	3	2	3	2	One transient. 95% + 500 rpm and one at 95% - 500 rpm.
	15				1								
	20	6		1									
100%	5				1								
	10	6	1	1	1	1		1		1			
101%	-4		6		1(1)	1		1		2		1	
	-4		2(2)		2					1		1	With flange coolant.
	-3				1								
	0		6		1(1)	1		1		2		1	
	5		6		1(1)	2		2		2		1	

(1) Additional stall transient performed with impeller exit cobra probe at approximately 15% from the shroud wall.

(2) Eight additional steady-states at near stall with various backface ΔP's.

Inlet guide vane traverse data were obtained at near-stall points for all speedlines at 70% speed or greater. Near-stall points were set as outlined for steady-state points. The inlet guide vane exit probe was first traversed radially inwards between inlet guide vane wakes from the shroud to the probe's maximum travel at 2.0% span (from hub). The probe was then retracted to the 10% span position and circumferentially traversed to include one IGV gap with a strut wake and one IGV gap without a strut wake. Circumferential traverses were then similarly performed at 30, 50, 70, and 90% spans to complete the inlet guide vane survey for that point.

Inducer exit radial traverses were performed by running the probe in to its limit and then recording data while slowly retracting the probe back out of the flow path.

Impeller exit traverse data were obtained on each speedline at the maximum possible back pressure with the traverse probe in the flow path. This point was set by decreasing the back pressure in small increments until the probe could be traversed across the span without causing the rig to surge. Data were then recorded while slowly traversing the probe from the hub wall back into the shroud. A steady-state point was recorded to coincide with each impeller exit traverse point. At the completion of impeller exit traversing with the air angle and total pressure cobra probe, this probe was replaced with a total temperature probe, and data were obtained at the same rig operating points.

One special test sequence involved performing stall transients with the impeller exit cobra probe, located at approximately 15% span. Data were recorded on six speedlines from wide-open discharge valve into stall at 1 scan/sec and from near stall into stall at 65 scans/sec.

Special Instrumentation Data Acquisition

High-frequency response data were obtained at 70 and 78% of design-corrected speed. Data were recorded on analog magnetic tape during a stall transient and near-stall steady-state point for each speedline. Transients and steady-state points were set as outlined in the overall performance data acquisition section.

DATA REDUCTION PROCEDURES

The reduction of data was accomplished in three steps: (1) reduction of overall performance data, (2) calculation of component performance and velocity triangles, and (3) reduction of high-frequency response and rig vibration data. The arithmetic mean value of data from redundant instrumentation was used for all calculations except where otherwise noted, and all performance data except orifice and plenum data were corrected to standard day inlet conditions as follows:

$$\text{corrected pressure} = \frac{\text{recorded pressure}}{\delta}$$

$$\text{corrected temperature} = \frac{\text{recorded temperature}}{\theta}$$

Under this system, inlet temperatures and pressures are always standard day conditions (T_o = 518.688°R, P_{to} = 14.694 psia).

Overall Performance

The reduction of overall performance data was accomplished through the use of an IBM 360-75 computer program. A DRIL (Data Reduction Input Language) program converts raw test data into engineering units, ratios, pressures, and temperatures to standard day inlet conditions, averages data from redundant instrumentation and from successive data recording cycles, and performs overall performance calculations. Actual weight flow was calculated from the orifice equation

$$w_{act} = 14.675 \left[1 - 0.302 \left(\frac{\Delta P}{P}\right)\right] \left[\frac{P \cdot \Delta P}{T_o}\right]^{1/2}$$

where

P = upstream orifice static pressure
ΔP = orifice differential static pressure
T_o = plenum total temperature

Both weight flow and speed were corrected to standard day inlet conditions as follows:

$$w_{cor} = w_{act} \frac{\sqrt{\theta}}{\delta}$$

and

$$N_{cor} = \frac{N}{\sqrt{\theta}}$$

Overall temperature ratio, total-to-static pressure ratio, and adiabatic efficiency are given, respectively, by

$$T_r = T_3/518.688$$

$$P_r = P_3/14.694$$

and

$$\eta = \frac{\text{ideal (isentropic) enthalpy change}}{\text{actual enthalpy change}} = \frac{\Delta hf(P_r)}{\Delta hf(T_r)}$$

where $\Delta hf(P_r)$ and $\Delta hf(T_r)$ were determined by fourth degree curve fits of change in enthalpy vs pressure ratio and temperature ratio data from Table I (Dry Air Tables) in Keenan and Kaye Gas Tables. Two separate pressure ratios and corresponding efficiencies were defined, depending on the type of data point. For steady-state points, the average of six collector static pressure taps was used for the values of P_3 in the pressure ratio equation. During stall transients, the pressure ratio was based on the value of a single collector static pressure tap read through a close-coupled pressure transducer. The value of this tap generally agreed to within less than 0.3% of the collector average during steady-state points.

Inlet Guide Vane Performance

Inlet guide vane performance was calculated by an inlet guide vane update routine to the main DRIL program, which includes the effects of the inlet struts, located upstream of the guide vanes. The static pressure distribution behind the inlet guide vanes was assumed to be a constant equal to the measured shroud static pressure at each point, and the temperature was assumed constant across the vanes.

Guide vane discharge total pressure and air angle traverse data were mass-averaged over both one gap including a strut wake and one gap without any strut effects at 10, 30, 50, 70, and 90% spans. These values were then weighted, based on the relative number of struts to number of inlet guide vanes, and combined to give a single mass-averaged value at each percent span as follows:

$$\overline{P}_t = \frac{3\overline{P}_{ts} + 7\overline{P}_{tv}}{10}$$

and

$$\overline{\alpha} = \frac{3\overline{\alpha}_s + 7\overline{\alpha}_v}{10}$$

where: the subscripts s and v pertain to gaps including a strut wake and gaps not including a strut wake, respectively. A spanwise mass-average total pressure ($\overline{P}_{t1}$) and mass-average air angle ($\overline{\alpha}_1$) were then calculated from these weighted values. The mass-average of any quantity (X) is given by

$$\overline{X} = \frac{\sum_{i=1}^{n} \Delta wX}{\sum_{i=1}^{n} \Delta w}$$

where

$$\Delta w = \frac{K(\Delta A)P_t}{\sqrt{\overline{T}}} \sin \alpha$$

Losses were calculated based on the values of $\overline{P}_{ts}$, $\overline{P}_{tv}$, and $\overline{P}_t$ at each percent span and an overall loss was calculated, based on the spanwise mass-average total pressure. These losses were all of the form

$$\text{loss} = \frac{14.694 - P_t}{14.694}$$

Weight flow was calculated by two separate methods for comparison with the orifice flow calculation. The first method involved integrating the incremental flows, ΔW_S and ΔW_V, which were obtained during the inlet guide vane total pressure and air angle circumferential mass-average calculations across the blade passage. The results of these integrations were then weighted to reflect the relative number of struts and vanes and summed to yield an integrated flow. The second flow calculation was based on the IGV exit spanwise mass average total pressure:

$$w_{cal} = \frac{KA\ (\bar{P}_{t1})\ \sin \bar{\alpha}_1}{\sqrt{T_1}}$$

where

A = cross-sectional flow path area at the IGV exit
T_1 = 518.688, same as inlet

Based on this calculated weight flow, an inlet flow coefficient was determined as follows:

$$C_d = \frac{w_{cal}}{w_{cor}}$$

Inlet guide vane exit velocity triangles were calculated by an IBM 1130 digital computer program, Centrifugal Compressor Data Reduction Program (CCDRP). Again, static pressure was assumed constant across the span. The ratio of specific heats (γ) was determined from a curve fit of γ vs static temperature (T_s) data and involved an iteration on the value of T_s to satisfy the following:

$$\frac{\bar{P}_{t1}}{P_1} = \left(\frac{T_1}{T_{s1}}\right)^{\gamma/\gamma-1}$$

The absolute Mach number (Mo) was calculated at each percent span by iterating on the value of Mo until

$$\frac{\bar{P}_t}{P_1} = \left(1 + \frac{\gamma - 1}{2} Mo^2\right)^{\gamma/\gamma-1}$$

The local speed of sound was calculated by

$$a = (\gamma GRT_s)^{1/2}$$

From Mo, a, and $\bar{\alpha}$ the components of the velocity triangles as defined below at each percent span were then calculated.

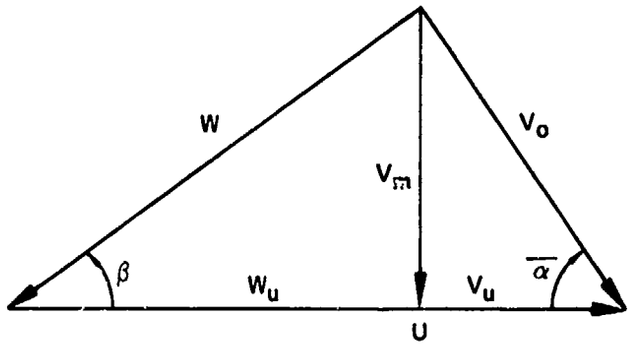

Inducer incidence (i) was determined at each percent span by

$$i = \beta^{+} - \beta$$

where β^{+} is the inducer leading edge metal angle at the corresponding percent span.

Inducer Performance

Total pressure, total temperature, and air angle data from each inducer traverse were first plotted vs percent span on a CALCOMP plotter. Up to 25 points from each plot were then selected and input into the 1130 CCDRP program. A constant spanwise static pressure distribution equal to the measured shroud static was assumed. Values of γ, T_s, and Mo were calculated for each point by the same iteration methods used in the inlet guide vane section. Total temperatures were corrected for Mach number effects by dividing the recorded temperatures by a recovery factor. The recovery factor used in the calculations was a linear approximation of the actual probe recovery factor vs Mach number calibration data. The maximum error created by this assumption is approximately 0.1% of the temperature reading.

Total pressure and total temperature were then mass-averaged across the span. The sum of the incremental weight flows from the mass-averaging routine was checked against the corresponding orifice flow, and an iteration was performed on the air angle values until the two flow calculations agreed. This air angle check was necessary since errors of 1 or 2 deg in the alignment of the air angle traverse probes on the test stand are not uncommon. Final mass-average total pressure ($\overline{P}_{t1.5}$) and total temperature ($\overline{T}_{1.5}$) values were then calculated, based on the adjusted air angle profile. Inducer pressure ratio and temperature ratio were calculated as follows:

$$P_{r(1-1.5)} = \frac{\overline{P}_{t1.5}}{\overline{P}_{t1}}$$

$$T_{r(1-1.5)} = \frac{\overline{T}_{1.5}}{518.7}$$

Inducer efficiency was calculated by the same methods as the overall efficiency. Inducer exit velocity triangles at 10, 30, 50, 70, and 90% span were determined by the same methods as in the inlet guide vane section.

Near-stall traverse data at 100% speed, 10-deg IGV setting and 101% speed, -4-deg IGV setting were also input into a streamline analysis computer program to calculate the actual spanwise static pressure distribution. This program satisfies the equations of motion and radial equilibrium using input values of total pressure and air angle, a description of the flow path, and a design blockage distribution. The blockages were adjusted until the measured shroud static pressures were matched. Linear approximations of the resulting static pressure distributions were then input into the IBM 1130 CCDRP program, and new velocity triangles and inducer performance parameters were calculated for these two points.

Impeller Performance

Impeller exit traverse data were reduced by nearly the same methods as the inducer exit data. Static pressure was assumed to vary linearly between the measured values at the hub and shroud. Total temperature was input in the form of traverse data and also as a single value equal to the collector total temperature, which was assumed constant across the span.

Flow at the impeller exit was supersonic across much of the span at the higher speed points, which would cause a shock to form in front of the traverse probe. For data taken where the local value of P_t/P was less than 1.893, the flow was assumed subsonic and impeller performance parameters and velocity triangles were calculated as in the inducer section. For values of P_t/P greater than 1.893, the flow was assumed supersonic, and a shock correction procedure was incorporated assuming a normal shock to determine the upstream flow conditions.

The mass-average radial velocity ($\bar{V}_m$) and mass-average tangential velocity ($\bar{V}_u$) were calculated, and from these a mass-average air angle was determined:

$$\bar{\alpha}_2 = \tan^{-1}\left(\frac{\bar{V}_m}{\bar{V}_u}\right)$$

The slip factor at the instrumentation station was calculated by

$$\text{slip factor} = \frac{\bar{V}_u}{U}$$

The slip factor at the actual impeller tip was determined from the instrumentation station slip factor by assuming constant angular momentum. Combined inducer-impeller performance was also defined by an internal flow analysis involving a solution of the equations of continuity and momentum. Input for the analysis consisted of overall total pressure ratio and total temperature ratio, rotor speed, mass flow, impeller exit static pressure, configuration geometry, flow factors at the leading edge of the inlet guide vanes and impeller exit, and a calculated temperature rise due to shroud friction, based on rotor speed, density, surface area, and friction coefficient for bladed disks.

Diffuser Performance

Diffuser discharge coefficient was calculated as

$$C_d^* = \frac{w_{cor}}{w}$$

$$\text{where } W = \frac{KA^*P_{t2}}{\sqrt{T_3}}$$

A^* = throat area

P_{t2} = maximum P_t at impeller exit from traverse data

Throat blockage was then determined by:

$$B^* = 1 - C_d^*$$

Diffuser static pressure recovery coefficients were defined from the impeller exit to the collector and from the throat to the collector, respectively, as follows:

$$C_p = \frac{P_3 - P_2}{\bar{P}_{t2} - P_2}$$

$$C_p^* = \frac{P_3 - P^*}{\bar{P}_{t2} - P^*}$$

Diffuser effectiveness was defined as

$$\epsilon = \frac{C_p^*}{C_{pi}^*}$$

where C_{pi}^* is the ideal pressure recovery coefficient that would be obtained with a one-dimensional, isentropic flow through the same diffuser. For the C_{pi}^* calculation, a throat Mach number of 1.0 and a γ of 1.4 were assumed.

Diffuser losses were documented by the following:

$$\text{Diffuser loss (total-to-static)} = \frac{\bar{P}_{t2} - P_3}{\bar{P}_{t2}}$$

$$\text{Diffuser loss (total-to-total)} = \frac{\bar{P}_{t2} - \bar{P}_{t3}}{\bar{P}_{t2}}$$

$$\text{Diffuser loss coefficient} = \frac{\bar{P}_{t2} - P_3}{\bar{P}_{t2} - P_2}$$

$$\text{Dump loss} = \frac{\bar{P}_{t3} - P_3}{\bar{P}_{t3}}$$

where $\bar{P}_{t3}$ is the mass-average total pressure at the diffuser exit.

Diffuser performance was also obtained by separating from overall performance the impeller exit conditions calculated by the internal flow analysis, described in the impeller section. Performance derived from this analysis was compared to that obtained from traverse data.

The Mach number profile at the diffuser exit was calculated, based on diffuser exit total pressure data and collector static pressure and assuming a γ of 1.4. Total pressure data from different pipes was first adjusted to match a single average value at the center of each pipe to eliminate scatter in the absolute profiles of individual pipes for this presentation.

High-Frequency Response and Rig Vibration Data

High-frequency response (Kulite) data recorded on analog magnetic tape was processed using a digital Fourier analyzer system to determine the magnitude of pressure fluctuations, blade wake definition, and rotating stall characteristics. Resultant data plots included spectral plots (amplitude vs frequency), tracking plots (amplitude vs time), and various correlation plots.

Rig vibration data recorded prior to the installation of the digital Fourier analyzer system was processed in a similar manner, except that a wave analyzer system was used in which the data were not first digitized. Resultant data plots were similar to those mentioned in preceding paragraphs.

VALIDATION OF TEST DATA

Estimates of the uncertainty of the data acquired from the compressor test rig are presented in Table VIII. These estimates include both the uncertainty of the sensor and of the recording device. All uncertainty calculations, with the exception of those for weight flow and efficiency, are applicable to any reading. Weight flow and efficiency uncertainty were calculated at the design point. Uncertainty of air angle assumes no alignment error. Both bias and precision errors (precision errors are two standard deviations from the mean) were used in the uncertainty analysis; these errors are also presented in Table VIII. When multiple probes were available for redundant measurement, the precision error was calculated by statistically averaging individual measurements by the root-sum-square method as illustrated below.

$$u = \frac{e}{\sqrt{n}}$$

TABLE VIII. ESTIMATE OF INSTRUMENTATION ACCURACY

Variable	Location (Station)	Type Instrument	Range	Number of Probes Averaged	Bias ±	Precision ±	Uncertainty ±	Units
P	00	Transducer	0 to 15	3	0.04	0.01	0.05	psia
T	00	Resistance Thermometer	Ambient	5	0.27	0.07	0.34	°R
P	1 and 1.5	Pressure Scanner	0 to 15	4	0.05	0.02	0.07	psia
Air Angle	1, 1.5, and 2.0	Potentiometer	0 to 160	1	0.4	1.2	1.6	degree
P_t	1.5	Transducer	0 to 25	1	0.40	0.30	0.43	psia
T	1.5	CA/TC	0 to 600	1	3.0	1.2	4.2	°F
P	1.5 to 2.0	Pressure Scanner	0 to 55	1	0.28	0.09	0.37	psia
P_t	2.0	Transducer	0 to 170	1	0.46	0.29	0.74	psia
T	2.0	CA/TC	0 to 1150	1	3.5	1.5	5.0	°R
P	2.0 to 3.0 and 3.5	Pressure Scanner	0 to 150	1	0.43	0.34	0.77	psia
T	3.5	CA/TC	0 to 1150	4	1.08	0.49	1.57	°R
Flowrate	Inlet	Orifice	3.1	3ΔP, 3P, 5 temperature	0.024	0.037	0.059	lb/sec
Efficiency	00 to 3.5	-	75%	-	-	-	0.553	percent

where u = overall uncertainty of flow variable

e = uncertainty of individual sensor

n = number of sensors recording the same flow variable

Table VIII also includes the effect of the data uncertainty on the uncertainty of the overall efficiency performance calculation. This performance uncertainty estimate was calculated by differentiating the efficiency equation and inputting the uncertainty values of Table VIII in the resulting relationship. The uncertainty of the efficiency value was 0.55 point in efficiency, which was considered to be satisfactory. The uncertainty of the weight flow was calculated by combining the total bias and precision involved in measuring weight flow with the inlet and instrumentation used for this program. The total uncertainty of ±0.059 lb/sec is based on the design flow of 3.1 lb/sec.

At each steady-state point, approximately 20 scans of data recorded over a 2-sec interval were averaged. A typical printout from a near-stall, steady-state point at 101% design speed and -4-deg inlet guide vane setting is shown in Table IX. A 2-sec average value, the maximum and the minimum value recorded, and 3 sigma (three standard deviations from the mean) are also listed for each instrumentation. These provide a measure of the actual scatter in the data due both to the uncertainty in measurement and to slight speed and flow variations that may have occurred while recording the steady-state.

Integrated flows calculated from traverse data at each instrumentation station were checked for correspondence with the inlet orifice flow as is shown in Figures 46 through 48 for Build No. 6. Calculated weight flows, based on mass-averaged values of the total pressure and air angle, are also included on the inlet guide vane flow correspondence plot in Figure 46. The approximate 0.40 lb_m/sec shift in the inducer exit integrated flow shown in Figure 47 can be attributed to two factors. The first of these is the constant spanwise static pressure distribution that was assumed for the reduction of most of the traverse data at this instrumentation station. As can be seen in Figure 47, the flow correspondence improved for the two near-stall points at 100 and 101% speed, which were reduced assuming a linear static pressure profile, which more closely approximated the calculated static pressure distribution at that station. The impeller exit integrated flow shown in Figure 48 correlates well with the orifice flow over most of the flow range, but falls off slightly at the higher flow rates. This can be attributed to larger differences between the actual static pressure profile and the assumed linear static pressure profile for these points.

Prior to the calculation of component performance parameters and velocity triangles, the inducer exit and the impeller exit integrated flows were adjusted to match the inlet orifice flow, and thus satisfy continuity requirements. This was accomplished by adding a constant value to the measured air angles so that the impeller exit airflow matched that measured. It was felt that the absolute value of the air angle measurement was the least accurate of the data used in the weight flow calculation, although the profile was considered accurate. However, as pointed out earlier, the assumed static pressure profiles at the inducer exit and the impeller exit and the assumed total temperature profile at the impeller exit also contributed significantly to the initial integrated flow variations, especially at the higher speed, higher pressure ratio points.

TABLE IX. TYPICAL PRINTOUT FOR A NEAR-STALL, STEADY-STATE POINT AT 101% DESIGN SPEED AND -4-DEG INLET GUIDE VANE SETTING

[illegible] TIME 2305 [illegible] NO. 1973 [illegible] NO. 2588 BUILD 06 RUN NO. 004.02 B-02

AVERAGE FOR ENG TIME INTERVAL BEGINNING AT 8865.224

[illegible]	UNITS	CHANNEL	AVERAGES	SIGMA	MAXIMUM	MINIMUM	SCANS USED	SCANS ELIMINATED
[illegible]	PSID	0	0.[illegible]	0.7[illegible]	0.242	-0.[illegible]	10	0
[illegible]	CRIS	1	0.0	0.0	0.0	0.0	10	0
[illegible]	PSIA	2	14.565	0.037	14.596	14.562	10	0
[illegible]	PSIA	3	14.607	0.020	14.619	14.604	10	0
[illegible]	PSIA	4	14.614	0.018	14.627	14.611	10	0
[illegible]	PERF---	5	14.[illegible]	0.020	14.613	14.592	10	0
[illegible]	PSID	6	1.492	0.007	1.497	1.486	10	0
[illegible]	PSID	7	1.[illegible]	0.007	1.521	1.484	10	0
[illegible]	PSID	8	1.[illegible]	0.007	1.[illegible]	1.[illegible]	10	0
[illegible]	PERF---	9	1.[illegible]	0.020	1.[illegible]	1.495	10	0
[illegible]	DEGT	10	528.[illegible]	0.164	528.760	528.[illegible]	10	0
[illegible]	DEGT	11	525.[illegible]	0.151	525.[illegible]	525.746	10	0
[illegible]	DEGT	12	526.[illegible]	0.[illegible]	526.[illegible]	526.[illegible]	10	0
[illegible]	DEGT	13	526.[illegible]	0.[illegible]	526.[illegible]	526.[illegible]	10	0
[illegible]	DEGT	14	527.[illegible]	0.[illegible]	527.[illegible]	527.[illegible]	10	0
[illegible]	PERF---	15	526.[illegible]	0.[illegible]	526.[illegible]	526.[illegible]	10	0
[illegible]	PSIA	16	13.[illegible]	0.[illegible]	13.[illegible]	13.[illegible]	10	0
[illegible]	PSIA	17	13.[illegible]	0.[illegible]	13.[illegible]	13.[illegible]	10	0
[illegible]	PSIA	18	13.[illegible]	0.[illegible]	13.[illegible]	13.[illegible]	10	0
[illegible]	PERF---	19	13.[illegible]	0.[illegible]	13.[illegible]	13.[illegible]	10	0
[illegible]	PERF---	20	1.[illegible]	0.0	1.[illegible]	1.[illegible]	10	0
[illegible]	PERF---	21	24.[illegible]	0.[illegible]	24.[illegible]	24.[illegible]	10	0
[illegible]	PERF---	22	1.[illegible]	0.[illegible]	1.[illegible]	1.[illegible]	10	0
[illegible]	QUID	23	508.[illegible]	0.0	508.[illegible]	508.[illegible]	10	0
[illegible]	PERF---	24	82.[illegible]	0.[illegible]	82.[illegible]	81.[illegible]	10	0
[illegible]	PERF---	25	618.[illegible]	0.[illegible]	618.[illegible]	617.[illegible]	10	0
[illegible]	QUID	26	1.[illegible]	0.[illegible]	1.[illegible]	1.[illegible]	10	0
[illegible]	QUID	27	97.[illegible]	0.[illegible]	97.[illegible]	97.[illegible]	10	0
[illegible]	PERF---	28	18.[illegible]	0.[illegible]	18.[illegible]	18.[illegible]	10	0
[illegible]	PERF---	29	782.[illegible]	0.[illegible]	783.[illegible]	782.[illegible]	10	0
[illegible]	QUID	30	0.[illegible]	0.[illegible]	0.[illegible]	0.[illegible]	10	0
[illegible]	PERF---	31	60.[illegible]	0.[illegible]	60.[illegible]	60.[illegible]	10	0
[illegible]	PERF---	32	57.[illegible]	0.[illegible]	57.[illegible]	57.[illegible]	10	0
[illegible]		33	222.[illegible]	0.0	222.[illegible]	222.[illegible]	10	0
[illegible]	PERF---	34	149.[illegible]	0.[illegible]	149.[illegible]	148.[illegible]	10	0
[illegible]	PERF---	35	142.[illegible]	0.[illegible]	143.[illegible]	141.[illegible]	10	0
[illegible]	PERF---	36	151.[illegible]	0.[illegible]	152.[illegible]	150.[illegible]	10	0
[illegible]	RPM	37	66633.[illegible]	115.[illegible]	66650.[illegible]	66349.[illegible]	10	0
[illegible]	RPM	38	66667.[illegible]	0.[illegible]	66557.[illegible]	66[illegible].[illegible]	10	0
[illegible]	PERF---	39	83.[illegible]	0.[illegible]	83.[illegible]	82.[illegible]	10	0
[illegible]	PERF---	40	1163.[illegible]	1.[illegible]	1166.[illegible]	1162.[illegible]	10	0
[illegible]	PERF---	41	1160.[illegible]	1.[illegible]	1160.[illegible]	1159.[illegible]	10	0
[illegible]	PERF---	42	1155.[illegible]	0.[illegible]	1155.[illegible]	1154.[illegible]	10	0
[illegible]	PERF---	43	1153.[illegible]	1.[illegible]	1153.[illegible]	1152.[illegible]	10	0
[illegible]	PERF---	44	1152.[illegible]	0.[illegible]	1153.[illegible]	1152.[illegible]	10	0
[illegible]		45	360.[illegible]	0.0	361.[illegible]	360.[illegible]	10	0
[illegible]	PERF---	46	1121.[illegible]	1.[illegible]	1121.[illegible]	1120.[illegible]	10	0
[illegible]	PERF---	47	942.[illegible]	0.[illegible]	942.[illegible]	941.[illegible]	10	0
[illegible]	PERF---	48	14.[illegible]	0.[illegible]	14.[illegible]	14.[illegible]	10	0
[illegible]	PERF---	49	141.[illegible]	0.[illegible]	141.[illegible]	141.[illegible]	10	0

TABLE IX, CONTINUED

[illegible]	[illegible]	[illegible]	[illegible]	[illegible]	[illegible]	[illegible]	[illegible]	[illegible]

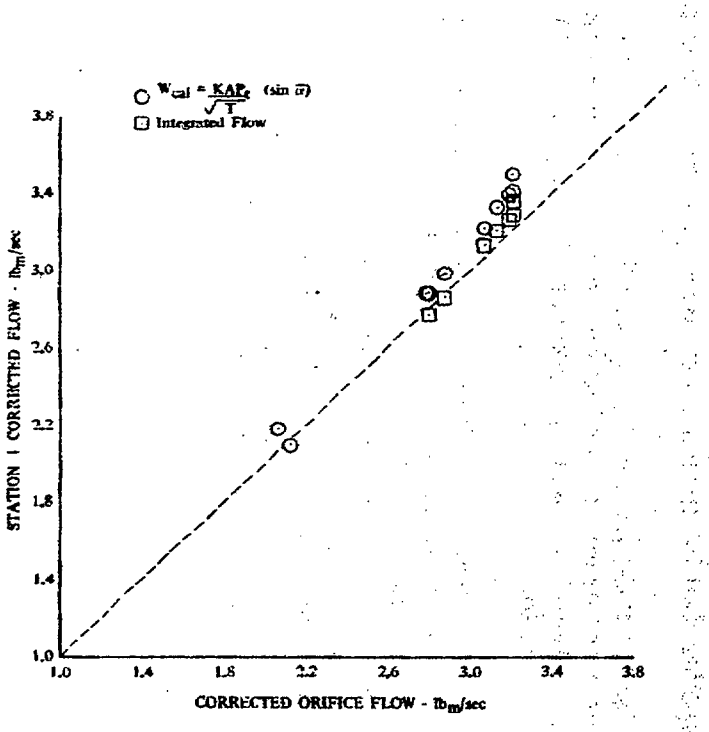

Figure 46. Inlet Guide Vane Exit Flow Correspondence, Build No. 6.

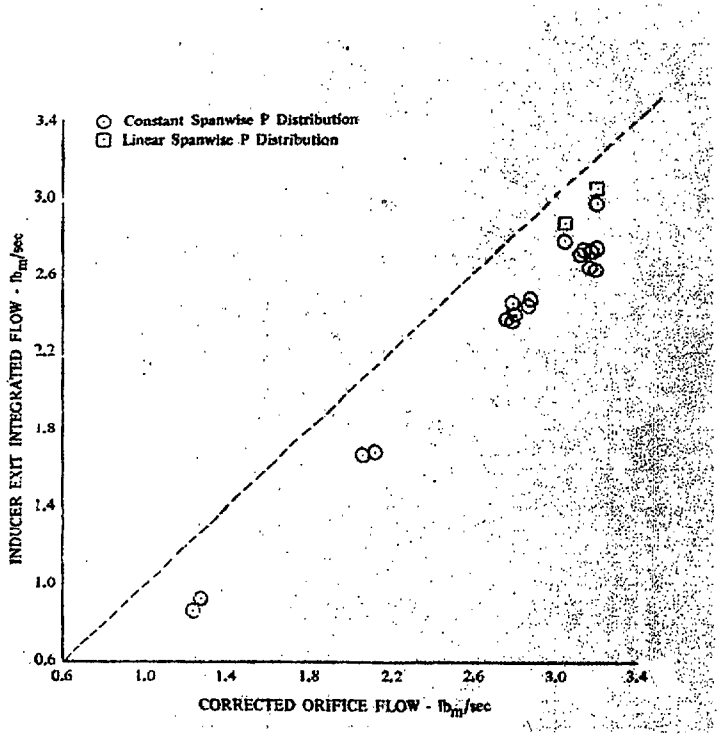

Figure 47. Inducer Exit Integrated Flow Correspondence, Build No. 6.

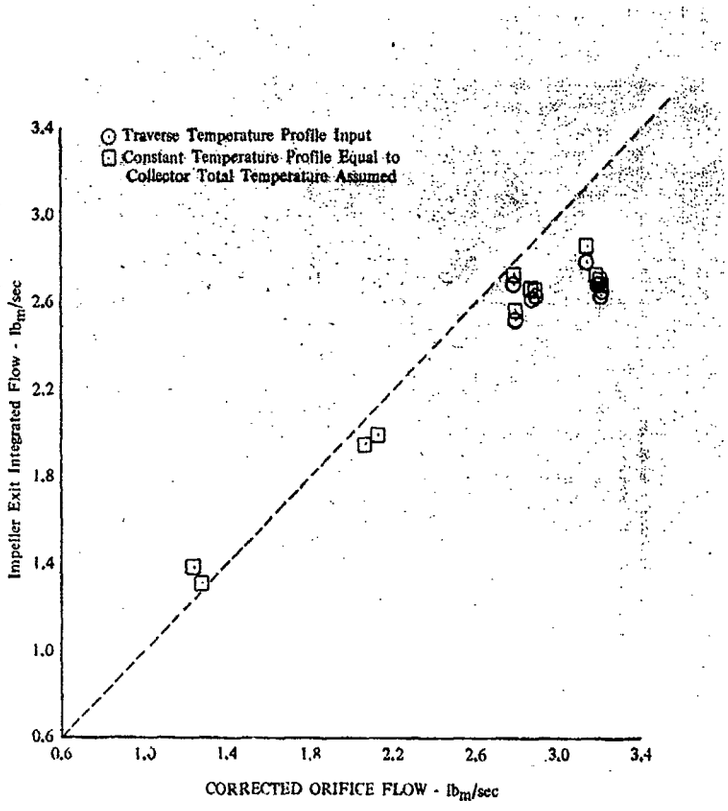

Figure 48. Impeller Exit Integrated Flow Correspondence, Build No. 6.

Measured collector static pressure readings from all taps were within the estimated precision of ±0.34 psia and generally read within ±0.1 psia. The measured collector temperatures exhibited an observed maximum deviation of ±0.75% about the average at the same condition.

Combined inlet guide vane, inducer, and impeller performance obtained from traverse data showed the same trends as the performance generated by an internal flow analysis as previously defined in the Data Reduction Section, although the absolute performance levels from the traverse data were higher. Table X compares the performance obtained from traverse data and that obtained from the internal flow analysis for near-stall points at 95% speed and 10-deg inlet guide vane setting and 101% speed and 0-deg inlet guide vane. Also shown in the table are the diffuser losses obtained by subtracting the above inlet guide vane, inducer, and impeller performance from the overall performance at those points.

TABLE X. TRAVERSE DATA - INTERNAL FLOW ANALYSIS PERFORMANCE COMPARISON

	101% Speed, 0-Deg IGV rpm = 65,953 Flow = 3.185		95% Speed, 10-Deg IGV rpm = 62,426 Flow = 2.783	
	Traverse Data	Internal Flow Analysis	Traverse Data	Internal Flow Analysis
IGV, Inducer, Impeller Pressure Ratio, P_o/P_{t2}	11.812	11.210	9.655	9.260
IGV, Inducer, Impeller Adiabatic Efficiency, %	81.5	79.4	85.8	82.7
Diffuser Loss, $\frac{P_{t2} - P_3}{P_{t2}}$	0.182	0.139	0.167	0.115

RESULTS AND DISCUSSION

Initial Performance

Overall performance data obtained during the Build No. 2 shakedown test indicated the existence of a performance deficiency, which data analyses revealed to be caused by an impeller-diffuser mismatch. These analyses resulted in a decision to bore out the diffuser throat to provide a better match for the impeller discharge conditions.

The overall performance data indicated that, if the compressor had operated at design speed, the compressor would have been down appreciably in efficiency (Figure 49) and flow (Figure 50). The test data were used in conjunction with analytical computer programs to separate the impeller and diffuser performance characteristics to isolate the cause of this degradation in performance. This analysis resulted in two conclusions. First, the diffuser was setting the maximum flow rate for the compressor, as indicated by the diffuser loss characteristics shown in Figure 51. Vertical diffuser loss characteristics, such as those in Figure 51, are commonly associated with a flow-limited diffuser. The second conclusion was that, as a result of the reduced inlet flow rate caused by the choked diffuser, the impeller incidence values were higher than design, resulting in a loss in impeller efficiency.

Further analysis of the diffuser revealed that the diffuser was flow limited due to greater than anticipated throat blockages at 70, 80, and 85% of design speed, as can be seen in Figure 52. Extrapolating the throat blockage data to 100% speed indicates the blockage will be 14% compared to the design value of 8%. By assuming a 14% blockage at 100% design rotor speed and that the impeller will meet its design goals at design flow rate, i.e., incidence, it was determined that a diffuser throat area 7% greater than the current design was required. Therefore, it was decided to bore out the diffuser throat by 7% but to retain the diffuser design throat length-to-diameter ratio of 0.5 by also reboring the 3-deg cone. Changes in diffuser leading edge radius ratio, leading edge Mach number, and diffuser exit conditions resulting from the increased throat area were considered negligible.

OVERALL PERFORMANCE

Overall performance data for Builds No. 3 and 6 of the compressor are presented in this section. Build No. 6 of the compressor was tested with a damaged diffuser, and its performance was somewhat impaired. An analytical representation of the performance that this stage would have produced without this damage was prepared using diffuser performance from Build No. 3; it is also presented in this section.

Data for Build No. 3 at the design inlet guide vane setting of 10 deg are presented in Figure 53 and for inlet guide vane angles of 0 and 20 deg in Figures 54 and 55. At the 10-deg design IGV setting, the flow rate was 3.03 lb/sec, compared to the goal of 3.1 lb/sec, an indication that the inducer-impeller was producing less pressure than anticipated. The maximum pressure ratio at design speed was 9.34 at an efficiency of 77.6%. A rotor speed of 95% of design produced a pressure ratio exceeding the required 8:1 pressure ratio at an efficiency slightly less than the 80% goal, 79.6%.

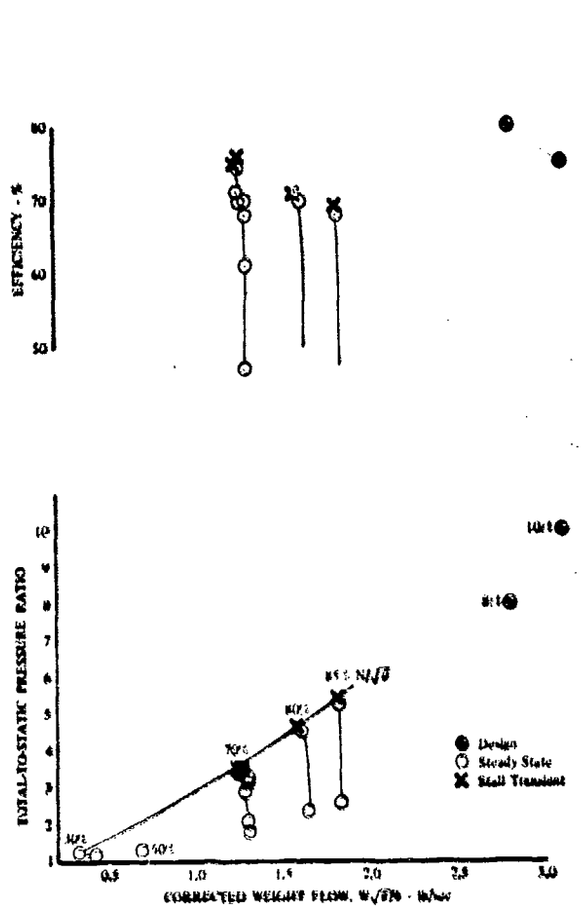

Figure 49. Overall Performance, Build No. 2 Shakedown Test.

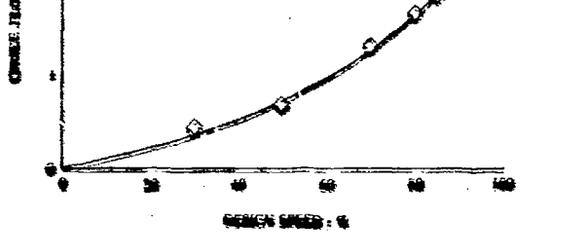

Figure 50. High-Speed Centrifugal Compressor Flow Characteristics.

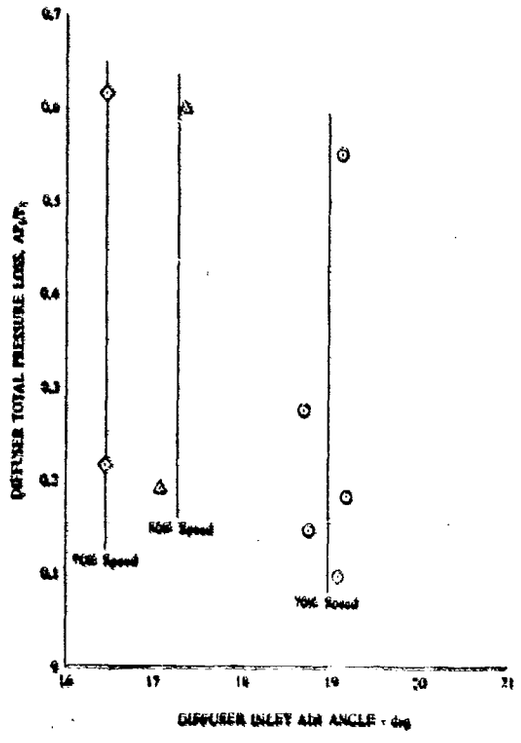

Figure 51. Diffuser Loss Characteristic, Build No. 2 Shakedown Test.

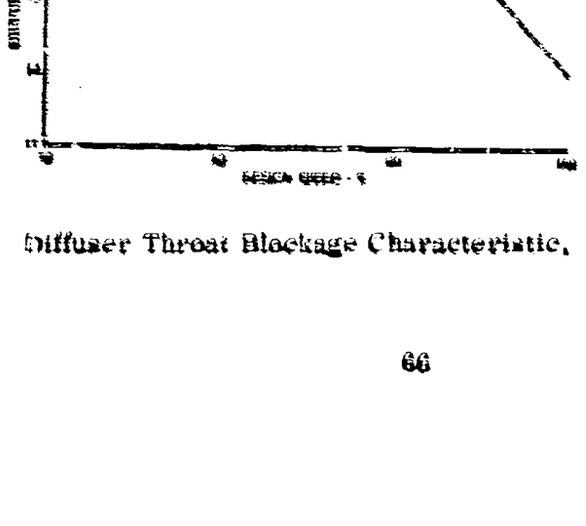

Figure 52. Diffuser Throat Blockage Characteristic, Build No. 2 Shakedown Test.

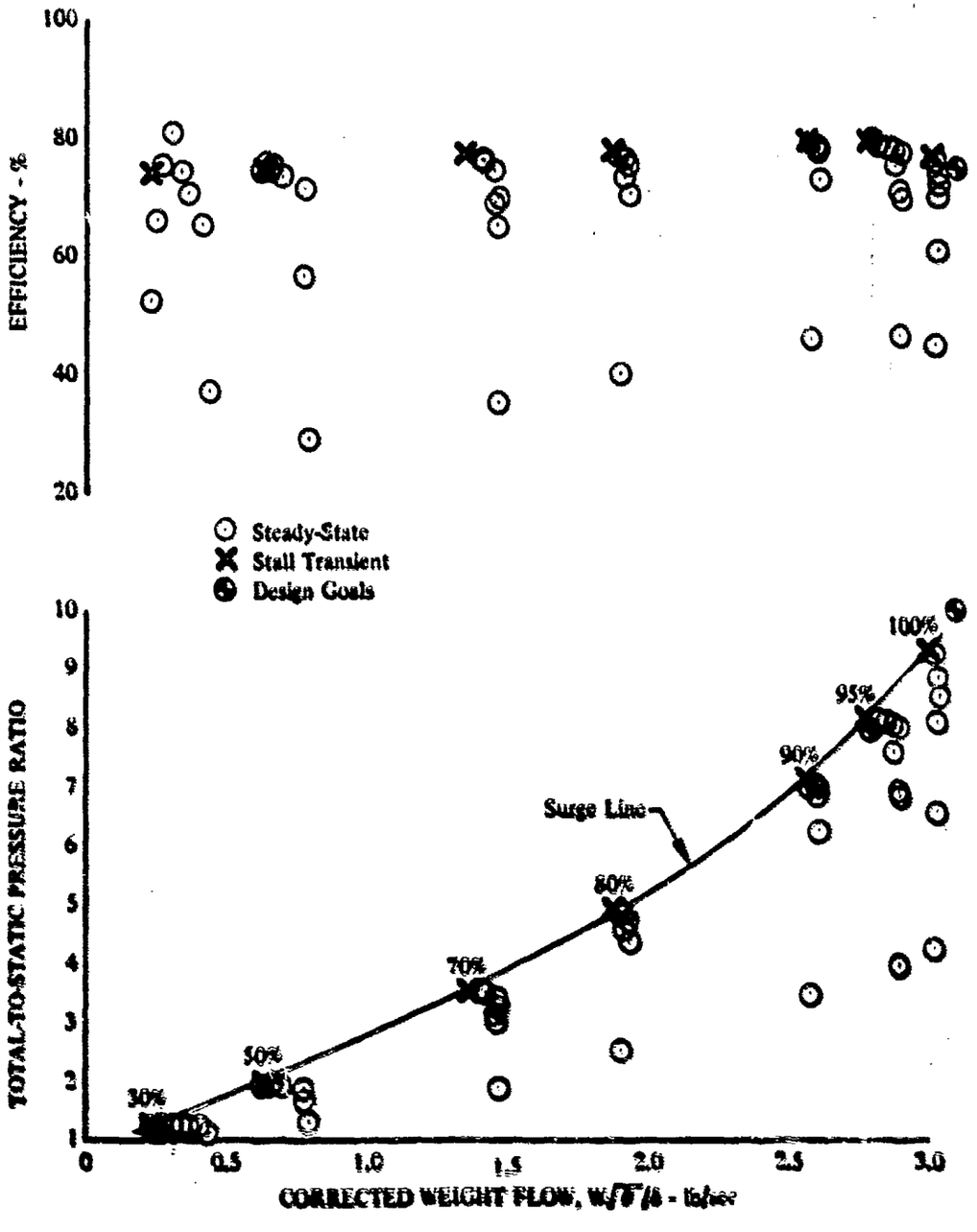

Figure 53. Overall Performance, Build No. 3, 10-deg IGV.

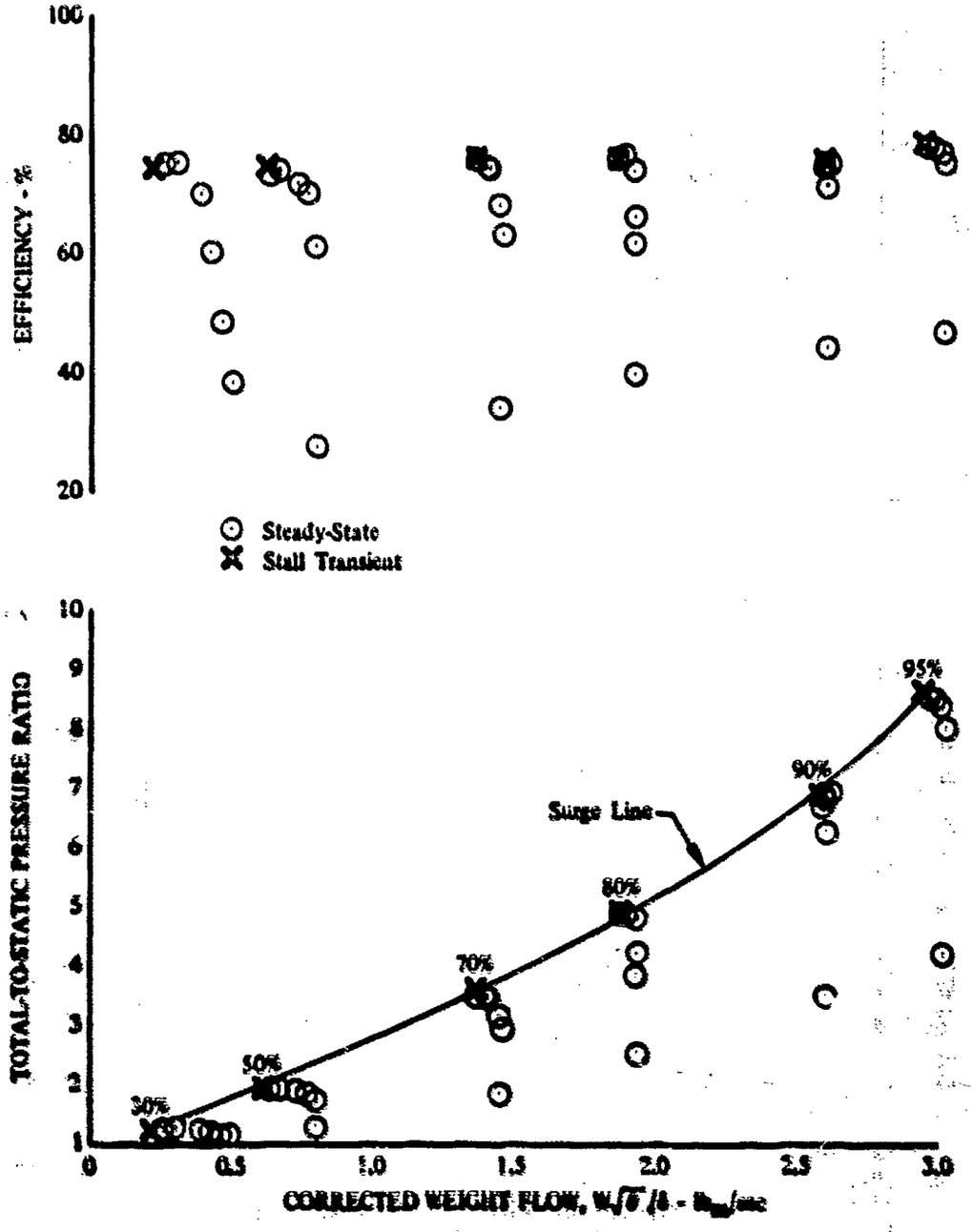

Figure 54. Overall Performance, Build No. 3, 0-deg IGV.

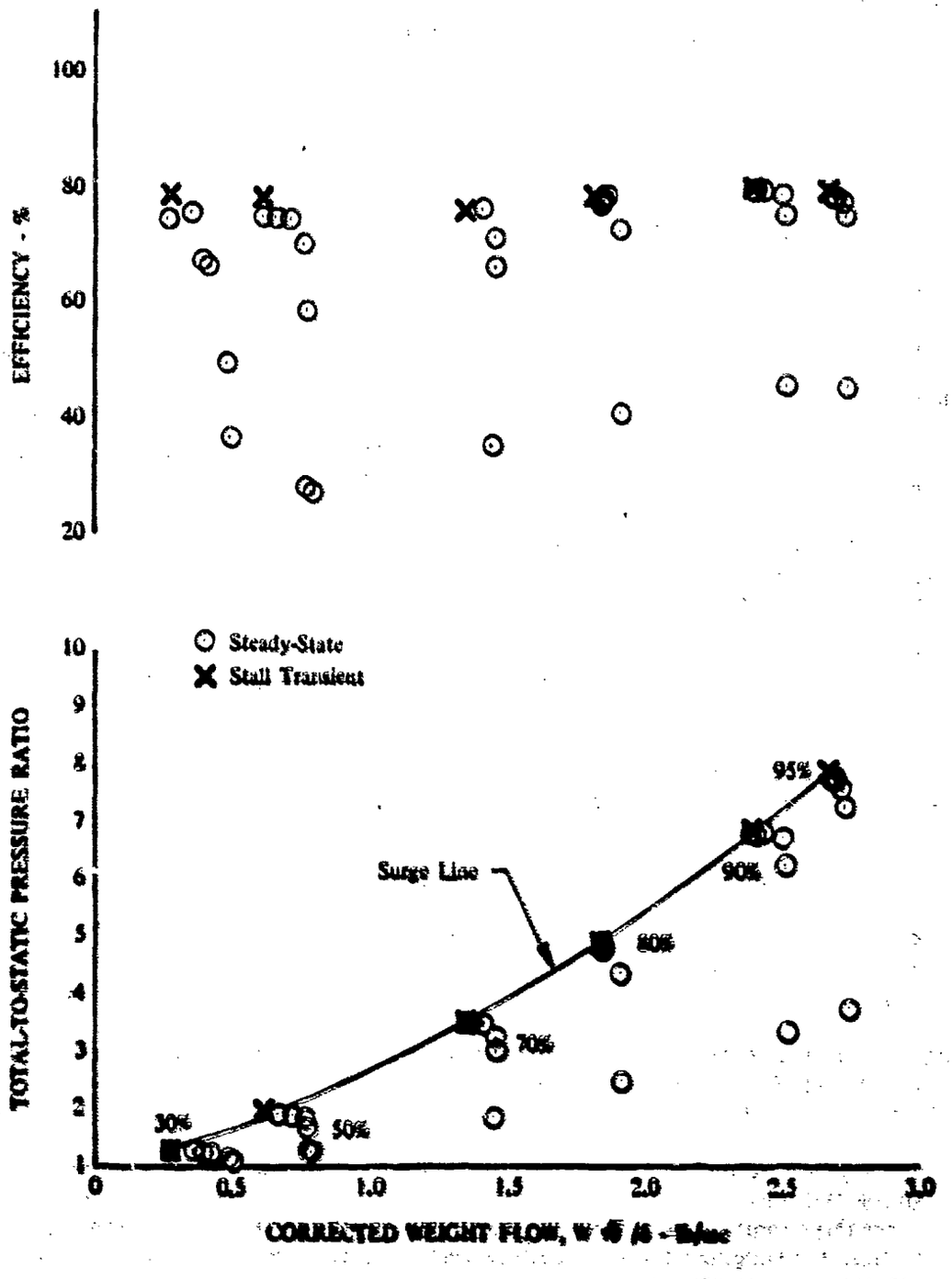

Figure 55. Build No. 3 Overall Performance, 20-deg IGV.

The trends exhibited by these data lead to an interesting speculation that the design conditions may have been attained by overspeeding the rotor approximately 2% at the design inlet guide vane setting. High rig vibrations prevented further high-speed testing.

The compressor maps obtained with inlet guide vane settings ±10 deg from the nominal were limited to a maximum speed of 95% of design due to rotor vibrations. The higher rotor work capability of the 0-deg IGV setting raised the maximum pressure ratio from 8.2 for the design IGV setting at 95% of design speed to over 8.6 without mensurable loss in efficiency. This change in IGV angle also increased airflow by 4.5%. The improved performance at the 0-deg IGV setting indicated that this setting may have offered the best compromise for attaining the performance goals at high-rotor speeds. Testing of Build No. 3 was, however, terminated due to a bearing failure associated with the vibration problems.

Performance testing of Build No. 6 after the redesign of the rig bearing and rotor system completed the high speed tests initiated with Build No. 3. Data are presented in Figure 56 for the various combinations of IGV settings and rotor speeds that were tested. The data show that the maximum pressure ratio reached at a -4-deg IGV setting was slightly above the design goal (10:03) at a rotor speed of 1% in excess of design, and the corresponding maximum efficiency was 1.2 percentage points low. At the 8:1 pressure ratio point, the efficiency decrement was 2 points below the goal.

Comparing this efficiency loss with the previous data led to the conclusion that the damage sustained by the diffuser was more serious than expected. Damage occurred when portions of the silver plating on the impeller shroud broke off and impinged on the leading edges of the diffuser during an earlier impeller-to-shroud rub. A complete discussion of the problem is presented in the diffuser component section. The Build No. 6 testing also included a special test in which nitrogen was used to cool a thermal dam machined between the impeller shroud flange and the inducer shroud flange to eliminate heat transfer and to create a thermal environment similar to that of Build No. 3 or a gas generator with thin cases.

This test generated a pressure ratio of 10.04:1 and an efficiency of 74.3% at 101% of design speed and -4-deg IGV setting. This was an improvement of 0.5% due to the thermal dam.

Using data from Builds No. 3 and 6 compressor tests, a composite performance map was formulated for this compressor. This map, Figure 57, uses the Build No. 3 data at rotor speeds of 95% of design and below. At design speed, data from a Build No. 6 stall transient (no steady-state data points were recorded) were used, but were adjusted to compensate for the reduced performance of the damaged diffuser using Build No. 3 diffuser performance data. This composite data map shows that the compressor achieved its major pressure ratio and efficiency goals. The efficiency throughout the speed range was optimized by varying the inlet guide vanes as noted on the figure.

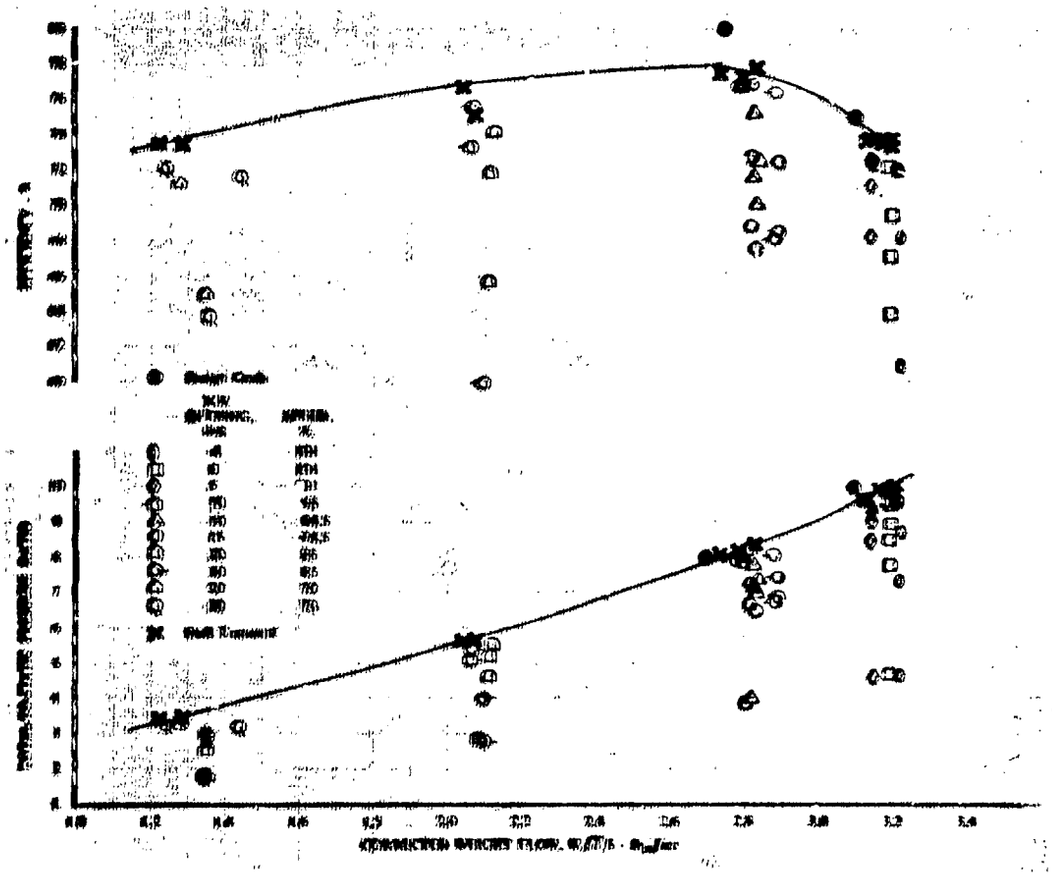

Figure 56. Build No. 6 Overall Performance.

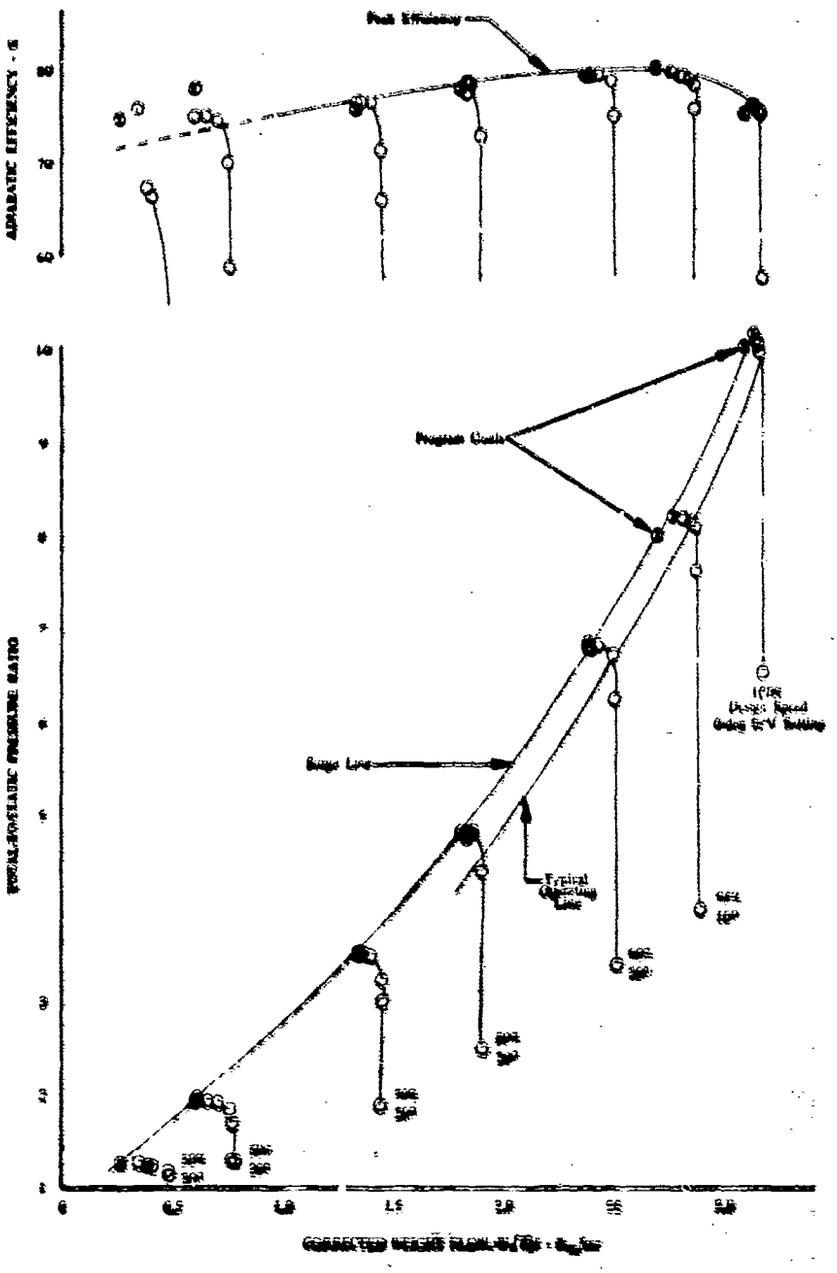

Figure 37. Composite Overall Performance Map.

COMPONENT PERFORMANCE

A discussion of the performance of each compressor stage component is presented in this section. A representation of the cumulative performance at various stage component interfaces is presented in Figure 58 to provide a perspective on the contributions of the various components to the overall stage performance. Data from both Builds No. 3 and 6 are used in this representation. It may be noted that the inlet section, including the IGV losses, has a small effect on overall performance and that the impeller performance is not sensitive to operating conditions throughout the speed-flow regime. On the other hand, the inducer performance peaks at about 2.9 lb/sec flow and then drops sharply at higher flow, suggesting that a significant improvement in efficiency may be possible through an evaluation of the cause of this loss and the accomplishment of corrective modifications.

Inlet and Inlet Guide Vanes

The inlet and inlet guide vanes were analyzed for the Builds No. 3 and 6 configurations. Tabulations of all inlet guide vane data are presented in Appendix I and can be used to further define the characteristics of individual vanes and struts. Inlet guide vane turning for the Build No. 6 configuration is shown in Figure 59 as mass average turning angle vs inlet guide vane setting. These data show that the mass average angles agree well with predicted turning angles. Although the average turning matches the design prediction, the flow was underturned at the tip, compensating for general overturning over the rest of the span, as demonstrated in Figure 60. This figure presents mass average exit air angle at five spanwise positions for the 10-deg IGV setting at three rotor speeds for Build No. 6 and one for Build No. 3. The different distribution is evidently related to the Build No. 6 converging configuration, since the Build No. 3 data using the same guide vanes and setting produced a more nearly constant distribution with slight overturning at the tip.

The redesigned inlet also produced a greater loss than the original design. Mass-averaged total pressure data from Builds No. 6 and 3, as shown in Figure 61, demonstrate this increase in inlet losses. A sample plot of the circumferential total pressure traverses used to generate this loss data is shown in Figure 62. A sample radial traverse is shown in Figure 63. The probe has been shimmed away from the hub wall by approximately 0.020 in. These data show the trend to increasing losses toward the tip of the guide vanes. This may also be seen in Figure 64 in which the losses from the hub through midspan are low, while 70 and 90% span losses are quite high for data taken at 100 and 101% of design speed. There is a considerable increase in losses generated when the guide vanes were set to produce negative turning. The increase in loss at 90% span with increasing prewhirl may be a function of the clearance between the vane end and the outer wall, which increased in any position except axial. At other spanwise locations the losses minimize at 10 deg, which was the design setting.

The inducer inlet conditions generated by the guide vanes are described completely for every traverse point in tabulations in Appendix I. A typical tabulation (e.g., 100% speed and 10 deg of prewhirl) is presented in Table XI. Inlet relative Mach number and incidence are presented as a function of spanwise position in Figure 65.

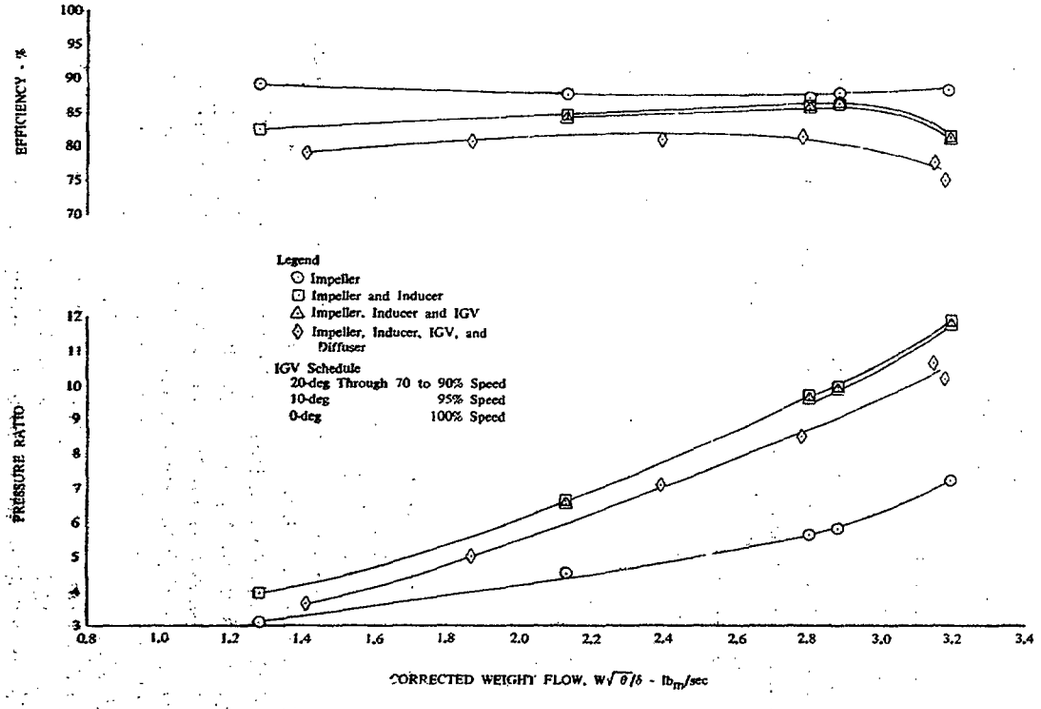

Figure 58. Component Efficiency Representation.

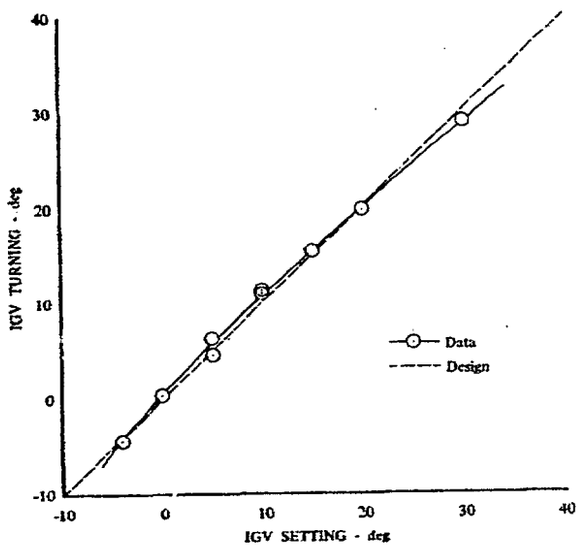

Figure 59. IGV Turning vs Setting, Build No. 6.

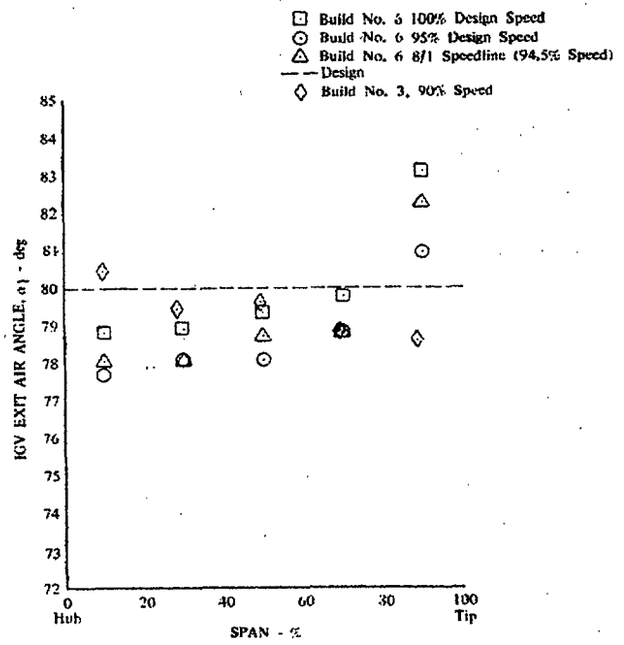

Figure 60. IGV Exit Prewhirl Distribution, 10-deg IGV.

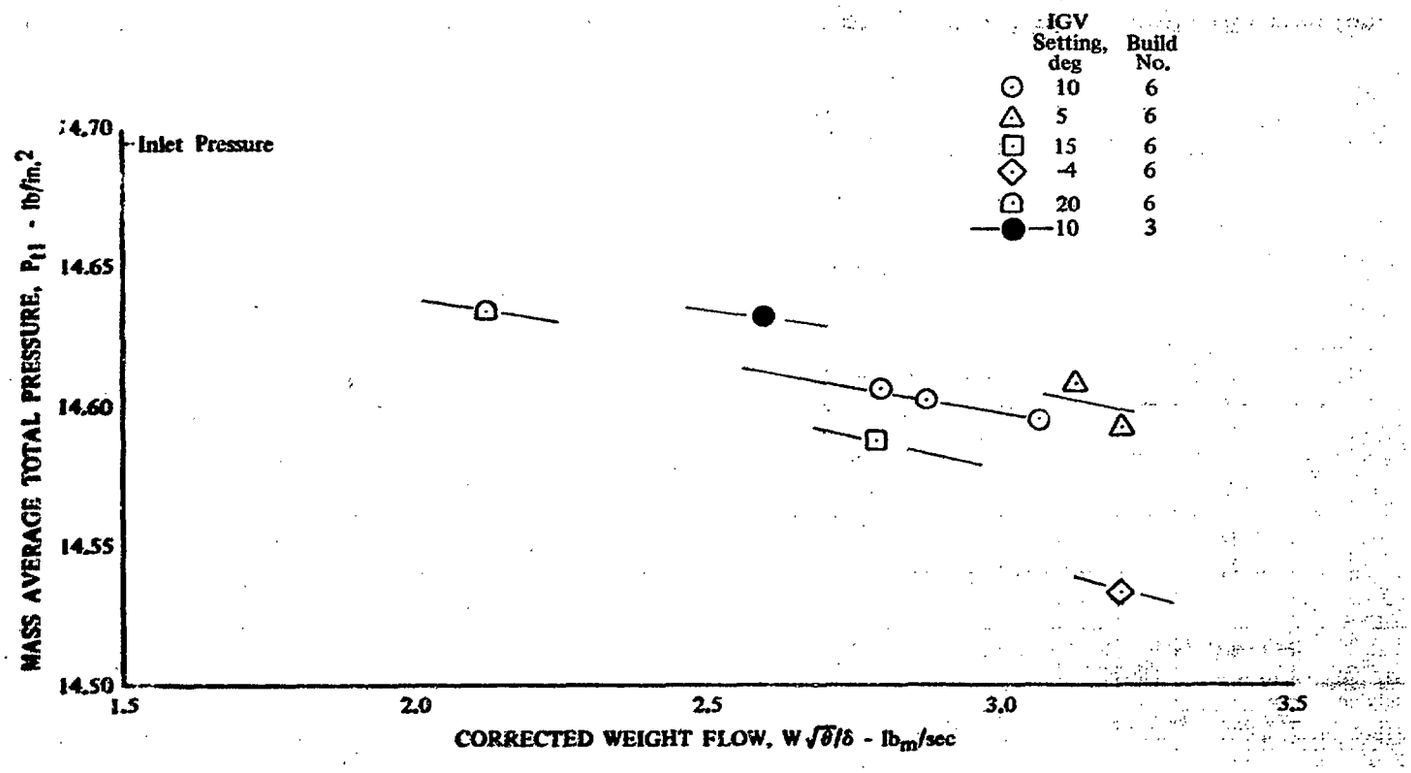

Figure 61. Inlet Section Total Pressure Loss Characteristics.

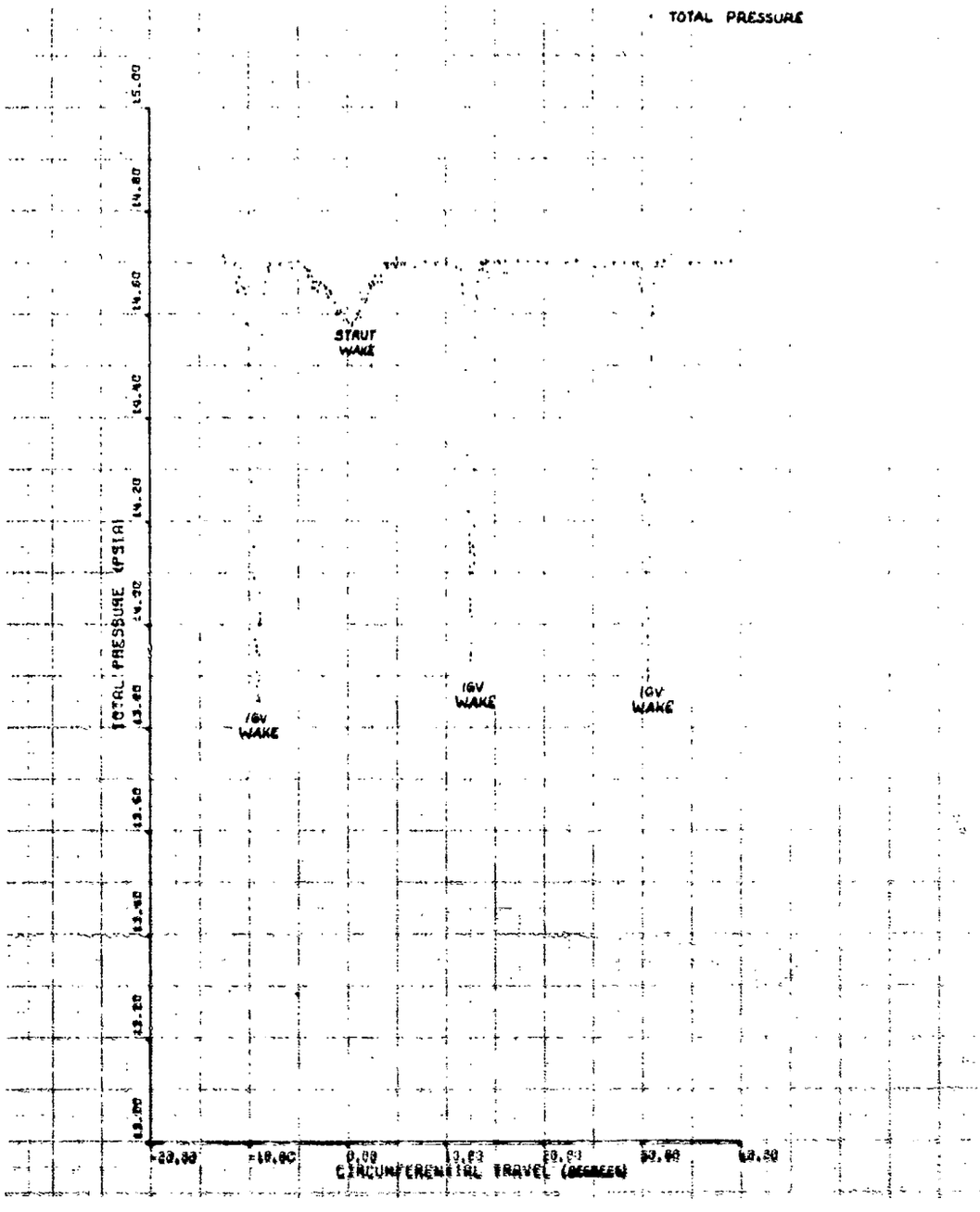

Figure 62. IGV Circumferential Traverse, Build No. 6, 100% Speed, 10-deg IGV, 50% Span.

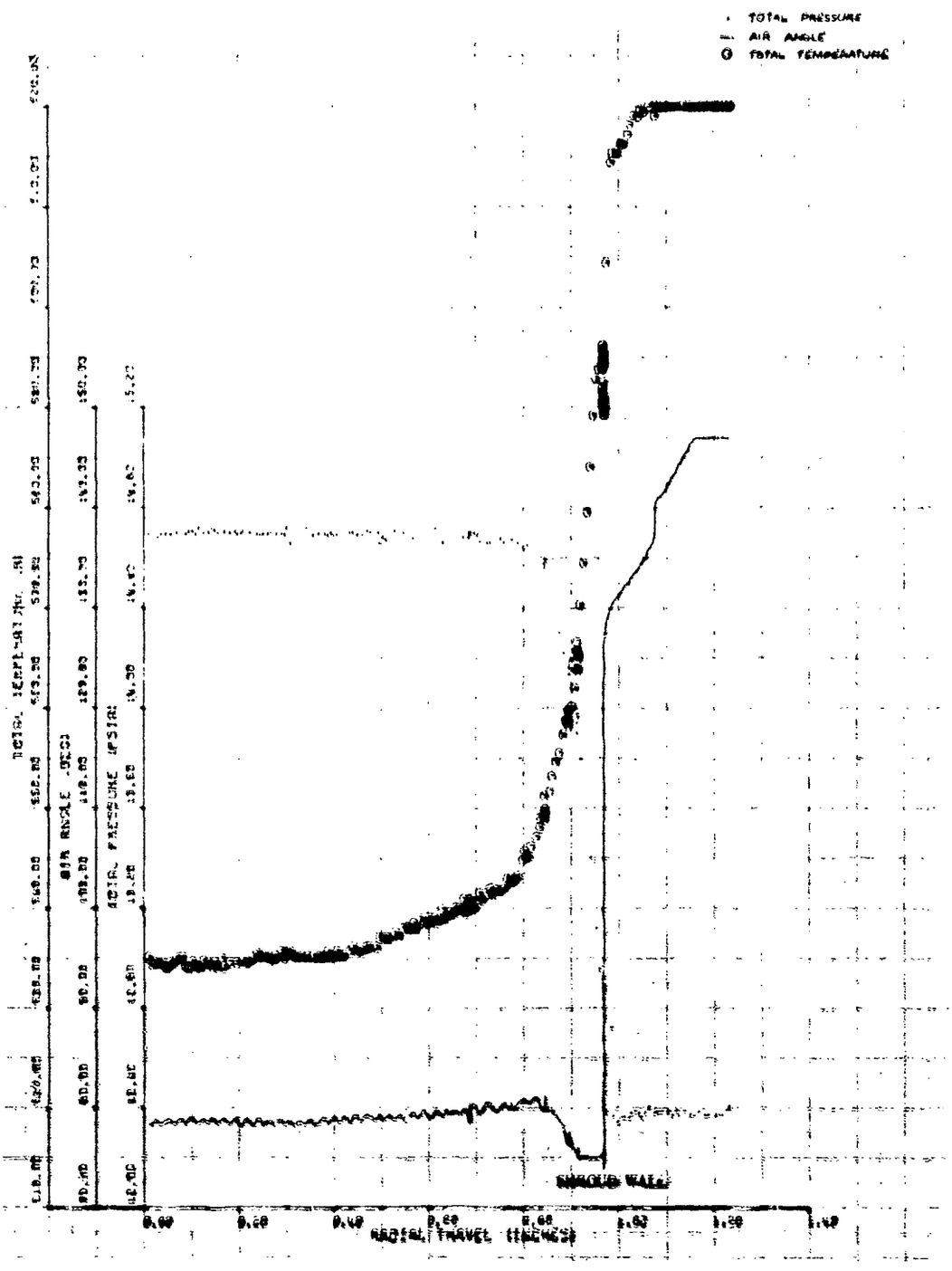

Figure 63. IGV Exit Radial Traverse, Build No. 6, 100% Speed, 10-deg IGV, Near Stall.

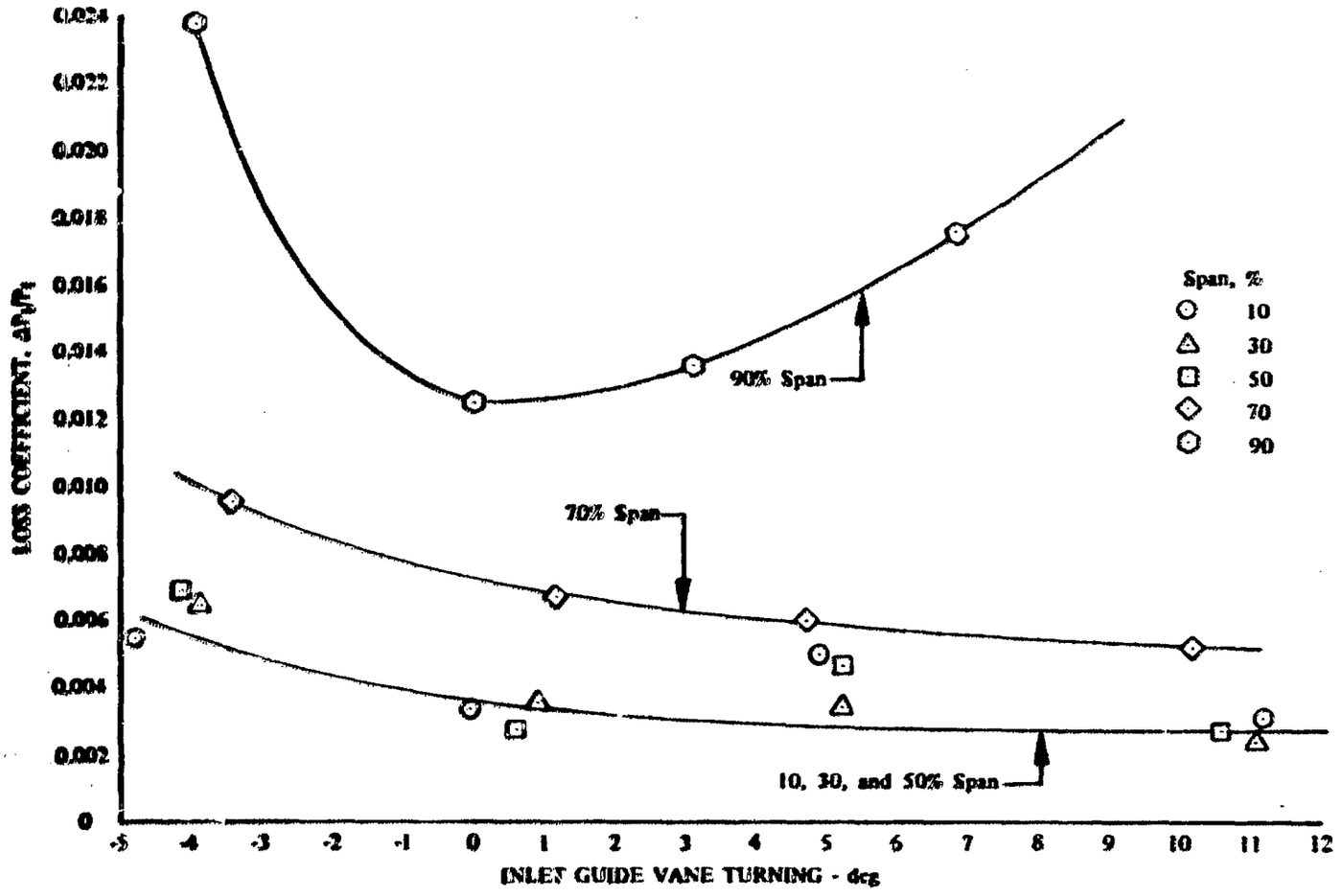

Figure 64. Build No. 6, Inlet Guide Vane Losses at Approximately 0.46 Mach Number.

TABLE XI. INLET GUIDE VANE CIRCUMFERENTIAL TRAVERSE DATA - 100% SPEED, 10-DEG IGV SETTING

Circumferentially Integrated Quantities

Percent Span	10.1389	30.2170	50.2768	70.4209	90.2630
Strut Average Radial Travel	0.1014	0.3022	0.5028	0.7042	0.9026
Vane Average Radial Travel	0.1003	0.3018	0.5020	0.7046	0.9022
Average Hub Static Pressure	12.4440	12.4440	12.4440	12.4440	12.4440
Average Shroud Static Pressure	12.4440	12.4440	12.4440	12.4440	12.4440
Spanwise Static Pressure	12.4440	12.4440	12.4440	12.4440	12.4440
Incremental Flow (S)	0.0246	0.0294	0.0319	0.0354	0.0362
Incremental Flow (V)	0.0239	0.0293	0.0314	0.0355	0.0360
Mass Average Pressure (S)	14.5850	14.6153	14.6169	14.5801	14.4525
Mass Average Pressure (V)	14.6720	14.6751	14.6684	14.6332	14.4308
Mass Average Angle (S)	78.7595	78.9085	79.0077	79.6817	82.6728
Mass Average Angle (V)	78.8080	78.9434	79.5941	79.8631	83.2852
Weighted Pressure	14.6459	14.6572	14.6529	14.6172	14.4373
Weighted Angle	78.7934	78.9329	79.4182	79.8086	83.1014
Weighted Flow	0.0241	0.0293	0.0315	0.0355	0.0360
Loss Coefficient (S)	0.007419	0.005357	0.005250	0.007751	0.016435
Loss Coefficient (V)	0.001500	0.001283	0.001743	0.004141	0.017910
Weighted Loss Coefficient	0.003276	0.002505	0.002795	0.005224	0.017458

Total Integrated Quantities

Total Incremental Flow	0.15652
Spanwise Mass Average Total Pressure	14.59489
Spanwise Mass Average Air Angle	79.94775
Total Pressure Loss	0.00674
Integrated Flow	3.13035
Flow Coefficient of Inlet	0.95331
Mach Number In	0.43984
Guide Vane Angle	96.67302

NOTE:

(S) denotes parameter pertaining to gaps containing both IGV and strut wakes.
(V) pertains to gaps containing IGV wakes only.

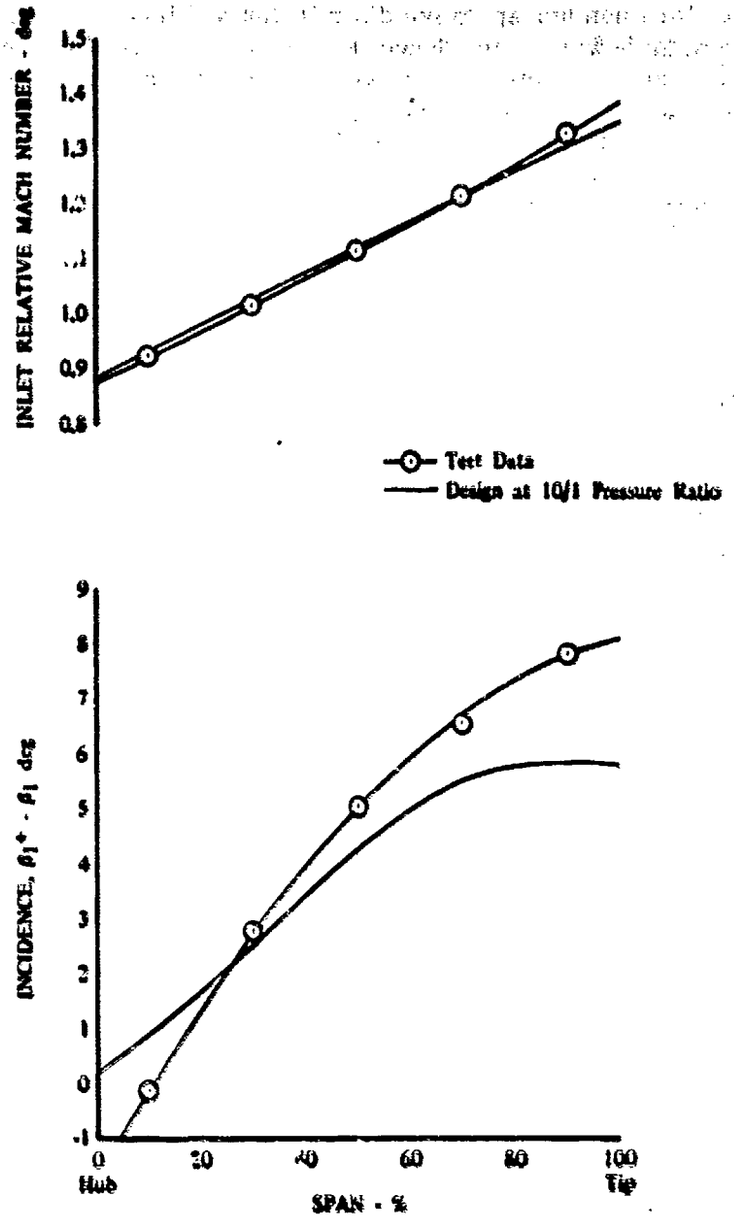

Figure 65. Inducer Inlet Conditions, 100% Speed, 10-deg IGV.

The inlet relative Mach number spanwise distribution and level are both in close agreement with design; however, incidence is more positive (stalled) in the outer half of the passage than anticipated. Increasing the speed and reducing the prewhirl (for instance, to 101% speed and -4-deg of prewhirl) raises the relative Mach number and increases the amount of stall incidence, as shown in Figure 66.

Static pressure profiles generated by wall taps through the inlet are presented in Appendix I for both Builds No. 3 and 6 at comparative conditions.

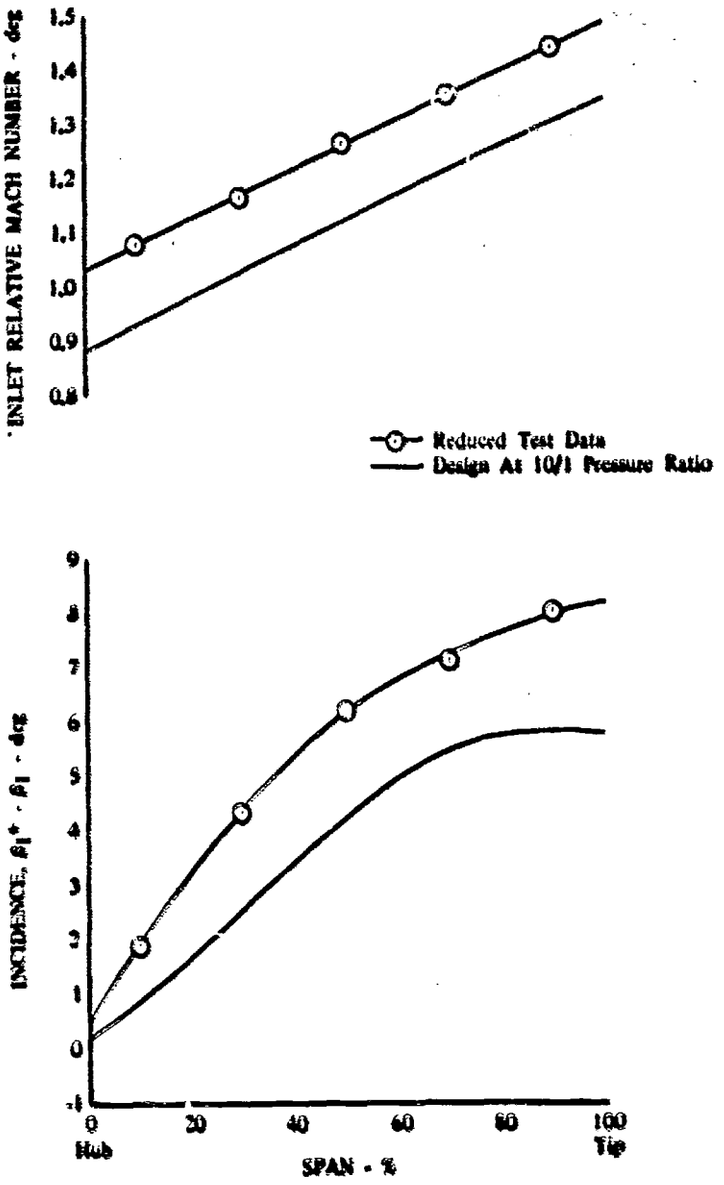

Figure 66. Inducer Inlet Conditions, 101% Speed, -4-deg IGV.

Inducer

Analysis of inducer performance was divided into Builds No. 3 and 6, with a majority of the traverse data used obtained in Build No. 6. Build No. 3 inducer data at 95% speed and 10 deg of prewhirl were reduced using inlet conditions from the only available inlet guide vane traverse point during that build. These data are shown in Figure 67. Inlet relative Mach number distribution was in good agreement with design values, but lower overall due to the decreased speed (95%). The average inducer incidence angle was about 2 deg above the design value because flow rate and, consequently, axial velocity were slightly below design. The inducer pressure ratio and efficiency for this point were 1.67 and 85.6%, respectively.

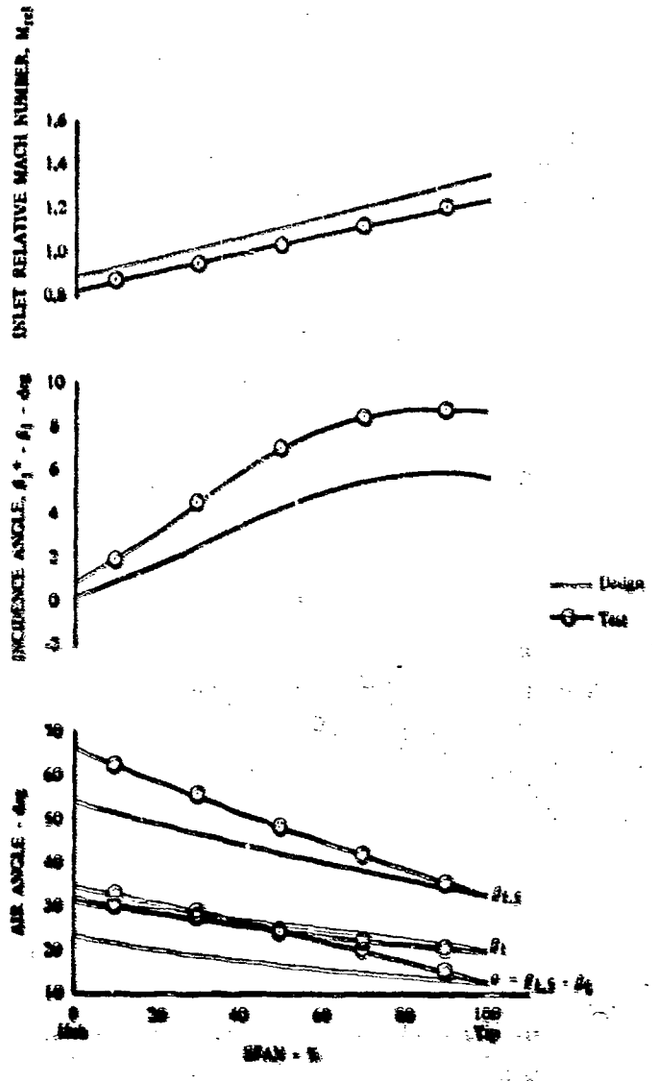

Figure 67. Inducer Inlet Conditions, Build No. 3, 95% Speed, 10-deg IGV, Near Stall.

The inducer discharge conditions calculated for this point indicated that the impeller was operating below design incidence over most of the span. The low incidence in the hub region was caused by overturning in the hub region of the inducer.

Sufficient data were obtained in Build No. 6 to completely define the blade element and overall performance of the inducer. Inducer pressure ratio and efficiency are presented as functions of weight flow in Figure 68. The inducer exceeded its design pressure ratio, but at a lower than goal efficiency. The efficiency of the inducer decreased markedly with speed above 95% of design speed; pressure ratio also decreased for constant inlet guide vane settings. The low prewhirls at 101% speed increased the pressure ratio and flow of the inducer, but efficiency monotonically decreased with increasing flow. Inducer exit traverse data also help explain the loss in performance at high speed. A traverse plot at 101% speed and -4-deg inlet guide vane setting in Figure 69 shows that a severe inducer exit air angle and total pressure profiles were generated when the inducer was operated at an inlet relative Mach number considerably higher than design. The radial travel increases from the hub to shroud, with the shroud wall being at approximately 0.62 in. Tabulated data for this point are presented in Table XII.

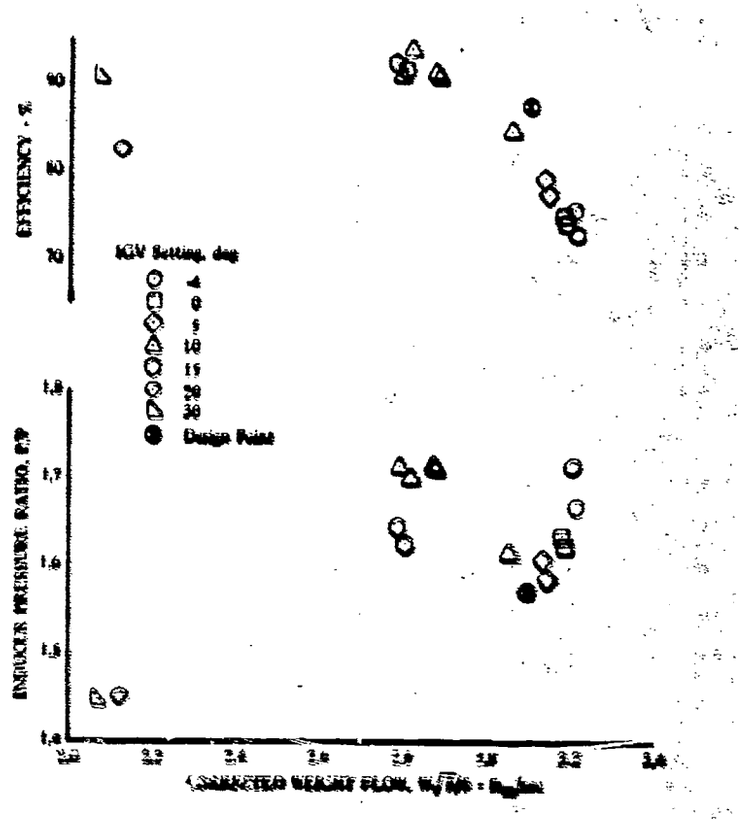

Figure 68. Inducer Performance, Build No. 6.

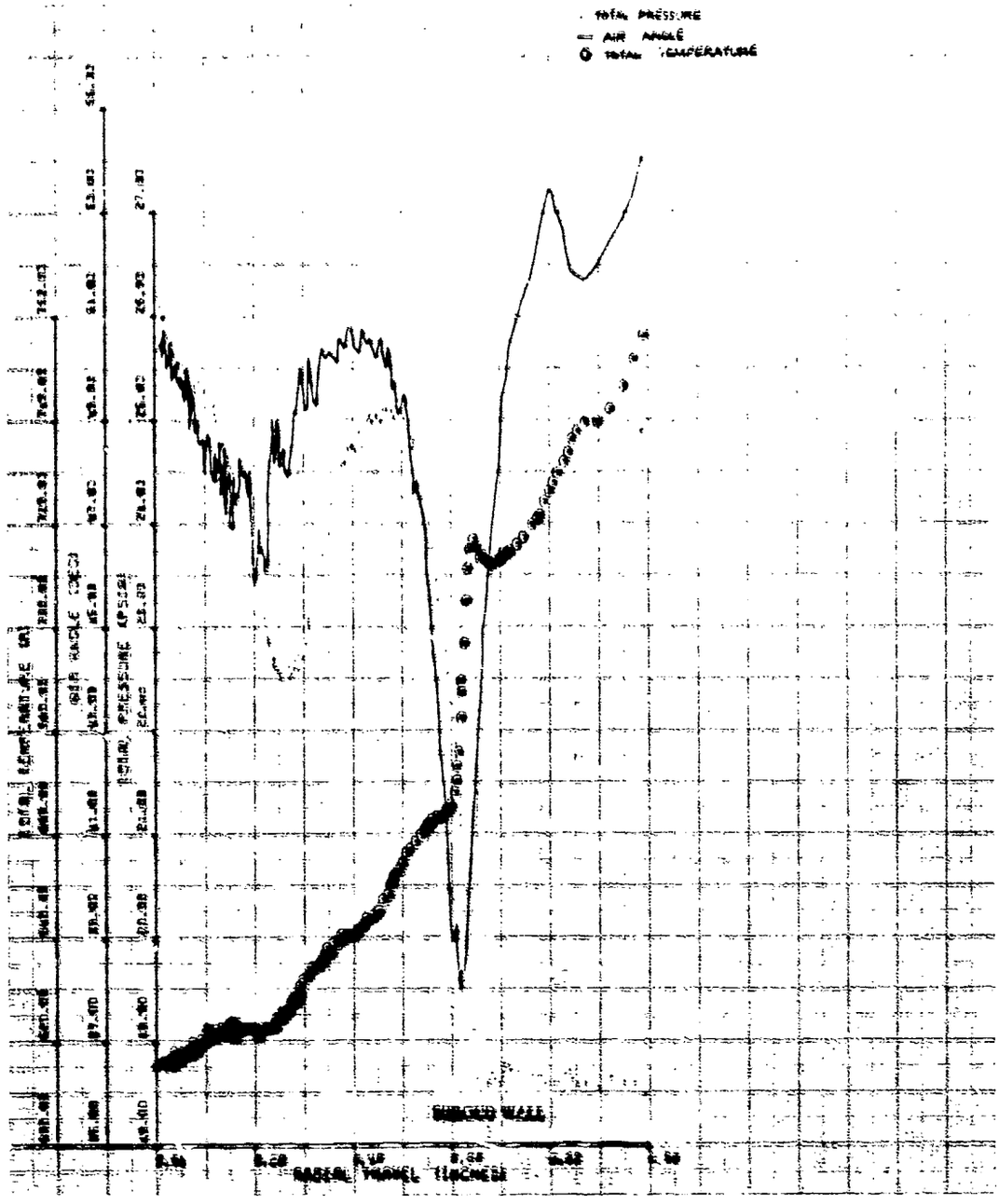

Figure 69. Inducer Exit Traverse, Build No. 6, 101% Speed, -4-deg IGV, Wide Open Discharge.

Reducing speed to 100% of design and increasing prewhirl to 10 deg, which allows the inducer to operate at design inlet Mach number, improved the midspan problem with the inducer. The majority of the inducer inefficiency at the design point appears near the tip as total pressure loss, overturning, and excessive temperature rise, as shown in Figure 70 and Table XIII. A further decrease in speed to 95% of design speed, as shown in Figure 71, continued to improve the performance of the inducer, allowing it to reach efficiencies of over 90% at pressure ratios of over 1.7:1.

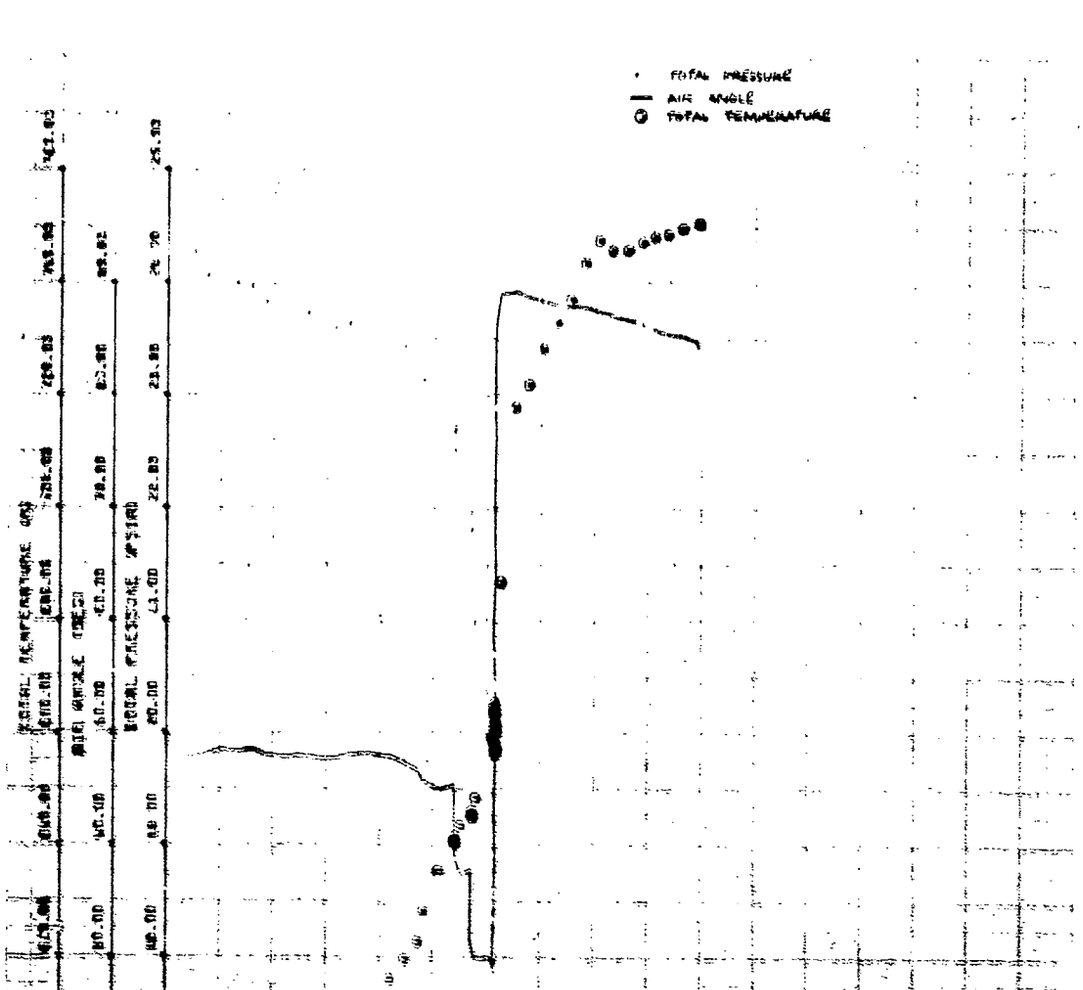

Figure 70. Inducer Exit Traverse, Build No. 6, 100% Speed, 10-deg IGV.

TABLE XII. INDUCER EXIT TRAVERSE DATA, 101% SPEED, -4-DEG IGV SETTING

* * * Inducer Exit * * *

Mass Average Total Pressure	24.923
Mass Average Total Temperature	631.963
Inducer Pressure Ratio	1.696
Inducer Temperature Ratio	1.218
Inducer Efficiency	0.745

Inducer Exit Velocity Triangles

	MO	VO	ALPHA	VM	VU	U	WU	B	WO	MREL	I	VO/VOMAX
10	0.697	808.673	35.740	472.362	656.374	1044.047	387.672	50.623	611.078	0.526	3.076	0.969
30	0.716	834.029	58.747	713.002	432.702	1126.575	693.872	45.779	994.903	0.854	3.620	1.000
50	0.582	691.862	53.639	557.156	410.182	1209.103	798.920	34.891	974.011	0.819	10.138	0.829
70	0.649	770.935	62.441	683.462	356.677	1291.630	934.953	36.167	1158.127	0.975	4.032	0.924
90	0.560	680.815	54.008	550.852	400.089	1374.158	974.069	29.488	1119.039	0.921	6.161	0.816

TABLE XIII. INDUCER EXIT TRAVERSE DATA, 100% SPEED, 10-DEG IGV SETTING

* * * Inducer Exit * * *

Mass Average Total Pressure	23.577
Mass Average Total Temperature	607.093
Inducer Pressure Ratio	1.604
Inducer Temperature Ratio	1.170
Inducer Efficiency	0.850

Inducer Exit Velocity Triangles

	MO	VO	ALPHA	VM	VU	U	WU	B	WO	MREL	I	VO/VOMAX
10	0.708	812.781	55.115	666.729	464.848	1032.187	567.338	49.604	875.444	0.762	4.095	1.000
30	0.697	798.528	54.707	651.771	461.347	1113.778	652.430	44.971	922.210	0.805	4.428	0.982
50	0.683	785.786	54.003	635.744	461.831	1195.368	733.536	40.914	970.694	0.844	4.115	0.966
70	0.678	785.521	54.269	637.668	458.718	1276.959	818.240	37.929	1037.370	0.895	2.270	0.966
90	0.607	717.287	46.915	523.867	489.963	1358.549	868.586	31.095	1014.337	0.858	4.554	0.882

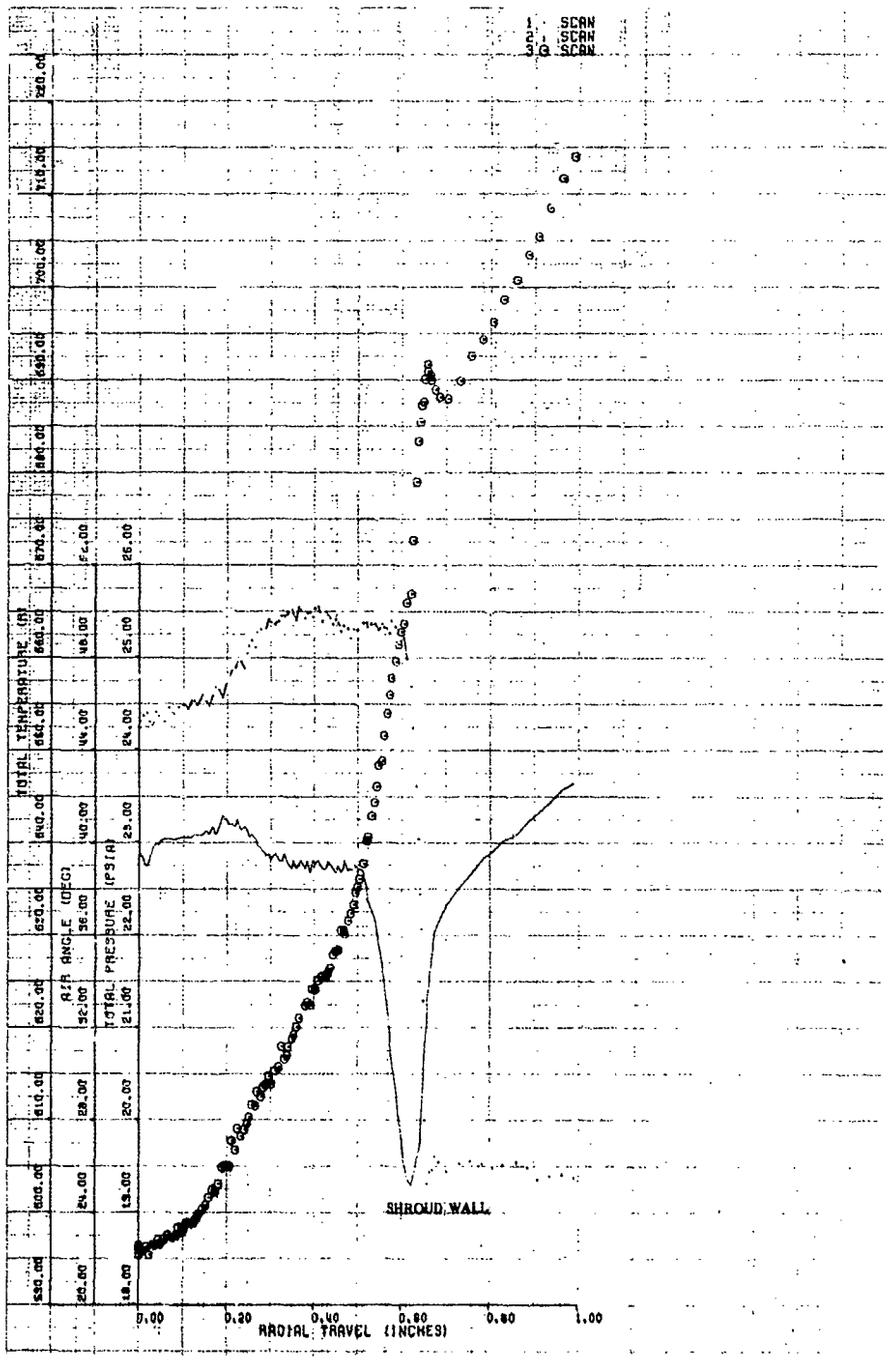

Figure 71. Inducer Exit Traverse, Build No. 6, 95% Speed, 10-deg IGV, Near Stall.

Inducer loss coefficient is presented in Figure 72 to demonstrate the level of improvement from overspeed (101%) to design (100%) conditions in conventional terms. The effect of the higher inlet Mach number and incidence on the inducer losses is easily seen in this figure. These data, coupled with the fact that the falloff in inducer efficiency at high flow shows a dependence on inlet guide vane setting, lead to the conclusion that these losses are largely dependent upon the high inlet relative Mach number.

Inducer exit traverse data are compared with impeller design inlet conditions in Figures 73 and 74 for 100% speed and 10 deg of prewhirl. Impeller inlet relative Mach number distribution and level agree well with the predicted design values; however, the incidence distribution shows the impeller incidence to be more negative than the design value, as did the data available from Build No. 3. The hub side overturning that causes this negative incidence is most apparent in Figure 74. Similar information is presented for the 101% design speed, -4-deg prewhirl condition in Figures 75 and 76.

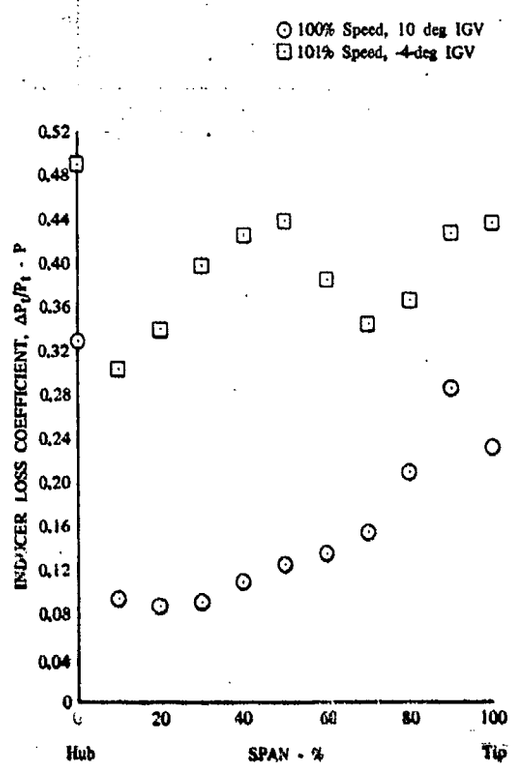

Figure 72. Inducer Losses.

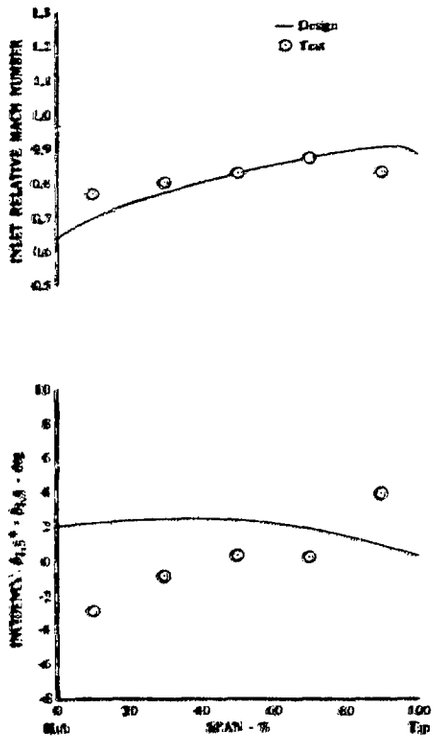

Figure 73. Impeller Inlet Conditions, 100% Design Speed, 10-deg IGV.

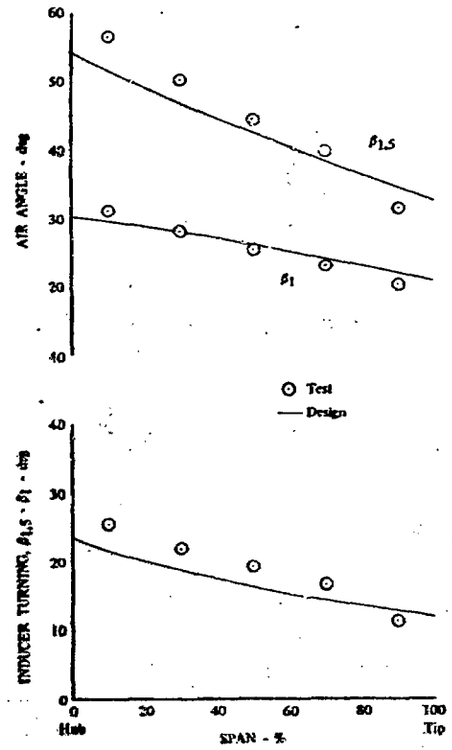

Figure 74. Inducer Exit Air Angle Profile, 100% Design Speed, 10-deg IGV.

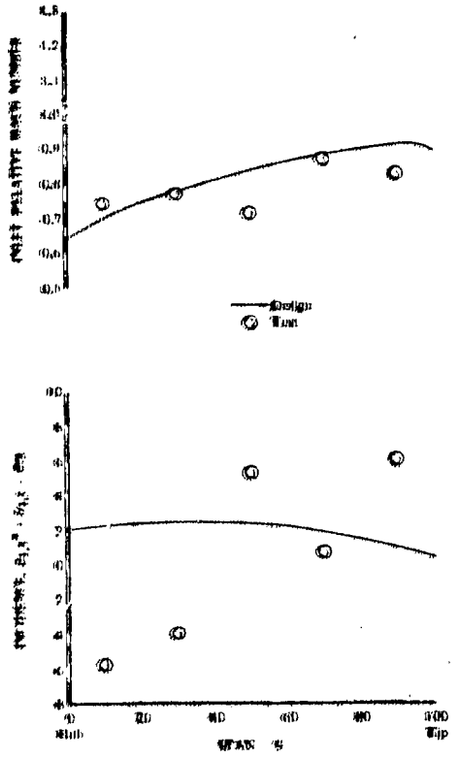

Figure 75. Impeller Inlet Conditions, 101% Speed, -4-deg IGV.

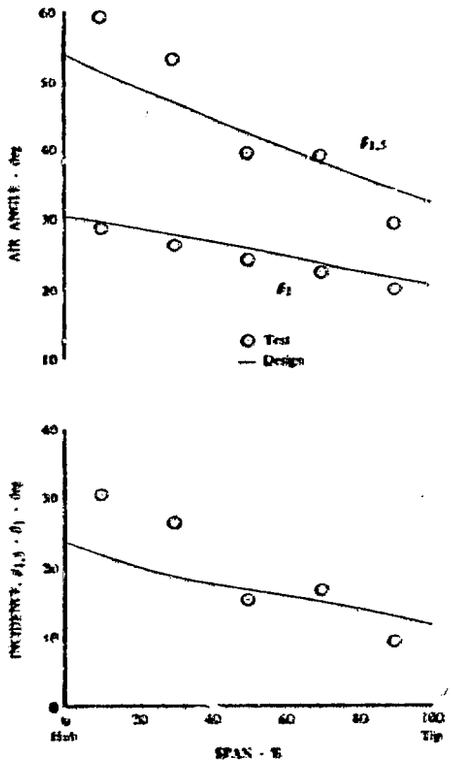

Figure 76. Inducer Exit Air Angle Profile, 101% Speed, -4-deg IGV.

The bulk of the traverse data were reduced by assuming that the static pressure across the span behind the inlet guide vanes was a constant pressure equal to that of the shroud wall behind the inducer. This assumption was necessary due to the lack of static pressure taps on the hub wall or static pressure traverse data. Performance in these planes was also reduced for some points using static pressure distributions generated by inputting geometric and aerodynamic information into a streamline analysis computer program. The static pressure profile comparison for the IGV exit (inducer inlet) is shown in Figure 77, and the inducer exit static pressure distribution comparison is shown in Figure 78.

Since the data reduction program would only accept linear distribution of static pressure, the profile generated by the streamline analysis was approximated as shown by a straight line from hub to shroud. Use of these static pressures in the data reduction program resulted in the profiles previously presented in Figures 72 through 76. The use of the initial constant pressure assumption yielded the results shown in Figures 79 and 80. There was only a small effect on impeller inlet relative Mach number; however, the change in calculated hub incidence was quite large. Incidence at 10% span from the hub was increased. Relative inducer exit air angle was, of course, similarly affected. This difference in inducer exit conditions should be considered during use of any of the standard reduction printouts presented in Appendix I.

The effect of the inducer on overall performance, other than its pressure ratio and efficiency characteristics, was evaluated in terms of any limitations it may have imposed on the impeller or overall performance. The effect of the poor high-speed inducer performance on the impeller was minimal, and is discussed in the following impeller component performance section. With respect to overall performance, the inducer was initially thought to be the flow-limiting component in the compressor. The correlation of maximum or choke flow presented in Figure 81 is composed of Build No. 3 data and was used to develop this logic. The slope of the speed-flow curve decreases sharply above 95% speed at 0-deg prewhirl, above 90 to 95% at 10-deg prewhirl, and above 90% speed at 20-deg prewhirl. This change in slope is generally a precursor to choking of the annulus and was considered to be evidence of inducer choking. The vertically common maximum flow at lower speeds, regardless of prewhirl, is due to diffuser choking.

The same relationship for the Build No. 6 data (Figure 82) did not exhibit similar characteristics. Choke flow at 70% speed was somewhat lower than Build No. 3, possibly from increased blockage in the diffuser due to the leading-edge damage. The slope of the curve did not fall off rapidly at high speed and continued to increase with lower prewhirl at maximum speed. The high-speed choke flow in Build No. 6 exceeded that projected for Build No. 3.

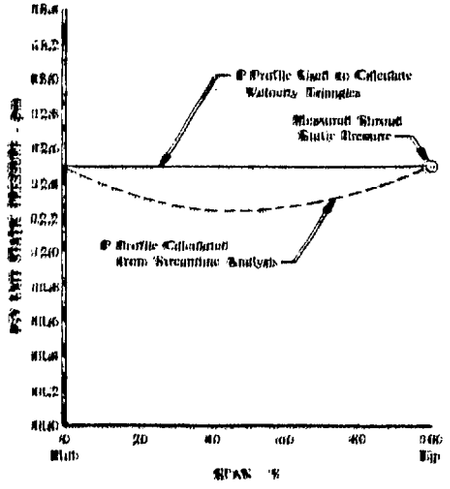

Figure 77. IGV Exit Static Pressure Profile, 100% Speed, 10-deg IGV.

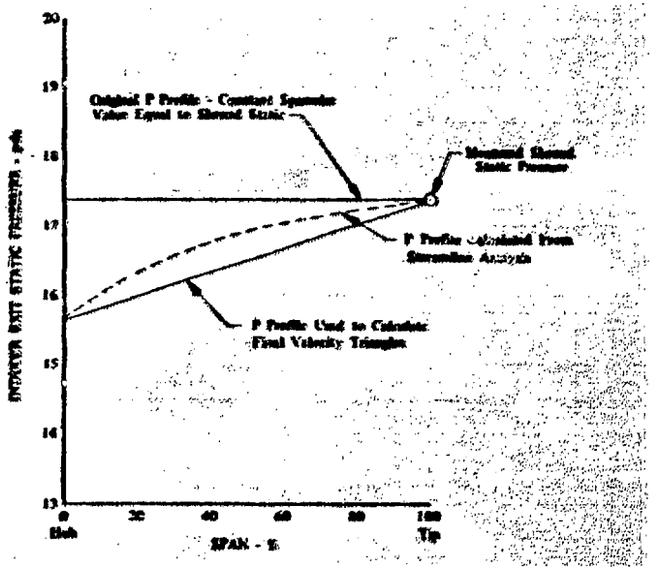

Figure 78. Inducer Exit Static Pressure Profile, 100% Speed, 10-deg IGV.

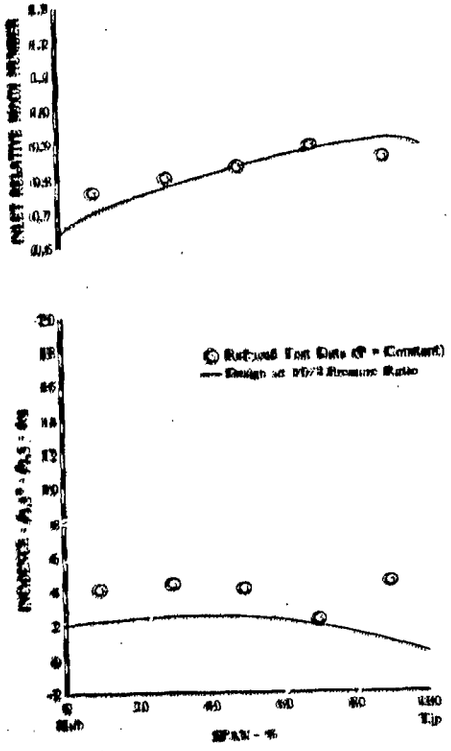

Figure 79. Impeller Inlet Conditions, 100% Speed, 10-deg IGV.

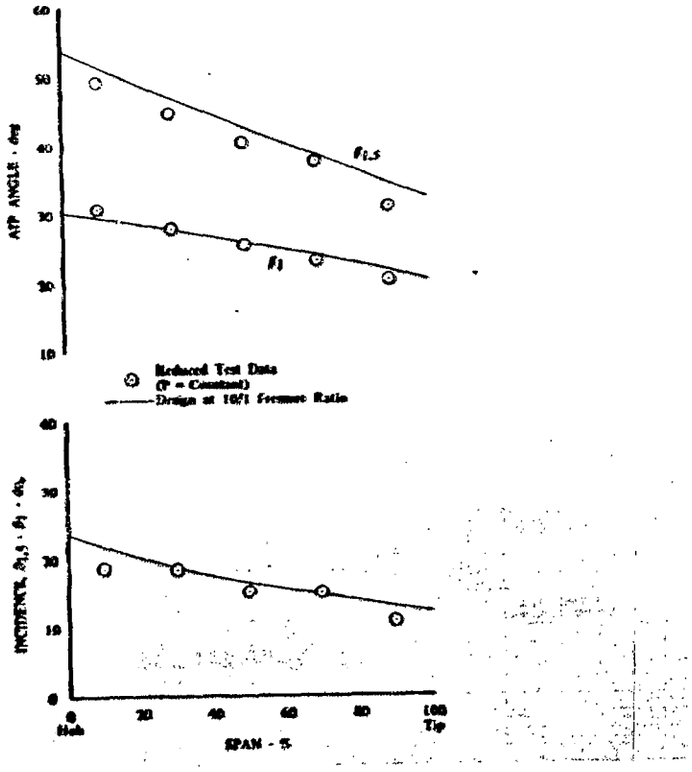

Figure 80. Inducer Exit Air Angle Profile, 100% Speed, 10-deg IGV.

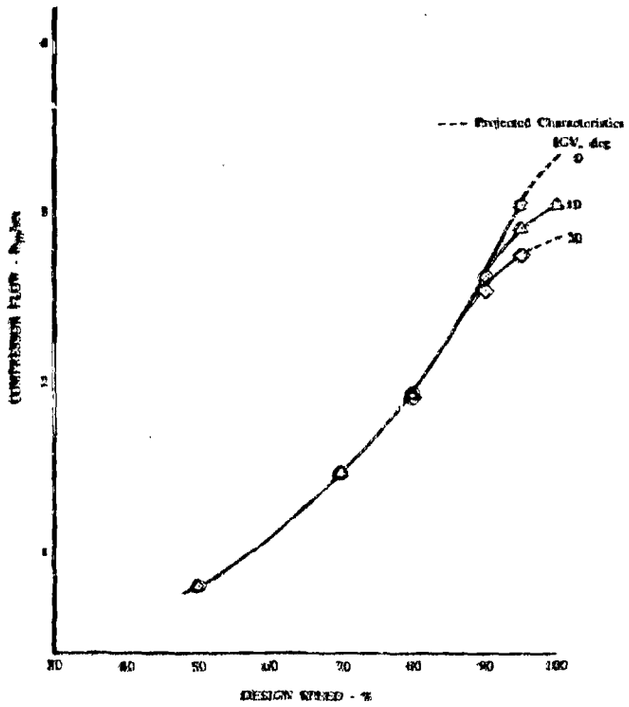

Figure 81. Choke Point Flow as a Function of Rotor Speed, Build No. 3.

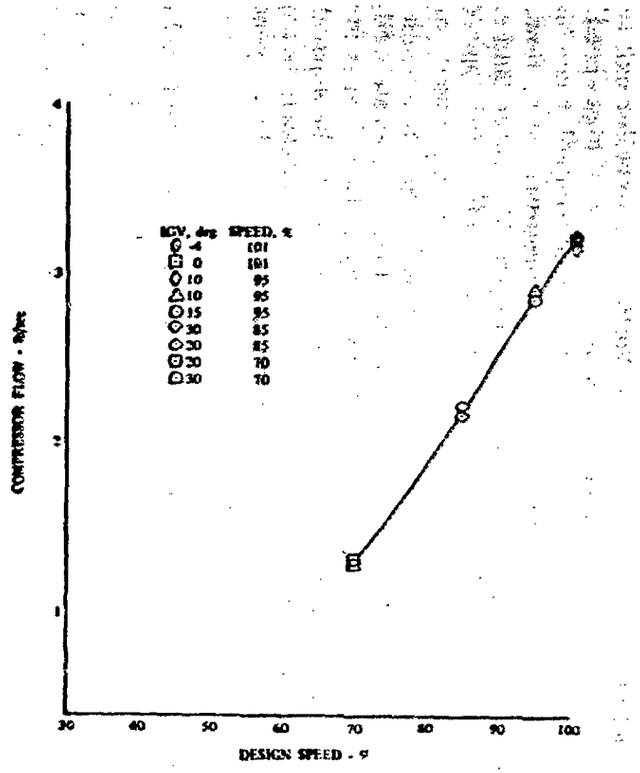

Figure 82. Build No. 6 Choke Point Flow as a Function of Rotor Speed.

Impeller

Impeller performance was well defined from a combination of Builds No. 3 and 6 data. Low-speed definition was available from Build No. 3 impeller exit traverses, and Build No. 6 impeller exit traverses defined its operation at high speed. An internal flow analysis was also used to analyze the inducer-impeller combination and was available for every data point. The impeller pressure ratio, flow, and efficiency data from Build No. 6 are presented in Figure 83. These data showed that the impeller produced its design pressure ratio at an efficiency approximately 5 percentage points higher than its design goal and at a flow rate slightly higher than design. The consistent high efficiency of the impeller and the smooth pressure rise characteristic showed that the impeller continued to operate well, even when its inlet conditions were being affected by the large inducer losses at high speed. This good high-speed performance was due, in part, to the separate inducer-impeller concept as the impeller performance demonstrated its capability to work efficiently at conditions that would have severely affected a conventionally designed impeller with an integral inducer.

The tabulated data for the impeller performance can be found on the impeller traverse printouts in Appendix I. Since insufficient data were obtained to properly separate the impeller and inducer performance generated in Build No. 3, the combined performance is shown in Figure 84 with comparative Build No. 6 results. The Build No. 6 inducer-impeller pressure ratio was slightly higher than that of Build No. 3, possibly due in part to the Build No. 6 impeller having a 0.020-in. larger diameter.

Build No. 3 inducer and impeller performances from an internal flow analysis program are shown in Figure 85. Similar Build No. 6 inducer and impeller performance are shown in Figure 86.

Inducer and impeller efficiency as a function of incidence was also generated by the internal performance analysis and is presented in Figure 87 for Build No. 3 data and in Figure 88 for Build No. 6 data. A limited amount of data that were obtained in Build No. 2 with an undersized diffuser is also presented in Figure 87 for comparative purposes. The lower efficiency was due to the inducer operating in a stalled condition. Low-speed characteristics are essentially identical for Builds No. 3 and 6. The inducer-impeller was operating on the stalled side of its performance characteristic and efficiency decreased with increasing incidence. It appeared from the Build No. 3 characteristics, that the inducer-impeller and diffuser were matched at 95% speed, and at 100% speed and 10-deg prewhirl, the match may be on the negative or choke side of the incidence characteristics. Build No. 6 data could be interpreted similarly if only 10-deg IGV setting data were obtained at 100% speed; however, other 101% speed data at different prewhirls behaved in a manner no different than that observed at lower speeds. Build No. 6 data at 95% speed also failed to exhibit the peaking effect demonstrated in Build No. 3, hence it is probable that Build No. 6 operated at slightly positive (stall) incidence at 95 to 101% speeds.

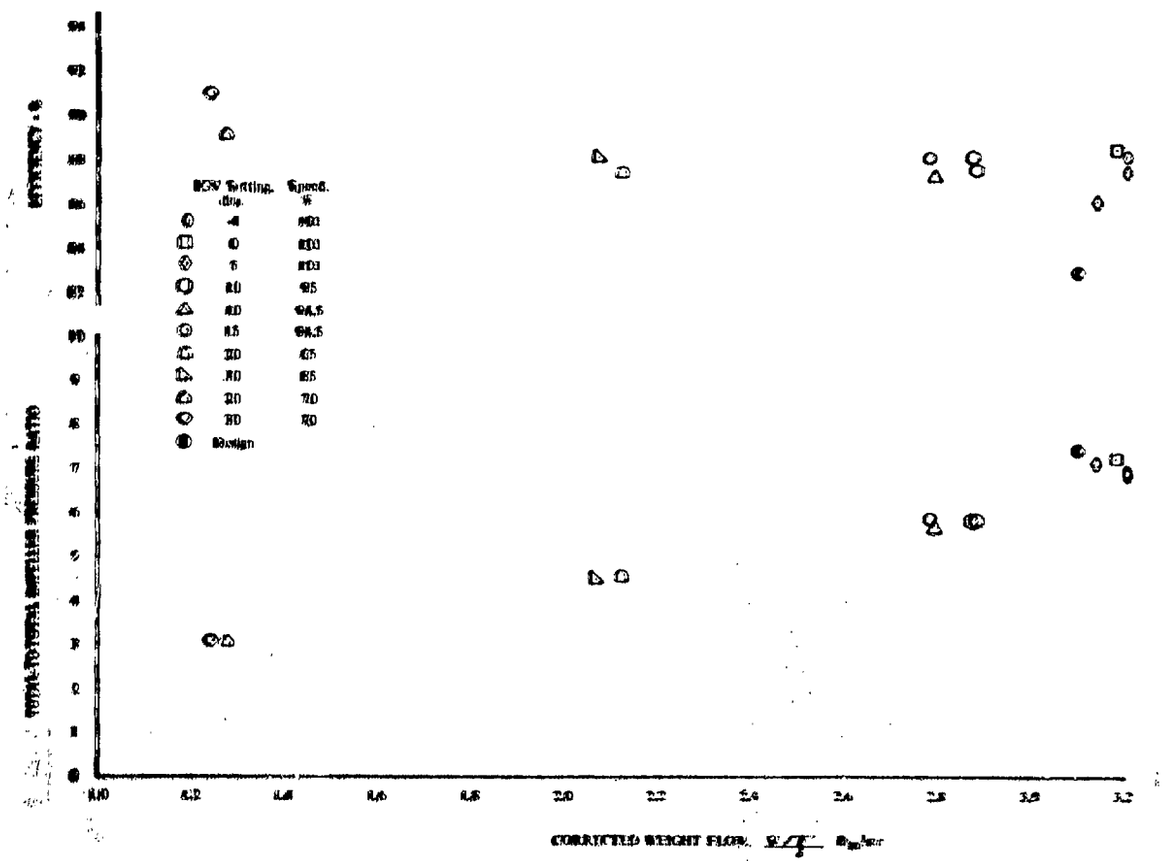

Figure 83. Build No. 6 Impeller Performance Derived From Traverse Data.

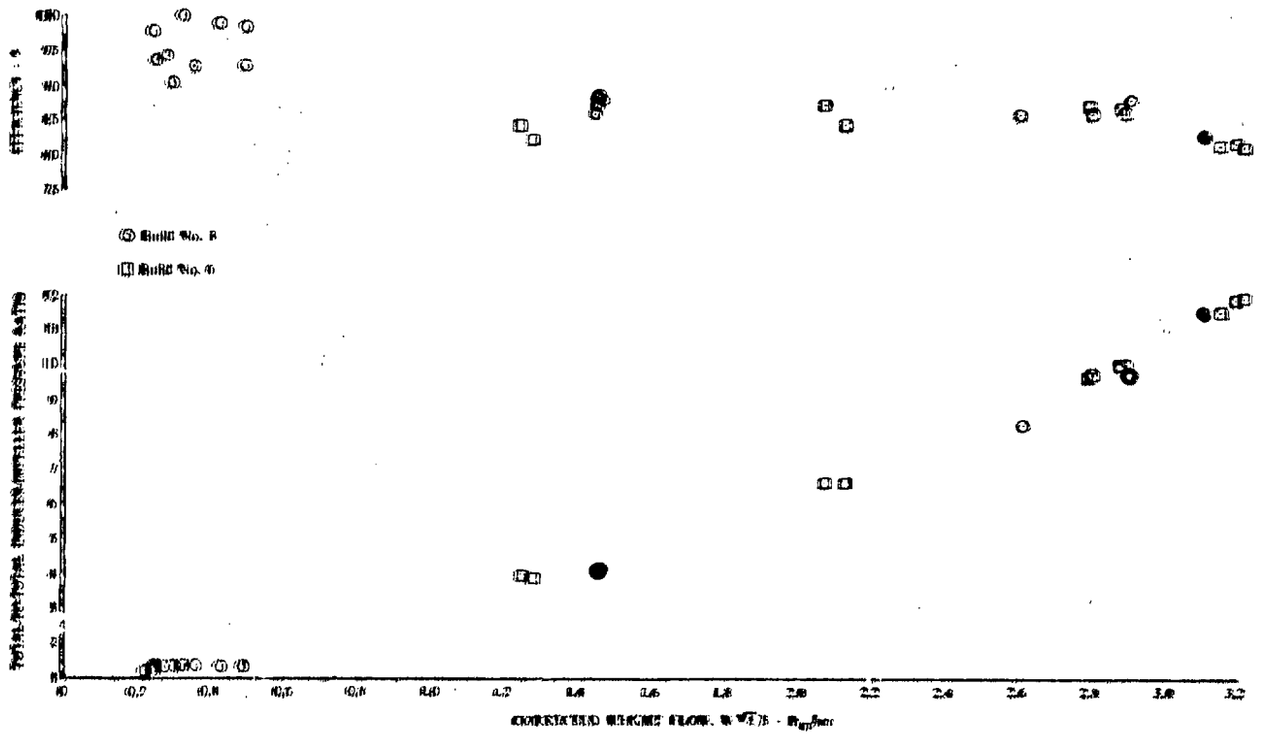

Figure 64. Inducer-Impeller Performance Derived From Traverse Data.

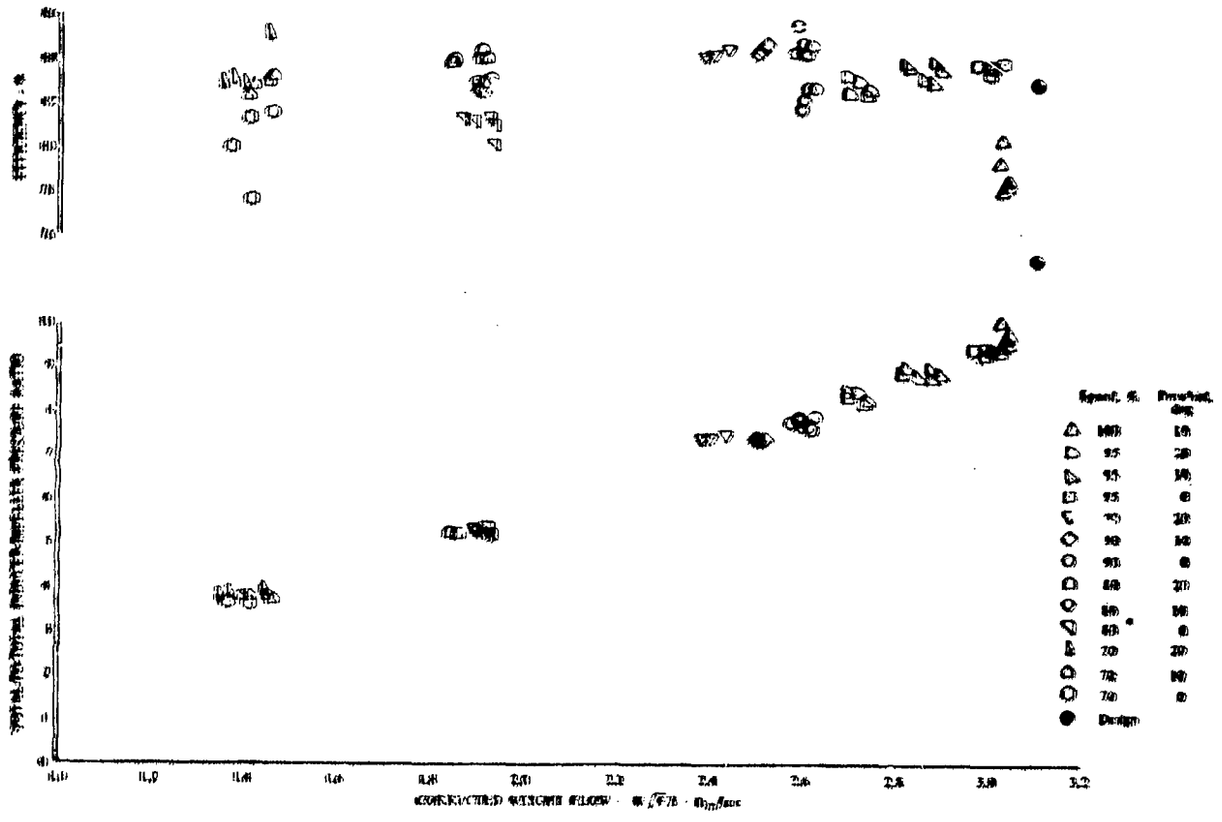

Figure 65. Build No. 3 Impeller Performance Map Derived From Internal Flow Analysis.

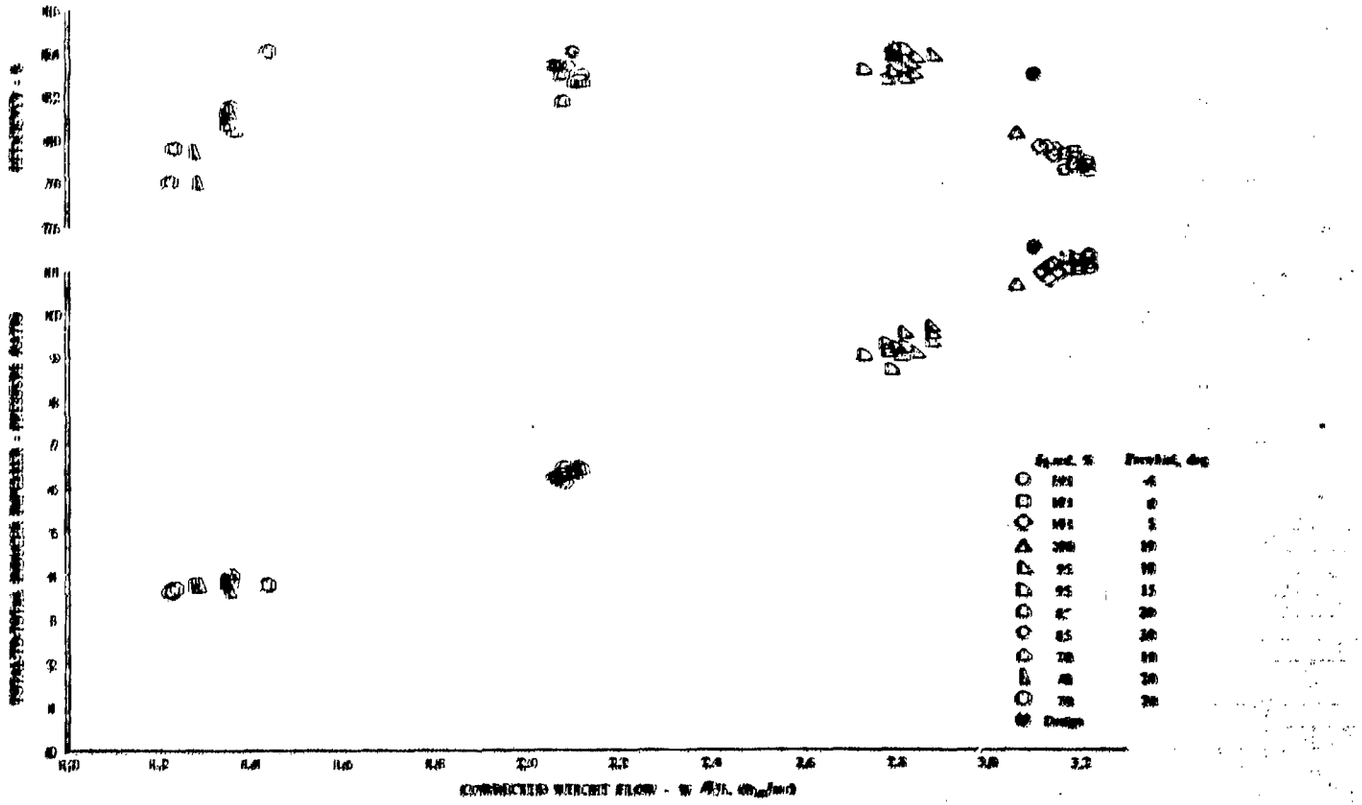

Figure 66. Build No. 6 Inducer-Impeller Performance Map Derived From Internal Analysis.

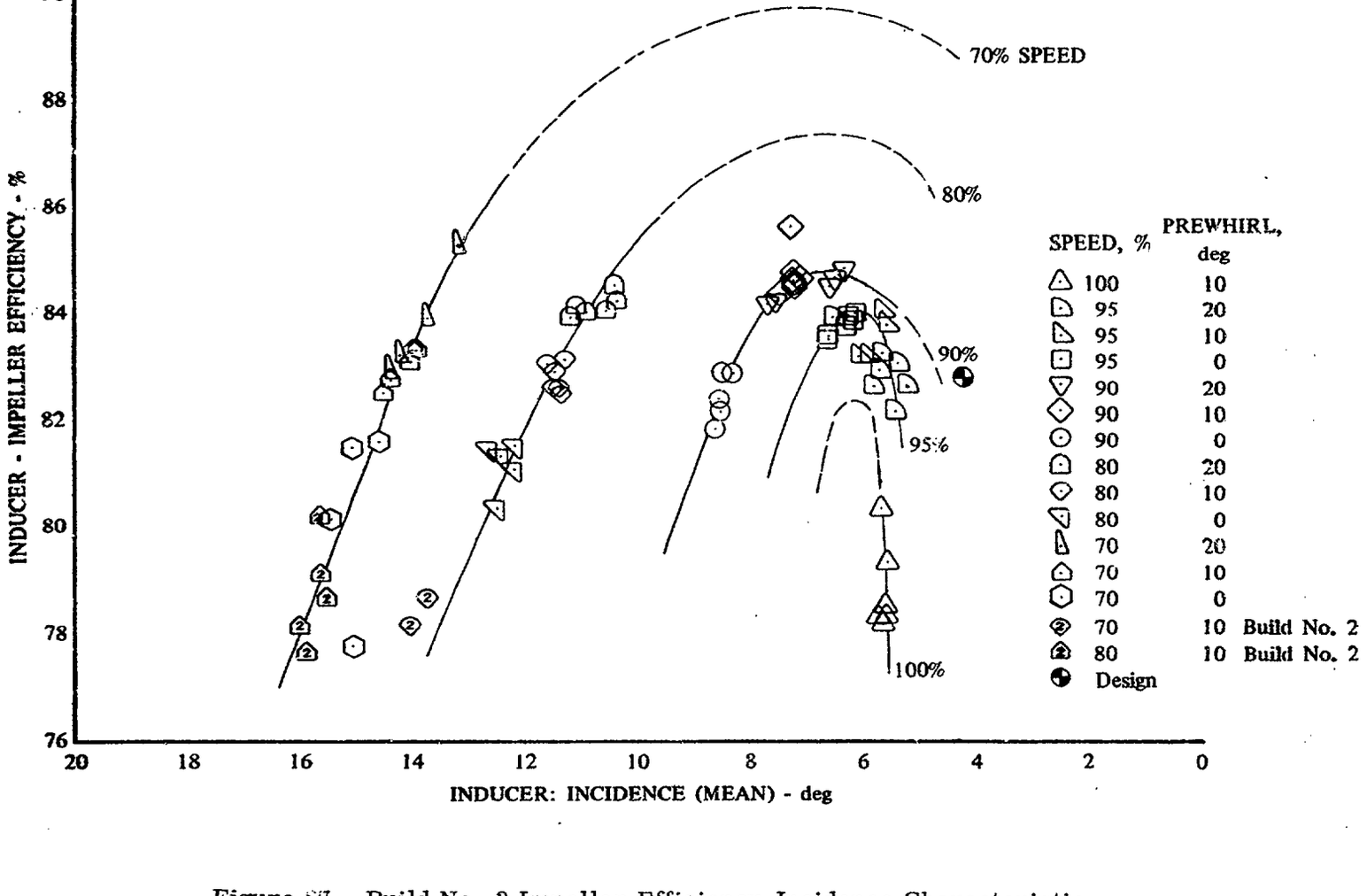

Figure 87. Build No. 3 Impeller Efficiency-Incidence Characteristic.

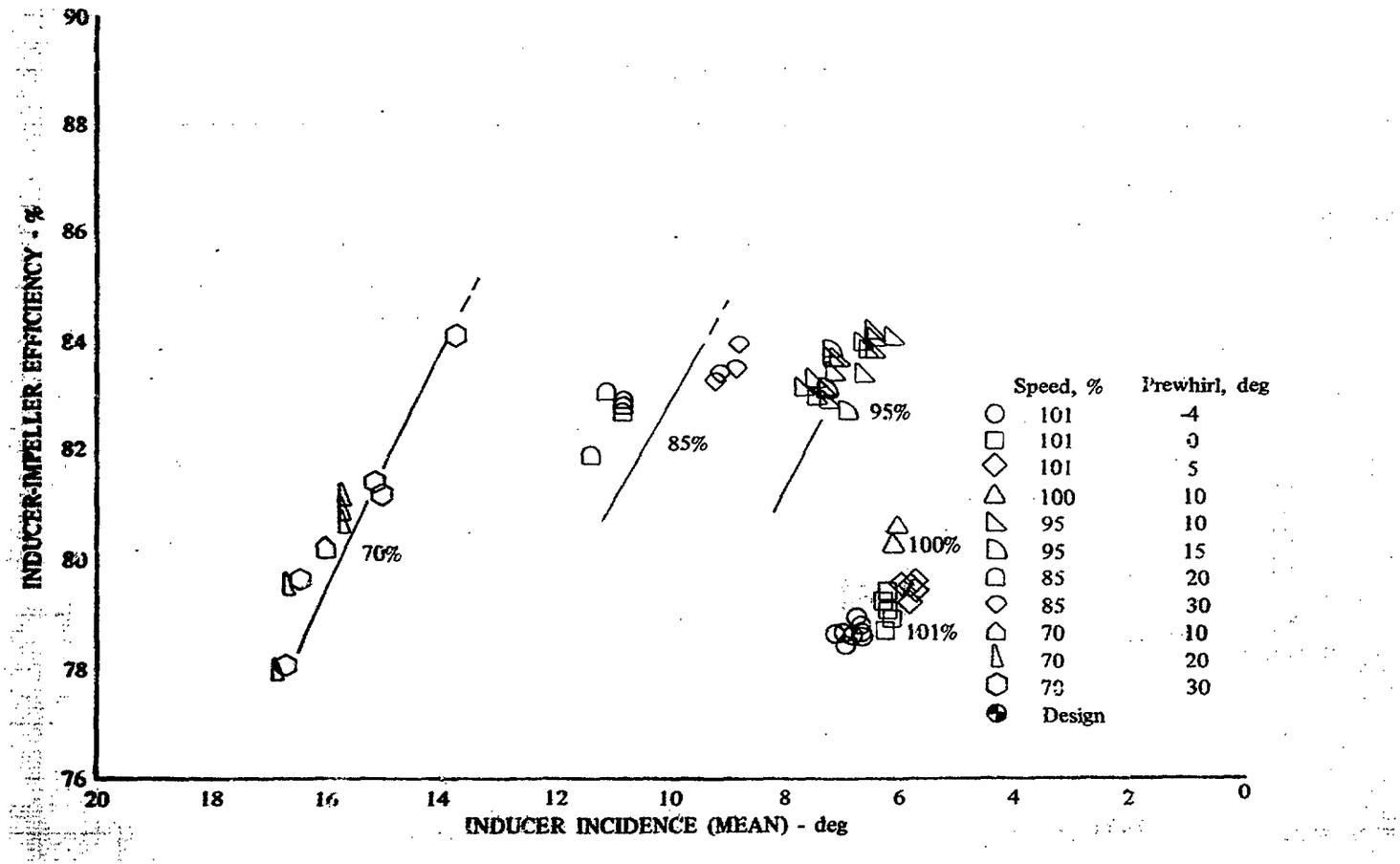

Figure 88. Build No. 6 Inducer-Impeller Efficiency-Incidence Characteristic.

The internal performance analysis was also used to demonstrate the effect of prewhirl on inducer-impeller performance, as shown in Figure 89 at 101% speed. The increase in efficiency with prewhirl was due to reduced shock losses as the inlet relative Mach number was lowered, and also due to reduced profile losses as the incidence was improved. The 100% speed Build No. 3 data showed nearly the same incidence and efficiency.

Comparison of the two builds at 95% speed is shown in Figure 90. The Build No. 6 inducer-impeller was operating at a more positive incidence most probably because of the reduced airflow at this speed caused by the smaller effective diffuser throat area in the damaged Build No. 6 diffuser.

Slip factor calculated at the impeller tip (discharge) from traverse data of Builds No. 3 and 6 is presented as a function of corrected flow rate in Figure 91. The general trend of both data sets was similar and the level at near design was also similar. Low-speed data exhibit an indication of higher slip factors for the Build No. 6 testing. Impeller exit discharge coefficients calculated by using impeller exit mass average data to generate weight flow which is compared to orifice flow are presented for the same data in Figure 92. These discharge coefficients were used to generate input for the internal flow analysis for both builds. While levels varied from build to build, both exhibited the trend of high blockage at low speed, which decreased with an increase in speed and flowed to a low blockage value at flow rates corresponding to 90 to 95%. Higher speed and flow conditions again showed a considerable increase in blockage.

Impeller exit traverse data summaries for every traverse point from Builds No. 3 and 6 are presented in Appendix I. An example of these data are presented in Figure 93 for 101% speed and -4 deg of prewhirl. Examples of impeller exit traverse data for 95% speed 10-deg prewhirl from Builds No. 3 and 6 are shown in Figures 94 and 95, respectively. Impeller exit total pressure data indicated a larger boundary layer development on the shroud side than on the hub. The air angles shifted toward tangential on both hub and shroud sides, corresponding roughly to areas of falloff in total pressure. Normalized distributions of radial velocity for Build No. 6 101% speed, -4-deg prewhirl and Builds No. 3 and 6 at 95% speed are shown in Figures 96 through 98, respectively. Builds No. 3 and 6 show essentially the same characteristic as the higher speed Build No. 6 data. Generally, velocity was less than design on the shroud side, with a peak greater than design near the hub.

Temperature traverses were also obtained behind the impeller. All of the temperature traverse data are presented in Appendix I. These data were input into the traverse reduction deck and a mass average temperature was calculated. This temperature was considerably different from the average temperature measured in the exhaust collector; for example, at 101% speed and 0-deg prewhirl, the average impeller exit temperature was 40-deg hotter than the collector. Since the impeller exit temperature was measured with a one-of-a-kind experimental thermocouple and since the resultant data differed not only in level from the average collector temperature but also in profile characteristics from the checkout of this probe during a previous test, the data were considered faulty.

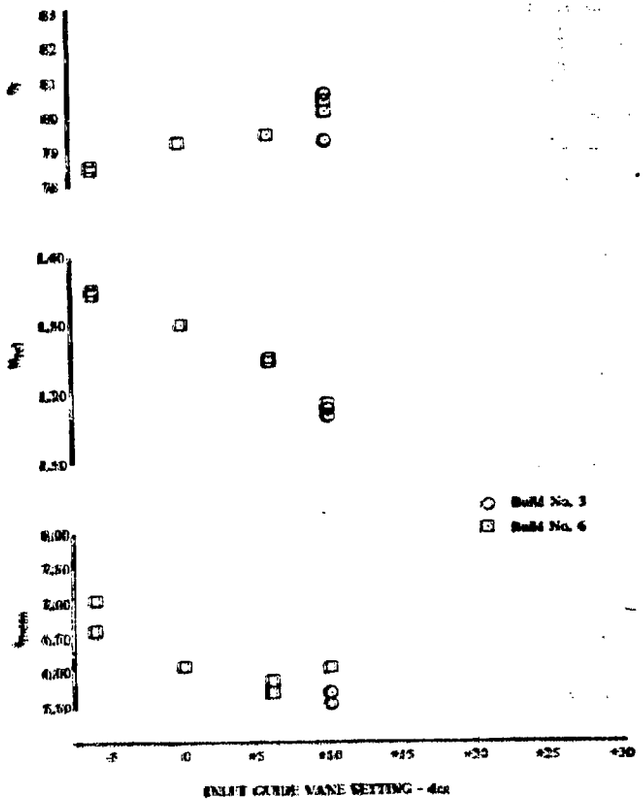

Figure 89. Effect of Prewhirl on Inducer-Impeller Performance Near 10:1 Pressure Ratio.

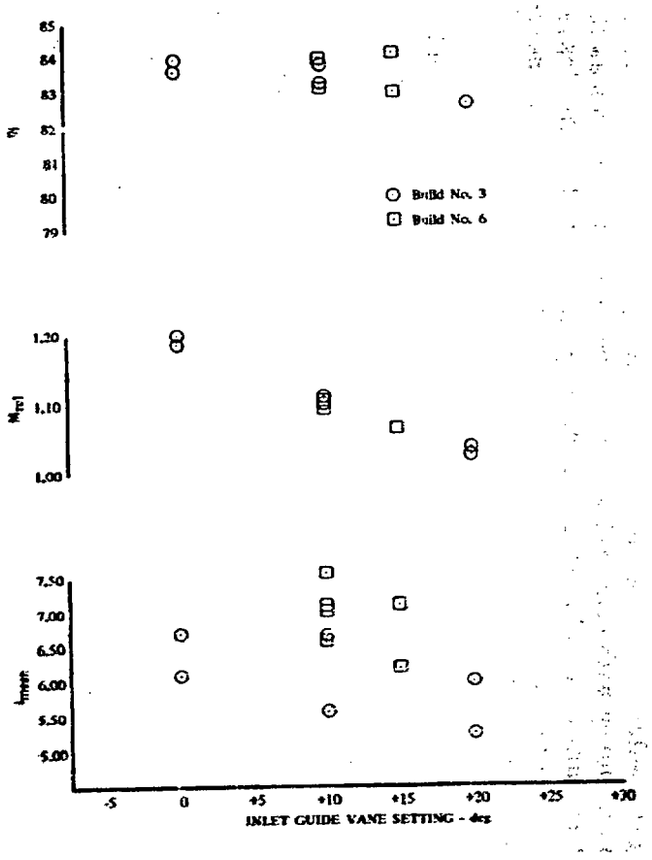

Figure 90. Effect of Prewhirl on Inducer-Impeller Performance Near 8:1 Pressure Ratio.

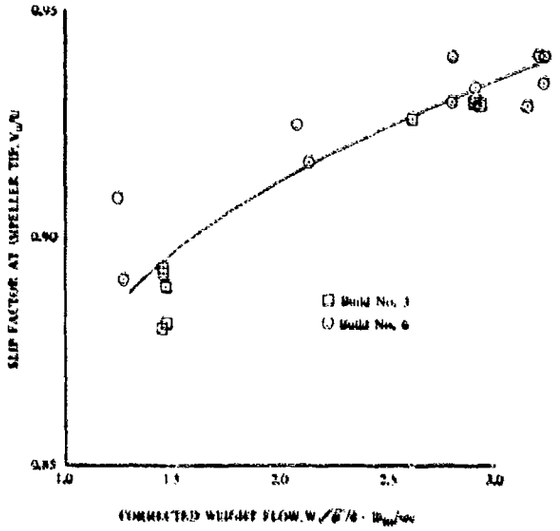

Figure 91. Impeller Exit Slip Factor.

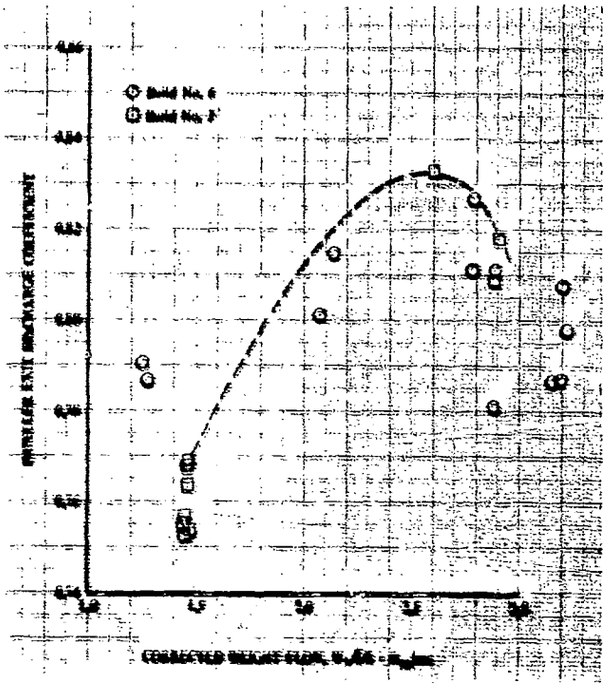

Figure 92. Impeller Exit Discharge Coefficient.

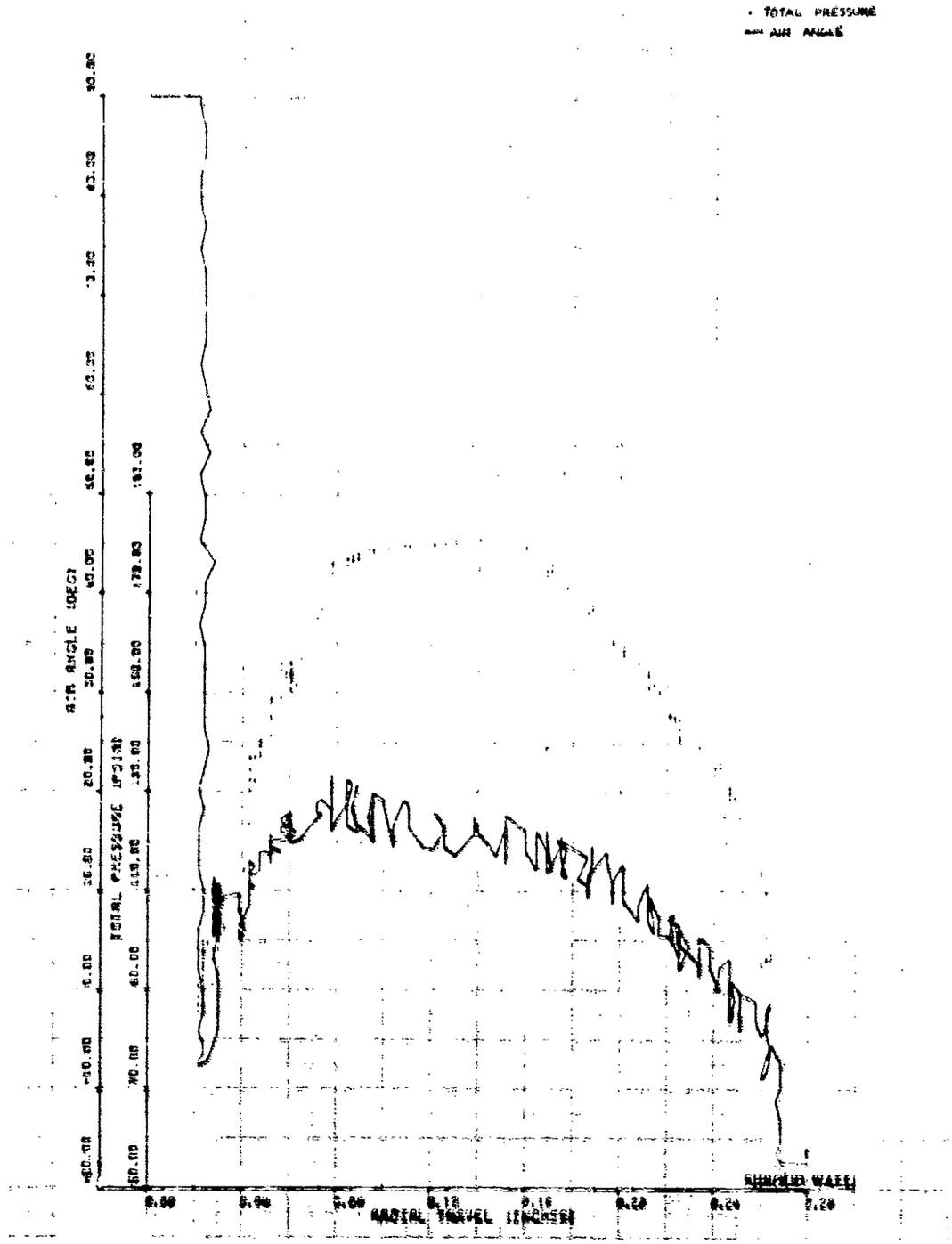

Figure 93. Impeller Exit Traverse, Build No. 6, 101% Speed, -4-deg IGV, Near Stall.

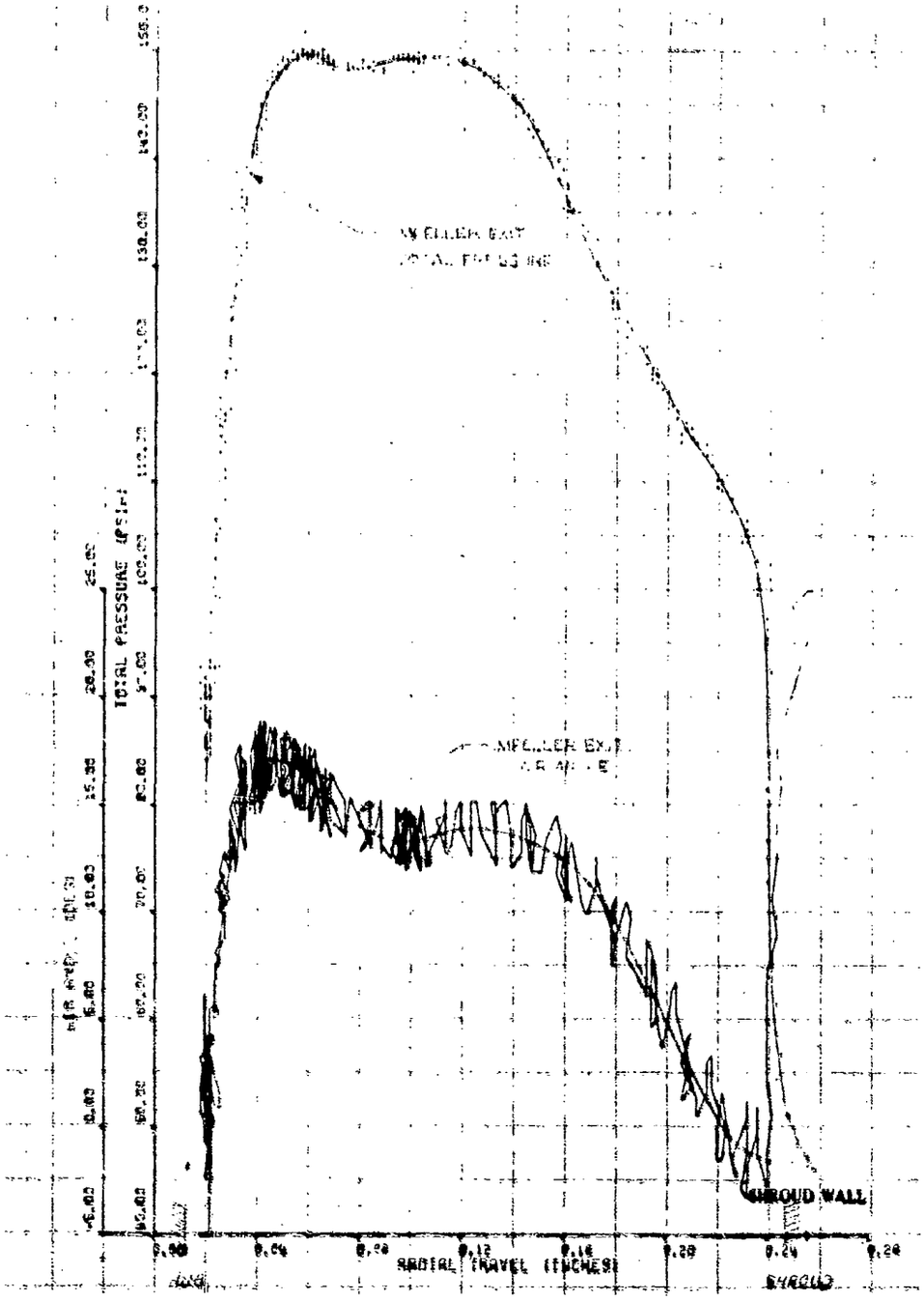

Figure 94. Impeller Exit Traverse, Build No. 3, 95% Speed, 10-deg IGV, Near Stall.

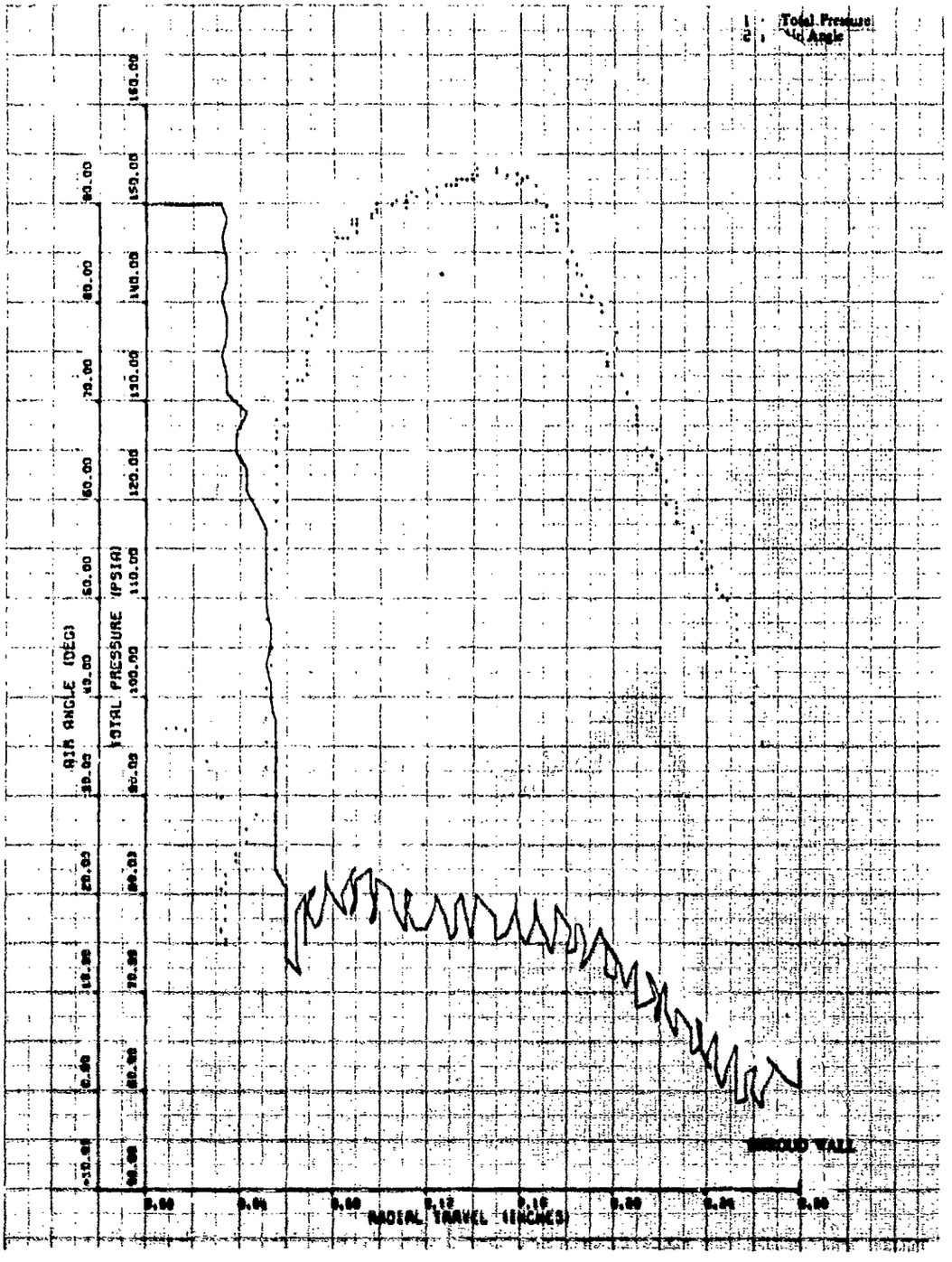

Figure 95. Impeller Exit Traverse, Build No. 6, 95% Speed, 10-deg IGV, Near Stall.

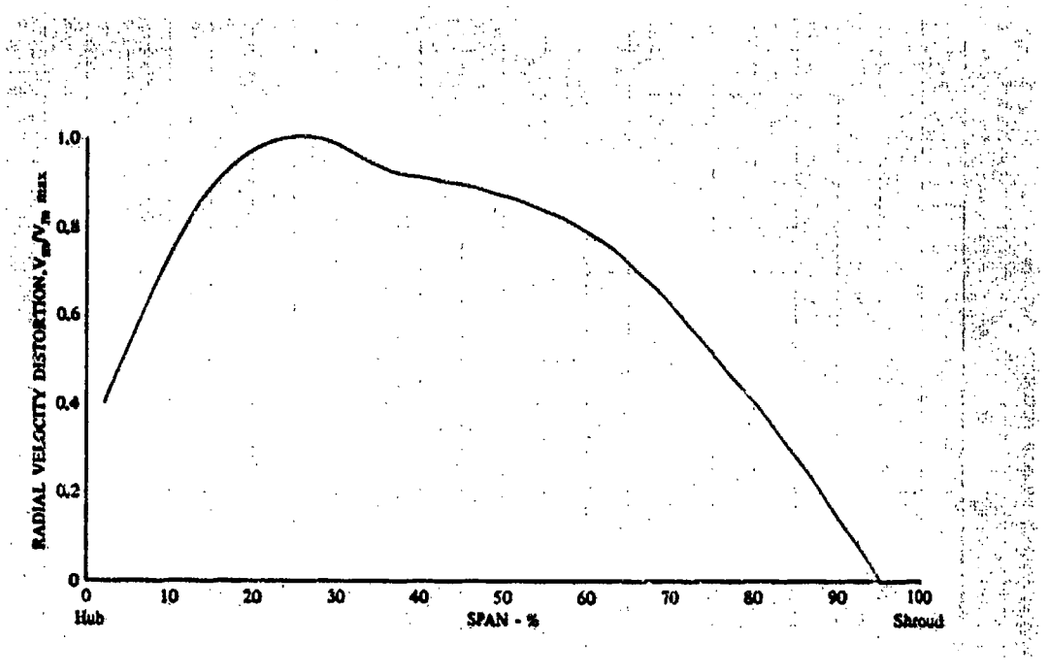

Figure 96. Normalized Radial Velocity Distribution, Build No. 6, 101% Speed, -4-deg IGV.

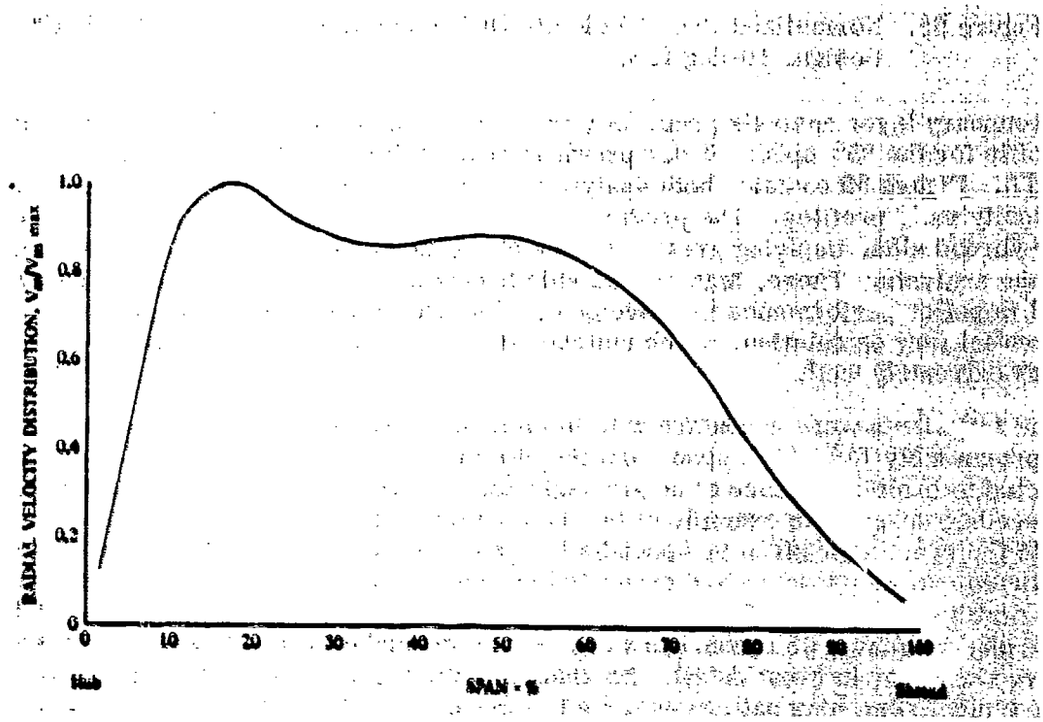

Figure 97. Normalized Radial Velocity Distribution, Build No. 3, 95% Speed, 10-deg IGV.

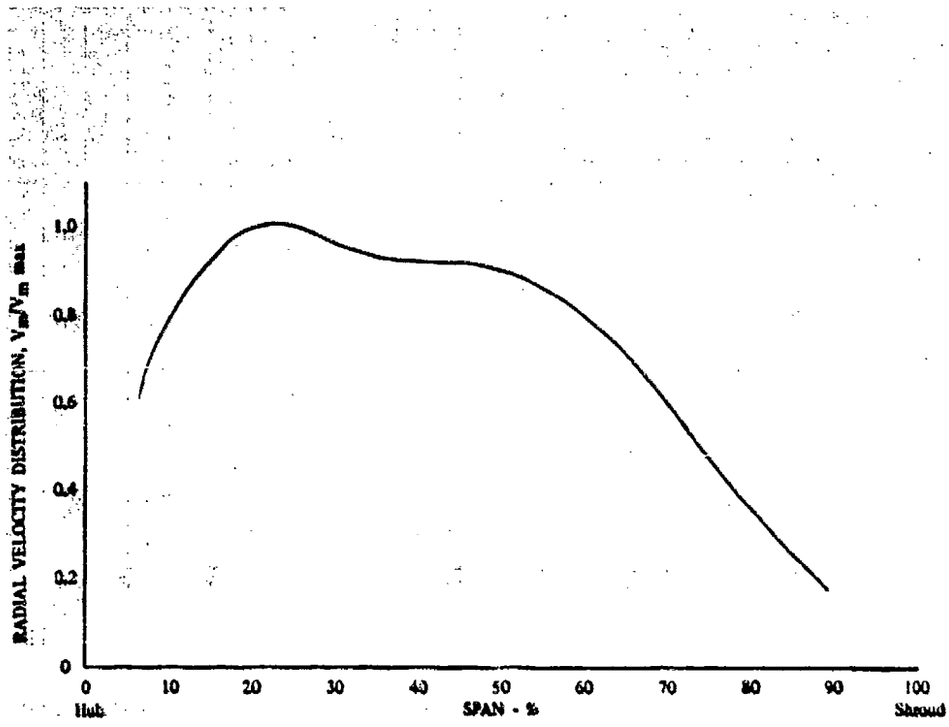

Figure 98. Normalized Radial Velocity Distribution, Build No. 6, 95% $N/\sqrt{\theta}$ Design, 10-deg IGV.

A boundary layer analysis program was used to predict the impeller exit velocity profile for the 95% speed 10-deg prewhirl near stall points for both Builds No. 3 and 6. Figure 99 contains both analytical predictions and experimentally obtained velocity ratio profiles. The predicted boundary layer thickness was too small on the shroud side, implying greater losses along the shroud wall than were assumed in the analysis. There, high shroud side losses also pointed to an area for potential impeller performance improvement. The predictions allowed an accurate potential flow calculation, which matched the experimental profile from 20 to 60% span extremely well.

Stall transients were conducted with the impeller exit traverse probe positioned at approximately 15% of the span from the shroud wall. These transients were expected to exhibit evidence of an air angle shift toward tangential flow immediately preceding surge. An example of the data obtained is presented in Figure 100, with the remainder given in Appendix I. Impeller exit total pressure, angle, and collector static pressure are presented vs time. A tabulation of speed and flow vs time is also given. Data from two different transients at scanning rates of 1 and approximately 65 scans/sec were used to describe overall trends and to show surge behavior in great detail. No change in air angle could be determined from the typical searching pattern observed in these data. In nearly every case, there was a drop in impeller exit total pressure accompanied by an increase in speed

and a slight decrease in weight flow before surge. Collector static pressure continued to rise even though the impeller exit total pressure decreased, which indicated either a shift in the impeller exit profile causing a pressure decrease at 15% span or that the diffusion efficiency increased faster than the rate of impeller exit pressure decrease.

Static pressure information was recorded along the shroud wall for every steady-state data point. Figure 101 shows Builds No. 3, 6, and design data for the 95% speed, 10-deg IGV setting condition. The trend of static pressure showed no significant change from build to build. True evaluation of the significance of these profiles was difficult since it was not possible to separate the contribution due to impeller work and diffusion; however, no obvious discontinuity showing areas of separation was visible. Most of the static pressure rise occurred after the transition from axial to radial flow, with some decrease in the magnitude of pressure rise near the exit of the impeller.

The five static pressure taps near the exit were located in such a way as to allow determination of the effect of diffuser pipes on the static pressure distribution in the impeller. No effect was seen, most likely due to the large vaneless space. Other examples of this static pressure distribution are presented in Appendix I. All show the same trends as the examples. The distribution and level do not change from near stall to wide open discharge; however, at a constant speed the level of static pressure is highest for the inlet guide vane setting that allows the impeller to do the most work.

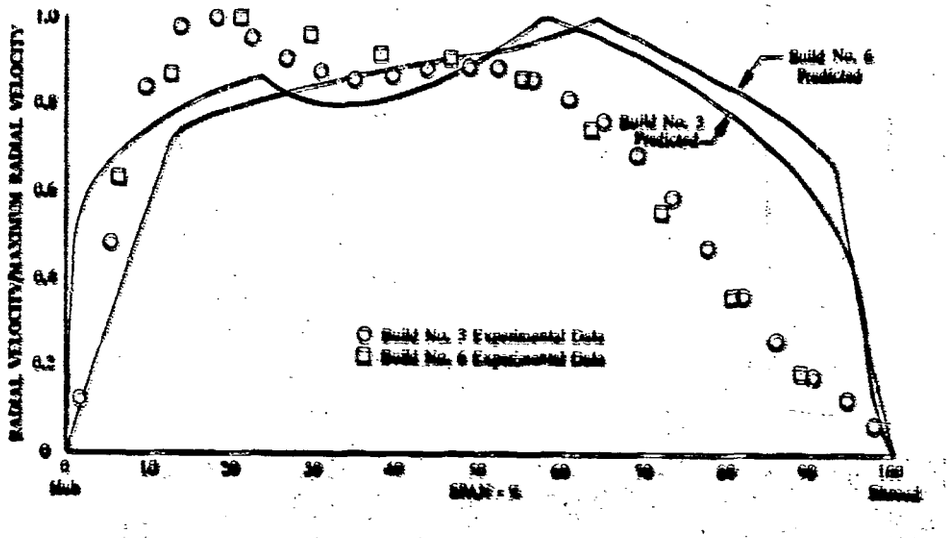

Figure 99. Discharge Velocity Ratio Comparisons.

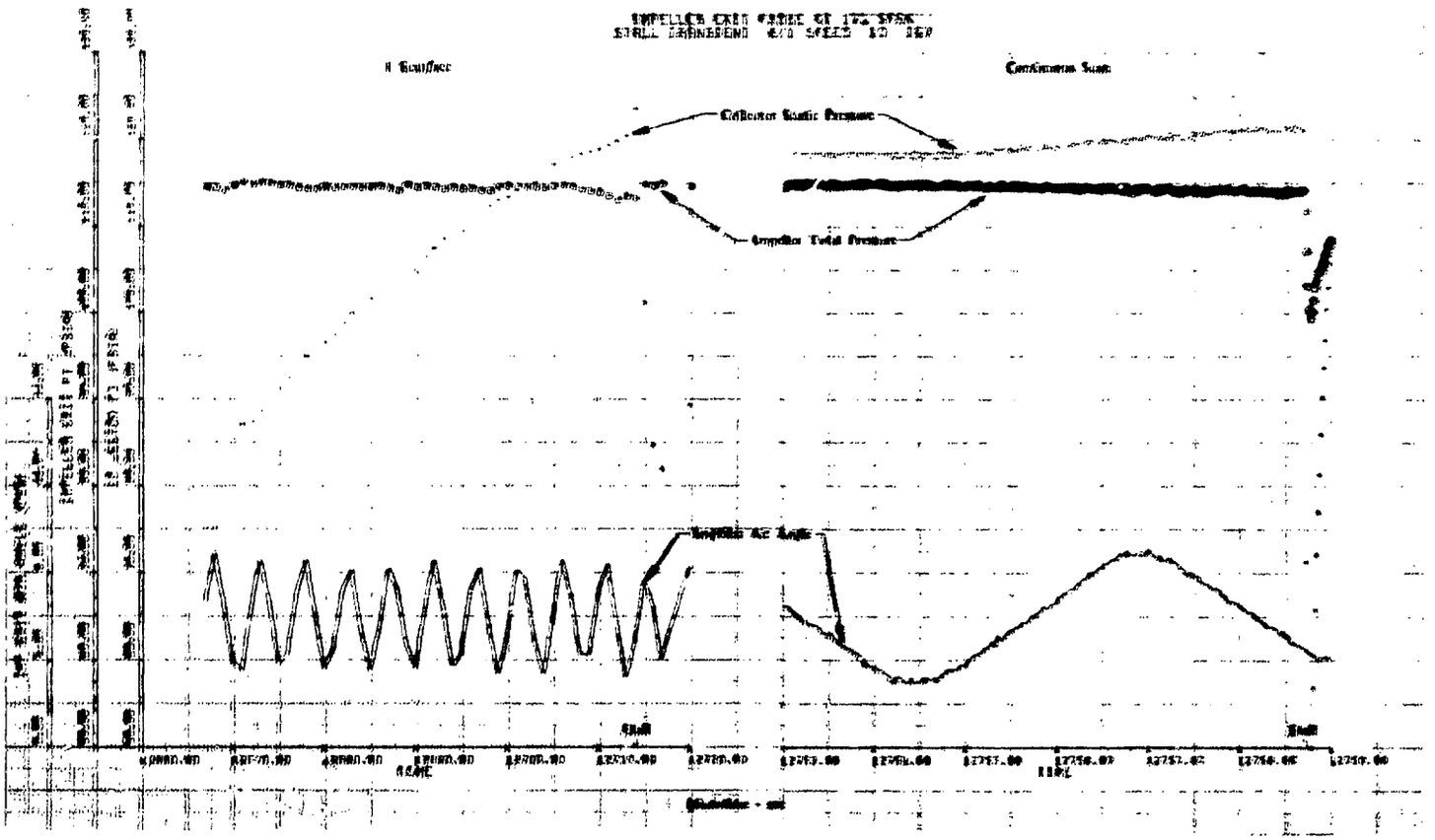

Figure 100. Stall Transient Data at 1 Scan/sec and Continuous Scan.

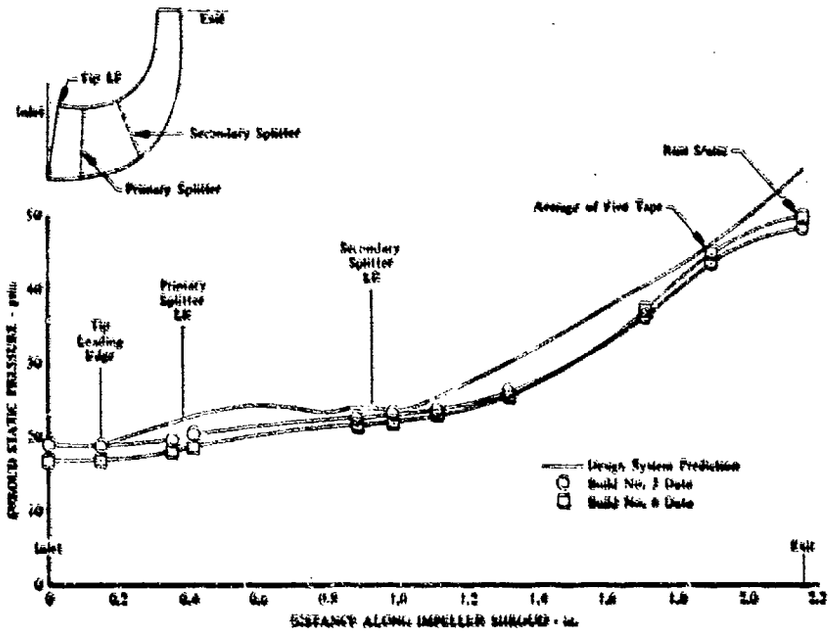

Figure 101. Static Pressure Variation Along Impeller Shroud, 95% Speed, Near Stall, 10-deg IGV.

Diffuser Performance

Diffuser performance evaluation, including an evaluation of the diffusion process and an assessment of the total pressure losses incurred during the diffusion process, will be presented in the form of static pressure distributions throughout the diffuser, total pressure profiles at the diffuser exit, and various loss correlations. Since the diffuser was damaged prior to the Build No. 6 performance testing, the discussion will include the Build No. 3 diffuser performance, the nature of the damage to the diffuser, and the resulting performance losses seen in Build No. 6. All diffuser performance data are available from tabulations of performance in Appendix I.

Build No. 3 static pressure distributions along the length of the diffuser pipes on the shroud side are shown at near stall and at minimum back pressure for 95% speed and 10-deg IGV and at near stall for 100% speed and 10-deg IGV in Figures 102 and 103. The strong normal shock, located approximately 1 in. from the diffuser exit at minimum back pressure, moves upstream of the throat to slightly strengthen the inlet shock in that region at near stall as is shown in Figure 102. The near stall static pressure distribution plots at 95 and 100% speed in Figures 102 and 103 show that the effective throat (i.e., where the diffusion process begins) is located approximately 0.230-in. upstream of the geometric throat. The region between the tangency point and the effective throat is essentially a region for flow adjustment and alignment and is marked by shock wave-boundary-layer interactions and areas of flow acceleration so that there is little if any diffusion. Figure 104 presents the static pressure distributions on the hub and shroud walls across one diffuser gap at the tangency radius for several points and

illustrates the complex nature of the flow in this region. This is also evident in the diffuser shroud side isobar map in Figure 105. The representations shown in Figures 104 and 105 are composites generated from static pressure information from several locations and may, therefore, contain scatter as a result of pipe-to-pipe variation. Downstream of the effective throat, where essentially all the diffusion takes place, no evidence of separation is noted. The circumferential static pressure distribution at the geometric throat, as shown in Figure 106 for 95% speed and 10-deg IGV, is fairly uniform especially near stall.

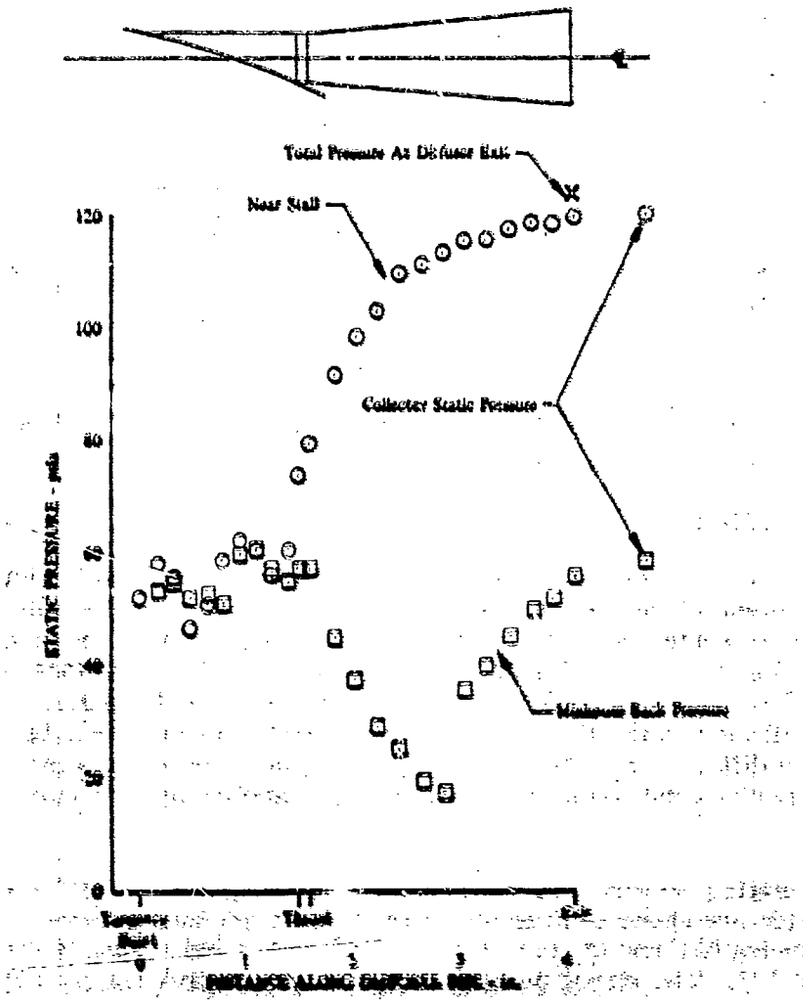

Figure 102. Diffuser Static Pressure Profile: Build No. 3, 95% Speed, 10-deg IGV.

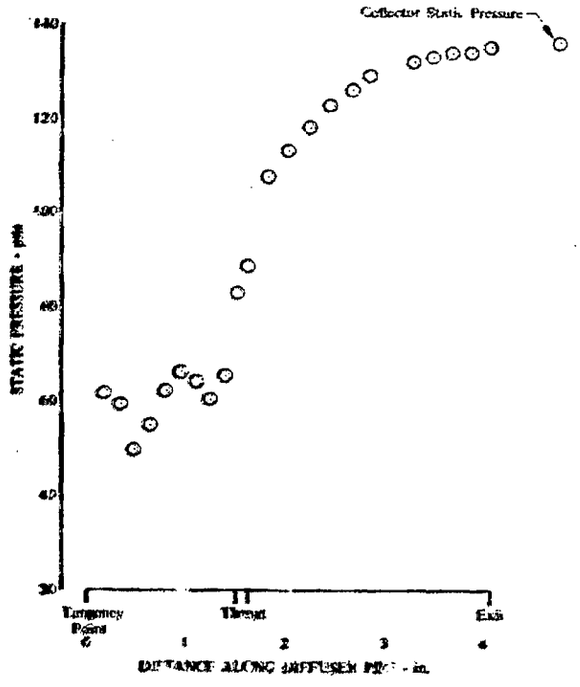

Figure 103. Diffuser Static Pressure Profile: Build No. 3, 100% Speed, 10-deg IGV, Near Stall.

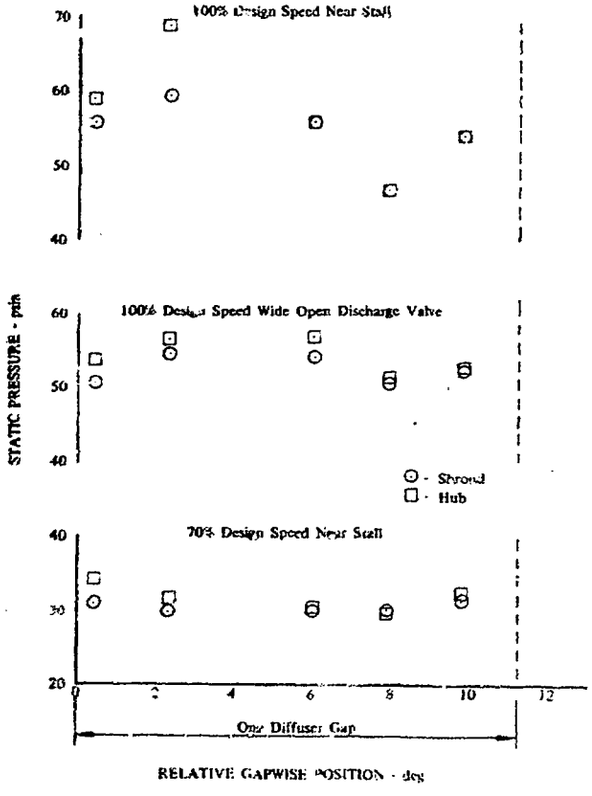

Figure 104. Diffuser Gapwise Static Pressure Distributions Along the Tangency Radius: Build No. 3, 10-deg IGV Setting.

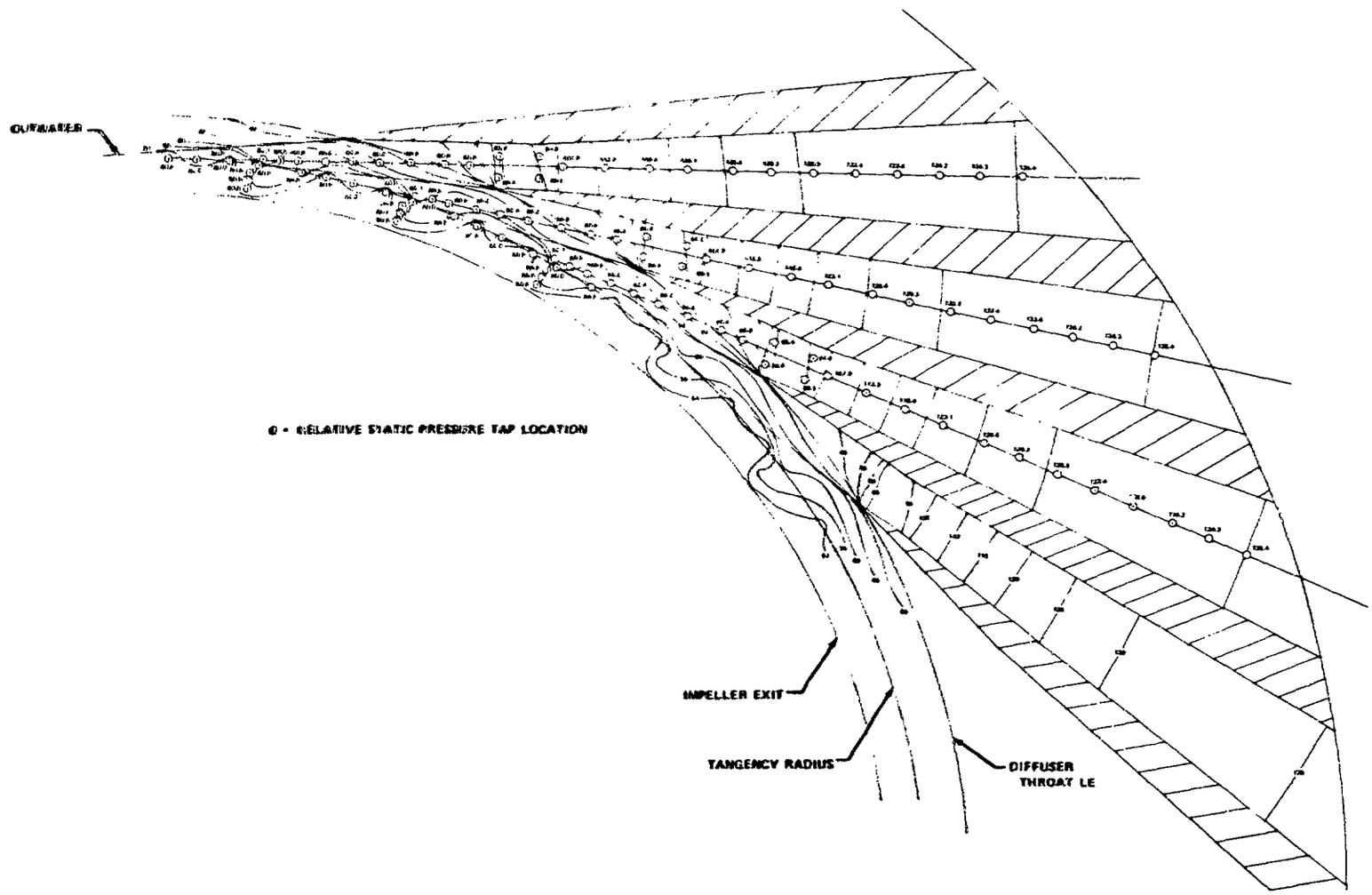

Figure 165. Diffuser Shroud Static Pressure Contours: Build No. 3, 100% Speed, 10-deg IGV.

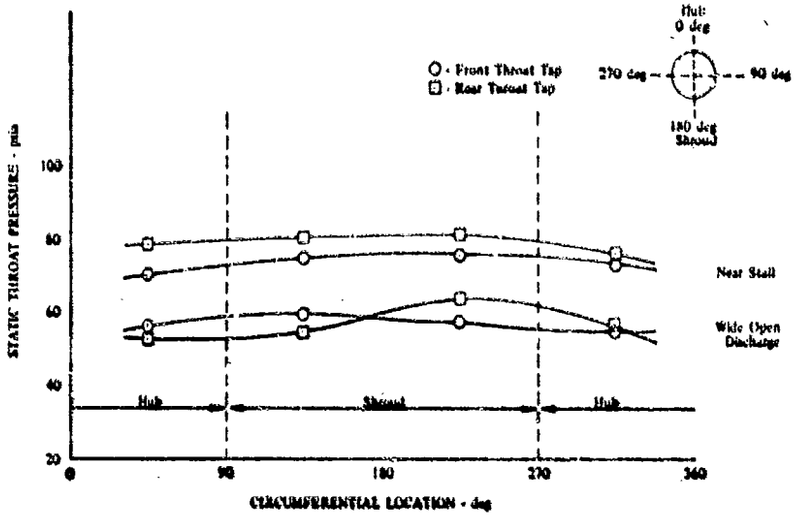

Figure 106. Diffuser Throat Static Pressure Distribution: Build No. 3, 95% Speed, 10-deg IGV.

During Build No. 4 testing (mechanical checkout of redesigned rig bearing and rotor system), a rub occurred between the impeller and the stationary shroud, spewing pieces of the shroud silver plating through the diffuser and causing damage to the diffuser pipe throat leading edges. Photographs of this damage from several typical pipes are shown in Figure 107. For comparison, a photograph of an undamaged diffuser pipe is shown in Figure 108. Prior to the Build No. 6 performance tests, all the diffuser pipes were polished to remove any burrs extending into the flow path along the damaged throat leading edges. One diffuser pipe found to be slightly oversized was nickel plated to the same size as the rest of the pipes. At the completion of the Build No. 6 testing during the rig teardown, it was discovered that a considerable amount of rust had formed in the diffuser pipes, as is shown in Figure 109. This rust probably also contributed to the loss in performance noted in Build No. 6, although it is impossible to predict the degree to which the diffuser pipes were rusted at any given point in the test program. The diffuser material, 410 Stainless Steel, was chosen because its thermal expansion closely matched that of the titanium impeller; however, it appears that for aerodynamic reasons a corrosion-resistant material would be better.

The effects of the damaged diffuser can be seen in the Build No. 6 static pressure distribution plots for 95 and 100% speeds and 10-deg IGV in Figures 110 and 111. The effective throat region has moved downstream from its Build No. 3 location and nearly coincides with the geometric throat. Also, regions of flow separation are now evident in some of the pipes toward the diffuser exit. The individual points shown on the plots are not necessarily from the same diffuser pipe, so the inconsistent nature of the static pressure data near the diffuser exit indicates

varying amounts of separation from pipe to pipe for those pipes in which separation does occur. Figure 112 shows Build No. 6 static pressure distributions for 101% speed and -4-deg IGV at both near stall and minimum back pressure.

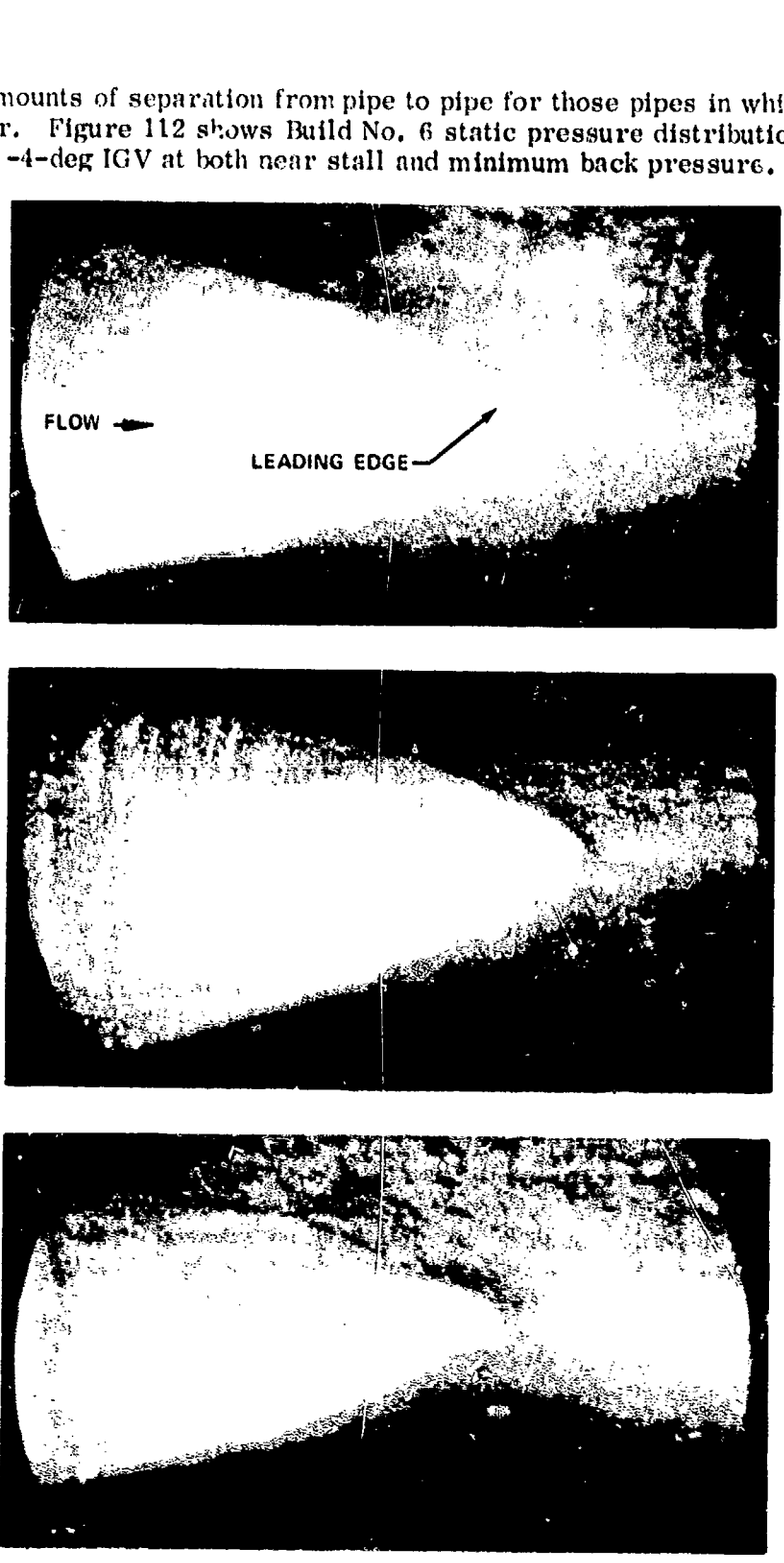

Figure 107. Damaged Diffuser Pipe Leading Edges.

Figure 108. Typical Undamaged Diffuser Pipe Leading Edge.

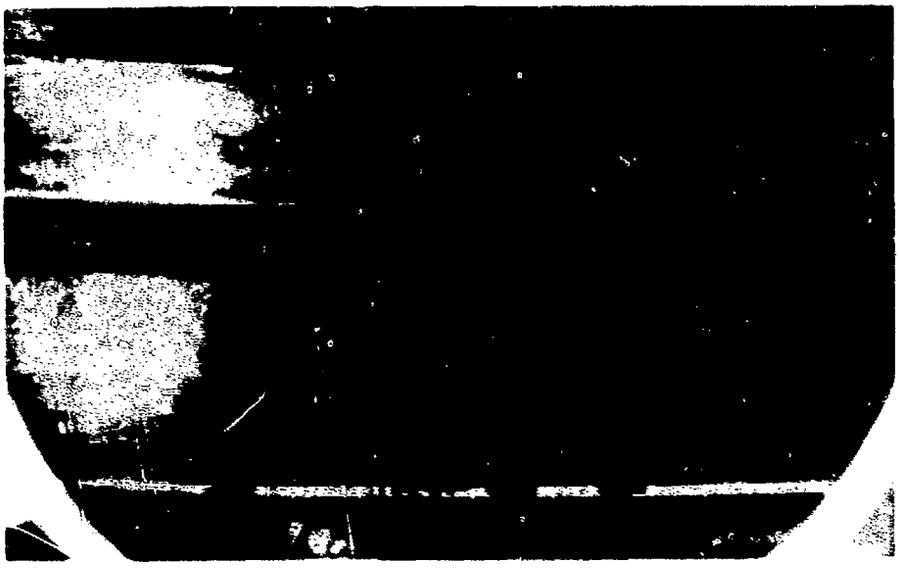

Figure 109. Post-Test Condition of Diffuser.

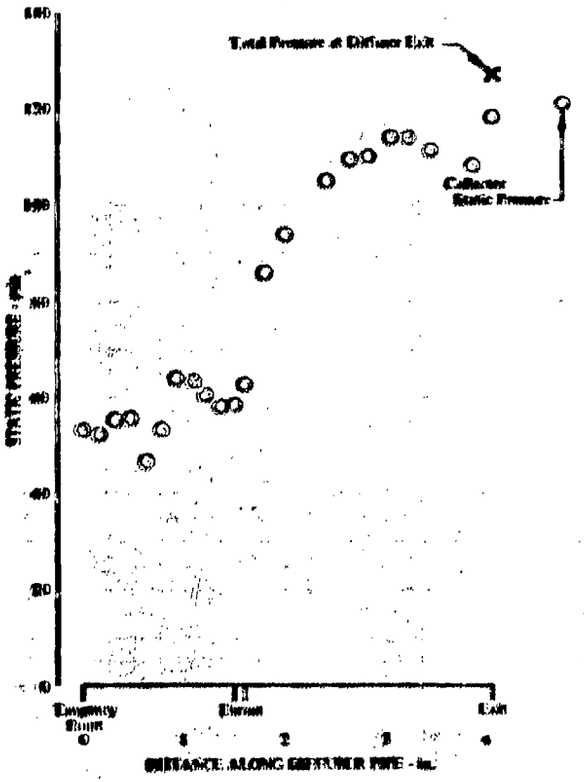

Figure 110. Diffuser Static Pressure Profile: Build No. 6, 95% Speed, 10-deg IGV, Near Stall.

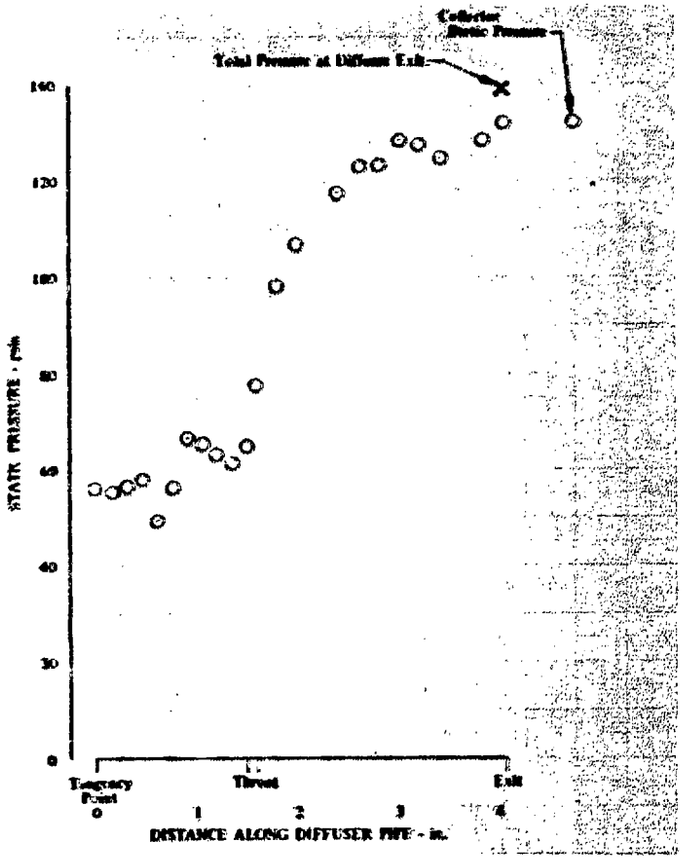

Figure 111. Diffuser Static Pressure Profile: Build No. 6, 100% Speed, 10-deg IGV, Near Stall.

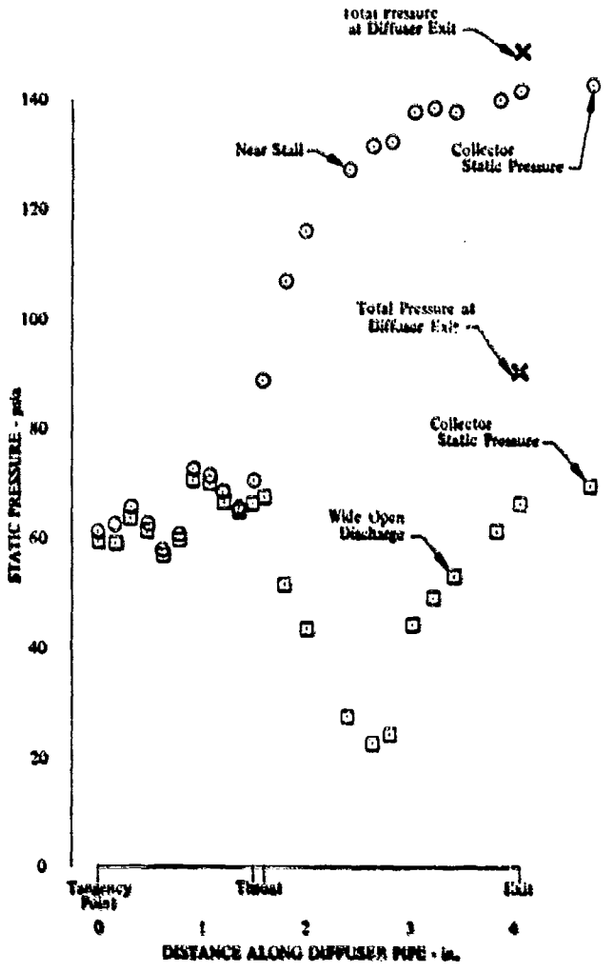

Figure 112. Diffuser Static Pressure Profile: Build No. 6, 101% Speed, -4-deg IGV.

Diffuser exit Mach number profiles were generated, based on diffuser exit total pressure rake data and collector static pressure. A resultant profile for Build No. 3 at 95% speed, near stall, and 10-deg IGV is shown in Figure 113. The profile is marked by a large low-diffusion region on the shroud side and by a low-flow region on the hub side, which probably represents a large boundary layer and flow separation. The Build No. 6 profile for the same point is presented in Figure 114 and has the same high-loss region on the hub side, but has a commensurately larger low-diffusion zone than Build No. 3. Profiles at 100 and 101% speed from Build No. 6, shown in Figures 115 and 116, have the same general characteristics as the 95% speed profile. Figure 117 shows the diffuser exit Mach number profile at minimum back pressure at 101% speed, which is characterized by very low diffusion with large high-loss regions.

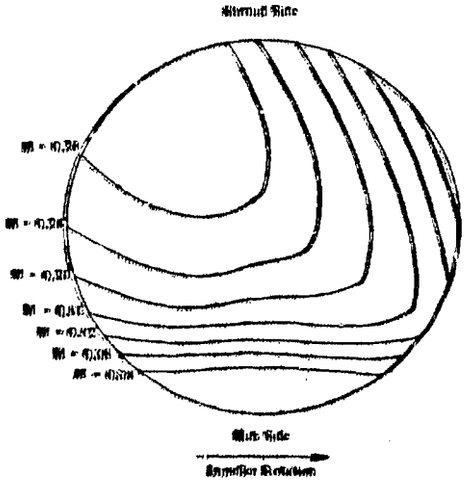

Figure 113. Diffuser Exit Mach Number Profile: Build No. 3, 95% Speed, $N/\sqrt{\theta}$ 10-deg IGV, Near Stall.

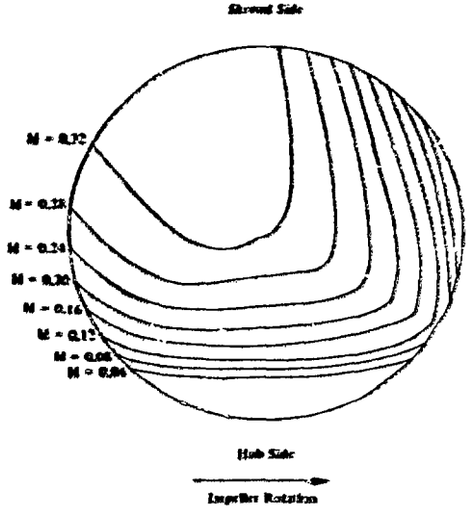

Figure 114. Diffuser Exit Mach Number Profile: Build No. 6, 95% Speed, 10-deg IGV, Near Stall.

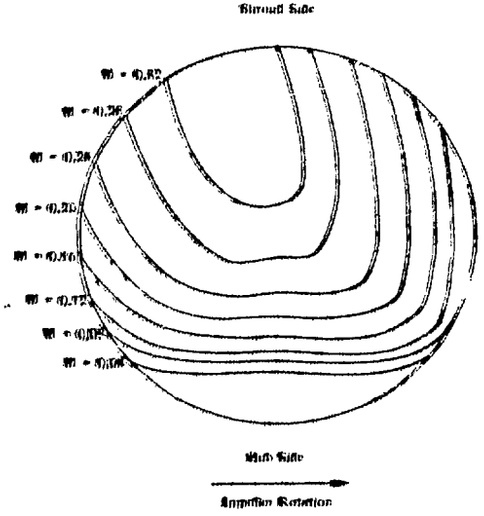

Figure 115. Diffuser Exit Mach Number Profile: Build No. 6, 100% Speed, 10-deg IGV, Near Stall.

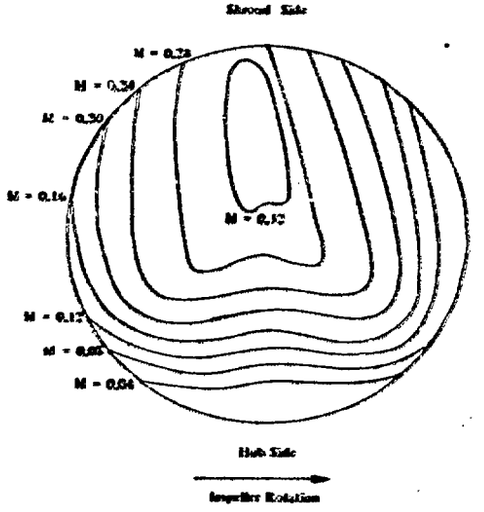

Figure 116. Diffuser Exit Mach Number Profile: Build No. 6, 101% Speed, -4-deg IGV, Near Stall.

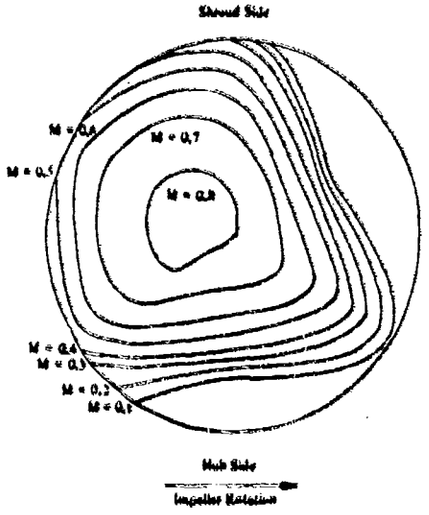

Figure 117. Diffuser Exit Mach Number Profile: Build No. 6, 101% Speed, -4-deg IGV, Wide Open Discharge.

Diffuser total pressure and diffuser dump losses are plotted as a function of corrected weight flow and impeller exit Mach number for both Builds No. 3 and 6 in Figures 118 and 119. The total pressure diffuser losses were essentially identical for both builds, although the Build No. 6 dump losses were higher. This can be directly attributed to the lower diffusion levels and resultant higher diffuser exit Mach numbers for Build No. 6, as is shown in Figure 120. The Build No. 6 static pressure rise coefficient values were considerably lower than the Build No. 3 levels, as shown in Figure 121.

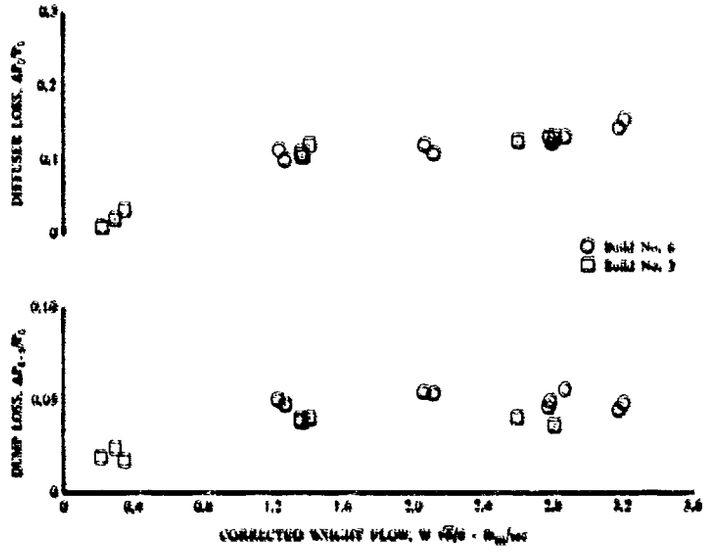

Figure 118. Diffuser Losses vs Corrected Weight Flow, Near Stall.

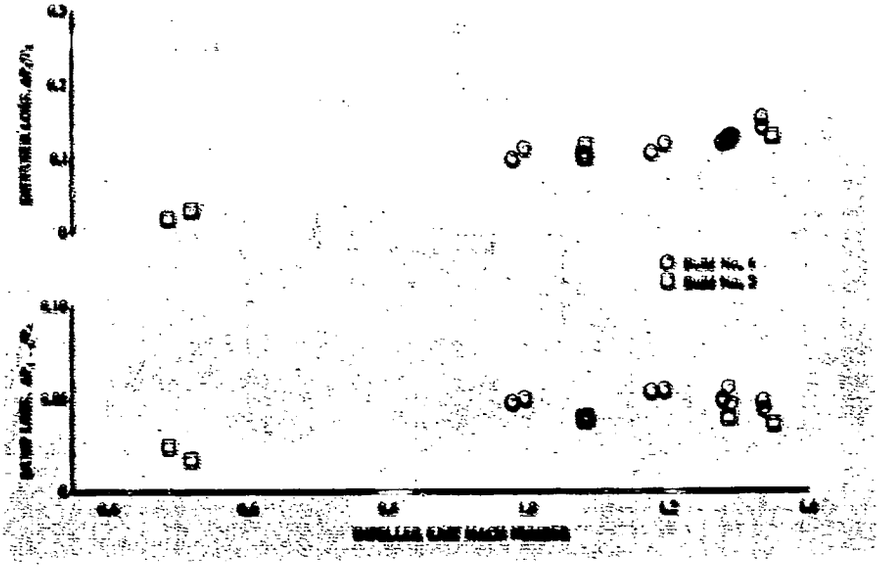

Figure 119. Diffuser Losses vs Impeller Exit Mach Number, Near Stall.

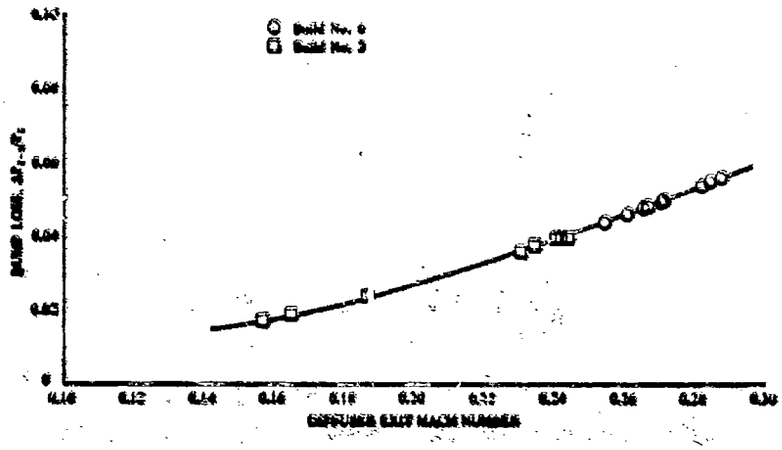

Figure 120. Diffuser Dump Losses Near Stall.

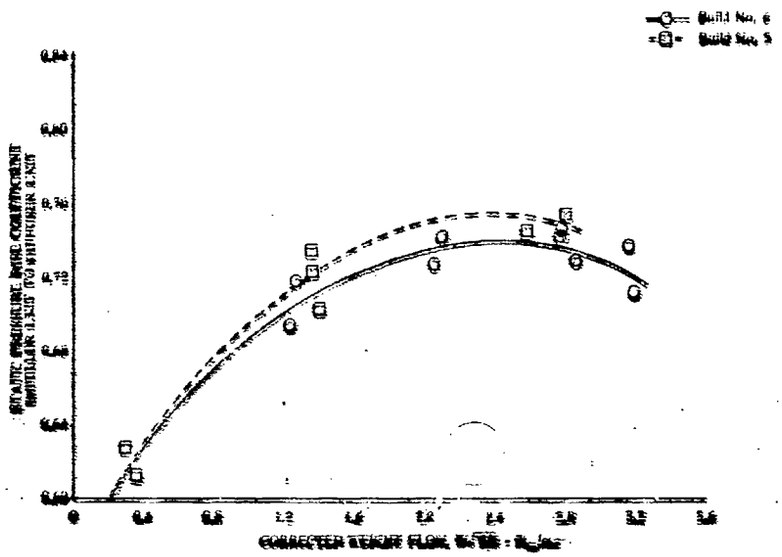

Figure 121. Diffuser Static Pressure Rise Coefficient vs Corrected Weight Flow.

HIGH-FREQUENCY RESPONSE DATA

High-frequency response data were recorded at two speeds, 70 and 78% of design speed, during Build No. 6 testing. These speeds were selected because they were the highest speeds for which performance data were available and which did not exceed the temperature limitations of the high-response KULITE™ pressure transducers. Data were recorded at steady-state conditions, near stall and during transient operation into stall for the following four pressures:

1. Total pressure at the impeller exit
2. Two static pressures in the vaneless space
3. Static pressure at the diffuser discharge.

These pressures were recorded using KULITE pressure transducers capable of frequencies from dc to 100,000 Hz; however, due to the high magnetic tape speed required to attain resolution at the high frequencies, data below 200 Hz are not reliable.

Typical data are presented in Figures 122 and 123 for 70 and 78% of design speed, respectively, and show the response of the four measured pressures during a 10-ms period including the surge event. Typically, these data define surge both in the form of an amplitude change and a frequency change. The amplitude difference between the two vaneless space static measurements is believed to be due to a faulty gain setting on one channel (PSDVK1); however, the wave form is unaffected.

Additional data from each of the high-response probes during the steady-state point and at 2.5-ms increments into the stall transient are presented in Appendix I in the form of pressure amplitude vs time and pressure amplitude vs frequency. These data indicate the presence of strong discrete fluctuations at frequencies corresponding to 12 E, 24 E, and 48 E (E - rotor speed). These frequencies correspond to excitations from the impeller blading, which has 12 full blades, 12 primary splitters, and 24 secondary splitters. Prior to surge, the dominant frequency observed was generally 24 E which seems to indicate a differential work input between the secondary splitters and the full blades and primary splitters. Correlations which were performed on these data, however, failed to identify the 24 E signal with the various types of blades and splitters.

Following surge, the dominant frequency became 48 E, which appears to be the pressure field associated with the stalled blading. This pattern of frequency change was observed for both the 70 and 78% speed. No evidence of rotating stall prior to surge was noted; however, the local distortion of the impeller discharge flow field due to the insertion of the relatively large high-frequency pressure probe caused surge to occur significantly below the undistorted surge line. This asymmetry may have prevented the formation of rotating stall cells.

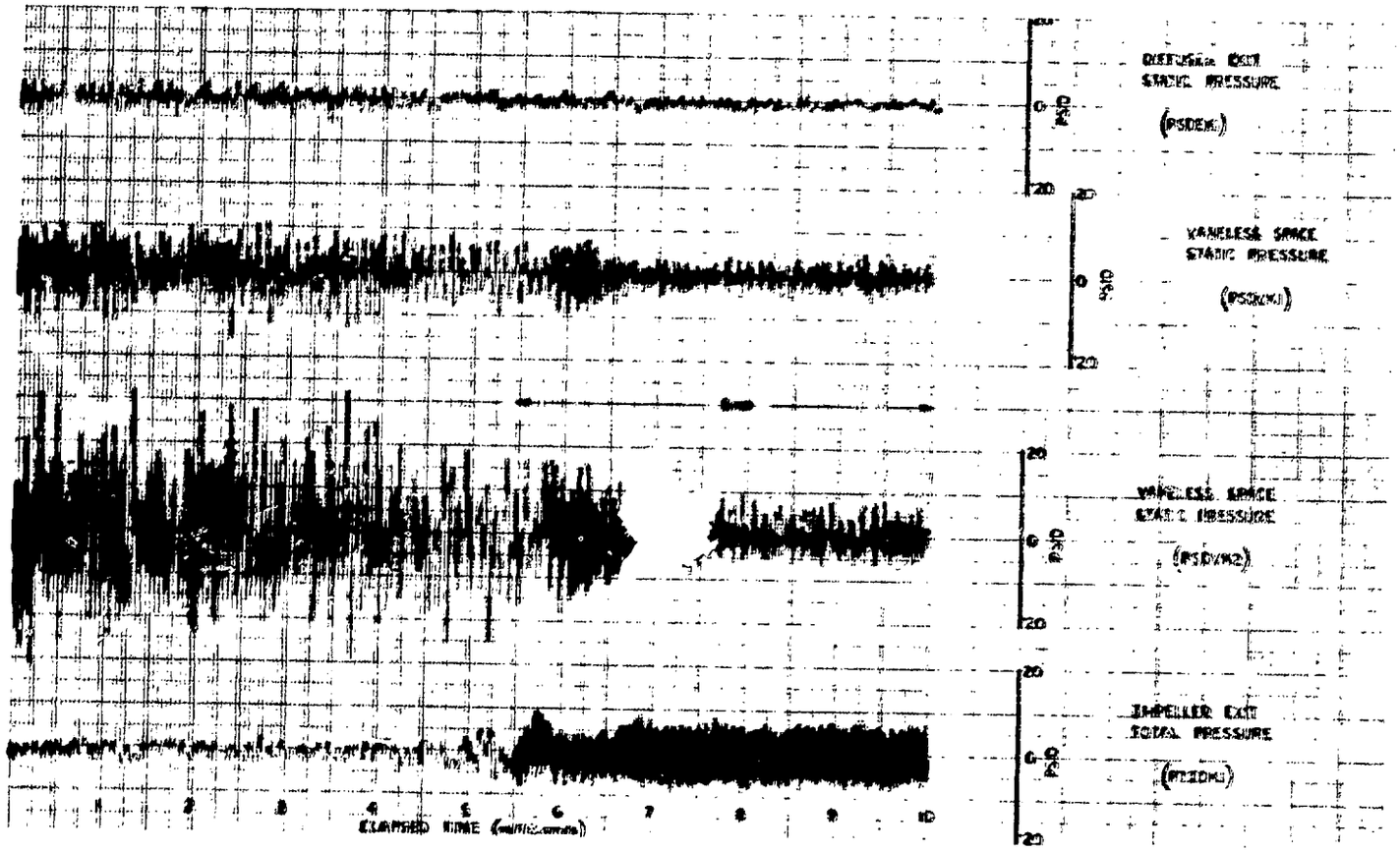

Figure 122. High-Frequency Response Data at 70% Speed.

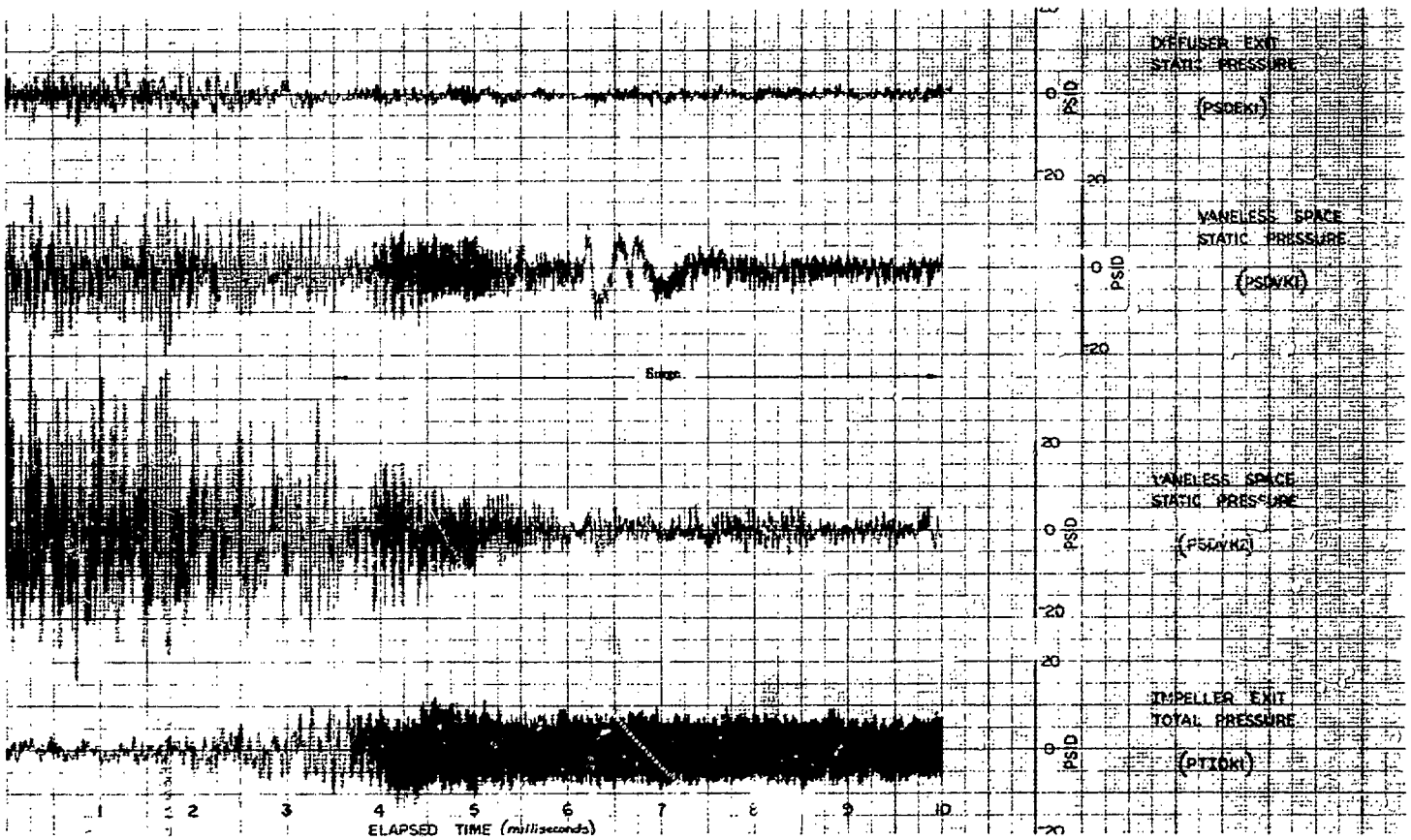

Figure 123. High-Frequency Response Data at 73% Speed.

CONCLUSIONS

The overall total-to-static pressure ratio and efficiency of this compressor came very close to meeting design goals and, for all practical purposes has demonstrated that high-pressure ratio, high-efficiency, single-stage centrifugal compressors can be developed. If the diffuser had not been damaged, the 10:1 pressure ratio 75% efficiency goal likely would have been surpassed, as shown by the composite compressor map generated assuming undamaged diffuser losses on the overall compressor performance.

The basic approach taken for the aerodynamic design has proven to be sound. The use of variable inlet guide vanes has allowed obtaining optimum performance data throughout the range of operating speeds and generation of an inlet guide vane schedule for potential use of this compressor in a gas generator configuration.

The inducer operated well until it was run at conditions beyond its intended design. When it was discovered that the overall pressure ratio was low at design speed and prewhirl, it was necessary to produce more work in the inducer-impeller. This involved a decrease in prewhirl, an increase in speed, or both. Either condition increased the inlet relative Mach number into the inducer and forced a more stalled incidence, generating high losses and resulting in low efficiency. The remote inducer, which was included in the design to accept shock losses should they be higher than expected and to allow separation on the inducer without destroying impeller performance, also functioned properly in this situation as the impeller operation was not influenced by the poor inducer exit characteristics.

The inlet guide vanes were set to produce less prewhirl, and rotor speed was increased to produce the required rotor pressure ratio. The impeller efficiency was above predicted, indicating that additional tip diameter would also have obtained the design performance.

The diffuser, including the entry region, is the most critical element in the performance of this compressor. The mismatch caused by the undersized diffuser in Build No. 2 and the resulting improved performance obtained in Build No. 3 by only increasing the throat diameters from 0.228 to 0.235 in. demonstrates the small latitude in dimensioning the diffuser throat and predicting impeller exit conditions and diffuser throat blockage.

The losses and static pressure rise generated by the resized diffuser were quite good and would have allowed the overall performance goal of 10:1 pressure ratio at 75% efficiency to have been surpassed in Build No. 3 at a lower prewhirl than 10 deg if the rig had functioned properly mechanically. Damage to the leading edge region of the diffuser, resulting from silver impingement when the impeller rubbed the shroud in a mechanical checkout of the redesigned bearing support and rotor system, resulted in enough change in the diffuser characteristics to cause the performance to be short of the goal. The change in throat blockage causes the flow rate to change and the static pressure rise to decrease. This behavior also points to the critical nature of the diffuser in a compressor such as this.

RECOMMENDATIONS

Analysis of the data obtained during this program to design and test a 10:1 pressure ratio single-stage centrifugal compressor leads to the following recommendations to improve its aerodynamic performance:

1. The inducer should be redesigned to operate efficiently at the conditions required to produce 10:1 pressure ratio. The inducer redesign would be based on the optimum inlet guide vane exit conditions and the desired impeller inlet conditions and could improve the design speed efficiency up to three points.

2. The modified inducer should be tested with a new diffuser to eliminate the detrimental effects of the damage leading edges of the current diffuser.

3. The potential performance increase that could be attained through reducing impeller blade-to-shroud friction heating should be evaluated. This friction heating could be minimized through the use of a shrouded impeller. The shrouded impeller also would eliminate the problem of impeller-to-shroud rubs encountered in this and other programs as a result of the small clearances required for conventional open-faced impellers to achieve good performance. A shrouded impeller would also permit extension of hub and shroud walls to form a mechanically practical rotating vaneless space to reduce diffuser entrance losses.

4. Means for improving the range characteristics of this compressor should be evaluated. The useful performance of the compressor in an engine or gas generator application would be substantially improved if peak efficiency could be achieved off the surge line. Several approaches have shown potential for improving the near-vertical speedline characteristics of high-pressure-rise, single-stage centrifugal compressors. Particular attention should be given to the impeller exit/diffuser entrance region, which, to a large degree, controls range from choke to surge. Specific recommendations at the 10:1 pressure ratio design point include reducing the number of diffuser passages to increase range, as well as using sweptback impeller blading.

APPENDIX I
OVERALL PERFORMANCE TABULATIONS

The tabulations of overall performance data used to construct the performance plots in the text are shown in Tables XIV through XVII. Table XIV contains data through the range of operation for Build No. 3 zero degrees of prewhirl. All steady-state data points and the incipient stall point located by stall transients are included. Similar Build No. 3 data for 10- and 20-deg inlet guide vane settings are shown on Tables XV and XVI, respectively. Table XVII contains similar data for all prewhirl conditions during Build No. 6. Data points are listed in sequential order down the speedline from the incipient stall point.

TABLE XIV. OVERALL PERFORMANCE TABULATION - BUILD NO. 3, 0-DEG PREWHIRL

Speed, %	IGV Setting, deg	Weight Flow, lb/sec	Pressure Ratio	Efficiency, %
30	0	0.213	1.257	0.747
		0.253	1.272	0.753
		0.302	1.281	0.758
		0.389	1.259	0.704
		0.425	1.218	0.606
		0.466	1.168	0.487
		0.494	1.142	0.383
50	0	0.620	1.953	0.751
		0.638	1.942	0.736
		0.667	1.959	0.742
		0.737	1.907	0.721
		0.769	1.877	0.704
		0.794	1.749	0.617
		0.801	1.301	0.276
70	0	1.370	3.603	0.764
		1.369	3.539	0.756
		1.412	3.515	0.748
		1.414	3.505	0.747
		1.452	3.196	0.686
		1.464	2.999	0.638
		1.454	1.878	0.346
80	0	1.879	4.904	0.767
		1.873	4.872	0.769
		1.897	4.878	0.771
		1.932	4.812	0.745
		1.936	4.202	0.669
		1.934	3.861	0.623
		1.938	2.531	0.402
90	0	2.597	6.935	0.761
		2.600	6.921	0.761
		2.624	6.926	0.760
		2.603	6.865	0.761
		2.597	6.714	0.751
		2.604	6.296	0.719
		2.605	3.496	0.446
95	0	2.954	8.661	0.791
		2.965	8.563	0.788
		2.969	8.555	0.786
		2.989	8.520	0.784
		3.019	8.376	0.778
		3.031	8.019	0.755
		3.026	4.198	0.472

TABLE XV. OVERALL PERFORMANCE TABULATION - BUILD NO. 3, 10-DEG PREWHIRL

Speed, %	IGV Setting, deg	Weight Flow, lb/sec	Pressure Ratio	Efficiency, %
30	10	0.223	1.200	0.526
		0.246	1.223	0.662
		0.224	1.251	0.741
		0.269	1.261	0.756
		0.301	1.271	0.811
		0.337	1.251	0.746
		0.360	1.241	0.709
		0.407	1.226	0.653
		0.432	1.120	0.372
50	10	0.637	1.950	0.746
		0.625	1.941	0.747
		0.655	1.941	0.748
		0.663	1.955	0.753
		0.649	1.928	0.743
		0.646	1.947	0.759
		0.698	1.919	0.737
		0.777	1.871	0.717
		0.776	1.664	0.567
		0.790	1.305	0.291
70	10	1.355	3.555	0.772
		1.406	3.503	0.763
		1.417	3.480	0.762
		1.453	3.408	0.742
		1.462	3.202	0.697
		1.460	3.006	0.653
		1.457	3.152	0.688
		1.463	1.884	0.352
80	10	1.874	4.943	0.779
		1.898	4.851	0.769
		1.910	4.836	0.766
		1.930	4.720	0.752
		1.914	4.549	0.734
		1.933	4.384	0.708
		1.903	2.500	0.401
90	10	2.562	7.137	0.797
		2.575	7.046	0.790
		2.595	7.046	0.789
		2.605	6.973	0.786
		2.607	6.882	0.781
		2.611	6.258	0.734
		2.586	3.496	0.461

TABLE XV - Continued

Speed, %	IGV Setting, deg	Weight Flow, lb/sec	Pressure Ratio	Efficiency, %
95	10	2.778	8.192	0.796
		2.818	8.261	0.791
		2.816	8.176	0.791
		2.819	8.174	0.791
		2.854	8.145	0.788
		2.873	8.083	0.782
		2.902	8.006	0.777
		2.878	7.610	0.757
		2.895	6.927	0.710
		2.902	6.825	0.700
		2.898	3.990	0.467
		2.895	3.978	0.467
100	10	3.005	9.338	0.770
		3.025	9.288	0.762
		3.037	8.885	0.742
		3.039	8.575	0.723
		3.034	8.135	0.703
		3.033	6.594	0.611
		3.025	4.287	0.451

TABLE XVI. OVERALL PERFORMANCE TABULATION - BUILD NO. 3, 20-DEG PREWHIRL

Speed, %	IGV Setting, deg	Weight Flow, lb/sec	Pressure Ratio	Efficiency, %
30	20	0.275	1.253	0.785
		0.269	1.259	0.747
		0.358	1.272	0.759
		0.394	1.235	0.674
		0.419	1.229	0.664
		0.484	1.168	0.497
		0.494	1.119	0.367
50	20	0.614	1.976	0.780
		0.611	1.942	0.750
		0.664	1.923	0.750
		0.718	1.918	0.746
		0.762	1.842	0.701
		0.774	1.686	0.588
		0.790	1.289	0.274
		0.777	1.297	0.278

TABLE XVI - Continued

Speed, %	IGV Setting, deg	Weight Flow, lb/sec	Pressure Ratio	Efficiency, %
70	20	1.345	3.508	0.758
		1.372	3.506	0.764
		1.350	3.498	0.764
		1.409	3.488	0.764
		1.458	3.230	0.713
		1.459	3.004	0.660
		1.448	1.886	0.354
80	20	1.818	4.818	0.780
		1.841	4.817	0.783
		1.848	4.809	0.784
		1.865	4.817	0.784
		1.841	4.752	0.774
		1.910	4.393	0.727
		1.919	2.483	0.409
90	20	2.389	6.849	0.793
		2.388	6.805	0.792
		2.402	6.772	0.792
		2.436	6.821	0.794
		2.501	6.712	0.788
		2.510	6.232	0.751
		2.520	3.385	0.456
95	20	2.664	7.882	0.792
		2.697	7.749	0.783
		2.696	7.732	0.783
		2.691	7.726	0.783
		2.721	7.593	0.775
		2.733	7.236	0.752
		2.740	3.740	0.454

TABLE XVII. OVERALL PERFORMANCE TABULATION - BUILD NO. 6

Speed, %	IGV Setting, deg	Weight Flow, lb/sec	Pressure Ratio	Efficiency, %
70	30	1.227	3.405	0.735
		1.242	3.320	0.722
		1.441	3.255	0.717
		1.357	2.952	0.638
		1.346	1.874	0.349
70	20	1.288	3.500	0.734
		1.279	3.346	0.713
		1.353	3.044	0.650
		1.353	2.598	0.544
		1.359	1.829	0.334
85	30	2.044	5.624	0.767
		2.071	5.425	0.756
		2.065	5.168	0.733
		2.097	4.040	0.600
		2.101	2.866	0.426
85	20	2.078	5.690	0.751
		2.125	5.553	0.742
		2.117	5.234	0.719
		2.113	4.692	0.657
		2.088	2.925	0.422
94.5	15	2.734	8.079	0.775
		2.787	7.957	0.768
		2.797	7.913	0.768
		2.823	7.298	0.728
		2.819	6.703	0.689
		2.833	6.539	0.676
		2.807	3.945	0.461
94.5	10	2.792	8.169	0.773
		2.796	8.037	0.768
		2.827	7.808	0.753
		2.841	7.414	0.726
		2.828	7.273	0.717
		2.837	7.015	0.701
		2.823	4.059	0.471
95	10	2.833	8.388	0.778
		2.819	8.238	0.769
		2.883	8.122	0.764
		2.894	7.487	0.725
		2.894	6.897	0.686
		2.881	6.792	0.681

TABLE XVII - Continued

Speed, %	IGV Setting, deg	Weight Flow, lb/sec	Pressure Ratio	Efficiency, %
101	5	3.129	9.661	0.735
		3.136	9.693	0.737
		3.142	9.444	0.726
		3.147	9.360	0.724
		3.144	9.119	0.712
		3.142	8.520	0.683
		3.150	4.679	0.448
101	0	3.183	9.882	0.737
		3.185	9.649	0.727
		3.192	9.552	0.722
		3.197	8.993	0.695
		3.194	8.516	0.672
		3.195	7.830	0.639
		3.192	4.743	0.450
101	-4	3.196	10.034	0.738
		3.198	9.965	0.733
		3.209	9.698	0.721
		3.217	9.672	0.721
		3.221	8.786	0.682
		3.222	7.398	0.610
		3.221	4.728	0.442

TRAVERSE PLOTS

This section contains plots of traverse data obtained during Builds No. 3 and 6 testing. Total pressure and total temperature are ratioed to standard day conditions, but are otherwise uncorrected. The keys on the plots identify the correct scale to the symbol from right to left in increasing number. The temperature sensor on the Station 1 and 1.5 traverse probe is offset 0.045 in. from the pressure sensing ports. Both the Station 1 and 1.5 probes were stopped prior to the hub wall and traversed into recesses in the shroud wall.

Figures 124 through 152 contain Station 1 (inlet guide vane exit) radial plots of total pressure, air angle, total temperature, and circumferential plots of total pressure. The radial traverses are from hub to shroud, while the circumferential traverses were made at five discrete spanwise locations. Figures 153 through 174 contain Station 1.5 (inducer exit) radial traverses of total pressure, air angle, and temperature vs travel. Figures 175 through 210 contain Station 2 (impeller exit) traverse plots of total pressure and air angle from hub to shroud. The probe was traversed from a recess in the shroud wall to a recess in the hub wall, and data were recorded on the return traverse. Figures 211 through 219 are impeller exit temperature traverse plots taken in the same manner as total pressure and air angle.

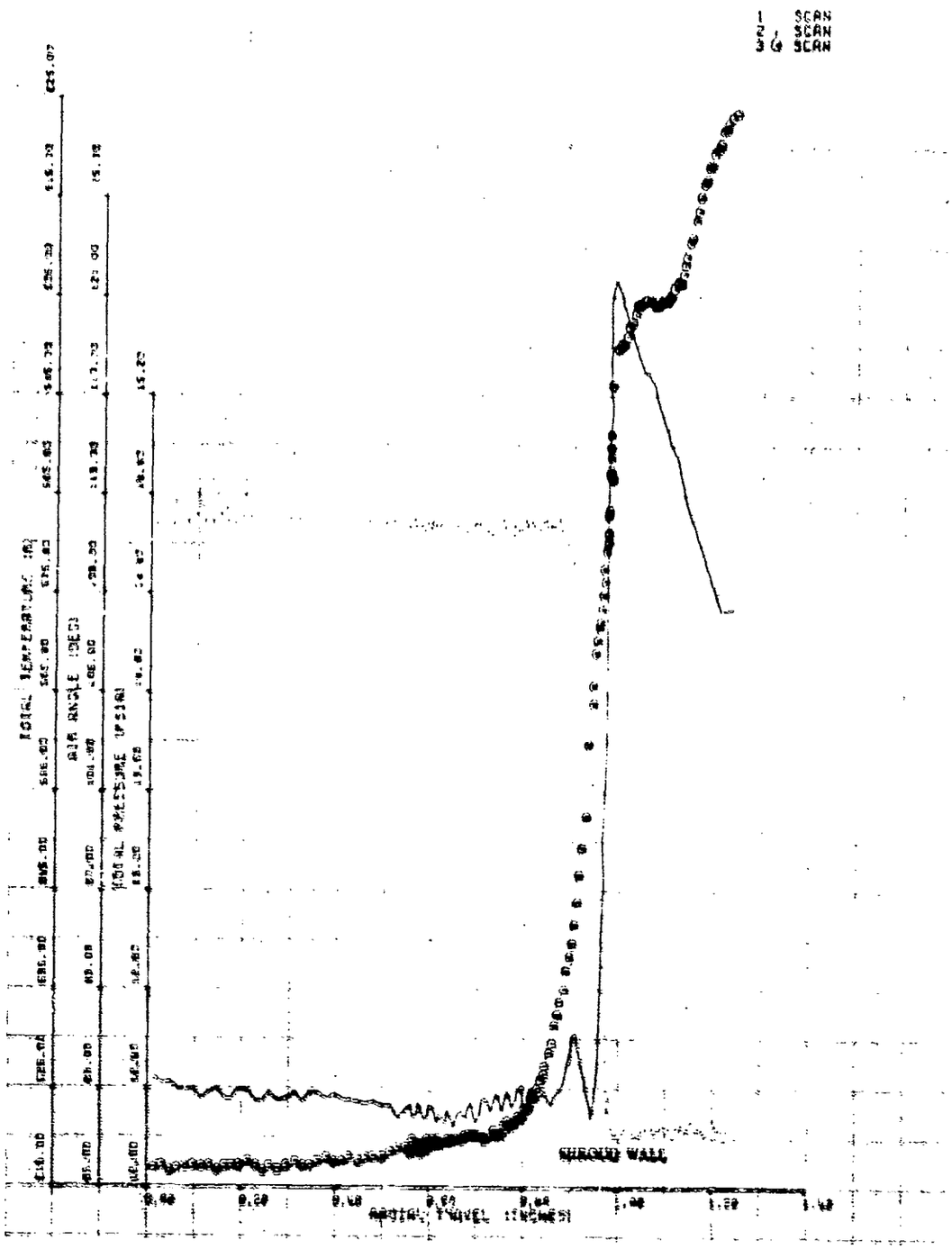

Figure 124. IGV Exit Radial Traverse, Build No. 6, 101% Speed, 0-deg IGV, Near Stall.

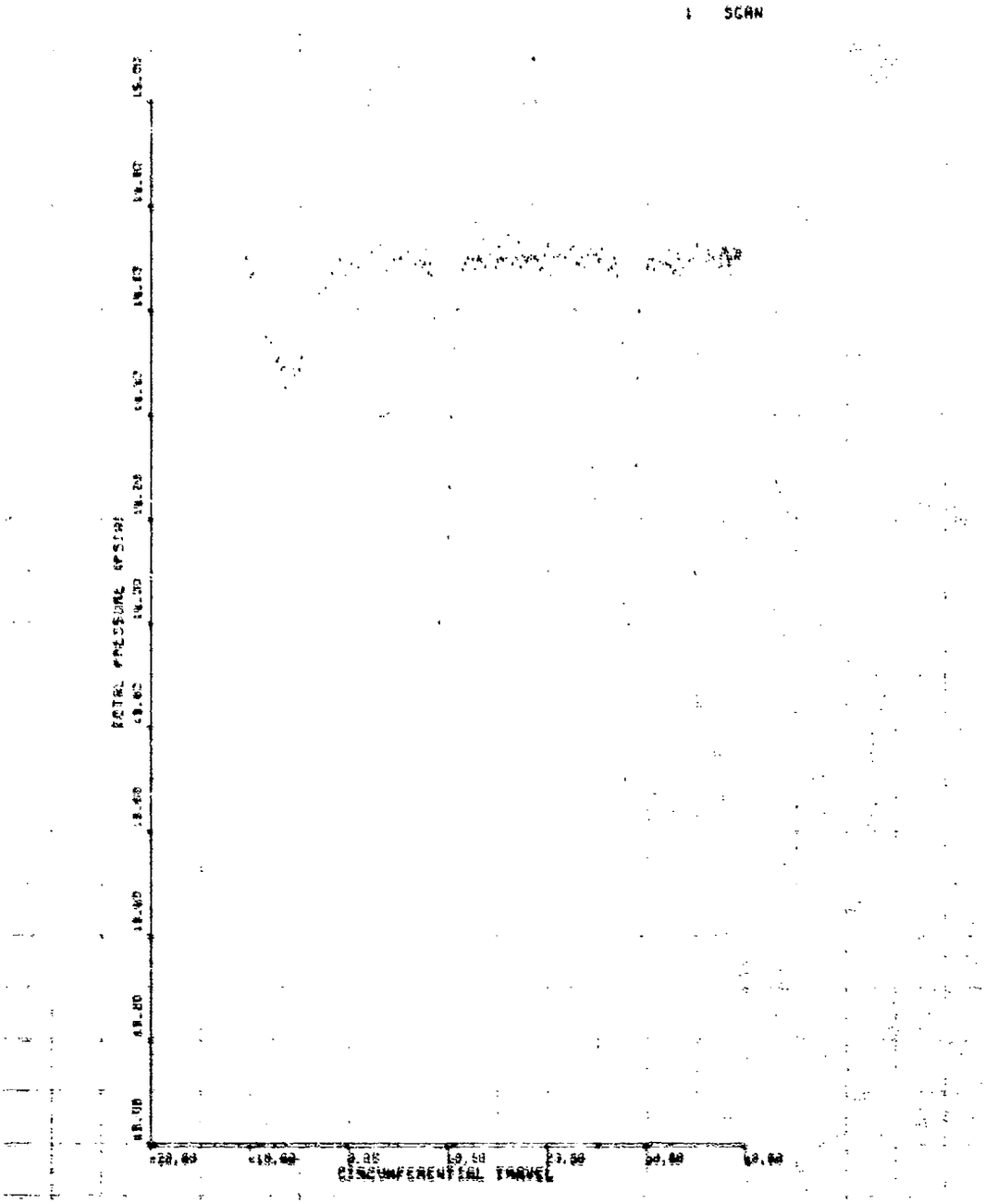

Figure 125. IGV Circumferential Traverse, Build No. 6, 101% Speed, 0-deg IGV, 10% Span.

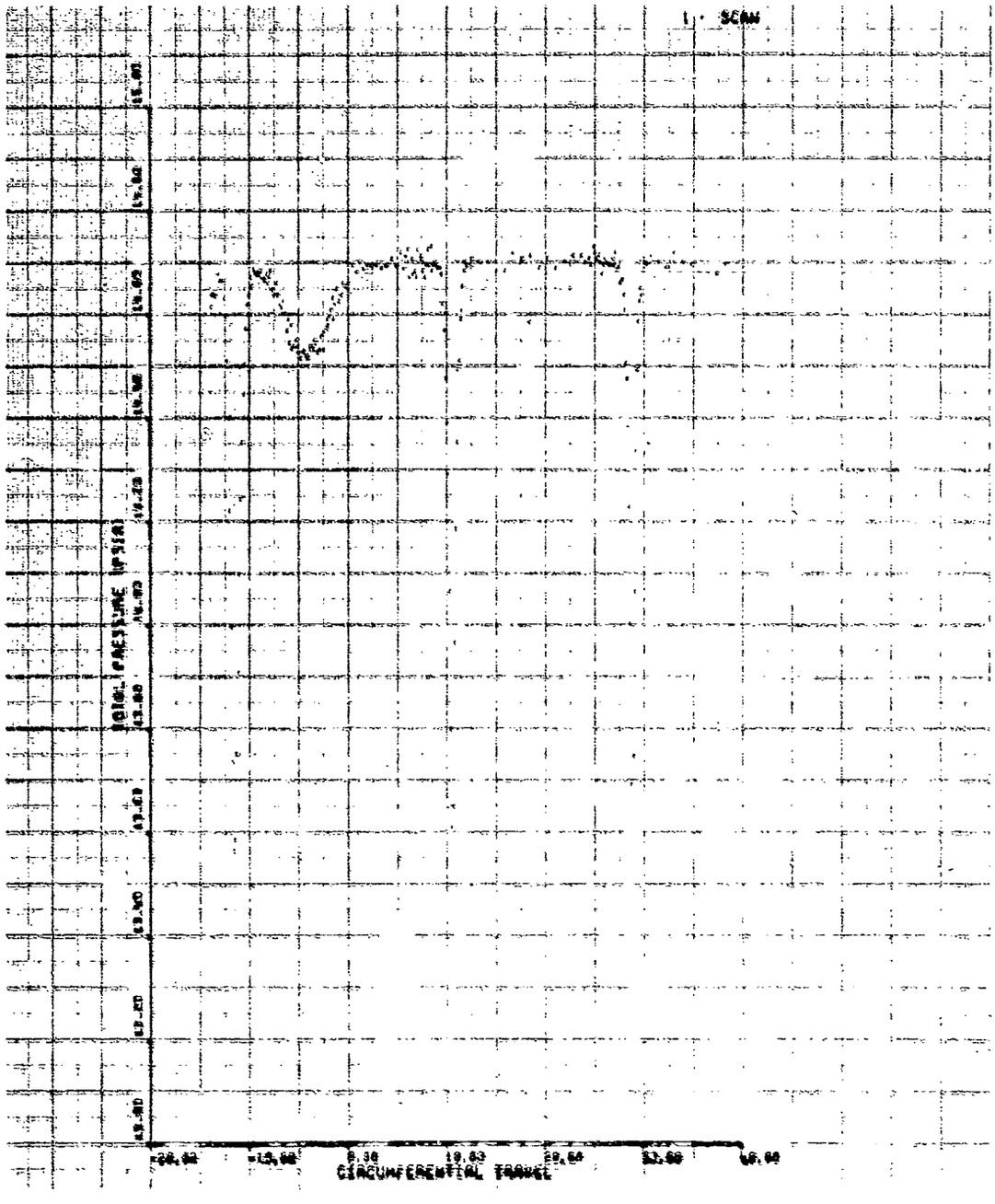

Figure 126. IGV Circumferential Traverse, Build No. 6, 101% Speed, 0-deg IGV, 30% Span.

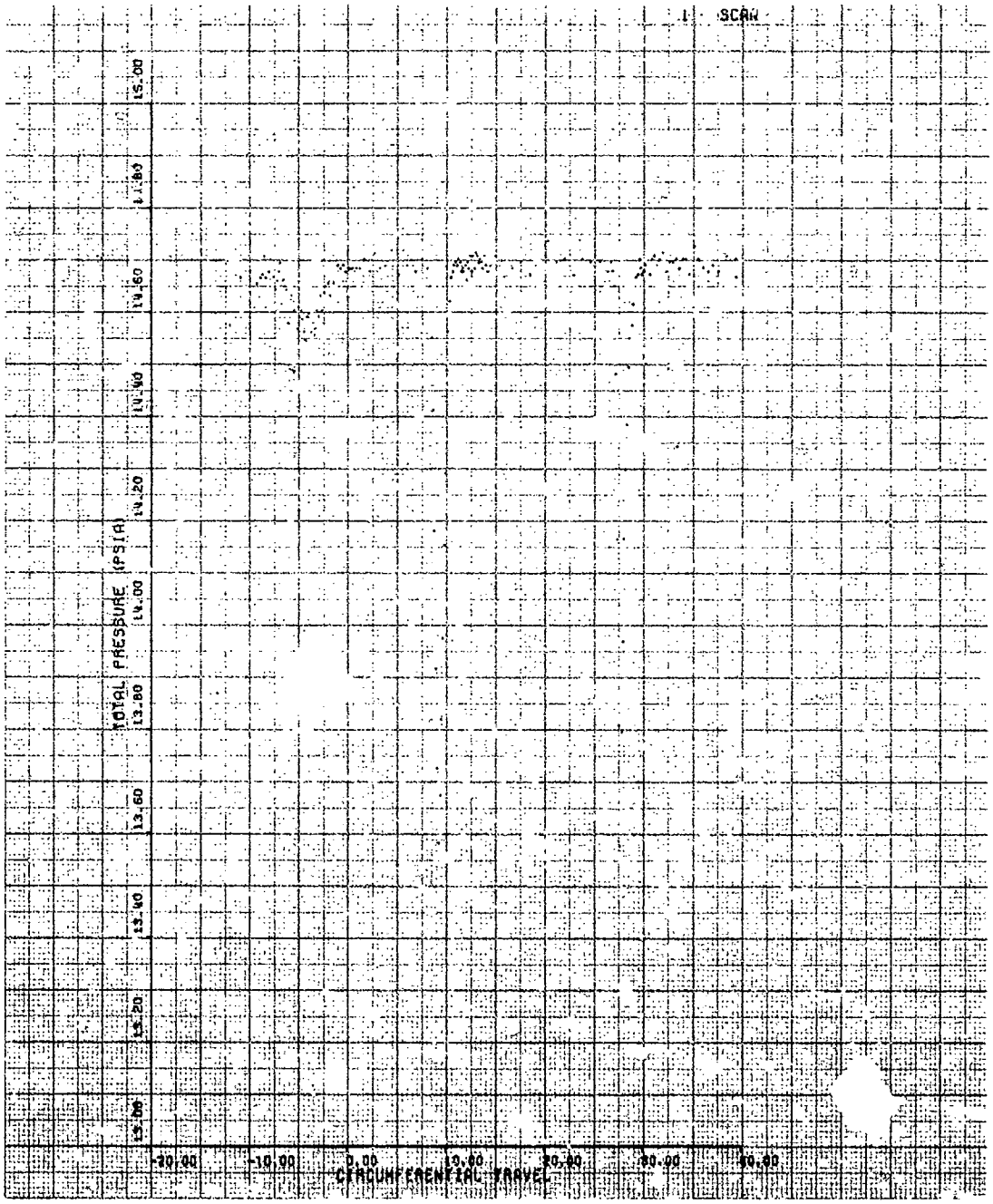

Figure 127. IGV Circumferential Traverse, Build No. 6, 101% Speed, 0-deg IGV, 50% Span.

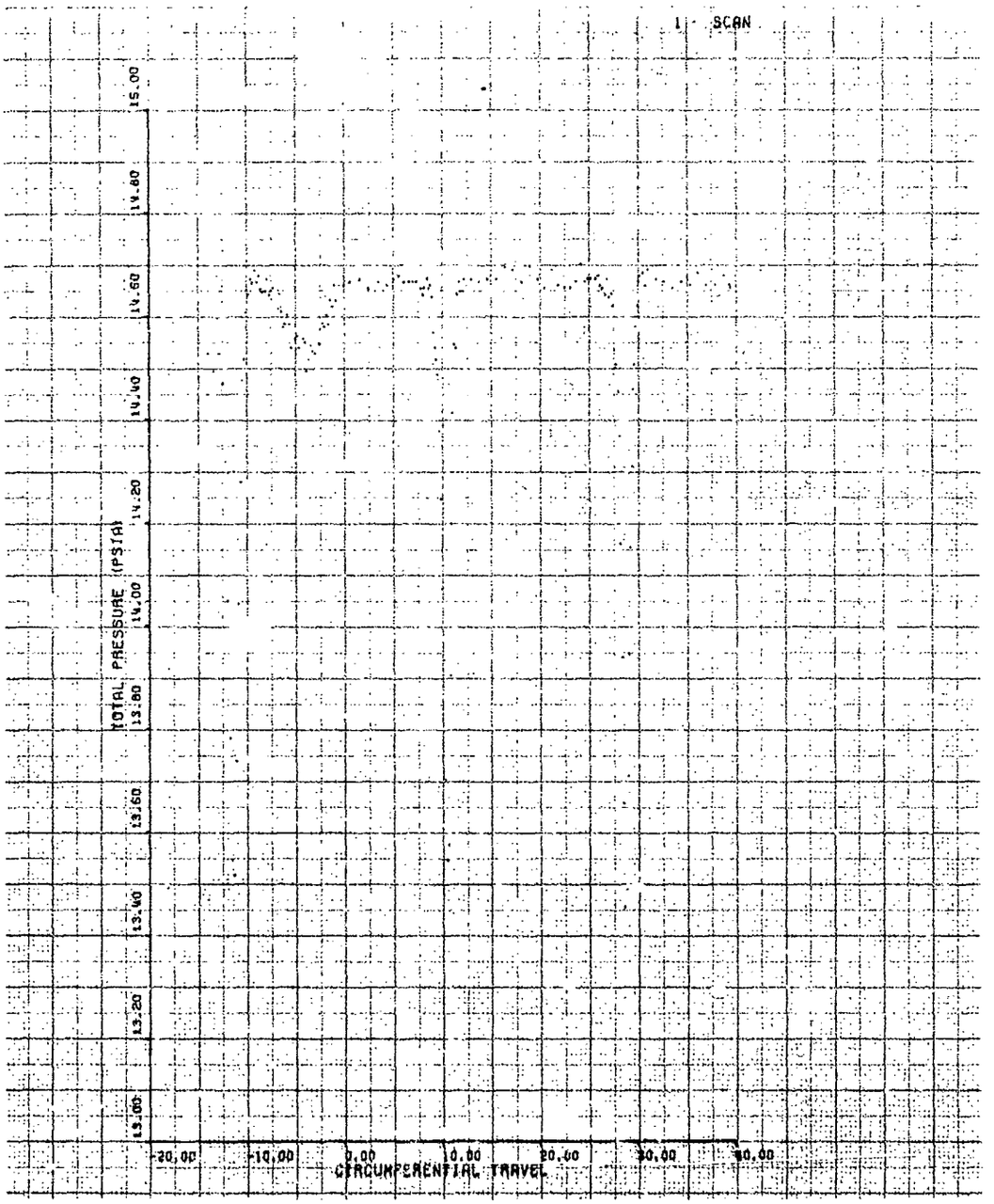

Figure 128. IGV Circumferential Traverse, Build No. 6, 101% Speed, 0-deg IGV, 70% Span.

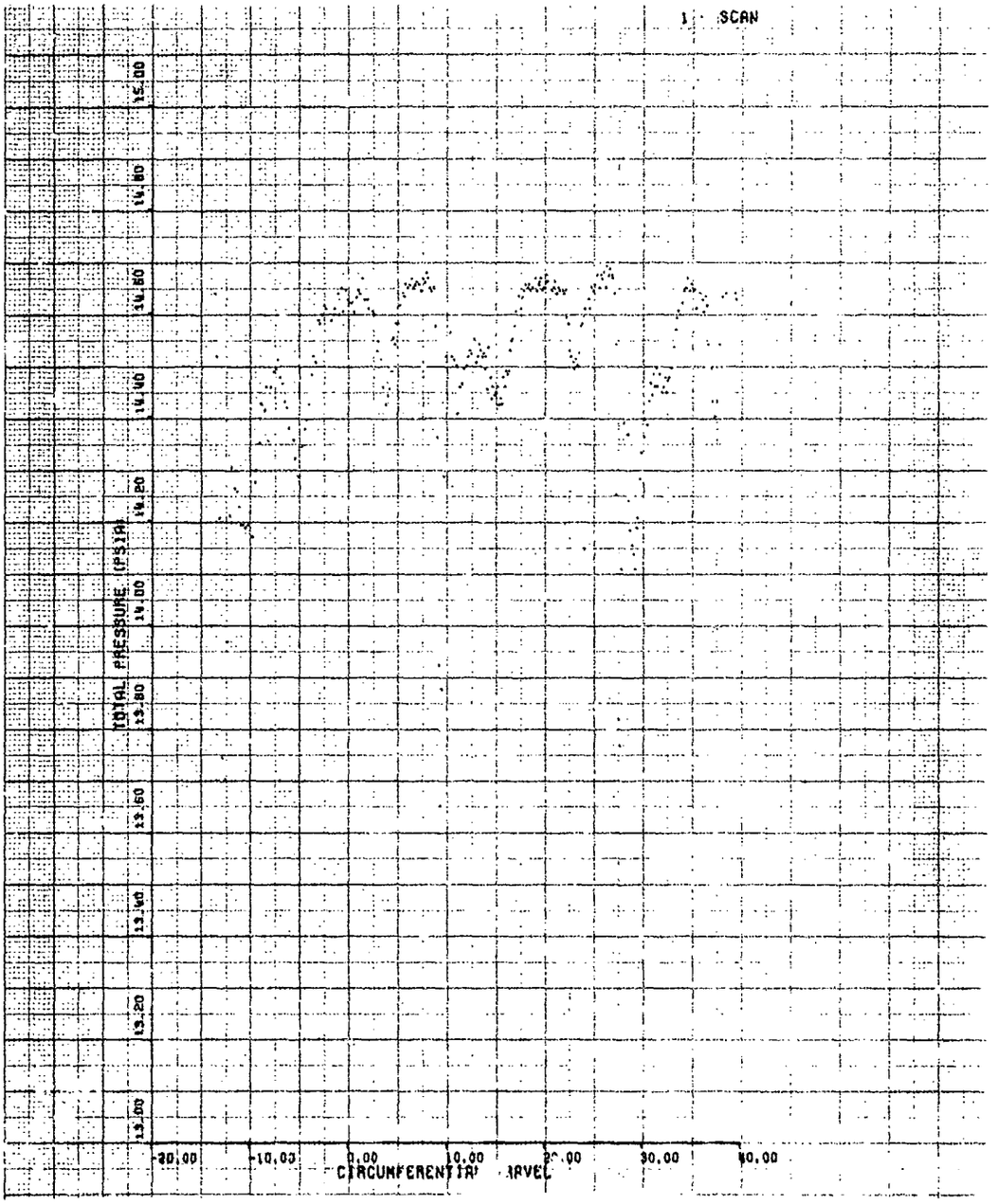

Figure 129. IGV Circumferential Traverse, Build No. 6, 101% Speed, 0-deg IGV, 90% Span.

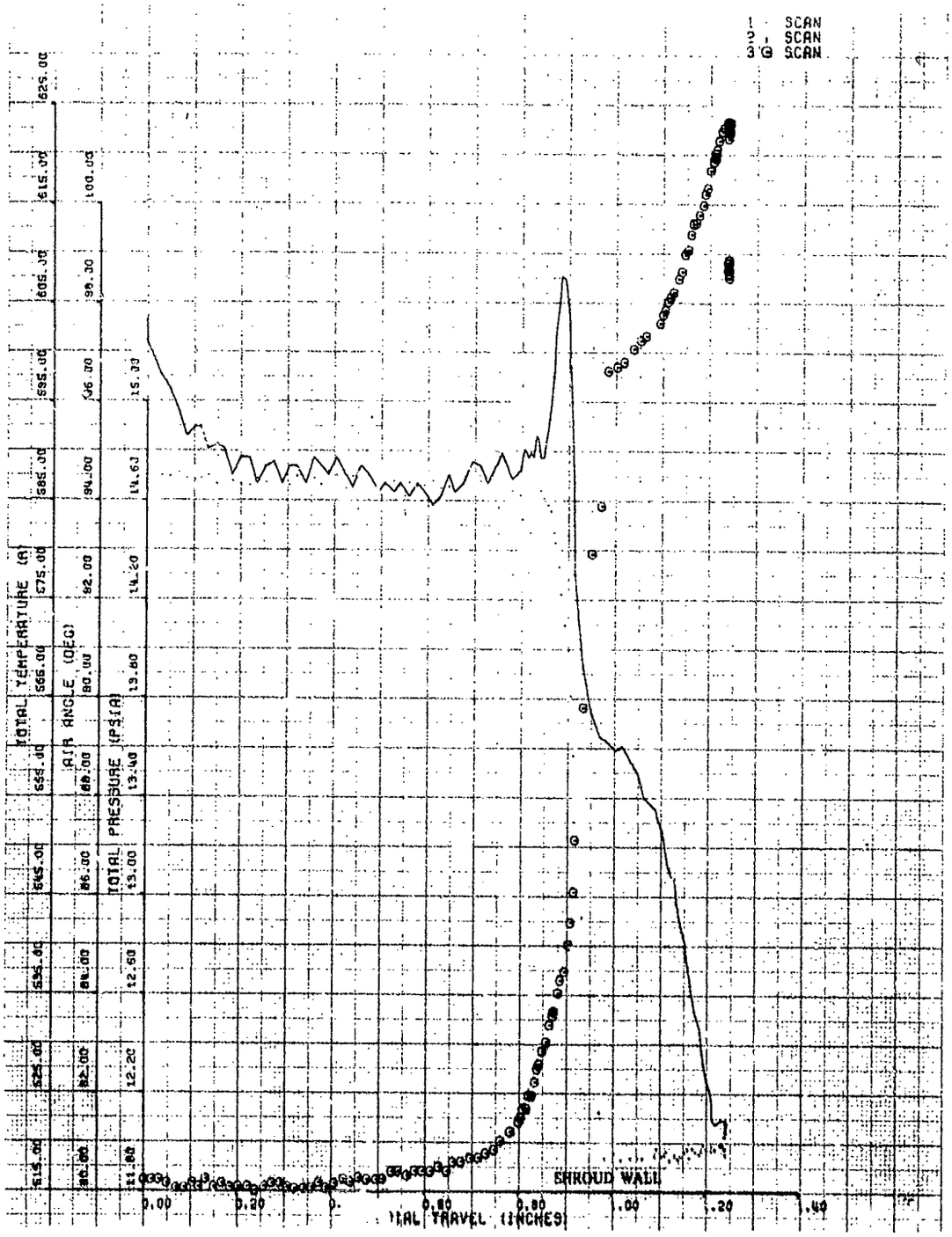

Figure 130. IGV Exit Radial Traverse, Build No. 6, 101% Speed, -4-deg IGV.

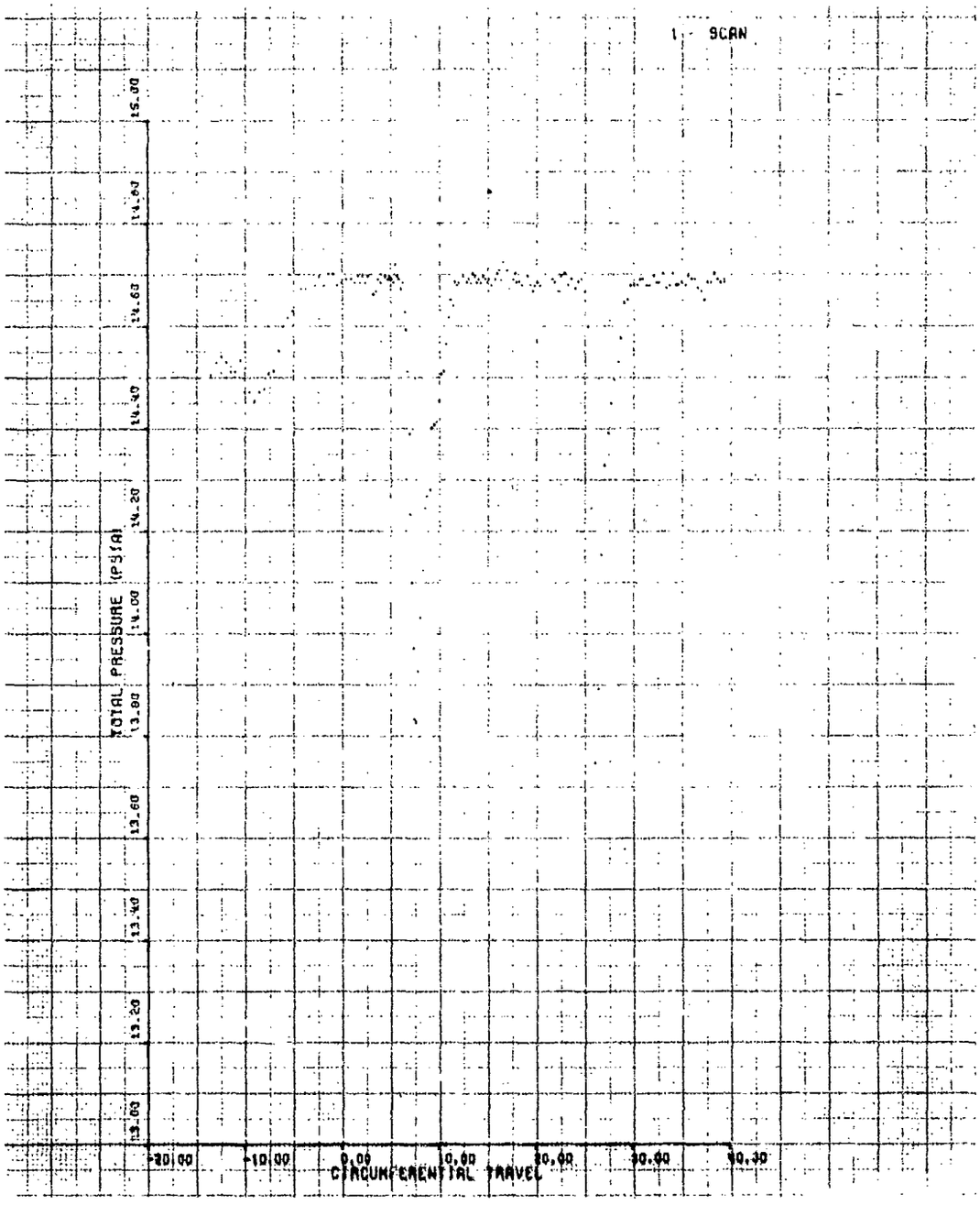

Figure 131. IGV Circumferential Traverse, Build No. 6, 101% Speed, -4-deg IGV, 10% Span.

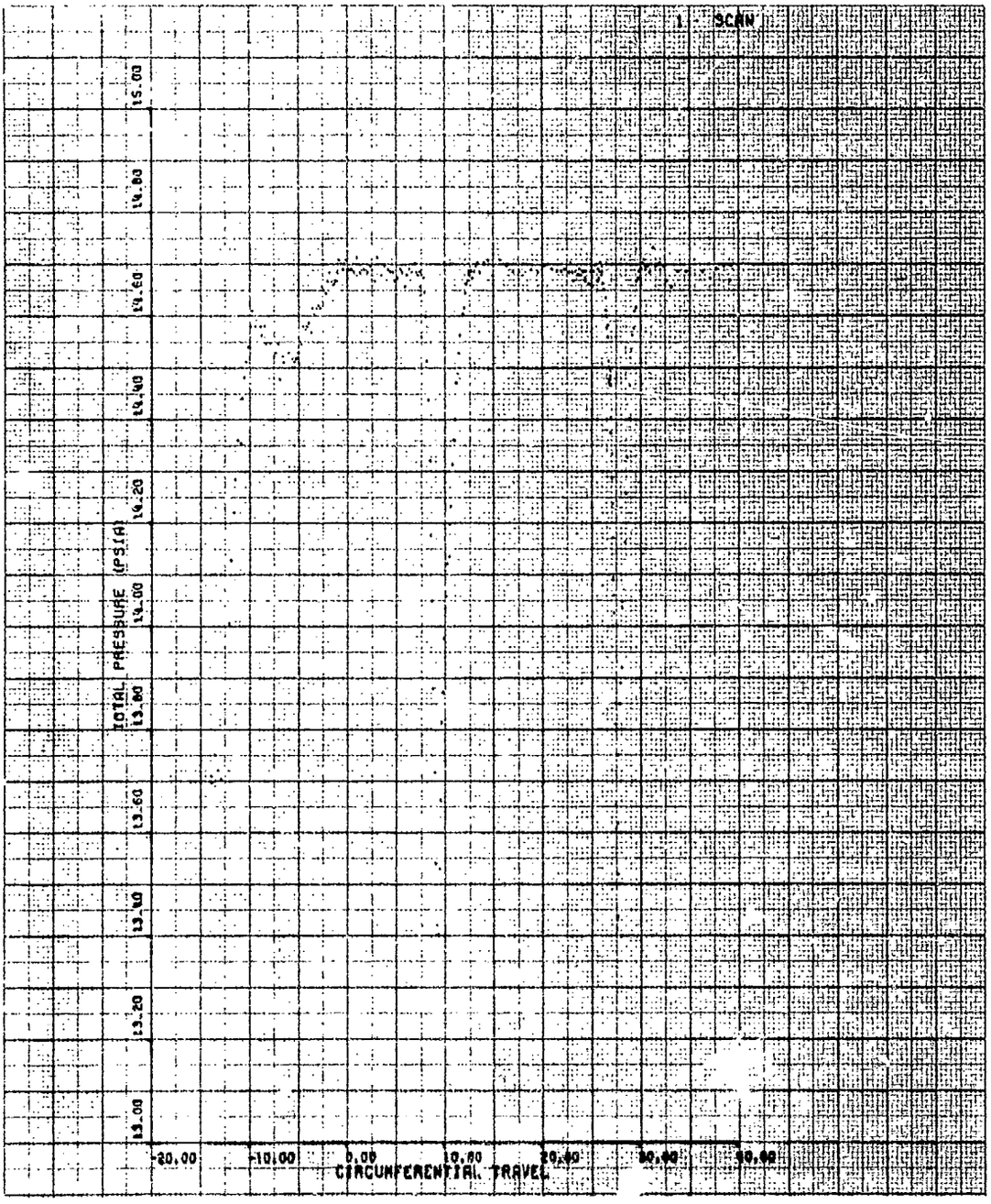

Figure 132. IGV Circumferential Traverse, Build No. 6, 101% Speed, -4-deg IGV, 30% Span.

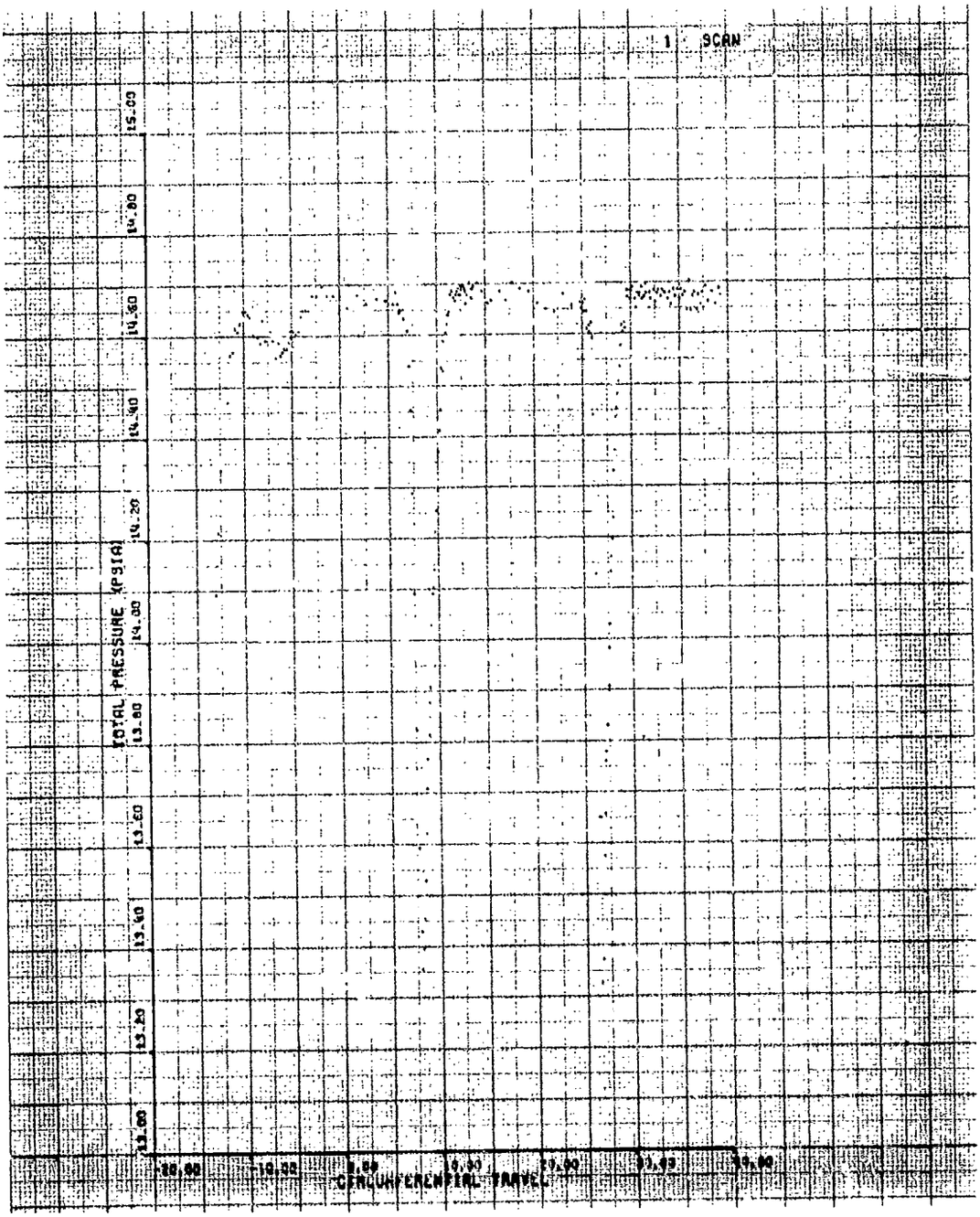

Figure 133. IGV Circumferential Traverse, Build No. 6, 101% Speed, -4-deg IGV, 50% Span.

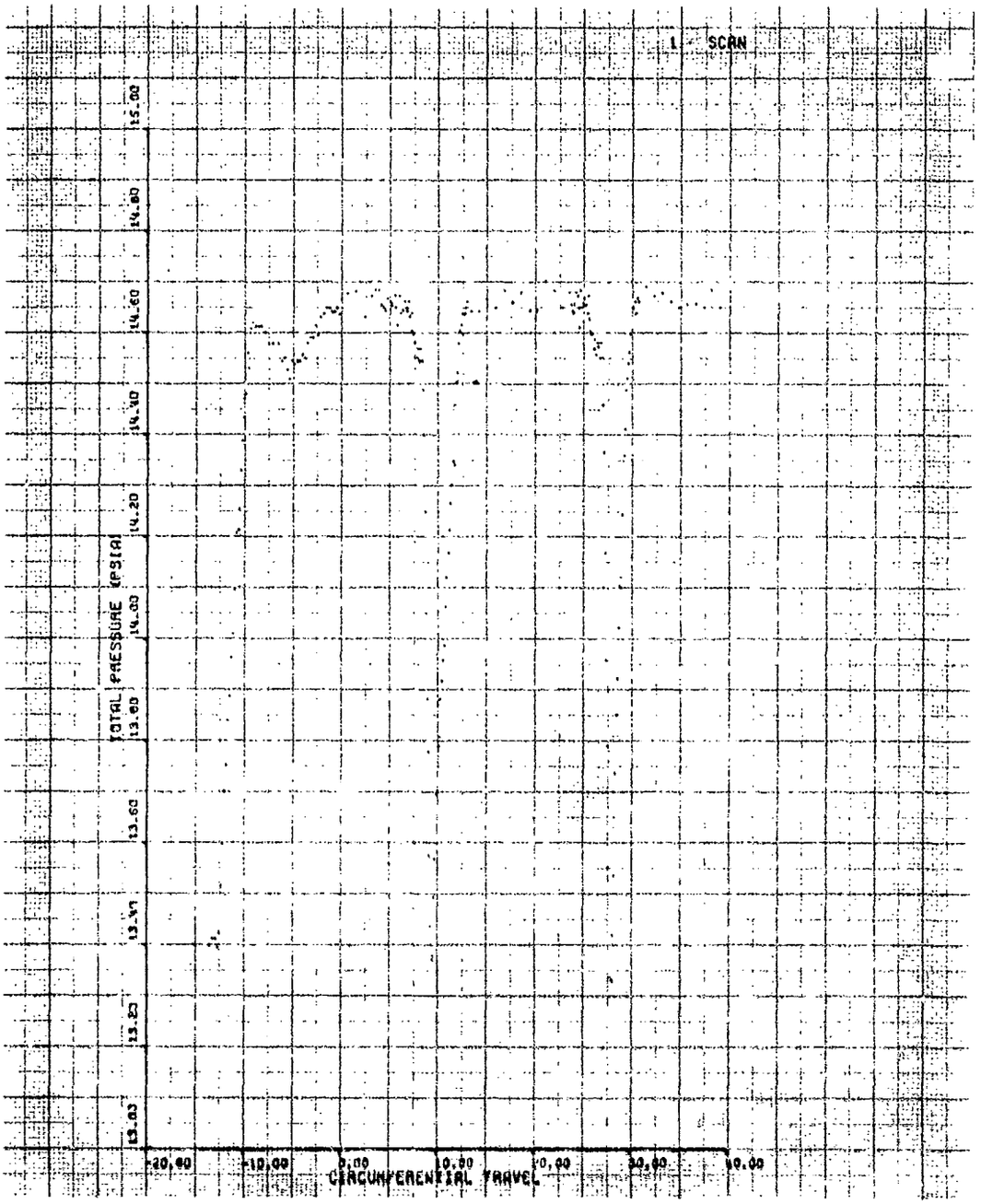

Figure 134. IGV Circumferential Traverse, Build No. 6, 101% Speed, -4-deg IGV, 70% Span.

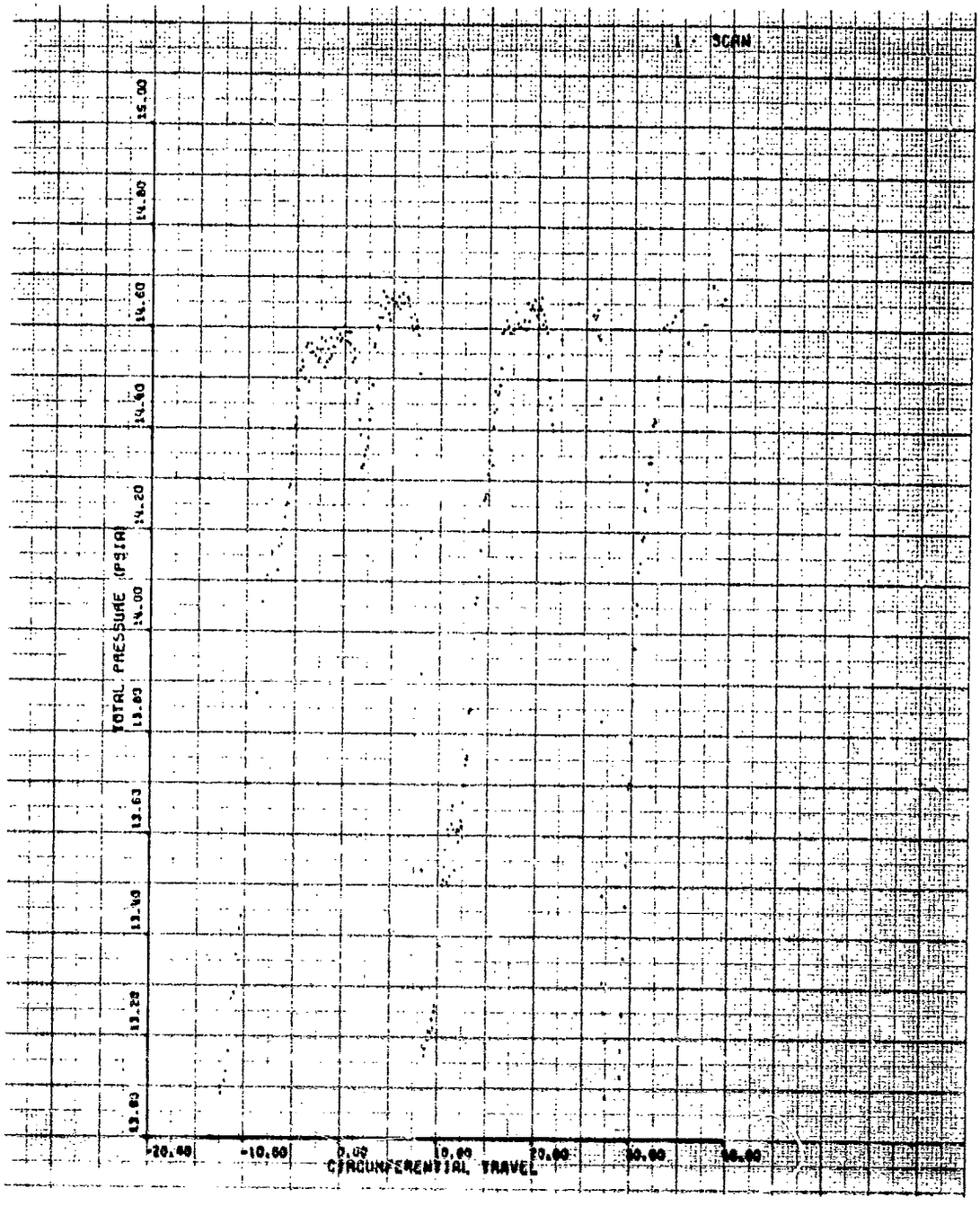

Figure 135. IGV Circumferential Traverse, Build No. 6, 101% Speed, -4-deg IGV, 90% Span.

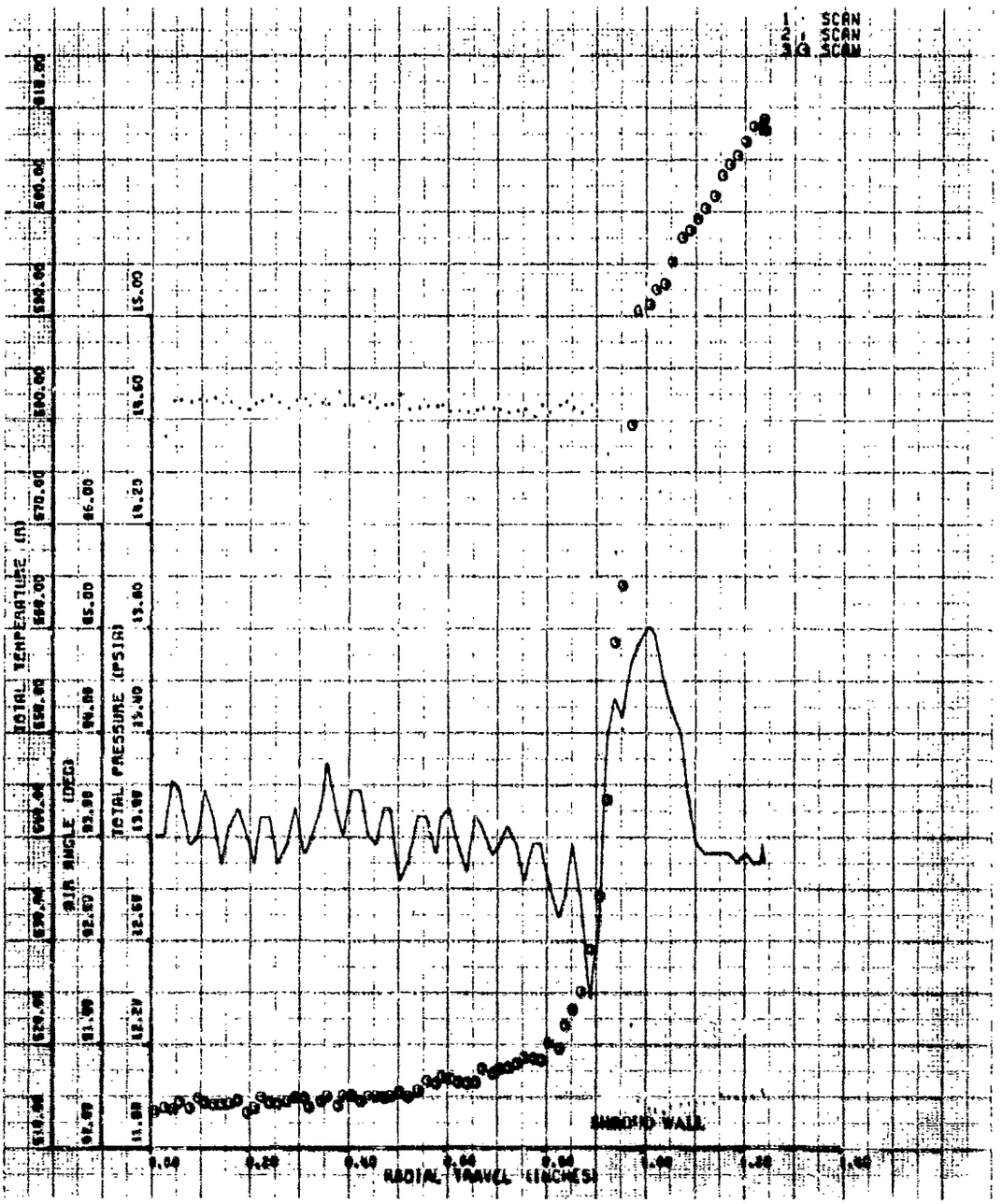

Figure 136. IGV Exit Radial Traverse, Build No. 6, 101% Speed, -5-deg IGV.

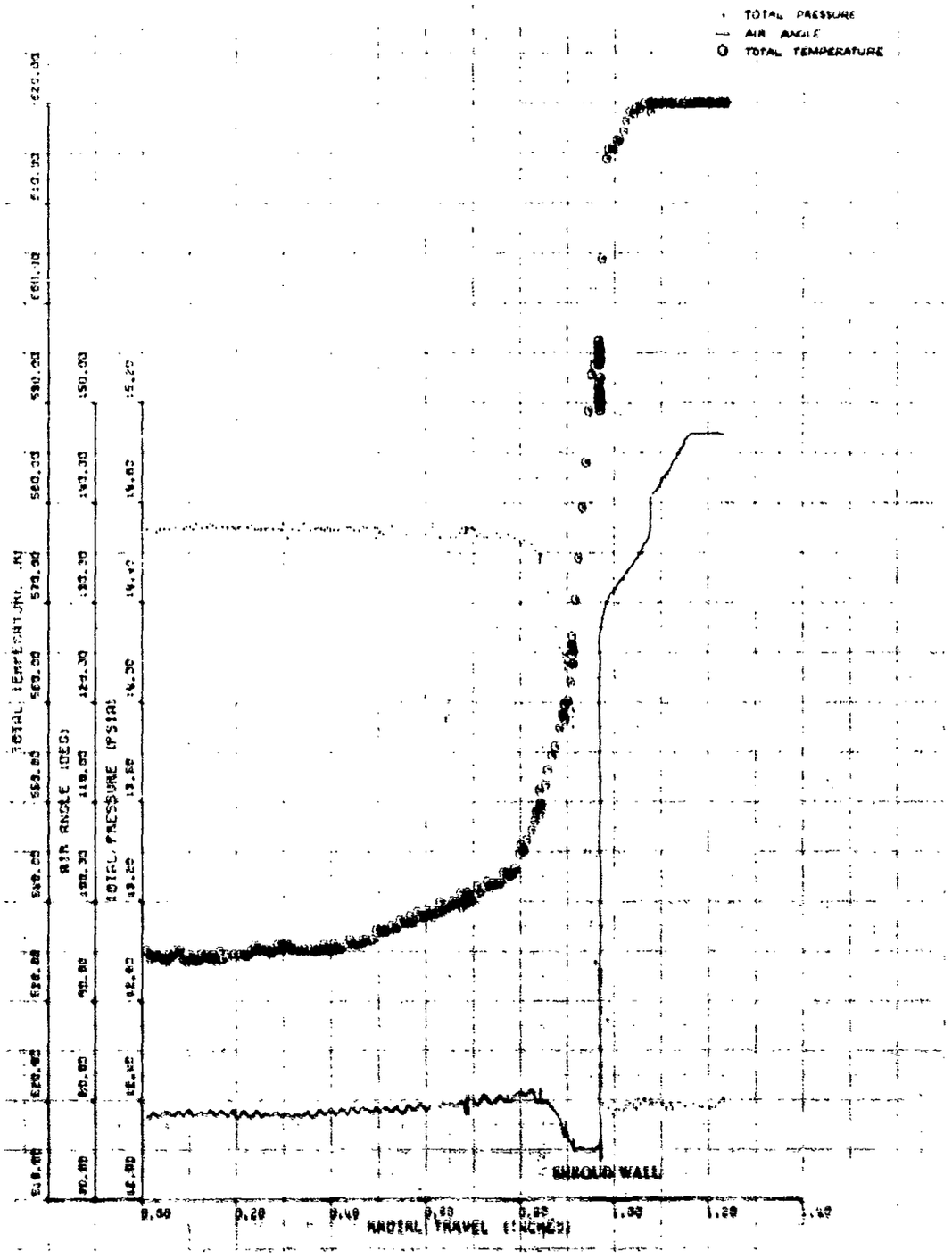

Figure 137. IGV Exit Radial Traverse, Build No. 6, 100% Speed, 10-deg IGV, Near Stall.

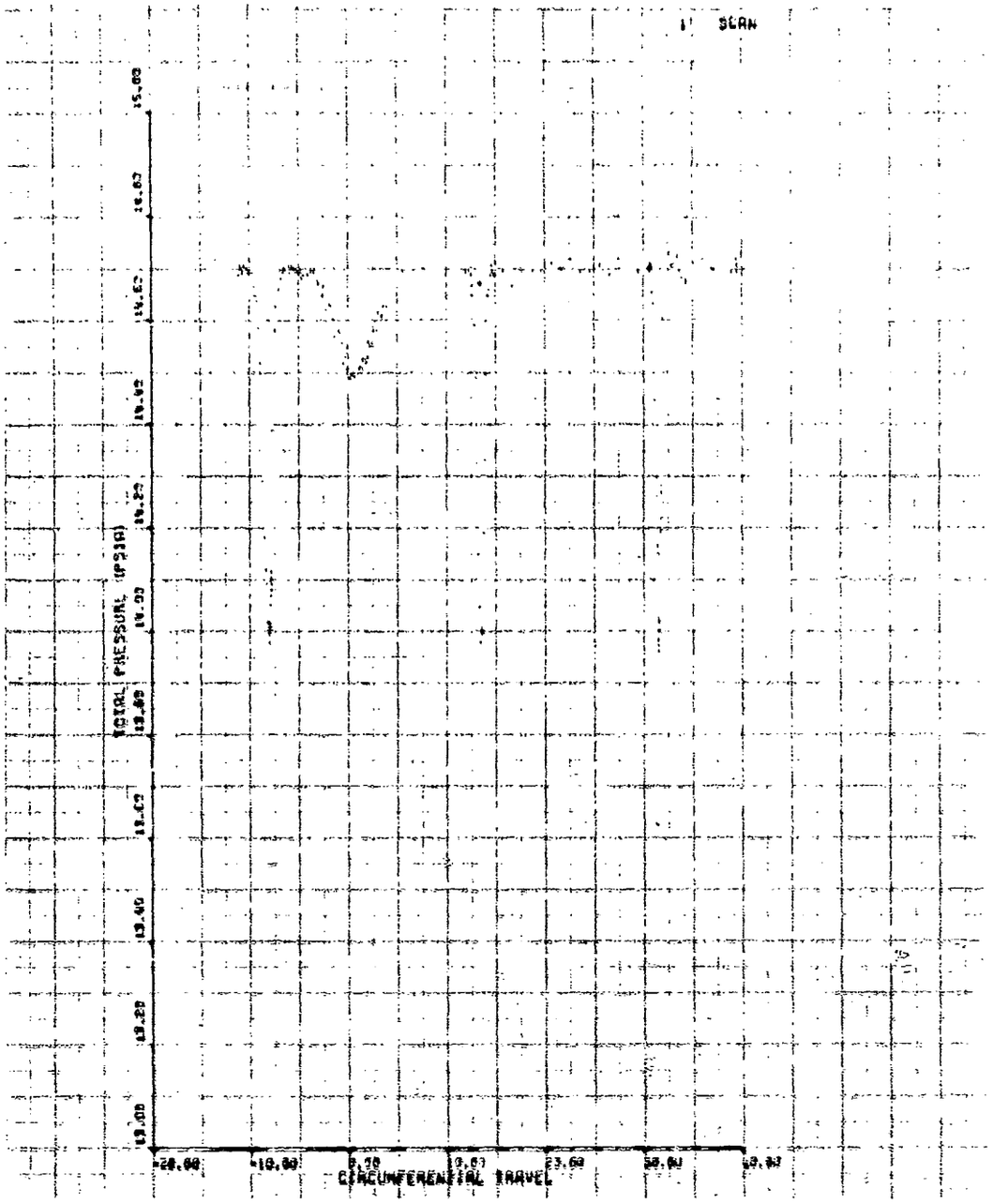

Figure 138. IGV Circumferential Traverse, Build No. 6, 100% Speed, 10-deg IGV, 10% Span.

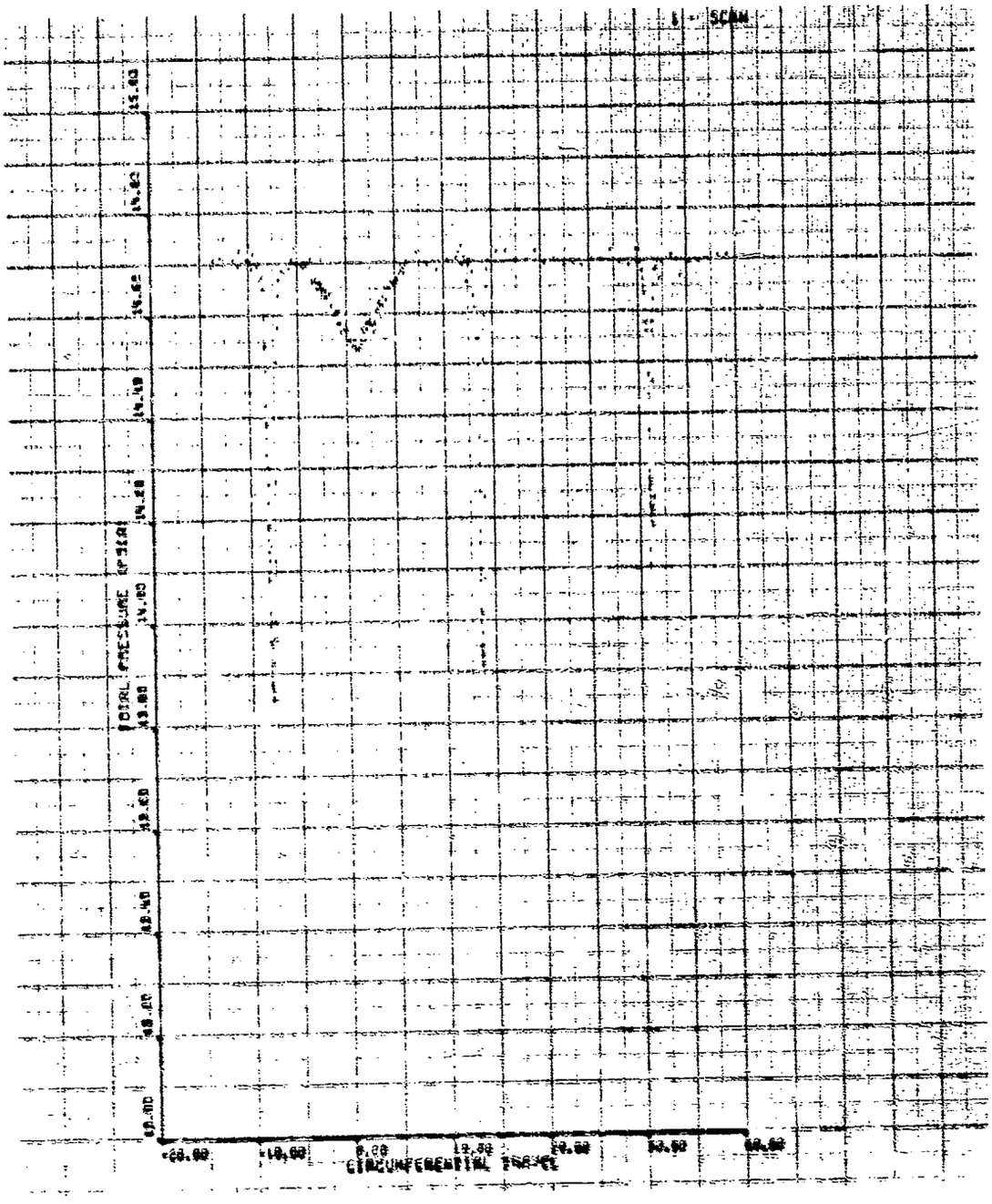

Figure 139. IGV Circumferential Traverse, Build No. 6, 100% Speed, 10-deg IGV, 30% Span.

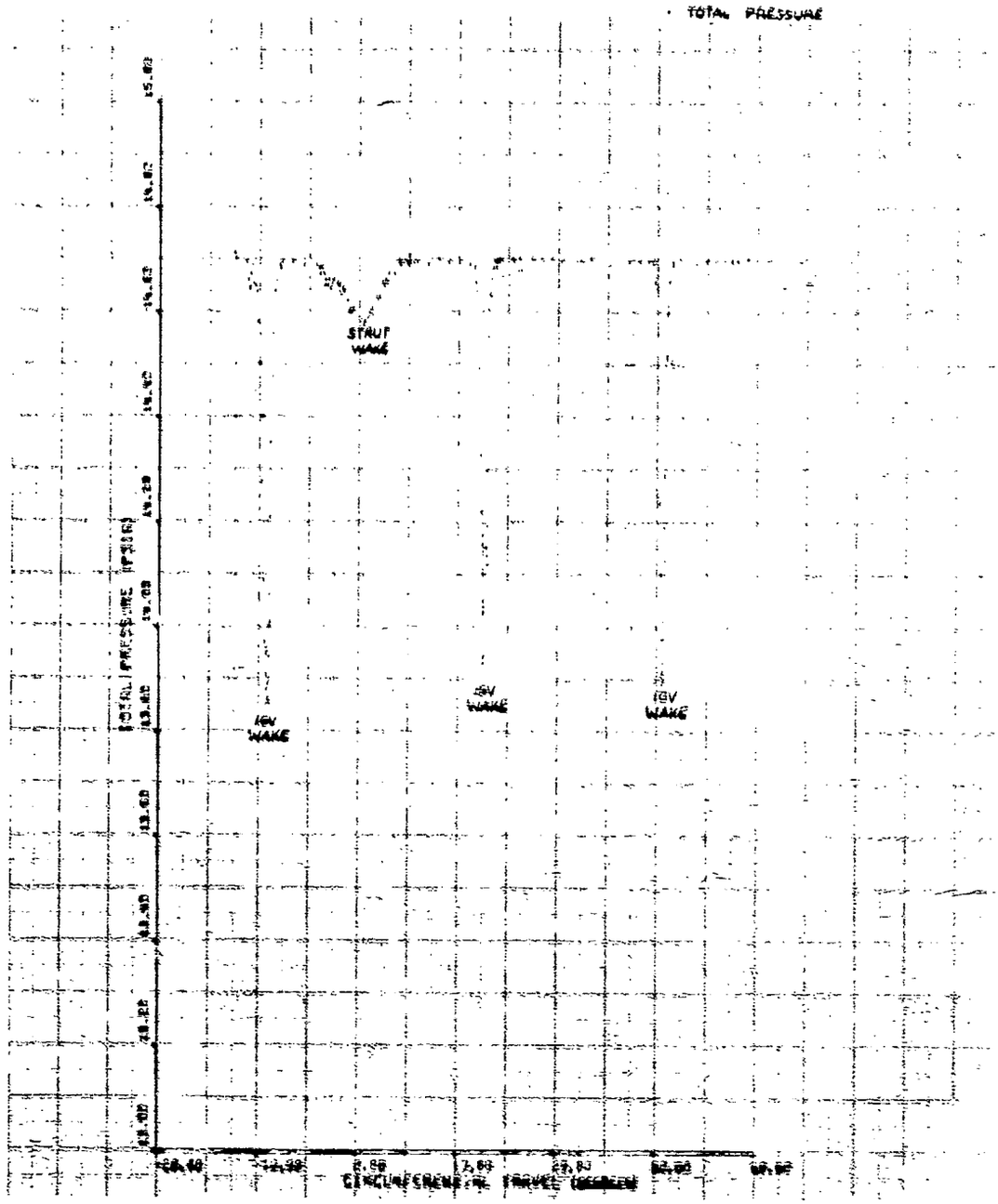

Figure 140. IGV Circumferential Traverse, Build No. 6, 100% Speed, 10-deg IGV, 50% Span.

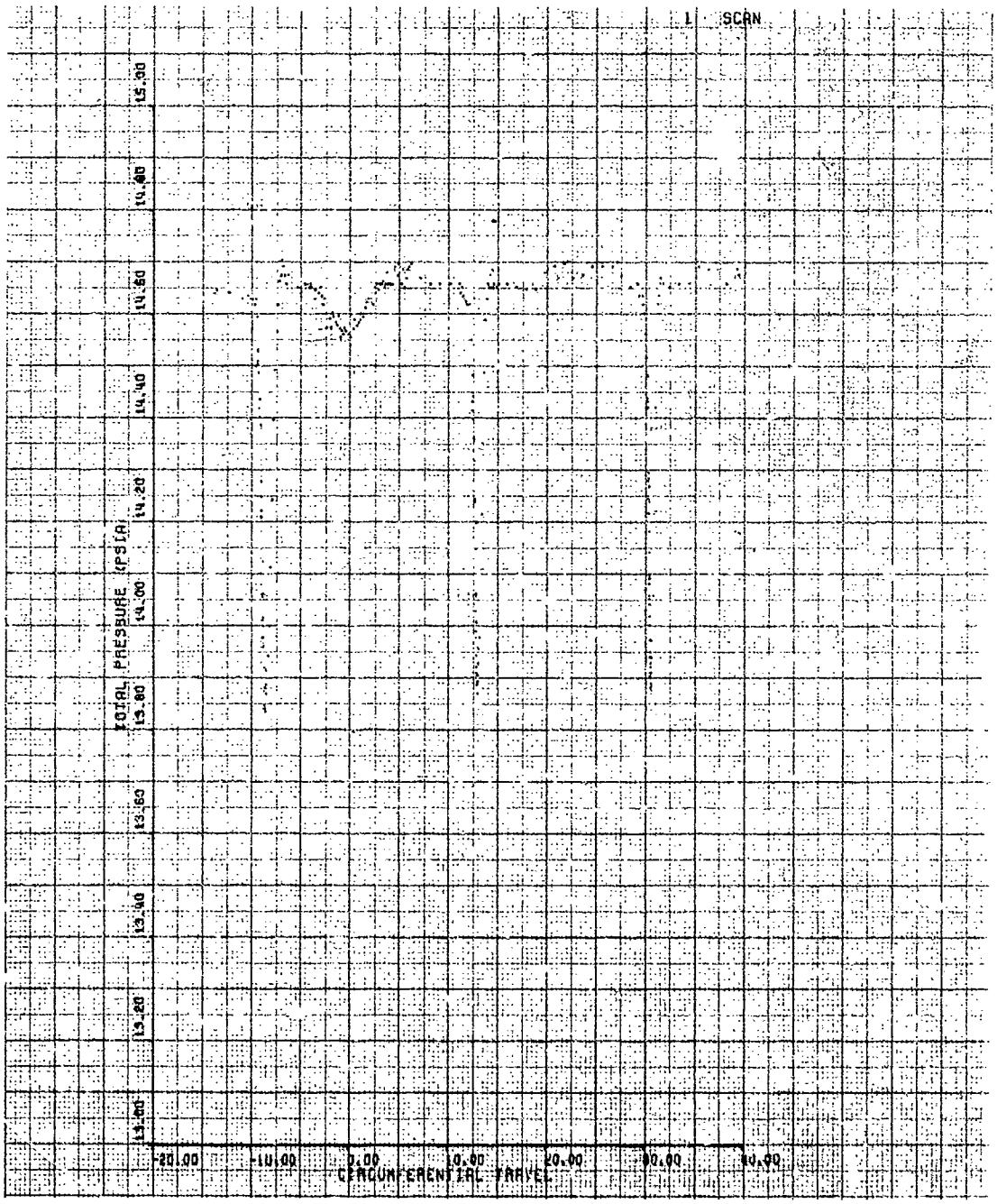

Figure 141. IGV Circumferential Traverse, Build No. 6, 100% Speed, 10-deg IGV, 70% Span.

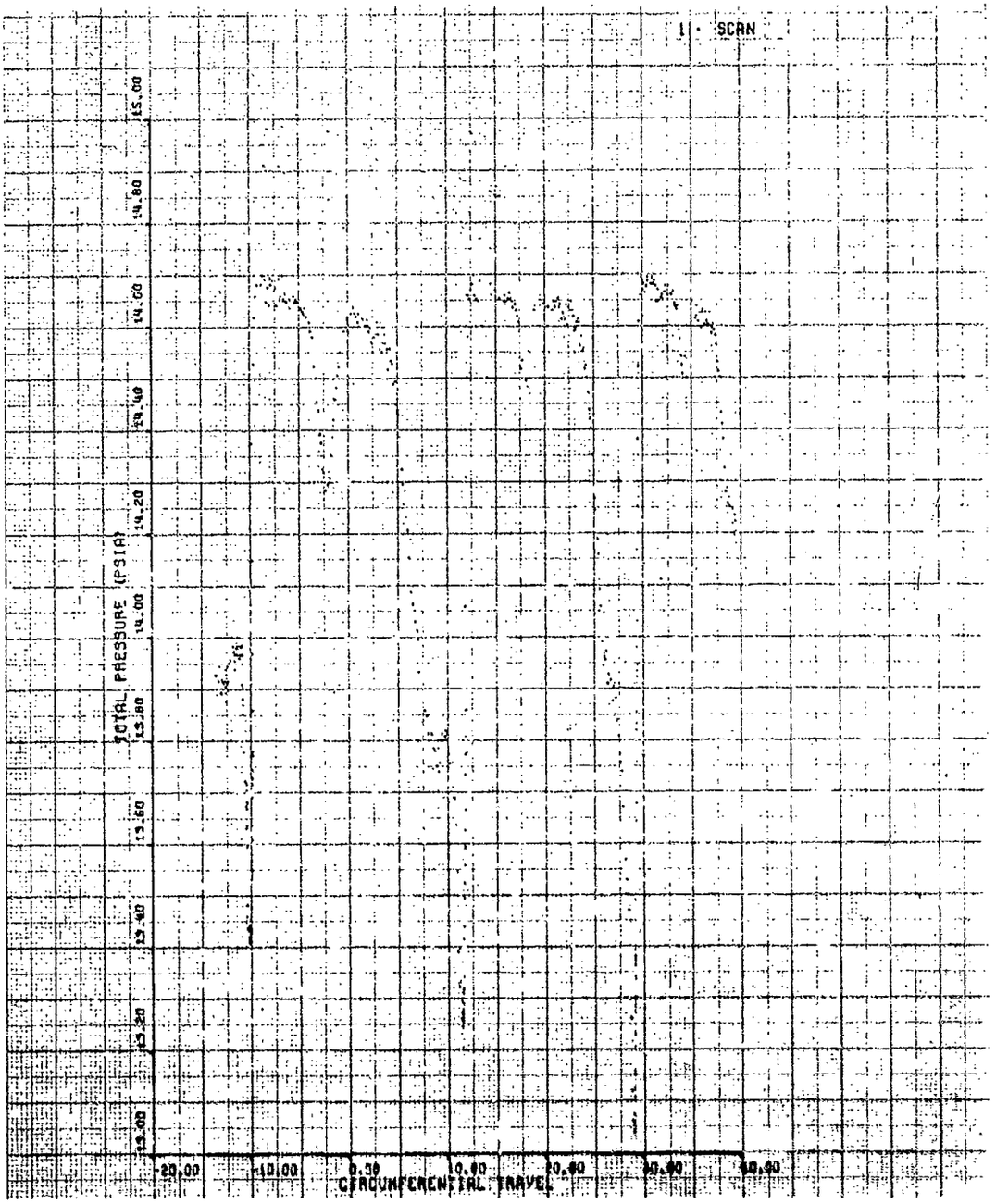

Figure 142. IGV Circumferential Traverse, Build No. 6, 100% Speed, 10-deg IGV, 90% Span.

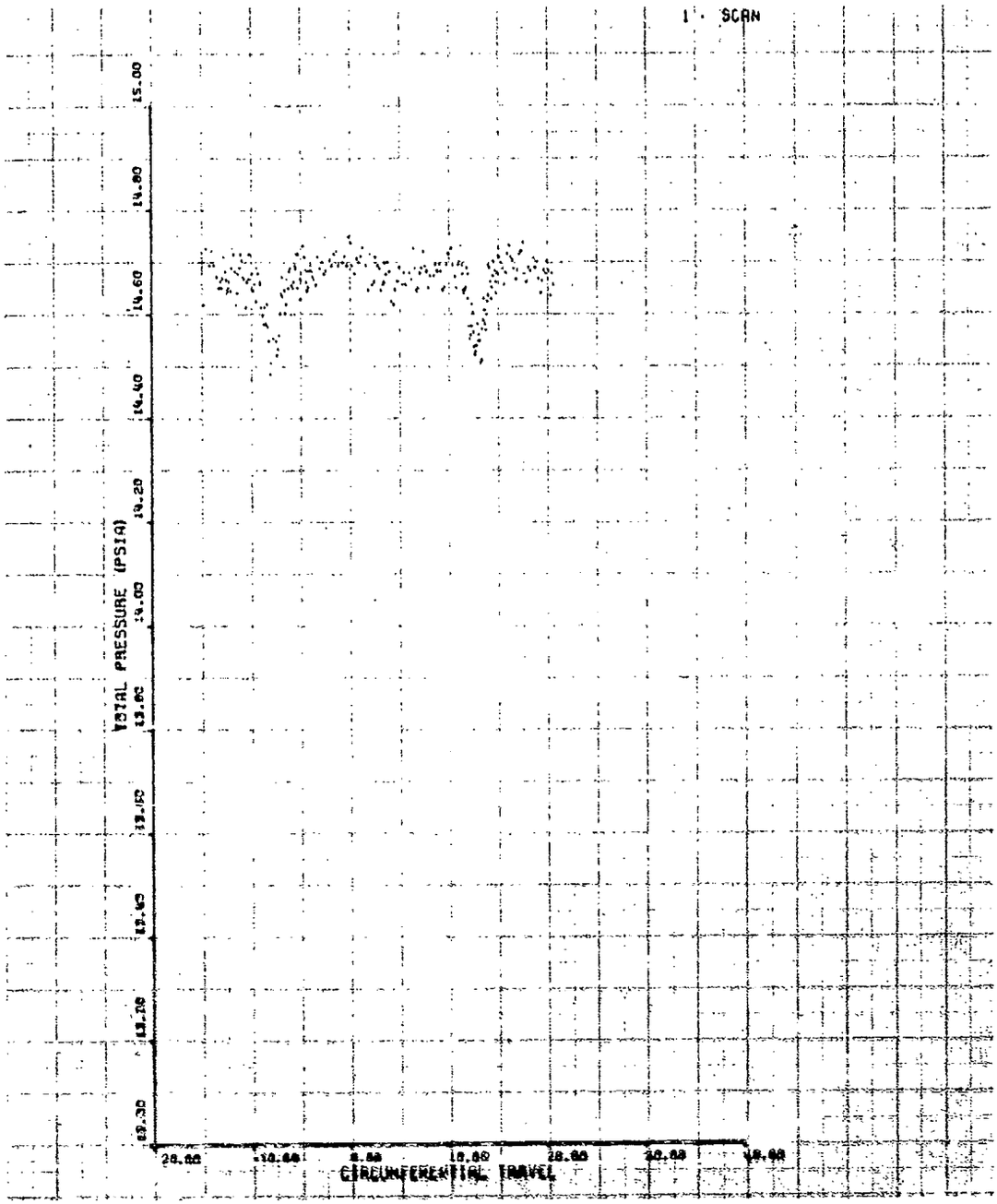

Figure 143. IGV Circumferential Traverse, Build No. 3, 70% Speed, 10-deg IGV, 10% Span.

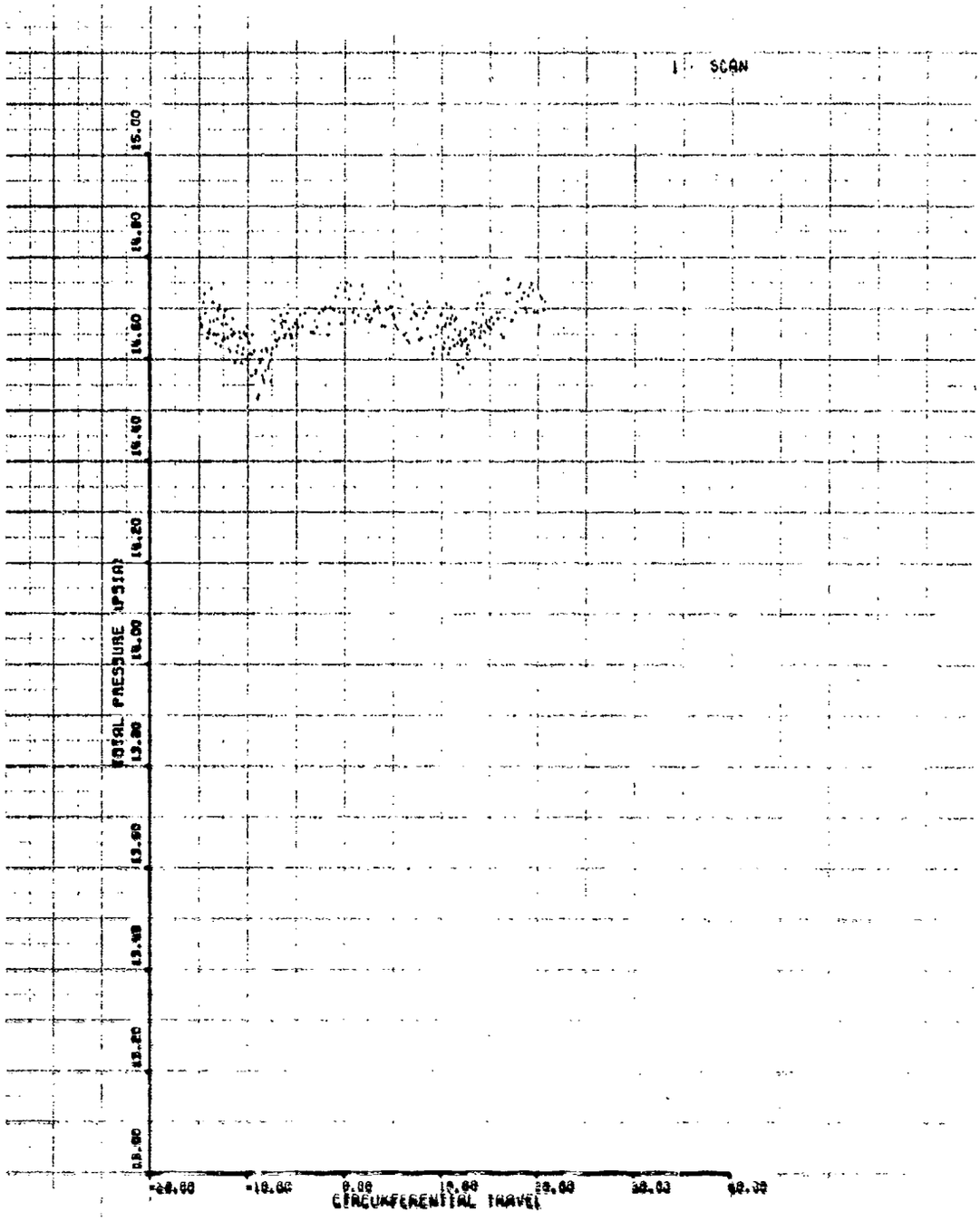

Figure 144. IGV Circumferential Traverse, Build No. 3, 70% Speed, 10-deg IGV, 30% Span.

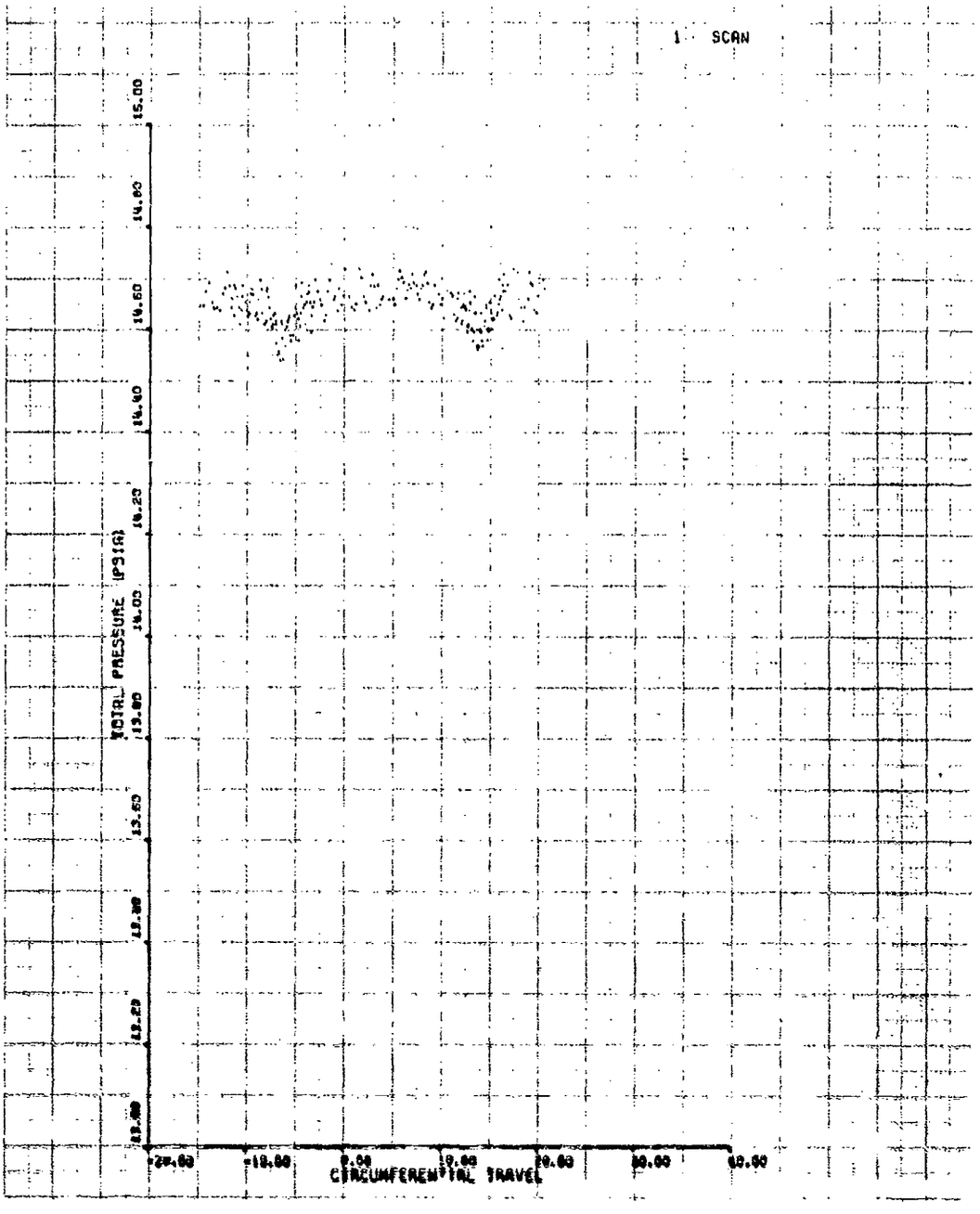

Figure 145. IGV Circumferential Traverse, Build No. 3, 70% Speed, 10-deg IGV, 50% Span.

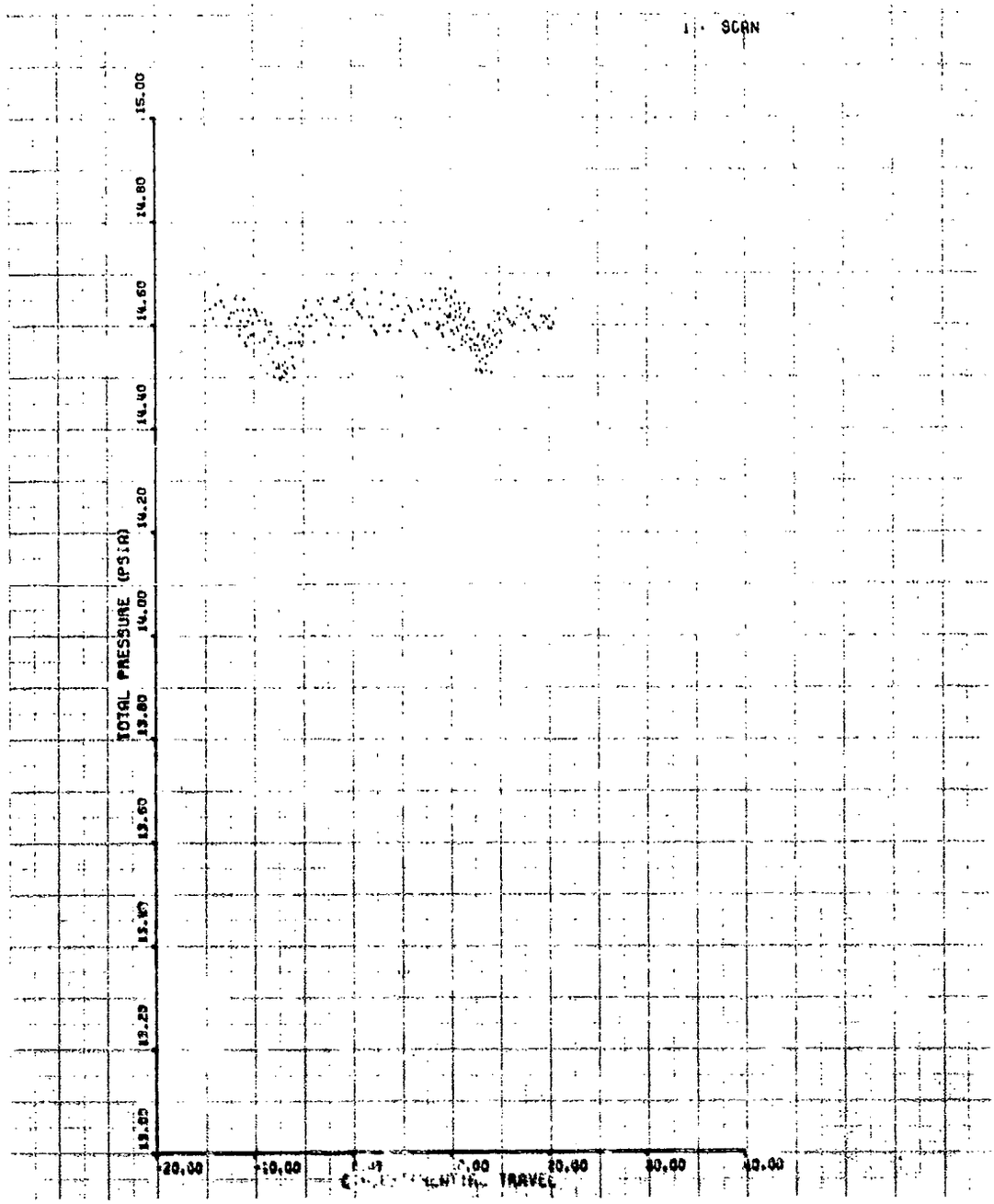

Figure 146. IGV Circumferential Traverse, Build No. 3, 70% Speed, 10-deg IGV, 70% Span.

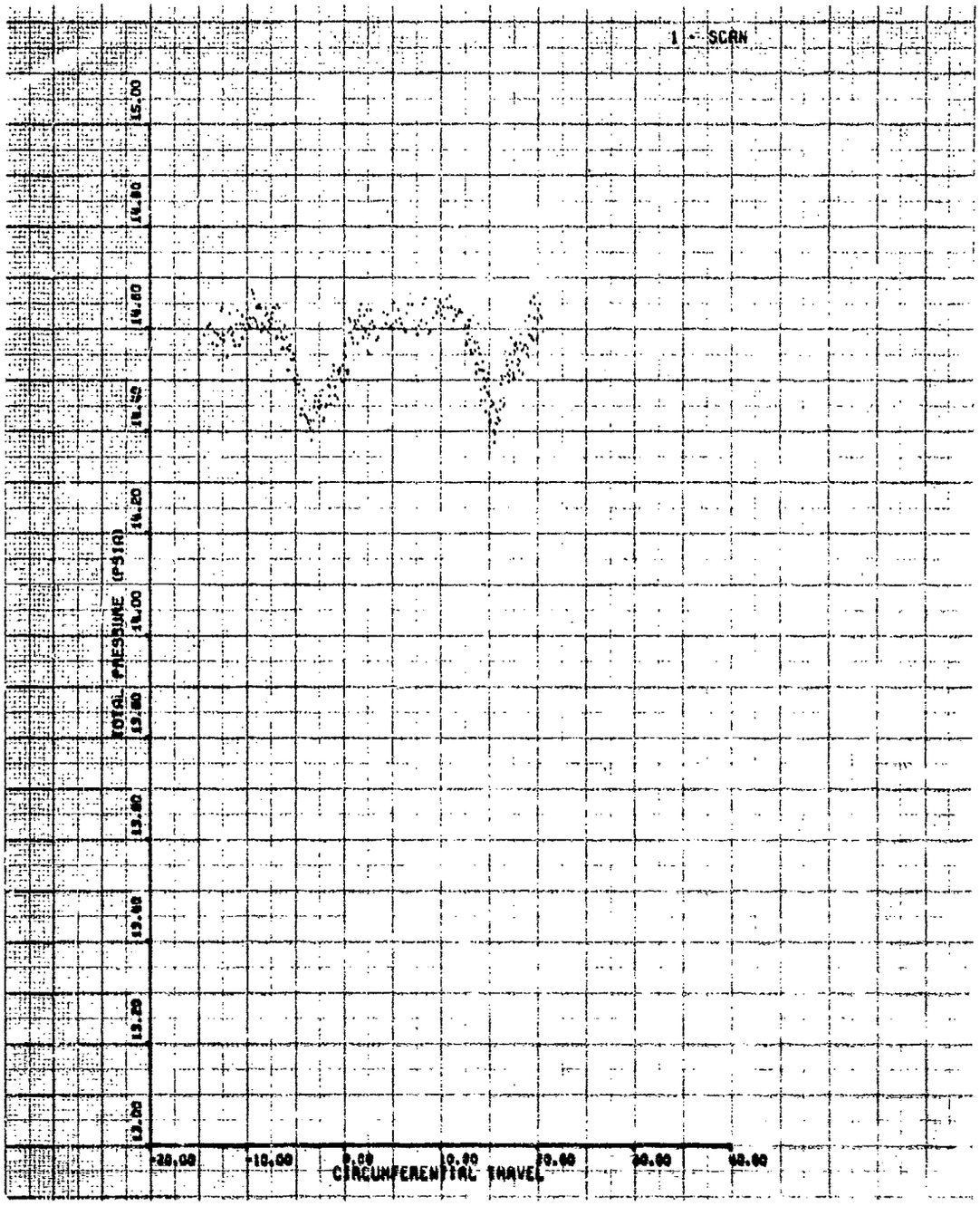

Figure 147. IGV Circumferential Traverse, Build No. 3, 70% Speed, 10-deg IGV, 90% Span.

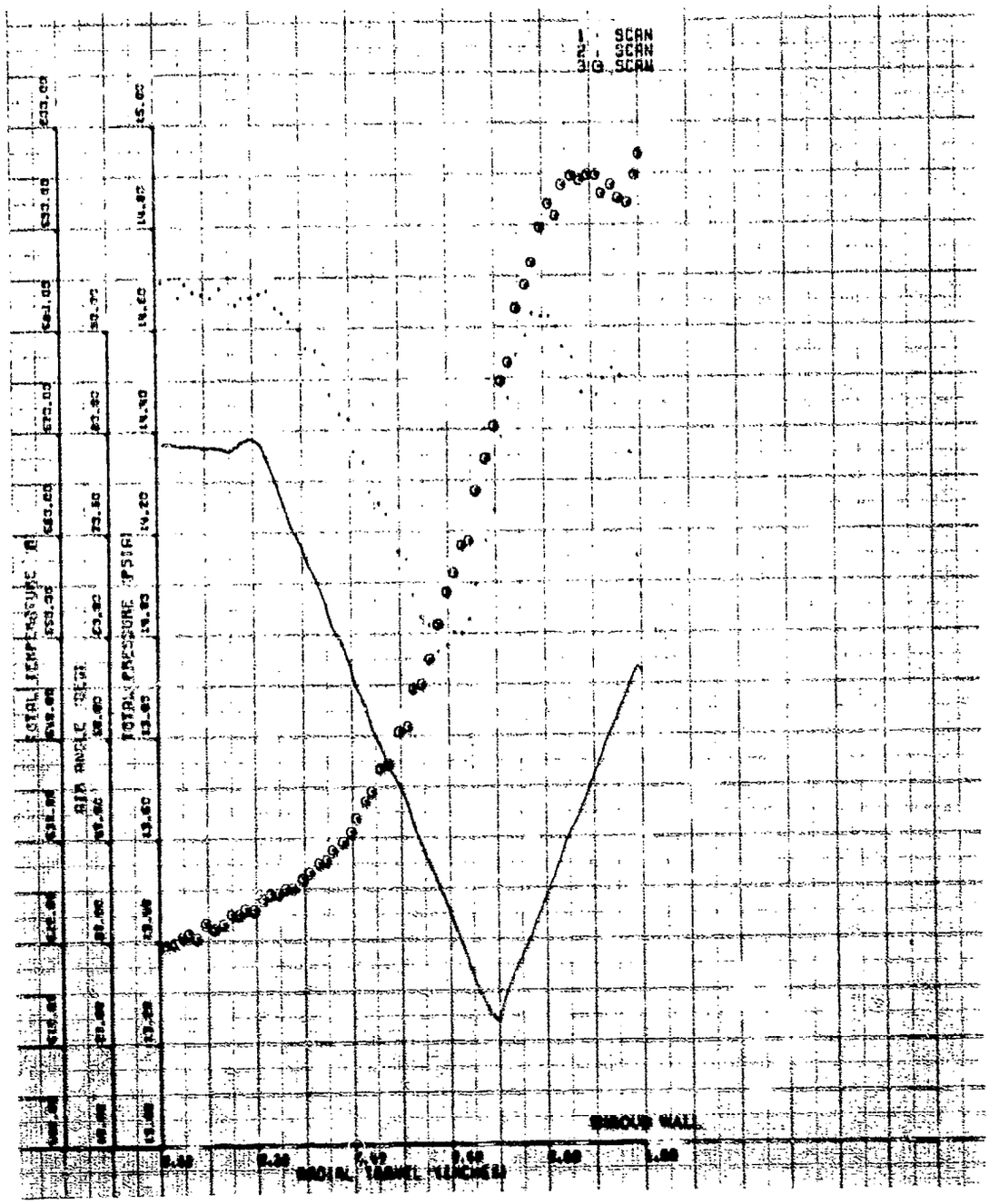

Figure 148. IGV Exit Radial Traverse, Build No. 6, 70% Speed, 10-deg IGV, Near Stall.

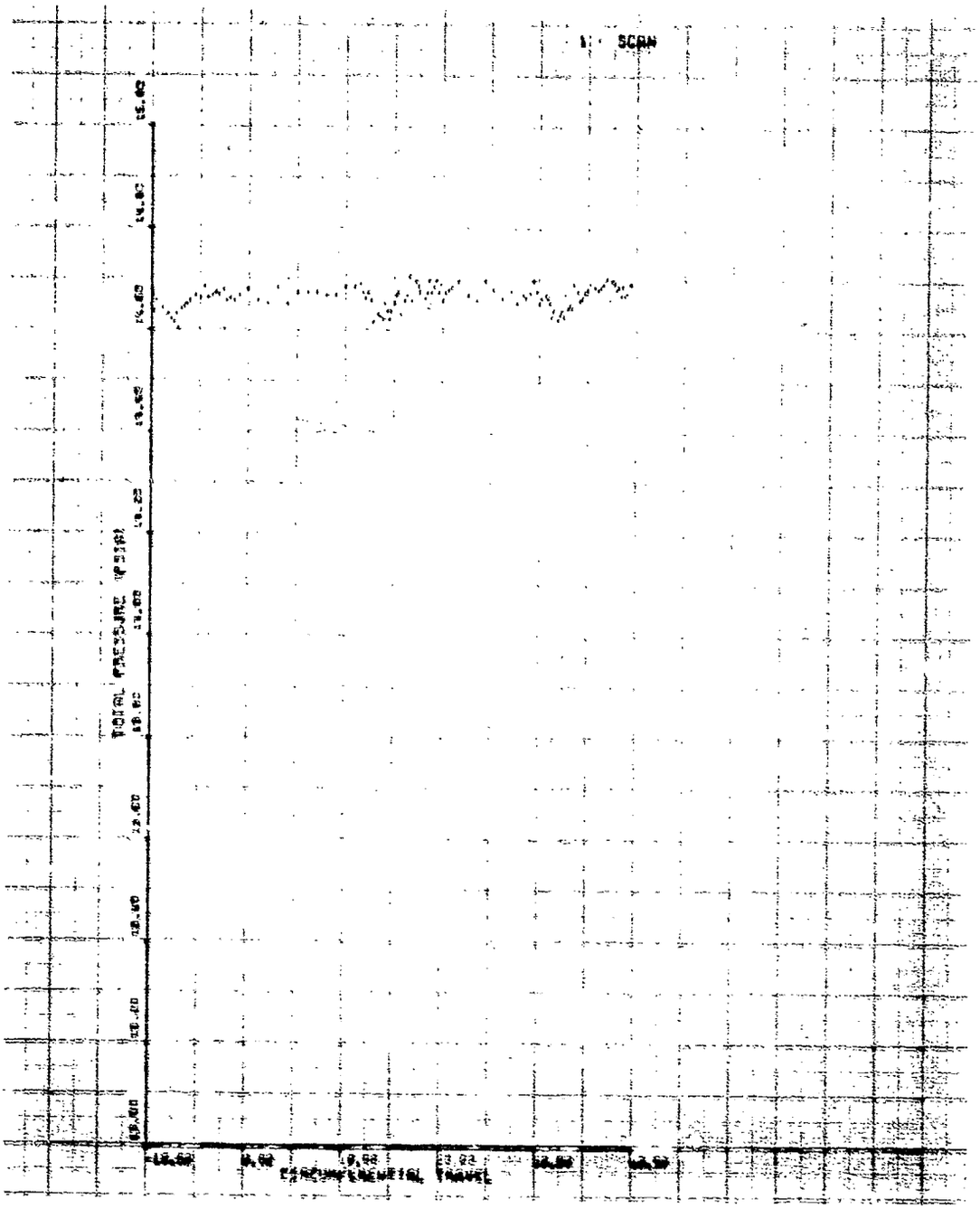

Figure 149. IGV Circumferential Trave, e, Build No. 6, 70% Speed, 10-deg IGV, 10% Span.

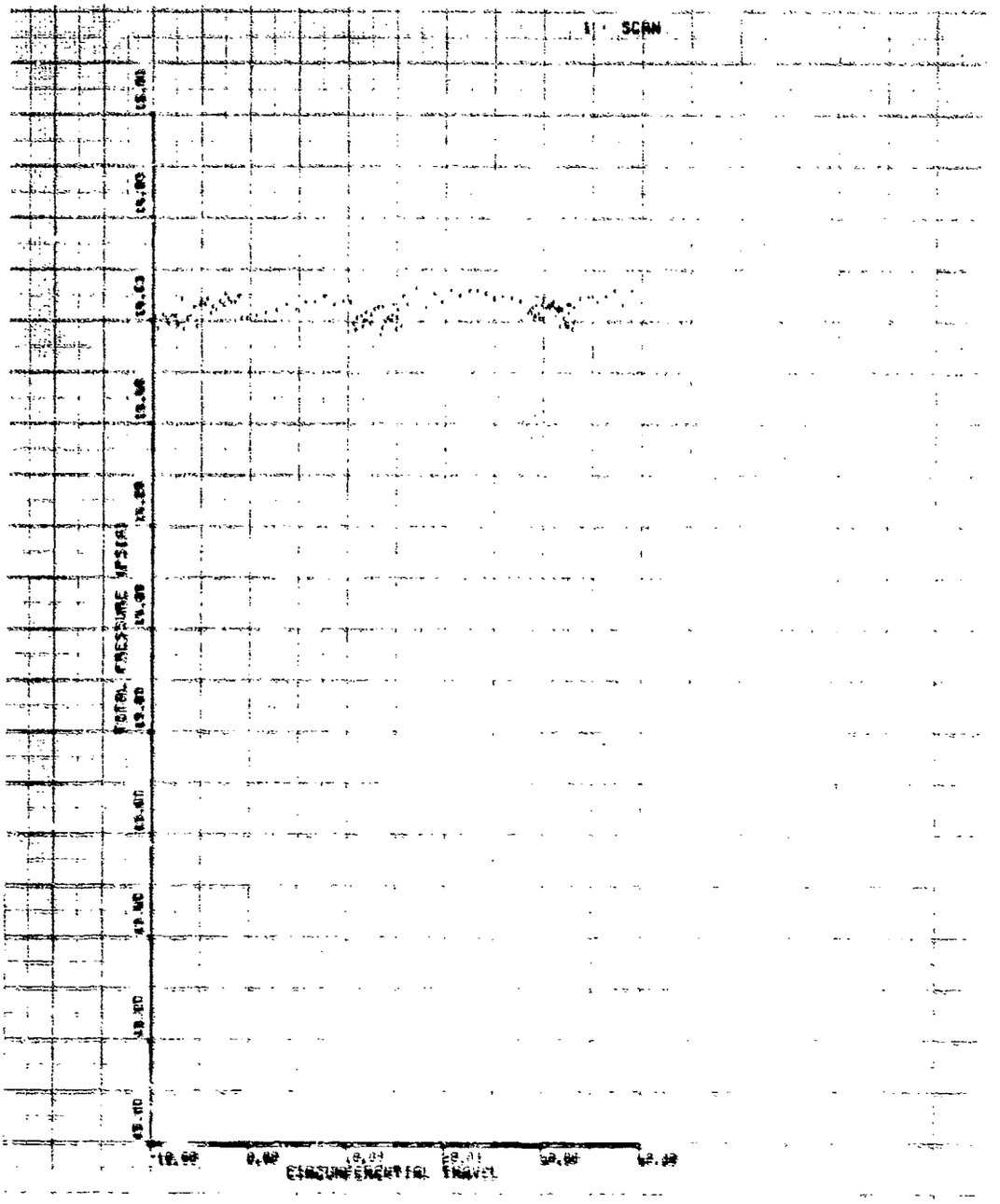

Figure 150. IGV Circumferential Traverse, Build No. 6, 70% Speed, 10-deg IGV, 30% Span.

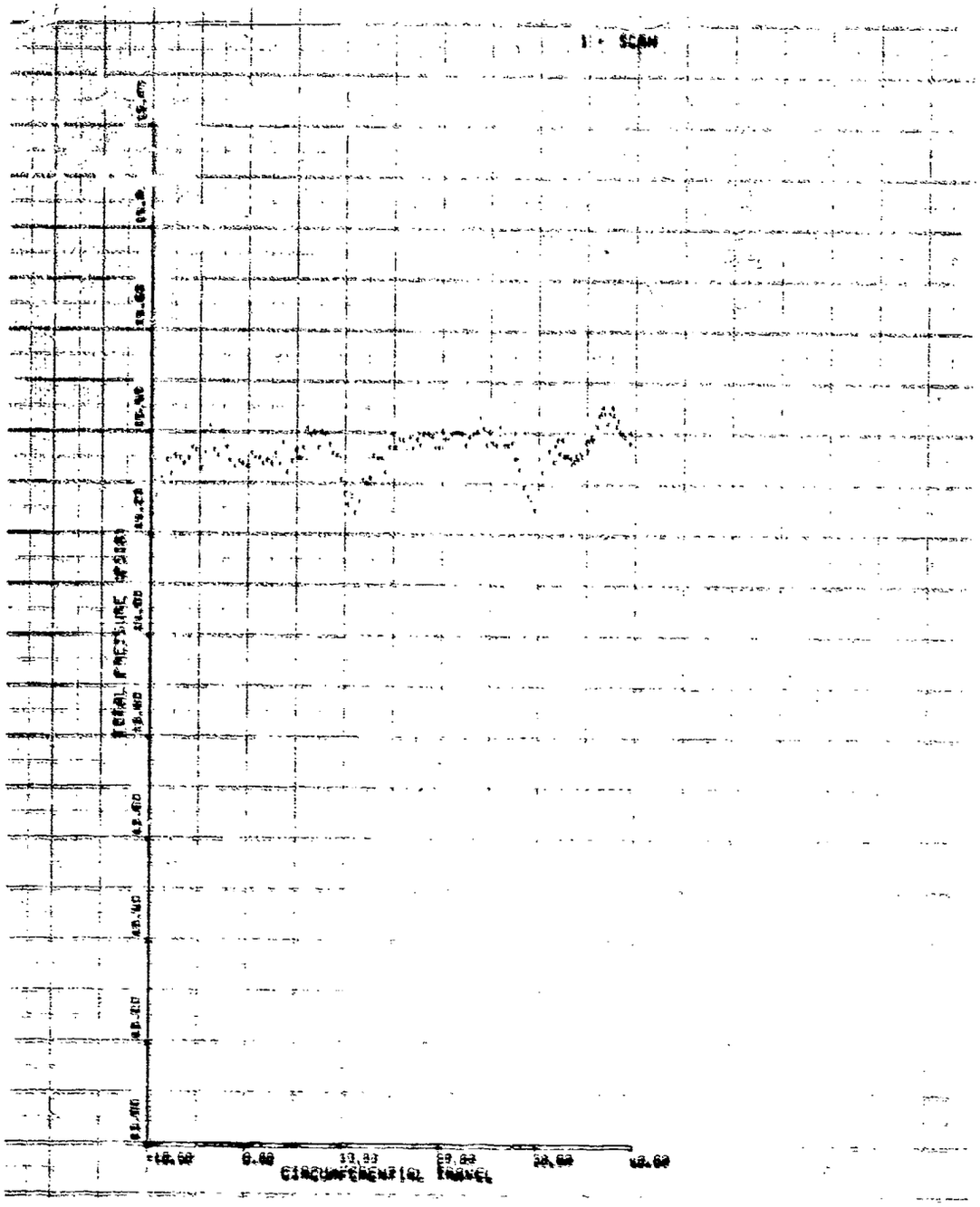

Figure 181. IGV Circumferential Traverse, Build No. 6, 70% Speed, 40-deg IGV, 50% Span.

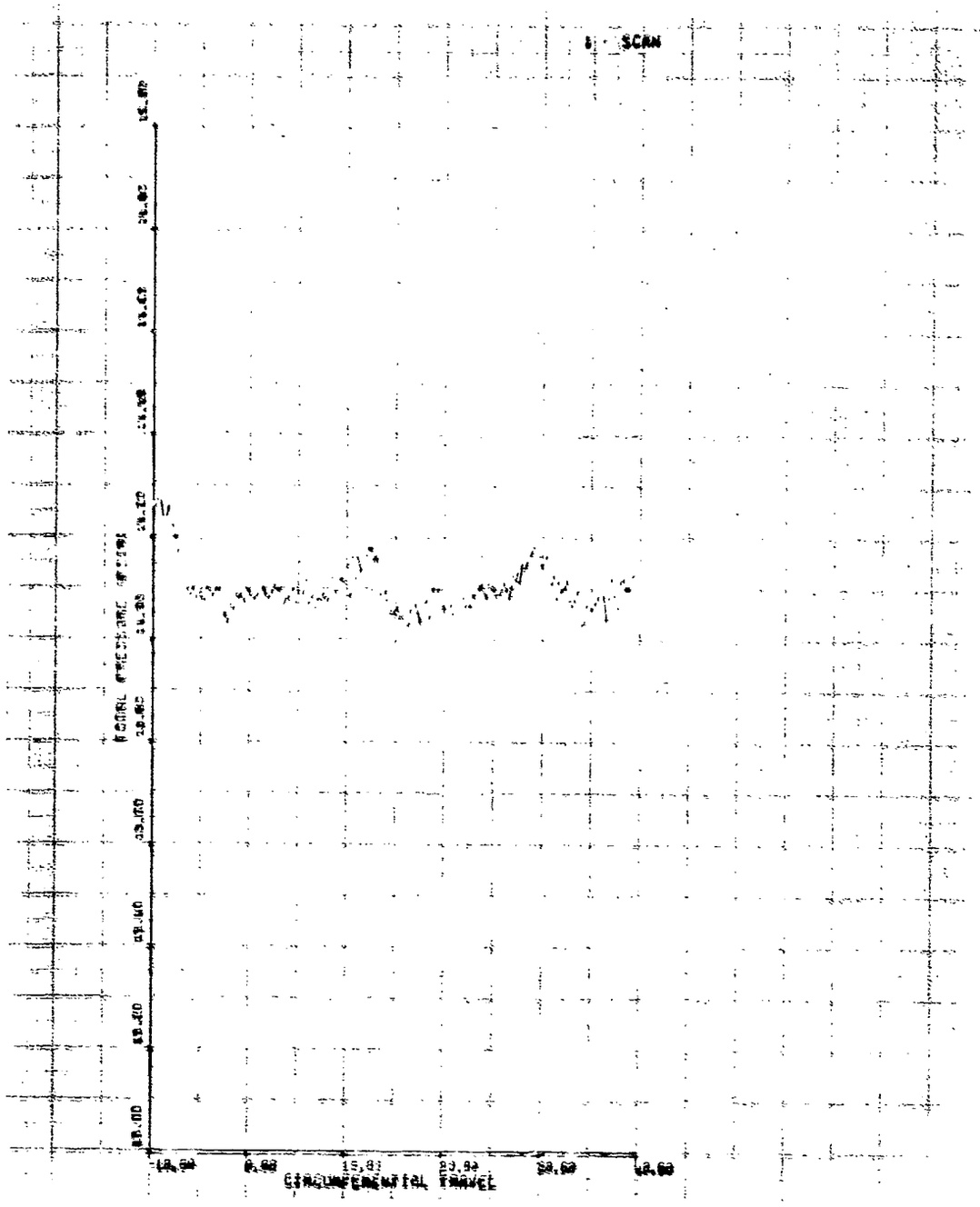

Figure 152. IGV Circumferential Traverse, Build No. 6, 70% Speed, 10-deg IGV, 70% Span.

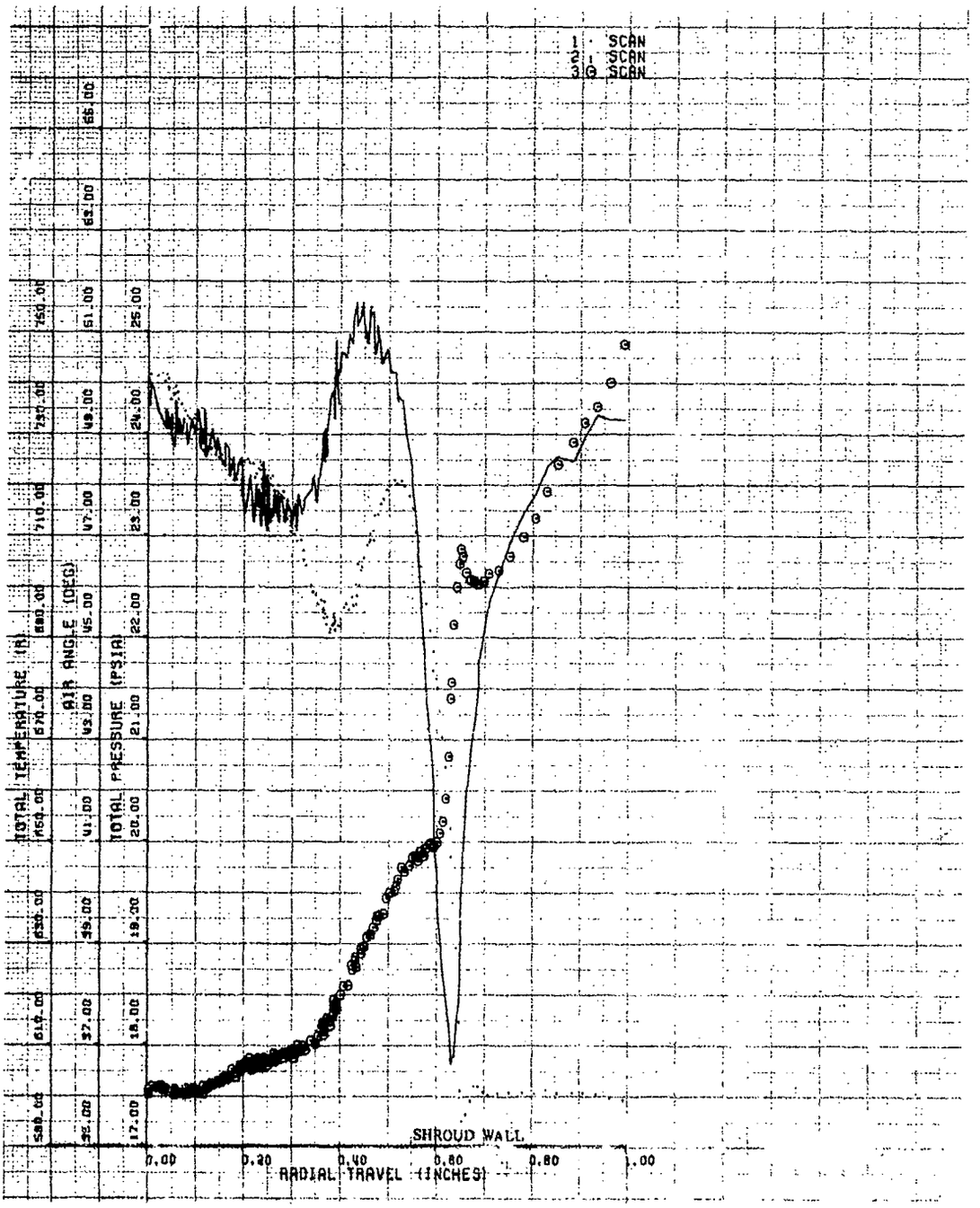

Figure 153. Inducer Exit Traverse, Build No. 6, 101% Speed, 5-deg IGV, Wide Open Discharge.

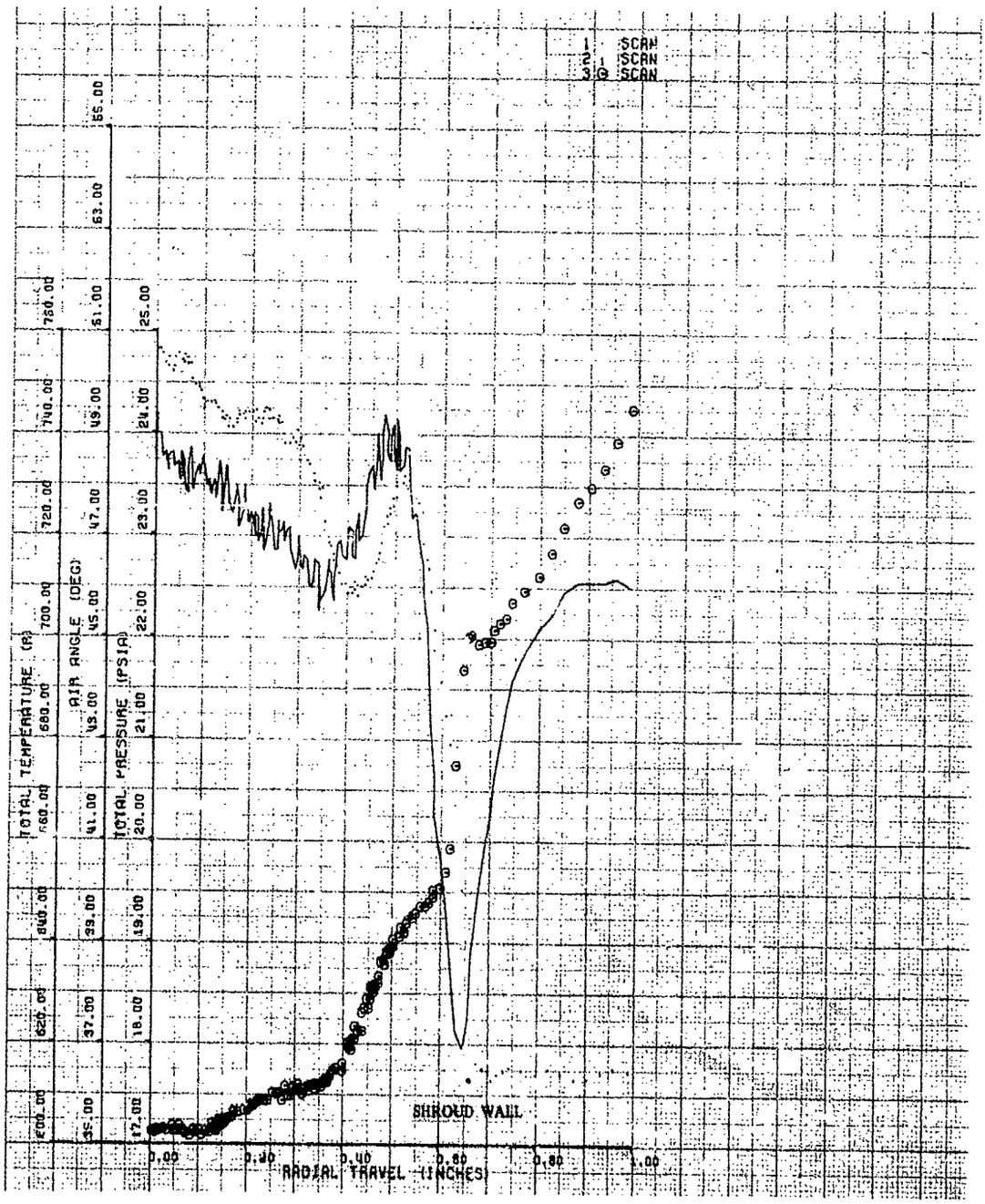

Figure 154. Inducer Exit Traverse, Build No. 6, 101% Speed, 5-deg IGV, Near Stall.

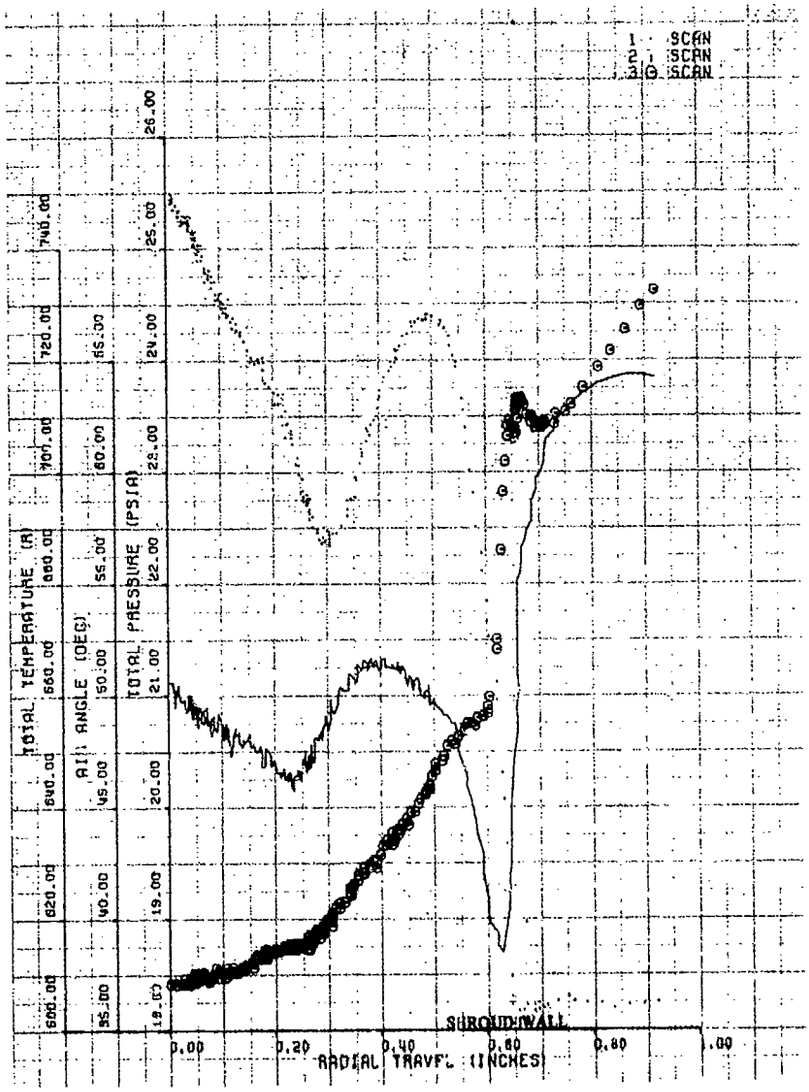

Figure 155. Inducer Exit Traverse, Build No. 6, 101% Speed, 0-deg IGV, Wide Open Discharge.

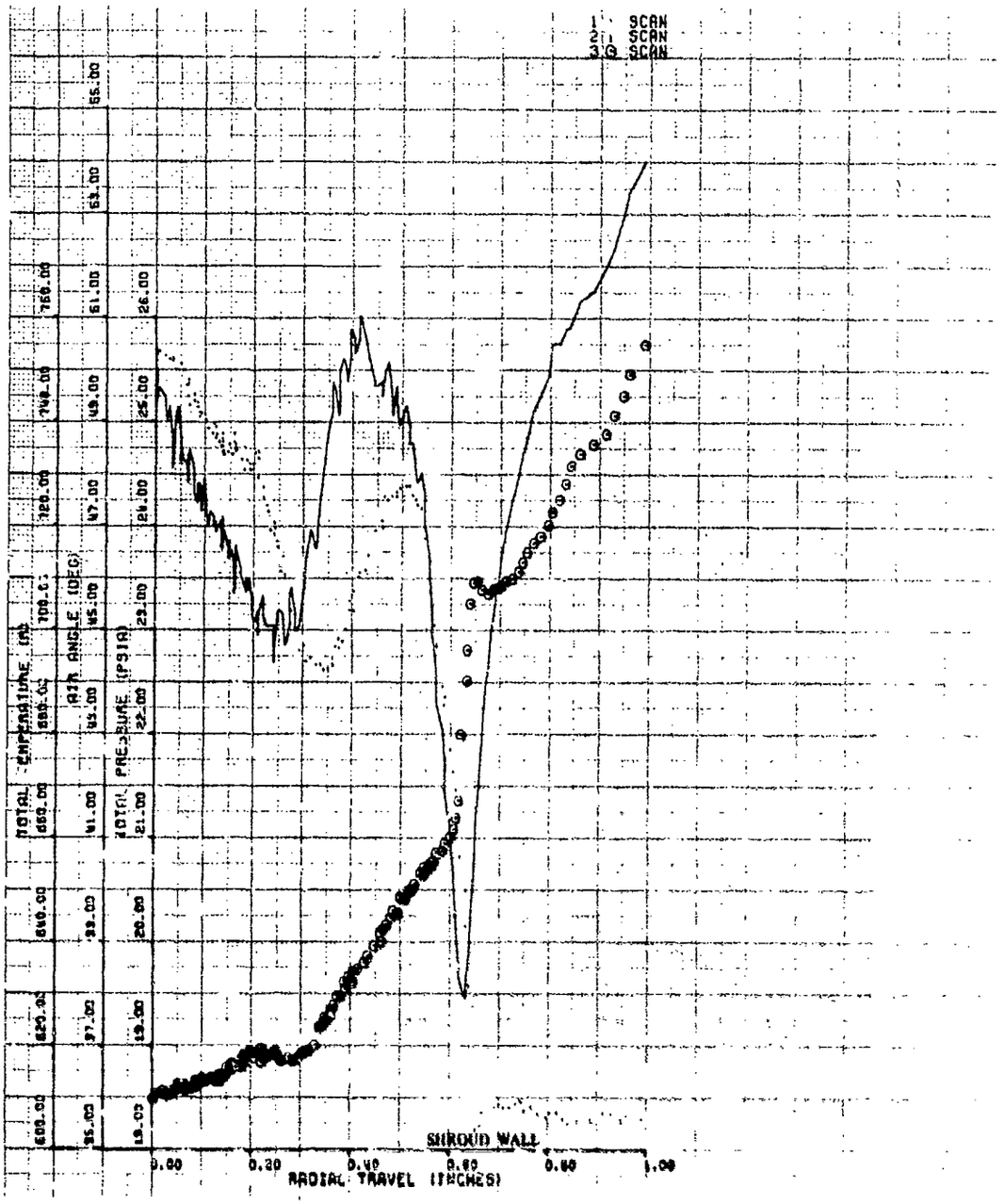

Figure 156. Inducer Exit Traverse, Build No. 6, 101% Speed, 0-deg IGV, Near Stall.

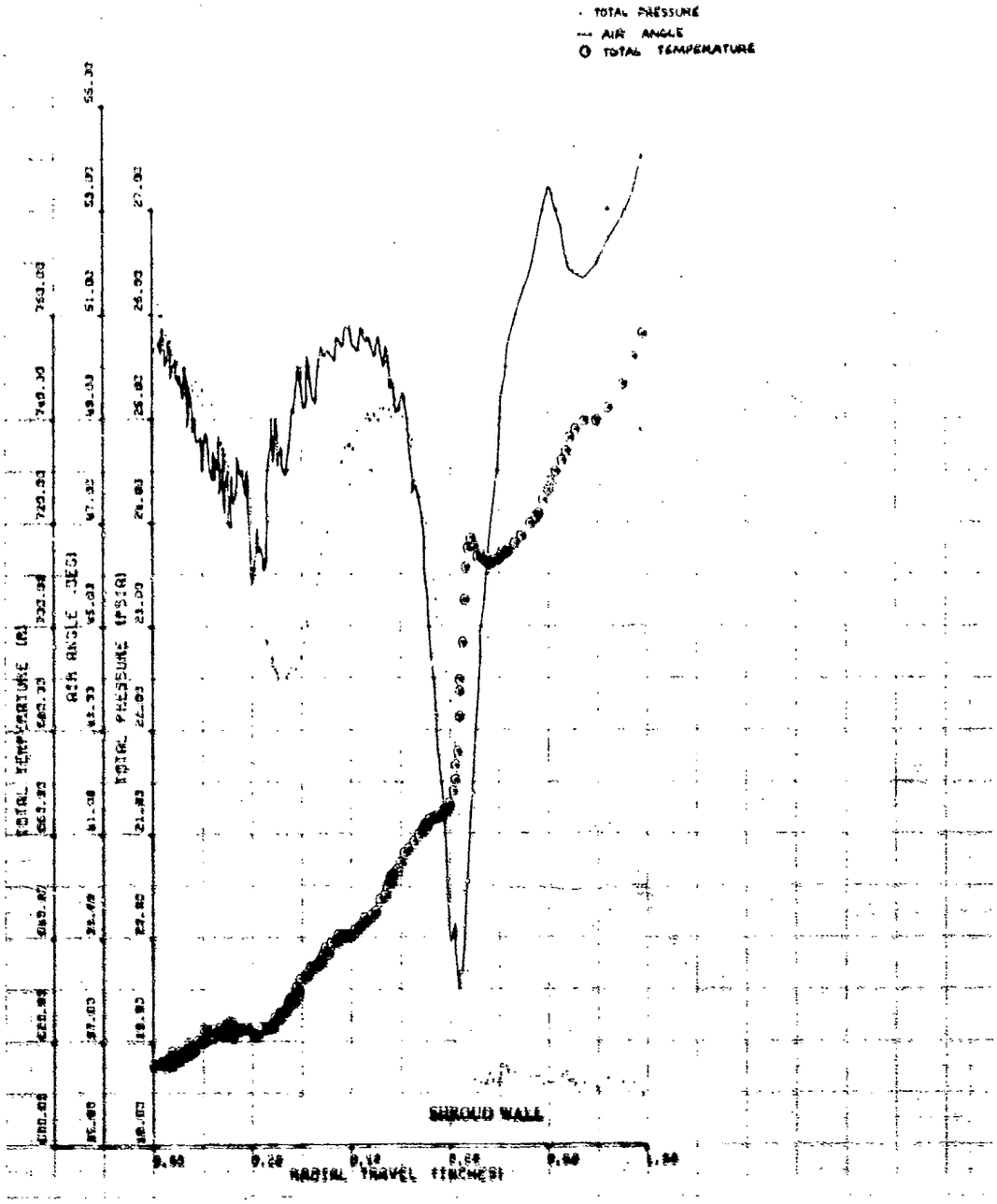

Figure 157. Inducer Exit Traverse, Build No. 6, 101% Speed, -4-deg IGV, Wide Open Discharge.

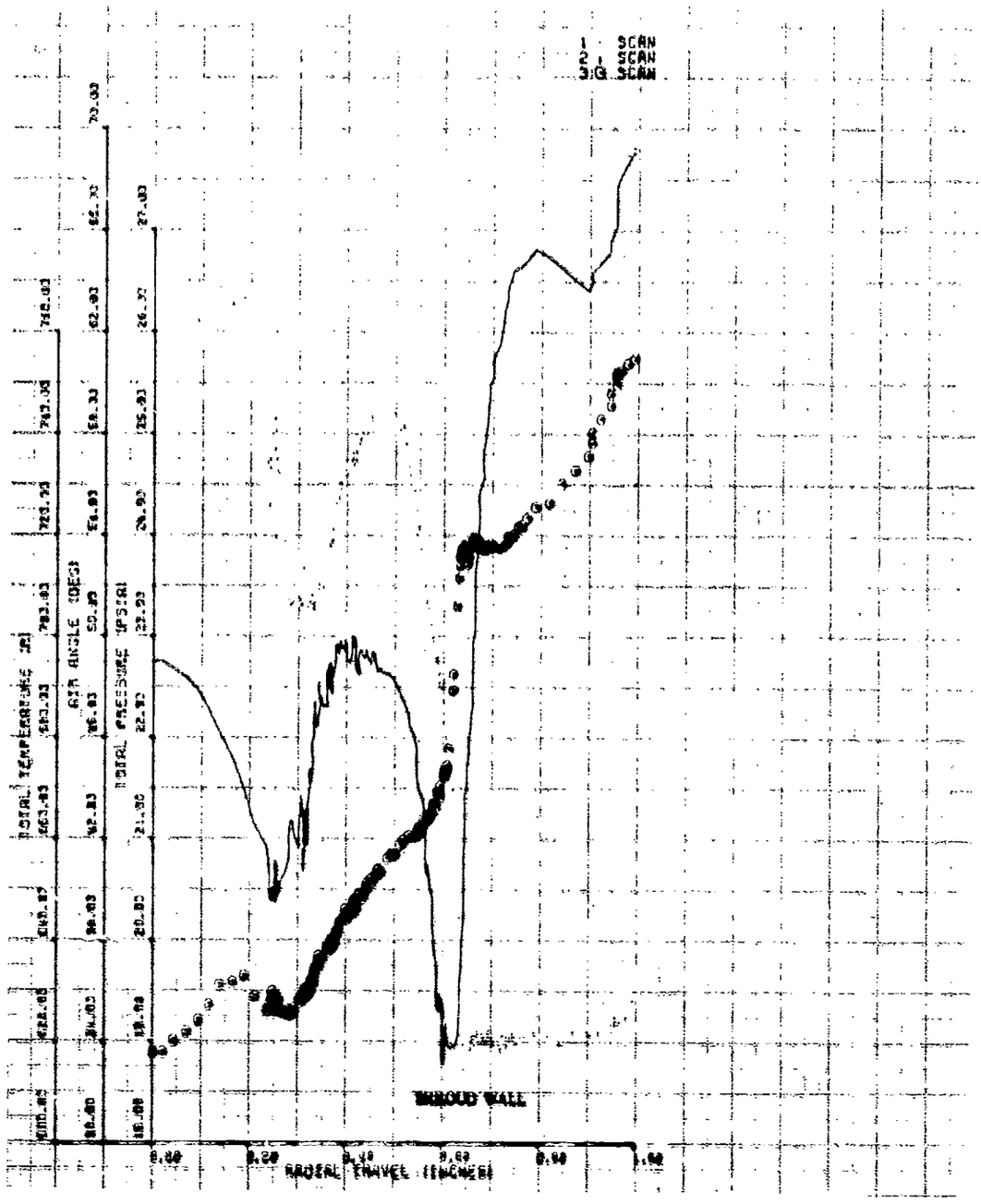

Figure 158. Inducer Exit Traverse, Build No. 6, 101% Speed, -4-deg IGV, Near Stall.

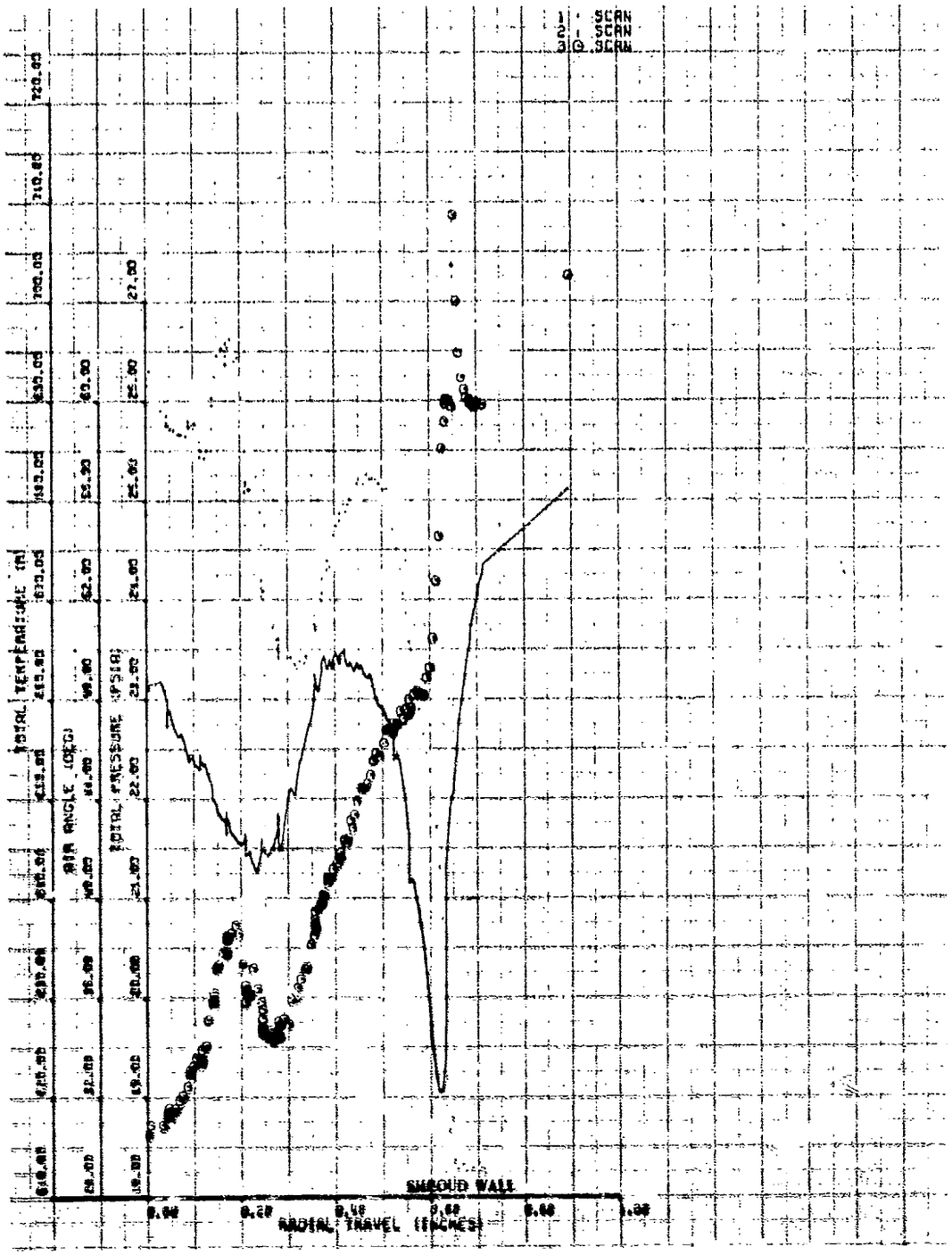

Figure 159. Inducer Exit With Coolant, Build No. 6, 101% Speed, -4-deg IGV, Near Stall.

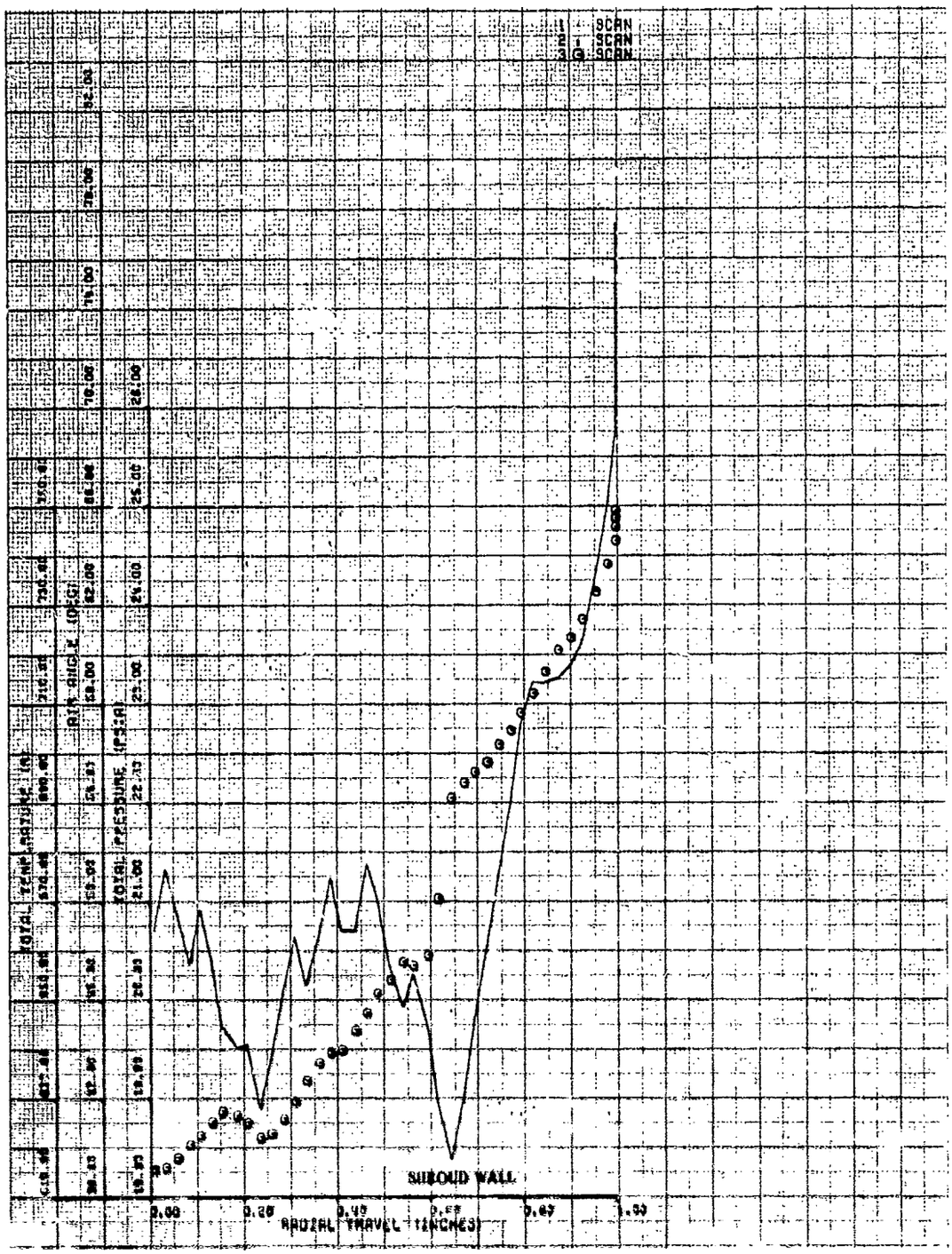

Figure 160. Inducer Exit Traverse, Build No. 6, 101% Speed, -5-deg IGV.

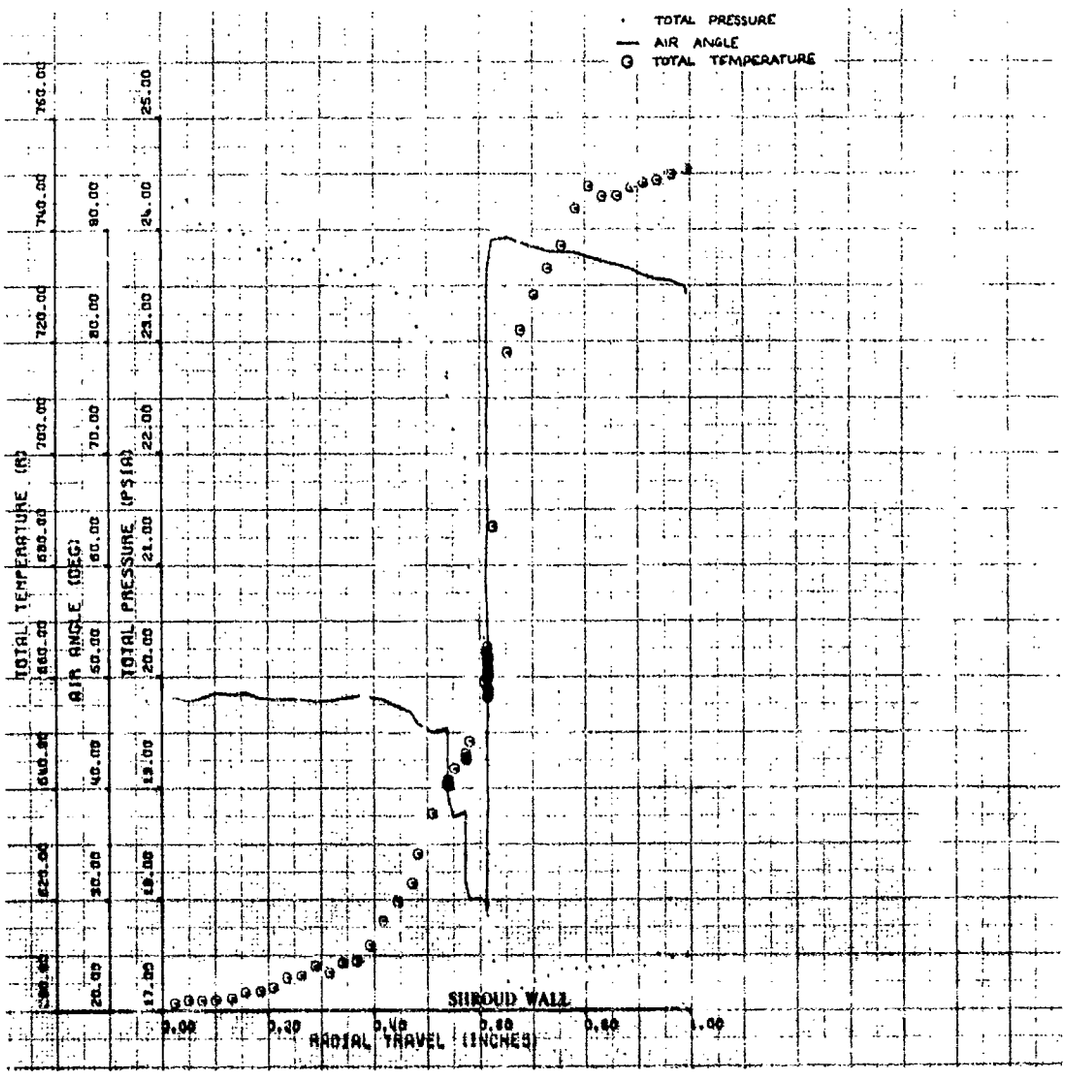

Figure 161. Inducer Exit Traverse, Build No. 6, 100% Speed, 10-deg IGV.

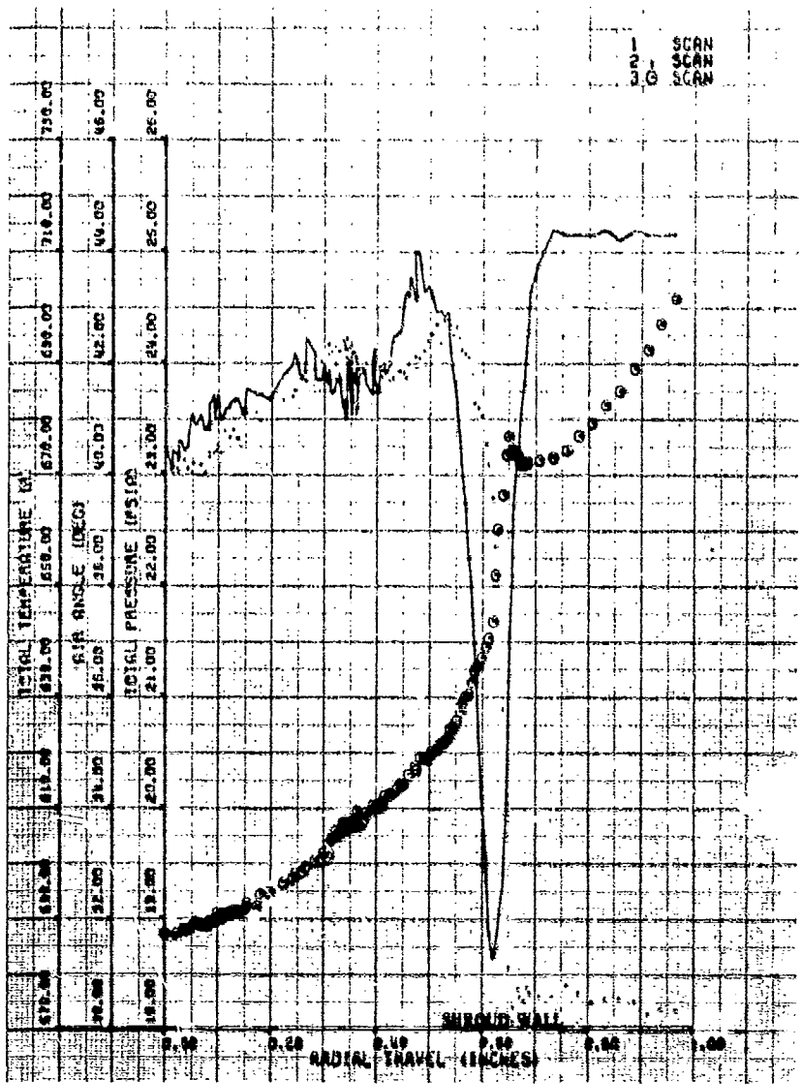

Figure 162. Inducer Exit Traverse, Build No. 6, 95% Speed, 15-deg IGV, Wide Open Discharge.

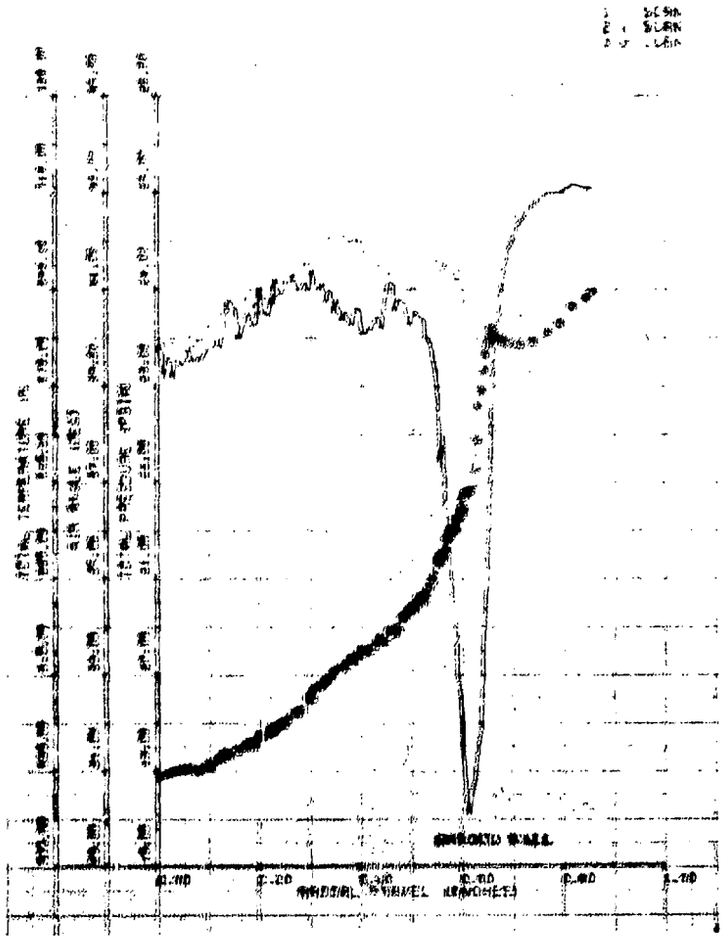

Figure 163. Inducer Exit Traverse, Build No. 6, 95% Speed, 15-deg IGV, Near Stall.

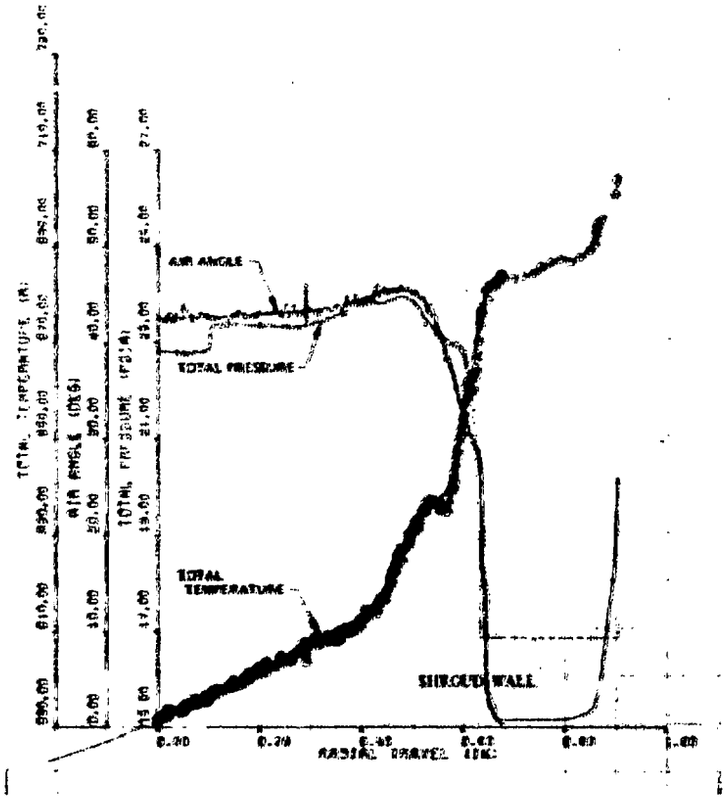

Figure 164. Inducer Exit Traverse, Build No. 3, 95% Speed, 10-deg IGV, Wide Open Discharge.

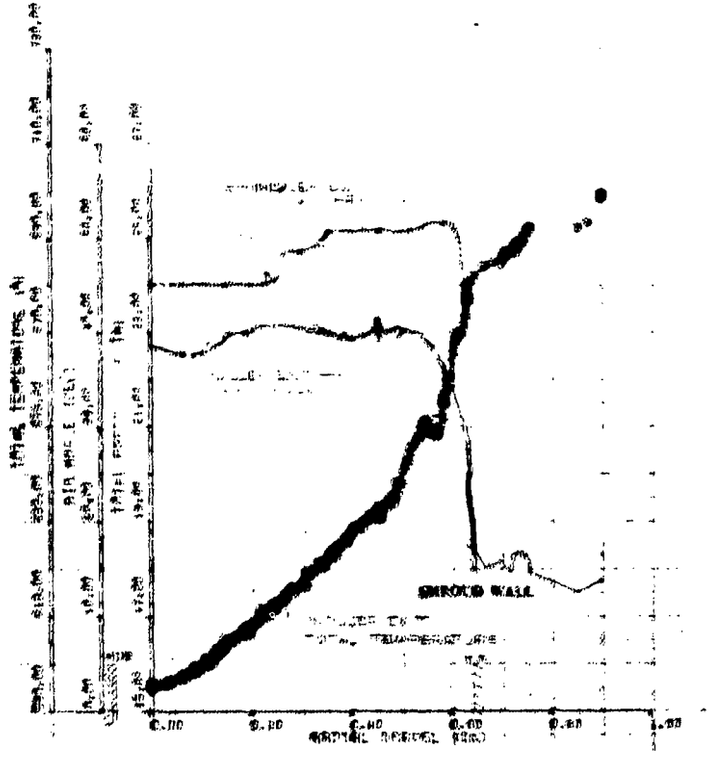

Figure 165. Inducer Exit Traverse, Build No. 3, 95% Speed, 10-deg IGV, Near Stall.

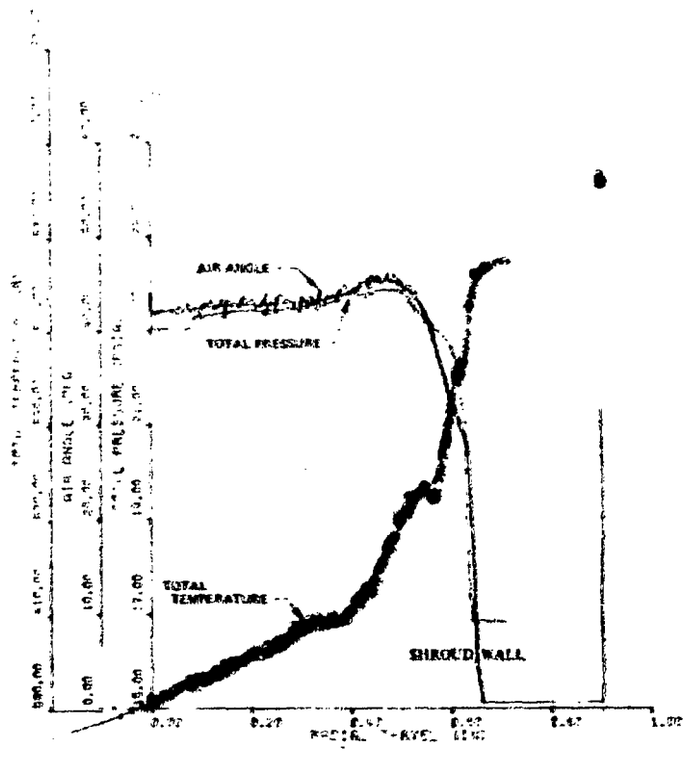

Figure 166. Inducer Exit Traverse, Build No. 3, 95% Speed, 10-deg IGV, Below Near Stall.

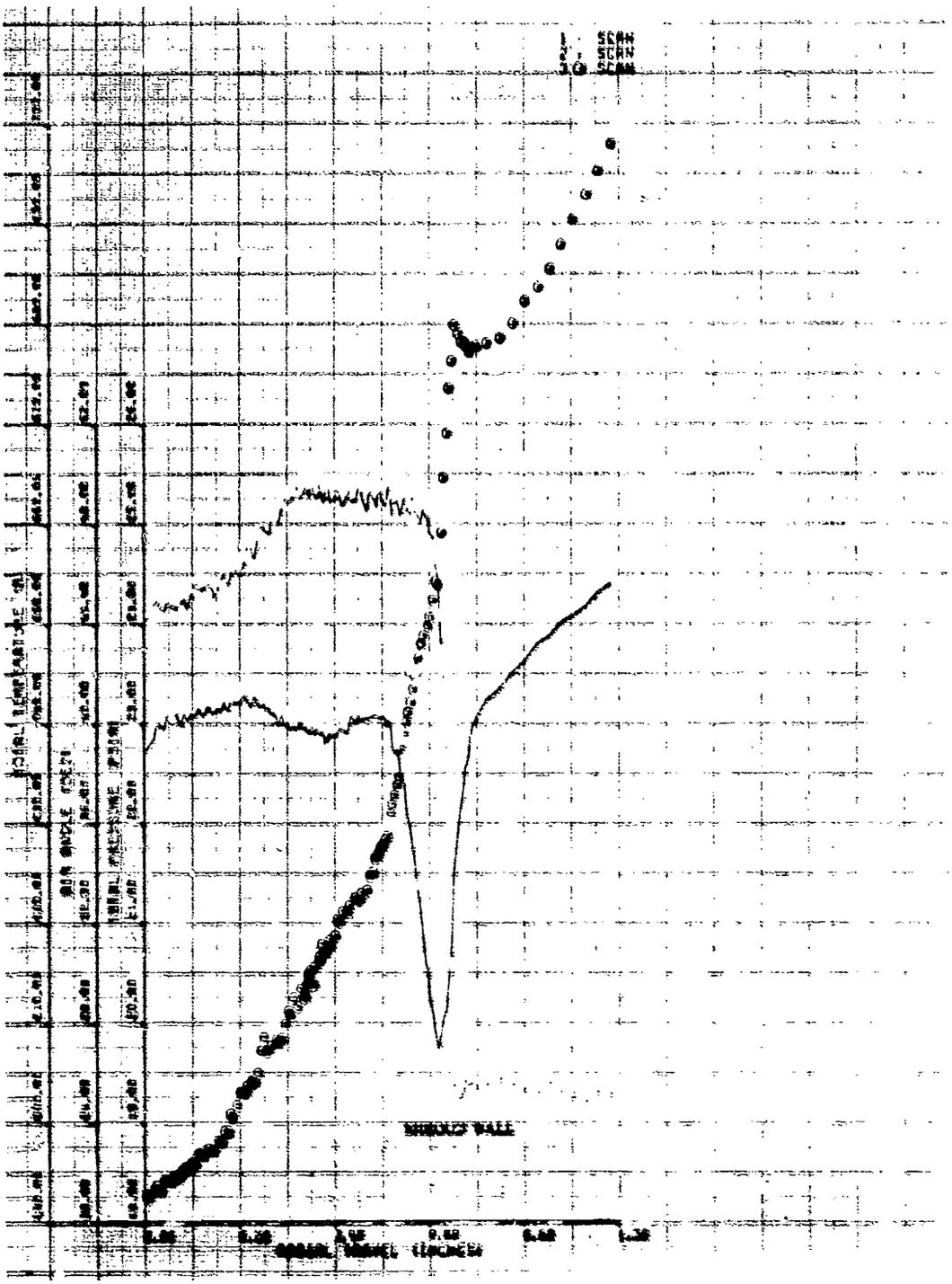

Figure 167. Inducer Exit Traverse, Build No. 6, 95% Speed, 10-deg IGV, Wide Open Discharge.

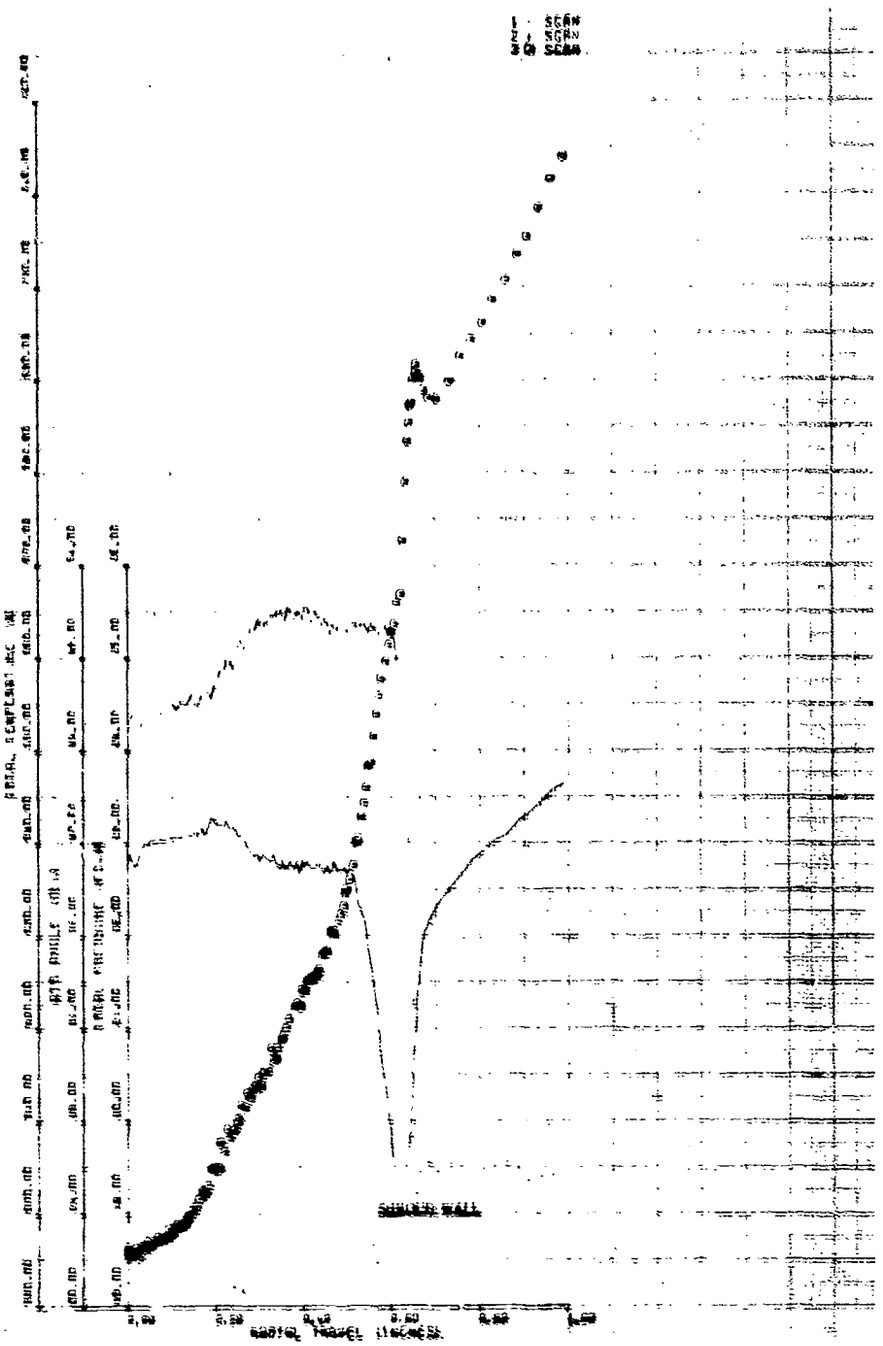

Figure 168. Inducer Exit Traverse, Build No. 6, 95% Speed, 19-deg IGV, Near Stall.

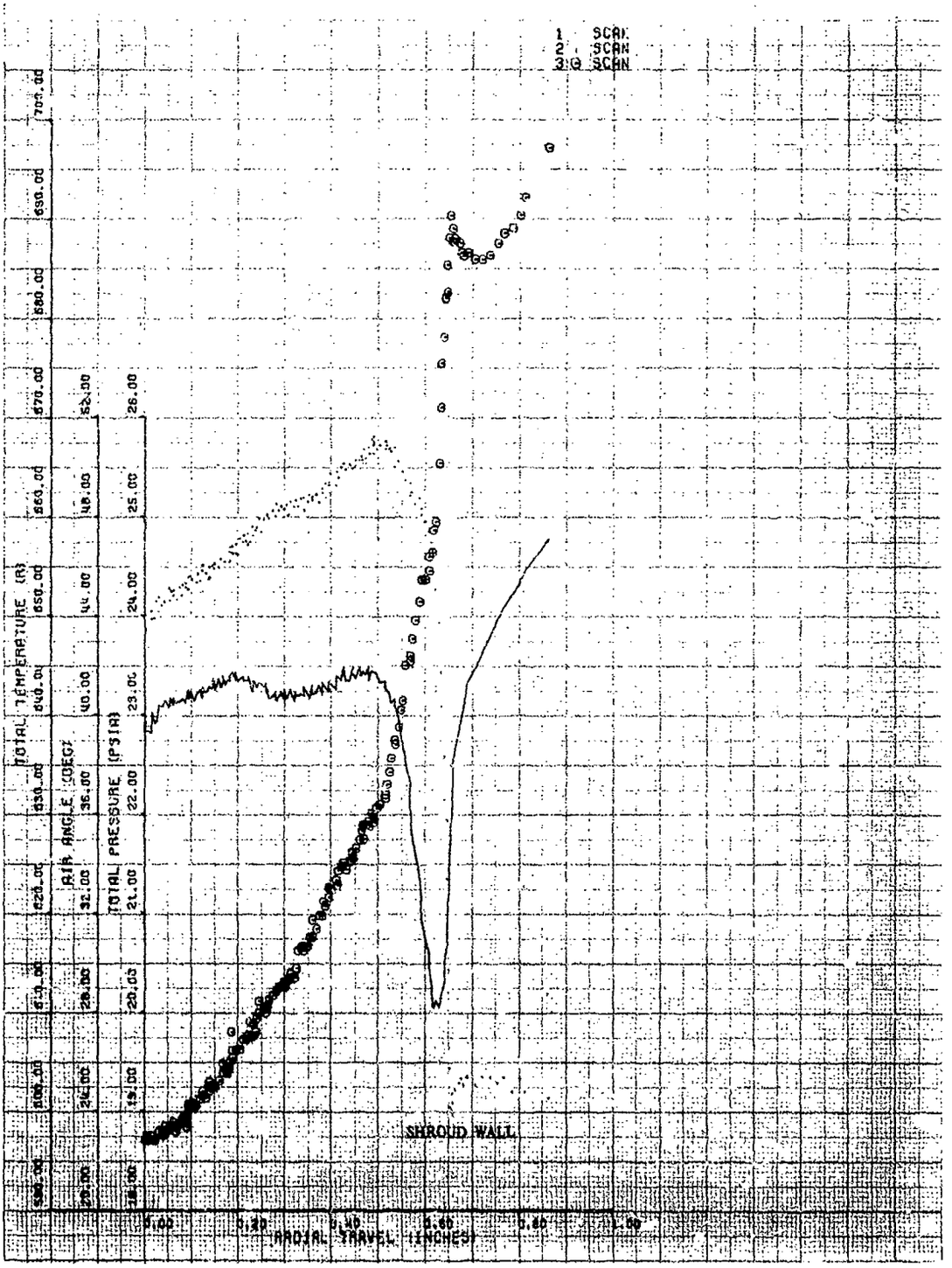

Figure 169. Inducer Exit Traverse, Build No. 6, 95% Speed, 10-deg IGV, Wide Open Discharge.

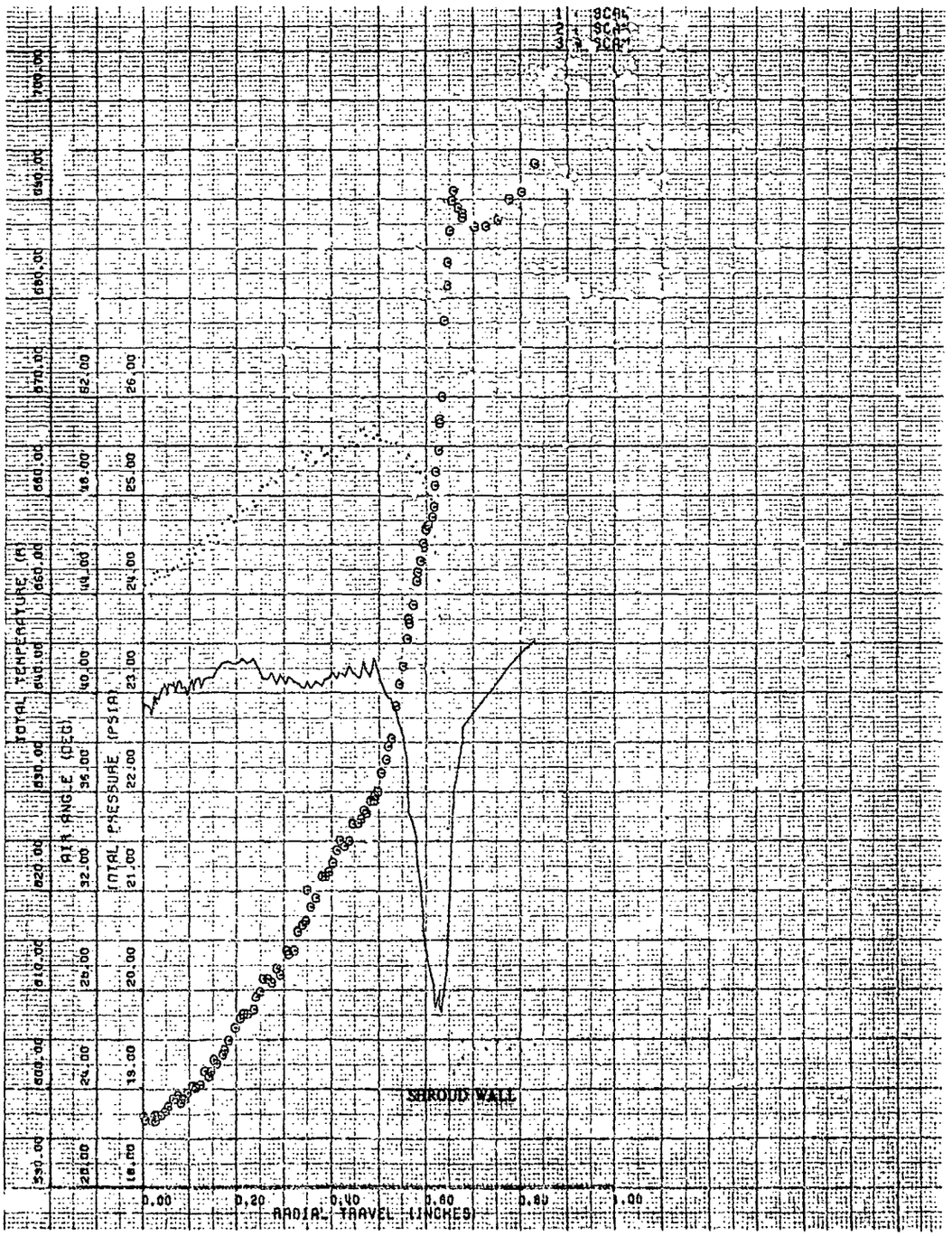

Figure 170. Inducer Exit Traverse, Build No. 6, 95% Speed, 10-deg IGV, Near Stall.

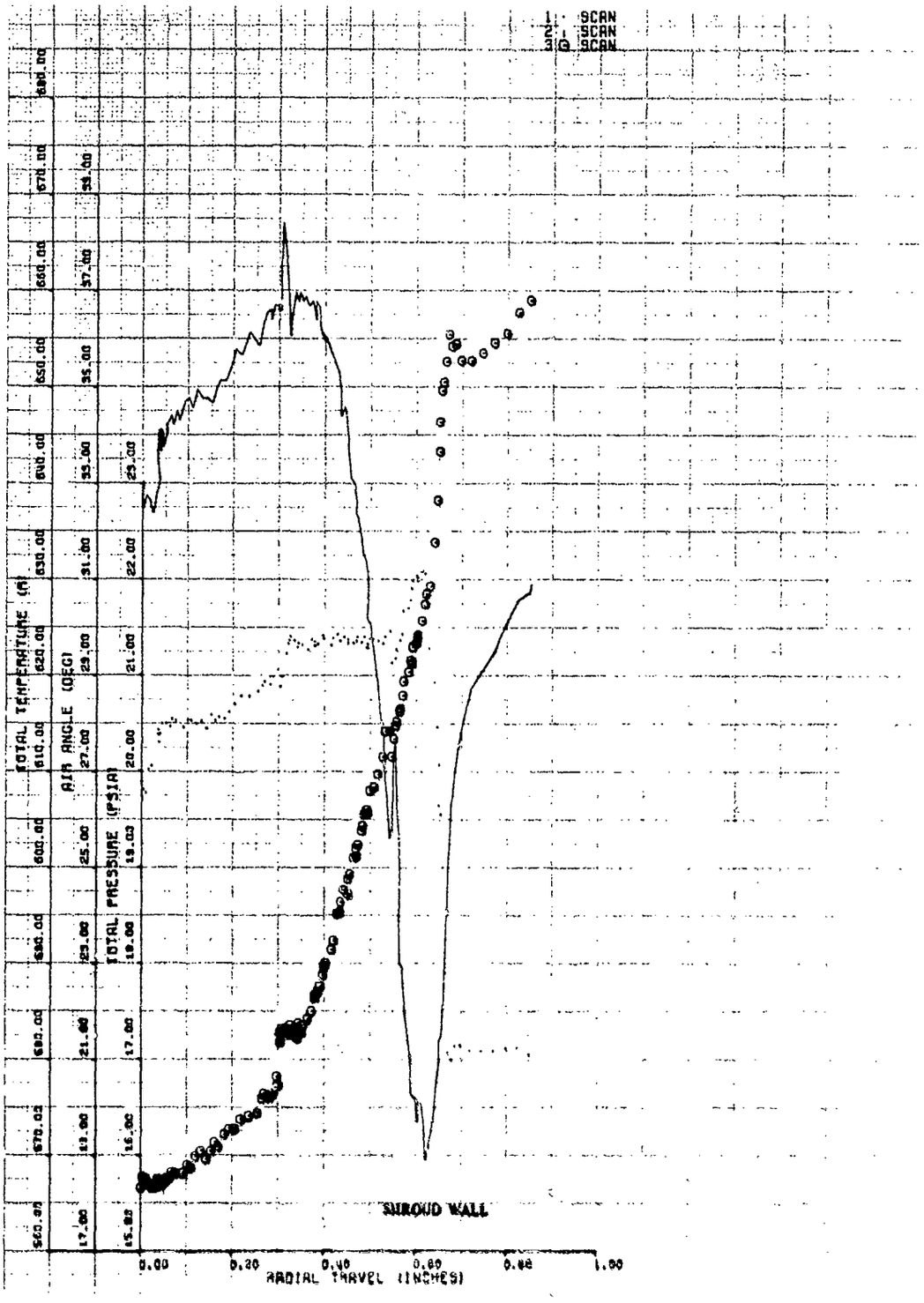

Figure 171. Inducer Exit Traverse, Build No. 6, 85% Speed, 30-deg IGV, Near Stall.

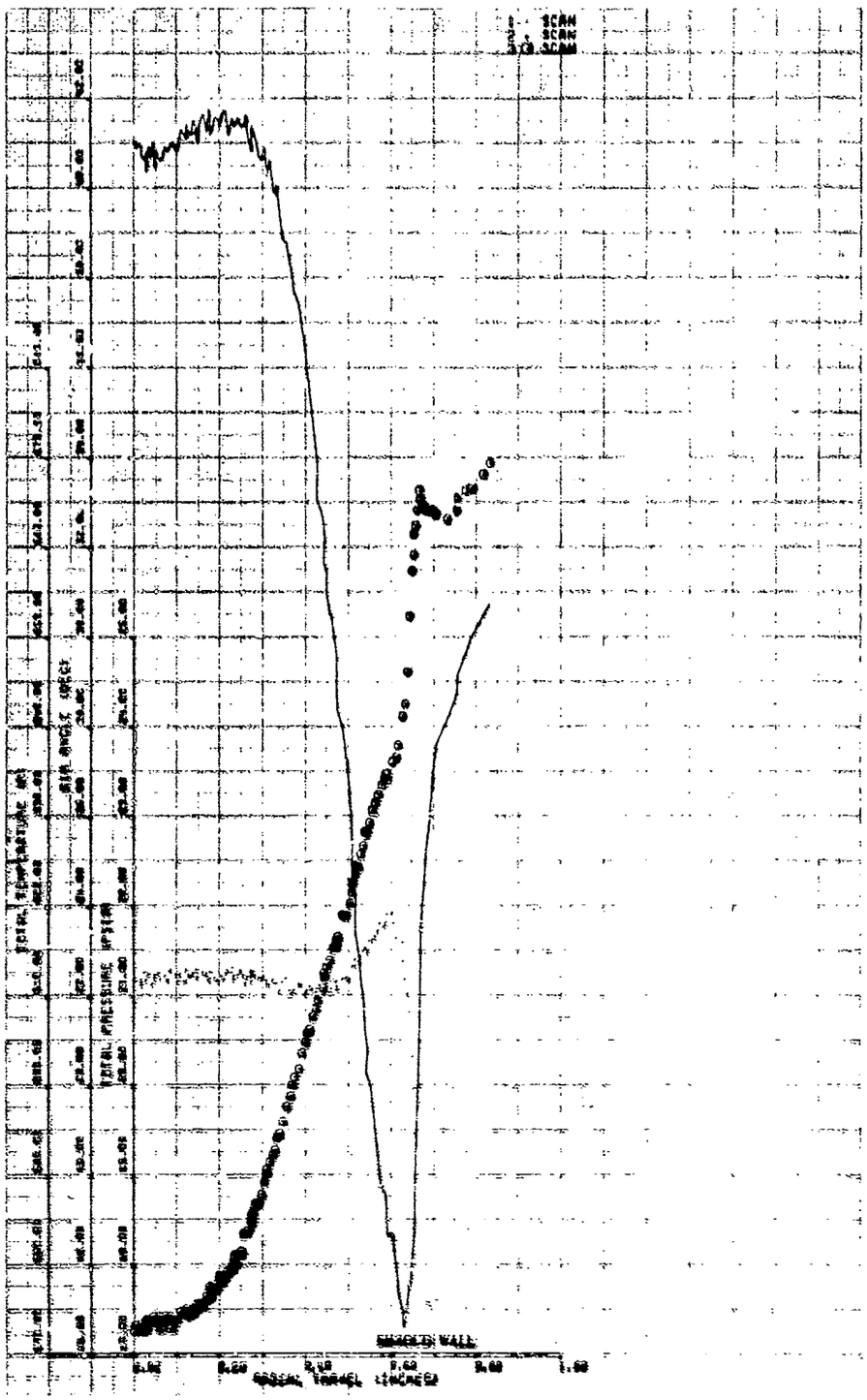

Figure 172. Inducer Exit Traverse, Build No. 6, 85% Speed, 20-deg IGV, Near Stall.

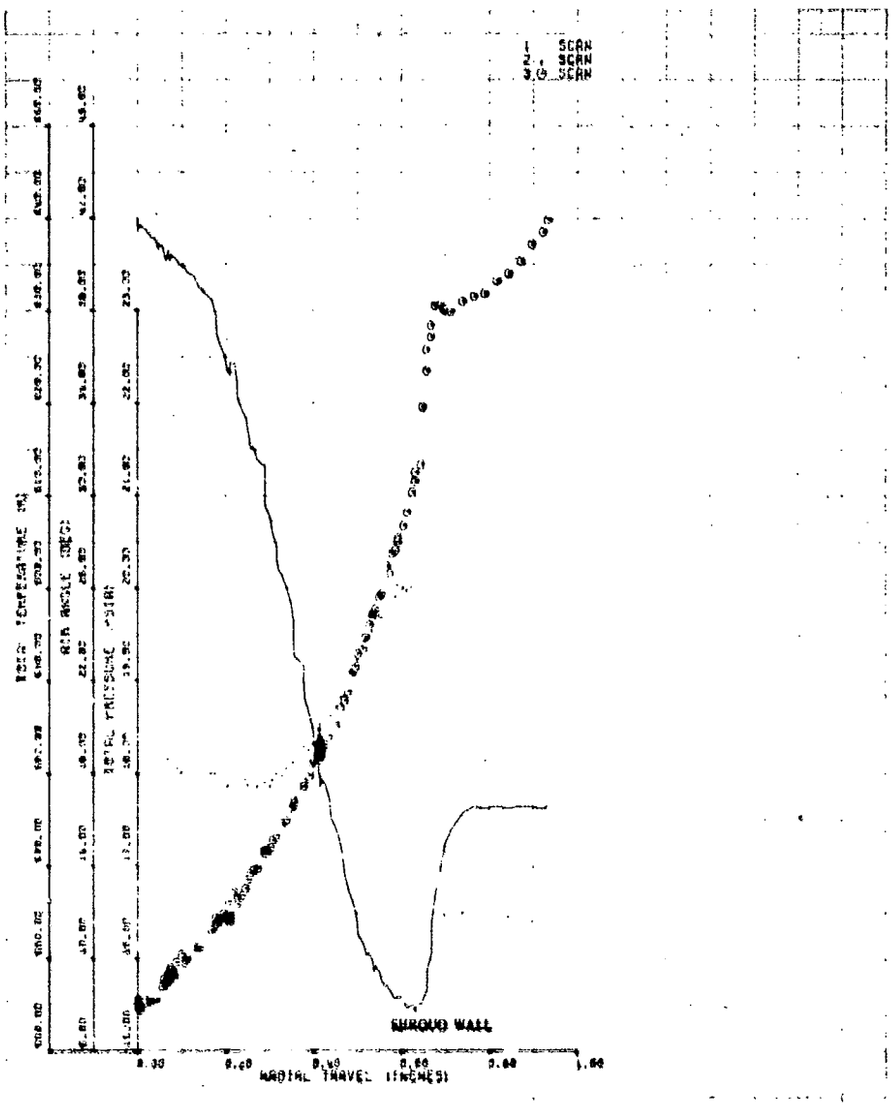

Figure 173. Inducer Exit Traverse, Build No. 6, 70% Speed, 30-deg IGV, Near Stall.

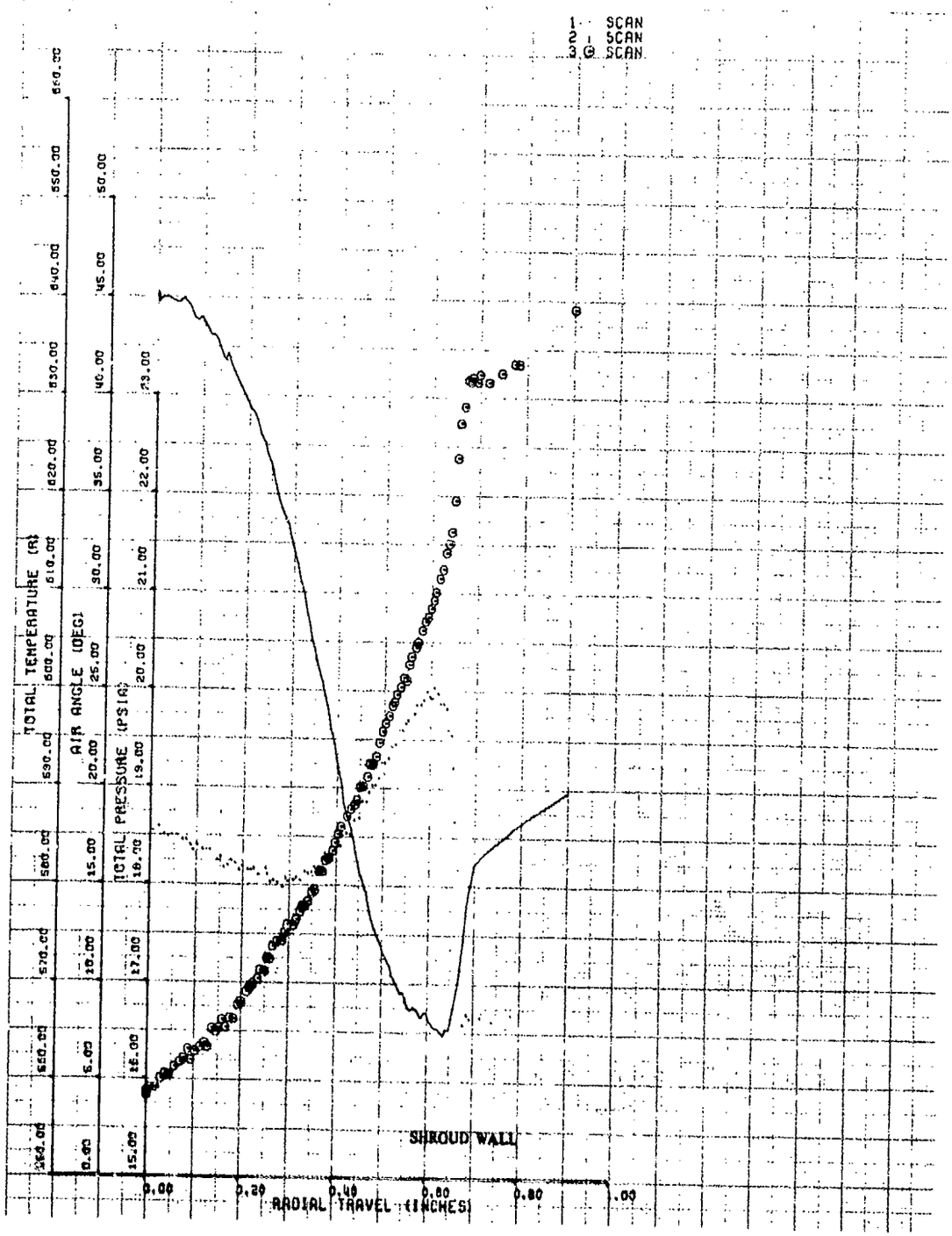

Figure 174. Inducer Exit Traverse, Build No. 6, 70% Speed, 20-deg IGV, Near Stall.

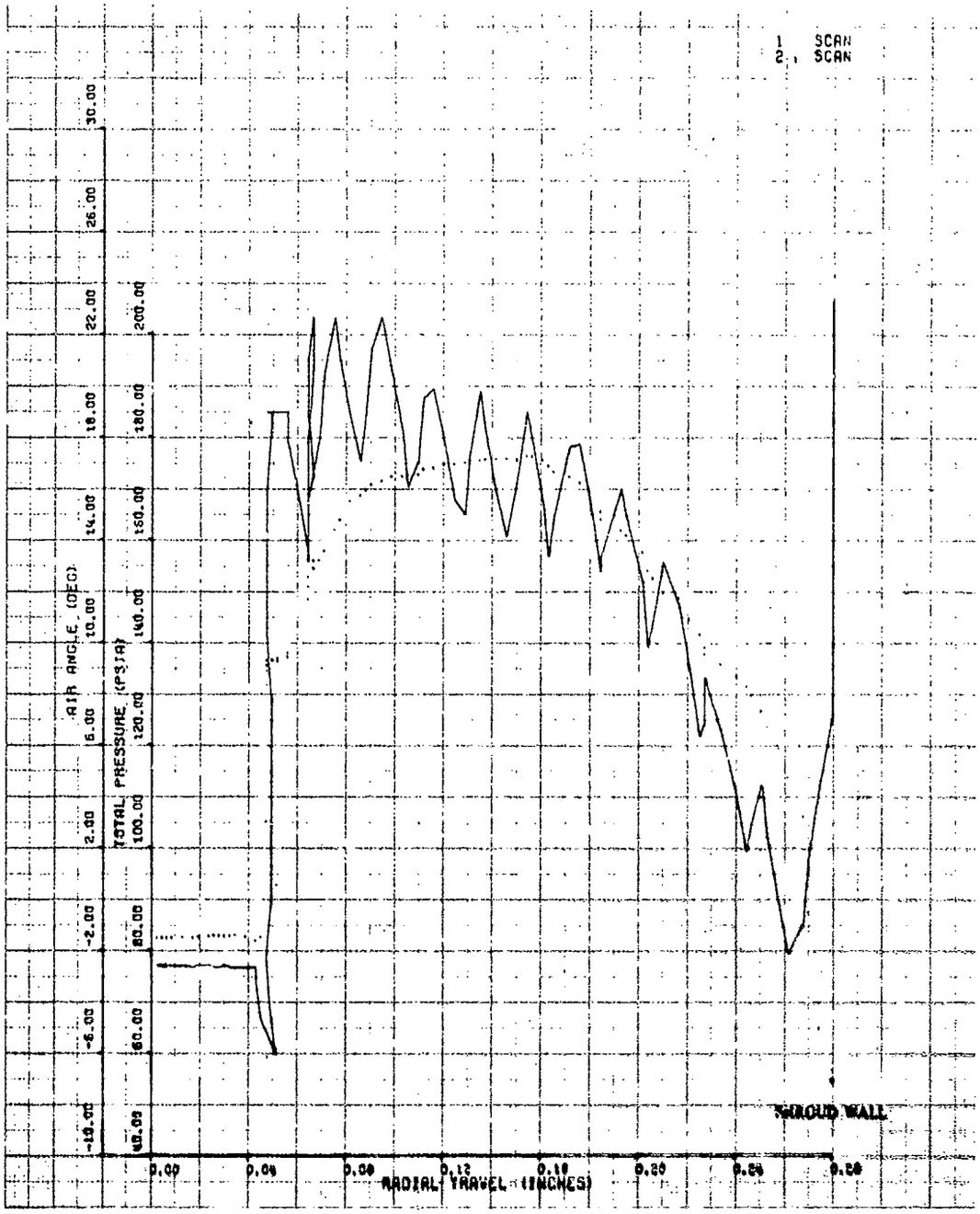

Figure 175. Impeller Exit Traverse, Build No. 6, 101% Speed, 5-deg IGV, Near Stall.

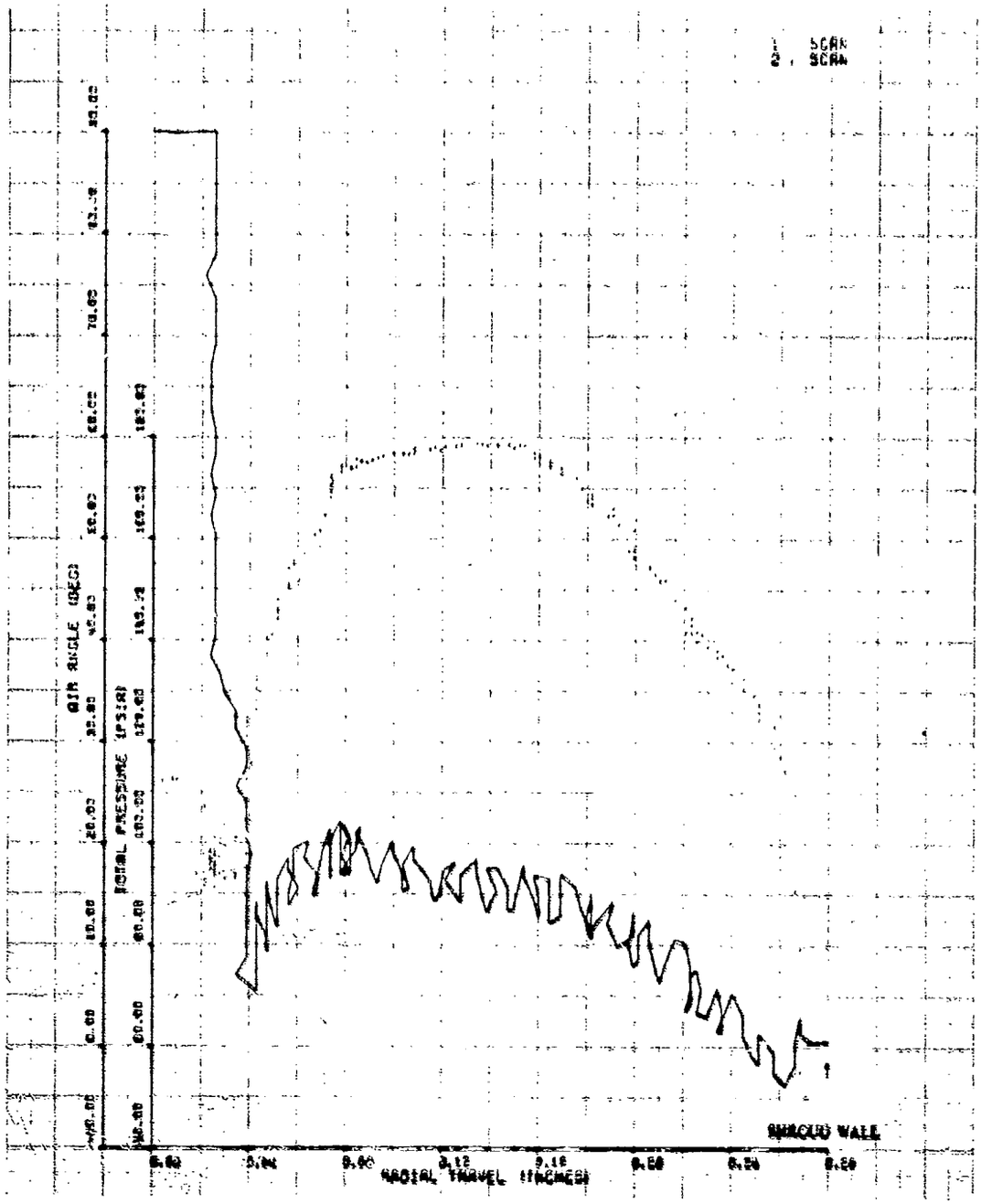

Figure 176. Impeller Exit Traverse, Build No. 6, 101% Speed, 0-deg IGV, Near Stall.

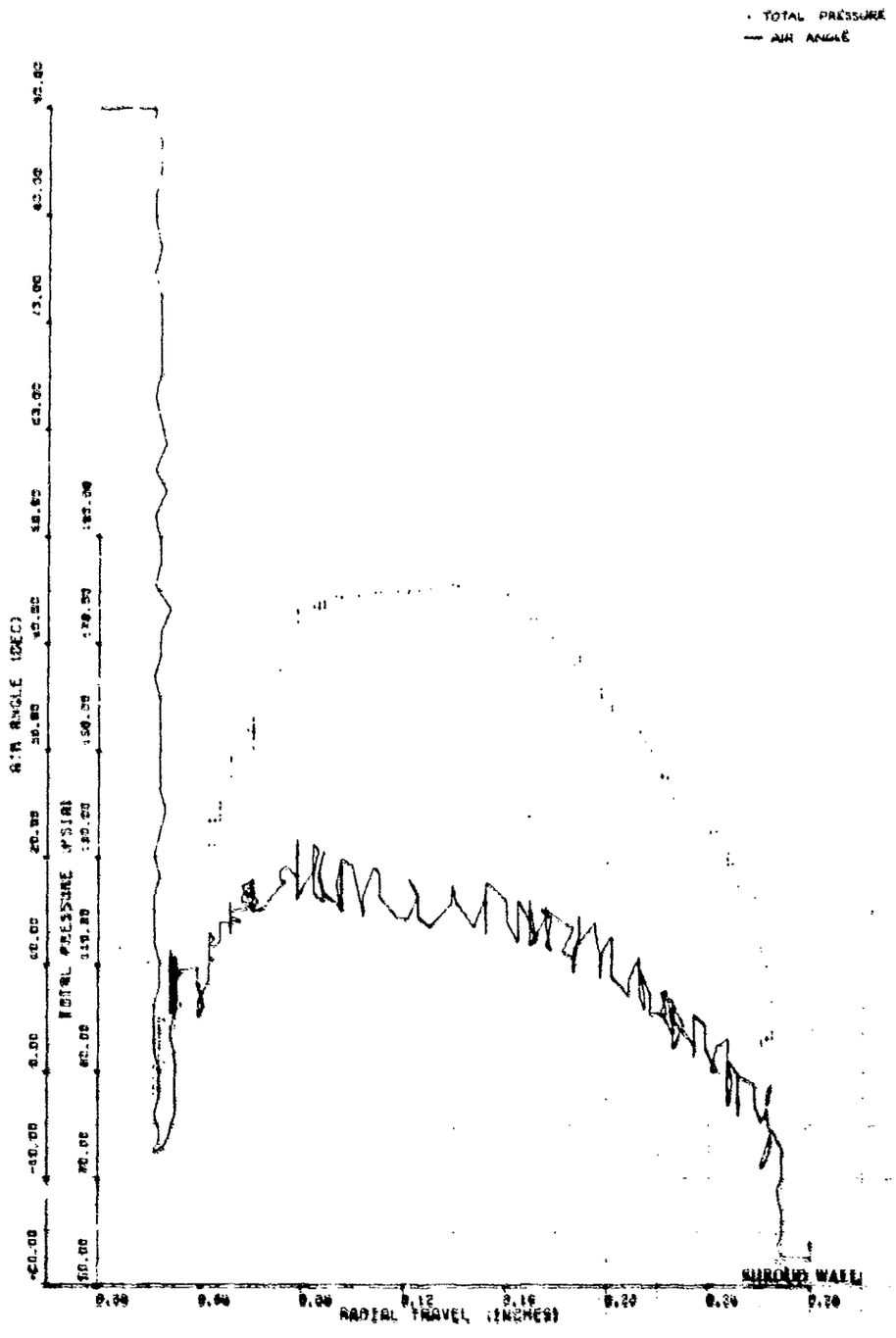

Figure 177. Impeller Exit Traverse, Build No. 6, 101% Speed, -4-deg IGV, Near Stall.

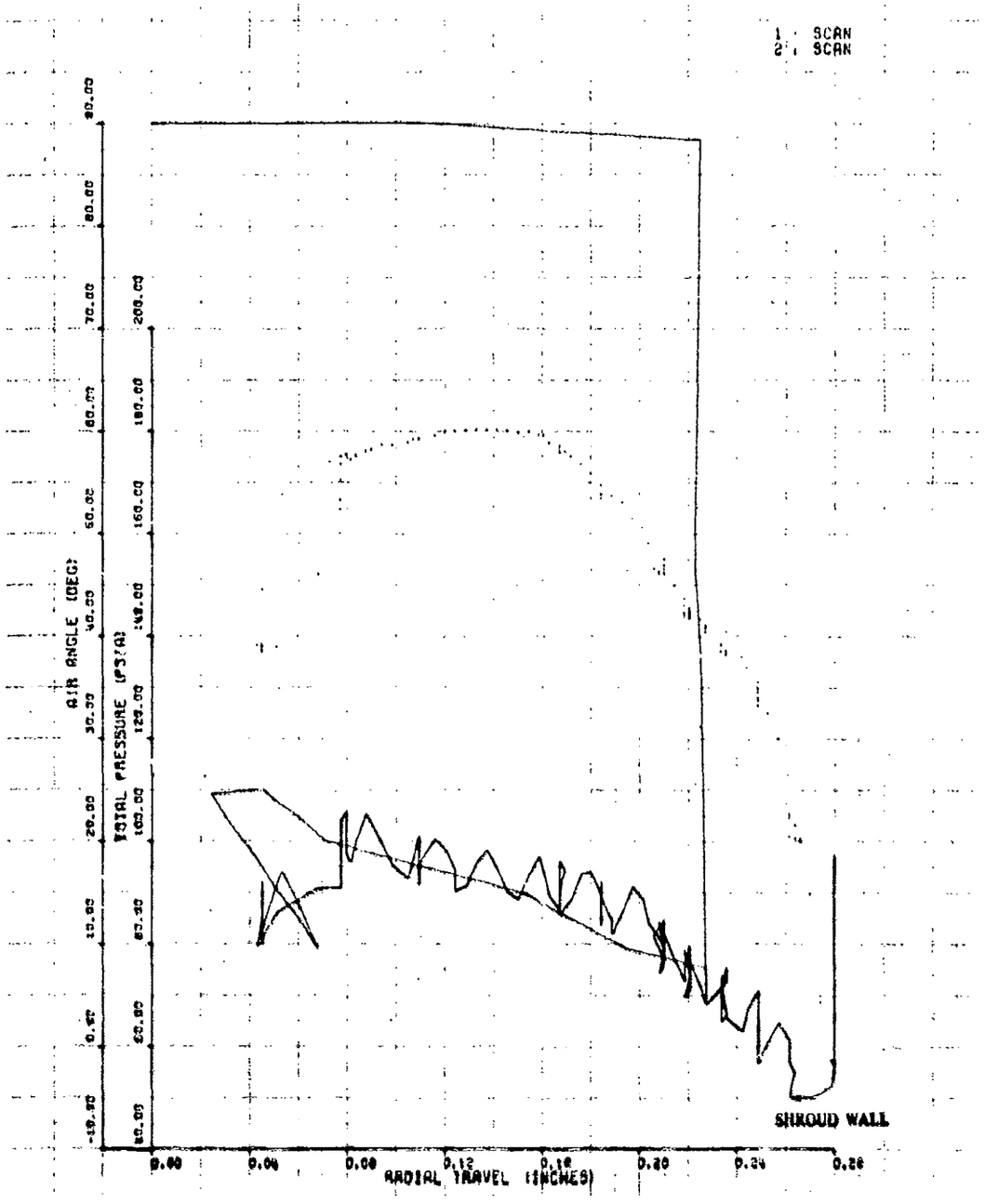

Figure 178. Impeller Exit Traverse With Flange Coolant, Build No. 6, 101% Speed, -4-deg IGV.

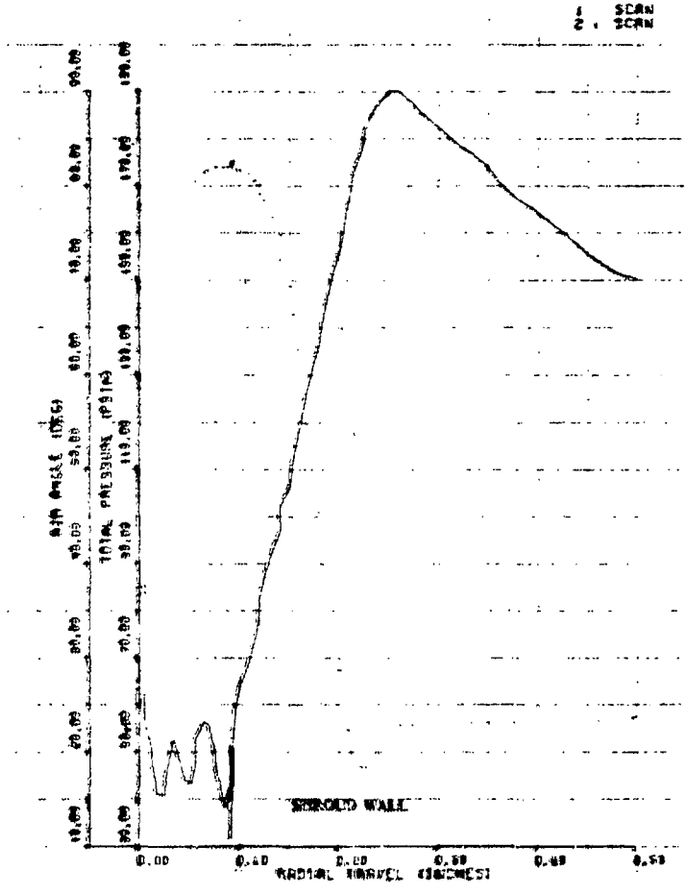

Figure 179. Impeller Exit Traverse, Build No. 6, 101% Speed, -5-deg IGV.

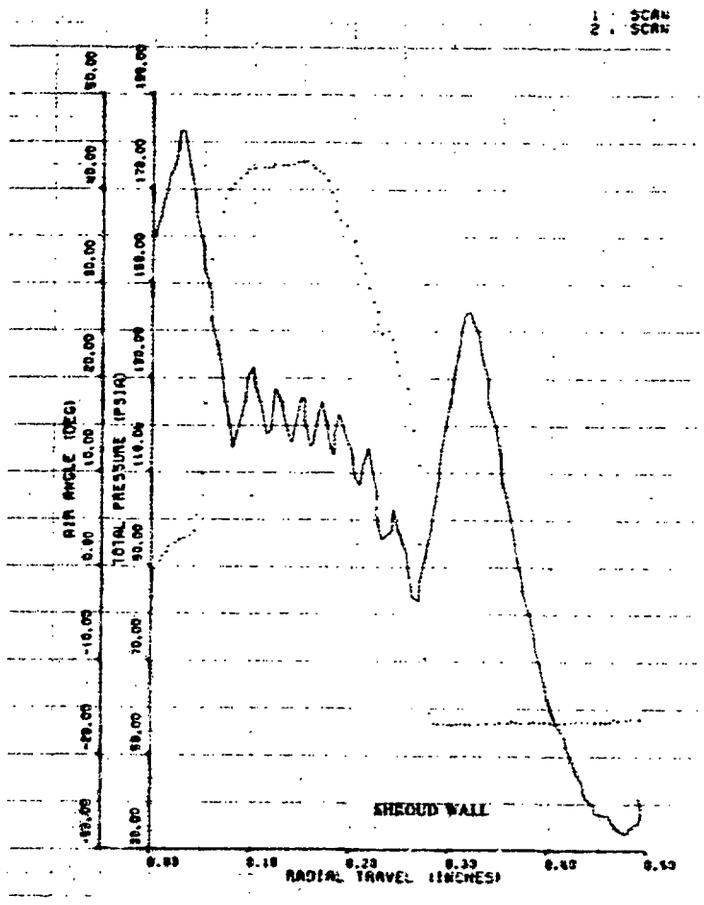

Figure 180. Impeller Exit Traverse, Build No. 6, 101% Speed, -5-deg IGV.

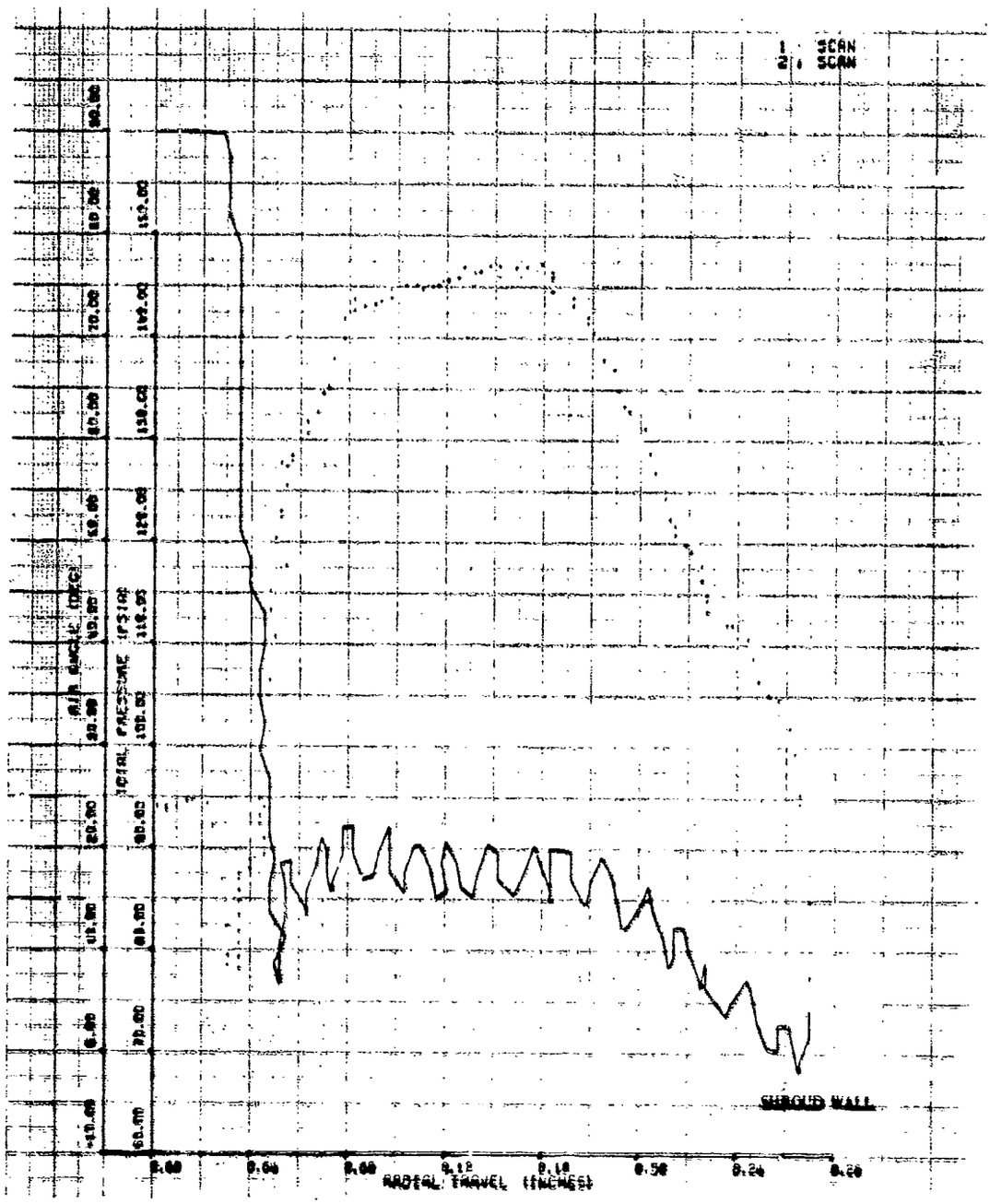

Figure 181. Impeller Exit Traverse, Build No. 6, 95% Speed, 15-deg IGV.

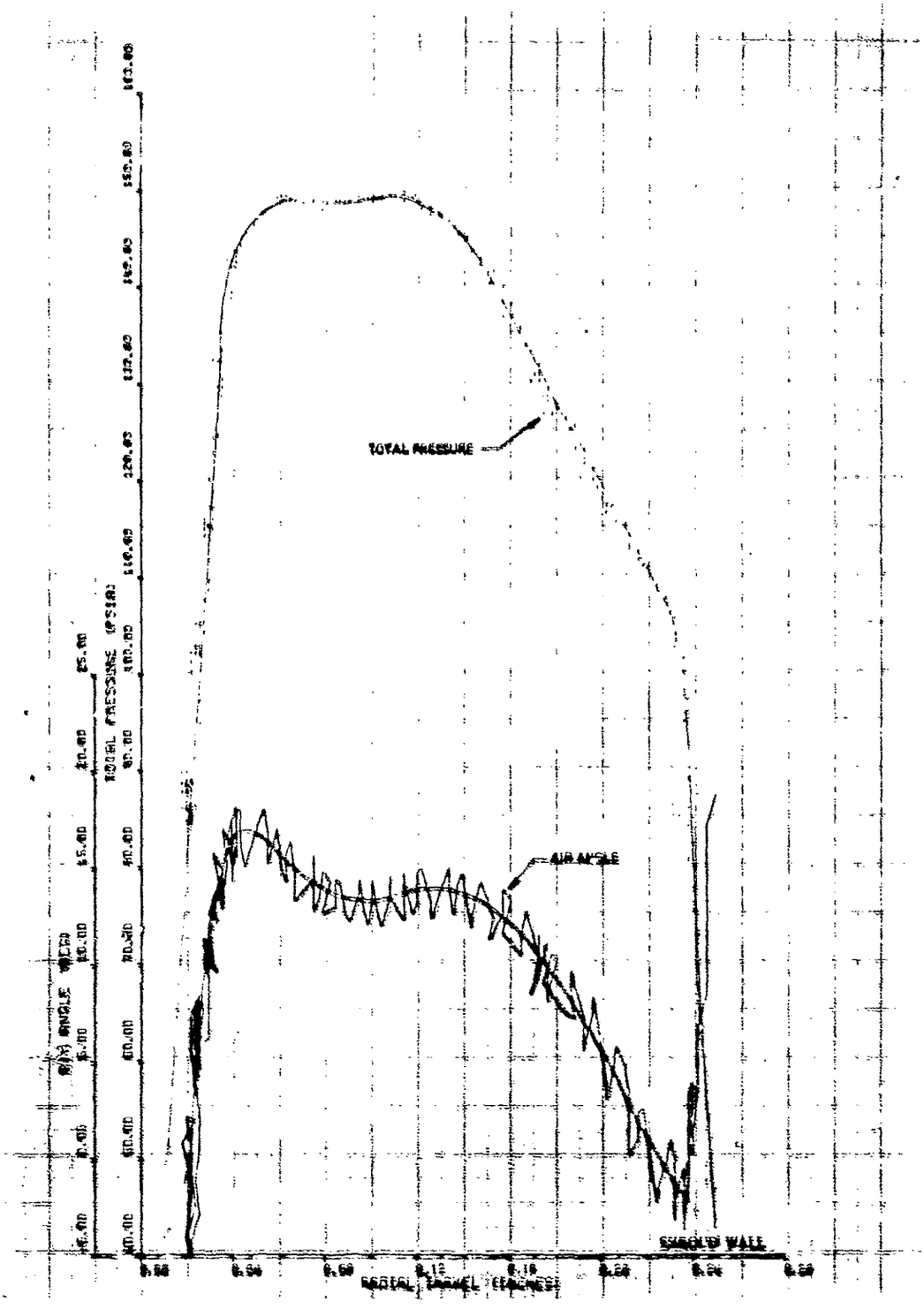

Figure 183. Impeller Exit Traverse, Build No. 3, 95% Speed, 10-deg IGV, Wide Open Discharge.

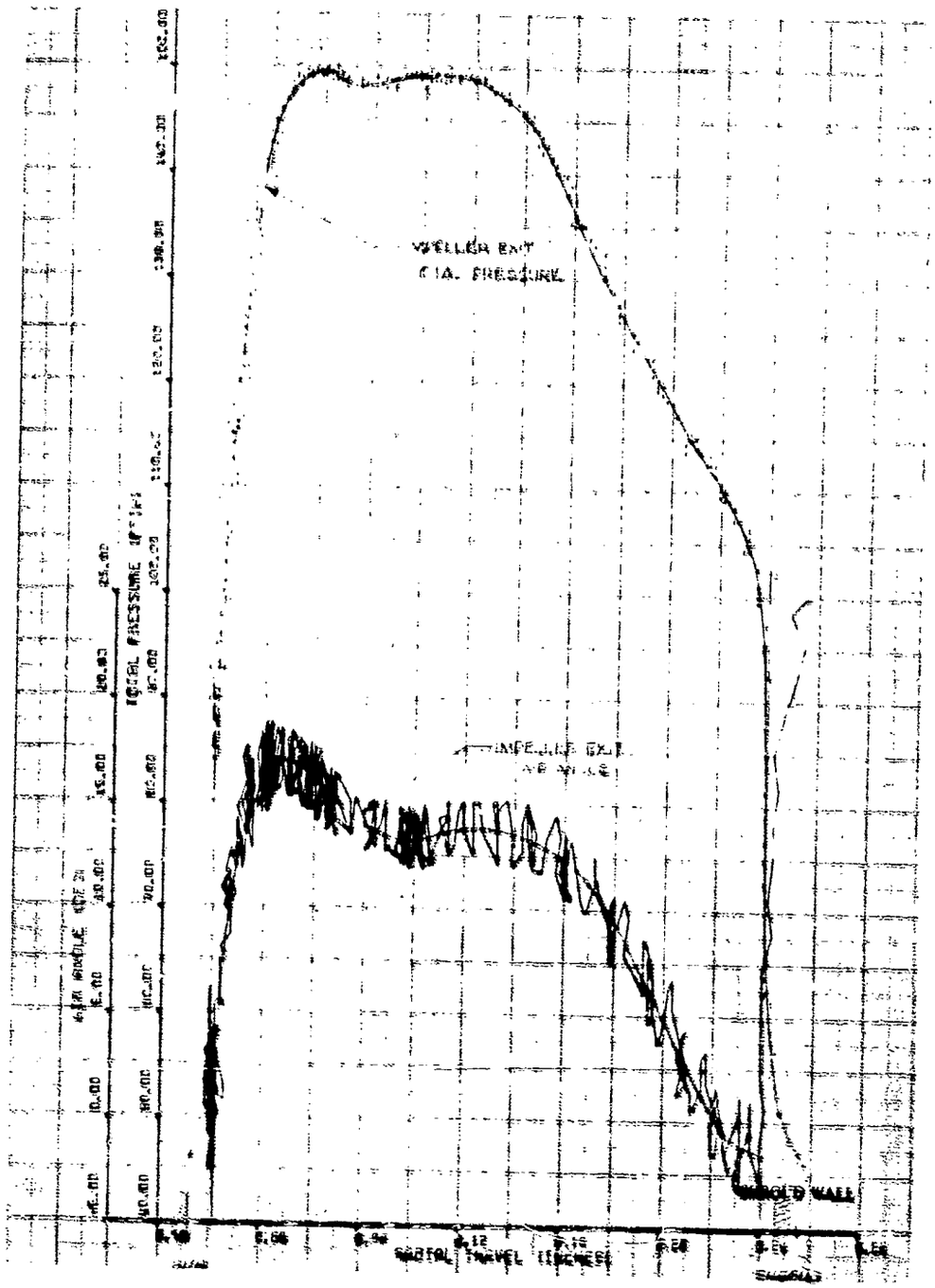

Figure 183. Impeller Exit Traverse, Build No. 3, 85% Speed, 10-deg IGV, Near Stall.

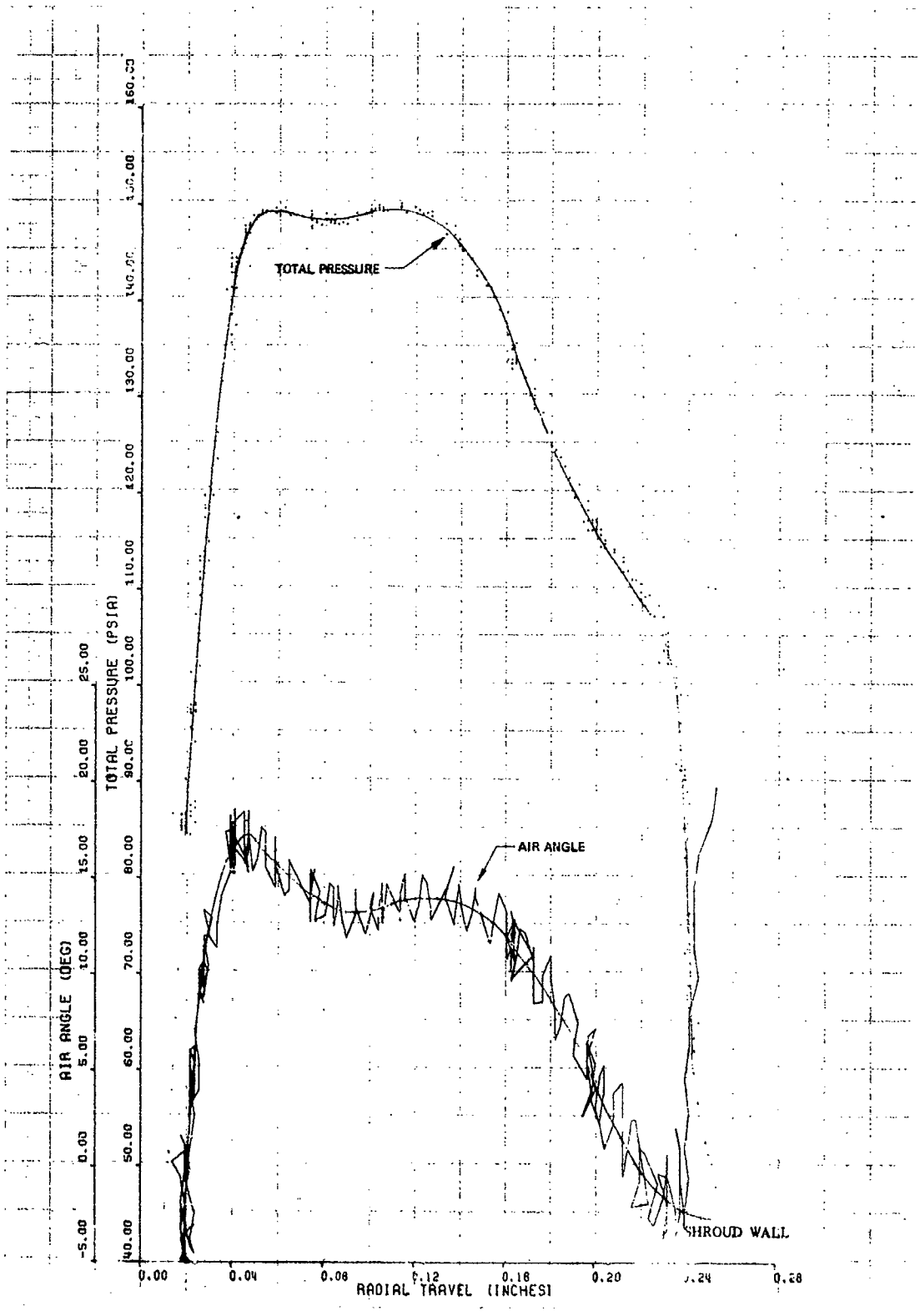

Figure 184. Impeller Exit Traverse, Build No. 3, 95% Speed, 10-deg IGV, Below Near Stall.

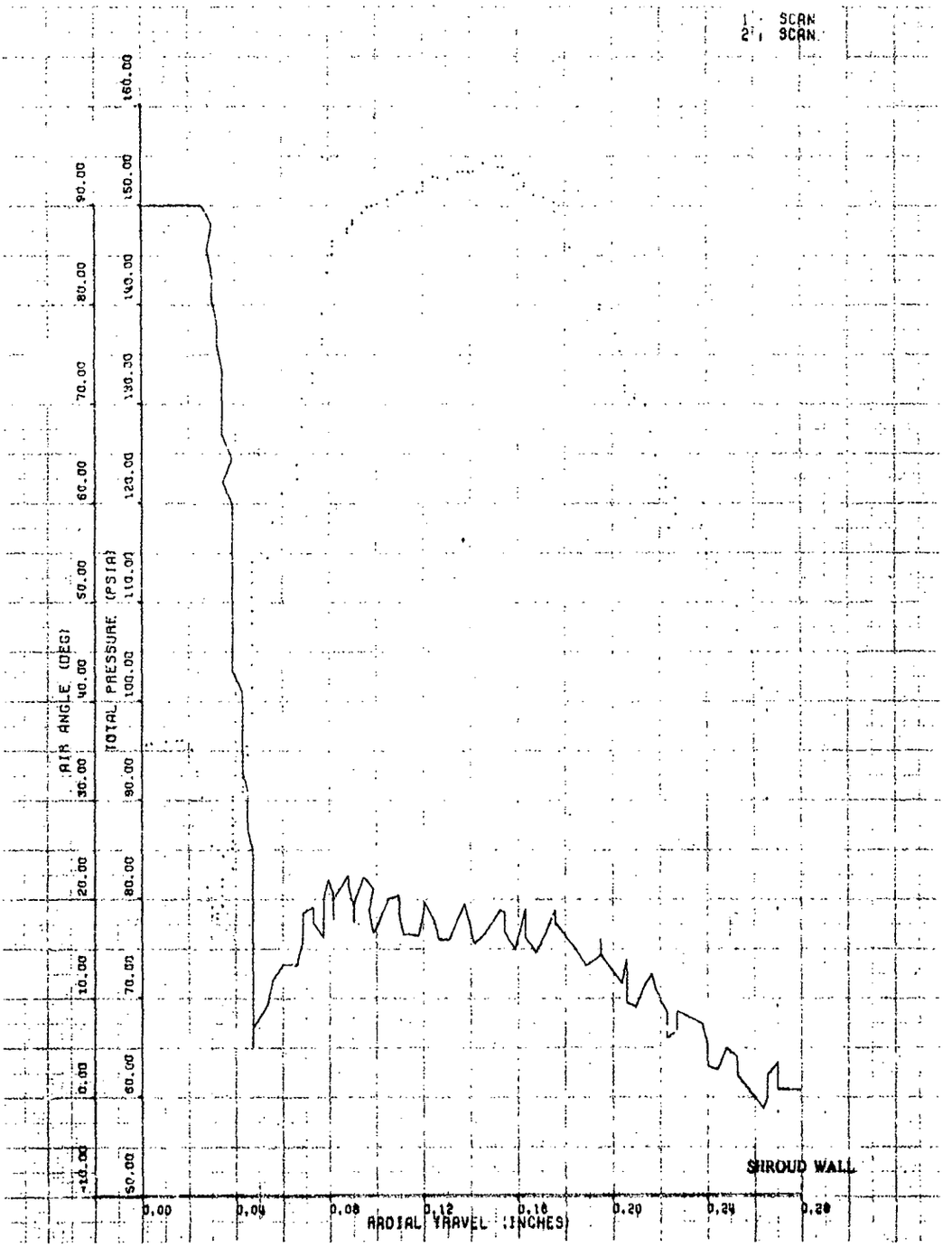

Figure 185. Impeller Exit Traverse, Build No. 6, 95% Speed, 10-deg IGV, Wide Open Discharge.

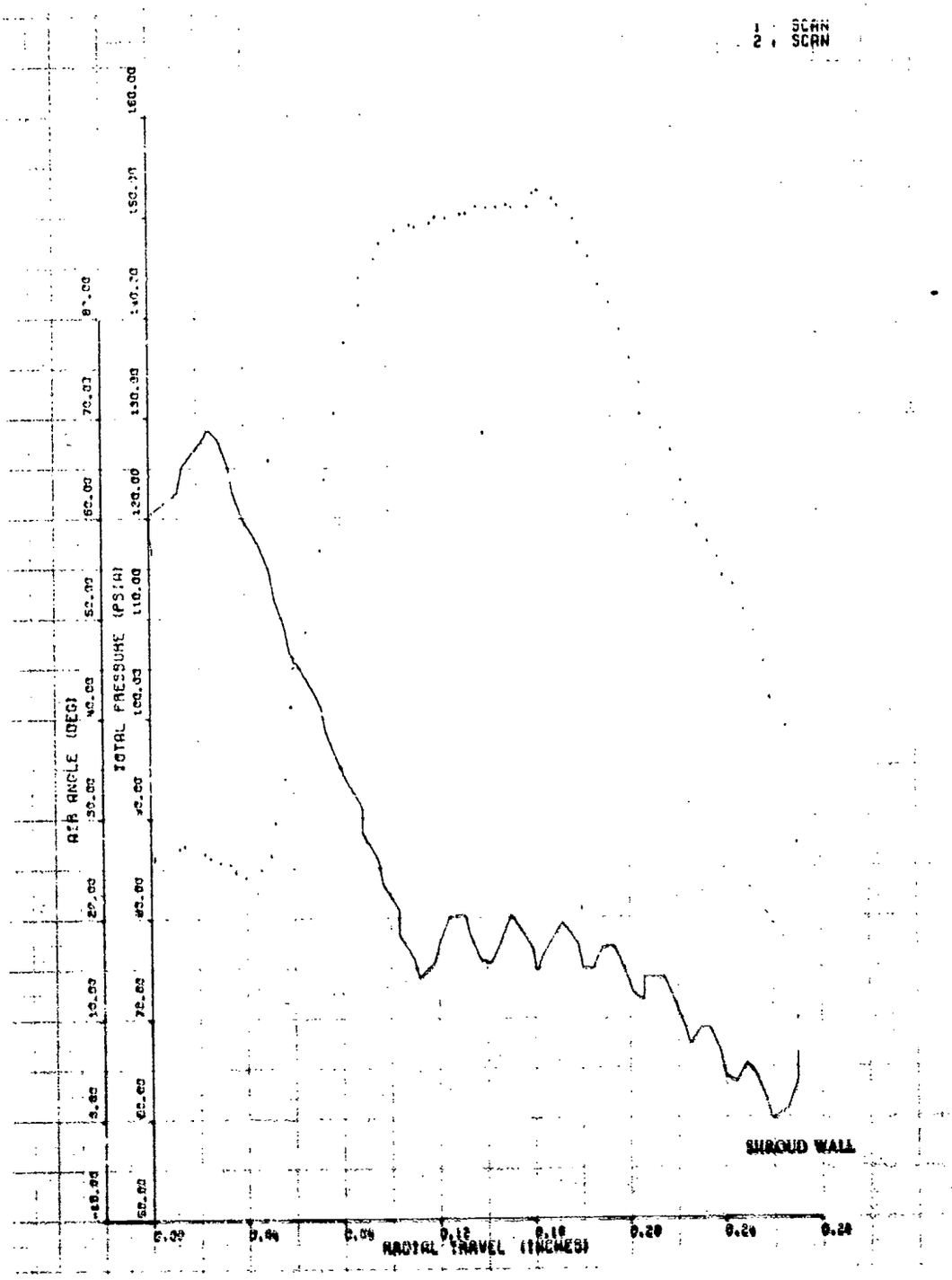

Figure 186. Impeller Exit Traverse, Build No. 6, 95% Speed, 10-deg IGV.

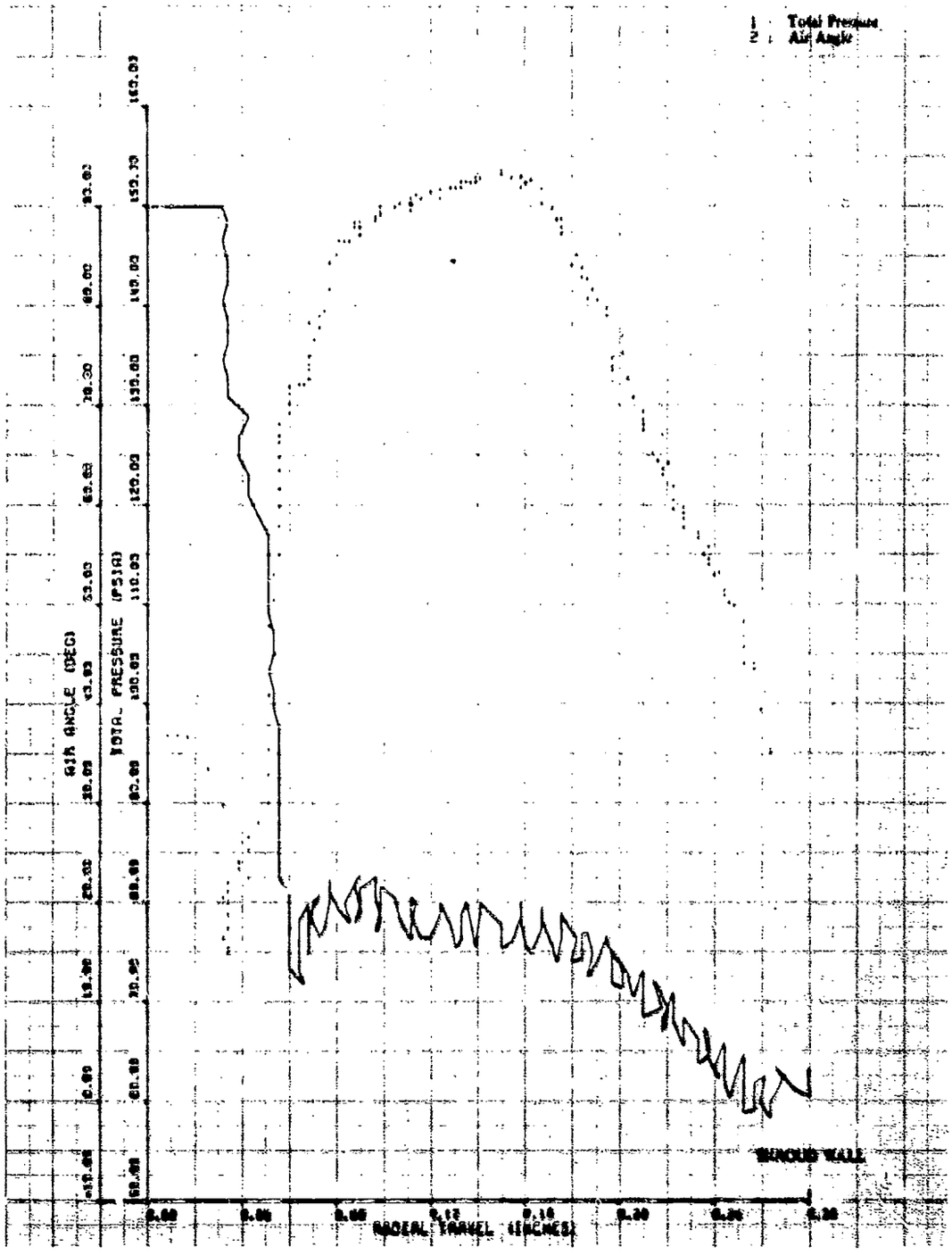

Figure 187. Impeller Exit Traverse, Build No. 6, 95% Speed, 10-deg IGV, Near Stall.

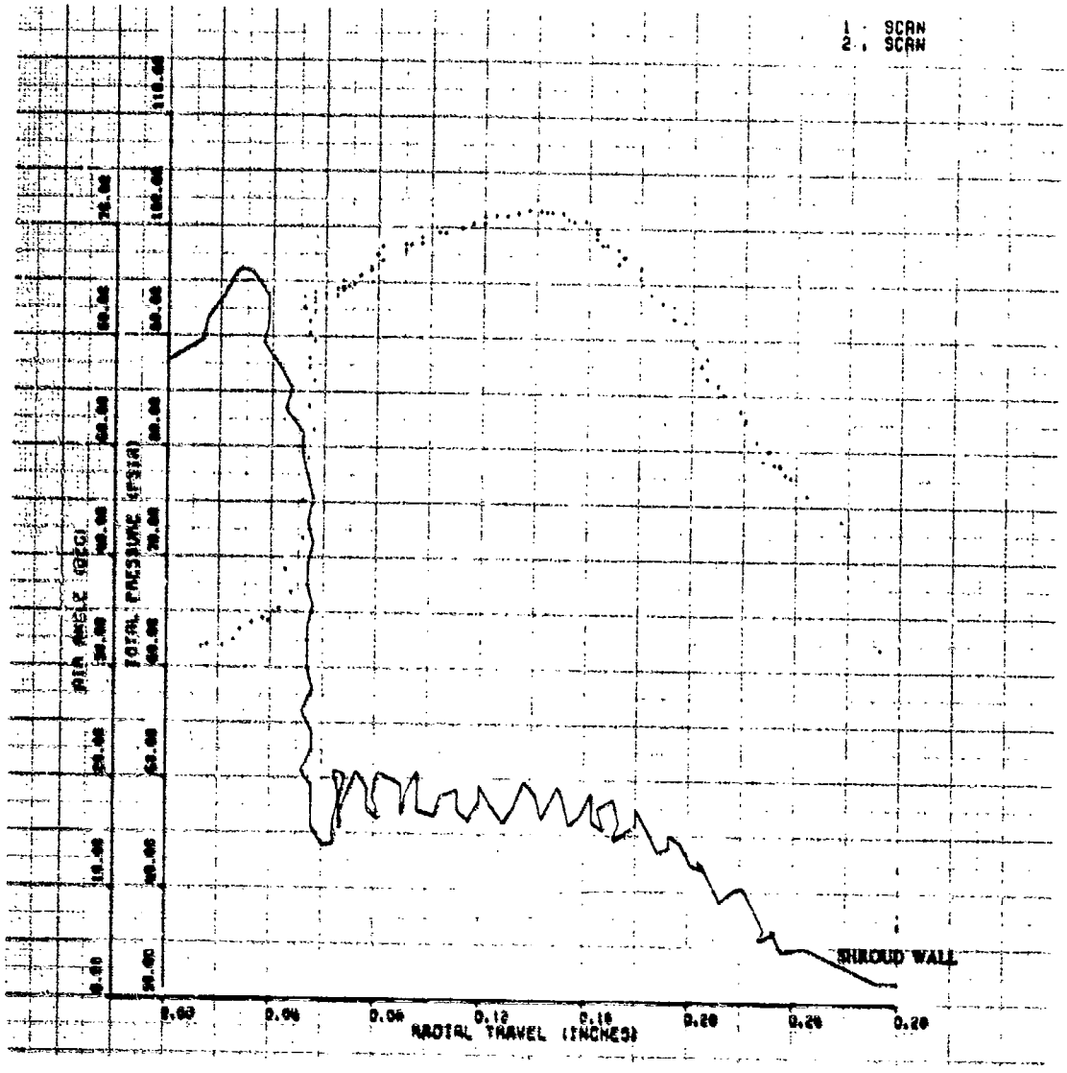

Figure 188. Impeller Exit Traverse, Build No. 6, 85% Speed, 30-deg IGV.

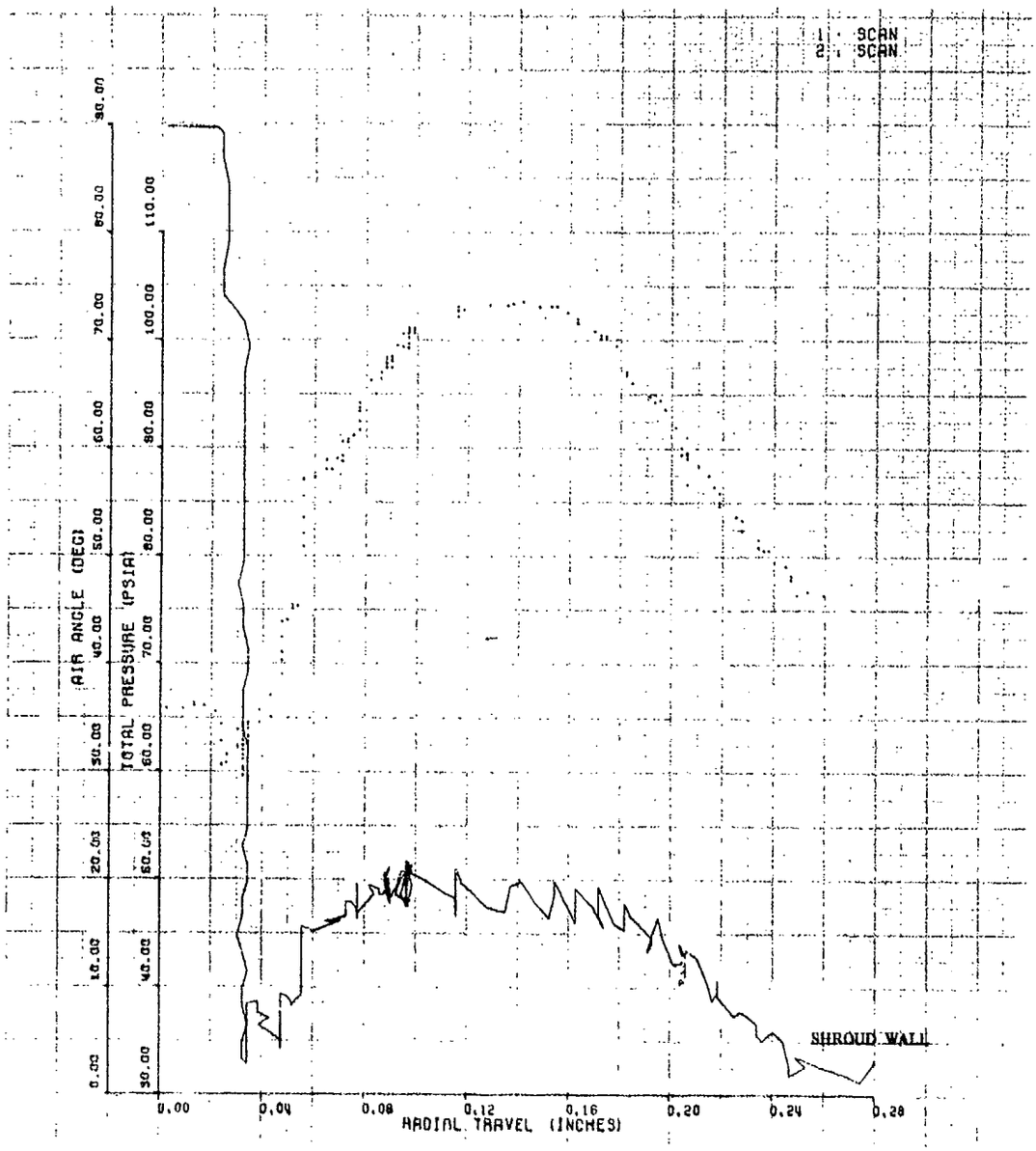

Figure 189. Impeller Exit Traverse, Build No. 6, 85% Speed, 20-deg IGV, Near Stall.

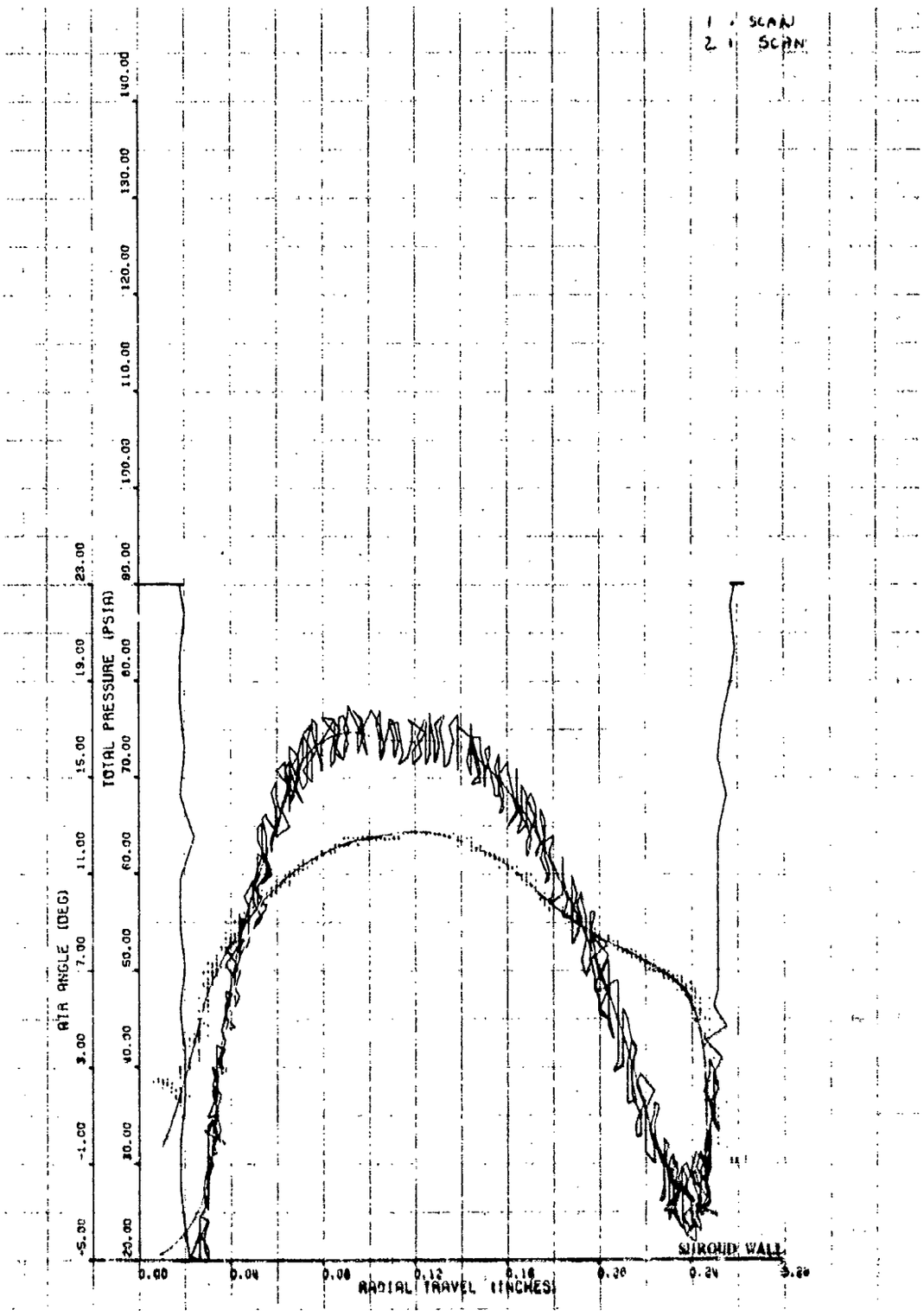

Figure 190. Impeller Exit Traverse, Build No. 3, 70% Speed, 20-deg IGV, Wide Open Discharge.

Figure 191. Impeller Exit Traverse, Build No. 3, 70% Speed, 20-deg IGV, Near Stall.

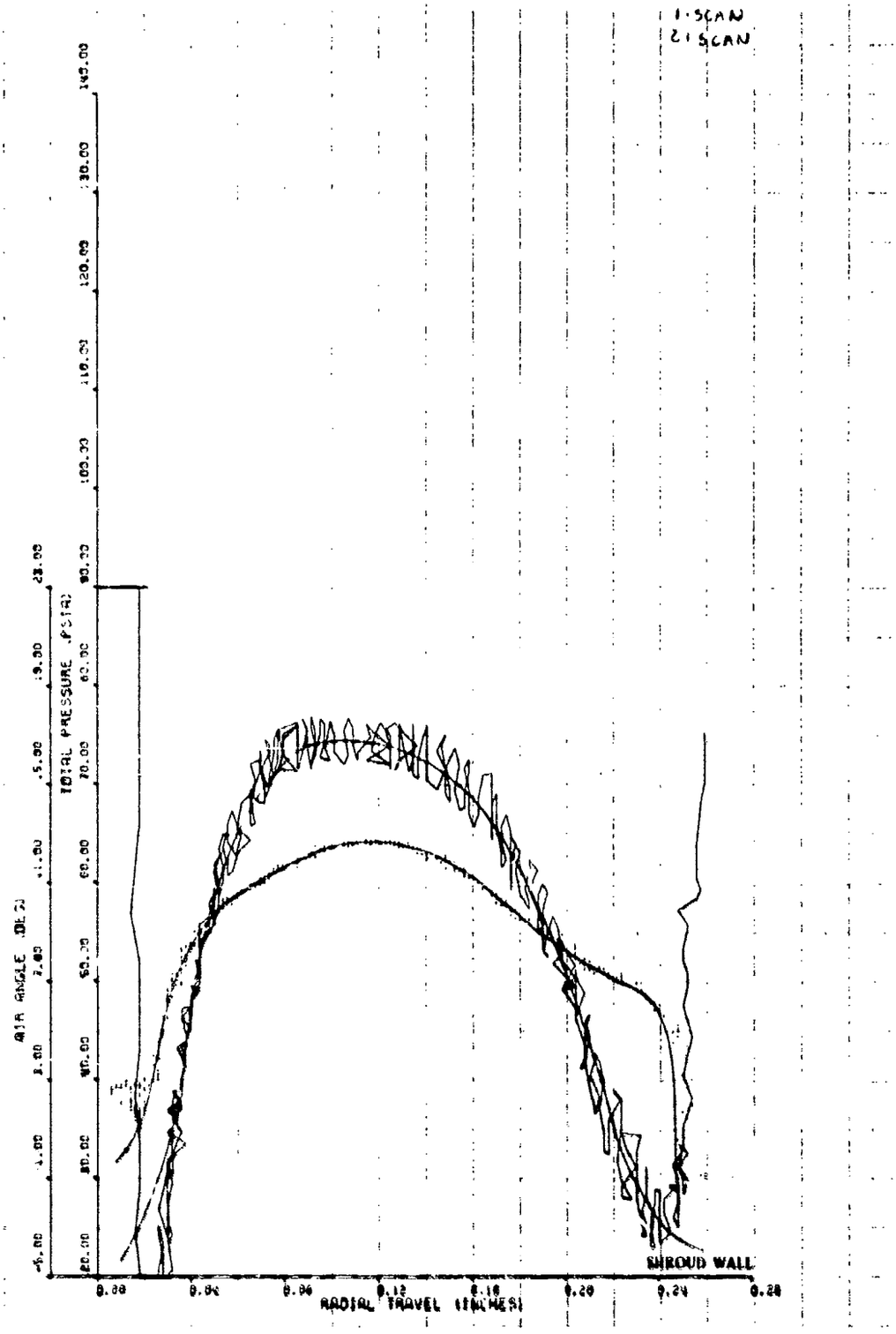

Figure 192. Impeller Exit Traverse, Build No. 3, 70% Speed, 20-deg IGV, Below Near Stall.

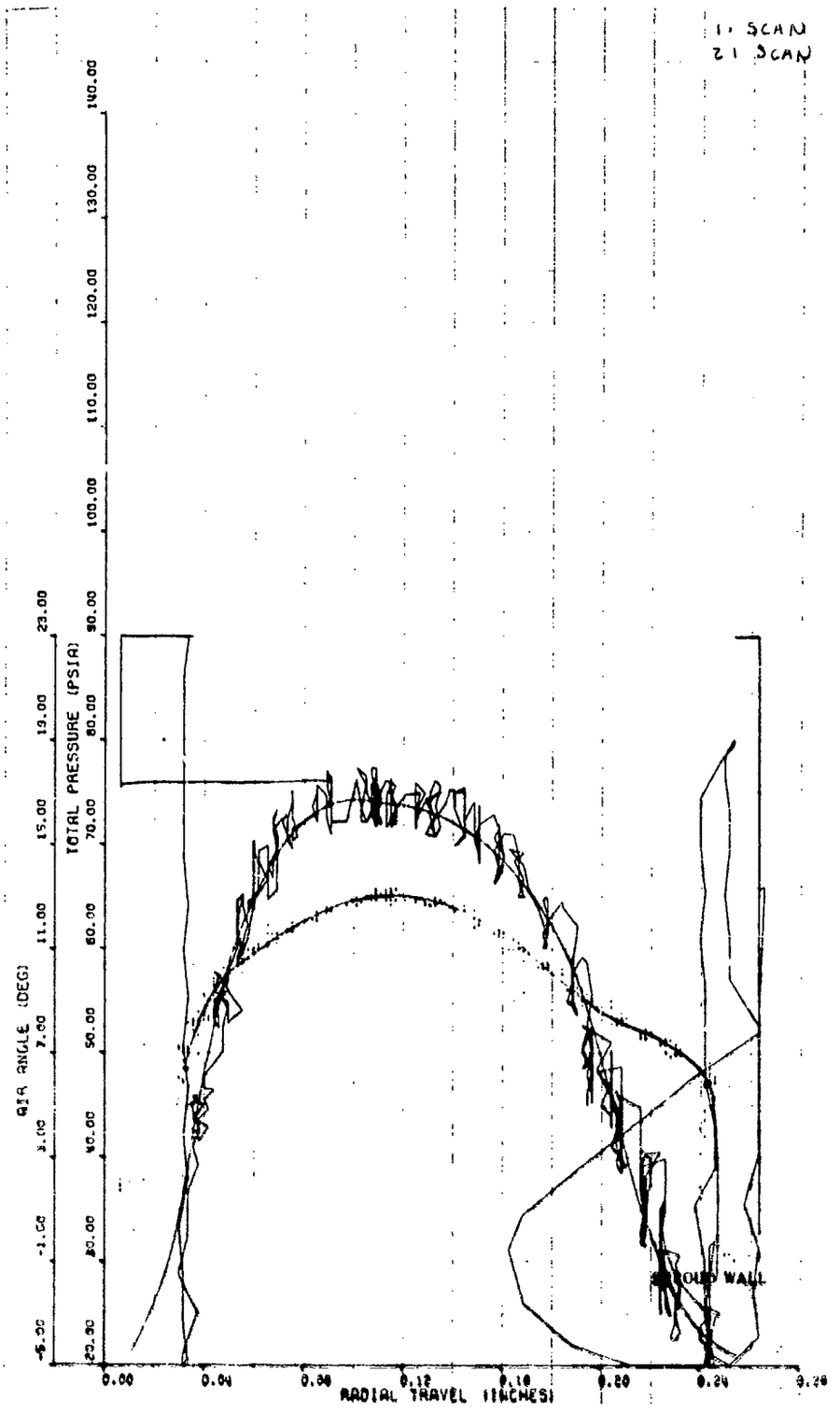

Figure 193. Impeller Exit Traverse, Build No. 3, 70% Speed, 10-deg IGV, Wide Open Discharge.

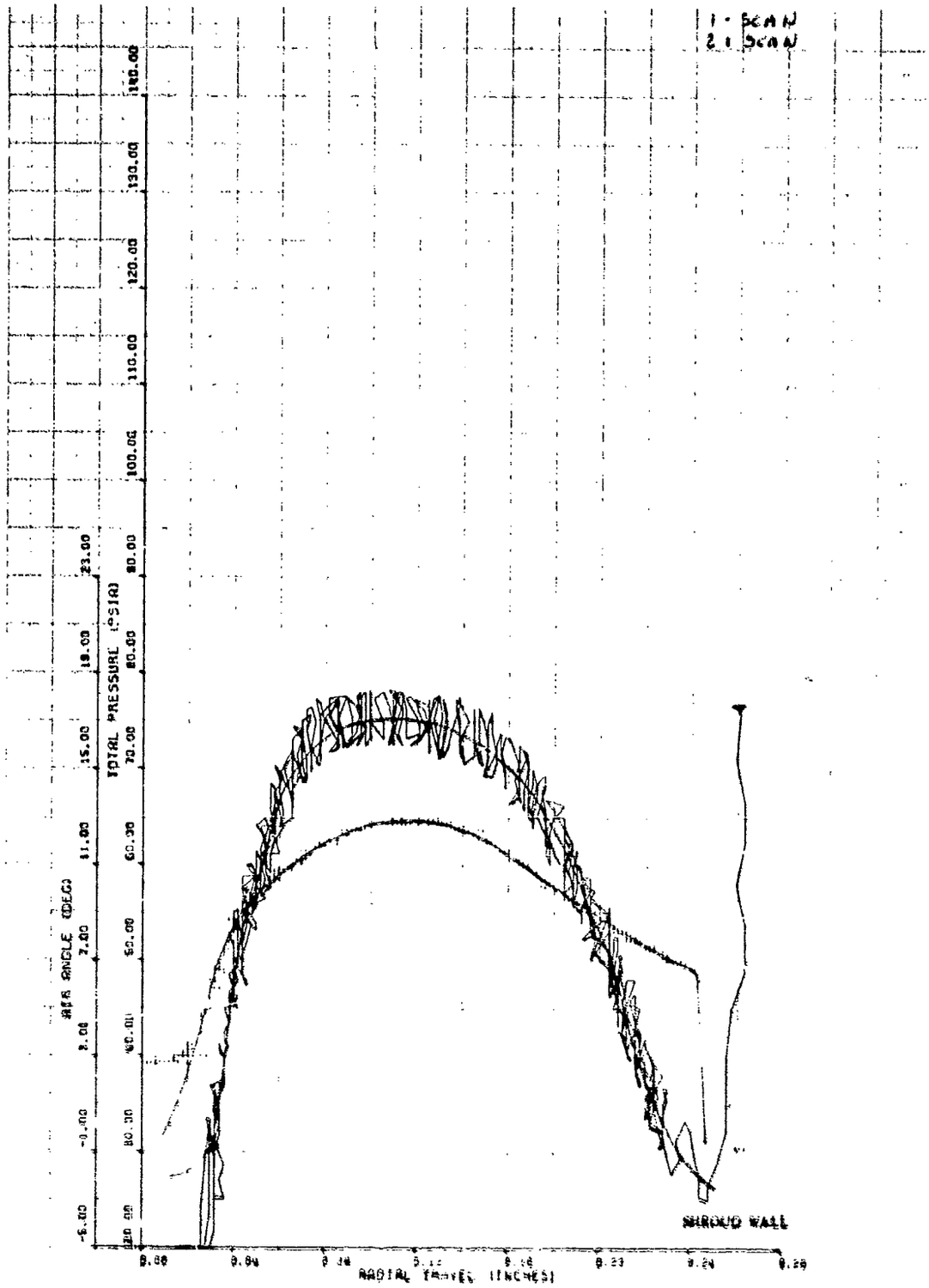

Figure 194. Impeller Exit Traverse, Build No. 3, 70% Speed, 10-deg IGV, Near Stall.

Figure 195. Impeller Exit Traverse, Build No. 3, 70% Speed, 10-deg IGV, Below Near Stall.

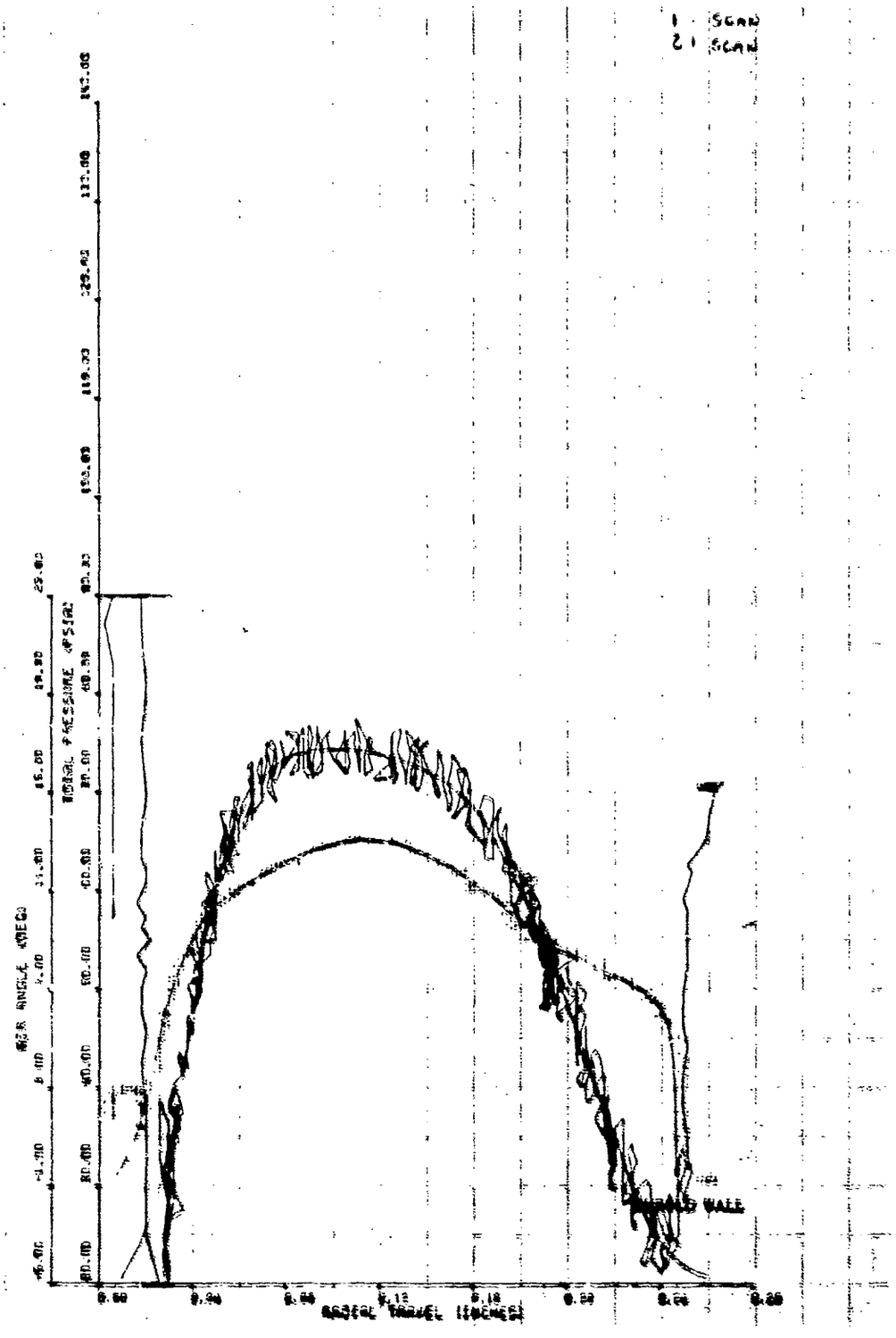

Figure 186. Impeller Exit Traverse, Build No. 3, 70% Speed, 0-deg IGV, Wide Open Discharge.

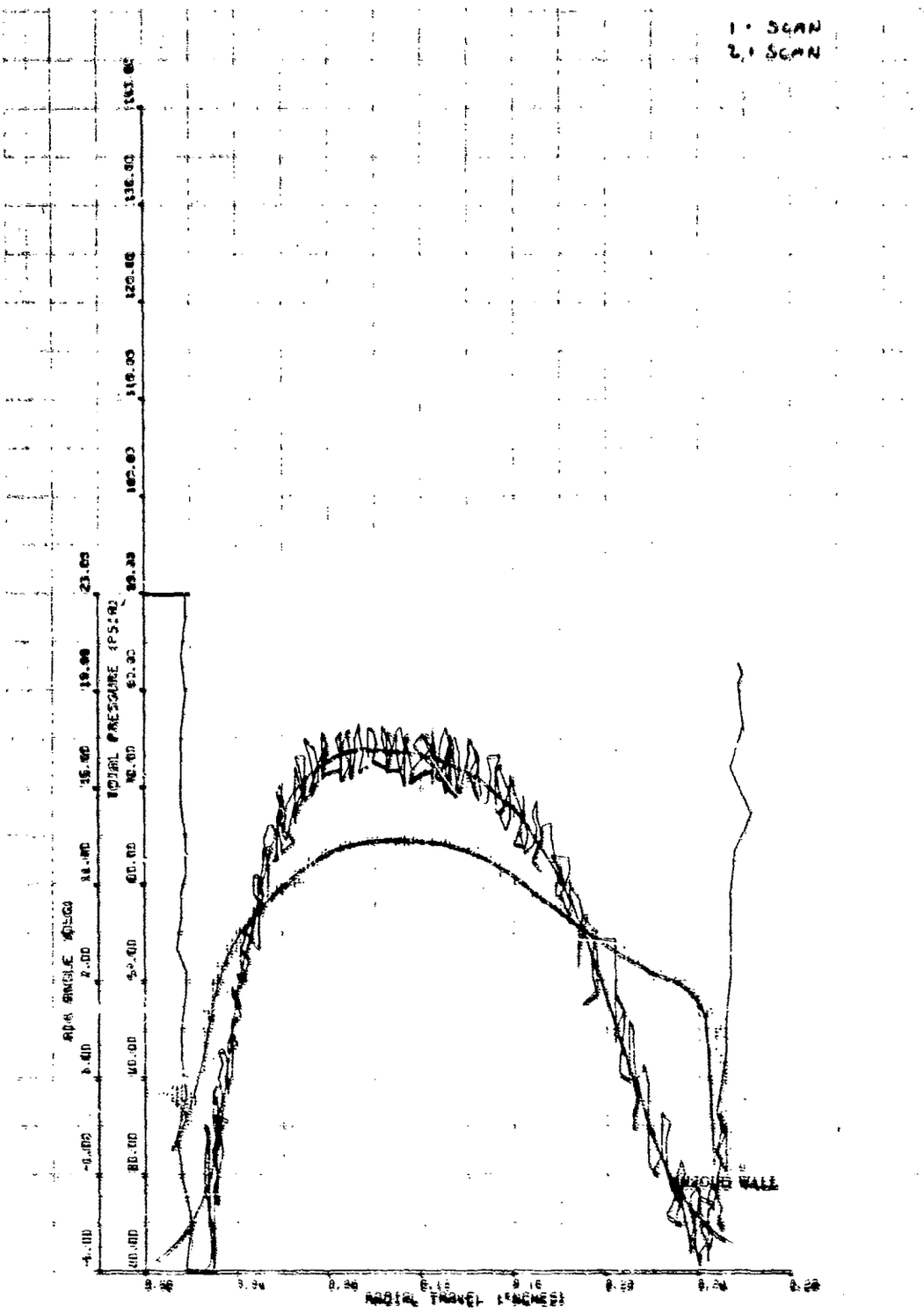

Figure 197. Impeller Exit Traverse, Build No. 3, 70% Speed, 0-deg IGV, Near Stall.

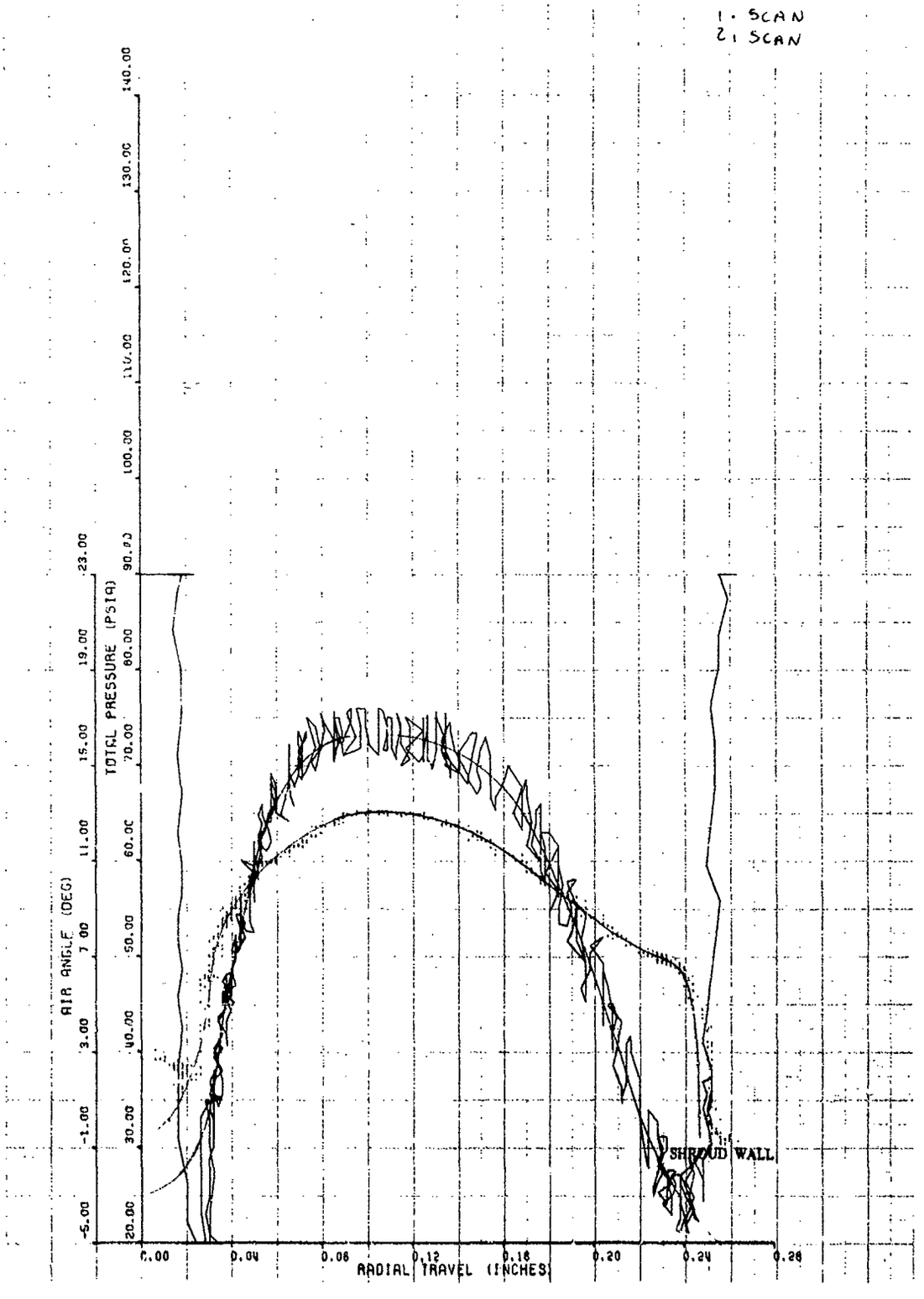

Figure 198. Impeller Exit Traverse, Build No. 3, 70% Speed, 0-deg IGV, Below Near Stall.

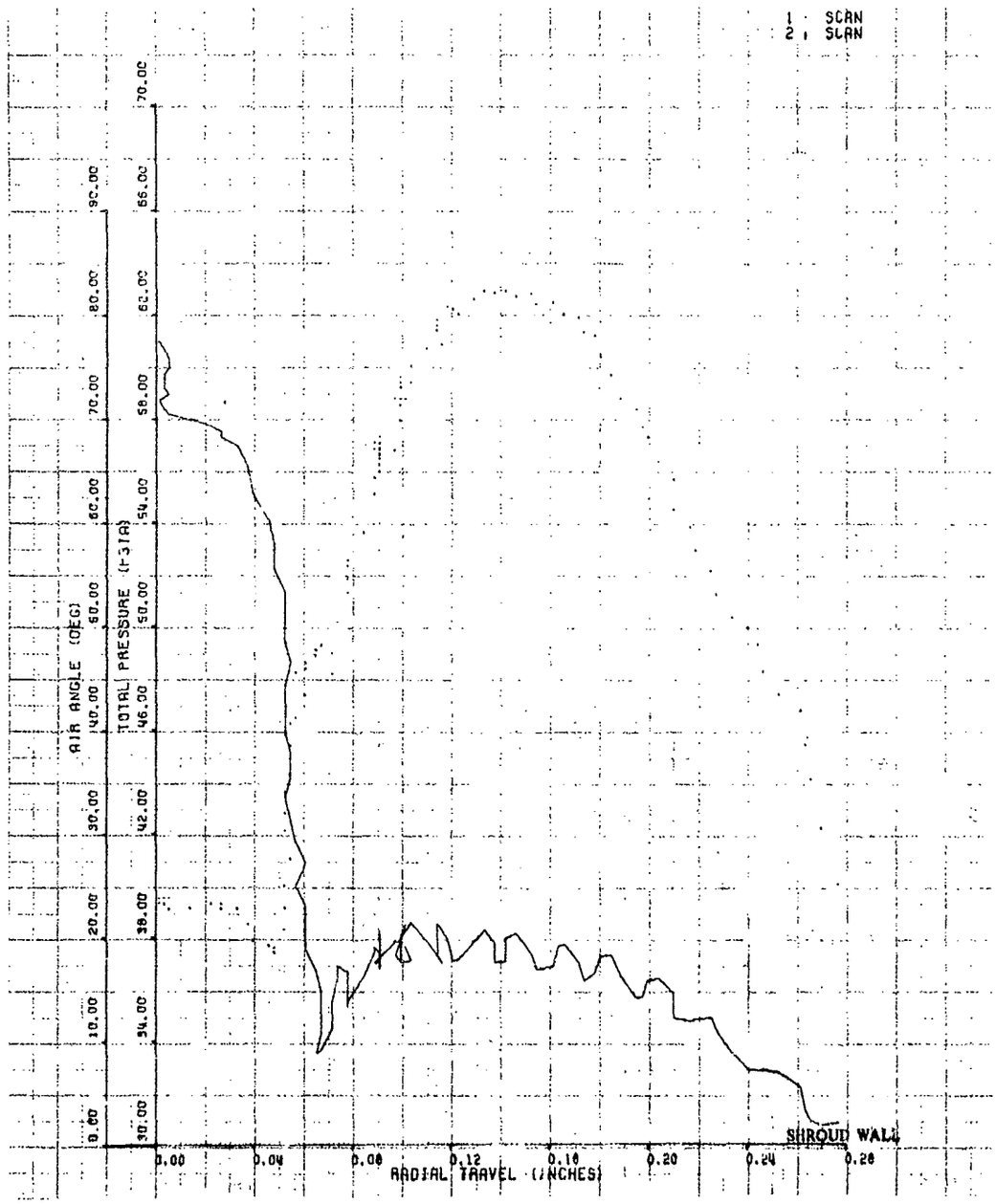

Figure 159. Impeller Exit Traverse, Build No. 6, 70% Speed, 30-deg IGV.

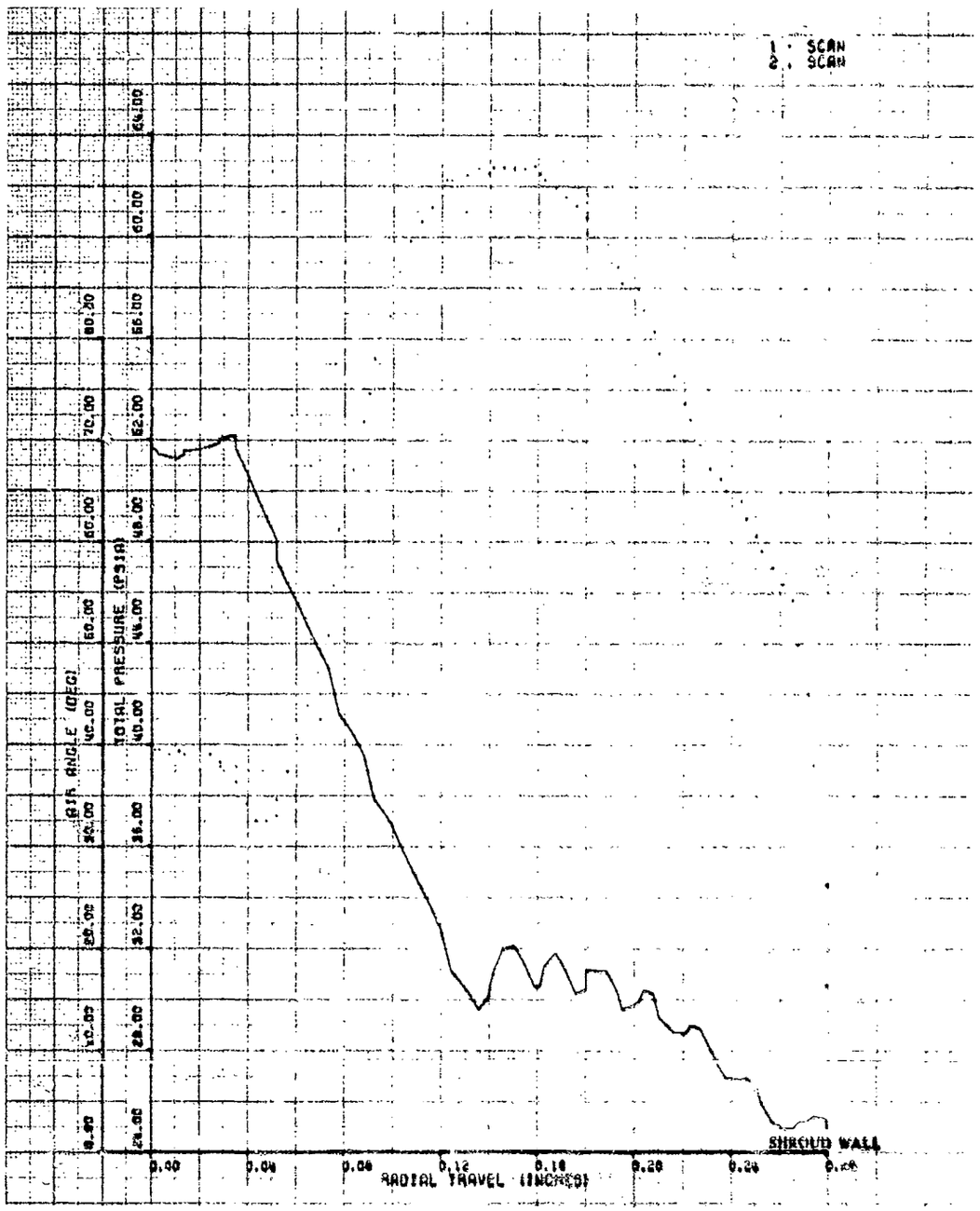

Figure 200. Impeller Exit Traverse, Build No. 6, 70% Speed, 20-deg IGV.

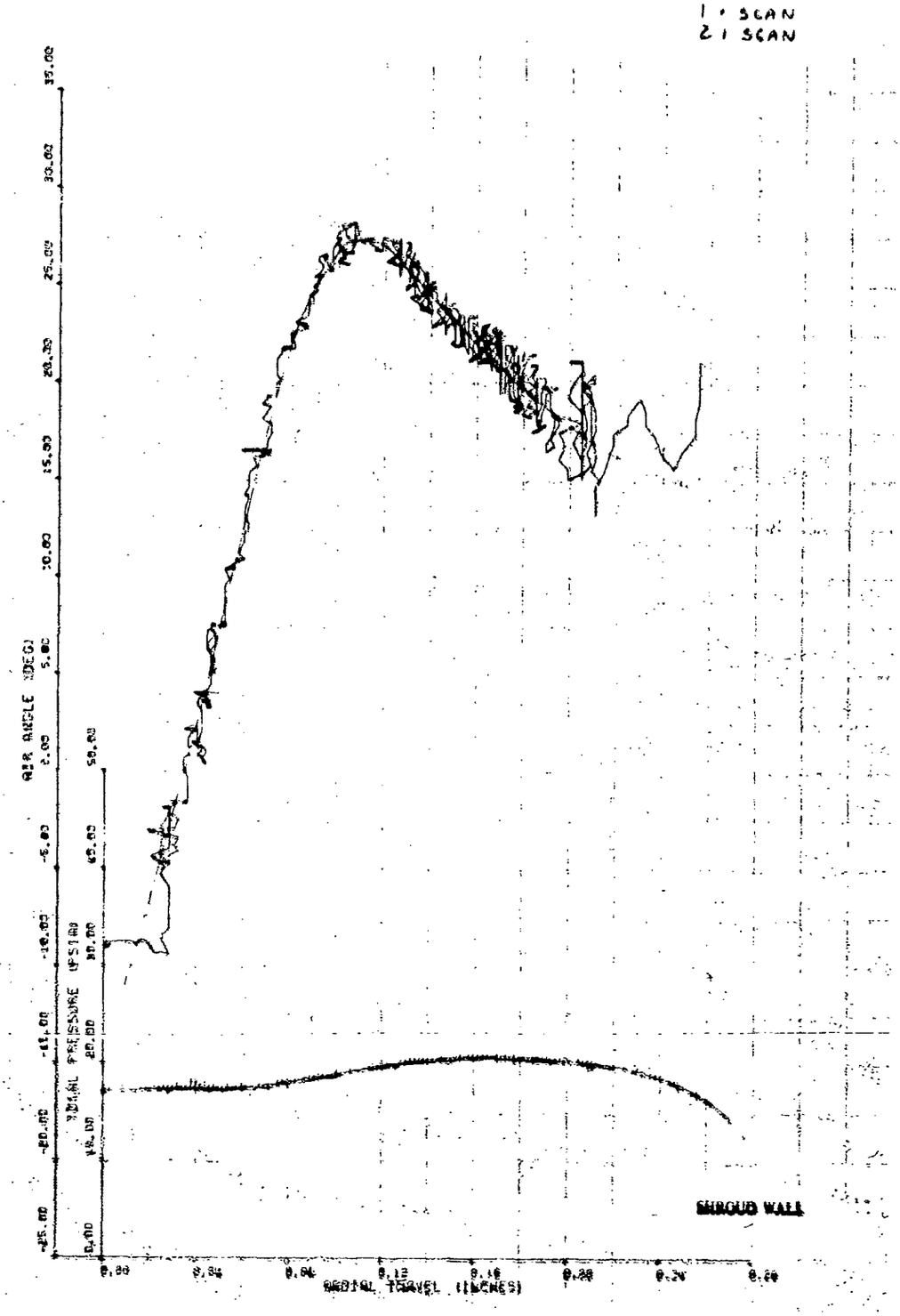

Figure 201. Impeller Exit Traverse, Build No. 3, 30% Speed, 20-deg IGV, Wide Open Discharge.

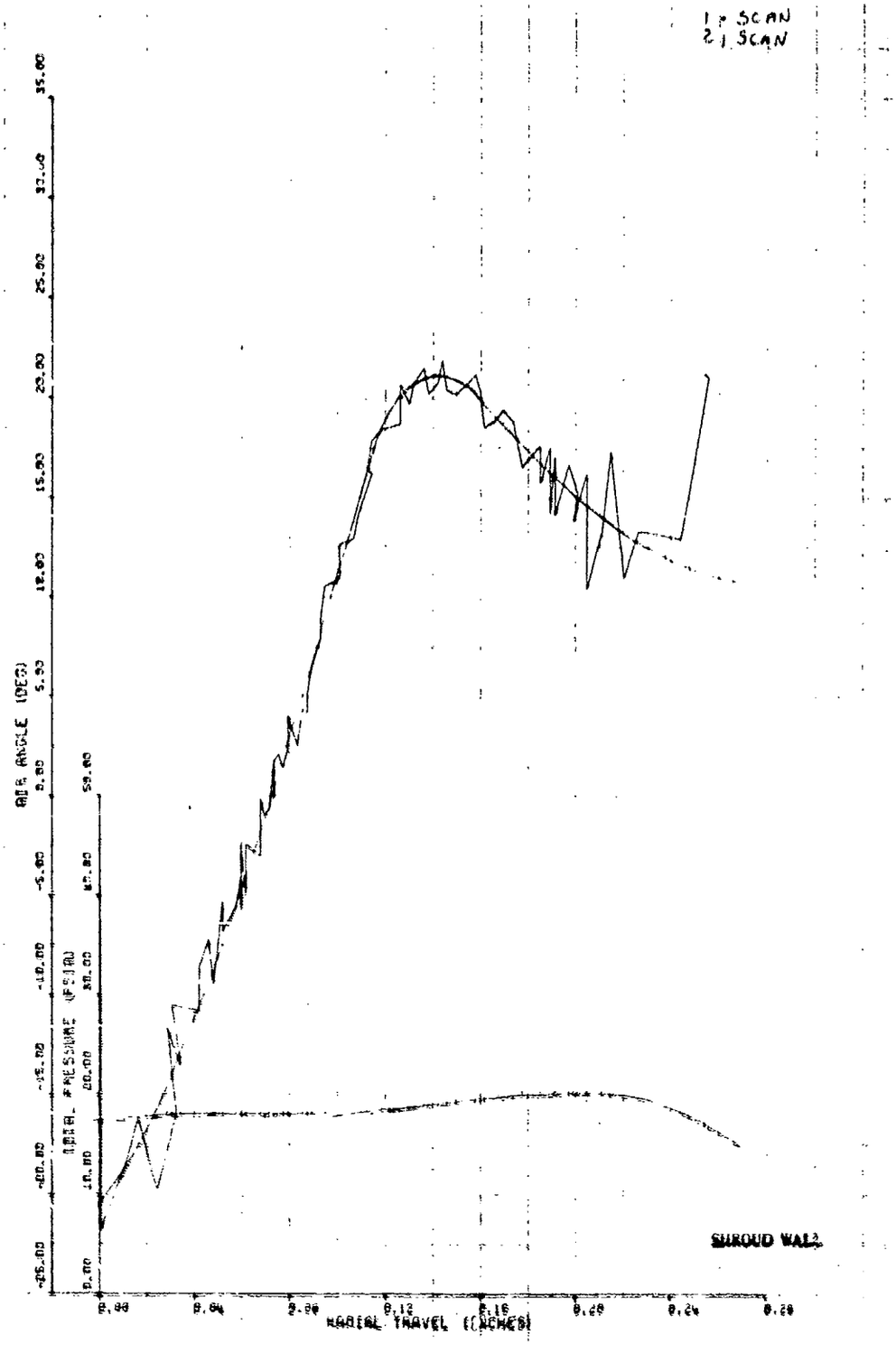

Figure 202. Impeller Exit Traverse, Build No. 3, 30% Speed, 20-deg IGV, Near Stall.

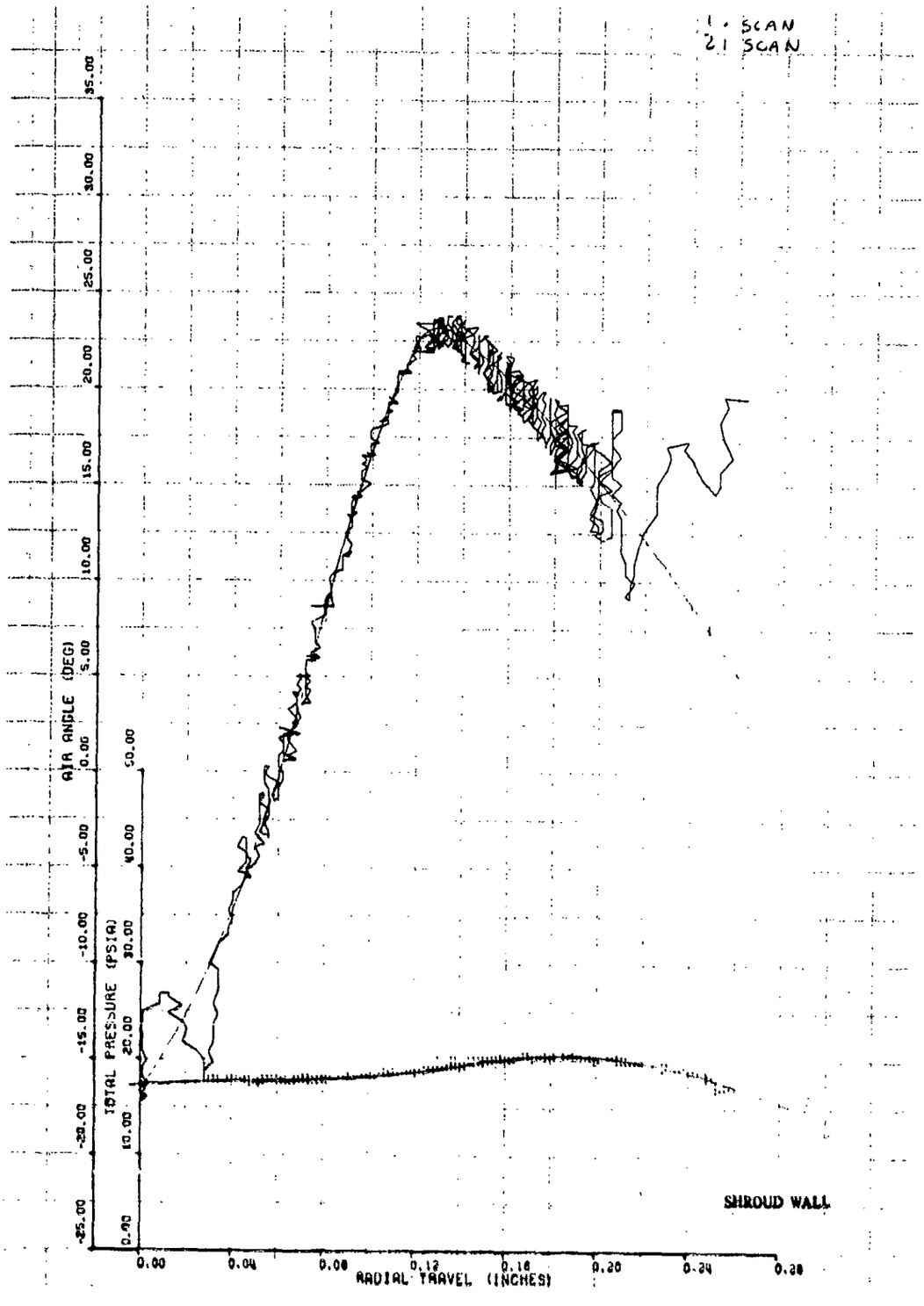

Figure 203. Impeller Exit Traverse, Build No. 3, 30% Speed, 20-deg IGV, Below Near Stall.

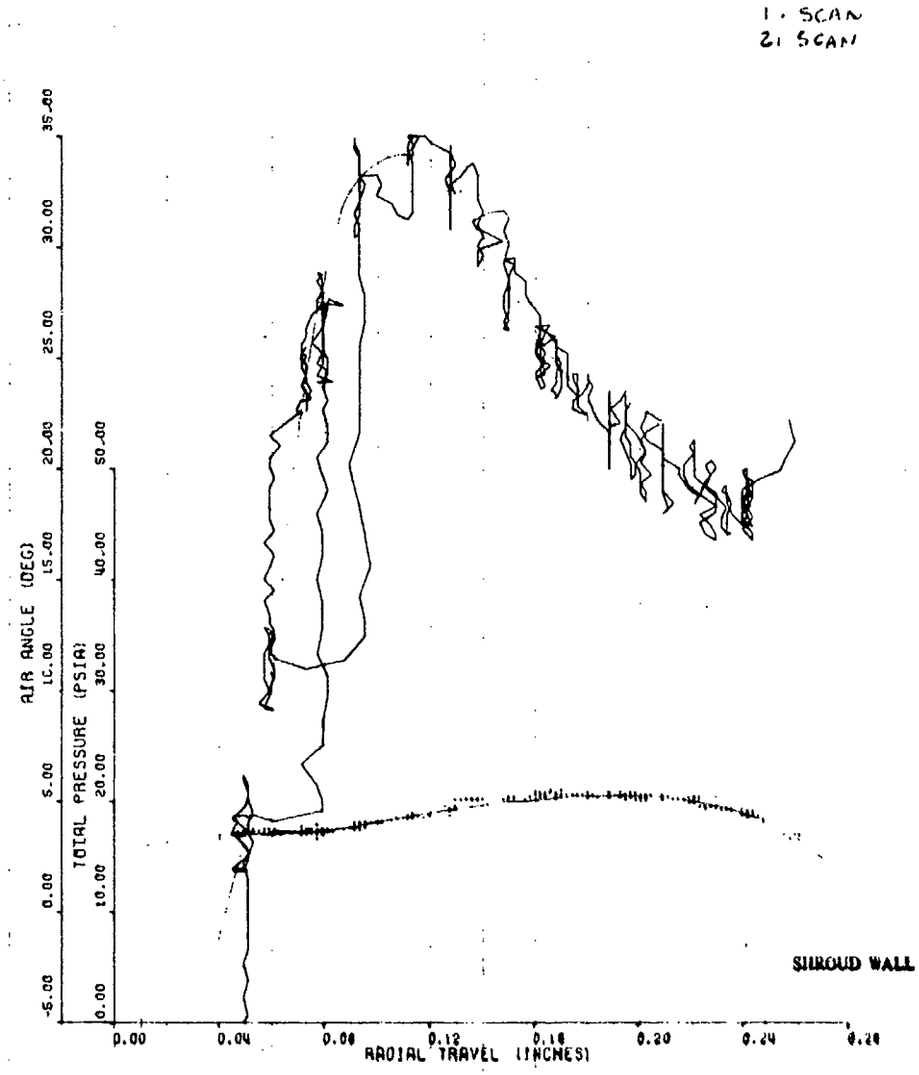

Figure 204. Impeller Exit Traverse, Build No. 3, 30% Speed, 10-deg IGV, Wide Open Discharge.

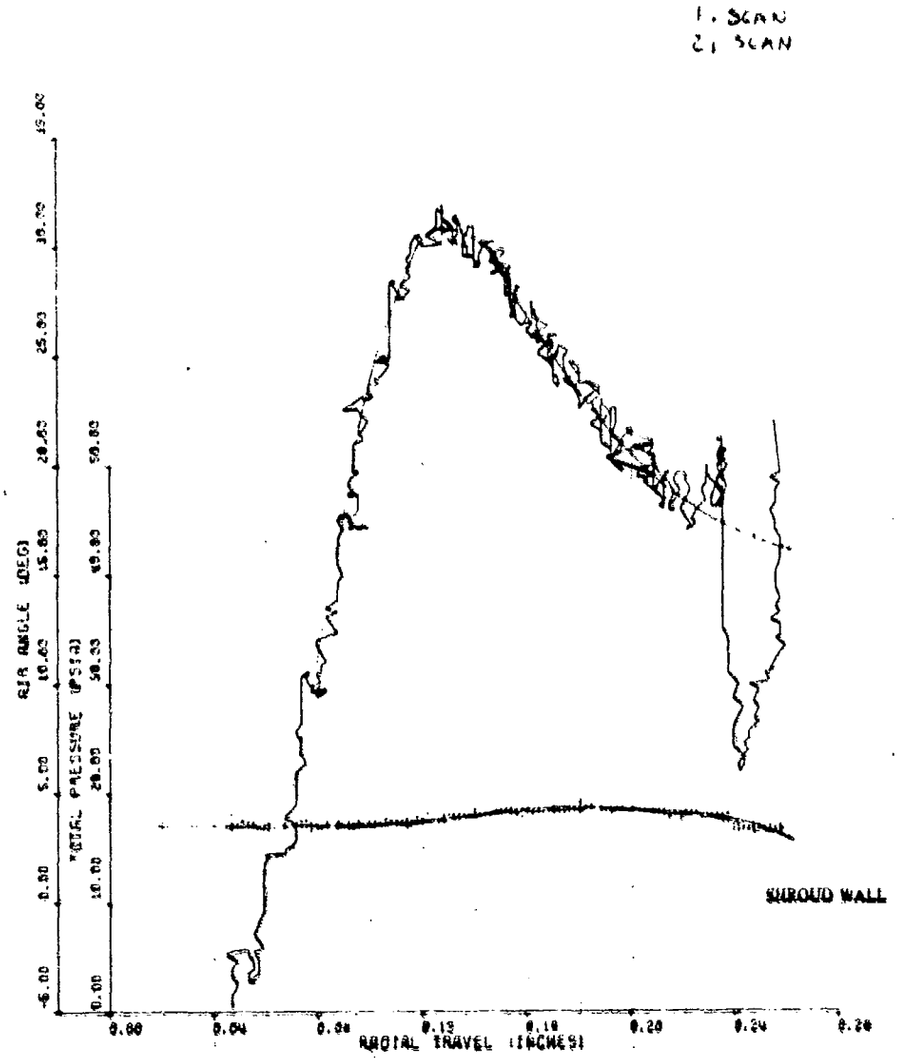

Figure 205. Impeller Exit Traverse, Build No. 3, 30% Speed, 10-deg IGV, Near Stall.

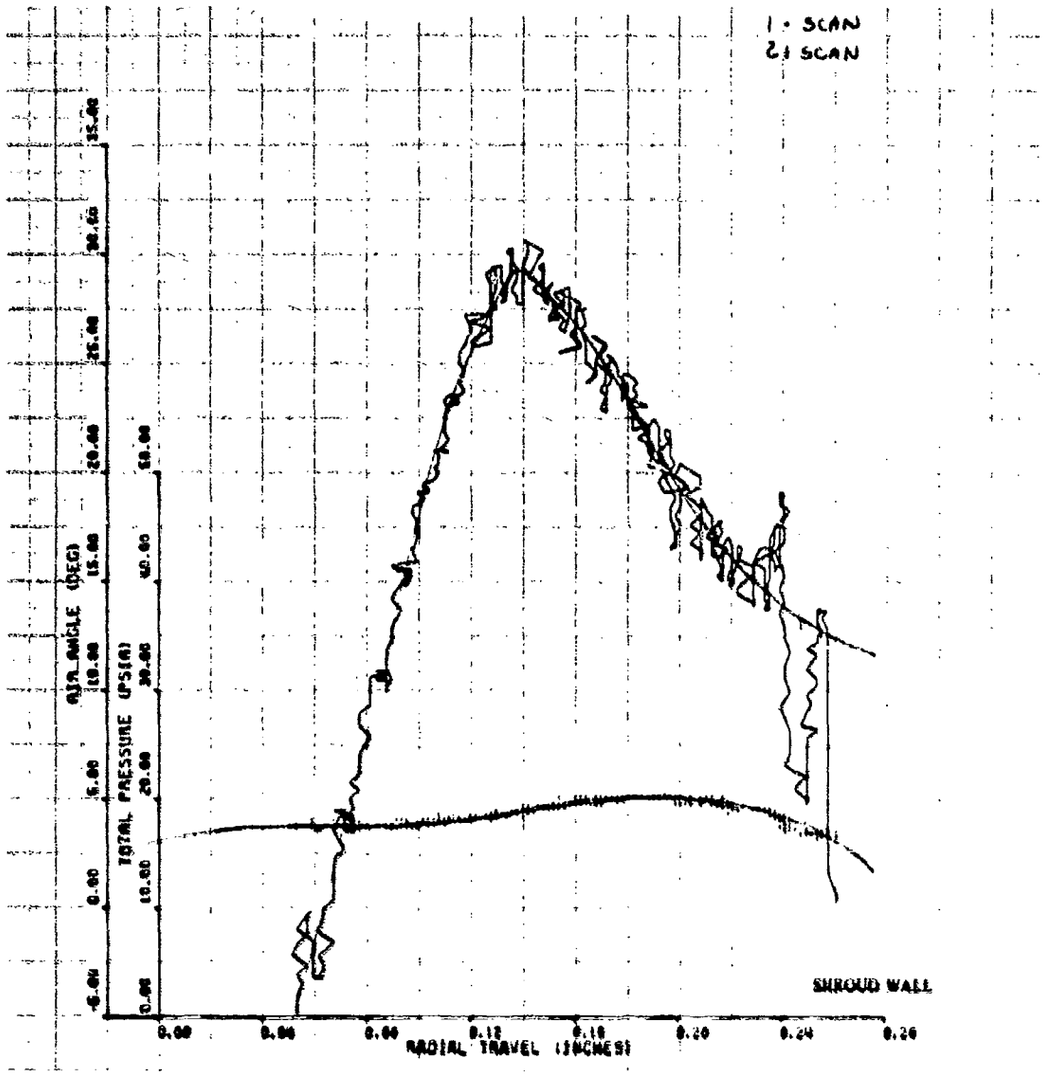

Figure 206. Impeller Exit Traverse, Build No. 3, 30% Speed, 10-deg IGV, Below Near Stall.

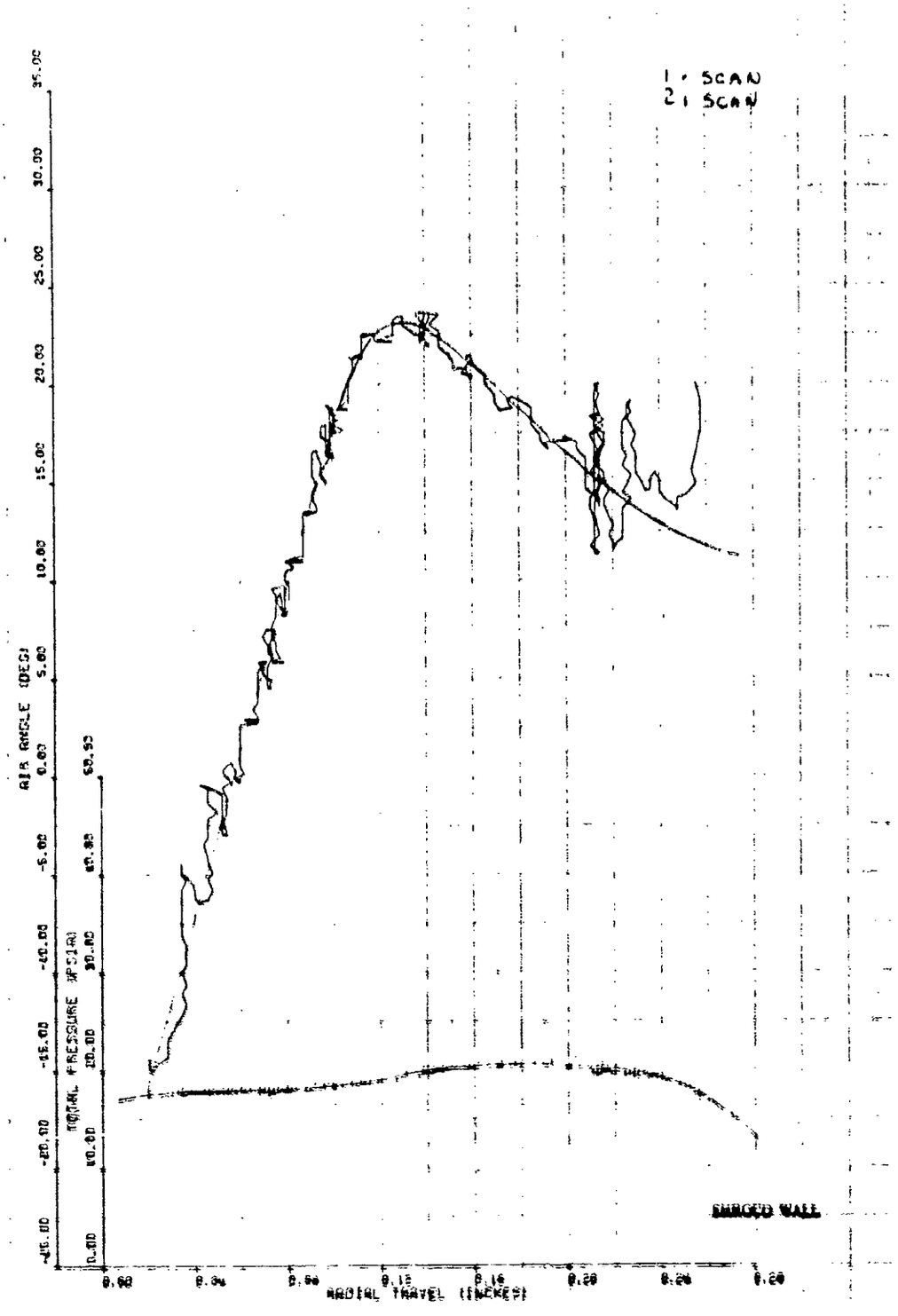

Figure 207. Impeller Exit Traverse, Build No. 3, 30% Speed, 10-deg IGV, Below Near Stall.

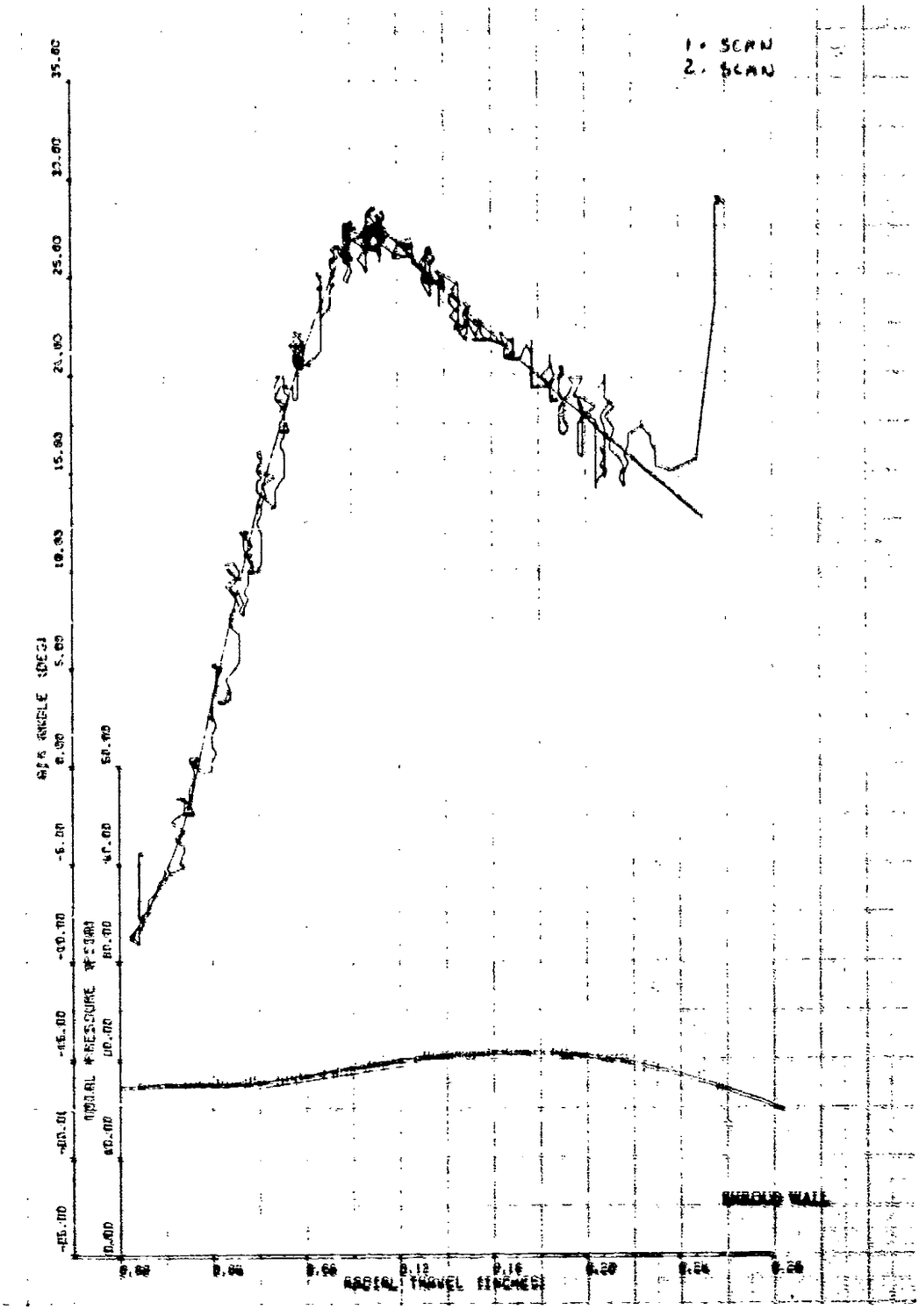

Figure 20s. Impeller Exit Traverse, Build No. 3, 30% Speed, 0-deg IGV, Wide Open Discharge.

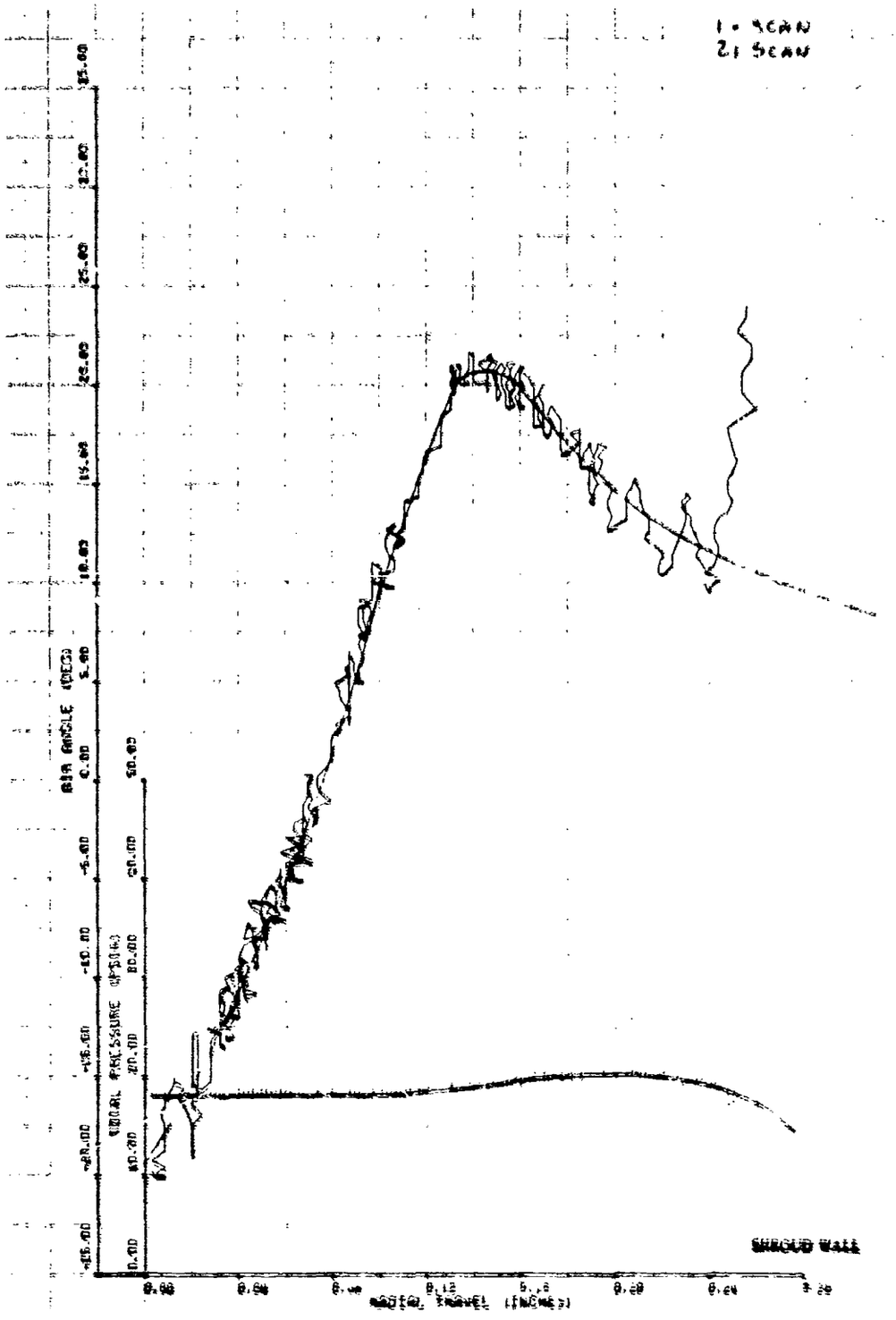

Figure 209. Impeller Exit Traverse, Build No. 3, 30% Speed, 0-deg IGV, Near Stall.

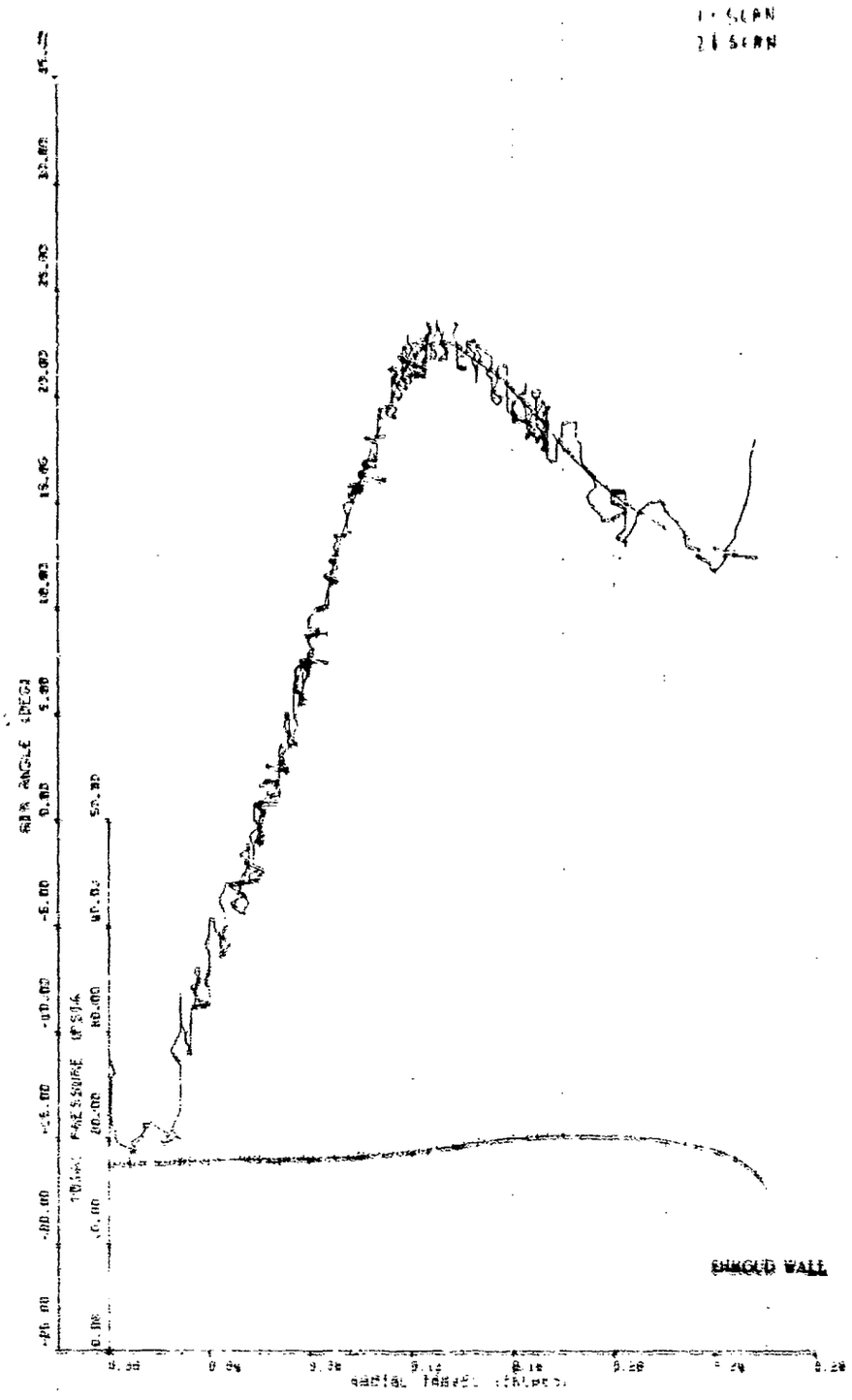

Figure 210. Impeller Exit Traverse, Build No. 3, 30% Speed, Peak Eff, 0 deg IGV, Below Near Stall.

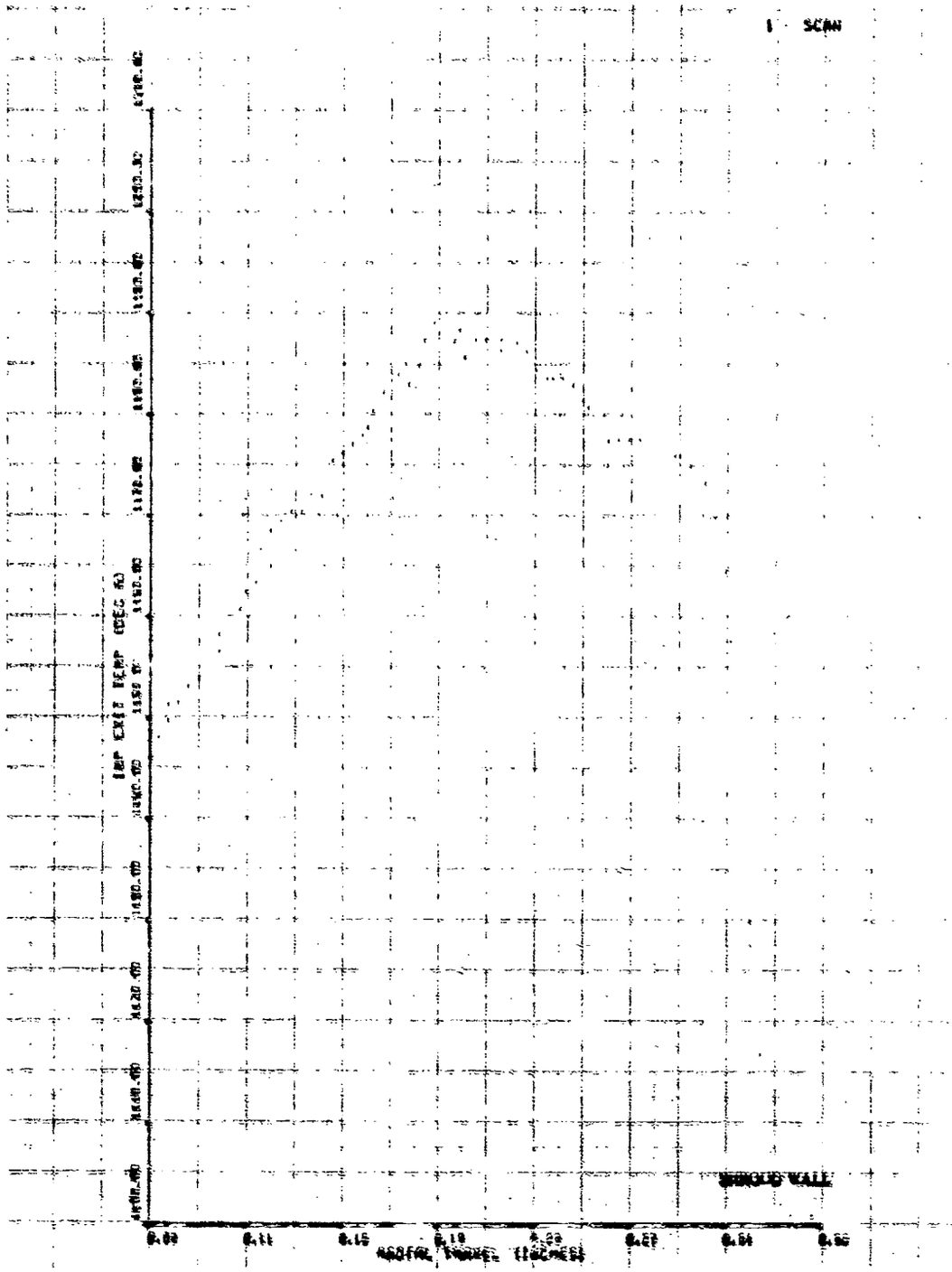

Figure 211. Impeller Exit Temperature Traverse, Build No. 6, 101 Speed, 5-deg IGV.

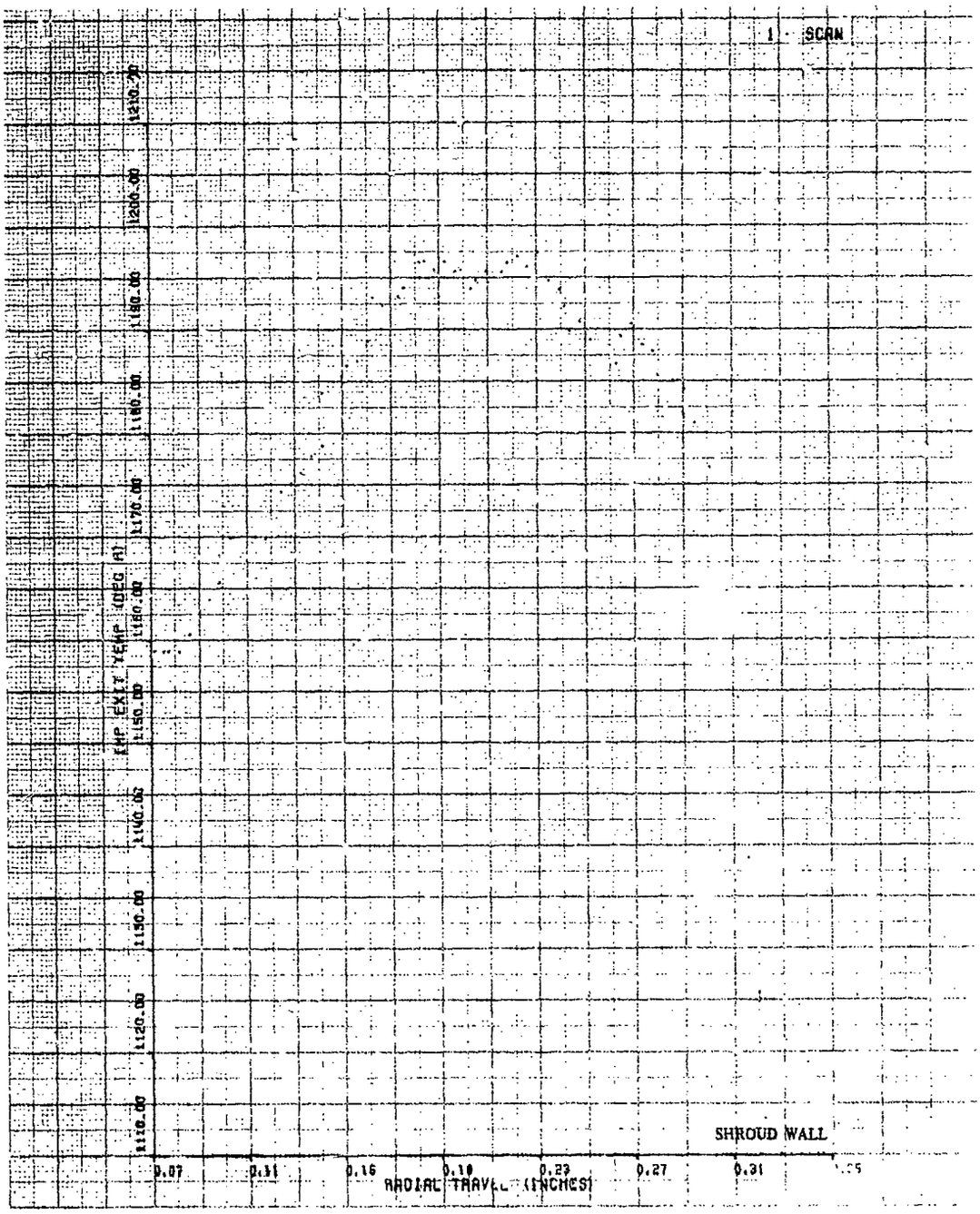

Figure 212. Impeller Exit Temperature Traverse, Build No. 6, 101% Speed, 0-deg IGV.

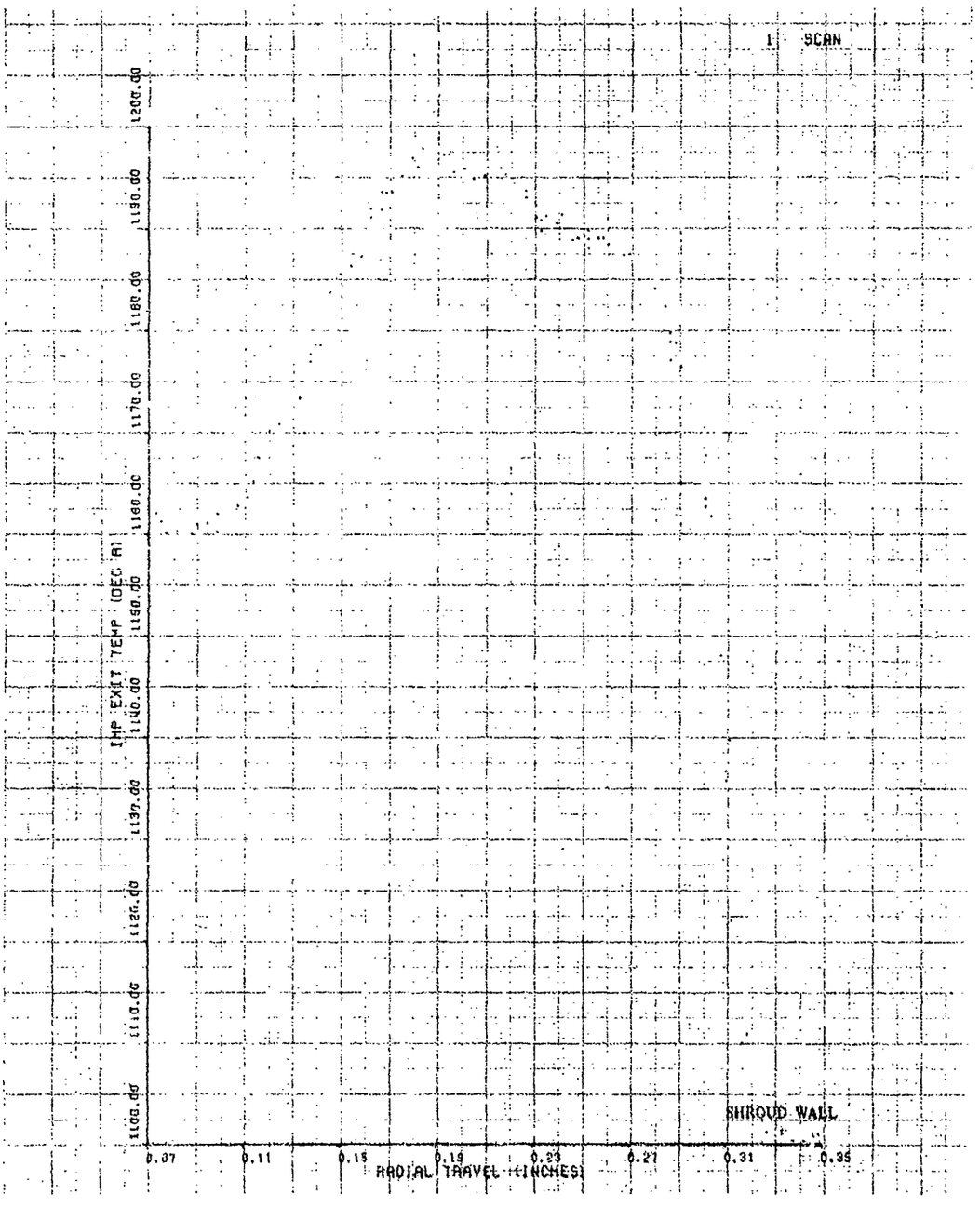

Figure 213. Impeller Exit Traverse With Coolant, Build No. 6, 101% Speed, -4-deg IGV.

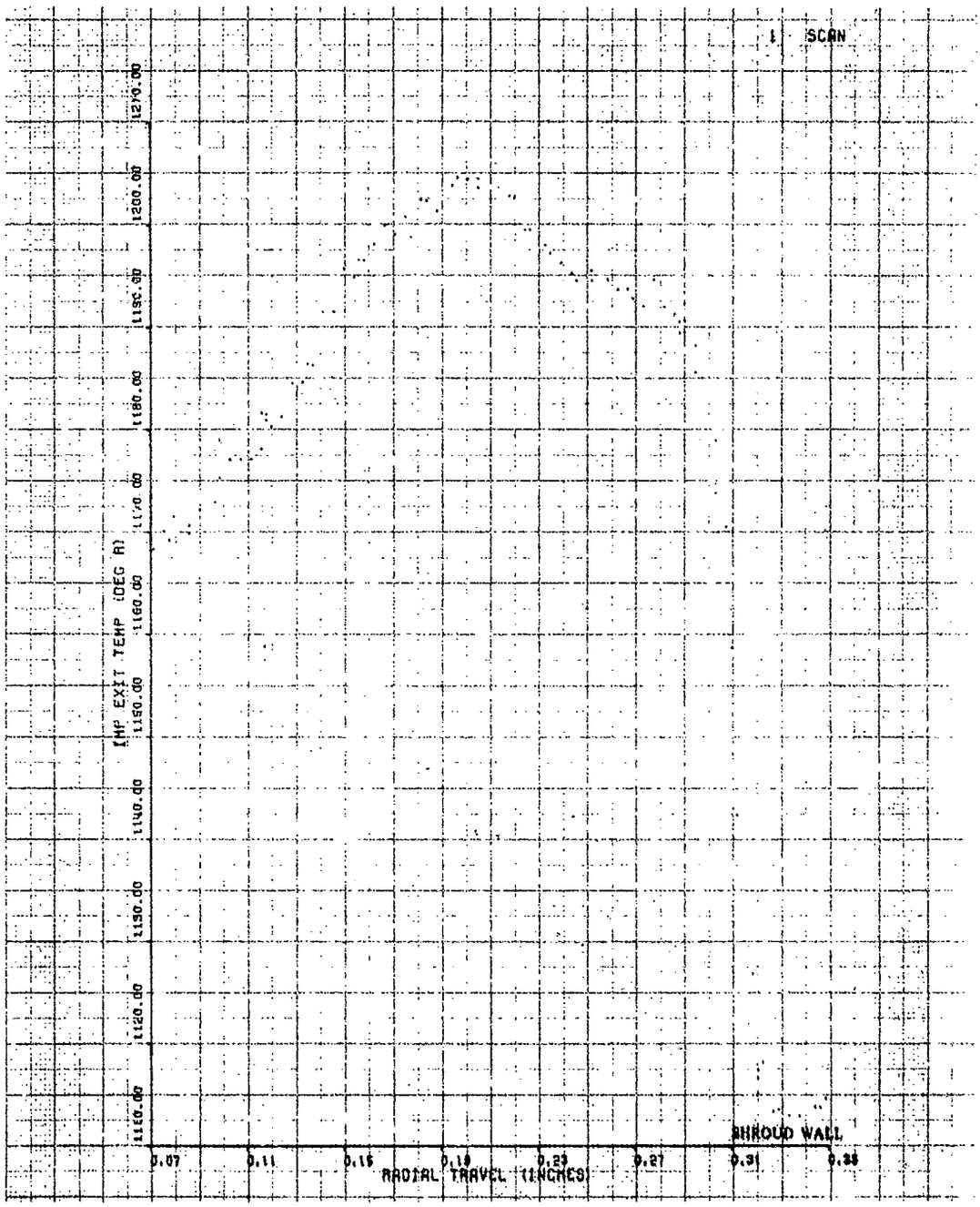

Figure 214. Impeller Exit Traverse With Coolant, Build No. 6, 101% Speed, -4-deg IGV.

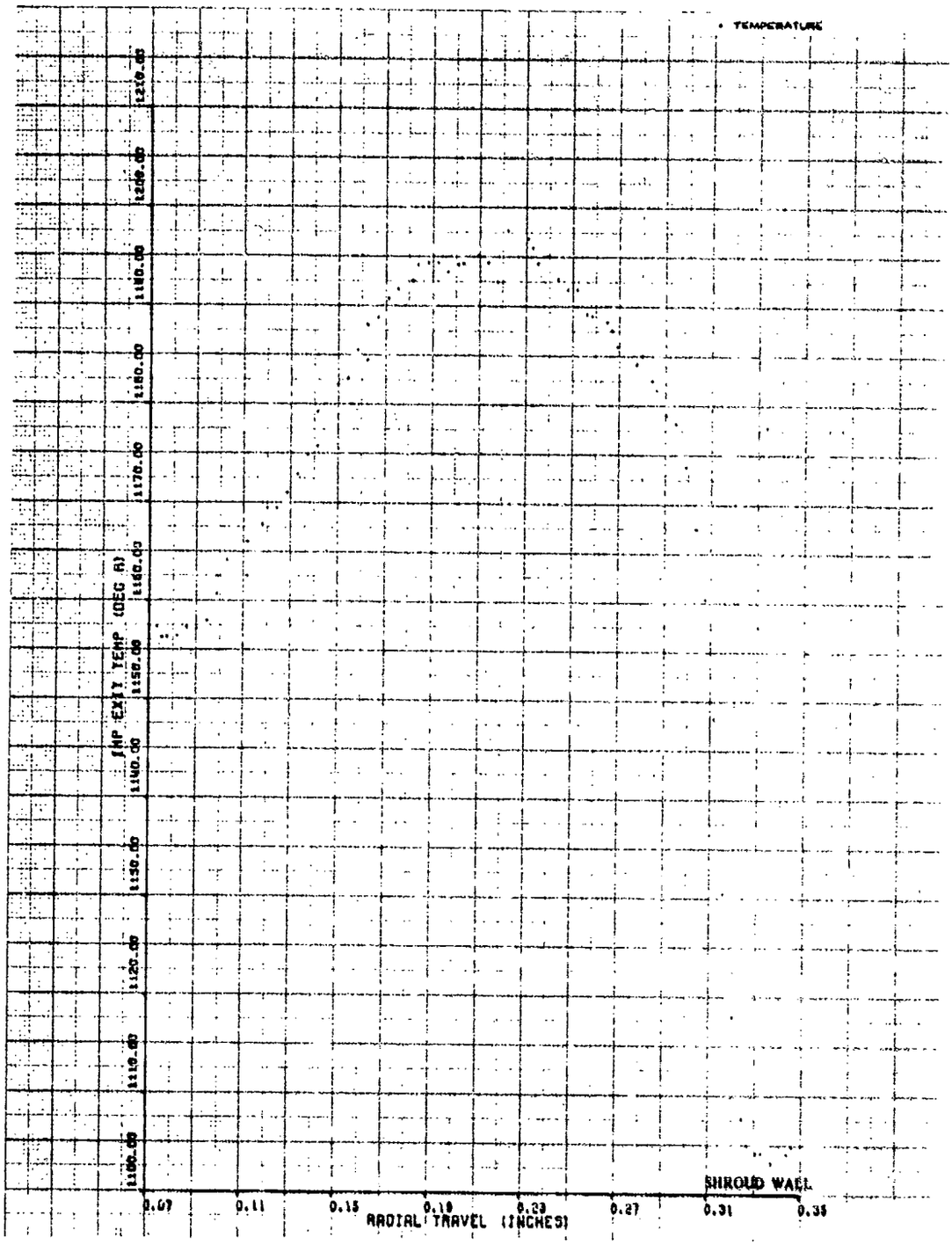

Figure 215. Impeller Exit Temperature Traverse, Build No. 6, 101% Speed, -4-deg IGV.

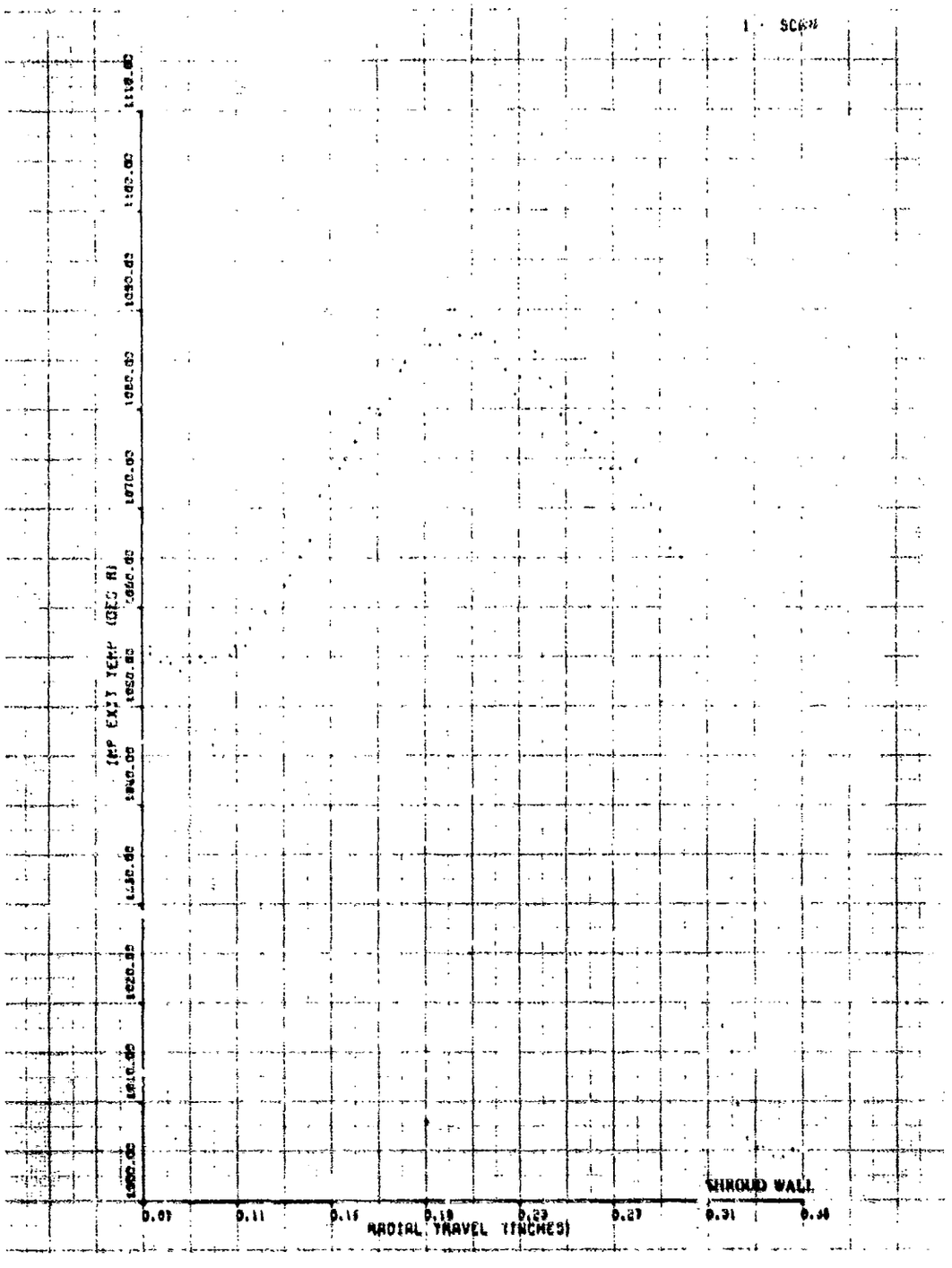

Figure 216. Impeller Exit Temperature Traverse, Build No. 6, 94.5% Speed, 15-deg IGV.

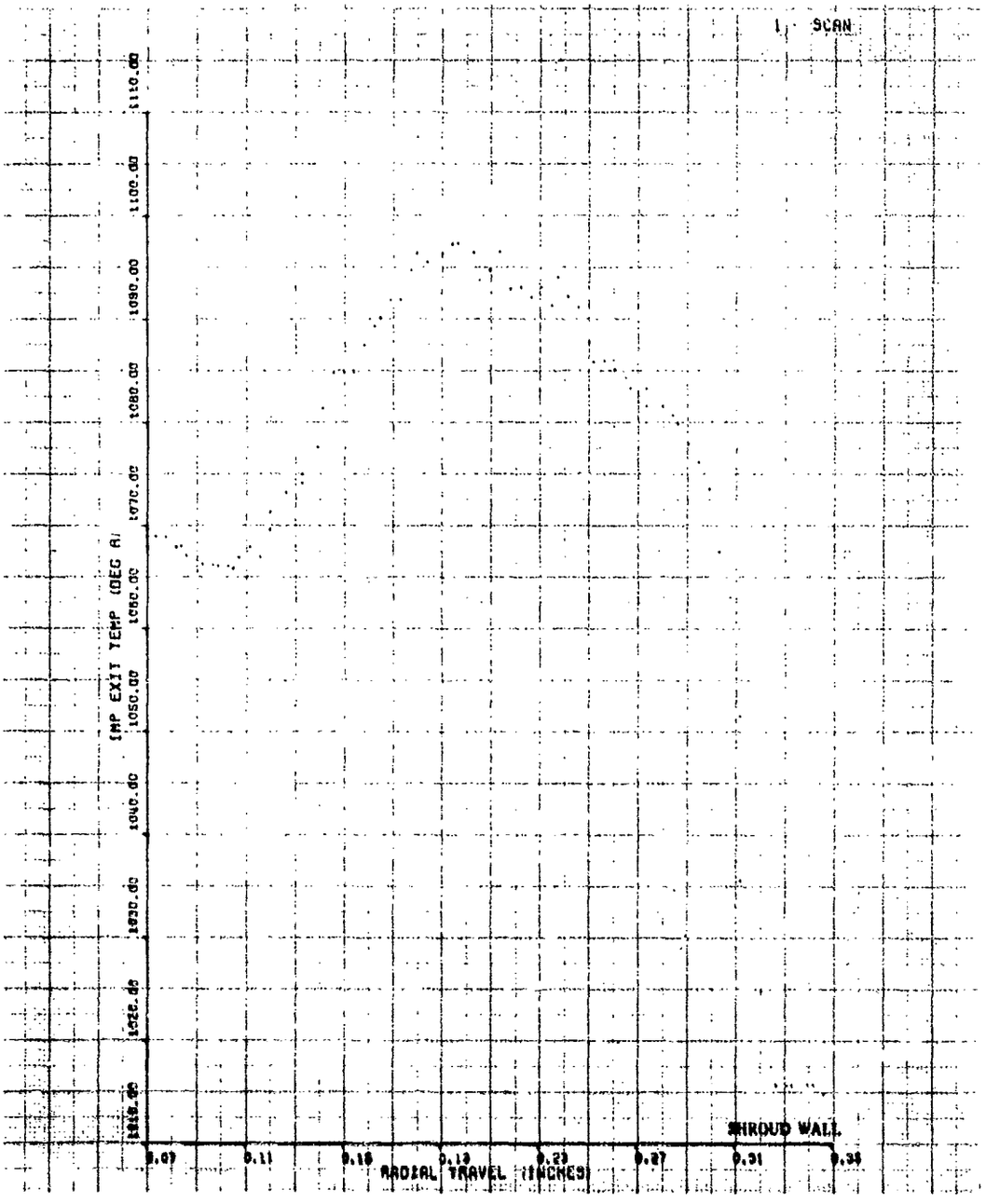

Figure 217. Impeller Exit Temperature Traverse, Build No. 6, 94.5% Speed, 10-deg IGV.

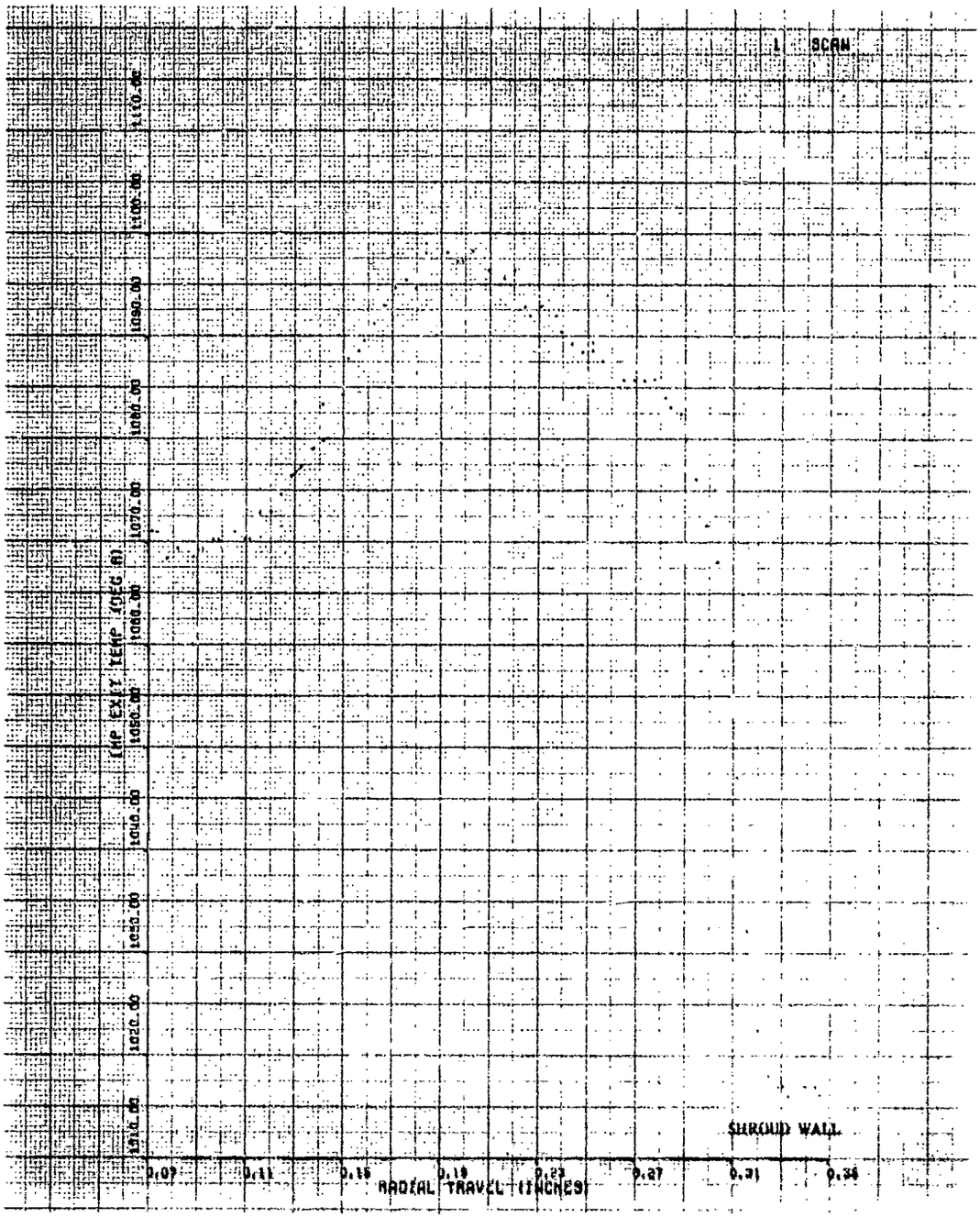

Figure 218. Impeller Exit Temperature Traverse, Build No. 6, 95% Speed, 10-deg IGV, Wide Open Discharge.

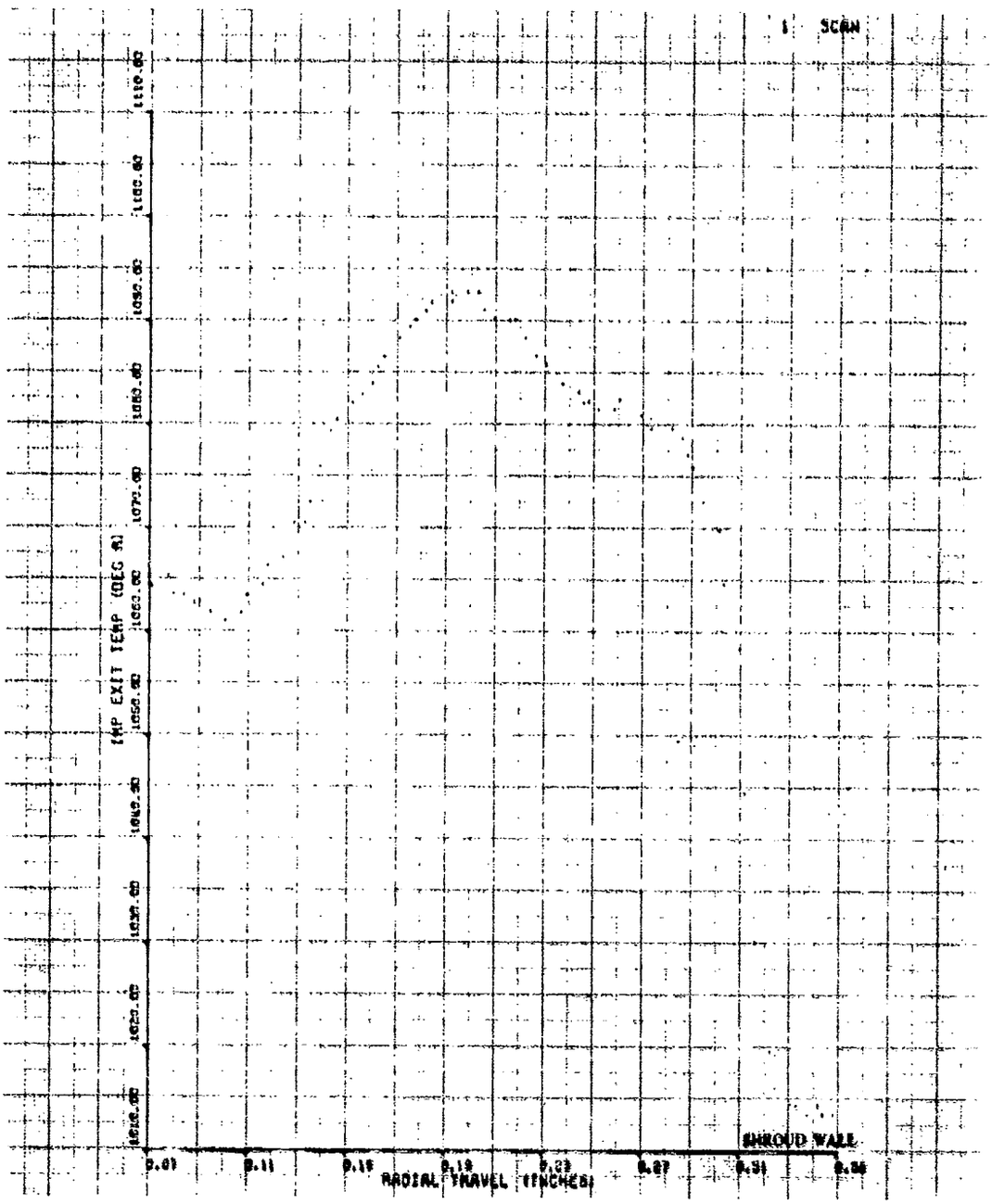

Figure 219. Impeller Exit Temperature Traverse, Build No. 6, 95% Speed, 10-deg IGV.

INLET GUIDE VANE PERFORMANCE PRINTOUTS

Summary printouts from the inlet guide vane circumferential traverse data reduction program are shown in Tables XVIII through XXIX for Builds No. 3 and 6. Parameters pertaining to inlet guide vane gaps, including both a strut wake and an inlet guide vane wake, are denoted by an (S), and those parameters pertaining to gaps that include only an inlet guide vane wake are denoted by a (V). Values of these parameters were then weighted, based on the relative number of struts to number of inlet guide vanes, and combined to yield the "weighted" values at each percent span. All other parameters listed in the printout are self-explanatory. A complete discussion of the data reduction procedures can be found in the main body of this report.

TABLE XVIII. INLET GUIDE VANE PERFORMANCE PRINTOUT, 70% SPEED, 16-DEG IGV, NEAR STALL, BUILD NO. 3

CIRCUMFERENTIALLY INTEGRATED QUANTITIES

PERCENT SPAN	6.0674	27.7380	47.4821	67.2579	86.9221
STRUT AVG RADIAL TRAVEL	C.0EC7	C.2774	C.4748	0.6726	C.8692
VANE AVG RADIAL TRAVEL	C.C8CE	C.2775	C.4752	0.6724	0.8691
AVG HUB STATIC PRESS	14.1174	14.1174	14.1174	14.1174	14.1174
AVG SHROUD STATIC PRESS	14.4541	14.4541	14.4541	14.4541	14.4541
SPANWISE STATIC PRESS	14.1418	14.2073	14.2736	14.3405	14.406C
INCREMENTAL FLOW (S)	C.C1C8	0.0167	C.0115	0.0145	0.0112
INCREMENTAL FLOW (V)	C.C111	C.C170	0.0118	0.0148	0.0122
MASS AVG PRESS (S)	14.6707	14.6646	14.6488	14.6057	14.5791
MASS AVG PRESS (V)	14.6764	14.6776	14.6587	14.6062	14.5963
MASS AVG ANGLE (S)	79.9365	78.9362	79.2388	78.4661	78.7722
MASS AVG ANGLE (V)	EC.5531	79.6017	79.7161	78.9684	78.2834
WEIGHTED PRESS	14.67C:	14.6750	14.6567	14.6061	14.5928
WEIGHTED ANGLE	EC.4297	79.4686	79.6206	78.8680	78.3811
WEIGHTED FLOW	C.011C	C.0169	0.0118	0.0147	0.012C
LOSS COEFFICIENT (S)	C.GC15E7	C.CC2001	C.003074	0.006008	0.0C781E
LOSS COEFFICIENT (V)	C.C016C5	C.CC1113	0.002405	0.005976	0.006652
WEIGHTED LOSS COEFFICIENT	C.C016C2	C.CC1291	C.002539	C.CC5983	0.006886

TOTAL INTEGRATED QUANTITIES

TOTAL INCREMENTAL FLOW	0.06640
SPANWISE MASS AVG TOTAL PRESS	14.64088
SPANWISE MASS AVG AIR ANGLE	79.02205
TOTAL PRESSURE LOSS	0.00361
INTEGRATED FLOW	1.32801
FLOW COEFFICIENT OF INLET	1.06268
MACH NUMBER IN	0.[illegible]6
GUIDE VANE ANGLE	50.7[illegible]0

TABLE XIX. INLET GUIDE VANE PERFORMANCE PRINTOUT, 90% SPEED, 10-DEG IGV, NEAR STALL, BUILD NO. 3

CIRCUMFERENTIALLY INTEGRATED QUANTITIES

PERCENT SPAN	18.7715	36.5858	45.2982	63.0581	80.8795
STRUT AVG RADIAL TRAVEL	0.1877	0.3659	0.4530	0.6306	0.8088
VANE AVG RADIAL TRAVEL	0.1882	0.3659	0.4535	0.6305	0.8088
AVG HUB STATIC PRESS	13.2041	13.2041	13.2041	13.2041	13.2041
AVG SHROUD STATIC PRESS	13.3549	13.3549	13.3549	13.3549	13.3549
SPANWISE STATIC PRESS	13.2307	13.2578	13.2714	13.2979	13.3243
INCREMENTAL FLOW (S)	0.0404	0.0007	0.0217	0.0266	0.0398
INCREMENTAL FLOW (V)	0.0422	0.0005	0.0221	0.0250	0.0419
MASS AVG PRESS (S)	14.6328	14.6303	14.6579	14.6136	14.5291
MASS AVG PRESS (V)	14.6767	14.6747	14.6792	14.6370	14.5824
MASS AVG ANGLE (S)	78.0359	82.1828	83.5815	74.8915	82.3078
MASS AVG ANGLE (V)	81.9529	82.9576	83.6800	75.7240	83.7035
WEIGHTED PRESS	14.6679	14.6659	14.6748	14.6327	14.5717
WEIGHTED ANGLE	81.1694	82.8026	83.6402	75.9574	83.4249
WEIGHTED FLOW	0.0418	0.0005	0.0220	0.0254	0.0414
LOSS COEFFICIENT (S)	0.004164	0.004334	0.002486	0.005334	0.011226
LOSS COEFFICIENT (V)	0.001177	0.001311	0.001010	0.003877	0.007598
WEIGHTED LOSS COEFFICIENT	0.001774	0.001916	0.001305	0.004168	0.008324

TOTAL INTEGRATED QUANTITIES

TOTAL INCREMENTAL FLOW	0.13118
SPANWISE MASS AVG TOTAL PRESS	14.63187
SPANWISE MASS AVG AIR ANGLE	79.72418
TOTAL PRESSURE LOSS	0.00423
INTEGRATED FLOW	2.62368
FLOW COEFFICIENT OF INLET	0.97841
MACH NUMBER IN	0.35615
GUIDE VANE ANGLE	96.32941

TABLE XX. INLET GUIDE VANE PERFORMANCE PRINTOUT, 85% SPEED, 20-DEG IGV, NEAR STALL, BUILD NO. 6

CIRCUMFERENTIALLY INTEGRATED QUANTITIES

PERCENT SPAN	10.0683	30.1750	50.2230	70.3277	90.1872
STRUT AVG RADIAL TRAVEL	0.1009	0.3018	0.5022	0.7033	0.9019
VANE AVG RADIAL TRAVEL	0.1008	0.3015	0.5013	0.7028	0.9019
AVG HUB STATIC PRESS	13.6100	13.6100	13.6100	13.6100	13.6100
AVG SHROUD STATIC PRESS	13.6100	13.6100	13.6100	13.6100	13.6100
SPANWISE STATIC PRESS	13.6100	13.6100	13.6100	13.6100	13.6100
INCREMENTAL FLOW (S)	0.0171	0.0202	0.0210	0.0245	0.0212
INCREMENTAL FLOW (V)	0.0174	0.0205	0.0220	0.0248	0.0224
MASS AVG PRESS (S)	14.6352	14.6660	14.6545	14.6350	14.4871
MASS AVG PRESS (V)	14.6572	14.6692	14.6826	14.6718	14.5358
MASS AVG ANGLE (S)	67.6903	68.0322	69.1018	70.2325	75.7120
MASS AVG ANGLE (V)	68.3452	68.6462	69.5150	70.5767	74.2330
WEIGHTED PRESS	14.6506	14.6688	14.6743	14.6607	14.5212
WEIGHTED ANGLE	68.1487	68.4620	69.3910	70.4734	74.6767
WEIGHTED FLOW	0.0173	0.0204	0.0217	0.0247	0.0220
LOSS COEFFICIENT (S)	0.004001	0.001769	0.002688	0.004018	0.014082
LOSS COEFFICIENT (V)	0.002503	0.001689	0.000761	0.001514	0.010764
WEIGHTED LOSS COEFFICIENT	0.002953	0.001713	0.001339	0.002265	0.011760

TOTAL INTEGRATED QUANTITIES

TOTAL INCREMENTAL FLOW	0.10607
SPANWISE MASS AVG TOTAL PRESS	14.63443
SPANWISE MASS AVG AIR ANGLE	70.30234
TOTAL PRESSURE LOSS	0.00405
INTEGRATED FLOW	2.12135
FLOW COEFFICIENT OF INLET	1.01750
MACH NUMBER IN	0.26409
GUIDE VANE ANGLE	106.94604

TABLE XXI. INLET GUIDE VANE PERFORMANCE PRINTOUT, 85% SPEED, 30-DEG IGV, NEAR STALL, BUILD NO. 6

CIRCUMFERENTIALLY INTEGRATED QUANTITIES

PERCENT SPAN	10.1117	30.0473	50.1771	70.3378	90.2058
STAGT AVG RADIAL TRAVEL	0.1011	0.3005	0.5018	0.7034	0.9021
VANE AVG RADIAL TRAVEL	0.1003	0.3023	0.5018	0.7034	0.9021
AVG HUB STATIC PRESS	13.1000	13.1000	13.1000	13.1000	13.1000
AVG SHROUD STATIC PRESS	13.1000	13.1000	13.1000	13.1000	13.1000
SPANWISE STATIC PRESS	13.1000	13.1000	13.1000	13.1000	13.1000
INCREMENTAL FLOW (S)	0.0181	0.0197	0.0223	0.0238	0.0211
INCREMENTAL FLOW (V)	0.0183	0.0220	0.0226	0.0274	0.0244
MASS AVG PRESS (S)	14.6005	14.5950	14.5141	14.4904	14.2913
MASS AVG PRESS (V)	14.5927	14.6351	14.5572	14.5608	14.4411
MASS AVG ANGLE (S)	55.8160	56.9463	59.5749	60.6313	71.3820
MASS AVG ANGLE (V)	56.3248	57.9069	60.6605	62.4249	69.0164
WEIGHTED PRESS	14.5951	14.6230	14.5443	14.5397	14.3961
WEIGHTED ANGLE	56.1121	57.6187	60.3348	61.8868	69.7261
WEIGHTED FLOW	0.0183	0.0213	0.0225	0.0263	0.0234
LOSS COEFFICIENT (S)	0.006364	0.006740	0.012240	0.013856	0.027405
LOSS COEFFICIENT (V)	0.008692	0.004019	0.009307	0.009064	0.017214
WEIGHTED LOSS COEFFICIENT	0.006774	0.004829	0.010187	0.010503	0.020271

TOTAL INTEGRATED QUANTITIES

TOTAL INCREMENTAL FLOW	0.11182
SPANWISE MASS AVG TOTAL PRESS	14.53548
SPANWISE MASS AVG AIR ANGLE	61.14932
TOTAL PRESSURE LOSS	0.01079
INTEGRATED FLOW	2.23641
FLOW COEFFICIENT OF INLET	.95170
MACH NUMBER IN	0.27533
GUIDE VANE ANGLE	117.612.0

TABLE XXII. INLET GUIDE VANE PERFORMANCE PRINTOUT, 8/1 SPEED, 10-DEG IGV, NEAR STALL, BUILD NO. 6

CIRCUMFERENTIALLY INTEGRATED QUANTITIES

PERCENT SPAN	10.0552	30.2590	50.1402	70.3766	90.2529
STRUT AVG RADIAL TRAVEL	0.1006	0.3026	0.5014	0.7038	0.9025
VANE AVG RADIAL TRAVEL	0.0998	0.3027	0.5022	0.7036	0.9021
AVG HUB STATIC PRESS	12.9410	12.9410	12.9410	12.9410	12.9410
AVG SHROUD STATIC PRESS	12.9410	12.9410	12.9410	12.9410	12.9410
SPANWISE STATIC PRESS	12.9410	12.9410	12.9410	12.9410	12.9410
INCREMENTAL FLOW (S)	0.0221	0.0268	0.0261	0.0318	0.0315
INCREMENTAL FLOW (V)	0.0229	0.0263	0.0276	0.0325	0.0298
MASS AVG PRESS (S)	14.6063	14.6262	14.6315	14.6058	14.4885
MASS AVG PRESS (V)	14.6670	14.6744	14.6679	14.6471	14.4332
MASS AVG ANGLE (S)	77.8664	77.8808	78.3391	78.5037	81.5074
MASS AVG ANGLE (V)	78.1397	78.1188	78.6947	78.9413	82.5757
WEIGHTED PRESS	14.6488	14.6599	14.6570	14.6347	14.4498
WEIGHTED ANGLE	78.0577	78.0474	78.7280	78.8100	82.2551
WEIGHTED FLOW	0.0226	0.0265	0.0271	0.0323	0.0303
LOSS COEFFICIENT (S)	0.005968	0.004611	0.004257	0.006004	0.013985
LOSS COEFFICIENT (V)	0.001834	0.001335	0.001776	0.003139	0.017745
WEIGHTED LOSS COEFFICIENT	0.003074	0.002318	0.002521	0.004034	0.016617

TOTAL INTEGRATED QUANTITIES

TOTAL INCREMENTAL FLOW	0.13892
SPANWISE MASS AVG TOTAL PRESS	14.60585
SPANWISE MASS AVG AIR ANGLE	78.90396
TOTAL PRESSURE LOSS	0.00600
INTEGRATED FLOW	2.77640
FLOW COEFFICIENT OF INLET	0.97114
MACH NUMBER IN	0.39162
GUIDE VANE ANGLE	98.49242

TABLE XXIII. INLET GUIDE VANE PERFORMANCE PRINTOUT, 8/1 SPEED, 15-DEG IGV, NEAR STALL, BUILD NO. 6

CIRCUMFERENTIALLY INTEGRATED QUANTITIES

PERCENT SPAN	10.0495	30.3265	50.2566	70.4075	90.2598
STRUT AVG RADIAL TRAVEL	0.1005	0.3033	0.5026	0.7041	0.9026
VANE AVG RADIAL TRAVEL	0.1003	0.3035	0.5031	0.7041	0.9027
AVG HUB STATIC PRESS	12.8556	12.8556	12.8556	12.8556	12.8556
AVG SHROUD STATIC PRESS	12.8556	12.8556	12.8556	12.8556	12.8556
SPANWISE STATIC PRESS	12.8556	12.8556	12.8556	12.8556	12.8556
INCREMENTAL FLOW (S)	0.0219	0.0266	0.0267	0.0322	0.0287
INCREMENTAL FLOW (V)	0.0226	0.0261	0.0277	0.0308	0.0297
MASS AVG PRESS (S)	14.5899	14.6359	14.6251	14.6040	14.3389
MASS AVG PRESS (V)	14.6366	14.6714	14.6548	14.6587	14.4054
MASS AVG ANGLE (S)	72.7570	72.9513	73.4628	74.0750	78.5647
MASS AVG ANGLE (V)	73.3160	73.2807	74.2171	74.5319	78.3494
WEIGHTED PRESS	14.6226	14.6607	14.6459	14.6423	14.3855
WEIGHTED ANGLE	73.1483	73.1819	73.9508	74.3948	78.4140
WEIGHTED FLOW	0.0224	0.0262	0.0274	0.0312	0.0294
LOSS COEFFICIENT (S)	0.007086	0.003956	0.004690	0.006124	0.024163
LOSS COEFFICIENT (V)	0.003906	0.001538	0.002665	0.002402	0.019640
WEIGHTED LOSS COEFFICIENT	0.004860	0.002264	0.003273	0.003519	0.020997

TOTAL INTEGRATED QUANTITIES

TOTAL INCREMENTAL FLOW	0.13662
SPANWISE MASS AVG TOTAL PRESS	14.58814
SPANWISE MASS AVG AIR ANGLE	74.48524
TOTAL PRESSURE LOSS	0.00720
INTEGRATED FLOW	2.73239
FLOW COEFFICIENT OF INLET	0.96963
MACH NUMBER IN	0.38997
GUIDE VANE ANGLE	103.82545

TABLE XXIV. INLET GUIDE VANE PERFORMANCE PRINTOUT, 101% SPEED, 5-DEG IGV, BELOW NEAR STALL, BUILD NO. 6

CIRCUMFERENTIALLY INTEGRATED QUANTITIES

PERCENT SPAN	10.1119	30.2659	50.3228	70.4516	90.2988
STRUT AVG RADIAL TRAVEL	0.1011	0.3027	0.5032	0.7045	0.9030
VANE AVG RADIAL TRAVEL	0.1015	0.3027	0.5032	0.7033	0.9032
AVG HUB STATIC PRESS	12.1371	12.1371	12.1371	12.1371	12.1371
AVG SHROUD STATIC PRESS	12.1371	12.1371	12.1371	12.1371	12.1371
SPANWISE STATIC PRESS	12.1371	12.1371	12.1371	12.1371	12.1371
INCREMENTAL FLOW (S)	0.0268	0.0302	0.0327	0.0359	0.0368
INCREMENTAL FLOW (V)	0.0266	0.0300	0.0379	0.0371	0.0385
MASS AVG PRESS (S)	14.5646	14.5786	14.6200	14.5716	14.5138
MASS AVG PRESS (V)	14.6423	14.6674	14.6250	14.6172	14.4867
MASS AVG ANGLE (S)	85.4214	84.5930	85.0027	85.4967	86.2876
MASS AVG ANGLE (V)	84.9313	84.8281	84.6319	85.1310	87.0897
WEIGHTED PRESS	14.6190	14.6408	14.6235	14.6035	14.4948
WEIGHTED ANGLE	85.0783	84.7576	84.7431	85.2407	86.8490
WEIGHTED FLOW	0.0267	0.0301	0.0364	0.0368	0.0380
LOSS COEFFICIENT (S)	0.008809	0.007851	0.005037	0.008330	0.012265
LOSS COEFFICIENT (V)	0.003518	0.001809	0.004695	0.005226	0.014109
WEIGHTED LOSS COEFFICIENT	0.005105	0.003622	0.004798	0.006157	0.013556

TOTAL INTEGRATED QUANTITIES

TOTAL INCREMENTAL FLOW	0.16786
SPANWISE MASS AVG TOTAL PRESS	14.59239
SPANWISE MASS AVG AIR ANGLE	85.39484
TOTAL PRESSURE LOSS	0.00692
INTEGRATED FLOW	3.35720
FLOW COEFFICIENT OF INLET	0.91697
MACH NUMBER IN	0.45503
GUIDE VANE ANGLE	91.96770

TABLE XXV. INLET GUIDE VANE PERFORMANCE PRINTOUT, 95% SPEED, 10-DEG IGV, NEAR STALL, BUILD NO. 6

CIRCUMFERENTIALLY INTEGRATED QUANTITIES

PERCENT SPAN	10.1383	30.2356	50.2806	70.3858	90.2598
STRUT AVG RADIAL TRAVEL	0.1014	0.3024	0.5028	0.7039	0.9026
VANE AVG RADIAL TRAVEL	0.1020	0.3023	0.5016	0.7037	0.9024
AVG HUB STATIC PRESS	12.8193	12.8193	12.8193	12.8193	12.8193
AVG SHROUD STATIC PRESS	12.8193	12.8193	12.8193	12.8193	12.8193
SPANWISE STATIC PRESS	12.8193	12.8193	12.8193	12.8193	12.8193
INCREMENTAL FLOW (S)	0.0242	0.0262	0.0282	0.0317	0.0313
INCREMENTAL FLOW (V)	0.0239	0.0268	0.0291	0.0334	0.0307
MASS AVG PRESS (S)	14.6256	14.6206	14.6461	14.6077	14.4051
MASS AVG PRESS (V)	14.6731	14.6716	14.6740	14.6551	14.4139
MASS AVG ANGLE (S)	77.5509	77.8978	77.8740	78.4593	81.4951
MASS AVG ANGLE (V)	77.7449	78.1520	78.1554	78.9947	80.6293
WEIGHTED PRESS	14.6588	14.6563	14.6656	14.6409	14.4112
WEIGHTED ANGLE	77.6866	78.0757	78.0710	78.8340	80.8891
WEIGHTED FLOW	0.0240	0.0266	0.0289	0.0329	0.0309
LOSS COEFFICIENT (S)	0.004657	0.004993	0.003262	0.005872	0.019662
LOSS COEFFICIENT (V)	0.001423	0.001524	0.001360	0.002645	0.019063
WEIGHTED LOSS COEFFICIENT	0.002393	0.002565	0.001931	0.003613	0.019243

TOTAL INTEGRATED QUANTITIES

TOTAL INCREMENTAL FLOW	0.14317
SPANWISE MASS AVG TOTAL PRESS	14.60225
SPANWISE MASS AVG AIR ANGLE	78.73923
TOTAL PRESSURE LOSS	0.00624
INTEGRATED FLOW	2.86339
FLOW COEFFICIENT OF INLET	0.96458
MACH NUMBER IN	0.40224
GUIDE VANE ANGLE	97.09309

TABLE XXVI. INLET GUIDE VANE PERFORMANCE PRINTOUT, 100% SPEED, 10-DEG IGV, NEAR STALL, BUILD NO. 6

CIRCUMFERENTIALLY INTEGRATED QUANTITIES

PERCENT SPAN	10.1389	30.2170	50.2768	70.4209	90.2630
STRUT AVG RADIAL TRAVEL	0.1014	0.3022	0.5028	0.7042	0.9026
VANE AVG RADIAL TRAVEL	0.1003	0.3018	0.5020	0.7046	0.9022
AVG HUB STATIC PRESS	12.4440	12.4440	12.4440	12.4440	12.4440
AVG SHROUD STATIC PRESS	12.4440	12.4440	12.4440	12.4440	12.4440
SPANWISE STATIC PRESS	12.4440	12.4440	12.4440	12.4440	12.4440
INCREMENTAL FLOW (S)	0.0246	0.0294	0.0319	0.0354	0.0362
INCREMENTAL FLOW (V)	0.0239	0.0293	0.0314	0.0355	0.0360
MASS AVG PRESS (S)	14.5350	14.6153	14.6169	14.5801	14.4525
MASS AVG PRESS (V)	14.6720	14.6751	14.6684	14.6332	14.4308
MASS AVG ANGLE (S)	78.7595	78.9085	79.0077	79.6817	82.6728
MASS AVG ANGLE (V)	78.8080	78.9434	79.5941	79.8631	83.2852
WEIGHTED PRESS	14.6459	14.6572	14.6529	14.6172	14.4373
WEIGHTED ANGLE	78.7934	78.9329	79.4182	79.8086	83.1014
WEIGHTED FLOW	0.0241	0.0293	0.0315	0.0355	0.0360
LOSS COEFFICIENT (S)	0.007419	0.005357	0.005250	0.007751	0.016435
LOSS COEFFICIENT (V)	0.001500	0.001283	0.001743	0.004141	0.017910
WEIGHTED LOSS COEFFICIENT	0.003276	0.002505	0.002795	0.005224	0.017468

TOTAL INTEGRATED QUANTITIES

TOTAL INCREMENTAL FLOW	0.15652
SPANWISE MASS AVG TOTAL PRESS	14.59489
SPANWISE MASS AVG AIR ANGLE	79.94775
TOTAL PRESSURE LOSS	0.00674
INTEGRATED FLOW	3.13035
FLOW COEFFICIENT OF INLET	0.95331
MACH NUMBER IN	0.43984
GUIDE VANE ANGLE	96.67302

TABLE XXVII. INLET GUIDE VANE PERFORMANCE PRINTOUT, 101% SPEED, -4-DEG IGV, NEAR STALL, BUILD NO. 6

CIRCUMFERENTIALLY INTEGRATED QUANTITIES

PERCENT SPAN	9.8964	30.2122	50.3212	70.3874	90.2370
STRUT AVG RADIAL TRAVEL	0.0990	0.3021	0.5032	0.7039	0.9024
VANE AVG RADIAL TRAVEL	0.0991	0.3007	0.5016	0.7039	0.9016
AVG HUB STATIC PRESS	12.1129	12.1129	12.1129	12.1129	12.1129
AVG SHROUD STATIC PRESS	12.1129	12.1129	12.1129	12.1129	12.1129
SPANWISE STATIC PRESS	12.1129	12.1129	12.1129	12.1129	12.1129
INCREMENTAL FLOW (S)	0.0271	0.0321	0.0326	0.0383	0.0355
INCREMENTAL FLOW (V)	0.0267	0.0318	0.0317	0.0376	0.0360
MASS AVG PRESS (S)	14.6131	14.5628	14.6225	14.5173	14.2661
MASS AVG PRESS (V)	14.6115	14.6120	14.5774	14.5673	14.3767
MASS AVG ANGLE (S)	94.6648	94.4430	94.0580	93.9955	95.0706
MASS AVG ANGLE (V)	94.8274	93.6026	94.1533	93.1720	93.4334
WEIGHTED PRESS	14.6120	14.5973	14.5909	14.5523	14.3435
WEIGHTED ANGLE	94.7786	93.8547	94.1247	93.4190	93.9245
WEIGHTED FLOW	0.0268	0.0319	0.0320	0.0378	0.0359
LOSS COEFFICIENT (S)	0.005506	0.008926	0.004863	0.012022	0.029119
LOSS COEFFICIENT (V)	0.005615	0.005579	0.007935	0.008620	0.021592
WEIGHTED LOSS COEFFICIENT	0.005582	0.006583	0.007014	0.009641	0.023850

TOTAL INTEGRATED QUANTITIES

TOTAL INCREMENTAL FLOW	0.16436
SPANWISE MASS AVG TOTAL PRESS	14.53274
SPANWISE MASS AVG AIR ANGLE	94.43839
TOTAL PRESSURE LOSS	0.01097
INTEGRATED FLOW	3.28720
FLOW COEFFICIENT OF INLET	0.94047
MACH NUMBER IN	0.46587
GUIDE VANE ANGLE	82.89236

TABLE XXVIII. INLET GUIDE VANE PERFORMANCE PRINTOUT, 101% SPEED, 0-DEG IGV, NEAR STALL, BUILD NO. 6

CIRCUMFERENTIALLY INTEGRATED QUANTITIES

PERCENT SPAN	9.9113	30.1065	50.1109	70.3106	90.1169
STRUT AVG RADIAL TRAVEL	0.0991	0.3011	0.5011	0.7031	0.9012
VANE AVG RADIAL TRAVEL	0.0993	0.3007	0.5013	0.7026	0.9010
AVG HUB STATIC PRESS	12.2522	12.2522	12.2522	12.2522	12.2522
AVG SHROUD STATIC PRESS	12.2522	12.2522	12.2522	12.2522	12.2522
SPANWISE STATIC PRESS	12.2522	12.2522	12.2522	12.2522	12.2522
INCREMENTAL FLOW (S)	0.0250	0.0318	0.0303	0.0370	0.0368
INCREMENTAL FLOW (V)	0.0263	0.0307	0.0314	0.0368	0.0385
MASS AVG PRESS (S)	14.6243	14.5840	14.6544	14.5578	14.4463
MASS AVG PRESS (V)	14.6494	14.6625	14.6495	14.6093	14.5373
MASS AVG ANGLE (S)	90.2377	89.3547	89.1071	89.0439	90.1648
MASS AVG ANGLE (V)	89.8768	88.9055	89.4831	88.6835	89.8621
WEIGHTED PRESS	14.6419	14.6390	14.6509	14.5939	14.5100
WEIGHTED ANGLE	89.9850	89.0402	89.3703	88.7916	89.9529
WEIGHTED FLOW	0.0260	0.0310	0.0311	0.0369	0.0380
LOSS [illegible]FFICIENT (S)	0.004742	0.007488	0.002695	0.009267	0.016858
LOSS COEFFICIENT (V)	0.003038	0.002140	0.003032	0.005761	0.010662
WEIGHTED LOSS COEFFICIENT	0.003549	0.003745	0.002931	0.006813	0.012521

TOTAL INTEGRATED QUANTITIES

TOTAL INCREMENTAL FLOW	0.16290
SPANWISE MASS AVG TOTAL PRESS	14.60144
SPANWISE MASS AVG AIR ANGLE	89.56659
TOTAL PRESSURE LOSS	0.00630
INTEGRATED FLOW	3.25810
FLOW COEFFICIENT OF INLET	0.93972
MACH NUMBER IN	0.46187
GUIDE VANE ANGLE	86.63223

TABLE XXIX. INLET GUIDE VANE PERFORMANCE PRINTOUT, 101% SPEED, 5-DEG IGV, NEAR STALL, BUILD NO. 6

CIRCUMFERENTIALLY INTEGRATED QUANTITIES

PERCENT SPAN	10.0578	30.2659	50.2744	70.3934	90.2602
STRUT AVG RADIAL TRAVEL	0.1006	0.3027	0.5027	0.7039	0.9026
VANE AVG RADIAL TRAVEL	0.1010	0.3026	0.5029	0.7039	0.9025
AVG HUB STATIC PRESS	12.3762	12.3762	12.3762	12.3762	12.3762
AVG SHROUD STATIC PRESS	12.3762	12.3762	12.3762	12.3762	12.3762
SPANWISE STATIC PRESS	12.3762	12.3762	12.3762	12.3762	12.3762
INCREMENTAL FLOW (S)	0.0247	0.0303	0.0313	0.0365	0.0372
INCREMENTAL FLOW (V)	0.0264	0.0303	0.0317	0.0360	0.0366
MASS AVG PRESS (S)	14.5844	14.6044	14.6155	14.5832	14.5323
MASS AVG PRESS (V)	14.6633	14.6736	14.6579	14.6298	14.5038
MASS AVG ANGLE (S)	83.9771	82.7935	83.0604	83.1970	85.5105
MASS AVG ANGLE (V)	82.9403	82.7175	83.4629	83.1833	85.8735
WEIGHTED PRESS	14.6396	14.6529	14.6452	14.6158	14.5123
WEIGHTED ANGLE	82.9813	82.7403	83.3421	83.1873	85.7646
WEIGHTED FLOW	0.0259	0.0303	0.0315	0.0362	0.0368
LOSS COEFFICIENT (S)	0.007461	0.006097	0.005343	0.007538	0.011008
LOSS COEFFICIENT (V)	0.002089	0.001385	0.002458	0.004372	0.012943
WEIGHTED LOSS COEFFICIENT	0.003701	0.002799	0.003324	0.005322	0.012362

TOTAL INTEGRATED QUANTITIES

TOTAL INCREMENTAL FLOW	0.16071
SPANWISE MASS AVG TOTAL PRESS	14.60872
SPANWISE MASS AVG AIR ANGLE	83.60435
TOTAL PRESSURE LOSS	0.00580
INTEGRATED FLOW	3.21425
FLOW COEFFICIENT OF INLET	0.94337
MACH NUMBER IN	0.44827
GUIDE VANE ANGLE	92.37350

TRAVERSE DATA REDUCTION PRINTOUTS

Component performance parameters and velocity triangles calculated from traverse data are presented in Tables XXX through LXXXII for all Builds No. 3 and 6 traverse points. Tables XXX through LIV include all Build No. 3 traverse data reduction printouts, and Tables LV through LXXII include all the Build No. 6 traverse printouts in which the data were reduced following the basic set of assumptions and procedures set forth in the data reduction procedures section of this report. For both builds, tables are arranged in order of increasing speed. Information in the title is self-explanatory, with WOD (wide open discharge), knee, and near stall, referring to the back pressure condition on the speedline.

In Tables LXXIV and LXXV, the inducer exit traverse data were reduced assuming a linear spanwise static pressure distribution instead of a constant static pressure distribution for near-stall points at 100% speed, 10-deg IGV and 101% speed, -4-deg IGV, respectively. All impeller exit traverse data in Tables XXX through LXXV were reduced assuming a constant spanwise total temperature profile equal to the collector total temperature. Tables LXXVI through LXXXII include impeller exit printouts in which the traverse data were reduced using the total temperature profiles obtained from impeller exit total temperature traverses.

Component performance parameters and velocity triangle components are given in the summaries for each traverse station. Velocity triangle components listed in the tables are defined per the following.

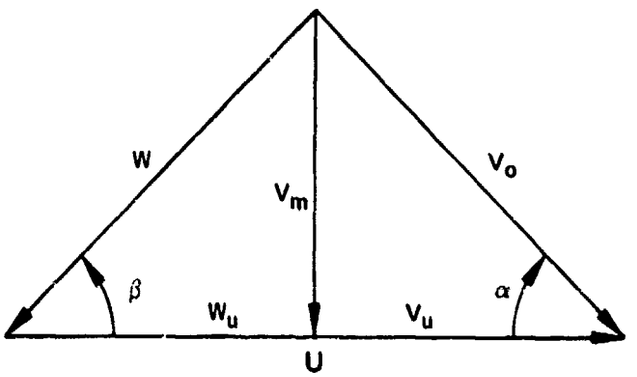

Other parameters calculated for each percent span include incidence (I), absolute Mach number (MO), and relative Mach number (MREL).

TABLE XXX.

10/1 CENT COMP, IMP TRAV 30 PCT SP, WDCV, RUN 3.06
IGV= 0 DEG
FLOW RATE = 0.494 SPEED = 19700.0

* * * IMPELLER EXIT * * * INITIAL INTEGRATED FLOW 0.461

PCENT SPAN	R	WO	VO	VO/VMAX	ALP	VM	VM/VMMAX	VU	U	WU	B	WO
0.0169	0.0040	0.2078	242.67	0.4074	-5.102	-21.58	-0.0841	241.71	605.62	363.90	33.593	-39.00
0.0764	0.0180	0.2078	242.55	0.4072	0.297	1.26	0.0049	242.55	605.62	363.07	33.744	2.27
0.1612	0.0380	0.2242	261.47	0.4390	9.697	44.04	0.1717	257.74	605.62	347.88	36.534	73.99
0.2461	0.0579	0.2734	318.00	0.5339	18.647	101.68	0.3964	301.30	605.62	304.31	44.715	144.51
0.3310	0.0779	0.3664	423.77	0.7115	25.397	181.75	0.7086	382.81	605.62	222.81	59.799	210.30
0.4159	0.0979	0.4457	512.06	0.8598	28.197	241.95	0.9433	451.29	605.62	154.33	71.120	255.71
0.5008	0.1179	0.4969	565.99	0.9503	26.947	256.49	1.0000	504.53	605.62	101.08	78.670	261.59
0.5857	0.1379	0.5195	592.65	0.9951	24.597	246.68	0.9617	538.86	605.62	66.75	82.938	248.57
0.6706	0.1579	0.5222	595.55	1.0000	22.347	226.44	0.8828	550.82	605.62	54.79	84.318	227.56
0.7555	0.1779	0.5085	580.58	0.9748	20.147	199.98	0.7796	545.06	605.62	60.56	83.659	201.21
0.8404	0.1979	0.4648	532.73	0.8945	18.097	165.48	0.6451	506.37	605.62	99.24	78.910	168.63
0.9252	0.2179	0.3773	435.43	0.7311	16.097	120.73	0.4707	418.35	605.62	187.26	65.885	132.28
0.9838	0.2317	0.3007	348.83	0.5857	14.647	88.21	0.3439	337.50	605.62	268.12	51.535	112.66

MASS AVERAGE TOTAL PRESSURE 19.838
MASS AVERAGE TOTAL TEMPERATURE 568.804
MASS AVG VM 203.033 VU 476.284 ANGLE 23.087
FLOW FACTOR 0.736 SLIP FACTOR INS. STA. 0.766 IMPELLER TIP 0.824
IMP. PRESS. RATIO 0.000 IMP. TEMP.RATIO 0.000 EFFICIENCY 0.000
IMP..IND. PRESS. RATIO 1.354 IMP.IND. TEMP. RATIO 1.096 EFFICIENCY 0.942
IMP..IND..IGV PRESS. RATIO 1.390 IMP..IND..IGV TEMP. RATIO 1.096 EFFICIENCY 0.930

* * * DIFFUSER * * *

CD DIFFUSER THROAT FRONT 0.808 REAR 0.768
STATIC PRESSURE RISE COEFFICIENT IMPELLER EXIT/DIFFUSER EXIT -0.112
DIFFUSER THROAT FRONT/DIFFUSER EXIT 0.473 DIFFUSER THROAT REAR/DIFFUSER EXIT 0.676
DIFFUSER LOSSES TOTAL TO STATIC 0.153 TOTAL TO TOTAL 0.121
DIFFUSER LOSS COEFFICIENT 1.112

TABLE XXXI.

10/1 CENTRIFUGAL COMPRESSOR, IMPELLER TRAVERSE 30 PCT SPEED, BELOW NEAR STALL.
RUN 3.06 IGV SETTING=0 DEG
FLOW RATE = 0.302 SPEED = 19420.0

* * * IMPELLER EXIT * * * INITIAL INTEGRATED FLOW 0.296

PCENT SPAN	R	RHO	VO	VO/VMAX	ALP	VM	VM/VMMAX	VU	U	WU	B	WO
0.0169	0.0040	0.2406	280.42	0.5009	-13.774	-66.75	-0.3555	272.35	597.01	324.66	39.993	-103.88
0.0764	0.0180	0.2824	305.59	0.5459	-9.874	-52.40	-0.2790	301.07	597.01	295.94	45.492	-73.48
0.1612	0.0380	0.2734	318.05	0.5682	-3.574	-19.82	-0.1055	317.43	597.01	279.57	48.628	-26.42
0.2461	0.0579	0.2734	317.04	0.5680	3.775	20.93	0.1115	317.25	597.01	279.75	48.594	27.91
0.3310	0.0779	0.3007	349.20	0.6238	12.025	72.75	0.3874	341.53	597.01	255.47	53.202	90.86
0.4159	0.0979	0.3390	392.62	0.7014	19.125	128.64	0.6850	370.95	597.01	226.06	58.641	150.64
0.5008	0.1178	0.3937	454.12	0.8113	22.225	171.77	0.9147	420.38	597.01	176.63	67.209	180.32
0.5857	0.1378	0.4457	511.79	0.9143	21.525	187.78	1.0000	476.09	597.01	120.92	75.748	193.74
0.6706	0.1578	0.4785	547.81	0.9786	19.225	180.39	0.9606	517.26	597.01	79.75	81.234	182.52
0.7555	0.1779	0.4894	559.73	1.0000	16.775	161.55	0.8603	535.91	597.01	61.10	83.495	162.60
0.8404	0.1979	0.4675	535.67	0.9570	14.825	137.07	0.7299	517.83	597.01	79.17	81.306	138.66
0.9252	0.2179	0.4074	468.90	0.8377	13.525	109.67	0.5840	455.90	597.01	141.11	72.801	114.80
0.9836	0.2317	0.3281	379.76	0.6784	12.925	84.94	0.4523	370.13	597.01	226.87	58.493	99.63

MASS AVERAGE TOTAL PRESSURE 19.706
MASS AVERAGE TOTAL TEMPERATURE 568.805
MASS AVG VM 186.456 VU 475.229 ANGLE 19.303
FLOW FACTOR 0.555 SLIP FACTOR INS. STA. 0.796 IMPELLER TIP 0.834
IMP. PRESS. RATIO 0.000 IMP. TEMP.RATIO 0.000 EFFICIENCY 0.000
IMP..IND. PRESS. RATIO 1.345 IMP.IND. TEMP. RATIO 1.096 EFFICIENCY 0.920
IMP..IND..IGV PRESS. RATIO 1.341 IMP..IND..IGV TEMP. RATIO 1.096 EFFICIENCY 0.909

* * * DIFFUSER * * *

CD DIFFUSER THROAT FRONT 0.625 REAR 0.625
STATIC PRESSURE RISE COEFFICIENT IMPELLER EXIT/DIFFUSER EXIT 0.627
DIFFUSER THROAT FRONT/DIFFUSER EXIT 0.668 DIFFUSER THROAT REAR/DIFFUSER EXIT 0.668
DIFFUSER LOSSES TOTAL TO STATIC 0.044 TOTAL TO TOTAL 0.021
DIFFUSER LOSS COEFFICIENT 0.372

TABLE XXXII.

10/1 CENTRIFUGAL COMPRESSOR, IMPELLER TRAVERSE 30 PCT SPEED, NEAR STALL, RUN 3.06
IGV SETTING=0 DEG
FLOW RATE = 0.293 SPEED = 19537.0

* * * IMPELLER EXIT * * * INITIAL INTEGRATED FLOW 0.223

PCENT SPAN	R	MD	VD	VD/VMAX	ALP	VM	VM/VMMAX	VU	U	WU	B	WD
0.0169	0.0040	0.2898	336.61	0.6020	-15.051	-87.41	-0.4660	325.07	600.61	275.54	49.714	-114.99
0.0764	0.0180	0.2898	336.61	0.6020	-11.801	-68.84	-0.3828	329.50	600.61	271.10	50.553	-89.15
0.1612	0.0380	0.2843	330.26	0.5906	-6.701	-38.54	-0.2143	328.01	600.61	272.60	50.270	-50.11
0.2461	0.0579	0.2789	323.91	0.5793	-0.651	-3.68	-0.0204	323.89	600.61	276.71	49.491	-4.84
0.3310	0.0779	0.2843	330.15	0.5904	6.648	38.22	0.2125	327.93	600.61	272.67	50.256	49.71
0.4159	0.0979	0.3117	361.27	0.6461	14.048	87.09	0.4876	350.46	600.61	250.14	54.483	107.74
0.5008	0.1179	0.3609	416.86	0.7455	19.698	140.51	0.7812	392.47	600.61	208.14	62.061	159.04
0.5857	0.1379	0.4183	481.07	0.8603	21.498	176.29	0.9802	447.60	600.61	153.01	71.127	186.31
0.6706	0.1579	0.4648	532.25	0.9519	19.768	179.84	1.0000	500.95	600.61	99.66	78.748	183.36
0.7555	0.1779	0.4894	559.13	1.0000	16.698	158.78	0.8829	536.11	600.61	64.49	83.140	159.93
0.8404	0.1979	0.4839	553.08	0.9891	14.348	137.06	0.7621	535.83	600.61	64.77	83.107	138.06
0.9252	0.2179	0.4320	495.82	0.8867	13.498	115.73	0.6435	482.13	600.61	118.48	76.193	119.17
0.9830	0.2317	0.3836	419.58	0.7504	12.698	92.23	0.5128	409.32	600.61	191.29	64.951	101.80

MASS AVERAGE TOTAL PRESSURE 19.756
MASS AVERAGE TOTAL TEMPERATURE 567.685
MASS AVG VM 174.800 VU 485.693 ANGLE 19.793
FLOW FACTOR 0.444 SLIP FACTOR INS. STA. 0.808 IMPELLER TIP 0.847
IMP. PRESS. RATIO 0.000 IMP. TEMP.RATIO 0.000 EFFICIENCY 0.000
IMP.+IND. PRESS. RATIO 1.349 IMP.+IND. TEMP. RATIO 1.094 EFFICIENCY 0.949
IMP.+IND.+IGV PRESS. RATIO 1.344 IMP.+IND.+IGV TEMP. RATIO 1.094 EFFICIENCY 0.938

* * * DIFFUSER * * *

CD DIFFUSER THROAT FRONT 0.546 REAR 0.565
STATIC PRESSURE RISE COEFFICIENT IMPELLER EXIT/DIFFUSER EXIT 0.583
DIFFUSER THROAT FRONT/DIFFUSER EXIT 0.548 DIFFUSER THROAT REAR/DIFFUSER EXIT 0.500
DIFFUSER LOSSES TOTAL TO STATIC 0.096 TOTAL TO TOTAL 0.031
DIFFUSER LOSS COEFFICIENT 0.416

TABLE XXXIII.

10/1 CENTRIFUGAL COMPRESSOR, IMPELLER TRAVERSE 30 PCT SPEED, WDCV, RUN 3.05
IGV SETTING=10 DEG
FLOW RATE = 0.432 SPEED = 19798.0

* * * IMPELLER EXIT * * * INITIAL INTEGRATED FLOW 0.511

PCENT SPAN	R	MO	VO	VO/VMAX	ALP	VM	VM/VMMAX	VU	U	WU	B	WO
0.0165	0.0060	0.1093	127.55	0.2120	-12.806	-28.27	-0.1172	124.37	608.63	484.25	14.404	-113.64
0.0784	0.0180	0.1312	152.95	0.2542	-8.306	-22.09	-0.0916	151.35	608.63	457.28	18.313	-70.32
0.1612	0.0380	0.1367	159.27	0.2647	0.843	2.34	0.0097	159.25	608.63	449.37	19.514	7.02
0.2461	0.0579	0.1804	209.91	0.3489	15.643	56.60	0.2346	202.14	608.63	406.49	26.440	127.12
0.3310	0.0779	0.2734	316.68	0.5263	27.343	145.46	0.6030	281.30	608.63	327.33	40.674	223.18
0.4159	0.0979	0.3691	424.84	0.7061	29.943	212.06	0.8791	368.13	608.63	240.49	56.843	253.30
0.5008	0.1179	0.4497	509.70	0.8471	28.243	241.20	1.0000	449.02	608.63	159.61	70.431	255.99
0.5857	0.1379	0.5003	569.48	0.9465	24.443	235.65	0.9769	518.44	608.63	90.19	80.130	239.19
0.6706	0.1579	0.5249	595.87	0.9904	20.443	212.02	0.8790	556.87	608.63	51.75	84.690	212.93
0.7555	0.1779	0.5304	601.84	1.0000	18.143	187.35	0.7767	571.73	608.63	36.90	86.306	187.74
0.8404	0.1979	0.5085	577.88	0.9604	16.243	161.64	0.6701	554.81	608.63	53.82	84.459	162.40
0.9252	0.2179	0.4347	497.19	0.8263	14.993	128.63	0.5332	480.26	608.63	128.36	73.035	133.14
0.9858	0.2317	0.3617	393.91	0.6540	14.443	98.15	0.4069	381.07	608.63	227.55	59.156	114.32

MASS AVERAGE TOTAL PRESSURE 19.993
MASS AVERAGE TOTAL TEMPERATURE 583.692
MASS AVG VM 199.579 VU 472.682 ANGLE 22.486
FLOW FACTOR 0.668 SLIP FACTOR INS. STA. 0.776 IMPELLER TIP 0.813
IMP. PRESS. RATIO 0.000 IMP. TEMP.RATIO 0.000 EFFICIENCY 0.000
IMP..IND. PRESS. RATIO 1.338 IMP.IND. TEMP. RATIO 1.086 EFFICIENCY 1.005
IMP..IND..IGV PRESS. RATIO 1.333 IMP..IND..IGV TEMP. RATIO 1.086 EFFICIENCY 0.992

* * * DIFFUSER * * *

CD DIFFUSER THROAT FRONT 0.698 REAR 0.672
STATIC PRESSURE RISE COEFFICIENT IMPELLER EXIT/DIFFUSER EXIT -0.218
DIFFUSER THROAT FRONT/DIFFUSER EXIT 0.678 DIFFUSER THROAT REAR/DIFFUSER EXIT 0.668
DIFFUSER LOSSES TOTAL TO STATIC 0.160 TOTAL TO TOTAL 0.121
DIFFUSER LOSS COEFFICIENT 1.218

TABLE XXXIV.

10/1 CENTRIFUGAL COMPRESSOR, IMPELLER TRAVERSE 30 PCT SPEED, KNEE, RUN 3.06
IGV SETTING=0.0 DEG
FLOW RATE = 0.357 SPEED = 19877.0

* * * IMPELLER EXIT * * * INITIAL INTEGRATED FLOW 0.350

RELAT BPA	M	MW	VW	VORTICITY	ALP	CM	VORTICITY	BU	U	WU	W	WQ
0.0189	0.0000	0.1859	216.20	0.3583	-17.969	-86.82	-0.3976	205.08	611.06	402.38	20.902	-147.25
0.0784	0.0180	0.2019	291.89	0.4988	-12.099	-81.13	-0.2822	262.17	611.06	329.08	41.166	-92.63
0.1012	0.0260	0.2043	349.12	0.5607	-3.699	-21.23	-0.0980	328.44	611.06	282.62	49.287	-28.01
0.2461	0.0679	0.2898	335.33	0.5731	4.800	28.06	0.1295	334.16	611.06	276.90	50.353	36.44
0.3810	0.0979	0.3144	363.17	0.6187	13.150	82.62	0.3815	353.65	611.06	257.41	53.950	102.19
0.4159	0.1079	0.3691	424.77	0.7236	20.900	151.53	0.6996	395.82	611.06	214.24	61.635	172.21
0.5008	0.1279	0.4429	506.75	0.8633	24.700	211.76	0.9777	462.39	611.06	150.67	71.876	222.61
0.5857	0.1479	0.4949	563.56	0.9600	22.600	216.57	1.0000	520.26	611.06	90.77	80.102	219.85
0.6706	0.1679	0.5183	591.19	0.9901	18.700	186.34	0.8603	550.51	611.06	60.54	83.723	187.46
0.7555	0.1779	0.5167	589.99	1.0000	16.450	164.22	0.7675	562.96	611.06	48.10	85.118	166.83
0.8404	0.1979	0.4976	566.67	0.9647	14.950	149.08	0.6749	547.10	611.06	63.96	83.331	147.08
0.9252	0.2179	0.4429	506.75	0.8627	13.050	114.34	0.5279	493.31	611.06	117.74	76.575	117.56
0.9838	0.2317	0.3718	427.54	0.7283	11.950	88.52	0.4087	418.27	611.06	192.78	65.254	97.46

MASS AVERAGE TOTAL PRESSURE 59.912
MASS AVERAGE TOTAL TEMPERATURE 564.585
MASS AVG VX 185.197 VU 509.405 ANGLE 19.976
FLOW FACTOR 0.360 SLIP FACTOR (US. ST. 0.833 IMPELLER TIP 0.876
IMP. PRESS. RATIO 0.000 IMP. TEMP. RATIO 0.000 EFFICIENCY 0.000
IMP.+IND. PRESS. RATIO 1.359 IMP.+IND. TEMP. RATIO 1.085 EFFICIENCY 1.042
IMP.+IND.+IGV PRESS. RATIO 0.355 IMP.+IND.+IGV TEMP. RATIO 1.088 EFFICIENCY 1.030

* * * DIFFUSER * * *

CD DIFFUSER THROAT FRONT 0.000 REAR 0.062
STATIC PRESSURE RISE COEFFICIENT IMPELLER EXIT/DIFFUSER EXIT 0.459
DIFFUSER THROAT FRONT/DIFFUSER EXIT 0.556 DIFFUSER THROAT REAR/DIFFUSER EXIT 0.564
DIFFUSER LOSSES TOTAL TO STATIC 0.076 TOTAL TO TOTAL 0.058
DIFFUSER LOSS COEFFICIENT 0.540

TABLE XXXV.

10/1 CENTRIFUGAL COMPRESSOR, IMPELLER TRAVERSE 30 PCT SPEED, BELOW HR ST.
RUN 3.00 IGV SETTING=10 DEG
FLOW RATE = 0.246 SPEED = 19647.0

* * * IMPELLER EXIT * * * INITIAL INTEGRATED FLOW 0.360

PCENT SPAN	R	RO	VU	VU/VUMAX	ALP	VR	VR/VRMAX	VU	U	RU	B	BO
0.0109	0.0000	0.1912	153.06	0.2658	-21.687	-58.54	-0.2816	142.17	403.99	461.81	17.111	-192.46
0.0596	0.0680	0.1916	222.67	0.3868	-17.737	-67.83	-0.3379	212.09	403.99	391.90	26.421	-142.53
0.1612	0.0360	0.2301	273.85	0.4745	-10.837	-51.34	-0.2557	268.18	403.99	335.80	38.612	-82.26
0.2661	0.0939	0.2408	279.31	0.4852	-2.187	-10.65	-0.0531	279.19	403.99	324.88	40.665	-16.34
0.3910	0.0779	0.2826	306.53	0.5287	7.962	40.05	0.1995	301.68	403.99	302.30	44.941	36.70
0.4159	0.0979	0.2882	334.07	0.6151	16.312	99.45	0.4954	339.81	403.99	264.17	52.138	125.96
0.5008	0.1179	0.3800	437.28	0.7596	21.982	163.54	0.8147	405.54	403.99	198.44	63.923	182.07
0.5857	0.1379	0.4586	522.92	0.9069	22.612	200.71	1.0000	481.89	403.99	122.09	75.782	207.86
0.6706	0.1579	0.4878	560.78	0.9766	19.612	190.24	0.9478	533.89	403.99	70.09	82.520	191.87
0.7555	0.1779	0.5658	575.69	1.0000	19.812	196.84	0.7814	553.82	403.99	20.17	84.823	157.49
0.8404	0.1979	0.4812	548.78	0.9534	12.162	115.42	0.5760	536.46	403.99	67.52	82.825	116.93
0.9252	0.2179	0.3992	458.16	0.7959	8.462	75.32	0.3752	451.93	403.99	192.05	71.403	78.47
0.9898	0.2317	0.2515	291.45	0.5063	8.112	41.13	0.2049	288.53	403.99	315.45	62.667	60.94

MASS AVERAGE TOTAL PRESSURE 19.689
MASS AVERAGE TOTAL TEMPERATURE 569.001
MASS AVG VM 188.918 VU 511.579 ANGLE 19.783
FLOW FACTOR 0.421 SLIP FACTOR INS. STA. 0.896 IMPELLER TIP 0.887
IMP. PRESS. RATIO 0.000 IMP. TEMP. RATIO 0.000 EFFICIENCY 0.000
IMP.+IND. PRESS. RATIO 1.366 IMP.+IND. TEMP. RATIO 1.089 EFFICIENCY 0.993
IMP.+IND.+IGV PRESS. RATIO 1.339 IMP.+IND.+IGV TEMP. RATIO 1.089 EFFICIENCY 0.981

* * * DIFFUSER * * *

CD DIFFUSER THROAT FRONT 0.401 REAR 0.501
STATIC PRESSURE RISE COEFFICIENT IMPELLER EXIT/DIFFUSER EXIT 0.355
DIFFUSER THROAT FRONT/DIFFUSER EXIT 0.428 DIFFUSER THROAT REAR/DIFFUSER EXIT 0.433
DIFFUSER LOSSES TOTAL TO STATIC 0.087 TOTAL TO TOTAL 0.080
DIFFUSER LOSS COEFFICIENT 0.644

TABLE XXXVI.

10/1 CENTRIFUGAL COMPRESSOR, IMPELLER TRAVERSE 30 PCT SPEED, N/S, RUN 3.05
IGV SETTING=10 DEG
FLOW RATE = 0.223 SPEED = 19422.0

* * * IMPELLER EXIT * * * INITIAL INTEGRATED FLOW 0.262

PCENT SPAN	R	MO	VO	VO/VMAX	ALP	VM	VM/VMMAX	VU	U	WU	B	WO
0.0169	0.0040	0.0874	102.47	0.2490	-16.834	-29.67	-0.1760	98.08	597.07	498.99	11.120	-153.87
0.0764	0.0180	0.0874	102.47	0.2490	-13.334	-23.63	-0.1401	99.71	597.07	497.36	11.336	-120.23
0.1612	0.0380	0.0874	102.47	0.2490	-6.834	-12.19	-0.0723	101.74	597.07	495.33	11.607	-60.60
0.2461	0.0579	0.0874	102.49	0.2491	2.665	4.76	0.0282	102.38	597.07	494.69	11.692	23.51
0.3310	0.0779	0.0984	115.24	0.2801	14.465	28.78	0.1707	111.59	597.07	485.48	12.945	128.50
0.4159	0.0979	0.1749	204.43	0.4969	23.865	82.70	0.4905	186.95	597.07	410.12	24.505	199.40
0.5008	0.1179	0.2734	318.05	0.7730	27.165	145.21	0.8613	282.97	597.07	314.10	42.015	216.95
0.5857	0.1379	0.3390	392.82	0.9548	25.415	168.59	1.0000	354.81	597.07	242.26	55.674	204.14
0.6706	0.1579	0.3554	411.40	1.0000	21.865	153.21	0.9088	381.81	597.07	215.26	60.585	175.89
0.7555	0.1779	0.3554	411.40	1.0000	18.715	132.00	0.7829	389.65	597.07	207.42	61.972	149.54
0.8404	0.1979	0.3363	389.66	0.9471	16.265	109.13	0.6473	374.06	597.07	223.01	59.197	127.06
0.9252	0.2179	0.2296	267.71	0.6507	14.515	67.10	0.3980	259.17	597.07	337.90	37.488	110.25
0.9838	0.2317	0.0437	51.24	0.1245	13.665	12.10	0.0718	49.79	597.07	547.28	5.198	133.61

MASS AVERAGE TOTAL PRESSURE 18.172
MASS AVERAGE TOTAL TEMPERATURE 571.141
MASS AVG VM 136.331 VU 334.721 ANGLE 22.160
FLOW FACTOR 0.518 SLIP FACTOR INS. STA. 0.960 IMPELLER TIP 0.587
IMP. PRESS. RATIO 0.000 IMP. TEMP.RATIO 0.000 EFFICIENCY 0.000
IMP.,IND. PRESS. RATIO 1.241 IMP.,IND. TEMP. RATIO 1.101 EFFICIENCY 0.630
IMP.,IND.,IGV PRESS. RATIO 1.236 IMP.,IND.,IGV TEMP. RATIO 1.101 EFFICIENCY 0.619

* * * DIFFUSER * * *

CD DIFFUSER THROAT FRONT 0.643 REAR 0.625
STATIC PRESSURE RISE COEFFICIENT IMPELLER EXIT/DIFFUSER EXIT 0.507
DIFFUSER THROAT FRONT/DIFFUSER EXIT 0.626 DIFFUSER THROAT REAR/DIFFUSER EXIT 0.656
DIFFUSER LOSSES TOTAL TO STATIC 0.029 TOTAL TO TOTAL 0.010
DIFFUSER LOSS COEFFICIENT 0.492

TABLE XXXVII.

10/1 CENT COMP, IMP TRAV
IGV=20 DEG
FLOW RATE = 0.494

30 PCT SP, WDCV, RUN 3.06
SPEED = 19874.0

* * * IMPELLER EXIT * * * INITIAL INTEGRATED FLOW 0.478

PCENT SPAN	R	MO	VO	VO/VMAX	ALP	VM	VM/VMMAX	VU	U	WU	B	WO
0.0169	0.0040	0.2132	248.21	0.4040	-7.667	-33.11	-0.1307	245.99	610.97	364.97	33.979	-59.25
0.0764	0.0180	0.2351	273.29	0.4449	-1.467	-7.00	-0.0276	273.20	610.97	337.76	38.967	-11.13
0.1612	0.0380	0.2460	285.80	0.4652	8.232	40.92	0.1615	282.86	610.97	328.10	40.764	62.67
0.2461	0.0579	0.2898	335.80	0.5466	18.082	104.22	0.4113	319.22	610.97	291.75	47.574	141.20
0.3310	0.0779	0.3718	428.59	0.6977	25.082	181.68	0.7170	388.17	610.97	222.79	60.146	209.48
0.4159	0.0979	0.4402	504.52	0.8213	27.532	233.21	0.9204	447.38	610.97	163.58	69.915	248.31
0.5008	0.1179	0.5003	570.20	0.9282	26.382	253.37	1.0000	510.81	610.97	100.15	78.906	258.19
0.5857	0.1379	0.5386	611.39	0.9953	24.482	253.36	0.9999	556.42	610.97	54.54	84.400	254.58
0.6706	0.1579	0.5414	614.27	1.0000	22.132	231.42	0.9133	569.01	610.97	41.95	85.782	232.05
0.7555	0.1779	0.5304	602.52	0.9808	19.432	200.45	0.7911	568.19	610.97	42.77	85.694	201.02
0.8404	0.1979	0.4949	563.86	0.9179	17.632	170.79	0.6741	537.37	610.97	73.59	82.201	172.39
0.9252	0.2179	0.4156	476.66	0.7759	16.332	134.04	0.5290	457.42	610.97	153.54	71.444	141.39
0.9838	0.2317	0.3171	366.27	0.5962	15.632	98.69	0.3895	352.72	610.97	258.24	53.790	122.32

MASS AVERAGE TOTAL PRESSURE 19.771
MASS AVERAGE TOTAL TEMPERATURE 565.383
MASS AVG VM 205.486 VU 493.754 ANGLE 22.595
FLOW FACTOR 0.733 SLIP FACTOR INS. STA. 0.808 IMPELLER TIP 0.847
IMP. PRESS. RATIO 0.000 IMP. TEMP.RATIO 0.000 EFFICIENCY 0.000
IMP.+IND. PRESS. RATIO 1.350 IMP.+IND. TEMP. RATIO 1.090 EFFICIENCY 0.999
IMP.+IND.+IGV PRESS. RATIO 1.345 IMP.+IND.+IGV TEMP. RATIO 1.090 EFFICIENCY 0.987

* * * DIFFUSER * * *

CD DIFFUSER THROAT FRONT 0.811 REAR 0.755
STATIC PRESSURE RISE COEFFICIENT IMPELLER EXIT/DIFFUSER EXIT -0.234
DIFFUSER THROAT FRONT/DIFFUSER EXIT 0.402 DIFFUSER THROAT REAR/DIFFUSER EXIT 0.643
DIFFUSER LOSSES TOTAL TO STATIC 0.168 TOTAL TO TOTAL 0.126
DIFFUSER LOSS COEFFICIENT 1.234

TABLE XXXVIII.

10/1 CENT COMP. IMP TRAV — 30 PCT SP. BELOW NR ST. RUN 3.06
ICV=20 DEG
FLOW RATE = 0.358 — SPEED = 19912.0

* * * IMPELLER EXIT * * * — INITIAL INTEGRATED FLOW 0.306

PCENT SPAN	R	MO	VO	VO/VMAX	ALP	VM	VM/VMMAX	VU	U	WU	B	WO
0.0169	0.0040	0.2187	254.49	0.4304	-11.332	-50.00	-0.2320	249.52	612.14	362.61	34.533	-88.21
0.0764	0.0180	0.2406	279.65	0.4730	-7.732	-37.62	-0.1746	277.10	612.14	335.03	39.594	-59.03
0.1612	0.0380	0.2734	317.23	0.5366	-1.382	-7.65	-0.0355	317.14	612.14	294.99	47.072	-10.45
0.2461	0.0579	0.2843	329.69	0.5577	6.517	37.42	0.1736	327.56	612.14	284.57	49.017	49.57
0.3310	0.0779	0.3007	348.35	0.5892	14.867	89.38	0.4148	336.69	612.14	275.44	50.713	115.48
0.4159	0.0979	0.3499	404.09	0.6835	21.867	150.50	0.6984	375.01	612.14	237.12	57.694	178.06
0.5008	0.1179	0.4101	471.38	0.7973	24.767	197.47	0.9164	428.02	612.14	184.11	66.725	214.97
0.5857	0.1379	0.4703	337.84	0.9098	23.617	215.47	1.0000	492.80	612.14	119.34	76.386	221.70
0.6706	0.1579	0.5113	582.45	0.9852	21.267	211.26	0.9804	542.79	612.14	69.35	82.719	212.98
0.7555	0.1779	0.5195	591.16	1.0000	18.717	189.70	0.8803	559.89	612.14	52.24	84.669	190.52
0.8404	0.1979	0.4867	555.61	0.9398	15.817	151.44	0.7028	534.58	612.14	77.56	81.744	153.02
0.9252	0.2179	0.4101	471.22	0.7971	13.117	106.94	0.4963	458.92	612.14	153.21	71.538	112.74
0.9838	0.2317	0.3390	391.46	0.6621	11.717	79.49	0.3689	383.30	612.14	228.83	59.162	92.58

MASS AVERAGE TOTAL PRESSURE 19.678
MASS AVERAGE TOTAL TEMPERATURE 567.340
MASS AVG VM 180.601 VU 483.062 ANGLE 20.499
FLOW FACTOR 0.610 SLIP FACTOR INS. STA. 0.789 IMPELLER TIP 0.827
IMP. PRESS. RATIO 0.000 IMP. TEMP.RATIO 0.000 EFFICIENCY 0.000
IMP.+IND. PRESS. RATIO 1.343 IMP.+IND. TEMP. RATIO 1.093 EFFICIENCY 0.943
IMP.+IND.+IGV PRESS. RATIO 1.339 IMP.+IND.+IGV TEMP. RATIO 1.093 EFFICIENCY 0.931

* * * DIFFUSER * * *

CD DIFFUSER THROAT FRONT 0.702 REAR 0.689
STATIC PRESSURE RISE COEFFICIENT IMPELLER EXIT/DIFFUSER EXIT 0.612
DIFFUSER THROAT FRONT/DIFFUSER EXIT 0.656 DIFFUSER THROAT REAR/DIFFUSER EXIT 0.677
DIFFUSER LOSSES TOTAL TO STATIC 0.050 TOTAL TO TOTAL 0.033
DIFFUSER LOSS COEFFICIENT 0.387

TABLE XXXIX.

10/1 CENT COMP. IMP TRAV — 30 PCT SP, NEAR STALL, RUN 3.06
IGV=20 DEG
FLOW RATE = 0.269 — SPEED = 19458.0

* * * IMPELLER EXIT * * * — INITIAL INTEGRATED FLOW 0.239

PCENT SPAN	R	RO	VO	VO/VMAX	ALP	VM	VM/VMMAX	VU	U	WU	B	WO
0.0169	0.0040	0.2570	297.99	0.5371	-16.243	-83.35	-0.4623	286.10	598.18	312.08	42.512	-123.35
0.0764	0.0180	0.2789	322.90	0.5821	-12.593	-70.40	-0.3904	315.13	598.18	283.04	48.071	-94.63
0.1612	0.0380	0.2898	335.33	0.6045	-6.593	-38.50	-0.2135	333.12	598.18	265.06	51.490	-49.20
0.2461	0.0579	0.2953	341.54	0.6157	0.456	2.72	0.0150	341.53	598.18	256.64	53.076	3.40
0.3310	0.0779	0.2953	341.54	0.6157	8.306	49.34	0.2736	337.96	598.18	260.22	52.405	62.27
0.4159	0.0979	0.3199	369.49	0.6660	16.306	103.74	0.5753	354.63	598.18	243.55	55.519	125.85
0.5008	0.1179	0.3718	427.99	0.7715	21.306	155.51	0.8625	398.74	598.18	199.44	63.426	173.88
0.5857	0.1379	0.4238	485.81	0.8757	21.706	179.67	0.9965	451.36	598.18	146.82	71.981	188.94
0.6706	0.1579	0.4648	530.83	0.9569	19.856	180.30	1.0000	499.27	598.18	98.90	78.794	183.80
0.7555	0.1779	0.4867	554.62	0.9998	17.506	166.83	0.9253	523.93	598.18	69.24	82.541	168.26
0.8404	0.1979	0.4867	554.72	1.0000	15.456	147.83	0.8199	534.66	598.18	63.52	83.224	148.87
0.9252	0.2179	0.4183	479.62	0.8646	13.806	114.45	0.6348	465.76	598.18	132.41	74.129	118.99
0.9838	0.2317	0.2953	341.30	0.6152	12.956	76.52	0.4244	332.61	598.18	265.56	51.396	97.92

MASS AVERAGE TOTAL PRESSURE 19.557
MASS AVERAGE TOTAL TEMPERATURE 565.596
MASS AVG VM 178.116 VU 479.570 ANGLE 20.375
FLOW FACTOR 0.472 SLIP FACTOR IMP. STA. 0.801 IMPELLER TIP 0.840
IMP. PRESS. RATIO 0.000 IMP. TEMP.RATIO 0.000 EFFICIENCY 0.000
IMP.+IND. PRESS. RATIO 1.335 IMP.+IND. TEMP. RATIO 1.090 EFFICIENCY 0.957
IMP.+IND.+IGV PRESS. RATIO 1.330 IMP.+IND.+IGV TEMP. RATIO 1.090 EFFICIENCY 0.945

* * * DIFFUSER * * *

CD DIFFUSER THROAT FRONT 0.590 REAR 0.614
STATIC PRESSURE RISE COEFFICIENT IMPELLER EXIT/DIFFUSER EXIT 0.556
DIFFUSER THROAT FRONT/DIFFUSER EXIT 0.537 DIFFUSER THROAT REAR/DIFFUSER EXIT 0.479
DIFFUSER LOSSES TOTAL TO STATIC 0.054 TOTAL TO TOTAL 0.034
DIFFUSER LOSS COEFFICIENT 0.443

TABLE XL.

10/1 CENTRIFUGAL COMPRESSOR, IMPELLER TRAVERSE
70 PCT SPEED, WIDE OPEN DISCHARGE, RUN 3.07
IGV TURNING= 0 DEG

FLOW RATE = 1.454 SPEED = 45557.0

* * * IMPELLER EXIT * * * INITIAL INTEGRATED FLOW 1.049

PCENT SPAN	R	MO	VO	VO/VMAX	ALP	VM	VM/VMMAX	VU	U	WU	B	WO
0.0169	0.0040	0.3281	449.50	0.3407	0.645	5.06	0.0107	449.47	1400.52	951.05	25.295	11.84
0.0551	0.0130	0.6439	857.79	0.6503	3.045	45.56	0.0967	856.58	1400.52	543.94	57.584	53.97
0.0976	0.0230	0.8312	1080.96	0.8195	7.445	140.06	0.2972	1071.85	1400.52	328.67	72.952	146.50
0.1400	0.0329	0.9132	1173.35	0.8895	12.795	259.85	0.5515	1144.21	1400.52	256.31	77.373	266.29
0.1825	0.0429	0.9556	1220.24	0.9250	16.795	352.58	0.7483	1168.19	1400.52	232.33	78.751	359.49
0.2249	0.0529	0.9830	1249.83	0.9475	19.045	407.83	0.8656	1181.41	1400.52	219.11	79.493	414.78
0.2674	0.0629	1.0042	1272.52	0.9647	20.245	440.33	0.9346	1193.90	1400.52	206.62	80.181	446.88
0.3098	0.0729	1.0218	1291.44	0.9790	20.745	457.44	0.9709	1207.71	1400.52	192.81	80.929	463.23
0.3522	0.0829	1.0347	1305.09	0.9894	20.945	466.53	0.9902	1218.85	1400.52	181.67	81.522	471.68
0.3947	0.0929	1.0441	1315.00	0.9969	20.995	471.14	1.0000	1227.70	1400.52	172.82	81.987	475.79
0.4371	0.1030	1.0476	1319.04	1.0000	20.845	469.37	0.9962	1232.71	1400.52	167.81	82.247	473.70
0.4796	0.1129	1.0441	1315.76	0.9975	20.595	462.83	0.9823	1231.67	1400.52	168.85	82.194	467.16
0.5220	0.1229	1.0359	1307.32	0.9911	20.245	452.38	0.9601	1226.56	1400.52	173.96	81.927	456.90
0.5645	0.1329	1.0242	1295.52	0.9821	19.745	437.67	0.9289	1219.35	1400.52	181.17	81.548	442.47
0.6069	0.1429	1.0066	1277.32	0.9683	18.995	415.75	0.8824	1207.76	1400.52	192.76	80.932	421.01
0.6494	0.1529	0.9843	1253.88	0.9505	17.795	383.20	0.8133	1193.89	1400.52	206.63	80.180	388.90
0.6918	0.1629	0.9583	1226.15	0.9295	16.145	340.95	0.7236	1177.79	1400.52	222.73	79.291	347.00
0.7342	0.1729	0.9296	1194.76	0.9057	14.145	291.97	0.6197	1158.53	1400.52	241.99	78.201	298.27
0.7767	0.1829	0.9050	1167.98	0.8854	11.795	238.74	0.5067	1143.32	1400.52	257.20	77.321	244.71
0.8191	0.1929	0.8832	1143.83	0.8671	9.195	182.78	0.3879	1129.13	1400.52	271.39	76.485	187.98
0.8616	0.2029	0.8640	1122.72	0.8511	6.545	127.97	0.2716	1115.40	1400.52	285.12	75.660	132.08
0.9040	0.2129	0.8421	1097.86	0.8323	4.045	77.44	0.1643	1095.12	1400.52	305.40	74.417	80.39
0.9465	0.2229	0.8121	1063.21	0.8060	1.845	34.23	0.0726	1062.66	1400.52	337.86	72.362	35.92
0.9825	0.2314	0.5769	777.80	0.5896	0.545	7.39	0.0157	777.76	1400.52	622.76	51.315	9.47

MASS AVERAGE TOTAL PRESSURE 60.960
MASS AVERAGE TOTAL TEMPERATURE 812.199
MASS AVG VM 388.346 VU 1191.270 ANGLE 18.055
FLOW FACTOR 0.755 SLIP FACTOR INS. STA. 0.850 IMPELLER TIP 0.891
IMP. PRESS. RATIO 0.000 IMP. TEMP.RATIO 0.000 EFFICIENCY 0.000
IMP..IND. PRESS. RATIO 4.163 IMP.IND. TEMP. RATIO 1.565 EFFICIENCY 0.879
IMP..IND..IGV PRESS. RATIO 4.148 IMP..IND..IGV TEMP. RATIO 1.565 EFFICIENCY 0.877

* * * DIFFUSER * * *

CD DIFFUSER THROAT FRONT 0.857 REAR 0.871
STATIC PRESSURE RISE COEFFICIENT IMPELLER EXIT/DIFFUSER EXIT -0.045
DIFFUSER THROAT FRONT/DIFFUSER EXIT -0.224 DIFFUSER THROAT REAR/DIFFUSER EXIT -0.039
DIFFUSER LOSSES TOTAL TO STATIC 0.547 TOTAL TO TOTAL 0.454
DIFFUSER LOSS COEFFICIENT 1.045

TABLE XLI.

10/1 CENTRIFUGAL COMPRESSOR. IMPELLER TRAVERSE
70 PCT SPEED. BELOW NEAR STALL. RUN 3.07
IGV TURNING= 0 DEG

FLOW RATE = 1.464 SPEED = 45712.0

* * * IMPELLER EXIT * * * INITIAL INTEGRATED FLOW 1.029

PCENT SPAN	R	MO	VO	VO/VMAX	ALP	VM	VM/VMMAX	VU	U	WU	B	WO
0.0169	0.0040	0.2624	361.69	0.2736	2.494	15.74	0.0334	361.34	1405.29	1043.94	19.092	48.12
0.0551	0.0130	0.5796	779.32	0.5896	4.094	55.64	0.1183	777.33	1405.29	627.95	51.067	71.52
0.0976	0.0230	0.8093	1057.93	0.8004	8.144	149.87	0.3186	1047.26	1405.29	358.02	71.126	158.38
0.1400	0.0329	0.9146	1177.39	0.8907	13.294	270.74	0.5756	1145.84	1405.29	259.44	77.241	277.59
0.1825	0.0429	0.9597	1227.21	0.9284	16.844	355.61	0.7561	1174.56	1405.29	230.73	78.886	362.60
0.2249	0.0529	0.9698	1239.59	0.9379	18.844	406.84	0.8650	1192.08	1405.29	213.20	79.859	413.30
0.2674	0.0629	1.0125	1284.02	0.9714	19.994	439.03	0.9335	1206.63	1405.29	198.66	80.650	446.95
0.3098	0.0729	1.0312	1304.04	0.9866	20.594	458.69	0.9753	1220.71	1405.29	184.58	81.401	463.90
0.3522	0.0829	1.0417	1315.10	0.9949	20.794	466.87	0.9927	1229.43	1405.29	175.85	81.859	471.62
0.3947	0.0929	1.0464	1320.25	0.9988	20.844	469.78	0.9988	1233.84	1405.29	171.44	82.089	474.29
0.4371	0.1030	1.0476	1321.73	1.0000	20.844	470.30	1.0000	1235.22	1405.29	170.06	82.160	474.74
0.4796	0.1129	1.0441	1318.44	0.9975	20.644	464.83	0.9883	1233.78	1405.29	171.51	82.085	469.30
0.5220	0.1229	1.0371	1311.45	0.9922	20.344	455.93	0.9694	1229.64	1405.29	175.64	81.870	460.56
0.5645	0.1329	1.0265	1300.73	0.9841	19.844	441.55	0.9388	1223.49	1405.29	181.79	81.548	446.60
0.6069	0.1429	1.0101	1283.61	0.9711	19.044	418.84	0.8905	1213.36	1405.29	191.93	81.011	424.06
0.6494	0.1529	0.9898	1262.10	0.9548	17.994	389.89	0.8290	1200.37	1405.29	204.92	80.312	395.53
0.6918	0.1629	0.9652	1235.94	0.9350	16.444	349.87	0.7439	1185.38	1405.29	219.90	79.490	355.84
0.7342	0.1729	0.9378	1206.31	0.9126	14.394	299.87	0.6376	1168.44	1405.29	236.85	78.541	305.97
0.7767	0.1829	0.9105	1176.66	0.8902	11.944	243.52	0.5177	1151.18	1405.29	254.10	77.552	249.38
0.8191	0.1929	0.8832	1146.34	0.8673	9.244	184.15	0.3915	1131.45	1405.29	273.84	76.394	189.46
0.8616	0.2029	0.8585	1118.64	0.8463	6.394	124.58	0.2648	1111.68	1405.29	293.60	75.205	128.85
0.9040	0.2129	0.8367	1093.67	0.8274	3.844	73.32	0.1559	1091.21	1405.29	314.07	73.942	76.30
0.9465	0.2229	0.8066	1059.44	0.8015	1.994	36.86	0.0783	1058.80	1405.29	346.49	71.879	38.79
0.9829	0.2314	0.5714	772.55	0.5845	0.844	11.38	0.0242	772.47	1405.29	632.82	50.675	14.71

MASS AVERAGE TOTAL PRESSURE 61.060
MASS AVERAGE TOTAL TEMPERATURE 815.582
MASS AVG VM 389.721 VU 1194.779 ANGLE 18.065
FLOW FACTOR 0.760 SLIP FACTOR INS. STA. 0.850 IMPELLER TIP 0.891
IMP. PRESS. RATIO 0.000 IMP. TEMP.RATIO 0.000 EFFICIENCY 0.000
IMP..IND. PRESS. RATIO 4.169 IMP.IND. TEMP. RATIO 1.572 EFFICIENCY 0.870
IMP..IND..IGV PRESS. RATIO 4.155 IMP..IND..IGV TEMP. RATIO 1.572 EFFICIENCY 0.868

* * * DIFFUSER * * *

CF DIFFUSER THROAT FACT 0.866 REAR 0.850
STATIC PRESSURE RISE COEFFICIENT IMPELLER EXIT/DIFFUSER EXIT 0.469
DIFFUSER THROAT FRONT/DIFFUSER EXIT 0.378 DIFFUSER THROAT REAR/DIFFUSER EXIT 0.471
DIFFUSER LOSSES TOTAL TO STATIC 0.278 TOTAL TO TOTAL 0.222
DIFFUSER LOSS COEFFICIENT .530

TABLE XLII.

10/1 CENTRIFUGAL COMPRESSOR. IMPELLER INAVERSE
70 PCT SPEED. NEAR STALL. RUN 3.07
IGV TURNING= 0 DEG

FLOW RATE = 1.452 SPEED = 45242.0

* * * IMPELLER EXIT * * * INITIAL INTEGRATED FLOW 1.027

PCENT SPAN	#	MD	VD	VD/VMAX	ALP	VM	VM/VMMAX	VU	U	WU	B	WD
0.0169	0.0040	0.3062	420.55	0.3196	0.992	7.28	0.0155	420.49	1400.06	979.57	23.231	18.47
0.0551	0.0130	0.6124	819.68	0.6229	2.692	38.51	0.0820	818.78	1400.06	581.28	54.627	47.22
0.0934	0.0230	0.8148	1063.36	0.8081	7.342	135.90	0.2896	1054.64	1400.06	345.42	71.865	143.00
0.1400	0.0329	0.9023	1162.84	0.8837	12.842	258.47	0.5508	1133.75	1400.06	266.31	76.781	265.51
0.1825	0.0429	0.9484	1214.26	0.9234	16.592	346.75	0.7389	1163.69	1400.06	236.37	78.567	353.83
0.2249	0.0529	0.9843	1252.64	0.9519	19.042	408.70	0.8709	1184.08	1400.06	215.97	79.662	419.44
0.2674	0.0629	1.0101	1280.31	0.9730	20.192	441.94	0.9417	1201.62	1400.06	198.44	80.622	447.92
0.3098	0.0729	1.0265	1297.74	0.9862	20.792	460.68	0.9817	1213.22	1400.06	186.84	81.246	466.11
0.3522	0.0829	1.0359	1307.70	0.9938	20.992	468.48	0.9983	1220.90	1400.06	179.16	81.651	473.50
0.3947	0.0929	1.0406	1312.84	0.9977	20.942	469.26	1.0000	1226.13	1400.06	173.93	81.926	473.96
0.4371	0.1030	1.0429	1315.81	1.0000	20.842	468.17	0.9976	1229.71	1400.06	170.35	82.112	472.84
0.4795	0.1129	1.0417	1314.72	0.9991	20.642	463.49	0.9877	1228.91	1400.06	169.75	82.144	467.88
0.5220	0.1229	1.0371	1309.94	0.9955	20.292	454.31	0.9681	1228.63	1400.06	171.43	82.056	458.71
0.5645	0.1329	1.0285	1298.24	0.9874	19.792	439.95	0.9375	1222.48	1400.06	177.28	81.739	444.26
0.6069	0.1429	1.0160	1282.51	0.9746	19.042	418.45	0.8917	1212.33	1400.06	187.73	81.197	423.44
0.6494	0.1529	0.9871	1258.24	0.9562	17.842	387.63	0.8260	1197.06	1400.06	203.00	80.375	393.16
0.6918	0.1629	0.9611	1240.34	0.9350	16.492	342.29	0.7443	1179.72	1400.06	220.34	79.420	355.22
0.7342	0.1729	0.9331	1202.46	0.9138	14.842	303.97	0.6477	1163.40	1400.06	236.66	78.501	310.19
0.7767	0.1829	0.9076	1172.48	0.8916	13.142	246.63	0.5255	1146.25	1400.06	253.81	77.514	252.40
0.8191	0.1929	0.8832	1140.98	0.8706	9.292	184.96	0.3941	1130.37	1400.06	269.69	76.580	190.15
0.8616	0.2029	0.8585	1121.43	0.8492	6.492	126.35	0.2692	1110.26	1400.06	289.80	75.371	130.59
0.9040	0.2129	0.8334	1095.77	0.8327	4.042	77.25	0.1646	1093.04	1400.06	307.01	74.310	80.24
0.9465	0.2229	0.8121	1064.83	0.8091	2.292	42.59	0.0907	1063.78	1400.06	336.28	72.427	44.07
0.9889	0.2329	0.7996	782.07	0.5943	1.342	12.32	0.0390	781.86	1400.06	618.20	51.807	23.36

MASS AVERAGE TOTAL PRESSURE 52.622
MASS AVERAGE TOTAL TEMPERATURE 514.003
MASS AVG VM 387.649 VM 1191.659 ANGLE 16.196
FLOW FACTOR 0.757 SLIP FACTOR 1.00- STA. 0.855 IMPELLER TIP 0.892
IMP. PRESS. RATIO 0.000 IMP. TEMP. RATIO 0.000 EFFICIENCY 0.000
IMP.+IND. PRESS. RATIO 4.140 IMP.+IND. TEMP. RATIO 1.569 EFFICIENCY 0.870
IMP.+IND.+DIV PRESS. RATIO 4.126 IMP.+IND.+DIV TEMP. RATIO 1.569 EFFICIENCY 0.867

* * * DIFFUSER * * *

LD DIFFUSER INLET FACT 0.850 MEAN 0.875
STATIC PRESSURE RISE COEFFICIENT IMPELLER EXIT/DIFFUSER EXIT 0.500
DIFFUSER INLET FACT/DIFFUSER EXIT 0.495 DIFFUSER INLET MEAN/DIFFUSER EXIT 0.509
DIFFUSER LOSS TOTAL TO STATIC 0.225 TOTAL TO TOTAL 0.175
DIFFUSER LOSS COEFFICIENT 0.438

TABLE XLIII.

10/1 CENTRIFUGAL COMPRESSOR. IMPELLER TRAVERSE
90 PCT SPEED. WIDE OPEN DISCHARGE. RUN 3.07
IGV TURNING=10 DEG

FLOW RATE = 1.463 SPEED = 45806.0

* * * IMPELLER EXIT * * * INITIAL INTEGRATED FLOW 1.037

PCENT SPAN	R	MD	VD	VD/VMAX	ALP	VM	VM/VMMAX	VU	U	MU	B	MD
0.0269	0.0040	0.2953	404.75	0.3060	1.086	7.67	0.0161	404.67	1408.18	1003.50	21.962	20.52
0.0551	0.0130	0.5766	776.96	0.5870	3.586	48.56	0.1022	774.84	1408.18	633.33	50.738	42.72
0.0876	0.0250	0.7988	1042.80	0.7885	7.236	149.09	0.3012	1033.03	1408.18	375.15	70.041	152.24
0.1400	0.0389	0.9805	1268.53	0.9595	12.686	256.63	0.5402	1140.00	1408.18	268.17	76.762	243.63
0.1825	0.0429	0.9542	1216.43	0.9197	16.136	338.08	0.7116	1168.51	1408.18	239.67	78.408	345.32
0.2249	0.0529	0.9826	1245.95	0.9420	18.236	389.91	0.8207	1183.37	1408.18	224.80	79.263	396.88
0.2674	0.0629	1.0078	1274.22	0.9634	19.686	429.25	0.9035	1199.74	1408.18	208.43	80.166	435.68
0.3098	0.0729	1.0253	1292.89	0.9775	20.636	455.66	0.9591	1209.93	1408.18	198.25	80.696	461.74
0.3522	0.0829	1.0394	1307.57	0.9886	21.086	470.43	0.9902	1220.01	1408.18	188.16	81.232	476.00
0.3947	0.0929	1.0488	1317.44	0.9961	21.136	475.06	1.0000	1228.81	1408.18	179.37	81.695	480.09
0.4371	0.1030	1.0535	1322.55	1.0000	21.036	474.75	0.9993	1234.41	1408.18	173.77	81.986	479.63
0.4796	0.1129	1.0523	1320.88	0.9990	20.836	470.19	0.9897	1235.40	1408.18	172.77	82.038	476.76
0.5220	0.1229	1.0476	1315.12	0.9946	20.486	460.97	0.9703	1233.82	1408.18	174.36	81.956	465.56
0.5644	0.1329	1.0382	1303.62	0.9857	19.986	446.94	0.9408	1228.86	1408.18	179.31	81.698	451.68
0.6069	0.1429	1.0230	1284.18	0.9710	19.286	426.79	0.8984	1219.96	1408.18	188.52	81.213	431.86
0.6493	0.1529	1.0007	1256.19	0.9501	18.286	398.11	0.8380	1204.72	1408.18	203.46	80.413	403.74
0.6918	0.1629	0.9748	1241.52	0.9387	16.986	362.70	0.7634	1187.35	1408.18	220.82	79.464	368.92
0.7342	0.1729	0.9465	1210.75	0.9154	15.286	319.21	0.6719	1167.91	1408.18	240.26	78.375	325.89
0.7767	0.1829	0.9187	1180.03	0.8929	12.786	261.38	0.5502	1151.74	1408.18	256.43	77.447	267.78
0.8191	0.1929	0.8955	1155.81	0.8735	9.386	188.42	0.3966	1139.84	1408.18	268.33	76.752	193.57
0.8615	0.2029	0.8777	1135.62	0.8588	5.986	120.46	0.2493	1129.62	1408.18	278.55	76.147	122.91
0.9040	0.2129	0.8585	1104.40	0.8426	3.286	63.89	0.1344	1112.96	1408.18	295.61	75.219	66.10
0.9464	0.2229	0.8344	1075.56	0.8232	1.436	26.96	0.0567	1075.22	1408.18	332.95	74.744	28.22
0.9825	0.2514	0.5906	765.43	0.5999	0.536	7.43	0.0156	793.39	1408.18	614.78	52.228	9.42

MASS AVERAGE TOTAL PRESSURE 60.914
MASS AVERAGE TOTAL TEMPERATURE 604.661
MASS AVG VM 395.065 VU 1155.334 ANGLE 18.202
FLOW FACTOR 0.759 S.IP FACTOR INS. STA. 0.648 IMPELLER TIP 0.889
IMP. PRESS. RATIO 4.000 IMP. TEMP. RATIO 2.000 EFFICIENCY 0.000
IMP.+IND. PRESS. RATIO 4.160 IMP.+IND. TEMP. RATIO 2.559 EFFICIENCY 0.889
IMP.+IND.+IGV PRESS. RATIO 4.345 IMP.+IND.+IGV TEMP. RATIO 2.559 EFFICIENCY 0.887

* * * DIFFUSER * * *

CD DIFFUSER THROAT FRONT 0.665 REAR 0.675
STATIC PRESSURE RISE COEFFICIENT IMPELLER EXIT/DIFFUSER EXIT -2.037
DIFFUSER THROAT FRONT/DIFFUSER EXIT -1.220 DIFFUSER THROAT REAR/DIFFUSER EXIT -2.042
DIFFUSER LOSSES TOTAL TO STATIC 0.545 TOTAL TO TOTAL 0.455
DIFFUSER LOSS COEFFICIENT 0.787

TABLE XLIV.

10/1 CENTRIFUGAL COMPRESSOR, IMPELLER TRAVERSE
70 PCT SPEED, BELOW NEAR STALL, RUN 3.07
IGV TURNING=10 DEG

FLOW RATE = 1.460 SPEED = 45883.0

* * * IMPELLER EXIT * * * INITIAL INTEGRATED FLOW 1.056

PERCENT SPAN	R	MD	VD	VD/VMAX	ALP	VM	VM/VMMAX	VU	V	MU	B	MQ
0.0189	0.0040	0.1968	291.07	0.2063	1.885	6.91	0.0189	270.92	1410.55	1139.62	13.372	38.55
0.0551	0.0830	0.5742	765.63	0.5859	3.535	47.45	0.1007	748.16	1410.55	642.38	50.095	81.84
0.0976	0.0930	0.6393	1054.23	0.8026	6.335	116.33	0.2469	1047.79	1410.55	382.75	70.903	123.10
0.1400	0.0529	0.6927	1149.23	0.8749	10.935	218.00	0.4627	1128.37	1410.55	282.17	75.959	224.72
0.1825	0.0429	0.8310	1191.50	0.9071	15.535	319.12	0.6774	1147.97	1410.55	262.57	77.116	327.36
0.2249	0.0529	0.9652	1228.56	0.9356	18.285	385.58	0.8185	1183.92	1410.55	243.62	78.207	393.80
0.2674	0.0629	0.9994	1265.60	0.9635	19.835	428.44	0.9110	1190.52	1410.55	220.02	79.529	436.71
0.3098	0.0729	1.0195	1286.99	0.9798	20.635	453.55	0.9628	1224.42	1410.55	208.12	80.288	460.15
0.3522	0.0829	1.0334	1300.62	0.9902	20.985	465.78	0.9887	1214.35	1410.55	198.19	80.822	471.82
0.3947	0.0929	1.0406	1309.43	0.9969	21.085	471.07	1.0000	1221.76	1410.55	188.79	81.216	476.66
0.4371	0.1030	1.0441	1313.47	1.0000	20.985	470.39	0.9985	1220.35	1410.55	184.19	81.458	475.66
0.4796	0.1129	1.0429	1312.38	0.9991	20.785	465.71	0.9886	1226.96	1410.55	183.58	81.490	470.90
0.5220	0.1229	1.0382	1306.80	0.9948	20.485	457.75	0.9717	1225.29	1410.55	185.26	81.402	462.95
0.5645	0.1329	1.0269	1292.45	0.9839	19.985	443.78	0.9420	1220.75	1410.55	190.29	81.136	448.14
0.6069	0.1429	1.0136	1282.55	0.9764	19.285	429.59	0.8991	1210.58	1410.55	199.96	80.620	429.33
0.6494	0.1529	0.9995	1260.86	0.9597	18.335	398.54	0.8417	1196.56	1410.55	212.98	79.860	402.83
0.6918	0.1629	0.9854	1241.42	0.9375	17.035	360.75	0.7658	1177.39	1410.55	233.15	78.798	367.76
0.7342	0.1729	0.9712	1208.69	0.9164	15.385	315.29	0.6693	1161.66	1410.55	248.88	77.907	322.45
0.7767	0.1829	0.9154	1176.91	0.8948	13.735	299.49	0.6360	1148.39	1410.55	264.15	77.024	265.88
0.8191	0.1929	0.8596	1149.84	0.8756	10.235	204.91	0.4337	1131.54	1410.55	279.00	76.148	219.43
0.8616	0.2029	0.8695	1127.05	0.8580	7.685	150.72	0.3199	1116.93	1410.55	293.61	75.271	155.84
0.9040	0.2129	0.8431	1096.08	0.8344	4.835	92.38	0.1961	1092.18	1410.55	318.37	73.748	96.23
0.9465	0.2229	0.8167	1061.56	0.8081	2.635	48.80	0.1036	1060.38	1410.55	350.16	71.725	51.39
0.9889	0.2329	0.7904	983.40	0.5964	1.485	20.30	0.0431	783.13	1410.55	627.41	51.299	26.91

MASS AVERAGE TOTAL PRESSURE 60.600
MASS AVERAGE TOTAL TEMPERATURE 809.458
MASS AVG VM 886.488 VU 1185.656 ANGLE 18.069
FLOW FACTOR 0.764 SLIP FACTOR INS. STA. 0.840 IMPELLER TIP 0.881
IMP. PRESS. RATIO 0.000 IMP. TEMP. RATIO 0.000 EFFICIENCY 0.000
IMP..IND. PRESS. RATIO 4.124 IMP. IND. TEMP. RATIO 1.560 EFFICIENCY 0.880
IMP..IND..IGV PRESS. RATIO 4.110 IMP..IND..IGV TEMP. RATIO 1.560 EFFICIENCY 0.878

* * * DIFFUSER * * *

CD DIFFUSER THROAT FRONT 0.668 REAR 0.881
STATIC PRESSURE RISE COEFFICIENT IMPELLER EXIT/DIFFUSER EXIT 0.463
DIFFUSER THROAT FRONT/DIFFUSER EXIT 0.996 DIFFUSER THROAT REAR/DIFFUSER EXIT 0.485
DIFFUSER LOSSES TOTAL TO STATIC 0.248 TOTAL TO TOTAL 0.214
DIFFUSER LOSS COEFFICIENT 0.506

TABLE XLV.

1CV1 CENTRIFUGAL COMPRESSOR. IMPELLER TRAVERSE
TO PCT SPEED. NEAR STALL. RUN 3.07
IGV TURNING=20 DEG

FLOW RATE = 1.461 SPEED = 45771.0

* * * IMPELLER EXIT * * * INITIAL INTEGRATED FLOW 1.101

PCENT SPAN	R	MU	WU	VOLVMAR	ALP	XM	XM/XMMAX	WR	U	WT	B	MU
0.0000	0.0000	0.8556	445.74	0.8571	1.477	26.41	0.8239	485.52	1407.1	921.58	27.781	36.14
0.0051	0.0080	0.8502	446.28	0.8565	2.477	26.31	0.8174	839.45	1407.10	567.65	55.432	43.84
0.0076	0.0120	0.8466	446.64	0.8565	3.277	26.22	0.8151	1045.3W	1407.10	361.80	78.907	123.42
0.0400	0.0629	0.8429	446.98	0.8740	11.677	25.55	0.7965	1129.98	1407.10	277.61	76.190	206.42
0.0625	0.0984	0.8466	446.70	0.8753	15.727	25.62	0.6985	1163.46	1407.1W	243.64	78.172	336.73
0.2500	0.0629	0.8775	444.54	0.8809	19.277	25.69	0.8309	1179.84	1407.10	227.26	79.096	356.83
0.3000	0.0719	1.0214	443.65	0.8764	20.327	25.76	0.8376	1190.87	1407.1W	216.23	80.137	432.16
0.3333	0.0829	1.0359	443.05	0.8883	20.677	25.82	0.8555	1209.62	1407.10	197.48	80.727	454.03
0.3667	0.0939	1.0459	442.65	0.8995	20.827	25.87	0.8626	1221.98	1407.10	185.12	81.332	466.13
0.4000	0.1050	1.0568	442.15	0.9059	20.827	25.92	0.8676	1229.29	1407.10	177.80	81.784	472.44
0.4333	0.1160	1.0666	441.64	0.9086	20.827	25.96	0.8699	1232.79	1407.10	174.30	81.952	473.62
0.4667	0.1270	1.0760	441.20	1.0000	20.677	26.00	0.8708	1233.37	1407.1W	173.73	82.087	474.73
0.5000	0.1380	1.0855	440.76	0.9804	20.377	26.04	0.8708	1233.37	1407.1W	173.73	81.982	469.85
0.5333	0.1490	1.0946	440.34	0.9772	19.877	26.07	0.8672	1225.94	1407.10	181.15	81.594	448.04
0.5667	0.1600	1.1029	439.96	0.9746	19.227	26.10	0.8637	1215.21	1407.10	191.89	81.026	429.08
0.6000	0.1710	1.1106	439.61	0.9572	18.327	26.12	0.8575	1199.91	1407.10	207.19	80.203	403.34
0.6333	0.1820	1.1184	439.26	0.9396	16.977	26.14	0.8475	1180.76	1407.10	226.34	79.481	384.50
0.6667	0.1930	1.1255	438.94	0.9222	15.277	26.16	0.8342	1159.27	1407.1W	247.82	78.841	324.95
0.7000	0.2040	1.1320	438.65	0.9048	13.027	26.17	0.8172	1136.26	1407.1W	270.84	77.989	274.45
0.7333	0.2150	1.1380	438.37	0.8827	10.427	26.18	0.7949	1106.32	1407.1W	300.78	77.183	216.34
0.7667	0.2260	1.1434	438.13	0.8634	7.377	26.19	0.7712	1073.23	1407.1W	333.87	76.235	154.66
0.8000	0.2370	1.1482	437.92	0.8435	4.077	26.20	0.7434	1033.12	1407.1W	374.01	75.023	94.01
0.8333	0.2480	1.1527	437.72	0.8252	2.877	26.20	0.7167	996.46	1407.10	410.66	73.722	57.02
0.8667	0.2590	1.1568	437.54	0.8195	1.877	26.19	0.6973	969.66	1407.10	437.46	72.772	37.03

MASS AVERAGE TOTAL PRESSURE 60.559
MASS AVERAGE TOTAL TEMPERATURE 604.967
MASS AVG VM 1.461 VU 1191.222 ANGLE 17.934
FLOW FACTOR 0.769 SLIP FACTOR INS. STA. 0.844 IMPELLER TIP 0.859
IMP. PRESS. RATIO 6.000 IMP. TEMP. RATIO 0.000 EFFICIENCY 0.000
IMP.-IND. PRESS. RATIO 4.938 IMP.-IND. TEMP. RATIO 1.561 EFFICIENCY 0.881
IMP.-IND.-IGV PRESS. RATIO 4.108 IMP.-IND.-IGV TEMP. RATIO 1.561 EFFICIENCY 0.878

* * * DIFFUSER * * *

ED DIFFUSER THROAT FRONT 0.966 REAR 0.882
STATIC PRESSURE RISE COEFFICIENT IMPELLER EXIT-DIFFUSER EXIT 0.573
DIFFUSER THROAT FRONT/DIFFUSER EXIT 0.808 DIFFUSER THROAT/DIFFUSER EXIT 0.573
DIFFUSER LOSSES TOTAL TO STATIC 0.222 TOTAL TO TOTAL 0.273
DIFFUSER LOSS COEFFICIENT 0.456

TABLE XXVI.

[illegible] CENTRIFUGAL COMPRESSOR, IMPELLER TRAVERSE
70 PCT SPEED, WIDE OPEN DISCHARGE, RUN 3.07
IGV TURNING 25 DEG

FLOW RATE = 1.444 SPEED = 4557.9

* * * IMPELLER EXIT * * * INITIAL INTEGRATED FLOW 1.245

POINT SPAN	R	MU	VU	VU/VMAX	ALP	VM	M/VMMAX	VR	V	MV	B	MU
0.0000	0.0000	0.0000	521.23	0.9999	0.000	0.39	0.0000	521.23	1401.05	0.00	37.443	0.77
0.0050	0.0050	0.0000	521.23	0.9999	0.000	0.39	0.0000	521.23	1401.05	0.00	37.443	0.77
0.0100	0.0100	0.0000	521.23	0.9999	0.000	0.39	0.0000	521.23	1401.05	0.00	37.443	0.77
0.0200	0.0200	0.0000	521.23	0.9999	0.000	0.39	0.0000	521.23	1401.05	0.00	37.443	0.77
0.0300	0.0300	0.0000	521.23	0.9999	0.000	0.39	0.0000	521.23	1401.05	0.00	37.443	0.77
0.0400	0.0400	0.0000	521.23	0.9999	0.000	0.39	0.0000	521.23	1401.05	0.00	37.443	0.77
0.0500	0.0500	0.0000	521.23	0.9999	0.000	0.39	0.0000	521.23	1401.05	0.00	37.443	0.77
0.0600	0.0600	0.0000	521.23	0.9999	0.000	0.39	0.0000	521.23	1401.05	0.00	37.443	0.77
0.0700	0.0700	0.0000	521.23	0.9999	0.000	0.39	0.0000	521.23	1401.05	0.00	37.443	0.77
0.0800	0.0800	0.0000	521.23	0.9999	0.000	0.39	0.0000	521.23	1401.05	0.00	37.443	0.77
0.0900	0.0900	0.0000	521.23	0.9999	0.000	0.39	0.0000	521.23	1401.05	0.00	37.443	0.77
0.1000	0.1000	0.0000	521.23	0.9999	0.000	0.39	0.0000	521.23	1401.05	0.00	37.443	0.77
0.1100	0.1100	0.0000	521.23	0.9999	0.000	0.39	0.0000	521.23	1401.05	0.00	37.443	0.77
0.1200	0.1200	0.0000	521.23	0.9999	0.000	0.39	0.0000	521.23	1401.05	0.00	37.443	0.77
0.1300	0.1300	0.0000	521.23	0.9999	0.000	0.39	0.0000	521.23	1401.05	0.00	37.443	0.77
0.1400	0.1400	0.0000	521.23	0.9999	0.000	0.39	0.0000	521.23	1401.05	0.00	37.443	0.77
0.1500	0.1500	0.0000	521.23	0.9999	0.000	0.39	0.0000	521.23	1401.05	0.00	37.443	0.77
0.1600	0.1600	0.0000	521.23	0.9999	0.000	0.39	0.0000	521.23	1401.05	0.00	37.443	0.77
0.1700	0.1700	0.0000	521.23	0.9999	0.000	0.39	0.0000	521.23	1401.05	0.00	37.443	0.77
0.1800	0.1800	0.0000	521.23	0.9999	0.000	0.39	0.0000	521.23	1401.05	0.00	37.443	0.77
0.1900	0.1900	0.0000	521.23	0.9999	0.000	0.39	0.0000	521.23	1401.05	0.00	37.443	0.77
0.2000	0.2000	0.0000	521.23	0.9999	0.000	0.39	0.0000	521.23	1401.05	0.00	37.443	0.77
0.2100	0.2100	0.0000	521.23	0.9999	0.000	0.39	0.0000	521.23	1401.05	0.00	37.443	0.77
0.2200	0.2200	0.0000	521.23	0.9999	0.000	0.39	0.0000	521.23	1401.05	0.00	37.443	0.77
0.2300	0.2300	0.0000	521.23	0.9999	0.000	0.39	0.0000	521.23	1401.05	0.00	37.443	0.77
0.2400	0.2400	0.0000	521.23	0.9999	0.000	0.39	0.0000	521.23	1401.05	0.00	37.443	0.77
0.2500	0.2500	0.0000	521.23	0.9999	0.000	0.39	0.0000	521.23	1401.05	0.00	37.443	0.77
0.2600	0.2600	0.0000	521.23	0.9999	0.000	0.39	0.0000	521.23	1401.05	0.00	37.443	0.77
0.2700	0.2700	0.0000	521.23	0.9999	0.000	0.39	0.0000	521.23	1401.05	0.00	37.443	0.77
0.2800	0.2800	0.0000	521.23	0.9999	0.000	0.39	0.0000	521.23	1401.05	0.00	37.443	0.77
0.2900	0.2900	0.0000	521.23	0.9999	0.000	0.39	0.0000	521.23	1401.05	0.00	37.443	0.77
0.3000	0.3000	0.0000	521.23	0.9999	0.000	0.39	0.0000	521.23	1401.05	0.00	37.443	0.77
0.3100	0.3100	0.0000	521.23	0.9999	0.000	0.39	0.0000	521.23	1401.05	0.00	37.443	0.77
0.3200	0.3200	0.0000	521.23	0.9999	0.000	0.39	0.0000	521.23	1401.05	0.00	37.443	0.77
0.3300	0.3300	0.0000	521.23	0.9999	0.000	0.39	0.0000	521.23	1401.05	0.00	37.443	0.77
0.3400	0.3400	0.0000	521.23	0.9999	0.000	0.39	0.0000	521.23	1401.05	0.00	37.443	0.77
0.3500	0.3500	0.0000	521.23	0.9999	0.000	0.39	0.0000	521.23	1401.05	0.00	37.443	0.77
0.3600	0.3600	0.0000	521.23	0.9999	0.000	0.39	0.0000	521.23	1401.05	0.00	37.443	0.77
0.3700	0.3700	0.0000	521.23	0.9999	0.000	0.39	0.0000	521.23	1401.05	0.00	37.443	0.77
0.3800	0.3800	0.0000	521.23	0.9999	0.000	0.39	0.0000	521.23	1401.05	0.00	37.443	0.77
0.3900	0.3900	0.0000	521.23	0.9999	0.000	0.39	0.0000	521.23	1401.05	0.00	37.443	0.77
0.4000	0.4000	0.0000	521.23	0.9999	0.000	0.39	0.0000	521.23	1401.05	0.00	37.443	0.77

MASS AVERAGE TOTAL PRESSURE 60.749
MASS AVERAGE TOTAL TEMPERATURE 827.571
MASS AVG VU 521.229 VU 521.229 ANGLE 68.150
FLOW FACTOR 0.356 SLIP FACTOR INC. EXP. 0.852 IMPELLER TIP 0.843
IMP. PRESS. RATIO 0.000 IMP. TEMP. RATIO 0.000 EFFICIENCY 0.000
IMP.+DIF. PRESS. RATIO 4.006 IMP.+DIF. TEMP. RATIO 1.556 EFFICIENCY 0.885
DIF.+INT.+IGV PRESS. RATIO 4.004 IMP.+DIF.+IGV TEMP. RATIO 1.556 EFFICIENCY 0.882

* * * DIFFUSER * * *

CL DIFFUSER THROAT FINISH 0.000 NEAR 0.870
FANNO PRESSURE LOSS COEFFICIENT IMPELLER EXIT/DIFFUSER EXIT -0.026
DIFFUSER THROAT FANNO/DIFFUSER EXIT -0.026 DIFFUSER THROAT NEAR/DIFFUSER EXIT -0.026
DIFFUSER LOSSES TOTAL TO STATIC 0.000 TOTAL TO TOTAL 0.054
DIFFUSER LOSS COEFFICIENT 0.00

TABLE XLVII.

[illegible] COMPRESSOR, IMPELLER INLEASE
90 PCT SPEED BELOW DESIGN STALL MASS 3.27
[illegible] 20 DEG

FLOW RATE = [illegible] SPEED = [illegible]

* * * IMPELLER EXIT * * * RADIAL INTEGRATED FLOW [illegible]

RELAT SPAN	R	RO	RO	RO/RTMAX	ALF	RM	VM/VTMAX	VM	U	RV	R	RV
[illegible]												
[illegible]												
[illegible]												

TABLE XLVIII.

10/1 CENTRIFUGAL COMPRESSOR, IMPELLER TRAVERSE
70 PCT SPEED, NEAR STALL, RUN 3.07
IGV TURNING= 20 DEG

FLOW RATE = 1.458 SPEED = 45913.0

* * * IMPELLER EXIT * * * INITIAL INTEGRATED FLOW 1.057

PCENT SPAN	R	MO	VO	VO/VMAX	ALP	VM	VM/VMMAX	VU	U	WU	B	BO
0.0169	0.0040	0.3554	484.59	0.3698	1.344	11.37	0.0242	484.46	1411.47	927.01	27.591	24.55
0.0551	0.0130	0.6453	856.73	0.6539	3.544	52.97	0.1131	855.09	1411.47	556.37	56.949	63.20
0.0976	0.0230	0.8271	1072.70	0.8188	7.744	144.56	0.3086	1062.92	1411.47	348.55	71.844	152.13
0.1400	0.0329	0.9037	1159.11	0.8847	12.344	247.81	0.5291	1132.31	1411.47	279.16	76.150	255.23
0.1825	0.0429	0.9433	1202.83	0.9181	15.894	329.42	0.7034	1156.84	1411.47	254.62	77.586	337.31
0.2249	0.0529	0.9734	1235.54	0.9431	18.494	391.94	0.8368	1171.73	1411.47	239.74	78.436	400.06
0.2674	0.0629	0.9980	1262.06	0.9633	19.944	430.51	0.9192	1186.36	1411.47	225.11	79.255	438.19
0.3098	0.0729	1.0160	1281.07	0.9778	20.694	452.72	0.9666	1198.41	1411.47	213.06	79.918	459.82
0.3522	0.0829	1.0289	1294.68	0.9882	20.994	463.86	0.9904	1208.73	1411.47	202.73	80.478	470.34
0.3947	0.0929	1.0371	1303.48	0.9949	21.044	468.08	0.9994	1216.54	1411.47	194.93	80.896	474.05
0.4371	0.1030	1.0406	1307.14	0.9977	20.994	468.33	1.0000	1220.36	1411.47	191.11	81.099	474.03
0.4796	0.1129	1.0429	1310.08	1.0000	20.794	465.11	0.9931	1224.74	1411.47	186.73	81.331	470.48
0.5220	0.1229	1.0371	1304.24	0.9955	20.444	455.58	0.9727	1222.09	1411.47	189.38	81.191	461.02
0.5645	0.1329	1.0277	1294.71	0.9882	19.944	441.65	0.9430	1217.06	1411.47	194.41	80.924	447.25
0.6069	0.1429	1.0148	1281.44	0.9781	19.194	421.31	0.8996	1210.20	1411.47	201.26	80.557	427.10
0.6494	0.1529	0.9966	1262.51	0.9636	18.194	394.22	0.8417	1199.38	1411.47	212.09	79.971	400.33
0.6918	0.1629	0.9734	1238.01	0.9449	16.944	360.82	0.7704	1184.26	1411.47	227.20	79.139	367.40
0.7342	0.1729	0.9483	1211.52	0.9247	15.244	318.56	0.6802	1168.88	1411.47	242.58	78.275	325.35
0.7767	0.1829	0.9242	1185.08	0.9045	12.994	266.48	0.5690	1154.73	1411.47	256.73	77.465	272.39
0.8191	0.1929	0.8968	1154.83	0.8814	10.244	205.39	0.4385	1136.42	1411.47	275.04	76.394	211.32
0.8616	0.2029	0.8649	1131.03	0.8633	7.094	139.69	0.2982	1122.37	1411.47	289.09	75.556	144.25
0.9040	0.2129	0.8531	1106.39	0.8445	4.244	81.89	0.1748	1103.36	1411.47	308.11	74.397	85.03
0.9465	0.2229	0.8121	1059.51	0.8087	2.244	41.50	0.0886	1058.69	1411.47	352.77	71.571	43.74
0.9825	0.2314	0.5769	774.86	0.5914	1.144	15.48	0.0330	774.71	1411.47	636.76	50.582	20.04

MASS AVERAGE TOTAL PRESSURE 59.796
MASS AVERAGE TOTAL TEMPERATURE 806.000
MASS AVG VM 386.852 VU 1185.619 ANGLE 18.070
FLOW FACTOR 0.768 SLIP FACTOR INS. STA. 0.839 IMPELLER TIP 0.880
IMP. PRESS. RATIO 0.000 IMP. TEMP.RATIO 0.000 EFFICIENCY 0.000
IMP.+IND. PRESS. RATIO 4.083 IMP.+IND. TEMP. RATIO 1.553 EFFICIENCY 0.883
IMP.+IND.+IGV PRESS. RATIO 4.069 IMP.+IND.+IGV TEMP. RATIO 1.553 EFFICIENCY 0.881

* * * DIFFUSER * * *

CD DIFFUSER THROAT FRONT 0.878 REAR 0.888
STATIC PRESSURE RISE COEFFICIENT IMPELLER EXIT/DIFFUSER EXIT 0.603
DIFFUSER THROAT FRONT/DIFFUSER EXIT 0.530 DIFFUSER THROAT REAR/DIFFUSER EXIT 0.602
DIFFUSER LOSSES TOTAL TO STATIC 0.206 TOTAL TO TOTAL 0.155
DIFFUSER LOSS COEFFICIENT 0.396

TABLE XLIX.

10/1 CENTRIFUGAL COMPRESSOR, IMPELLER EXIT TRAVERSE
90 PCT SPEED, NEAR STALL, RUN 3.08
IGV TURNING = 0 DEG

FLOW RATE = 2.604 SPEED = 58529.6

* * * INLET GUIDE VANE EXIT * * *

	MO	VO	ALPHA	VM	VU	U	WU	B	WO	MREL	I	VO/VOMAX
10	0.380	418.452	90.000	418.452	0.000	868.998	868.997	25.712	964.499	0.876	5.187	1.000
30	0.371	409.658	90.000	409.657	0.000	971.233	971.232	22.869	1054.093	0.956	8.030	0.978
50	0.366	403.789	90.000	403.789	0.000	1073.468	1073.467	20.614	1146.899	1.040	9.946	0.964
70	0.360	397.915	90.000	397.915	0.000	1175.703	1175.702	18.698	1241.215	1.125	10.971	0.950
90	0.355	392.036	90.000	392.036	0.000	1277.938	1277.937	17.054	1336.719	1.212	11.095	0.936

* * * INDUCER EXIT * * * INITIAL INTEGRATED FLOW 2.268

MASS AVERAGE TOTAL PRESSURE 24.129
MASS AVERAGE TOTAL TEMPERATURE 627.447
INDUCER PRESSURE RATIO 1.642
INDUCER TEMPERATURE RATIO 1.209
INDUCER EFFICIENCY 0.725

INDUCER EXIT VELOCITY TRIANGLES

	MO	VO	ALPHA	VM	VU	U	WU	B	WO	MREL	I	VO/VOMAX
10	0.576	670.063	50.474	520.846	426.446	926.096	499.649	32.706	593.795	0.511	20.993	0.898
30	0.576	673.292	51.821	528.466	416.167	999.399	583.232	42.179	787.042	0.674	7.220	0.903
50	0.604	711.078	50.908	551.898	448.375	1072.701	624.325	41.476	833.291	0.708	3.553	0.953
70	0.601	720.104	47.302	529.243	488.325	1146.004	657.678	38.824	844.180	0.725	1.375	0.965
90	0.609	745.462	34.470	445.780	614.573	1219.306	604.733	36.395	751.280	0.614	-0.745	1.000

TABLE XLIX. (Continued)

* * * IMPELLER EXIT * * * INITIAL INTEGRATED FLOW 1.799

PCENT SPAN	R	MO	VO	VO/VMAX	ALP	VM	VM/VMMAX	VU	U	WU	B	WO
0.0148	0.0035	0.3773	575.41	0.3302	6.810	68.23	0.1203	571.35	1799.33	1227.98	24.951	161.74
0.0488	0.0114	0.7628	1119.44	0.6424	11.010	213.79	0.3770	1098.83	1799.33	700.50	57.482	253.54
0.0912	0.0214	1.0664	1495.13	0.8580	14.760	380.92	0.6718	1445.79	1799.33	353.54	76.259	392.14
0.1358	0.0319	1.2164	1661.52	0.9535	17.410	497.14	0.8768	1585.40	1799.33	213.92	82.315	501.65
0.1782	0.0419	1.2585	1705.24	0.9786	18.960	534.05	0.9772	1612.72	1799.33	186.61	83.399	557.74
0.2419	0.0569	1.2714	1718.84	0.9864	19.260	536.97	1.0000	1622.64	1799.33	176.69	83.785	570.32
0.3056	0.0719	1.2773	1725.04	0.9900	18.960	530.48	0.9885	1631.45	1799.33	167.88	84.124	563.44
0.3480	0.0820	1.2832	1731.22	0.9935	18.810	528.20	0.9845	1638.76	1799.33	160.57	84.403	560.87
0.3904	0.0919	1.2902	1738.52	0.9977	18.810	530.55	0.9886	1645.67	1799.33	153.66	84.665	562.99
0.4329	0.1019	1.2937	1742.38	1.0000	18.810	531.80	0.9908	1649.32	1799.33	150.01	84.803	564.12
0.4753	0.1120	1.2914	1740.10	0.9986	18.810	531.06	0.9895	1647.16	1799.33	152.17	84.721	563.45
0.5178	0.1219	1.2832	1731.65	0.9938	18.810	528.34	0.9847	1639.17	1799.33	160.16	84.419	561.00
0.5602	0.1319	1.2703	1718.12	0.9860	18.810	523.98	0.9770	1626.35	1799.33	172.97	83.928	557.10
0.6027	0.1419	1.2562	1704.17	0.9780	18.810	519.48	0.9691	1613.16	1799.33	186.17	83.416	553.13
0.6451	0.1519	1.2363	1683.78	0.9663	18.110	523.39	0.9231	1600.37	1799.33	198.96	82.913	527.42
0.6876	0.1620	1.2117	1657.54	0.9513	15.910	454.38	0.8014	1594.05	1799.33	205.28	82.661	458.13
0.7300	0.1719	1.1835	1627.71	0.9341	13.110	369.20	0.6511	1585.28	1799.33	214.05	82.310	372.55
0.7724	0.1819	1.1519	1593.31	0.9144	10.810	298.83	0.5270	1565.03	1799.33	234.30	81.485	302.16
0.8149	0.1920	1.1214	1559.61	0.8951	8.360	226.76	0.3999	1543.03	1799.33	256.29	80.569	229.86
0.8573	0.2019	1.0992	1534.73	0.8808	6.760	180.66	0.3186	1524.06	1799.33	275.27	79.761	183.58
0.8998	0.2119	1.0804	1513.45	0.8686	5.810	153.21	0.2702	1505.67	1799.33	293.65	78.963	156.09
0.9422	0.2220	1.0464	1474.28	0.8461	4.910	126.19	0.2225	1468.87	1799.33	330.46	77.320	129.34
0.9741	0.2294	0.9570	1367.76	0.7849	4.810	114.69	0.2022	1362.94	1799.33	436.38	72.245	120.43
0.9910	0.2334	0.6535	973.18	0.5585	4.810	81.60	0.1439	969.76	1799.33	829.57	49.454	107.39

MASS AVERAGE TOTAL PRESSURE 121.325
MASS AVERAGE TOTAL TEMPERATURE 1010.599
MASS AVG VM 490.723 VU 1590.881 ANGLE 17.142
FLOW FACTOR 0.834 SLIP FACTOR INS. STA. 0.884 IMPELLER TIP 0.926
IMP. PRESS. RATIO 5.028 IMP. TEMP.RATIO 1.610 EFFICIENCY 0.950
IMP.-IND. PRESS. RATIO 8.256 IMP.IND. TEMP. RATIO 1.948 EFFICIENCY 0.859
IMP.-IND.-IGV PRESS. RATIO 8.256 IMP.-IND.-IGV TEMP. RATIO 1.948 EFFICIENCY 0.859

* * * DIFFUSER * * *

CD DIFFUSER THROAT FRONT 0.957 REAR 0.892
STATIC PRESSURE RISE COEFFICIENT IMPELLER EXIT/DIFFUSER EXIT 0.623
DIFFUSER THROAT FRONT/DIFFUSER EXIT 0.578 DIFFUSER THROAT REAR/DIFFUSER EXIT 0.572
DIFFUSER LOSSES TOTAL TO STATIC 0.238 TOTAL TO TOTAL 0.237
DIFFUSER LOSS COEFFICIENT 0.376

TABLE L.

10/1 CENTRIFUGAL COMPRESSOR, IND AND IMP TRAV 8/1 LINE, WIDE OPEN DISCHARGE,
RUN 3.09 IGV TURNING=10 DEG
FLOW RATE = 2.898 SPEED = 61877.0

* * * INLET GUIDE VANE EXIT * * *

	MO	VO	ALPHA	VM	VU	U	WU	B	WO	MREL	I	VO/VOMAX
10	0.451	493.938	80.450	487.092	81.949	918.697	836.748	30.204	968.198	0.884	0.695	1.000
30	0.448	491.040	79.450	482.739	89.907	1026.780	936.872	27.260	1053.930	0.962	3.639	0.994
50	0.442	485.241	79.600	477.269	87.596	1134.862	1047.265	24.500	1150.892	1.050	6.059	0.982
70	0.434	476.533	78.850	467.538	92.152	1242.944	1150.791	22.110	1242.141	1.133	7.559	0.964
90	0.432	473.721	78.620	464.407	93.473	1351.026	1257.553	20.268	1340.565	1.222	7.881	0.959

* * * INDUCER EXIT * * * INITIAL INTEGRATED FLOW 2.879

MASS AVERAGE TOTAL PRESSURE 23.133
MASS AVERAGE TOTAL TEMPERATURE 605.739
INDUCER PRESSURE RATIO 1.574
INDUCER TEMPERATURE RATIO 1.167
INDUCER EFFICIENCY 0.826

INDUCER EXIT VELOCITY TRIANGLES

	MO	VO	ALPHA	VM	VU	U	WU	B	WO	MREL	I	VO/VOMAX
10	0.797	893.467	42.474	603.320	659.005	979.061	320.056	62.054	682.958	0.609	-8.354	1.000
30	0.782	883.420	42.972	602.182	646.380	1056.556	410.175	55.739	728.607	0.644	-6.339	0.988
50	0.741	846.064	43.720	584.841	611.379	1134.051	522.671	48.212	784.363	0.686	-3.182	0.946
70	0.735	847.143	45.567	604.926	593.056	1211.546	618.489	44.364	865.138	0.751	-4.164	0.948
90	0.661	780.083	39.170	492.722	604.776	1289.041	684.264	35.756	843.204	0.715	-0.106	0.873

TABLE L. (Continued)

* * * IMPELLER EXIT * * * INITIAL INTEGRATED FLOW 2.034

PCENT SPAN	R	MO	VO	VO/VMAX	ALP	VM	VM/VMMAX	VU	U	WU	B	WO
0.0169	0.0040	0.6343	962.17	0.5242	2.192	36.81	0.0558	961.46	1902.24	940.77	45.623	51.50
0.0551	0.0130	1.0195	1466.70	0.7992	10.192	259.54	0.3938	1443.55	1902.24	458.68	72.372	272.33
0.0976	0.0230	1.2351	1711.63	0.9326	18.692	548.56	0.8324	1621.34	1902.24	280.89	80.171	556.73
0.1400	0.0329	1.3265	1806.67	0.9844	21.392	658.99	1.0000	1682.20	1902.24	220.04	82.547	664.61
0.1825	0.0429	1.3419	1823.62	0.9936	20.892	650.33	0.9868	1703.71	1902.24	198.52	83.353	654.73
0.2249	0.0529	1.3476	1828.17	0.9961	19.792	619.05	0.9393	1720.17	1902.24	182.07	83.958	622.50
0.2674	0.0629	1.3488	1829.76	0.9970	18.792	589.44	0.8944	1732.22	1902.24	170.02	84.394	592.28
0.3098	0.0729	1.3499	1831.35	0.9978	18.192	571.77	0.8676	1739.81	1902.24	162.43	84.666	574.25
0.3522	0.0829	1.3511	1832.03	0.9982	17.992	565.90	0.8587	1742.44	1902.24	159.80	84.760	568.28
0.3947	0.0929	1.3535	1834.75	0.9997	18.092	569.79	0.8646	1744.04	1902.24	158.20	84.816	572.13
0.4371	0.1030	1.3535	1835.21	1.0000	18.392	579.05	0.8786	1741.46	1902.24	160.77	84.725	581.52
0.4796	0.1129	1.3476	1829.08	0.9966	18.592	583.17	0.8849	1733.61	1902.24	168.62	84.444	585.93
0.5220	0.1229	1.3371	1818.80	0.9910	18.392	573.88	0.8708	1725.89	1902.24	176.35	84.165	576.86
0.5645	0.1329	1.3207	1802.66	0.9822	17.892	553.84	0.8404	1715.48	1902.24	186.76	83.786	557.11
0.6069	0.1429	1.2972	1778.44	0.9690	17.192	525.68	0.7977	1698.98	1902.24	203.26	83.177	529.43
0.6494	0.1529	1.2726	1753.55	0.9555	16.092	486.07	0.7375	1684.84	1902.24	217.40	82.647	490.09
0.6918	0.1629	1.2445	1723.80	0.9392	14.592	434.30	0.6590	1668.20	1902.24	234.04	82.013	438.55
0.7342	0.1729	1.2164	1693.59	0.9228	12.892	377.88	0.5734	1650.90	1902.24	251.34	81.343	382.23
0.7767	0.1829	1.1882	1662.93	0.9061	10.992	317.09	0.4811	1632.42	1902.24	269.82	80.614	321.39
0.8191	0.1929	1.1578	1629.26	0.8877	8.792	249.04	0.3779	1610.11	1902.24	292.13	79.716	253.11
0.8616	0.2029	1.1273	1595.06	0.8691	6.592	183.12	0.2778	1584.51	1902.24	317.73	78.661	186.77
0.9040	0.2129	1.1308	1599.31	0.8714	4.592	128.05	0.1943	1594.17	1902.24	308.06	79.062	130.42
0.9465	0.2229	0.9884	1431.88	0.7802	2.692	67.26	0.1020	1430.30	1902.24	471.93	71.739	70.83
0.9825	0.2314	0.5742	878.12	0.4784	1.392	21.34	0.0323	877.86	1902.24	1024.37	40.595	32.79

MASS AVERAGE TOTAL PRESSURE 143.471
MASS AVERAGE TOTAL TEMPERATURE 1049.316
MASS AVG VM 527.176 VU 1690.640 ANGLE 17.318
FLOW FACTOR 0.809 SLIP FACTOR INS. STA. 0.888 IMPELLER TIP 0.931
IMP. PRESS. RATIO 6.201 IMP. TEMP.RATIO 1.732 EFFICIENCY 0.924
IMP.-IND. PRESS. RATIO 9.797 IMP.-IND. TEMP. RATIO 2.022 EFFICIENCY 0.883
IMP.-IND.-IGV PRESS. RATIO 9.763 IMP.-IND.-IGV TEMP. RATIO 2.022 EFFICIENCY 0.881

* * * DIFFUSER * * *

CD DIFFUSER THROAT FRONT 0.889 REAR 0.889
STATIC PRESSURE RISE COEFFICIENT IMPELLER EXIT/DIFFUSER EXIT 0.120
DIFFUSER THROAT FRONT/DIFFUSER EXIT 0.012 DIFFUSER THROAT REAR/DIFFUSER EXIT 0.013
DIFFUSER LOSSES TOTAL TO STATIC 0.591 TOTAL TO TOTAL 0.503
DIFFUSER LOSS COEFFICIENT 0.879

TABLE LI.

10/1 CENTRIFUGAL COMPRESSOR, INDUCER TRAVERSE 8/1 LINE, BELOW NEAR STALL, RUN 3.09
IGV TURNING=10 DEG
FLOW RATE = 2.902 SPEED = 61921.0

* * * INLET GUIDE VANE EXIT * * *

	MO	VO	ALPHA	VM	VU	U	WU	B	WO	MREL	I	VO/VOMAX
10	0.448	490.944	80.450	484.140	81.452	919.351	837.898	30.019	967.712	0.883	0.380	0.999
30	0.448	491.040	79.450	482.739	89.907	1027.510	937.602	27.242	1054.579	0.963	3.657	1.000
50	0.442	485.241	79.600	477.269	87.596	1135.668	1048.072	24.483	1151.626	1.051	6.076	0.988
70	0.437	479.530	78.850	470.479	92.731	1243.827	1151.096	22.230	1243.532	1.134	7.439	0.976
90	0.432	473.721	78.620	464.407	93.473	1351.987	1258.513	20.254	1341.466	1.223	7.895	0.964

* * * INDUCER EXIT * * * INITIAL INTEGRATED FLOW 2.894

MASS AVERAGE TOTAL PRESSURE 23.268
MASS AVERAGE TOTAL TEMPERATURE 604.322
INDUCER PRESSURE RATIO 1.583
INDUCER TEMPERATURE RATIO 1.165
INDUCER EFFICIENCY 0.851

INDUCER EXIT VELOCITY TRIANGLES

	MO	VO	ALPHA	VM	VU	U	WU	B	WO	MREL	I	VO/VOMAX
10	0.803	899.789	41.807	599.828	670.691	979.757	309.066	62.739	674.771	0.602	-9.039	1.000
30	0.782	880.994	42.579	596.091	648.711	1057.307	408.596	55.570	722.686	0.641	-6.170	0.975
50	0.746	850.630	42.888	578.920	623.235	1134.857	511.622	48.531	772.597	0.678	-3.501	0.945
70	0.731	843.454	44.549	591.707	601.079	1212.407	611.327	41.80	850.787	0.737	-3.865	0.937
90	0.657	775.248	38.240	479.854	608.892	1289.957	681.065	35.167	833.132	0.706	0.482	0.861

TABLE LII.

10/1 CENTRIFUGAL COMPRESSOR, IMPELLER TRAVERSE
8/1 LINE, BELOW NEAR STALL, RUN 3.09
IGV TURNING=10 DEG

FLOW RATE = 2.902 SPEED = 61904.0

* * * IMPELLER EXIT * * * INITIAL INTEGRATED FLOW 2.002

PCENT SPAN	R	MO	VO	VO/VMAX	ALP	VM	VM/VMMAX	VU	U	WU	B	WO
0.0169	0.0040	0.6480	981.95	0.5349	4.299	73.61	0.1111	979.19	1903.07	923.87	46.665	101.20
0.0551	0.0130	1.0453	1498.21	0.8161	11.899	308.92	0.4666	1466.02	1903.07	437.05	73.399	322.35
0.0976	0.0230	1.2421	1719.74	0.9368	19.199	565.54	0.8542	1624.09	1903.07	278.97	80.293	573.83
0.1400	0.0329	1.3253	1806.41	0.9840	21.499	662.03	1.0000	1680.72	1903.07	222.35	82.463	667.80
0.1825	0.0429	1.3476	1828.62	0.9961	21.099	658.28	0.9943	1706.03	1903.07	197.04	83.411	662.65
0.2249	0.0529	1.3488	1830.21	0.9970	19.899	622.94	0.9409	1720.93	1903.07	182.13	83.958	626.42
0.2674	0.0629	1.3476	1829.53	0.9966	18.999	595.61	0.8996	1729.86	1903.07	173.21	84.282	598.59
0.3098	0.0729	1.3476	1829.53	0.9966	18.399	577.47	0.8722	1736.00	1903.07	167.06	84.503	580.13
0.3522	0.0829	1.3499	1831.80	0.9978	18.199	572.11	0.8641	1740.17	1903.07	162.90	84.652	574.61
0.3947	0.0929	1.3535	1835.66	1.0000	18.299	576.36	0.8706	1742.83	1903.07	160.23	84.747	578.79
0.4371	0.1030	1.3535	1835.66	1.0000	18.599	585.48	0.8843	1739.79	1903.07	163.27	84.638	588.05
0.4796	0.1129	1.3499	1832.26	0.9981	18.799	590.45	0.8918	1734.51	1903.07	168.55	84.449	593.23
0.5220	0.1229	1.3406	1823.13	0.9931	18.699	584.50	0.8828	1726.90	1903.07	176.17	84.175	587.53
0.5645	0.1329	1.3253	1807.73	0.9847	18.199	564.60	0.8528	1717.30	1903.07	185.76	83.826	567.89
0.6069	0.1429	1.3019	1784.01	0.9718	17.299	530.50	0.8013	1703.31	1903.07	199.76	83.310	534.13
0.6494	0.1529	1.2679	1749.18	0.9528	15.999	482.12	0.7282	1681.43	1903.07	221.64	82.490	486.29
0.6918	0.1629	1.2281	1706.71	0.9297	14.399	424.42	0.6410	1653.09	1903.07	249.97	81.401	429.24
0.7342	0.1729	1.1953	1671.61	0.9106	12.599	364.63	0.5507	1631.35	1903.07	271.71	80.543	369.65
0.7767	0.1829	1.1636	1636.38	0.8914	10.299	292.57	0.4419	1610.01	1903.07	293.05	79.683	297.37
0.8191	0.1929	1.1355	1605.21	0.8744	7.799	217.83	0.3290	1590.36	1903.07	312.70	78.876	222.00
0.8616	0.2029	1.1097	1575.85	0.8584	5.299	145.54	0.2198	1569.11	1903.07	333.95	77.984	148.80
0.9040	0.2129	1.0804	1541.79	0.8399	3.399	91.42	0.1380	1539.07	1903.07	363.99	76.693	93.94
0.9465	0.2229	0.9570	1393.74	0.7592	2.399	58.34	0.0881	1392.51	1903.07	510.55	69.865	62.14
0.9825	0.2314	0.6343	964.40	0.5253	1.899	31.96	0.0482	963.86	1903.07	939.20	45.742	44.62

MASS AVERAGE TOTAL PRESSURE 143.401
MASS AVERAGE TOTAL TEMPERATURE 1050.140
MASS AVG VM 533.751 VU 1686.440 ANGLE 17.562
FLOW FACTOR 0.800 SLIP FACTOR INS. STA. 0.886 IMPELLER TIP 0.928
IMP. PRESS. RATIO 0.000 IMP. TEMP.RATIO 0.000 EFFICIENCY 0.000
IMP..IND. PRESS. RATIO 9.793 IMP.IND. TEMP. RATIO 2.024 EFFICIENCY 0.881
IMP..IND..IGV PRESS. RATIO 9.759 IMP..IND..IGV TEMP. RATIO 2.024 EFFICIENCY 0.880

* * * DIFFUSER * * *

CD DIFFUSER THROAT FRONT 0.891 REAR 0.890
STATIC PRESSURE RISE COEFFICIENT IMPELLER EXIT/DIFFUSER EXIT 0.553
DIFFUSER THROAT FRONT/DIFFUSER EXIT 0.498 DIFFUSER THROAT REAR/DIFFUSER EXIT 0.497
DIFFUSER LOSSES TOTAL TO STATIC 0.300 TOTAL TO TOTAL 0.253
DIFFUSER LOSS COEFFICIENT 0.446

TABLE LIII.

10/1 CENTRIFUGAL COMPRESSOR, INDUCER T 8/1 LINE, NEAR STALL.
RUN 3.09 IGV TURNING=10 DEG
FLOW RATE = 2.818 SPEED = 62035.0

* * * INLET GUIDE VANE EXIT * * *

	MD	VD	ALPHA	VM	VU	U	WU	B	WD	MREL	I	VD/VDMAX
10	0.432	473.721	80.450	467.155	78.594	921.043	842.448	29.009	963.304	0.878	1.890	1.000
30	0.432	473.721	79.450	465.712	86.736	1029.401	942.665	26.291	1051.431	0.958	4.608	1.000
50	0.423	464.997	79.600	457.357	83.941	1137.760	1053.818	23.460	1148.786	1.047	7.099	0.981
70	0.415	456.351	78.850	447.737	88.249	1246.117	1157.868	21.141	1241.422	1.130	8.528	0.963
90	0.410	450.521	78.620	441.664	88.895	1354.476	1265.580	19.238	1340.433	1.220	8.911	0.951

* * * INDUCER EXIT * * * INITIAL INTEGRATED FLOW 2.823

MASS AVERAGE TOTAL PRESSURE 24.553
MASS AVERAGE TOTAL TEMPERATURE 614.449
INDUCER PRESSURE RATIO 1.670
INDUCER TEMPERATURE RATIO 1.184
INDUCER EFFICIENCY 0.856

INDUCER EXIT VELOCITY TRIANGLES

	MD	VD	ALPHA	VM	VU	U	WU	B	WD	MREL	I	VD/VDMAX
10	0.765	865.835	38.641	540.666	676.276	981.561	305.284	60.549	620.902	0.549	-6.849	1.000
30	0.724	827.332	38.982	520.465	643.112	1059.254	416.141	51.355	666.376	0.583	-1.955	0.955
50	0.716	825.388	40.639	537.568	626.327	1136.947	510.619	46.472	741.426	0.643	-1.442	0.953
70	0.705	823.548	39.296	521.578	637.329	1214.639	577.310	42.096	778.030	0.666	-1.896	0.951
90	0.675	803.224	37.251	486.200	639.358	1292.332	652.974	36.671	814.104	0.684	-1.021	0.927

TABLE LIV.

10/1 CENTRIFUGAL COMPRESSOR, IMPELLER TRAV 8/1 LINE, NEAR STALL.

RUN 3.09 IGV TURNING=10 DEG

FLOW RATE = 2.895 SPEED = 62126.0

* * * IMPELLER EXIT * * * INITIAL INTEGRATED FLOW 2.040

PCENT SPAN	R	MO	VO	VO/VMAX	ALP	VM	VM/VMMAX	VU	U	WU	B	WO
0.0169	0.0040	0.6535	979.43	0.5311	4.841	82.66	0.1262	975.94	1909.89	933.95	46.259	114.41
0.0551	0.0130	1.0558	1495.26	0.8108	12.091	313.22	0.4782	1462.09	1909.89	447.80	72.971	327.58
0.0976	0.0230	1.2856	1727.06	0.9366	18.641	552.05	0.8428	1636.46	1909.89	273.43	80.514	559.70
0.1400	0.0329	1.3335	1796.94	0.9744	20.891	640.79	0.9783	1678.81	1909.89	231.08	82.162	646.83
0.1825	0.0429	1.3558	1820.04	0.9870	21.091	654.95	1.0000	1698.11	1909.89	211.78	82.890	660.03
0.2249	0.0529	1.3593	1823.83	0.9890	19.991	623.53	0.9520	1713.93	1909.89	195.96	83.477	627.59
0.2674	0.0629	1.3593	1824.76	0.9895	18.991	593.83	0.9066	1725.43	1909.89	184.46	83.897	597.21
0.3098	0.0729	1.3640	1830.12	0.9924	18.741	572.67	0.8746	1738.15	1909.89	171.74	84.357	575.66
0.3522	0.0829	1.3699	1836.58	0.9959	17.841	562.70	0.8591	1748.26	1909.89	161.63	84.717	565.10
0.3947	0.0929	1.3746	1841.93	0.9988	17.941	567.40	0.8663	1752.36	1909.89	157.53	84.863	569.69
0.4371	0.1030	1.3757	1843.97	1.0000	18.241	577.20	0.8812	1751.30	1909.89	158.59	84.825	579.57
0.4796	0.1129	1.3734	1842.23	0.9990	18.391	581.24	0.8874	1748.14	1909.89	161.75	84.713	583.72
0.5220	0.1229	1.3675	1837.63	0.9965	18.241	575.22	0.8782	1745.28	1909.89	164.61	84.611	577.77
0.5645	0.1329	1.3535	1826.25	0.9893	17.841	558.92	0.8533	1736.51	1909.89	173.38	84.298	561.70
0.6069	0.1429	1.3389	1800.50	0.9764	17.241	533.67	0.8148	1719.59	1909.89	190.30	83.684	536.92
0.6494	0.1529	1.3007	1772.87	0.9614	16.341	498.82	0.7616	1701.24	1909.89	208.65	83.007	502.55
0.6918	0.1629	1.2726	1744.71	0.9461	14.941	449.84	0.6868	1685.72	1909.89	224.17	82.424	453.80
0.7342	0.1729	1.2457	1716.82	0.9310	12.941	384.49	0.5870	1673.22	1909.89	236.67	81.948	388.32
0.7767	0.1829	1.2210	1691.34	0.9172	10.591	310.88	0.4746	1662.52	1909.89	247.37	81.537	314.30
0.8191	0.1929	1.1953	1664.23	0.9025	8.241	238.56	0.3642	1647.04	1909.89	262.85	80.932	241.58
0.8616	0.2029	1.1718	1639.59	0.8891	5.991	171.14	0.2613	1630.63	1909.89	279.26	80.281	173.63
0.9040	0.2129	1.1497	1608.73	0.8724	4.241	118.98	0.1816	1604.33	1909.89	305.56	79.216	121.12
0.9465	0.2229	0.9748	1410.87	0.7651	3.291	81.00	0.1236	1408.54	1909.89	501.35	72.407	85.98
0.9825	0.2314	0.5988	910.88	0.4939	2.841	45.15	0.0689	909.76	1909.89	1000.13	62.290	67.10

MASS AVERAGE TOTAL PRESSURE 143.537
MASS AVERAGE TOTAL TEMPERATURE 1049.316
MASS AVG VM 528.091 VU 1696.397 ANGLE 17.291
FLOW FACTOR 0.817 SLIP FACTOR INS. STA. 0.888 IMPELLER TIP 0.931
IMP. PRESS. RATIO 0.000 IMP. TEMP.RATIO 0.000 EFFICIENCY 0.000
IMP.+IND. PRESS. RATIO 9.892 IMP.IND. TEMP. RATIO 2.022 EFFICIENCY 0.883
IMP.+IND.+IGV PRESS. RATIO 9.768 IMP.+IND.+IGV TEMP. RATIO 2.022 EFFICIENCY 0.882

* * * DIFFUSER * * *

CD DIFFUSER THROAT FRONT 0.889 REAR 0.888
STATIC PRESSURE RISE COEFFICIENT IMPELLER EXIT/DIFFUSER EXIT 0.567
DIFFUSER THROAT FRONT/DIFFUSER EXIT 0.513 DIFFUSER THROAT REAR/DIFFUSER EXIT 0.512
DIFFUSER LOSSES TOTAL TO STATIC 0.290 TOTAL TO TOTAL 0.245
DIFFUSER LOSS COEFFICIENT 0.432

TABLE LV.

10/1 CENTRIFUGAL COMPRESSOR, IND AND IMP TRAV
70 PCT SPEED, NEAR STALL, 20 DEG IGV TURNING
BUILD 6

FLOW RATE = 1.279 SPEED = 45948.9

* * * INDUCER EXIT * * * INITIAL INTEGRATED FLOW 0.926

MASS AVERAGE TOTAL PRESSURE 18.603
MASS AVERAGE TOTAL TEMPERATURE 573.003
INDUCER PRESSURE RATIO 1.266
INDUCER TEMPERATURE RATIO 1.104
INDUCER EFFICIENCY 0.667

INDUCER EXIT VELOCITY TRIANGLES

	MD	WD	ALPHA	VM	VU	U	WU	B	WD	MREL	I	VD/VDMAX
10	0.382	630.690	35.283	358.950	248.701	720.667	471.965	37.254	592.956	0.519	16.445	0.720
30	0.380	613.962	31.558	324.219	257.351	777.633	520.281	31.929	613.034	0.534	17.470	0.683
50	0.364	588.671	41.448	263.769	298.672	834.599	535.926	26.205	597.320	0.516	18.824	0.657
70	0.415	683.032	25.801	210.242	434.877	891.565	456.687	24.719	502.758	0.432	15.480	0.797
90	0.519	805.971	18.616	193.443	574.265	948.531	374.266	27.332	421.302	0.361	8.317	1.000

TABLE LV. (Continued)

* * * IMPELLER EXIT * * * INITIAL INTEGRATED FLOW 1.309

STEAM LINE	R	MD	VD	VD/VMAX	ALP	VM	VM/VMAX	VU	U	WJ	B	BD
1.0000	0.0000	1.0000	779.00	0.1856	9.168	124.26	0.2690	769.96	1400.28	630.29	50.696	160.61
0.9867	0.0200	0.7574	1014.47	0.7528	12.668	219.79	0.5111	977.77	1400.28	422.50	60.630	239.43
0.9667	0.0400	0.9146	1182.91	0.8866	17.168	349.19	0.8120	1130.22	1400.28	270.05	76.561	359.02
0.9466	0.0600	0.9889	1285.76	0.9659	16.918	416.88	0.9694	1216.32	1400.28	183.96	81.399	421.62
0.9265	0.0799	1.0476	1326.31	0.9784	18.918	430.03	1.0000	1254.66	1400.28	145.61	83.380	432.91
0.9064	0.1000	1.0528	1331.10	1.0000	18.168	415.06	0.9651	1264.73	1400.28	135.54	83.882	417.44
0.8863	0.1199	1.0417	1325.41	0.9919	16.918	384.26	0.8935	1263.26	1400.28	137.01	83.809	386.51
0.8662	0.1399	1.0101	1297.17	0.9670	15.418	342.25	0.7958	1240.94	1400.28	159.33	82.683	345.06
0.8461	0.1599	0.9570	1229.90	0.9239	13.418	285.42	0.6637	1196.32	1400.28	203.95	80.325	289.54
0.8260	0.1800	0.8814	1157.81	0.8696	10.168	204.37	0.4752	1139.43	1400.28	260.84	77.105	209.66
0.8059	0.1999	0.8189	1071.74	0.8076	5.918	110.82	0.2577	1069.01	1400.28	331.26	72.783	116.02
0.7858	0.2150	0.7800	1002.77	0.7285	2.918	49.38	0.1148	988.51	1400.28	431.76	65.972	54.08
0.7750	0.2249	0.7085	892.49	0.5202	0.918	11.10	0.0258	692.40	1400.28	707.87	44.367	15.88

MASS AVERAGE TOTAL PRESSURE 57.488
MASS AVERAGE TOTAL TEMPERATURE 814.000
MASS AVG VM 344.648 VU 1181.258 ANGLE 16.135
FLOW FACTOR 0.787 SLIP FACTOR INS. STA. 0.850 IMPELLER TIP 0.891
IMP. PRESS. RATIO 5.085 IMP. TEMP.RATIO 1.421 EFFICIENCY 0.892
IMP.+IND. PRESS. RATIO 3.910 IMP.+IND. TEMP. RATIO 1.570 EFFICIENCY 0.825
IMP.+IND.+IGV PRESS. RATIO 3.910 IMP.+IND.+IGV TEMP. RATIO 1.570 EFFICIENCY 0.825

* * * DIFFUSER * * *

CD DIFFUSER THROAT FRONT 0.785 REAR 0.788
STATIC PRESSURE RISE COEFFICIENT IMPELLER EXIT/DIFFUSER EXIT 0.618
DIFFUSER THROAT FRONT/DIFFUSER EXIT 0.614 DIFFUSER THROAT REAR/DIFFUSER EXIT 0.621
DIFFUSER LOSSES TOTAL TO STATIC 0.164 TOTAL TO TOTAL 0.101
DIFFUSER LOSS COEFFICIENT 0.281

TABLE LVI.

10/1 CENTRIFUGAL COMPRESSOR, IND AND IMP TRAV
TO PCT SPEED, NEAR STALL, 90 DEG IGV TURNING
BUILD 6

FLOW RATE = 1.242 SPEED = 45528.7

* * * INDUCER EXIT * * * INITIAL INTEGRATED FLOW 0.869

MASS AVERAGE TOTAL PRESSURE 18.462
MASS AVERAGE TOTAL TEMPERATURE 570.390
INDUCER PRESSURE RATIO 1.256
INDUCER TEMPERATURE RATIO 1.099
INDUCER EFFICIENCY 0.877

INDUCER EXIT VELOCITY TRIANGLES

%D	VD	ALPHA	VM	VU	U	WU	B	MO	MREL	I	VD/VDMAX
10	0.880	632.481	51.768	339.721	267.437	720.348	452.710	36.885	566.001	0.497	16.814	0.684
30	0.869	600.544	48.427	289.655	265.787	777.289	511.502	30.363	592.813	0.518	19.236	0.634
50	0.850	619.668	38.592	259.305	324.908	834.229	509.320	26.981	571.530	0.496	18.048	0.698
70	0.832	600.018	25.485	215.149	454.363	891.170	439.806	26.067	489.611	0.423	14.132	0.791
90	0.844	631.519	18.717	202.656	598.119	948.111	349.991	30.071	404.429	0.348	9.578	1.000

TABLE LVI. (Continued)

* * * IMPELLER EXIT * * * INITIAL INTEGRATED FLOW 1.387

PERCENT SPAN	R	RHO	VO	VO/VMAX	ALP	VM	VM/VMAX	VU	U	MU	B	MO
0.0833	0.0055	0.7123	945.42	0.7070	10.406	170.76	0.4106	929.87	1399.66	469.78	63.196	191.32
0.0848	0.0200	0.6634	1124.20	0.8411	12.906	251.23	0.6041	1096.38	1399.66	303.27	74.537	260.66
0.1297	0.0400	0.9781	1247.13	0.9328	16.406	352.24	0.8470	1196.35	1399.66	203.30	80.355	357.29
0.1346	0.0600	1.0359	1310.35	0.9799	18.406	413.74	0.9949	1243.11	1399.66	156.34	82.832	417.00
0.1395	0.0799	1.0593	1334.57	0.9980	18.156	415.86	1.0000	1268.13	1399.66	131.52	84.078	418.09
0.1444	0.1000	1.0817	1337.14	1.0000	17.156	394.42	0.9484	1277.64	1399.66	122.01	84.544	396.22
0.1893	0.1199	1.0693	1320.50	0.9874	15.906	361.84	0.8701	1269.75	1399.66	129.91	84.158	363.73
0.1942	0.1399	1.0078	1281.37	0.9582	14.406	318.79	0.7665	1241.07	1399.66	158.58	82.716	321.39
0.1991	0.1599	0.9515	1220.82	0.9130	12.156	257.07	0.6181	1193.45	1399.66	206.20	80.197	260.88
0.2440	0.1800	0.8814	1134.46	0.8483	9.156	183.70	0.4417	1119.75	1399.66	279.90	77.153	188.42
0.2488	0.1999	0.8353	1090.71	0.8157	5.406	102.76	0.2471	1085.86	1399.66	313.79	73.881	106.96
0.2938	0.2190	0.7804	1003.15	0.7502	2.156	37.74	0.0907	1002.44	1399.66	397.21	66.384	40.59
0.2990	0.2249	0.8382	877.23	0.6561	-0.343	-5.26	-0.0126	877.92	1399.66	522.33	59.231	-6.12

MASS AVERAGE TOTAL PRESSURE 0.000
MASS AVERAGE TOTAL TEMPERATURE 859.000
MASS AVG VM 333.086 MU 1214.361 ANGLE 15.379
FLOW FACTOR 0.795 SLIP FACTOR INS. STA. 0.867 IMPELLER TIP 0.909
IMP. PRESS. RATIO 2.149 IMP. TEMP. RATIO 1.421 EFFICIENCY 0.911
IMP.+IND. PRESS. RATIO 3.991 IMP.+IND. TEMP. RATIO 1.562 EFFICIENCY 0.845
IMP.+IND.+IGV PRESS. RATIO 3.991 IMP.+IND.+IGV TEMP. RATIO 1.562 EFFICIENCY 0.845

* * * DIFFUSER * * *

CD DIFFUSER THROAT FRONT 0.760 REAR 0.760
STATIC PRESSURE RISE COEFFICIENT IMPELLER EXIT/DIFFUSER EXIT 0.654
DIFFUSER THROAT FRONT/DIFFUSER EXIT 0.977 DIFFUSER THROAT REAR/DIFFUSER EXIT 0.581
DIFFUSER LOSSES TOTAL TO STATIC 0.160 TOTAL TO TOTAL 0.139
DIFFUSER LOSS COEFFICIENT 0.205

TABLE LVII.

10/1 CENTRIFUGAL COMPRESSOR, END AND IMP TRAV
85 PCT SPEED, NEAR STALL, 20 DEG IGV TURNING
BUILD 5

FLOW RATE = 2.125 SPEED = 55063.1

* * * INLET GUIDE VANE EXIT * * *

	MD	VD	ALPHA	VM	VU	U	WU	B	WD	MREL	I	VD/VDMAX
HD	0.908	339.694	68.148	311.761	125.020	826.868	701.848	23.950	767.975	0.693	8.969	0.991
MD	0.906	328.858	68.482	319.199	124.400	924.918	800.117	21.901	859.982	0.777	9.398	1.000
LD	0.906	336.781	69.291	317.110	119.251	1021.979	902.728	19.355	956.806	0.864	11.204	0.999
TD	0.906	338.858	70.475	319.367	[illegible]	1119.716	1006.495	17.805	1055.911	0.954	12.084	1.000
PD	0.278	309.013	76.578	298.227	81.661	1216.261	1134.599	14.717	1173.089	1.058	13.432	0.911

* * * INDUCER EXIT * * * INITIAL INTEGRATED FLOW 1.687

MASS AVERAGE TOTAL PRESSURE 21.209
MASS AVERAGE TOTAL TEMPERATURE 989.548
INDUCER PRESSURE RATIO 1.443
INDUCER TEMPERATURE RATIO 1.136
INDUCER EFFICIENCY 0.811

INDUCER EXIT VELOCITY TRIANGLES

	MD	VD	ALPHA	VM	VU	U	WU	B	WD	MREL	I	VD/VDMAX
LO	0.582	598.410	80.978	463.344	375.921	880.692	909.170	42.527	689.482	0.600	11.172	0.887
MD	0.824	599.894	81.752	478.098	371.367	950.307	978.980	39.134	748.406	0.653	10.265	0.892
MD	0.836	595.413	80.838	481.663	376.010	1019.923	649.912	35.639	792.311	0.687	9.390	0.886
TD	0.914	600.412	81.124	384.985	492.214	1089.538	637.324	31.787	769.786	0.641	8.412	0.893
PD	0.567	672.987	86.727	302.227	600.199	1159.153	558.954	28.400	635.430	0.536	7.249	1.000

TABLE LVII. (Continued)

* * * IMPELLER EXIT * * * INITIAL INTEGRATED FLOW 1.985

PCENT SPAN	R	MO	VO	VO/VM	ALP	VM	VM/VMMAX	VU	U	WU	B	WO
0.0233	0.0054	0.9078	1269.65	0.7757	8.507	187.82	0.3377	1255.57	1711.21	455.63	70.054	199.80
0.0636	0.0149	1.0382	1422.02	0.8689	13.007	320.07	0.5754	1385.53	1711.21	325.68	76.772	328.79
0.1273	0.0300	1.1343	1528.12	0.9337	17.007	446.97	0.8036	1461.29	1711.21	249.92	80.294	453.47
0.2122	0.0500	1.1929	1590.38	0.9718	19.757	537.61	0.9666	1496.75	1711.21	214.46	81.846	543.11
0.2971	0.0699	1.2269	1625.54	0.9932	20.007	556.17	1.0000	1527.43	1711.21	183.77	83.139	560.18
0.3820	0.0899	1.2374	1636.52	1.0000	19.507	546.49	0.9825	1542.58	1711.21	168.63	83.761	549.74
0.4668	0.1099	1.2351	1634.27	0.9986	19.007	532.27	0.9570	1545.16	1711.21	166.04	83.866	535.34
0.5517	0.1299	1.2152	1613.79	0.9861	18.007	498.89	0.8970	1534.74	1711.21	176.47	83.440	502.18
0.6366	0.1499	1.1730	1569.84	0.9592	15.757	426.32	0.7665	1510.84	1711.21	200.36	82.445	430.05
0.7215	0.1699	1.1132	1505.73	0.9200	12.007	313.26	0.5632	1472.78	1711.21	238.42	80.804	317.33
0.8064	0.1899	1.0523	1438.13	0.8787	8.007	200.34	0.3602	1424.10	1711.21	287.10	78.601	204.37
0.8913	0.2099	1.0054	1385.07	0.8463	4.757	114.88	0.2065	1380.20	1711.21	330.91	76.518	118.13
0.9550	0.2249	0.9624	1335.05	0.8157	2.757	64.23	0.1154	1333.51	1711.21	377.70	74.185	66.76

MASS AVERAGE TOTAL PRESSURE 96.838
MASS AVERAGE TOTAL TEMPERATURE 951.700
MASS AVG VM 459.504 VU 1497.800 ANGLE 17.055
FLOW FACTOR 0.815 SLIP FACTOR INS. STA. 0.875 IMPELLER TIP 0.917
IMP. PRESS. RATIO 4.565 IMP. TEMP.RATIO 1.614 EFFICIENCY 0.875
IMP.,IND. PRESS. RATIO 6.617 IMP,IND. TEMP. RATIO 1.834 EFFICIENCY 0.846
IMP.,IND.,IGV PRESS. RATIO 6.590 IMP.,IND.,IGV TEMP. RATIO 1.834 EFFICIENCY 0.844

* * * DIFFUSER * * *

CD DIFFUSER THROAT FRONT 0.862 REAR 0.862
STATIC PRESSURE RISE COEFFICIENT IMPELLER EXIT/DIFFUSER EXIT 0.742
DIFFUSER THROAT FRONT/DIFFUSER EXIT 0.684 DIFFUSER THROAT REAR/DIFFUSER EXIT 0.685
DIFFUSER LOSSES TOTAL TO STATIC 0.157 TOTAL TO TOTAL 0.109
DIFFUSER LOSS COEFFICIENT 0.257

TABLE LVIII.

10/1 CENTRIFUGAL COMPRESSOR, IND AND IMP TRAV
85 PCT SPEED, NEAR STALL, 30 DEG IGV TURNING
BUILD 6

FLOW RATE = 2.071 SPEED = 55505.1

* * * INLET GUIDE VANE EXIT * * *

	MO	VO	ALPHA	VM	VU	U	WU	B	WO	MREL	I	VO/VOMAX
10	0.352	389.096	56.112	323.000	216.948	824.635	607.686	27.991	688.195	0.623	2.908	0.992
30	0.355	392.036	57.618	331.075	209.956	921.275	711.319	24.959	784.593	0.711	5.940	1.000
50	0.344	380.266	60.334	330.425	188.206	1018.856	830.650	21.692	893.958	0.809	8.867	0.969
70	0.344	380.266	61.888	335.401	179.187	1116.587	937.400	19.667	995.597	0.902	9.982	0.969
90	0.322	356.600	69.726	334.507	123.565	1212.900	1089.334	17.070	1139.537	1.031	11.079	0.909

* * * INDUCER EXIT * * * INITIAL INTEGRATED FLOW 1.677

MASS AVERAGE TOTAL PRESSURE 21.018
MASS AVERAGE TOTAL TEMPERATURE 582.301
INDUCER PRESSURE RATIO 1.430
INDUCER TEMPERATURE RATIO 1.122
INDUCER EFFICIENCY 0.880

INDUCER EXIT VELOCITY TRIANGLES

	MO	VO	ALPHA	VM	VU	U	WU	B	WO	MREL	I	VO/VOMAX
10	0.481	549.178	37.670	335.614	434.695	878.193	443.498	37.116	556.172	0.487	16.583	0.789
30	0.511	581.828	46.027	418.724	403.973	947.610	543.637	37.604	686.200	0.603	11.795	0.836
50	0.552	629.403	48.446	471.003	417.498	1017.028	599.530	38.153	762.417	0.669	6.876	0.904
70	0.557	642.781	42.089	430.849	477.008	1086.446	609.438	35.258	746.355	0.647	4.941	0.923
90	0.596	695.748	29.660	344.295	604.587	1155.864	551.277	31.986	649.958	0.556	3.663	1.000

TABLE LVIII. (Continued)

* * * IMPELLER EXIT * * * INITIAL INTEGRATED FLOW 1.949

PCENT SPAN	R	MO	VO	VO/VMAX	ALP	VM	VM/VMMAX	VU	U	WU	B	WO
0.0636	0.0149	1.0722	1447.72	0.8868	17.420	433.43	0.8154	1381.32	1706.35	325.03	76.758	445.26
0.1273	0.0300	1.1988	1582.88	0.9696	18.670	506.73	0.9533	1499.58	1706.35	206.77	82.149	511.52
0.2122	0.0500	1.2234	1608.57	0.9853	19.295	531.54	1.0000	1518.21	1706.35	188.14	82.935	535.61
0.2971	0.0699	1.2374	1622.74	0.9940	19.045	529.53	0.9962	1533.90	1706.35	172.44	83.585	532.87
0.3820	0.0899	1.2468	1632.41	1.0000	18.920	529.32	0.9958	1544.21	1706.35	162.14	84.005	532.23
0.4668	0.1099	1.2457	1631.31	0.9993	18.420	515.48	0.9697	1547.73	1706.35	158.62	84.148	518.18
0.5517	0.1299	1.2234	1609.00	0.9856	17.170	475.01	0.8936	1537.28	1706.35	169.07	83.723	477.87
0.6366	0.1499	1.1789	1563.11	0.9575	15.170	409.06	0.7695	1508.63	1706.35	197.72	82.523	412.56
0.7215	0.1699	1.1203	1501.18	0.9196	11.920	310.08	0.5833	1468.81	1706.35	237.54	80.813	314.11
0.8064	0.1899	1.0570	1432.50	0.8775	7.920	197.40	0.3713	1418.83	1706.35	287.52	78.544	201.41
0.8913	0.2099	1.0031	1371.53	0.8401	4.920	117.64	0.2213	1366.48	1706.35	339.87	76.032	121.23
0.9550	0.2249	0.9296	1285.88	0.7877	3.420	76.72	0.1443	1283.59	1706.35	422.76	71.770	80.78

MASS AVERAGE TOTAL PRESSURE 96.112
MASS AVERAGE TOTAL TEMPERATURE 937.399
MASS AVG VM 460.575 VU 1506.133 ANGLE 17.003
FLOW FACTOR 0.801 SLIP FACTOR INS. STA. 0.882 IMPELLER TIP 0.925
IMP. PRESS. RATIO 4.572 IMP. TEMP.RATIO 1.609 EFFICIENCY 0.882
IMP.+IND. PRESS. RATIO 6.612 IMP.IND. TEMP. RATIO 1.807 EFFICIENCY 0.875
IMP.+IND.+IGV PRESS. RATIO 6.540 IMP.+IND.+IGV TEMP. RATIO 1.807 EFFICIENCY 0.869

* * * DIFFUSER * * *

CD DIFFUSER THROAT FRONT 0.845 REAR 0.850
STATIC PRESSURE RISE COEFFICIENT IMPELLER EXIT/DIFFUSER EXIT 0.727
DIFFUSER THROAT FRONT/DIFFUSER EXIT 0.643 DIFFUSER THROAT REAR/DIFFUSER EXIT 0.662
DIFFUSER LOSSES TOTAL TO STATIC 0.169 TOTAL TO TOTAL 0.121
DIFFUSER LOSS COEFFICIENT 0.272

TABLE LIX.

10/1 CENTRIFUGAL COMPRESSOR, INDUCER TRAVERSE
8/1 SPEEDLINE, WOD, 10 DEG IGV TURNING
BUILD 6

FLOW RATE = 2.823 SPEED = 61657.2

* * * INLET GUIDE VANE EXIT * * *

MD	VD	ALPHA	VM	VU	U	WU	B	WO	MREL	I	VO/VOMAX
10	0.437	479.530	78.057	469.151	99.228	915.792	816.504	29.881	941.691	0.859	1.018	1.000
30	0.437	479.437	78.047	469.042	99.293	1024.528	925.234	26.882	1037.333	0.946	4.017	0.999
50	0.437	479.437	78.728	470.189	93.714	1131.586	1037.871	24.372	1139.410	1.039	6.187	0.999
70	0.437	479.530	78.810	470.414	93.059	1240.557	1147.497	22.291	1240.178	1.131	7.378	1.000
90	0.415	456.440	82.255	452.276	61.511	1347.590	1286.078	19.375	1363.287	1.241	8.774	0.951

* * * INDUCER EXIT * * * INITIAL INTEGRATED FLOW 2.413

MASS AVERAGE TOTAL PRESSURE 24.844
MASS AVERAGE TOTAL TEMPERATURE 609.773
INDUCER PRESSURE RATIO 1.690
INDUCER TEMPERATURE RATIO 1.175
INDUCER EFFICIENCY 0.923

INDUCER EXIT VELOCITY TRIANGLES

MD	VD	ALPHA	VM	VU	U	WU	B	WO	MREL	I	VO/VOMAX
10	0.579	668.925	47.995	497.069	447.641	975.530	527.889	43.277	725.083	0.628	10.422	0.894
30	0.593	685.659	49.096	518.230	448.960	1052.642	603.682	40.644	795.610	0.688	8.755	0.916
50	0.627	727.050	48.597	545.346	480.831	1129.754	648.922	40.043	847.646	0.731	4.986	0.972
70	0.637	744.509	48.355	556.359	494.729	1206.866	712.136	37.998	903.700	0.773	2.201	0.995
90	0.631	747.979	39.527	476.044	576.935	1283.978	707.043	33.951	852.366	0.719	1.698	1.000

TABLE LX.

10/1 CENTRIFUGAL COMPRESSOR, IND AND IMP TRAV
8/1 SPEEDLINE, NEAR STALL, 10 DEG IGV TURNING
BUILD 6

FLOW RATE = 2.796 SPEED = 61819.2

* * * INLET GUIDE VANE EXIT * * *

MD	VC	ALPHA	VM	VU	U	WU	B	WO	MREL	I	VO/VOMAX
1D 0.423	484.997	78.057	454.932	96.220	918.137	821.916	28.964	939.421	0.856	1.935	0.993
3D 0.426	487.906	78.047	457.761	96.905	1027.219	930.314	26.199	1036.836	0.945	4.700	0.999
5D 0.426	487.997	78.728	458.969	91.478	1134.559	1043.080	23.750	1139.592	1.038	6.809	1.000
7D 0.421	482.087	78.810	453.302	89.674	1243.816	1154.142	21.442	1239.970	1.129	8.227	0.987
9D 0.389	438.847	82.255	434.843	59.140	1351.130	1291.989	18.601	1363.204	1.240	9.548	0.937

* * * INDUCER EXIT * * * INITIAL INTEGRATED FLOW 2.371

MASS AVERAGE TOTAL PRESSURE 25.029
MASS AVERAGE TOTAL TEMPERATURE 613.736
INDUCER PRESSURE RATIO 1.703
INDUCER TEMPERATURE RATIO 1.183
INDUCER EFFICIENCY 0.898

INDUCER EXIT VELOCITY TRIANGLES

MD	VO	ALPHA	VM	VU	U	WU	B	WO	MREL	I	VO/VOMAX
1D 0.582	674.075	47.813	499.467	452.669	978.093	525.423	43.549	724.940	0.626	10.150	0.888
3D 0.598	684.401	48.986	516.417	449.130	1055.407	606.277	40.423	796.404	0.687	8.976	0.902
5D 0.626	727.476	48.182	542.166	485.053	1132.722	647.668	39.932	844.641	0.727	5.097	0.959
7D 0.628	738.170	47.596	545.078	497.779	1210.036	712.257	37.426	896.895	0.764	2.773	0.973
9D 0.637	758.319	37.753	464.295	599.564	1287.351	687.786	34.021	829.831	0.697	1.628	1.000

TABLE LX. (Continued)

* * * IMPELLER EXIT * * * INITIAL INTEGRATED FLOW 2.560

PCENT SPAN	R	MO	VO	VO/VMAX	ALP	VM	VM/VMMAX	VU	U	WU	B	WO
0.0445	0.0104	0.9624	1407.03	0.7613	12.526	305.17	0.5150	1373.54	1900.46	526.92	69.011	326.86
0.1273	0.0300	1.1613	1642.40	0.8886	15.276	432.73	0.7303	1584.36	1900.46	316.10	78.716	441.26
0.2122	0.0500	1.2960	1787.98	0.9674	17.526	538.45	0.9087	1704.98	1900.46	195.48	83.459	541.97
0.2971	0.0699	1.3394	1832.27	0.9914	18.526	582.19	0.9825	1737.32	1900.46	163.14	84.635	584.75
0.3820	0.0899	1.3476	1840.80	0.9960	18.776	592.51	1.0000	1742.83	1900.46	157.62	84.832	594.93
0.4668	0.1097	1.3546	1848.15	1.0000	18.526	587.24	0.9910	1752.37	1900.46	148.09	85.169	589.33
0.5517	0.1299	1.3464	1840.10	0.9956	17.776	561.79	0.9481	1752.24	1900.46	148.22	85.164	563.80
0.6366	0.1499	1.3054	1797.90	0.9728	16.276	503.90	0.8504	1725.84	1900.46	174.62	84.222	506.48
0.7215	0.1699	1.2363	1725.35	0.9335	13.776	410.67	0.6934	1675.72	1900.46	224.74	82.361	414.55
0.8064	0.1897	1.1613	1643.14	0.8890	9.776	279.01	0.4709	1619.28	1900.46	281.18	80.148	283.19
0.8913	0.2099	1.0746	1543.24	0.8350	4.526	121.79	0.2055	1538.43	1900.46	362.03	76.757	125.12
0.9550	0.2249	0.9707	1417.83	0.7671	1.526	37.77	0.0637	1417.33	1900.46	483.13	71.176	39.90

MASS AVERAGE TOTAL PRESSURE 141.880
MASS AVERAGE TOTAL TEMPERATURE 1059.800
MASS AVG VM 498.571 VU 1687.611 ANGLE 16.458
FLOW FACTOR 0.827 SLIP FACTOR INS. STA. 0.887 IMPELLER TIP 0.930
IMP. PRESS. RATIO 5.668 IMP. TEMP.RATIO 1.726 EFFICIENCY 0.873
IMP..IND. PRESS. RATIO 9.713 IMP.IND. TEMP. RATIO 2.043 EFFICIENCY 0.861
IMP..IND..IGV PRESS. RATIO 9.655 IMP..IND..IGV TEMP. RATIO 2.043 EFFICIENCY 0.858

* * * DIFFUSER * * *

CD DIFFUSER THROAT FRONT 0.832 REAR 0.817
STATIC PRESSURE RISE COEFFICIENT IMPELLER EXIT/DIFFUSER EXIT 0.747
DIFFUSER THROAT FRONT/DIFFUSER EXIT 0.697 DIFFUSER THROAT REAR/DIFFUSER EXIT 0.669
DIFFUSER LOSSES TOTAL TO STATIC 0.167 TOTAL TO TOTAL 0.123
DIFFUSER LOSS COEFFICIENT 0.252

TABLE LXI.

10/1 CENTRIFUGAL COMPRESSOR, INDUCER TRAVERSE
8/1 SPEEDLINE, WOD, 15 DEG IGV TURNING
BUILD 6

FLOW RATE = 2.807 SPEED = 61605.6

* * * INLET GUIDE VANE EXIT * * *

MD	VO	ALPHA	VM	VU	U	WU	B	WO	MREL	I	VO/VOMAX
10 0.440	482.340	73.148	461.627	139.828	914.936	775.107	30.776	902.159	0.823	0.123	0.988
30 0.445	488.141	73.181	467.262	141.236	1024.033	882.796	27.892	998.831	0.911	3.007	1.000
50 0.442	485.241	73.990	466.422	133.826	1131.265	997.438	25.061	1101.105	1.005	5.498	0.994
70 0.442	485.335	74.394	467.445	130.559	1239.685	1109.125	22.853	1203.604	1.098	6.816	0.994
90 0.412	453.437	78.414	444.197	91.068	1346.498	1255.429	19.484	1331.697	1.212	8.665	0.928

* * * INDUCER EXIT * * * INITIAL INTEGRATED FLOW 2.455

MASS AVERAGE TOTAL PRESSURE 23.717
MASS AVERAGE TOTAL TEMPERATURE 602.838
INDUCER PRESSURE RATIO 1.614
INDUCER TEMPERATURE RATIO 1.162
INDUCER EFFICIENCY 0.905

INDUCER EXIT VELOCITY TRIANGLES

MD	VO	ALPHA	VM	VU	U	WU	B	WO	MREL	I	VO/VOMAX
10 0.593	680.376	47.731	503.477	457.626	974.713	517.086	44.236	721.711	0.629	9.463	0.909
30 0.609	700.055	48.824	526.928	460.894	1051.760	590.866	41.726	791.692	0.689	7.673	0.936
50 0.642	739.289	49.396	561.290	481.146	1128.808	647.662	40.913	857.037	0.744	4.116	0.988
70 0.639	742.718	50.191	570.548	475.505	1205.855	730.350	37.996	926.788	0.798	2.203	0.993
90 0.637	747.798	43.451	514.287	542.872	1282.903	740.030	34.797	901.186	0.767	0.852	1.000

TABLE LXII.

10/1 CENTRIFUGAL COMPRESSOR, IND AND IMP TRAV
8/1 SPEEDLINE, NEAR STALL, 15 DEG IGV TURNING
BUILD 6

FLOW RATE = 2.787 SPEED = 61700.7

* * * INLET GUIDE VANE EXIT * * *

	MD	VO	ALPHA	VM	VU	U	WU	B	WO	MREL	I	VO/VOMAX
10	0.432	473.721	73.148	453.378	137.330	916.350	779.019	30.158	901.345	0.822	0.701	0.987
30	0.437	479.530	73.181	459.020	138.745	1025.614	886.869	27.364	998.617	0.921	3.535	1.000
50	0.434	476.523	73.990	458.052	131.424	1133.012	1001.587	24.575	1101.358	1.004	5.984	0.993
70	0.434	476.533	74.394	458.967	128.191	1241.600	1113.408	22.402	1204.296	1.098	7.267	0.993
90	0.404	444.772	78.414	435.710	89.328	1348.578	1259.250	19.086	1332.499	1.212	9.063	0.927

* * * INDUCER EXIT * * * INITIAL INTEGRATED FLOW 2.386

MASS AVERAGE TOTAL PRESSURE 23.903
MASS AVERAGE TOTAL TEMPERATURE 605.103
INDUCER PRESSURE RATIO 1.632
INDUCER TEMPERATURE RATIO 1.166
INDUCER EFFICIENCY 0.904

INDUCER EXIT VELOCITY TRIANGLES

	MD	VO	ALPHA	VM	VU	U	WU	B	WO	MREL	I	VO/VOMAX
10	0.579	666.698	47.565	491.896	450.027	976.219	526.192	43.070	720.306	0.626	10.629	0.895
30	0.607	698.146	48.609	523.762	461.607	1053.385	591.777	41.510	790.271	0.687	7.889	0.937
50	0.637	734.801	49.662	560.097	475.629	1130.552	654.922	40.537	861.761	0.747	4.492	0.986
70	0.628	732.665	48.966	552.667	480.996	1207.718	726.722	37.252	912.998	0.783	2.947	0.984
90	0.631	744.500	42.493	502.915	548.960	1284.885	735.924	34.347	891.352	0.756	1.302	1.000

TABLE LXII. (Continued)

* * * IMPELLER EXIT * * * INITIAL INTEGRATED FLOW 2.729

PCENT SPAN	R	MO	VO	VO/VMAX	ALP	VM	VM/VMMAX	VU	U	WU	B	WO
0.0233	0.0054	1.0968	1562.07	0.8503	13.050	352.72	0.5878	1521.73	1896.82	375.09	76.153	363.27
0.0636	0.0149	1.2351	1715.67	0.9339	15.800	467.14	0.7785	1650.85	1896.82	245.97	81.525	472.30
0.1273	0.0300	1.2843	1768.00	0.9624	18.050	547.81	0.9129	1680.99	1896.82	215.83	82.683	552.31
0.2122	0.0500	1.3300	1815.46	0.9882	19.300	600.03	1.0000	1713.43	1896.82	183.39	83.890	603.46
0.2971	0.0699	1.3382	1823.98	0.9928	19.050	595.33	0.9921	1724.08	1896.82	172.73	84.278	598.31
0.3820	0.0899	1.3453	1831.31	0.9968	18.675	586.38	0.9772	1734.89	1896.82	161.93	84.667	588.[illegible]
0.4668	0.1099	1.3511	1837.02	1.0000	18.425	580.61	0.9676	1742.85	1896.82	153.97	84.951	582.87
0.5517	0.1299	1.3312	1817.06	0.9891	17.550	547.91	0.9131	1732.48	1896.82	164.33	84.581	550.37
0.6366	0.1499	1.2867	1772.08	0.9646	15.050	460.14	0.7668	1711.29	1896.82	185.52	83.812	462.84
0.7215	0.1699	1.2234	1704.98	0.9281	11.300	334.08	0.5567	1671.93	1896.82	224.89	82.339	337.09
0.8064	0.1899	1.1578	1632.98	0.8889	7.300	207.49	0.3458	1619.74	1896.82	277.08	80.292	210.51
0.8913	0.2099	1.0921	1558.51	0.8483	3.300	89.71	0.1495	1555.92	1896.82	340.89	77.641	91.84
0.9550	0.2249	1.0007	1449.40	0.7889	0.800	20.23	0.0337	1449.26	1896.82	447.56	72.838	21.18

MASS AVERAGE TOTAL PRESSURE 141.475
MASS AVERAGE TOTAL TEMPERATURE 1053.039
MASS AVG VM 514.998 VU 1701.057 ANGLE 16.843
FLOW FACTOR 0.811 SLIP FACTOR INS. STA. 0.896 IMPELLER TIP 0.940
IMP. PRESS. RATIO 5.896 IMP. TEMP.RATIO 1.740 EFFICIENCY 0.882
IMP.+IND. PRESS. RATIO 9.698 IMP.+IND. TEMP. RATIO 2.030 EFFICIENCY 0.872
IMP.+IND.+IGV PRESS. RATIO 9.628 IMP.+IND.+IGV TEMP. RATIO 2.030 EFFICIENCY 0.868

* * * DIFFUSER * * *

CD DIFFUSER THROAT FRONT 0.846 REAR 0.832
STATIC PRESSURE RISE COEFFICIENT IMPELLER EXIT/DIFFUSER EXIT 0.742
DIFFUSER THROAT FRONT/DIFFUSER EXIT 0.682 DIFFUSER THROAT REAR/DIFFUSER EXIT 0.632
DIFFUSER LOSSES TOTAL TO STATIC 0.172 TOTAL TO TOTAL 0.132
DIFFUSER LOSS COEFFICIENT 0.257

TABLE LXIII.

10/1 CENTRIFUGAL COMPRESSOR, IND AND IMP TRAV
95 PCT SPEED, NOD, 10 DEG IGV TURNING
BUILD 6

FLOW RATE = 2.885 SPEED = 62114.1

* * * INLET GUIDE VANE EXIT * * *

MO	VO	ALPHA	VM	VU	U	WU	B	WO	MREL	I	VO/VOMAX
10 8.446	491.048	77.888	479.764	104.719	922.986	818.268	30.383	948.518	0.866	0.516	0.999
30 8.448	491.136	78.079	480.538	101.478	1031.992	930.513	27.312	1047.269	0.956	3.587	1.000
50 8.448	491.060	78.071	480.436	101.498	1140.732	1039.234	24.811	1144.914	1.045	5.748	0.999
70 8.445	488.161	78.834	478.901	96.530	1249.799	1153.269	22.515	1250.597	1.141	7.194	0.993
90 8.418	459.264	80.889	453.470	72.723	1357.612	1284.889	19.439	1362.562	1.241	8.710	0.935

* * * INDUCER EXIT * * * INITIAL INTEGRATED FLOW 2.493

MASS AVERAGE TOTAL PRESSURE 24.976
MASS AVERAGE TOTAL TEMPERATURE 613.630
INDUCER PRESSURE RATIO 1.499
INDUCER TEMPERATURE RATIO 1.183
INDUCER EFFICIENCY 0.895

INDUCER EXIT VELOCITY TRIANGLES

MO	VO	ALPHA	VM	VU	U	WU	B	WO	MREL	I	VO/VOMAX
10 0.582	674.661	48.350	504.121	448.382	982.759	534.396	43.330	734.655	0.634	10.369	0.884
30 0.601	697.196	49.341	528.897	454.257	1060.442	606.184	41.104	804.482	0.694	8.295	0.914
50 0.626	727.977	48.757	547.388	479.913	1138.125	658.212	39.747	856.082	0.736	9.282	0.954
70 0.652	762.602	49.411	579.118	496.169	1215.809	719.639	38.824	923.720	0.789	1.373	1.000
90 0.639	758.195	41.294	500.351	569.656	1293.492	723.836	34.654	879.930	0.742	0.995	0.994

TABLE LXIII. (Continued)

* * * IMPELLER EXIT * * * INITIAL INTEGRATED FLOW 2.654

PCENT SPAN	R	MD	VD	VD/VMAX	ALP	VM	VM/VMMAX	VU	U	WU	B	WD
0.0233	0.0094	1.0160	1478.07	0.7995	8.224	211.43	0.3371	1462.87	1909.53	446.66	73.020	221.06
0.0636	0.0149	1.1355	1618.94	0.8757	12.224	342.79	0.5465	1582.24	1909.53	327.29	78.312	350.04
0.1273	0.0308	1.2328	1727.66	0.9345	17.224	511.57	0.8156	1650.14	1909.53	259.36	81.067	517.85
0.2122	0.0500	1.3148	1814.28	0.9813	20.224	627.18	1.0000	1702.43	1909.53	207.10	83.064	631.81
0.2971	0.0699	1.3371	1837.06	0.9937	19.724	619.99	0.9885	1729.27	1909.53	180.25	84.049	623.35
0.3820	0.0899	1.3488	1848.68	1.0000	18.974	601.08	0.9583	1748.24	1909.53	161.29	84.728	603.63
0.4668	0.1099	1.3488	1848.68	1.0000	18.474	585.80	0.9340	1753.42	1909.53	156.11	84.912	588.12
0.5517	0.1299	1.3324	1832.38	0.9911	17.724	557.84	0.8894	1745.40	1909.53	164.12	84.628	560.30
0.6366	0.1499	1.2902	1788.80	0.9676	15.724	484.77	0.7729	1721.86	1909.53	187.67	83.779	487.64
0.7215	0.1699	1.2140	1707.24	0.9234	12.224	361.48	0.5763	1668.53	1909.53	240.99	81.781	365.23
0.8064	0.1899	1.1484	1634.41	0.8840	8.224	259.79	0.3727	1617.60	1909.53	291.92	79.770	257.57
0.8913	0.2099	1.0851	1561.45	0.8446	4.474	121.80	0.1942	1556.69	1909.53	352.84	77.229	124.89
0.9350	0.2249	0.9488	1395.79	0.7549	2.224	54.16	0.0863	1394.70	1909.53	514.83	69.739	57.74

MASS AVERAGE TOTAL PRESSURE 144.016
MASS AVERAGE TOTAL TEMPERATURE 1067.799
MASS AVG VM 918.074 VU 1700.181 ANGLE 16.946
FLOW FACTOR 0.811 SLIP FACTOR INS. STA. 0.890 IMPELLER TIP 0.933
IMP. PRESS. RATIO 9.846 IMP. TEMP.RATIO 1.740 EFFICIENCY 0.876
IMP.+IND. PRESS. RATIO 9.997 IMP.+IND. TEMP. RATIO 2.038 EFFICIENCY 0.863
IMP.+IND.+IGV PRESS. RATIO 9.837 IMP.+IND.+IGV TEMP. RATIO 2.058 EFFICIENCY 0.880

* * * DIFFUSER * * *

CD DIFFUSER THROAT FRONT 0.878 REAR 0.866
STATIC PRESSURE RISE COEFFICIENT IMPELLER EXIT/DIFFUSER EXIT 0.132
DIFFUSER THROAT FRONT/DIFFUSER EXIT 0.042 DIFFUSER THROAT REAR/DIFFUSER EXIT 0.007
DIFFUSER LOSSES TOTAL TO STATIC 0.580 TOTAL TO TOTAL 0.457
DIFFUSER LOSS COEFFICIENT 0.857

TABLE LXIV.

10/1 CENTRIFUGAL COMPRESSOR, IND AND IMP TRAV
95 PCT SPEED, NEAR STALL, 10 DEG IGV TURNING
BUILD 6

FLOW RATE = 2.877 SPEED = 62138.8

* * * INLET GUIDE VANE EXIT * * *

	MD	VD	ALPHA	VM	VU	U	WU	B	WD	MREL	I	VD/VDMAX
1D	0.442	485.335	77.686	474.170	103.502	923.336	819.833	30.044	947.082	0.864	0.859	1.000
3D	0.442	485.335	78.075	474.862	100.280	1032.404	932.123	26.996	1046.111	0.954	3.903	1.000
5D	0.442	485.335	78.071	474.854	100.319	1141.187	1040.868	24.522	1144.069	1.044	6.037	1.000
7D	0.440	482.340	78.934	473.209	93.406	1250.298	1156.891	22.246	1249.925	1.140	7.423	0.993
9D	0.412	453.437	80.889	447.716	71.800	1358.154	1286.353	19.190	1362.041	1.240	8.959	0.934

* * * INDUCER EXIT * * * INITIAL INTEGRATED FLOW 2.453

MASS AVERAGE TOTAL PRESSURE 25.926
MASS AVERAGE TOTAL TEMPERATURE 613.670
INDUCER PRESSURE RATIO 1.703
INDUCER TEMPERATURE RATIO 1.183
INDUCER EFFICIENCY 0.898

INDUCER EXIT VELOCITY TRIANGLES

	MD	VD	ALPHA	VM	VU	U	WU	B	WD	MREL	I	VD/VDMAX
1D	0.574	665.505	47.972	494.348	445.531	983.150	537.599	42.600	730.337	0.630	11.099	0.887
3D	0.596	691.087	49.465	525.242	449.149	1060.865	611.715	40.630	806.273	0.695	8.749	0.922
5D	0.631	733.829	49.285	556.219	478.670	1138.579	659.908	40.126	869.052	0.742	6.903	0.979
7D	0.639	749.485	49.555	570.381	486.202	1216.293	730.091	37.998	926.482	0.790	2.201	1.000
9D	0.628	746.835	50.336	483.408	569.280	1294.008	724.727	33.704	871.156	0.733	1.945	0.996

TABLE LXIV, (Continued)

* * * IMPELLER EXIT * * * INITIAL INTEGRATED FLOW 2.659

PCENT SPAN	R	MD	VD	VD/VMAX	ALP	VM	VM/VMMAX	VU	U	WU	S	WD
0.0000	0.0849	1.0000	1581.38	0.8446	14.727	396.94	0.6106	1910.08	1910.29	400.20	75.156	410.65
0.0478	0.0800	1.0079	1780.03	0.9525	18.727	565.35	0.8696	1667.60	1910.29	242.68	81.719	571.31
0.0822	0.0900	1.0207	1815.83	0.9822	20.977	650.06	1.0000	1695.47	1910.29	214.81	82.779	655.27
0.0970	0.0899	1.0382	1834.23	0.9922	19.977	626.67	0.9640	1723.85	1910.29	186.43	83.827	630.33
0.0000	0.0899	1.0476	1843.49	0.9972	18.977	599.91	0.9222	1743.29	1910.29	167.00	84.528	602.25
0.0488	0.1099	1.0583	1848.56	1.0000	16.727	593.92	0.9130	1750.68	1910.29	159.60	84.790	599.98
0.0507	0.1299	1.0802	1827.68	0.9887	17.977	564.11	0.8677	1738.45	1910.29	171.84	84.354	566.86
0.0300	0.1499	1.0796	1774.18	0.9597	15.727	480.92	0.7397	1707.75	1910.29	202.53	83.236	484.29
0.7500	0.1699	1.1017	1701.60	0.9205	12.227	360.39	0.5543	1663.00	1910.29	247.27	81.541	364.36
0.0000	0.1899	1.1378	1619.04	0.8758	8.227	231.70	0.3564	1602.37	1910.29	307.91	79.122	239.94
0.0000	0.2099	1.0558	1525.91	0.8243	4.477	116.97	0.1800	1519.26	1910.29	391.03	75.566	122.85

MASS AVERAGE TOTAL PRESSURE 145.651
MASS AVERAGE TOTAL TEMPERATURE 1064.059
MASS AVG VM 598.980 VU 1697.650 ANGLE 19.613
FLOW FACTOR 0.781 SLIP FACTOR INS. STA. 0.886 IMPELLER TIP 0.931
IMP. PRESS. RATIO 5.831 IMP. TEMP.RATIO 1.733 EFFICIENCY 0.882
IMP.+IND. PRESS. RATIO 9.992 IMP.+IND. TEMP. RATIO 2.051 EFFICIENCY 0.868
IMP.+IND.+IGV PRESS. RATIO 9.932 IMP.+IND.+IGV TEMP. RATIO 2.051 EFFICIENCY 0.865

* * * DIFFUSER * * *

CD DIFFUSER THROAT FRONT 0.884 REAR 0.864
STATIC PRESSURE RISE COEFFICIENT IMPELLER EXIT/DIFFUSER EXIT 0.729
DIFFUSER THROAT FRONT/DIFFUSER EXIT 0.693 DIFFUSER THROAT REAR/DIFFUSER EXIT 0.665
DIFFUSER LOSSES TOTAL TO STATIC 0.180 TOTAL TO TOTAL 0.132
DIFFUSER LOSS COEFFICIENT 0.272

TABLE LXV.

&D/1 CENTRIFUGAL COMPRESSOR, INDUCER TRAVERSE
&DD PCT SPEED, NEAR STALL, 10 DEG IGV TURNING
BUILD 6

FLOW RATE = 3.058 SPEED = 6923N.1

* * * INLET GUIDE VANE EXIT * * *

	MD	VD	ALPHA	VM	VU	U	WU	B	WD	MREL	I	VD/VDMAX
ID	0.486	930.980	78.793	920.855	183.195	969.393	886.197	31.019	1010.737	0.926	-0.119	0.994
MD	0.489	933.963	78.932	924.032	182.499	1083.791	981.291	28.103	1112.449	1.019	2.796	1.000
SD	0.489	933.963	79.618	924.882	98.057	1198.085	1100.028	25.508	1218.837	1.117	5.091	1.000
TD	0.483	928.284	79.088	919.870	93.459	1312.859	1219.399	23.030	1323.394	1.214	6.579	0.989
9D	0.484	908.210	87.101	904.991	61.043	1425.913	1364.869	20.287	1455.156	1.330	7.002	0.991

* * * INDUCER EXIT * * * INITIAL INTEGRATED FLOW 2.779

MASS AVERAGE TOTAL PRESSURE 23.977
MASS AVERAGE TOTAL TEMPERATURE 609.276
INDUCER PRESSURE RATIO 1.494
INDUCER TEMPERATURE RATIO 1.174
INDUCER EFFICIENCY 0.829

INDUCER EXIT VELOCITY TRIANGLES

	MD	VD	ALPHA	VM	VU	U	WU	B	WD	MREL	I	VD/VDMAX
ID	0.788	818.781	55.458	669.903	460.865	1032.107	571.342	49.923	880.151	0.786	4.176	1.000
MD	0.807	788.928	54.865	653.956	459.554	1113.778	654.224	44.948	926.373	0.807	4.451	0.982
SD	0.868	789.786	54.174	637.889	459.974	1193.388	739.394	40.903	972.978	0.846	4.126	0.966
TD	0.878	789.321	54.445	639.071	458.782	1274.958	820.196	37.924	1039.776	0.897	2.275	0.966
9D	0.807	717.287	47.050	525.280	488.447	1358.549	870.101	31.119	1016.369	0.880	4.930	0.882

TABLE LXVI.

10/1 CENTRIFUGAL COMPRESSOR, INDUCER TRAVERSE
101 PCT SPEED, WOD, -4 DEG IGV TURNING
BUILD 6

FLOW RATE = 3.214 SPEED = 65934.3

* * * INLET GUIDE VANE EXIT * * *

	MO	VO	ALPHA	VM	VU	U	WU	B	WO	MREL	I	VO/VOMAX
10	0.527	573.572	94.778	571.578	-47.780	978.341	1026.122	29.119	1174.576	1.080	1.780	0.979
30	0.527	573.685	93.854	572.387	-38.565	1095.329	1133.895	26.784	1270.176	1.168	4.115	1.000
50	0.527	573.685	94.124	572.199	-41.262	1211.126	1252.388	24.555	1376.913	1.266	6.004	1.000
70	0.522	567.965	93.419	566.954	-33.870	1326.676	1360.547	22.622	1473.949	1.355	7.047	0.990
90	0.500	545.251	93.924	543.973	-37.317	1440.979	1478.296	20.202	1575.204	1.445	7.947	0.950

* * * INDUCER EXIT * * * INITIAL INTEGRATED FLOW 2.752

MASS AVERAGE TOTAL PRESSURE 24.234
MASS AVERAGE TOTAL TEMPERATURE 631.609
INDUCER PRESSURE RATIO 1.649
INDUCER TEMPERATURE RATIO 1.217
INDUCER EFFICIENCY 0.705

INDUCER EXIT VELOCITY TRIANGLES

	MO	VO	ALPHA	VM	VU	U	WU	B	WO	MREL	I	VO/VOMAX
10	0.721	834.748	62.465	740.199	385.886	1043.202	657.315	48.394	989.929	0.856	5.305	1.000
30	0.654	765.278	59.436	658.951	389.145	1125.663	736.518	41.818	988.269	0.845	7.581	0.916
50	0.568	674.954	61.525	593.302	321.798	1208.125	886.326	33.798	1066.575	0.898	11.231	0.808
70	0.686	810.987	62.591	719.948	373.327	1290.586	917.258	38.128	1136.057	0.986	2.071	0.971
90	0.587	711.554	54.599	580.006	412.190	1373.047	960.856	31.116	1122.343	0.927	4.533	0.852

TABLE LXVII.

10/1 CENTRIFUGAL COMPRESSOR, IND AND IMP TRAV
101 PCT SPEED, NEAR STALL, -- DEG IGV TURNING
BUILD 6

FLOW RATE = 3.209 SPEED = 65987.7

* * * INLET GUIDE VANE EXIT * * *

MO	VO	ALPHA	VM	VU	U	WU	B	WO	MREL	I	VG/VOMAX
10	0.524	570.826	94.778	568.842	-47.551	979.133	1026.685	28.988	1173.739	1.079	1.911	1.000
30	0.522	567.965	93.854	566.680	-38.181	1096.216	1134.397	26.544	1268.063	1.166	4.355	0.994
50	0.522	567.965	94.124	566.494	-40.851	1212.106	1252.958	24.328	1375.071	1.264	6.231	0.994
70	0.519	565.215	93.419	564.209	-33.706	1327.750	1361.457	22.509	1473.736	1.354	7.160	0.990
90	0.497	542.485	93.924	541.213	-37.127	1442.146	1479.274	20.095	1575.171	1.445	8.054	0.950

* * * INDUCER EXIT * * * INITIAL INTEGRATED FLOW 2.919

MASS AVERAGE TOTAL PRESSURE 25.044
MASS AVERAGE TOTAL TEMPERATURE 632.864
INDUCER PRESSURE RATIO 1.704
INDUCER TEMPERATURE RATIO 1.220
INDUCER EFFICIENCY 0.746

INDUCER EXIT VELOCITY TRIANGLES

MO	VO	ALPHA	VM	VU	U	WU	B	WO	MREL	I	VO/VOMAX
10	0.717	831.881	52.785	662.492	508.120	1044.047	540.926	50.768	855.277	0.737	2.931	1.000
30	0.713	830.845	52.853	662.262	501.710	1126.575	624.864	46.664	910.520	0.782	2.735	0.998
50	0.582	691.634	46.934	505.288	472.272	1209.103	736.830	34.440	893.440	0.752	10.589	0.831
70	0.650	772.558	55.676	638.028	435.620	1291.630	856.010	36.699	1067.629	0.899	3.500	0.928
90	0.583	684.136	47.931	507.868	458.380	1374.158	915.778	29.011	1047.177	0.862	6.438	0.822

TABLE LXVII. (Continued)

* * * IMPELLER EXIT * * * INITIAL INTEGRATED FLOW 2.678

PCENT SPAN	R	MO	VO	VO/VMAX	ALP	VM	VM/VMMAX	VU	U	WU	B	WO
0.0233	0.0055	0.9283	1414.74	0.7245	11.220	277.22	0.4067	1397.51	2028.41	631.10	65.696	304.17
0.0848	0.0200	1.1484	1761.52	0.8648	15.220	446.43	0.6550	1640.88	2028.61	387.73	76.705	458.72
0.1697	0.0399	1.3148	1888.65	0.9605	19.470	629.51	0.9237	1780.65	2028.61	247.96	82.072	635.58
0.2546	0.0600	1.3710	1948.67	0.9910	20.470	681.48	1.0000	1825.62	2028.61	202.99	83.655	685.68
0.3395	0.0799	1.3816	1959.71	0.9966	19.220	645.13	0.9466	1850.47	2028.61	178.14	84.501	648.11
0.4244	0.0999	1.3874	1966.25	1.0000	18.220	614.78	0.9021	1867.67	2028.61	160.94	85.074	617.06
0.5093	0.1200	1.3874	1965.80	0.9997	17.470	590.14	0.8659	1875.13	2028.61	153.48	85.320	592.12
0.5942	0.1400	1.3617	1939.24	0.9862	16.220	541.68	0.7948	1862.05	2028.61	166.56	84.888	543.84
0.6791	0.1599	1.3124	1867.34	0.9598	13.970	455.63	0.6685	1831.52	2028.61	197.09	83.858	458.26
0.7640	0.1800	1.2492	1817.71	0.9244	10.470	330.31	0.4847	1787.45	2028.61	241.16	82.316	333.31
0.8488	0.2000	1.1683	1725.07	0.8773	6.720	201.86	0.2962	1713.22	2028.61	315.39	79.569	205.25
0.9125	0.2150	1.1062	1651.35	0.8398	3.220	92.75	0.1361	1648.75	2028.61	379.86	77.025	95.18
0.9550	0.2250	1.0500	1582.36	0.8047	-0.029	-0.82	-0.0012	1582.36	2028.61	446.25	74.250	-0.85
0.9868	0.2325	0.8763	1356.32	0.6898	-2.529	-59.87	-0.0878	1355.00	2028.61	673.61	63.566	-56.86

MASS AVERAGE TOTAL PRESSURE 172.985
MASS AVERAGE TOTAL TEMPERATURE 1159.000
MASS AVG VM 550.241 VU 1808.291 ANGLE 16.924
FLOW FACTOR 0.808 SLIP FACTOR INS. STA. 0.891 IMPELLER TIP 0.934
IMP. PRESS. RATIO 6.903 IMP. TEMP.RATIO 1.831 EFFICIENCY 0.875
IMP..IND. PRESS. RATIO 11.902 IMP.IND. TEMP. RATIO 2.234 EFFICIENCY 0.812
IMP..IND..IGV PRESS. RATIO 11.772 IMP..IND..IGV TEMP. RATIO 2.234 EFFICIENCY 0.807

TABLE LXVIII.

10/1 CENTRIFUGAL COMPRESSOR, IND AND IMP TRAV
101 PCT SPEED, NS, -4 DEG IGV, WITH COOLANT
BUILD 6

FLOW RATE = 3.214 SPEED = 65779.6

* * * INLET GUIDE VANE EXIT * * *

	MD	VD	ALPHA	VM	VU	U	WU	B	WD	MREL	I	VD/VDMAX
10	0.526	570.826	94.778	568.842	-47.551	976.046	1023.598	29.062	1171.040	1.077	1.837	1.000
30	0.522	567.965	93.854	566.680	-38.181	1092.759	1130.940	26.614	1264.972	1.163	4.285	0.994
50	0.522	567.969	94.124	566.494	-40.851	1206.284	1249.135	24.394	1371.589	1.261	6.165	0.994
70	0.519	565.219	93.419	564.209	-33.706	1323.563	1357.270	22.572	1469.869	1.351	7.097	0.990
90	0.497	542.485	93.926	541.213	-37.127	1437.598	1474.726	20.152	1570.901	1.441	7.997	0.950

* * * INDUCER EXIT * * * INITIAL INTEGRATED FLOW 2.638

MASS AVERAGE TOTAL PRESSURE 24.773
MASS AVERAGE TOTAL TEMPERATURE 633.556
INDUCER PRESSURE RATIO 1.685
INDUCER TEMPERATURE RATIO 1.221
INDUCER EFFICIENCY 0.725

INDUCER EXIT VELOCITY TRIANGLES

	MD	VD	ALPHA	VM	VU	U	WU	B	WD	MREL	I	VD/VDMAX
10	0.674	991.689	62.661	880.925	455.432	1040.755	585.322	56.398	1057.654	0.933	-2.698	1.000
30	0.691	806.208	58.811	689.684	417.501	1123.022	705.521	44.349	986.623	0.846	9.050	0.812
50	0.560	669.158	57.408	563.781	360.443	1205.290	844.846	33.715	1015.685	0.850	11.314	0.674
70	0.661	760.192	64.248	684.693	330.284	1287.558	957.273	35.574	1176.936	0.992	4.623	0.766
90	0.564	662.961	55.341	545.319	377.020	1369.825	992.804	28.778	1132.711	0.929	6.871	0.668

TABLE LXVIII. (Continued)

* * * IMPELLER EXIT * * * INITIAL INTEGRATED FLOW 2.703

PCENT SPAN	R	MD	VD	VD/VMAX	ALP	VM	VM/VMMAX	VU	U	WU	S	WD
0.0742	0.0179	1.2714	1840.66	0.9363	19.124	603.03	0.8392	1739.07	2022.22	283.14	80.752	610.97
0.1497	0.0400	1.3734	1949.82	0.9919	21.624	718.94	1.0000	1812.59	2022.22	209.62	83.403	729.93
0.2546	0.0660	1.3825	1959.60	0.9969	20.124	674.21	0.9383	1839.97	2022.22	182.25	84.343	677.51
0.3395	0.0799	1.3886	1965.69	1.0000	19.374	652.09	0.9075	1854.38	2022.22	167.84	84.828	654.76
0.4244	0.1000	1.3874	1964.92	0.9996	18.374	619.39	0.8620	1864.74	2022.22	157.47	85.173	621.59
0.5093	0.1199	1.3687	1945.34	0.9896	17.124	572.79	0.7971	1859.10	2022.22	163.11	84.985	575.00
0.5942	0.1399	1.3242	1897.06	0.9655	15.624	511.17	0.7114	1827.83	2022.22	194.39	83.929	514.05
0.6791	0.1599	1.2539	1821.43	0.9266	13.374	390.33	0.5432	1779.12	2022.22	243.09	82.219	393.95
0.7640	0.1800	1.1859	1743.82	0.8871	8.374	253.97	0.3534	1725.23	2022.22	296.99	80.232	257.70
0.8278	0.1949	1.1414	1691.84	0.8606	5.624	165.80	0.2307	1683.69	2022.22	338.52	78.631	169.12
0.8701	0.2050	1.0911	1582.27	0.8049	3.624	100.02	0.1392	1579.10	2022.22	443.11	74.325	103.88

MASS AVERAGE TOTAL PRESSURE 174.954
MASS AVERAGE TOTAL TEMPERATURE 1156.100
MASS AVG VM 592.489 VU 1813.782 ANGLE 17.804
FLOW FACTOR 0.784 SLIP FACTOR INS. STA, 0.896 IMPELLER TIP 0.940
IMP. PRESS. RATIO 7.062 IMP. TEMP.RATIO 1.824 EFFICIENCY 0.895
IMP..IND. PRESS. RATIO 12.028 IMP.IND. TEMP. RATIO 2.229 EFFICIENCY 0.821
IMP..IND..IGV PRESS. RATIO 11.906 IMP..IND..IGV TEMP. RATIO 2.228 EFFICIENCY 0.816

* * * DIFFUSER * * *

CD DIFFUSER THROAT FRONT 0.865 REAR 0.841
STATIC PRESSURE RISE COEFFICIENT IMPELLER EXIT/DIFFUSER EXIT 0.712
DIFFUSER THROAT FRONT/DIFFUSER EXIT 0.675 DIFFUSER THROAT REAR/DIFFUSER EXIT 0.646
DIFFUSER LOSSES TOTAL TO STATIC 0.198 TOTAL TO TOTAL 0.157
DIFFUSER LOSS COEFFICIENT 0.287

TABLE LXIX.

10/1 CENTRIFUGAL COMPRESSOR, INDUCER TRAVERSE
101 PCT SPEED, WOD, 0 DEG IGV TURNING
BUILD 6

FLOW RATE = 3.192 SPEED = 65834.8

* * * INLET GUIDE VANE EXIT * * *

%D	WD	VD	ALPHA	VM	VU	U	WU	B	WO	MREL	I	VO/VOMAX
10	0.514	559.486	89.985	559.486	0.147	976.949	976.802	29.802	1125.685	1.034	1.097	1.000
30	0.514	559.486	89.040	559.408	9.372	1093.067	1083.694	27.303	1219.562	1.120	3.596	1.000
50	0.514	559.486	89.370	559.452	6.149	1208.088	1201.938	24.960	1325.761	1.218	5.599	1.000
70	0.508	553.753	88.791	553.630	11.679	1324.231	1312.552	22.869	1424.535	1.308	6.800	0.989
90	0.500	545.251	89.952	545.251	0.449	1438.113	1437.663	20.769	1537.588	1.411	7.380	0.974

* * * INDUCER EXIT * * * INITIAL INTEGRATED FLOW 2.738

MASS AVERAGE TOTAL PRESSURE 29.697
MASS AVERAGE TOTAL TEMPERATURE 622.874
INDUCER PRESSURE RATIO 1.612
INDUCER TEMPERATURE RATIO 1.200
INDUCER EFFICIENCY 0.728

INDUCER EXIT VELOCITY TRIANGLES

%D	WD	VD	ALPHA	VM	VU	U	WU	B	WO	MREL	I	VO/VOMAX
10	0.720	829.239	61.661	729.861	393.624	1041.627	648.002	48.400	976.015	0.848	5.300	1.000
30	0.660	765.596	59.270	658.096	391.210	1123.963	732.752	41.927	984.895	0.849	7.472	0.923
50	0.571	672.354	60.858	587.249	327.412	1206.300	878.888	33.749	1057.027	0.898	11.280	0.810
70	0.658	775.169	63.170	691.721	349.868	1288.636	938.768	36.384	1166.089	0.991	3.815	0.934
90	0.587	707.035	56.115	586.951	394.190	1370.973	976.783	31.001	1139.565	0.947	4.648	0.852

TABLE LXX.

10/1 CENTRIFUGAL COMPRESSOR, IND AND IMP TRAV
101 PCT SPEED, NEAR STALL, 0 DEG IGV TURNING
BUILD 6

FLOW RATE = 3.185 SPEED = 65952.8

* * * INLET GUIDE VANE EXIT * * *

	MO	VO	ALPHA	VM	VU	U	WU	B	WO	MREL	I	VO/VOMAX
10	0.511	556.730	89.985	556.730	0.146	978.702	978.555	29.636	1125.841	1.034	1.263	1.000
30	0.511	556.730	89.040	556.652	9.326	1095.028	1085.701	27.144	1220.085	1.120	3.759	1.000
50	0.511	556.620	89.370	556.586	6.118	1210.254	1204.136	24.807	1326.549	1.218	2.752	0.999
70	0.508	550.993	88.791	550.870	11.620	1326.606	1314.985	22.729	1425.709	1.308	6.940	0.989
90	0.497	542.485	89.952	542.485	0.446	1440.692	1440.245	20.639	1539.075	1.411	7.510	0.974

* * * INDUCER EXIT * * * INITIAL INTEGRATED FLOW 2.654

MASS AVERAGE TOTAL PRESSURE 23.891
MASS AVERAGE TOTAL TEMPERATURE 623.890
INDUCER PRESSURE RATIO 1.625
INDUCER TEMPERATURE RATIO 1.202
INDUCER EFFICIENCY 0.734

INDUCER EXIT VELOCITY TRIANGLES

	MO	WO	ALPHA	VM	VU	U	WU	B	WO	MREL	I	VO/VOMAX
10	0.708	817.653	64.302	736.783	354.552	1043.495	688.942	46.921	1008.707	0.873	6.778	1.000
30	0.684	771.151	61.066	674.896	373.080	1125.979	752.899	41.878	1011.109	0.871	7.527	0.943
50	0.568	670.260	60.157	581.381	333.533	1208.464	874.930	33.603	1050.479	0.891	11.426	0.819
70	0.612	724.952	64.928	656.644	307.203	1290.948	983.744	33.722	1182.766	0.999	6.477	0.886
90	0.552	668.835	57.991	565.452	353.457	1373.432	1019.974	29.003	1166.227	0.965	6.646	0.815

TABLE LXX. (Continued)

* * * IMPELLER EXIT * * * INITIAL INTEGRATED FLOW 2.726

PCENT SPAN	R	MD	VO	VO/VMAX	ALP	VM	VM/VMMAX	VU	U	WU	B	WO
0.0233	0.0054	1.0687	1605.56	0.8152	12.934	359.37	0.5193	1564.82	2027.54	462.71	73.527	374.75
0.0636	0.0149	1.2503	1819.42	0.9238	15.934	529.94	0.7659	1740.53	2027.54	287.01	80.636	537.10
0.1273	0.0300	1.3300	1906.36	0.9679	20.184	657.77	0.9506	1789.28	2027.54	238.25	82.415	663.57
0.2122	0.0500	1.3804	1958.92	0.9946	20.684	691.92	1.0000	1832.65	2027.54	194.88	83.929	695.82
0.2971	0.0699	1.3874	1966.25	0.9983	19.684	662.30	0.9571	1851.35	2027.54	176.19	84.563	665.29
0.3820	0.0899	1.3910	1969.45	1.0000	18.684	630.92	0.9118	1865.66	2027.54	161.88	85.041	633.29
0.4668	0.1099	1.3874	1965.36	0.9979	17.684	597.02	0.8628	1872.49	2027.54	155.05	85.266	599.06
0.5517	0.1299	1.3640	1940.84	0.9854	16.434	549.09	0.7935	1861.55	2027.54	165.99	84.904	551.27
0.6366	0.1499	1.3207	1894.58	0.9619	14.184	464.25	0.6709	1836.82	2027.54	190.72	84.072	466.74
0.7215	0.1699	1.2597	1828.00	0.9281	10.434	331.06	0.4784	1797.77	2027.54	229.77	82.716	333.75
0.8064	0.1899	1.1882	1746.54	0.8868	6.434	195.72	0.2828	1735.54	2027.54	292.00	80.449	198.47
0.8701	0.2049	1.1296	1677.53	0.8517	3.934	115.09	0.1663	1673.58	2027.54	353.96	78.057	117.64
0.9125	0.2150	1.0710	1606.54	0.8157	1.934	54.22	0.0783	1605.62	2027.54	421.92	75.276	56.06
0.9550	0.2249	0.7738	1212.52	0.6156	-0.065	-1.39	-0.0020	1212.52	2027.54	815.01	56.092	-1.67

MASS AVERAGE TOTAL PRESSURE 173.578
MASS AVERAGE TOTAL TEMPERATURE 1134.000
MASS AVG VM 565.468 VU 1821.763 ANGLE 17.244
FLOW FACTOR 0.787 SLIP FACTOR INS. STA. 0.898 IMPELLER TIP 0.941
IMP. PRESS. RATIO 7.269 IMP. TEMP.RATIO 1.849 EFFICIENCY 0.885
IMP.+IND. PRESS. RATIO 11.888 IMP.+IND. TEMP. RATIO 2.224 EFFICIENCY 0.818
IMP.+IND.+IGV PRESS. RATIO 11.812 IMP.+IND.+IGV TEMP. RATIO 2.224 EFFICIENCY 0.815

* * * DIFFUSER * * *

CD DIFFUSER THROAT FRONT 0.854 REAR 0.820
STATIC PRESSURE RISE COEFFICIENT IMPELLER EXIT/DIFFUSER EXIT 0.737
DIFFUSER THROAT FRONT/DIFFUSER EXIT 0.695 DIFFUSER THROAT REAR/DIFFUSER EXIT 0.631
DIFFUSER LOSSES TOTAL TO STATIC 0.182 TOTAL TO TOTAL 0.144
DIFFUSER LOSS COEFFICIENT 0.262

TABLE LXXI.

10/1 CENTRIFUGAL COMPRESSOR, INDUCER TRAVERSE
101 PCT SPEED, WOD, 5 DEG IGV TURNING
BUILD 6

FLOW RATE = 3.150 SPEED = 65974.5

• • • INLET GUIDE VANE EXIT • • •

MD	VO	ALPHA	VM	VU	U	WU	B	WO	MREL	I	VO/VOMAX
10	0.497	542.485	85.078	540.485	46.543	980.178	933.635	30.066	1078.796	0.989	0.833	0.994
30	0.500	545.251	84.757	542.970	49.820	1096.305	1046.485	27.422	1178.960	1.081	3.477	0.999
50	0.500	545.466	84.743	543.171	49.977	1211.872	1161.895	25.055	1282.589	1.176	5.504	1.000
70	0.497	542.435	85.240	540.614	45.011	1327.854	1282.842	22.851	1392.103	1.277	6.818	0.994
90	0.486	531.187	86.849	530.385	29.199	1442.212	1413.013	20.574	1509.277	1.382	7.575	0.973

• • • INDUCER EXIT • • • INITIAL INTEGRATED FLOW 2.740

MASS AVERAGE TOTAL PRESSURE 23.178
MASS AVERAGE TOTAL TEMPERATURE 613.436
INDUCER PRESSURE RATIO 1.577
INDUCER TEMPERATURE RATIO 1.182
INDUCER EFFICIENCY 0.761

INDUCER EXIT VELOCITY TRIANGLES

MD	VO	ALPHA	VM	VU	U	WU	B	WO	MREL	I	VO/VOMAX
10	0.719	824.311	60.936	716.280	407.960	1043.837	635.876	48.403	957.808	0.835	5.296	1.000
30	0.683	784.537	59.397	675.267	399.390	1126.348	726.958	42.888	992.197	0.864	6.511	0.951
50	0.645	746.344	58.006	632.981	395.428	1208.860	813.431	37.888	1030.697	0.894	7.141	0.905
70	0.617	723.861	61.575	636.593	344.563	1291.371	946.808	33.915	1140.919	0.974	6.284	0.878
90	0.612	729.147	54.565	594.094	422.737	1373.882	951.145	31.989	1121.439	0.942	3.660	0.884

TABLE LXXII.

10/1 CENTRIFUGAL COMPRESSOR. IND AND IMP TRAV
101 PCT SPEED. NEAR STALL. 5 DEG IGV TURNING
BUILD 6

FLOW RATE = 3.142 SPEED = 66122.6

* * * INLET GUIDE VANE EXIT * * *

MD		VD	ALPHA	VM	VU	U	WU	B	WD	MREL	I	VD/VDMAX
10	0.494	539.611	82.981	535.567	65.937	982.067	916.130	30.910	1061.191	0.973	0.589	0.994
30	0.497	542.485	82.740	538.136	68.553	1098.767	1030.214	27.580	1162.296	1.066	3.319	0.999
50	0.497	542.592	83.342	538.933	62.909	1214.314	1151.405	25.082	1271.292	1.166	5.477	1.000
70	0.492	536.735	83.187	532.945	63.670	1330.500	1266.829	22.816	1374.368	1.260	6.853	0.989
90	0.481	525.426	83.784	523.921	58.806	1449.229	1406.423	20.433	1500.864	1.374	7.716	0.968

* * * INDUCER EXIT * * * INITIAL INTEGRATED FLOW 2.716

MASS AVERAGE TOTAL PRESSURE 23.454
MASS AVERAGE TOTAL TEMPERATURE 614.369
INDUCER PRESSURE RATIO 1.596
INDUCER TEMPERATURE RATIO 1.184
INDUCER EFFICIENCY 0.775

INDUCER EXIT VELOCITY TRIANGLES

MD		VD	ALPHA	VM	VU	U	WU	B	WD	MREL	I	VD/VDMAX
10	0.713	819.057	59.688	707.084	413.313	1046.181	632.798	48.173	948.896	0.826	3.926	1.000
30	0.680	782.780	58.504	667.463	408.947	1128.878	719.931	42.834	981.737	0.853	6.565	0.955
50	0.671	775.305	56.839	649.039	424.683	1211.575	787.491	39.494	1020.488	0.883	9.330	0.946
70	0.697	719.215	58.845	610.354	368.077	1294.271	925.293	33.410	1108.488	0.943	6.789	0.870
90	0.569	659.509	52.578	523.772	400.768	1376.968	976.200	28.215	1107.838	0.923	7.434	0.805

TABLE LXXII. (Continued)

* * * IMPELLER EXIT * * * INITIAL INTEGRATED FLOW 2.662

PCENT SPAN	R	MO	VO	VO/VMAX	ALP	VM	VM/VMMAX	VU	U	WU	B	WO
0.0445	0.0105	1.0945	1626.31	0.8256	20.524	570.19	0.8525	1523.08	2032.76	509.68	71.497	601.27
0.1061	0.0250	1.3359	1600.40	0.9647	20.524	666.29	0.9962	1779.77	2032.76	252.99	81.909	672.99
0.1697	0.0400	1.3734	1939.30	0.9844	20.174	668.82	1.0000	1820.31	2032.76	212.44	83.343	673.36
0.2946	0.0600	1.3921	1959.07	0.9965	19.574	656.34	0.9813	1845.85	2032.76	186.91	84.217	659.70
0.3395	0.0799	1.3992	1965.81	0.9979	18.824	634.30	0.9483	1860.66	2032.76	172.10	84.719	637.01
0.4244	0.1000	1.4027	1969.84	1.0000	17.924	606.24	0.9064	1874.23	2032.76	158.52	85.165	608.40
0.5093	0.1199	1.3886	1955.91	0.9929	16.824	566.11	0.8464	1872.19	2032.76	160.57	85.097	568.19
0.5942	0.1399	1.3441	1909.94	0.9695	15.324	504.76	0.7547	1842.03	2032.76	190.73	84.088	507.46
0.6791	0.1599	1.2773	1837.99	0.9330	12.674	403.27	0.6029	1793.20	2032.76	239.55	82.390	406.65
0.7640	0.1800	1.2070	1760.05	0.8934	8.924	273.03	0.4082	1738.74	2032.76	294.02	80.402	276.91
0.8488	0.1999	1.1097	1645.94	0.8355	4.174	119.81	0.1791	1641.57	2032.76	391.18	76.596	123.16
0.9125	0.2150	0.9378	1429.91	0.7259	1.424	35.54	0.0531	1429.47	2032.76	603.29	67.118	38.98

MASS AVERAGE TOTAL PRESSURE 168.163
MASS AVERAGE TOTAL TEMPERATURE 1145.498
MASS AVG VM 557.524 VU 801.409 ANGLE 17.486
FLOW FACTOR 0.787 SLIP FACTOR INS. STA. 0.886 IMPELLER TIP 0.928
IMP. PRESS. RATIO 7.169 IMP. TEMP.RATIO 1.864 EFFICIENCY 0.862
IMP.+IND. PRESS. RATIO 11.924 IMP.+IND. TEMP. RATIO 2.208 EFFICIENCY 0.815
IMP.+IND.+IGV PRESS. RATIO 11.444 IMP.+IND.+IGV TEMP. RATIO 2.208 EFFICIENCY 0.812

TABLE LXXIII.

10/1 CENTRIFUGAL COMPRESSOR, INDUCER TRAVERSE
100 PCT SPEED, NEAR STALL, 10 DEG IGV TURNING
BUILD 6

FLOW RATE = 3.058 SPEED = 69238.1

* * * INLET GUIDE VANE EXIT * * *

	MD	VD	ALPHA	VM	VU	U	WU	B	WD	MREL	I	VD/VDMAX
10	0.488	930.698	78.793	928.853	183.193	989.393	886.197	31.019	1010.737	0.926	-0.119	0.994
30	0.489	933.963	78.932	926.032	182.499	1083.791	981.291	28.103	1112.449	1.019	2.796	1.000
90	0.489	933.963	79.418	926.882	98.097	1198.085	1100.028	25.508	1218.837	1.117	9.051	1.000
70	0.483	928.284	79.888	919.878	93.459	1312.859	1219.399	23.898	1323.594	1.214	6.579	0.989
90	0.484	908.219	83.181	904.991	81.903	1429.913	1384.869	20.287	1459.136	1.338	7.862	0.991

* * * INDUCER EXIT * * * INITIAL INTEGRATED FLOW 2.869

MASS AVERAGE TOTAL PRESSURE 23.988
MASS AVERAGE TOTAL TEMPERATURE 609.348
INDUCER PRESSURE RATIO 1.805
INDUCER TEMPERATURE RATIO 1.174
INDUCER EFFICIENCY 0.829

INDUCER EXIT VELOCITY TRIANGLES

	MD	VD	ALPHA	VM	VU	U	WU	B	WD	MREL	I	VD/VDMAX
10	0.806	919.383	82.889	727.628	892.110	1032.187	480.077	56.983	871.732	0.769	-2.883	1.000
30	0.778	888.284	82.656	701.696	931.925	1113.778	582.269	50.315	911.807	0.804	-0.915	0.963
90	0.761	869.610	82.339	669.340	916.759	1199.368	678.609	44.606	953.164	0.835	0.423	0.925
70	0.718	819.969	82.227	669.806	901.126	1278.959	775.892	39.912	1011.912	0.877	0.287	0.897
90	0.828	732.465	45.037	918.287	917.304	1358.549	840.935	31.644	987.830	0.837	4.005	0.[illegible]

TABLE LXXIV.

10/1 CENTRIFUGAL COMPRESSOR, IND AND INP TRAV
100 PCT SPEED, NEAR STALL, -4 DEG IGV TURNING
BUILD 6

FLOW RATE = 3.209 SPEED = 65987.7

* * * INLET GUIDE VANE EXIT * * *

	MD	WD	ALPHA	WM	WU	U	MU	B	WO	MREL	I	VO/VOMAX
ID	0.524	970.828	84.770	988.842	-47.551	979.133	1026.685	28.988	1173.739	1.079	1.911	1.000
3D	0.522	967.985	93.854	988.680	-38.161	1096.216	1134.397	26.344	1268.063	1.166	4.359	0.994
5D	0.522	967.985	84.124	988.[illegible]	-46.851	1242.106	1252.958	24.328	1375.071	1.264	6.231	0.994
7D	0.516	959.283	93.419	984.289	-33.706	1327.750	1361.457	22.559	1473.736	1.354	7.160	0.990
9D	0.497	942.465	93.526	961.213	-37.127	1442.146	1479.274	20.095	1575.171	1.445	8.054	0.950

* * * INDUCER EXIT * * * INITIAL INTEGRATED FLOW 3.051

MASS AVERAGE TOTAL PRESSURE 25.036
MASS AVERAGE TOTAL TEMPERATURE 632.918
INDUCER PRESSURE RATIO 1.705
INDUCER TEMPERATURE RATIO 1.220
INDUCER EFFICIENCY 0.767

INDUCER EXIT VELOCITY TRIANGLES

	MD	WD	ALPHA	WM	WU	U	MU	B	WO	MREL	I	VO/VOMAX
1D	0.835	952.979	69.827	727.875	614.493	1044.047	429.551	59.453	845.173	0.741	-5.793	1.000
3D	0.806	927.390	69.667	709.044	597.753	1126.575	528.821	53.283	884.531	0.769	-3.883	0.973
5D	0.658	775.819	63.958	538.820	358.183	1209.103	650.919	39.617	844.999	0.717	5.412	0.814
7D	0.604	689.133	52.694	652.344	497.056	1291.630	794.574	39.386	1028.057	0.870	9.814	0.680
9D	0.579	702.249	64.956	496.607	497.365	1374.158	876.793	29.526	1007.663	0.831	6.123	0.737

TABLE LXXIV. (Continued)

* * * IMPELLER EXIT * * * INITIAL INTEGRATED FLOW 2.678

PCENT SPAN	R	MD	VO	VO/VMAX	ALP	VM	VM/VMMAX	VU	U	WU	B	WO
0.0233	0.0095	0.9281	1424.74	0.7245	11.220	277.22	0.4067	1397.91	2028.61	631.10	65.696	304.17
0.0848	0.0200	1.1484	1700.92	0.8648	15.220	446.43	0.6550	1640.88	2028.61	387.73	76.705	458.72
0.1697	0.0295	1.3148	1888.89	0.9605	19.470	629.51	0.9237	1780.65	2028.61	247.96	82.072	639.58
0.2546	0.0400	1.3710	1948.87	0.9910	20.470	681.48	1.0000	1829.62	2028.61	202.99	83.655	685.68
0.3395	0.0799	1.3816	1959.71	0.9966	19.220	645.13	0.9466	1850.47	2028.61	178.14	84.801	648.11
0.4244	0.0999	1.3874	1966.29	1.0000	18.220	614.78	0.9021	1867.67	2028.61	160.94	85.074	617.06
0.5093	0.1200	1.3874	1965.80	0.9997	17.470	590.14	0.8659	1875.13	2028.61	153.48	85.320	592.12
0.5942	0.1400	1.3817	1959.24	0.9962	16.220	561.68	0.7946	1882.06	2028.61	146.56	84.888	563.84
0.6791	0.1599	1.3714	1887.34	0.9598	13.970	459.63	0.6685	1831.52	2028.61	197.09	83.858	458.26
0.7640	0.1800	1.2492	1817.71	0.9244	10.470	330.31	0.4847	1787.45	2028.61	241.16	82.316	333.31
0.8488	0.2000	1.1483	1725.07	0.8773	6.720	201.86	0.2962	1713.22	2028.61	315.39	79.369	203.23
0.9185	0.2197	1.1062	1691.39	0.8598	3.220	92.75	0.1361	1688.75	2028.61	339.86	77.029	93.18
0.9550	0.2350	1.0900	1582.36	0.8047	-0.029	-0.82	-0.0012	1582.36	2028.61	446.25	74.250	-0.85
0.9868	0.2329	0.8763	1356.32	0.6898	-2.529	-59.87	-0.0878	1355.00	2028.61	673.61	63.566	-66.66

MASS AVERAGE TOTAL PRESSURE 172.985
MASS AVERAGE TOTAL TEMPERATURE 1159.000
MASS AVG VM 590.2**1 VU 1808.291 ANGLE 18.924
FLOW FACTOR 0.808 SLIP FACTOR INS. ETA. 0.891 IMPELLER TIP 0.934
IMP. PRESS. RATIO 6.909 IMP. TEMP.RATIO 1.831 EFFICIENCY 0.875
IMP..IND. PRESS. RATIO 11.992 IMP.IND. TEMP. RATIO 2.234 EFFICIENCY 0.812
IMP..IND..IGV PRESS. RATIO 11.772 IMP..IND..IGV TEMP. RATIO 2.234 EFFICIENCY 0.807

TABLE LXXV.

10/1 CENTRIFUGAL COMPRESSOR, IMPELLER TRAVERSE
8/1 SPEEDLINE, NEAR STALL, 10 DEG IGV TURNING
BUILD 6

FLOW RATE = 2.796 SPEED = 61819.2

* * * IMPELLER EXIT * * * INITIAL INTEGRATED FLOW 2.518

PCENT SPAN	R	BO	VO	VO/VMAX	ALP	VM	VM/VMMAX	VU	U	WU	B	WO
0.0469	0.0104	0.9624	1415.57	0.7505	12.782	313.18	0.5110	1380.49	1900.46	519.97	69.360	334.66
0.1273	0.0300	1.1624	1660.31	0.8802	15.531	444.59	0.7254	1599.68	1900.46	300.78	79.351	452.38
0.2122	0.0500	1.2960	1812.13	0.9607	17.782	553.41	0.9030	1725.55	1900.46	174.91	84.212	556.25
0.2971	0.0699	1.3405	1866.56	0.9896	18.782	600.96	0.9806	1767.15	1900.46	133.31	85.685	602.67
0.3820	0.0899	1.3483	1879.28	0.9963	19.032	612.82	1.0000	1776.55	1900.46	123.90	86.010	614.31
0.4668	0.1099	1.3545	1886.12	1.0000	18.782	607.27	0.9909	1785.69	1900.46	114.77	86.322	608.52
0.5517	0.1299	1.3466	1875.14	0.9941	18.032	580.44	0.9471	1783.04	1900.46	117.42	86.232	581.70
0.6366	0.1499	1.3061	1830.26	0.9703	16.532	520.80	0.8498	1754.60	1900.46	145.86	85.247	522.59
0.7215	0.1699	1.2374	1753.29	0.9295	14.032	425.10	0.6936	1700.97	1900.46	199.49	83.310	420.02
0.8064	0.1899	1.1613	1664.49	0.8824	10.032	289.95	0.4731	1639.04	1900.46	261.41	80.938	293.61
0.8913	0.2099	1.0748	1545.60	0.8194	4.782	128.84	0.2102	1540.22	1900.46	360.24	76.835	132.32
0.9550	0.2269	0.9893	1394.79	0.7395	1.782	43.37	0.0707	1394.12	1900.46	506.34	70.038	46.14

MASS AVERAGE TOTAL PRESSURE 141.717
MASS AVERAGE TOTAL TEMPERATURE 1093.729
MASS AVG VR 913.392 VU 1712.168 ANGLE 16.691
FLOW FACTOR 0.617 SLIP FACTOR INS. STA. 0.900 IMPELLER TIP 0.944
IMP. PRESS. RATIO 0.000 IMP. TEMP.RATIO 0.000 EFFICIENCY 0.000
IMP.+IND. PRESS. RATIO 9.704 IMP.+IND. TEMP. RATIO 2.108 EFFICIENCY 0.808
IMP.+IND.+IGV PRESS. RATIO 9.644 IMP.+IND.+IGV TEMP. RATIO 2.108 EFFICIENCY 0.805

TABLE LXXVI.

10/1 CENTRIFUGAL COMPRESSOR, IMPELLER TRAVERSE
8/1 SPEEDLINE, NEAR STALL, 15 DEG IGV TURNING
BUILD 6

FLOW RATE = 2.787 SPEED = 61700.7

* * * IMPELLER EXIT * * * INITIAL INTEGRATED FLOW 2.690

PCENT SPAN	R	MD	VD	VD/VMAX	ALP	VM	VM/VMMAX	VU	U	WU	B	WD
0.0233	0.0054	1.0968	1569.58	0.8355	13.275	359.73	0.5863	1524.72	1896.82	372.10	76.285	370.28
0.0536	0.0149	1.2351	1725.32	0.9202	16.025	476.29	0.7762	1658.28	1896.82	238.54	81.814	481.19
0.1279	0.0300	1.2843	1781.10	0.9499	18.275	558.51	0.9103	1691.26	1896.82	205.56	83.070	562.62
0.2122	0.0500	1.3300	1835.74	0.9791	19.525	613.54	1.0000	1730.18	1896.82	166.64	84.498	616.38
0.2971	0.0699	1.3382	1851.90	0.9877	19.275	611.32	0.9963	1748.09	1896.82	148.73	85.136	613.53
0.3820	0.0898	1.3453	1864.72	0.9945	18.900	604.02	0.9844	1764.18	1896.82	132.64	85.700	605.72
0.4668	0.1099	1.3523	1874.91	1.0000	18.650	599.57	0.9772	1776.46	1896.82	120.36	86.123	600.95
0.5517	0.1298	1.3524	1852.95	0.9882	17.775	565.67	0.9219	1764.49	1896.82	132.32	85.711	567.26
0.6366	0.1499	1.2867	1802.35	0.9613	15.275	474.83	0.7739	1738.68	1896.82	158.14	84.802	476.79
0.7215	0.1699	1.2234	1731.02	0.9232	11.525	345.85	0.5637	1696.12	1896.82	200.70	83.251	348.26
0.8064	0.1899	1.1978	1652.88	0.8815	7.525	216.46	0.3528	1638.65	1896.82	258.17	81.046	219.13
0.8913	0.2099	1.0921	1563.68	0.8340	3.525	96.14	0.1567	1560.72	1896.82	336.10	77.846	98.34
0.9590	0.2249	1.0007	1432.18	0.7638	1.025	25.62	0.0417	1431.95	1896.82	464.87	72.014	26.93

MASS AVERAGE TOTAL PRESSURE 141.334
MASS AVERAGE TOTAL TEMPERATURE 1083.183
MASS AVG VM 928.134 VU 1723.003 ANGLE 17.041
FLOW FACTOR 0.803 SLIP FACTOR INS. STA. 0.908 IMPELLER TIP 0.952
IMP. PRESS. RATIO 9.008 IMP. TEMP.RATIO 0.000 EFFICIENCY 0.000
IMP..IND. PRESS. RATIO 9.689 IMP.IND. TEMP. RATIO 2.088 EFFICIENCY 0.823
IMP..IND..IGV PRESS. RATIO 9.619 IMP..IND..IGV TEMP. RATIO 2.088 EFFICIENCY 0.820

TABLE LXXVII.

10/1 CENTRIFUGAL COMPRESSOR. IMPELLER TRAVERSE
95 PCT SPEED. NOD. 10 DEG IGV TURNING
BUILD 6

FLOW RATE = 2.885 SPEED = 62114.1

* * * IMPELLER EXIT * * * INITIAL INTEGRATED FLOW 2.625

PCENT SPAN	R	MD	WD	VD/VMAX	ALP	VM	VM/VMMAX	VU	U	WU	B	WD
0.0233	0.0054	1.0140	1476.81	0.7866	8.382	215.30	0.3379	1461.04	1909.53	448.49	72.935	225.21
0.0638	0.0149	1.1935	1622.17	0.8640	12.382	347.86	0.5460	1584.44	1909.53	325.09	78.405	355.11
0.1273	0.0300	1.2528	1734.40	0.9238	17.382	518.16	0.8134	1655.19	1909.53	254.34	81.264	524.24
0.2122	0.0500	1.3148	1828.93	0.9741	20.382	637.00	1.0000	1714.42	1909.53	195.11	83.507	641.11
0.2971	0.0699	1.3371	1859.03	0.9902	19.882	632.25	0.9925	1748.22	1909.53	161.31	84.728	634.94
0.3820	0.0899	1.3488	1875.33	0.9988	19.132	614.65	0.9649	1771.73	1909.53	137.79	85.552	616.51
0.4668	0.1099	1.3489	1877.40	1.0000	18.632	599.83	0.9416	1778.99	1909.53	130.53	85.803	601.44
0.5517	0.1299	1.3305	1858.06	0.9896	17.882	570.55	0.8956	1768.29	1909.53	141.24	85.433	572.37
0.6366	0.1499	1.2902	1808.94	0.9635	15.882	495.05	0.7771	1739.88	1909.53	169.64	84.438	497.40
0.7215	0.1699	1.2152	1726.38	0.9195	12.382	370.21	0.5811	1686.22	1909.53	223.30	82.456	373.44
0.8064	0.1899	1.1484	1649.27	0.8786	8.382	240.44	0.3774	1631.64	1909.53	277.88	80.334	243.90
0.8913	0.2099	1.0851	1561.49	0.8317	4.632	126.11	0.1979	1596.39	1909.53	313.18	77.214	128.32
0.9550	0.2249	0.9488	1374.75	0.7322	2.382	57.15	0.0897	1573.56	1909.53	335.97	68.683	61.35

MASS AVERAGE TOTAL PRESSURE 145.894
MASS AVERAGE TOTAL TEMPERATURE 1089.831
MASS AVG VM 927.524 VU 1716.098 ANGLE 17.087
FLOW FACTOR 0.808 SLIP FACTOR INS. STA. 0.898 IMPELLER TIP 0.942
IMP. PRESS. RATIO 0.000 IMP. TEMP.RATIO 0.000 EFFICIENCY 0.000
IMP..IND. PRESS. RATIO 9.988 IMP.IND. TEMP. RATIO 2.101 EFFICIENCY 0.828
IMP..IND..IGV PRESS. RATIO 9.928 IMP..IND..IGV TEMP. RATIO 2.101 EFFICIENCY 0.825

TABLE LXXVIII.

10/1 CENTRIFUGAL COMPRESSOR, IMPELLER TRAVERSE
95 PCT SPEED, NEAR STALL, 10 DEG IGV TURNING
BUILD 6

FLOW RATE = 2.877 SPEED = 62138.8

* * * IMPELLER EXIT * * * INITIAL INTEGRATED FLOW 2.621

PCENT SPAN	R	MD	VD	VD/VMAX	ALP	VM	VM/VMMAX	VU	U	WU	S	WD
0.0536	0.0149	1.0886	1568.89	0.8328	14.994	405.92	0.6103	1515.47	1910.29	394.82	75.397	419.47
0.1273	0.0300	1.2679	1774.45	0.9419	18.994	577.55	0.8684	1677.82	1910.29	232.46	82.111	583.06
0.2122	0.0500	1.3218	1835.26	0.9742	21.244	665.01	1.0000	1710.54	1910.29	199.75	83.339	669.53
0.2971	0.0699	1.3394	1860.98	0.9879	20.244	643.95	0.9683	1746.01	1910.29	164.27	84.625	646.80
0.3820	0.0899	1.3476	1870.33	0.9930	19.244	618.44	0.9299	1771.48	1910.29	138.80	85.519	620.34
0.4668	0.1098	1.3523	1883.74	1.0000	18.994	613.12	0.9219	1781.17	1910.29	129.12	85.853	614.73
0.5517	0.1299	1.3312	1851.28	0.9830	16.244	582.72	0.8762	1767.71	1910.29	142.58	85.388	584.61
0.6366	0.1499	1.2808	1805.29	0.9583	15.994	497.44	0.7480	1735.40	1910.29	174.89	84.243	499.96
0.7215	0.1699	1.2117	1727.16	0.9168	12.494	373.67	0.5619	1686.25	1910.29	224.04	82.431	376.95
0.8064	0.1898	1.1390	1640.44	0.8708	8.494	242.32	0.3643	1622.44	1910.29	287.84	79.939	246.10
0.8913	0.2099	1.0558	1532.77	0.8136	4.744	126.78	0.1906	1527.52	1910.29	382.77	75.932	130.70

MASS AVERAGE TOTAL PRESSURE 149.845
MASS AVERAGE TOTAL TEMPERATURE 1094.412
MASS AVG VM 553.898 VU 1719.142 ANGLE 17.858
FLOW FACTOR 0.770 SLIP FACTOR INS. STA. 0.899 IMPELLER TIP 0.943
IMP. PRESS. RATIO 0.000 IMP. TEMP.RATIO 0.000 EFFICIENCY 0.000
IMP..IND. PRESS. RATIO 9.985 IMP.IND. TEMP. RATIO 2.109 EFFICIENCY 0.821
IMP..IND..IGV PRESS. RATIO 9.925 IMP..IND..IGV TEMP. RATIO 2.109 EFFICIENCY 0.816

TABLE LXXIX.

10/1 CENTRIFUGAL COMPRESSOR, IMPELLER TRAVERSE
101 PCT SPEED, NEAR STALL, -4 DEG IGV TURNING
BUILD 6

FLOW RATE = 1.209 SPEED = 65987.7

* * * IMPELLER EXIT * * * INITIAL INTEGRATED FLOW 2.635

PCENT SPAN	R	MD	VD	VD/VMAX	ALP	VM	VM/VMMAX	VU	U	WU	B	MD
0.0233	0.2055	0.9283	1628.75	0.7131	11.431	283.17	0.4053	1400.40	2028.61	628.21	65.839	310.36
0.0848	0.2200	1.1484	1713.64	0.8553	15.431	455.98	0.6527	1651.86	2028.61	376.75	77.152	467.69
0.1697	0.2399	1.3148	1908.73	0.9527	19.681	642.85	0.9202	1797.22	2028.61	231.39	82.663	648.15
0.2546	0.2600	1.3722	1978.01	0.9873	20.681	698.58	1.0000	1859.54	2028.61	178.07	84.503	701.81
0.3395	0.2799	1.3828	1995.37	0.9959	19.431	663.82	0.9502	1881.71	2028.61	146.90	85.536	665.84
0.4244	0.2998	1.3874	2002.57	0.9995	18.431	633.16	0.9063	1899.84	2028.61	128.77	86.122	634.61
0.5093	0.3200	1.3874	2003.43	1.0000	17.681	608.50	0.8710	1908.78	2028.61	119.82	86.407	609.70
0.5942	0.3400	1.3817	1975.51	0.9860	16.431	558.82	0.7999	1894.83	2028.61	133.78	85.961	560.21
0.6791	0.3599	1.3124	1919.89	0.9583	14.181	470.37	0.6733	1861.38	2028.61	167.23	84.866	472.26
0.7640	0.3800	1.2503	1847.33	0.9220	10.681	342.41	0.4901	1815.32	2028.61	213.29	83.298	344.76
0.8488	0.2000	1.1683	1744.42	0.8707	6.931	210.52	0.3013	1731.67	2028.61	296.94	80.269	213.60
0.9125	0.2150	1.1062	1647.38	0.8222	3.431	98.61	0.1411	1644.42	2028.61	384.18	76.849	101.26
0.9550	0.2250	1.0500	1557.30	0.7773	0.181	4.94	0.0070	1557.29	2028.61	471.32	73.161	5.16
0.9888	0.2325	0.8749	1328.10	0.6619	-2.318	-53.64	-0.0767	1325.02	2028.61	703.59	62.031	-60.73

MASS AVERAGE TOTAL PRESSURE 172.839
MASS AVERAGE TOTAL TEMPERATURE 1194.597
MASS AVG VM 564.387 VU 1833.951 ANGLE 17.108
FLOW FACTOR 0.600 SLIP FACTOR INS. STA. 0.909 IMPELLER TIP 0.947
IMP. PRESS. RATIO 0.000 IMP. TEMP.RATIO 0.000 EFFICIENCY 0.000
IMP..IND. PRESS. RATIO 11.892 IMP.IND. TEMP. RATIO 2.303 EFFICIENCY 0.768
IMP..IND..IGV PRESS. RATIO 11.782 IMP..IND..IGV TEMP. RATIO 2.303 EFFICIENCY 0.763

TABLE LXXX.

ID/1 CENTRIFUGAL COMPRESSOR, IMPELLER TRAVERSE
ID1 PCT SPEED, NS, -4 DEG IGV, WITH COOLANT
BUILD 6

FLOW RATE = 9.214 SPEED = 65779.6

* * * IMPELLER EXIT * * * INITIAL INTEGRATED FLOW 2.657

PCENT SPAN	R	MD	VD	VD/VMAX	ALP	VM	VM/VMMAX	VU	U	WU	B	WD
0.0742	0.0175	1.2714	1855.99	0.9256	19.395	616.36	0.8368	1750.65	2022.22	271.56	81.182	623.73
0.1697	0.0400	1.3748	1974.93	0.9849	21.895	736.49	1.0000	1832.47	2022.22	189.75	84.088	740.43
0.2546	0.0600	1.3839	1994.03	0.9944	20.395	694.92	0.9435	1869.02	2022.22	153.19	85.314	697.26
0.3395	0.0799	1.3886	2002.12	0.9999	19.645	674.13	0.9153	1888.40	2022.22	133.81	85.946	675.82
0.4244	0.1000	1.3874	2000.16	1.0000	18.645	641.08	0.8704	1899.91	2022.22	122.30	86.316	642.41
0.5093	0.1199	1.3837	1994.64	0.9896	17.395	593.29	0.8055	1893.68	2022.22	128.54	86.116	594.65
0.5942	0.1399	1.3253	1910.90	0.9654	15.895	530.22	0.7199	1861.87	2022.22	160.34	85.077	532.18
0.6791	0.1599	1.2550	1809.40	0.9293	12.645	406.19	0.9515	1810.39	2022.22	211.83	83.326	408.96
0.7640	0.1800	1.1871	1711.54	0.8849	8.645	266.76	0.3622	1754.37	2022.22	267.84	81.319	269.85
0.8276	0.1949	1.1425	1716.47	0.8560	5.895	176.31	0.2393	1707.39	2022.22	314.82	79.592	179.28
0.8701	0.2050	1.0911	1590.96	0.7934	3.895	108.09	0.1467	1587.27	2022.22	434.95	74.675	112.07

MASS AVERAGE TOTAL PRESSURE 174.860
MASS AVERAGE TOTAL TEMPERATURE 1196.437
MASS AVG VM 600.044 VU 1861.002 ANGLE 18.052
FLOW FACTOR 0.755 SLIP FACTOR INS. STA. 0.910 IMPELLER TIP 0.954
IMP. PRESS. RATIO 0.000 IMP. TEMP.RATIO 0.000 EFFICIENCY 0.000
IMP..IND. PRESS. RATIO 12.031 IMP.IND. TEMP. RATIO 2.302 EFFICIENCY 0.773
IMP..IND..IGV PRESS. RATIO 11.900 IMP..IND..IGV TEMP. RATIO 2.302 EFFICIENCY 0.768

TABLE LXXXI.

10/1 CENTRIFUGAL COMPRESSOR. IMPELLER TRAVERSE
101 PCT SPEED. NEAR STALL. 0 DEG IGV TURNING
BUILD 6

FLOW RATE = 3.185 SPEED = 65952.8

* * * IMPELLER EXIT * * * INITIAL INTEGRATED FLOW 2.679

PCENT SPAN	R	MD	VD	VD/VMAX	ALP	VM	VM/VMMAX	VU	U	WU	B	WD
0.0233	0.0094	1.0687	1613.46	0.8022	13.192	368.22	0.9189	1570.88	2027.54	456.66	73.790	383.47
0.0536	0.0149	1.2915	1836.50	0.9131	17.192	542.83	0.7650	1754.44	2027.54	273.10	81.152	549.37
0.1273	0.0300	1.3312	1927.59	0.9584	20.442	673.24	0.9488	1806.20	2027.54	221.34	83.013	678.27
0.2122	0.0500	1.3816	1983.03	0.9870	20.942	709.50	1.0000	1853.90	2027.54	173.63	84.649	712.61
0.2971	0.0699	1.3874	1998.23	0.9936	19.942	681.54	0.9605	1878.41	2027.54	149.13	85.460	683.69
0.3820	0.0899	1.3921	2011.07	1.0000	18.942	652.82	0.9201	1902.16	2027.54	125.38	86.228	654.24
0.4668	0.1099	1.3886	2009.88	0.9994	17.942	619.16	0.8726	1912.13	2027.54	115.41	86.545	620.29
0.5517	0.1299	1.3852	1984.84	0.9869	16.692	570.11	0.8035	1901.20	2027.54	126.34	86.198	571.36
0.6366	0.1499	1.3218	1936.46	0.9628	14.442	482.95	0.6806	1875.24	2027.54	152.29	85.356	484.55
0.7215	0.1699	1.2597	1864.23	0.9269	10.692	345.88	0.4874	1831.86	2027.54	195.67	83.902	347.84
0.8064	0.1899	1.1882	1779.12	0.8846	6.692	207.33	0.2922	1767.00	2027.54	260.54	81.612	209.57
0.8701	0.2049	1.1296	1706.65	0.8485	4.192	124.75	0.1758	1701.89	2027.54	325.65	79.167	127.01
0.9125	0.2150	1.0710	1631.79	0.8113	2.192	62.42	0.0879	1630.55	2027.54	396.98	76.316	64.24
0.9550	0.2249	0.7738	1221.61	0.6074	0.192	4.10	0.0057	1221.60	2027.54	805.94	56.585	4.91

MASS AVERAGE TOTAL PRESSURE 175.429
MASS AVERAGE TOTAL TEMPERATURE 1193.339
MASS AVG VM 382.262 VU 1850.259 ANGLE 17.468
FLOW FACTOR 0.778 SLIP FACTOR INS. STA. 0.912 IMPELLER TIP 0.956
IMP. PRESS. RATIO 0.000 IMP. TEMP.RATIO 0.000 EFFICIENCY 0.000
IMP..IND. PRESS. RATIO 11.877 IMP.IND. TEMP. RATIO 2.300 EFFICIENCY 0.768
IMP..IND..IGV PRESS. RATIO 11.802 IMP..IND..IGV TEMP. RATIO 2.300 EFFICIENCY 0.766

TABLE LXXXII.

10/1 CENTRIFUGAL COMPRESSOR, IMPELLER TRAVERSE
101 PCT SPEED, NEAR STALL, 5 DEG IGV TURNING
BUILD 6

FLOW RATE = 3.142 SPEED = 66122.6

* * * IMPELLER EXIT * * * INITIAL INTEGRATED FLOW 2.791

PCENT SPAN	R	MD	VD	VD/VMAX	ALP	VM	VM/VMMAX	VU	U	WU	B	MO
0.0445	0.0105	1.0957	1651.56	0.8143	20.931	590.02	0.8467	1542.57	2032.76	490.18	72.371	619.09
0.1061	0.0250	1.3359	1935.21	0.9542	20.931	691.35	0.9921	1807.50	2032.76	225.25	82.896	696.70
0.1697	0.0400	1.3746	1982.24	0.9774	20.581	696.83	1.0000	1855.72	2032.76	177.03	84.550	699.99
0.2546	0.0600	1.3921	2007.59	0.9899	19.981	686.02	0.9844	1886.74	2032.76	146.01	85.374	688.07
0.3395	0.0799	1.4003	2021.17	0.9966	19.231	665.74	0.9553	1908.38	2032.76	124.38	86.271	667.15
0.4244	0.1000	1.4039	2027.99	1.0000	18.331	637.82	0.9153	1925.08	2032.76	107.68	86.798	638.82
0.5093	0.1199	1.3898	2012.87	0.9925	17.231	596.27	0.8556	1922.52	2032.76	110.23	86.718	597.25
0.5942	0.1399	1.3441	1959.98	0.9664	15.731	531.40	0.7625	1886.56	2032.76	146.19	85.568	532.99
0.6791	0.1599	1.2785	1883.78	0.9290	13.081	426.81	0.6125	1836.84	2032.76	195.91	83.911	429.23
0.7640	0.1800	1.2070	1803.24	0.8891	9.331	292.38	0.4195	1779.38	2032.76	253.38	81.895	295.33
0.8488	0.1999	1.1109	1682.05	0.8294	4.581	134.35	0.1928	1676.68	2032.76	356.08	78.009	137.35
0.9125	0.2150	0.9378	1436.17	0.7081	1.831	45.89	0.0658	1435.44	2032.76	597.32	67.406	49.71

MASS AVERAGE TOTAL PRESSURE 167.975
MASS AVERAGE TOTAL TEMPERATURE 1201.682
MASS AVG VM 592.988 VU 1841.147 ANGLE 17.851
FLOW FACTOR 0.772 SLIP FACTOR INS. STA. 0.905 IMPELLER TIP 0.949
IMP. PRESS. RATIO 0.000 IMP. TEMP.RATIO 0.000 EFFICIENCY 0.000
IMP.+IND. PRESS. RATIO 11.911 IMP+IND. TEMP. RATIO 2.316 EFFICIENCY 0.746
IMP.+IND.+IGV PRESS. RATIO 11.491 IMP.+IND.+IGV TEMP. RATIO 2.316 EFFICIENCY 0.743

STATIC PRESSURE DISTRIBUTIONS

This section consists of static pressures along the entire flow path of the rig for Builds No. 3 and 6. Figures 220 through 229 consist of static pressure profiles along the inlet flow path; Figures 230 through 239 of static pressure variations along the impeller shroud; and Figures 240 and 241 of diffuser static pressure profiles.

Figures 220 through 225 are Build No. 3 data, which had a straight axial inlet, shroud, and hub static pressure taps from the inlet guide vane leading edge to the impeller. Figures 226 through 229 consist of Build No. 6 static pressures with the converging inlet, which had only shroud static taps. These taps range from the inlet guide vane trailing edge through the inducer. Figures 230 through 235 show Build No. 3 shroud static pressures along the impeller shroud and Figures 236 through 239 show the pressures for Build No. 6. Figure 240 is a Build No. 3 diffuser static pressure profile for 95% speed and inlet guide vanes of 0, 10, and 20 deg. Figure 241 is a Build No. 3 diffuser static pressure profile for a 10-deg inlet guide vane at speeds of 30, 70, 95, and 100%.

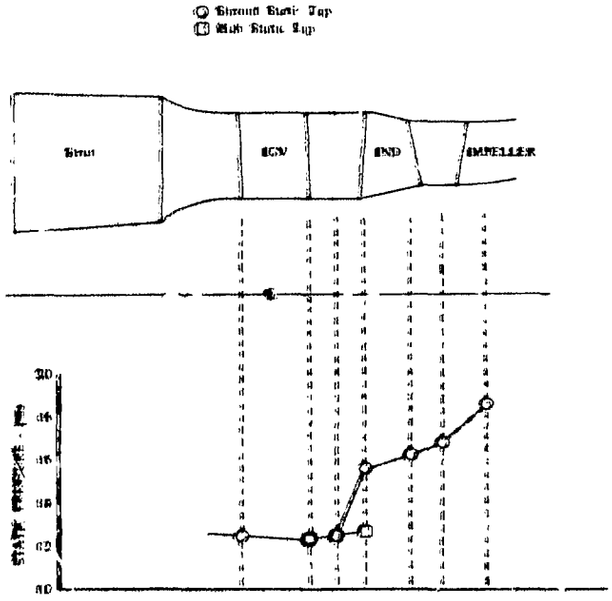

Figure 220. Static Pressure Profile Along Flow Path, Build No. 3, 109% Speed, 10-deg IGV, Near Stall.

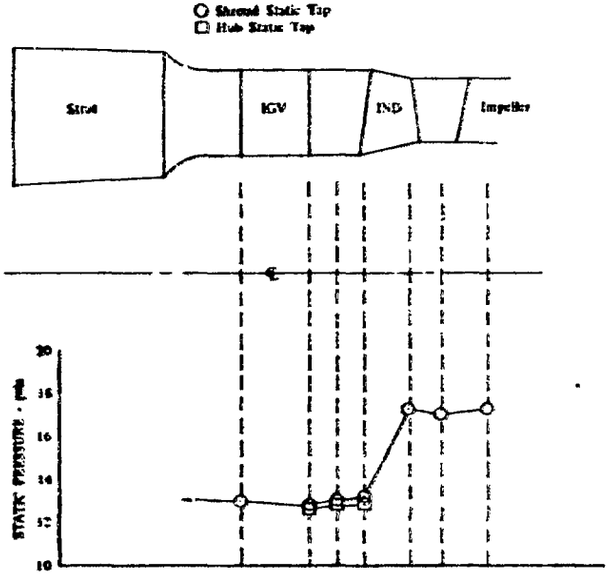

Figure 221. Static Pressure Profile Along Flow Path, Build No. 3, 95% Speed, 20-deg IGV, Near Stall.

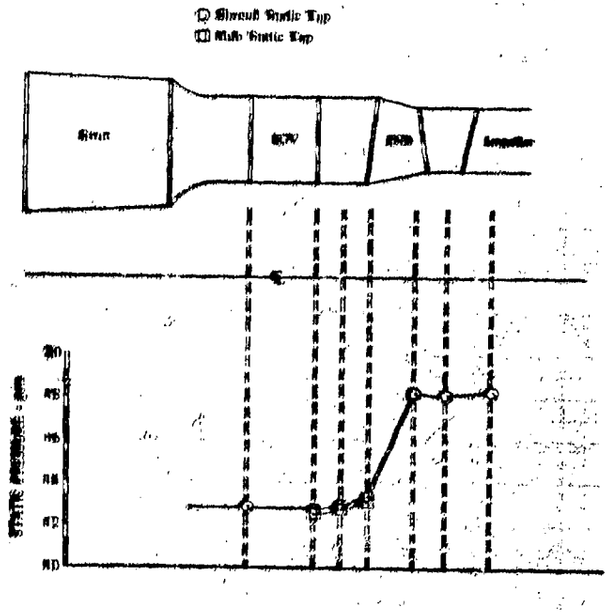

Figure 222. Static Pressure Profile Along Flow Path, Build No. 3, 95% Speed, 10-deg IGV, Wide Open Discharge.

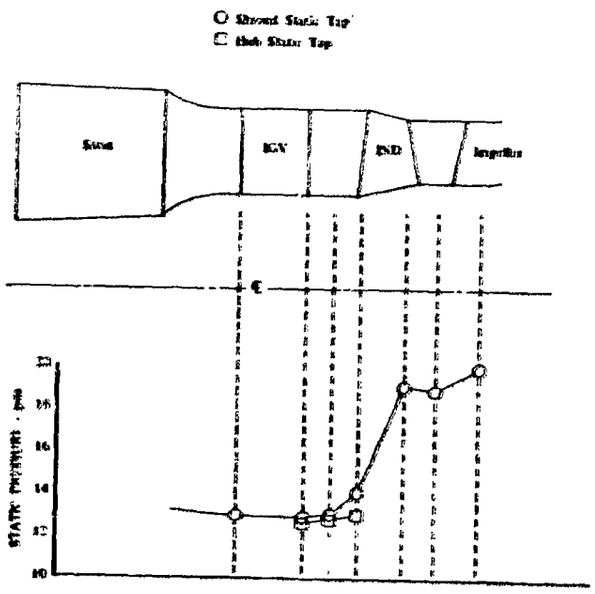

Figure 223. Static Pressure Profile Along Flow Path, Build No. 3, 95% Speed, 10-deg IGV, Near Stall.

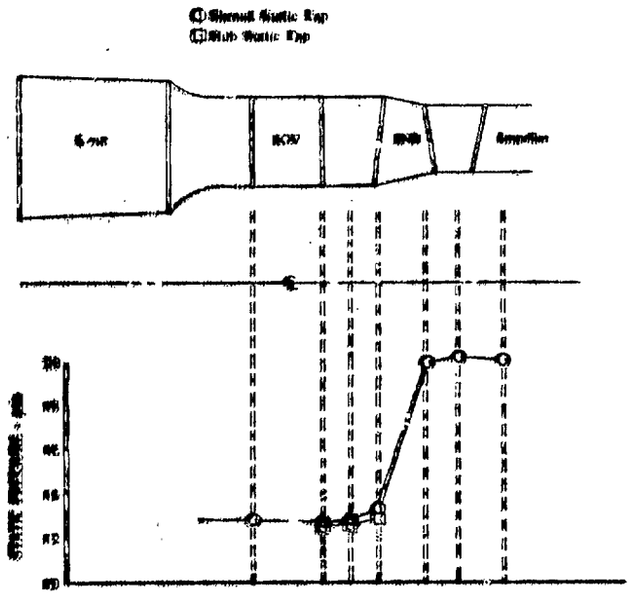

Figure 224. Static Pressure Profile Along Flow Path, Build No. 3, 95% Speed, 0-deg IGV, Near Stall.

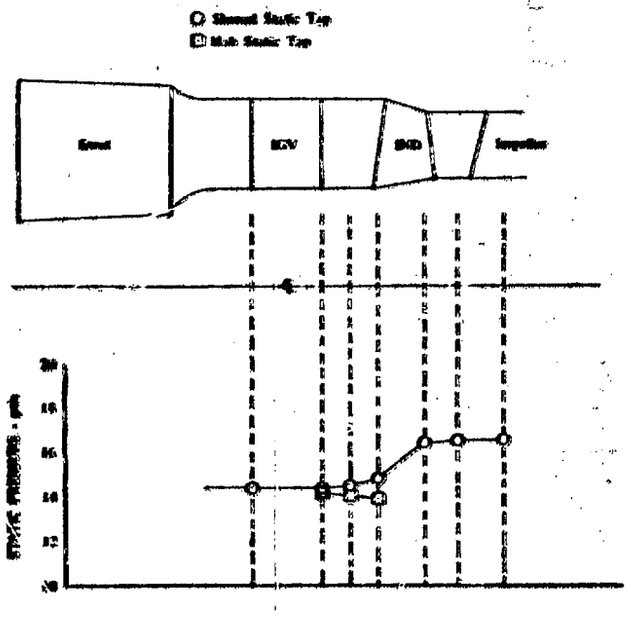

Figure 225. Static Pressure Profile Along Flow Path, Build No. 3, 70% Speed, 10-deg IGV, Near Stall.

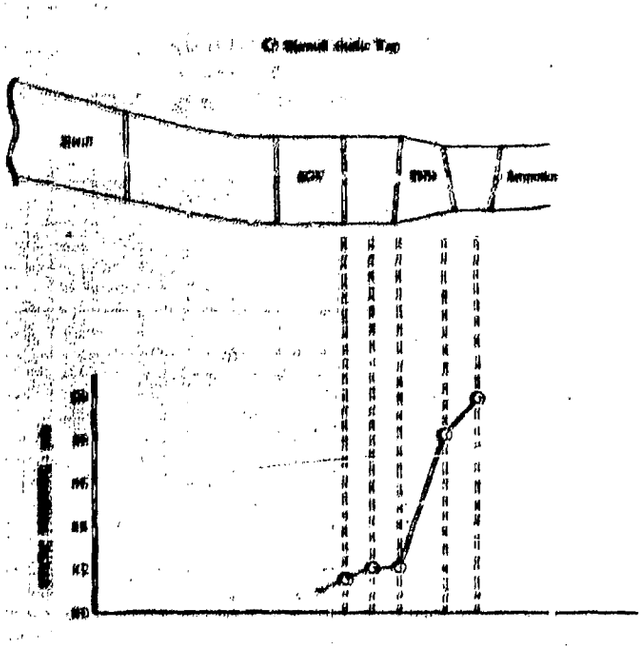

Figure 226. Static Pressure Profile Along Flow Path, Build No. 6, 101% Speed, -4-deg IGV, Wide Open Discharge.

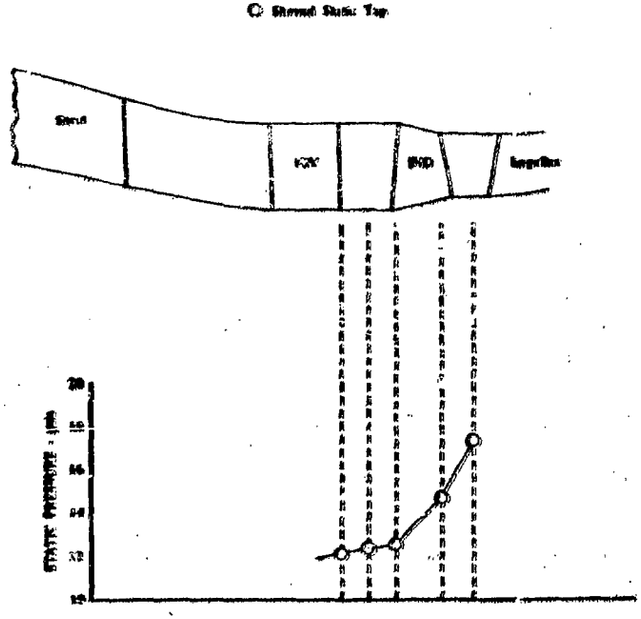

Figure 227. Static Pressure Profile Along Flow Path, Build No. 6, 100% Speed, 10-deg IGV, Near Stall.

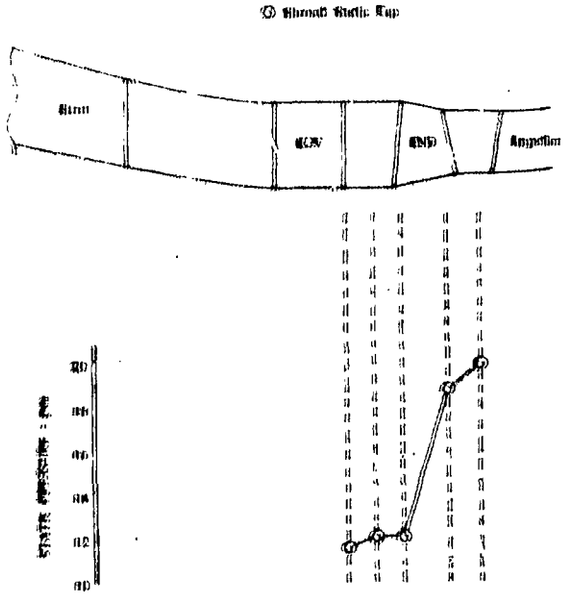

Figure 228. Static Pressure Profile Along Flow Path, Build No. 6, 101% Speed, -4-deg IGV, Near Stall.

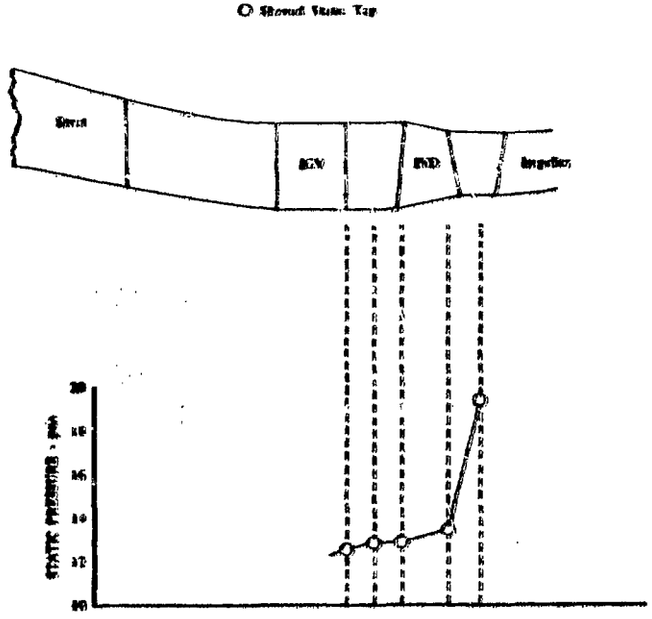

Figure 229. Static Pressure Profile Along Flow Path, Build No. 6, 95% Speed, 10-deg IGV, Near Stall.

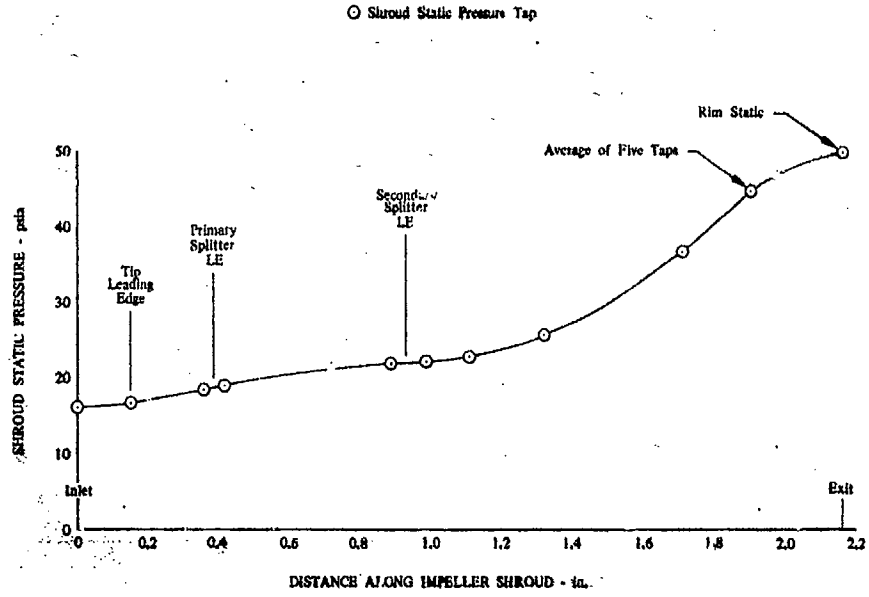

Figure 230. Static Pressure Variation Along Impeller Shroud, Build No. 3, 100% Speed, 10-deg IGV, Near Stall.

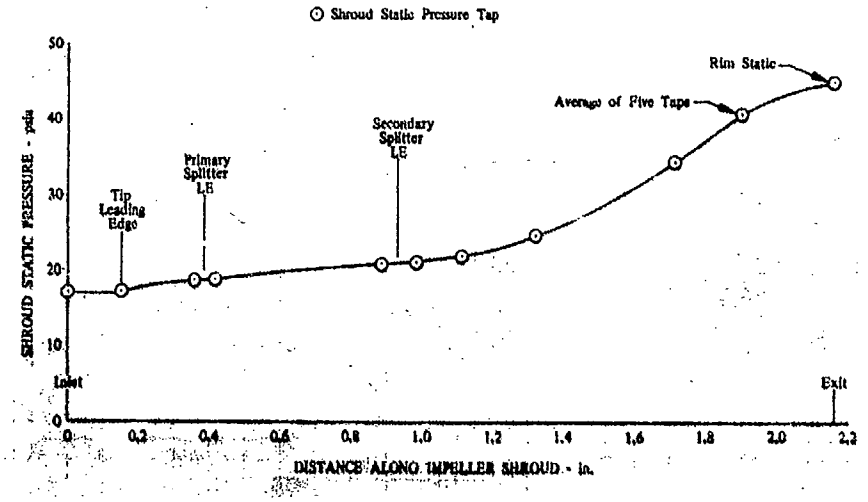

Figure 231. Static Pressure Variation Along Impeller Shroud, Build No. 3, 95% Speed, 20-deg IGV, Near Stall.

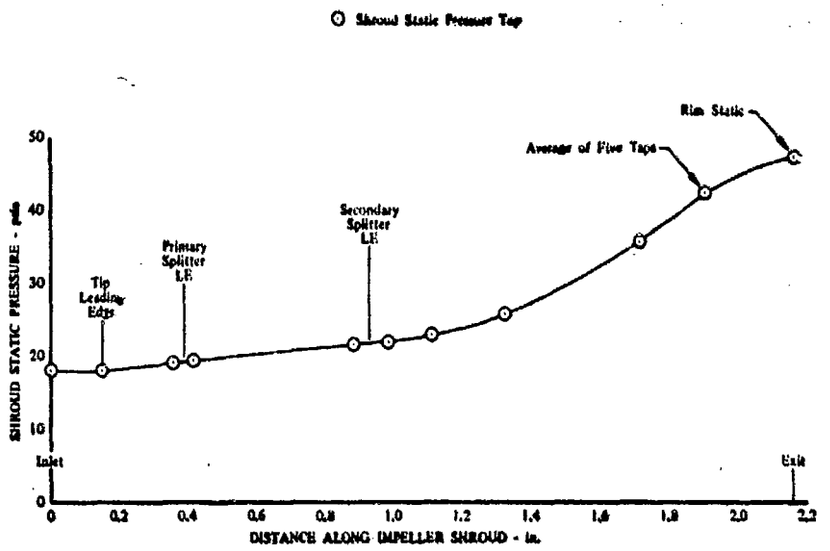

Figure 232. Static Pressure Variation Along Impeller Shroud, Build No. 3, 95% Speed, 10-deg IGV, Wide Open Discharge.

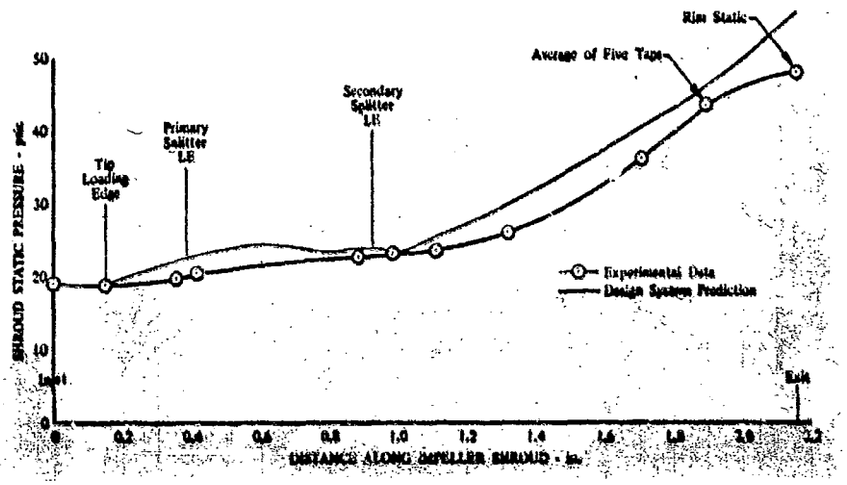

Figure 233. Static Pressure Variation Along Impeller Shroud, Build No. 3, 95% Speed, 10-deg IGV, Near Stall.

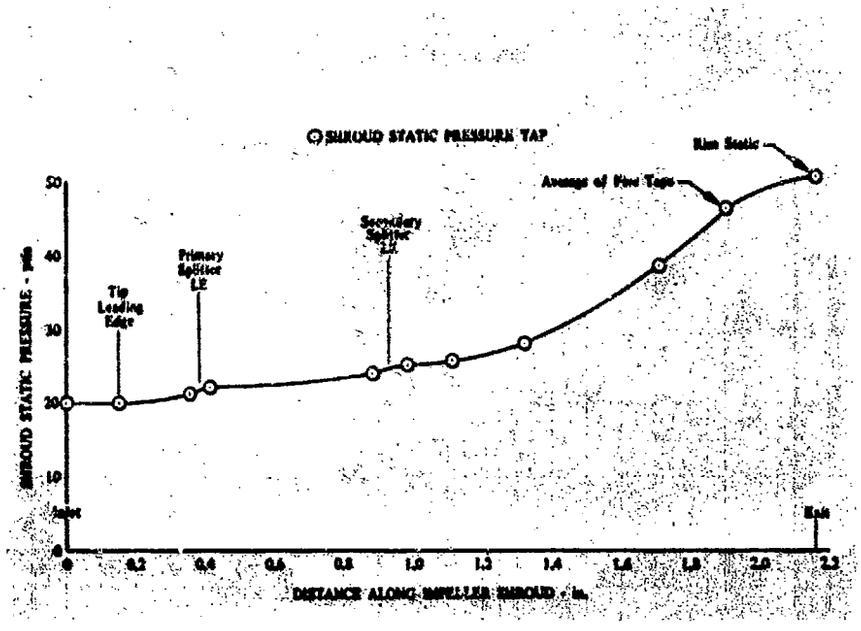

Figure 234. Static Pressure Variation Along Impeller Shroud, Build No. 3, 95% Speed, 0-deg IGV, Near Stall.

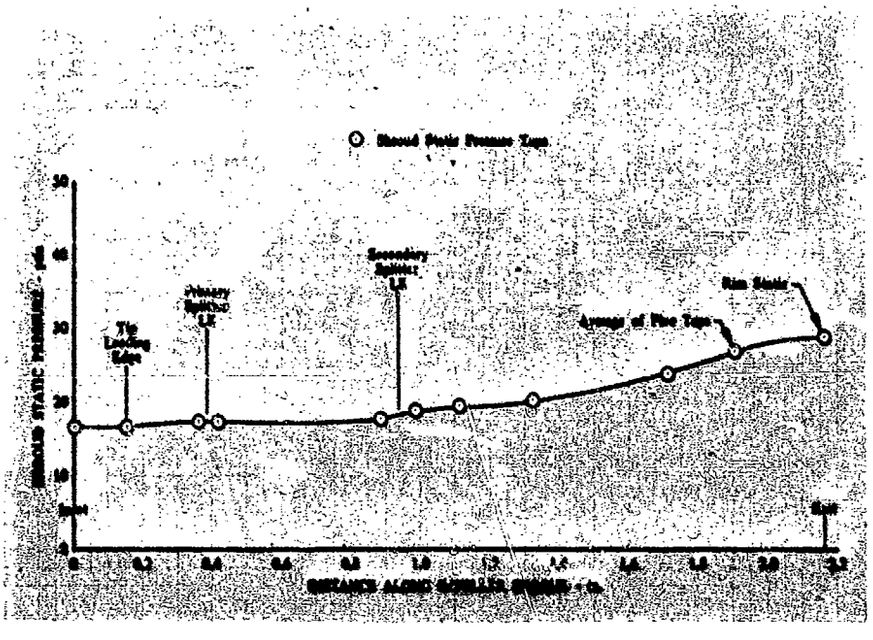

Figure 235. Static Pressure Variation Along Impeller Shroud, Build No. 3, 70% Speed, 10-deg IGV, Near Stall.

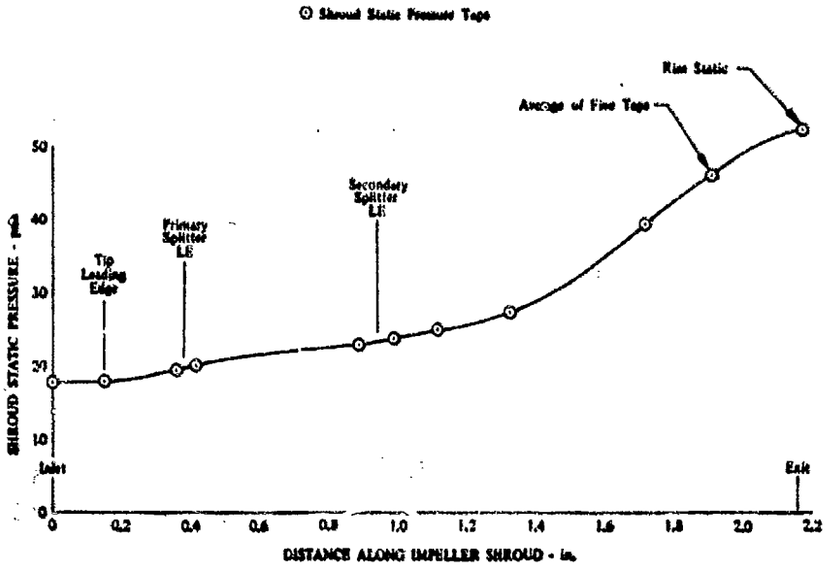

Figure 236. Static Pressure Variation Along Impeller Shroud, Build No. 6, 101% Speed, -4-deg IGV, Wide Open Discharge.

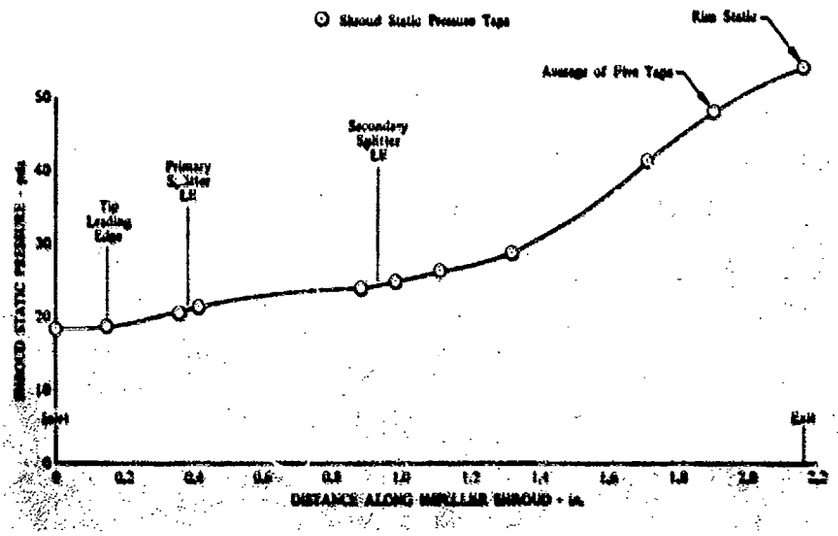

Figure 237. Static Pressure Variation Along Impeller Shroud, Build No. 6, 101% Speed, -4-deg IGV, Near Stall.

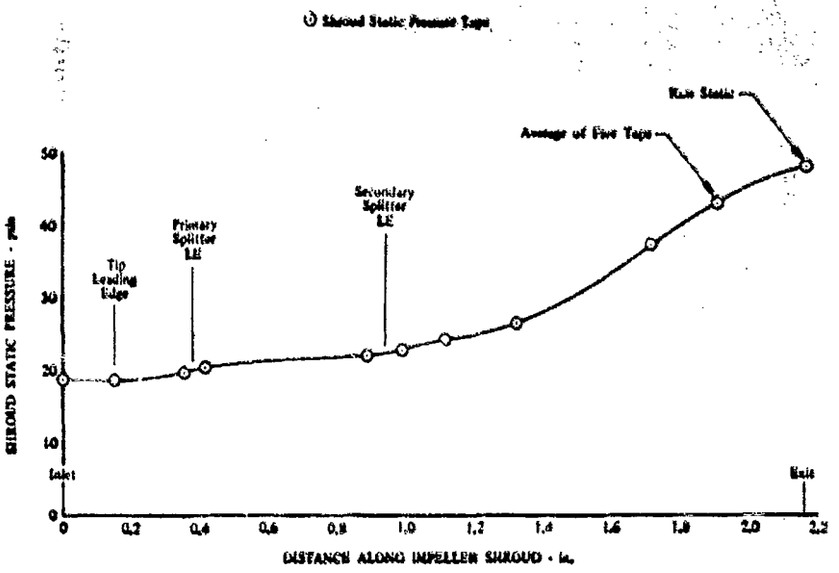

Figure 238. Static Pressure Variation Along Impeller Shroud, Build No. 6, 100% Speed, 10-deg IGV, Near Stall.

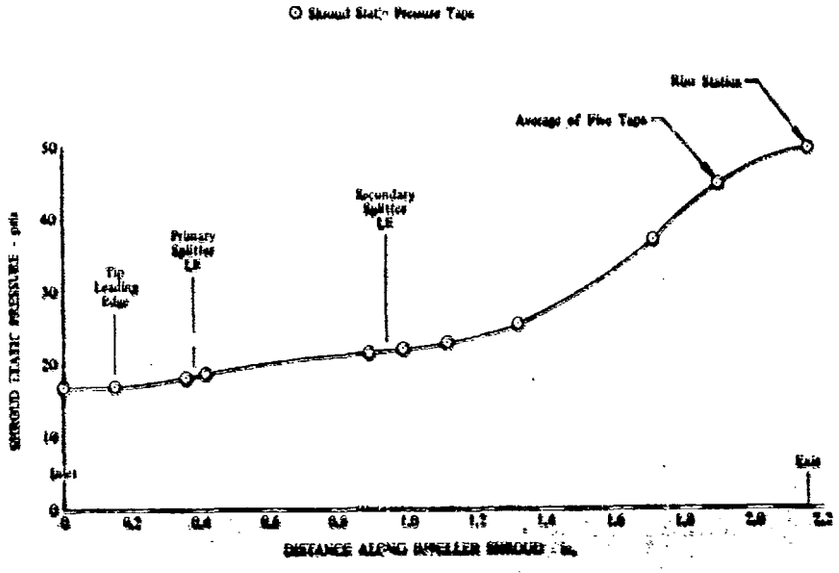

Figure 239. Static Pressure Variation Along Impeller Shroud, Build No. 6, 95% Speed, 10-deg IGV, Near Stall.

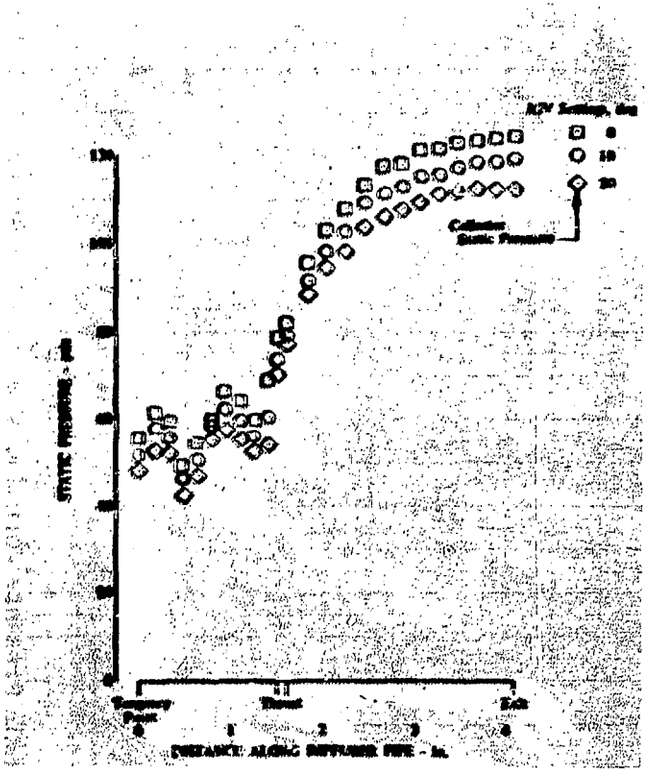

Figure 240. Diffuser Static Pressure Profile, Build No. 3, 95% Speed, Near Stall.

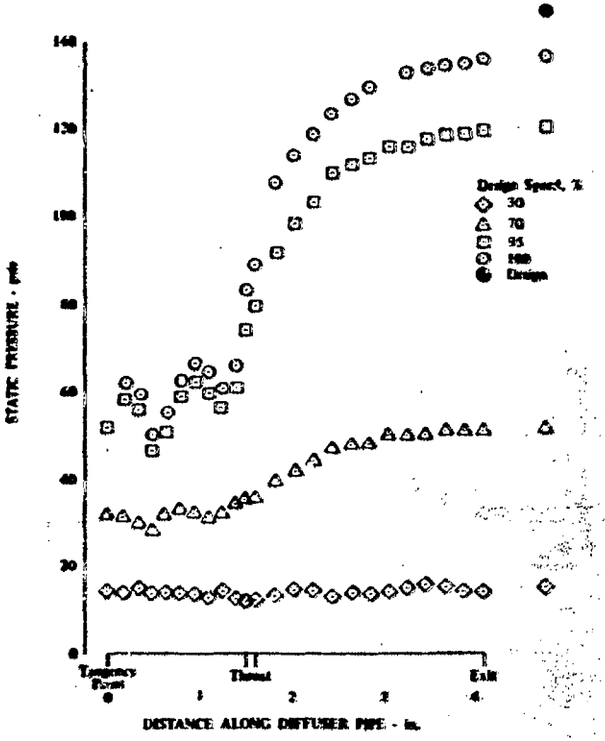

Figure 241. Diffuser Static Pressure Profile, Build No. 3, 10-deg IGV, Near Stall.

HIGH-FREQUENCY RESPONSE INSTRUMENTATION DATA PLOTS

High-response (Kulite) data were obtained during Build No. 6 testing at a near-stall, steady-state point and during a stall transient for both 70 and 78% design speeds. Data were recorded from one total pressure probe at the impeller exit (header PTIDK1), two static pressure probes in the diffuser vaneless space (PSDVK1 and PSDVK2), and one static pressure probe at the diffuser exit (PSDEK1).

Plots produced from the data are shown in Figures 242 through 296. Each figure includes a plot of pressure vs time, peak-to-peak pressure vs frequency, and a cross correlation. The cross correlation was generated to determine the commonality of the signals. It was accomplished as follows: Time samples of the two waveforms to be correlated were divided into a number of segments. The corresponding segments of the two waveforms were multiplied together and the resulting products were summed to obtain a value that was representative of the similarity of the two waveforms at time delay zero. The segments of one of the waveforms were shifted in time by a chosen amount. The corresponding segments of the first waveform and the time shifted segments of the second waveform were multiplied together and their products summed to obtain a value that was representative of the similarities of the first waveform and a time shifted version of the second waveform. The shift in time, multiplication, and summation were repeated for all time delays of interest. The cross-correlation plot is a plot of these similarities vs their corresponding time delays. Plots produced at a near-stall, steady-state point at 70% speed for each parameter are shown in Figures 242 through 245. Figures 246 through 251 show the plots produced from the total pressure Kulite data at successive time increments proceeding into stall at 70% speed. The time statement on each plot refers to the day of the year, hour of day, minute, second, and fraction of second. The fraction of second code is included in the title of each plot to aide in identification. Transient plots at the same successive time increments for PSDVK1, PSDVK2, and PSDEK1 are shown in Figures 252 through 257, Figures 258 through 263, and Figures 264 through 269, respectively. Near-stall, steady-state plots at 78% speed for each parameter are shown in Figures 270 through 273. The transient plots into stall for each parameter at 78% speed are as follows: PTIDK1, Figures 274 through 279; PSDVK1, Figures 280 through 285; PSDVK2, Figures 286 through 291; and PSDEK1, Figures 292 through 297.

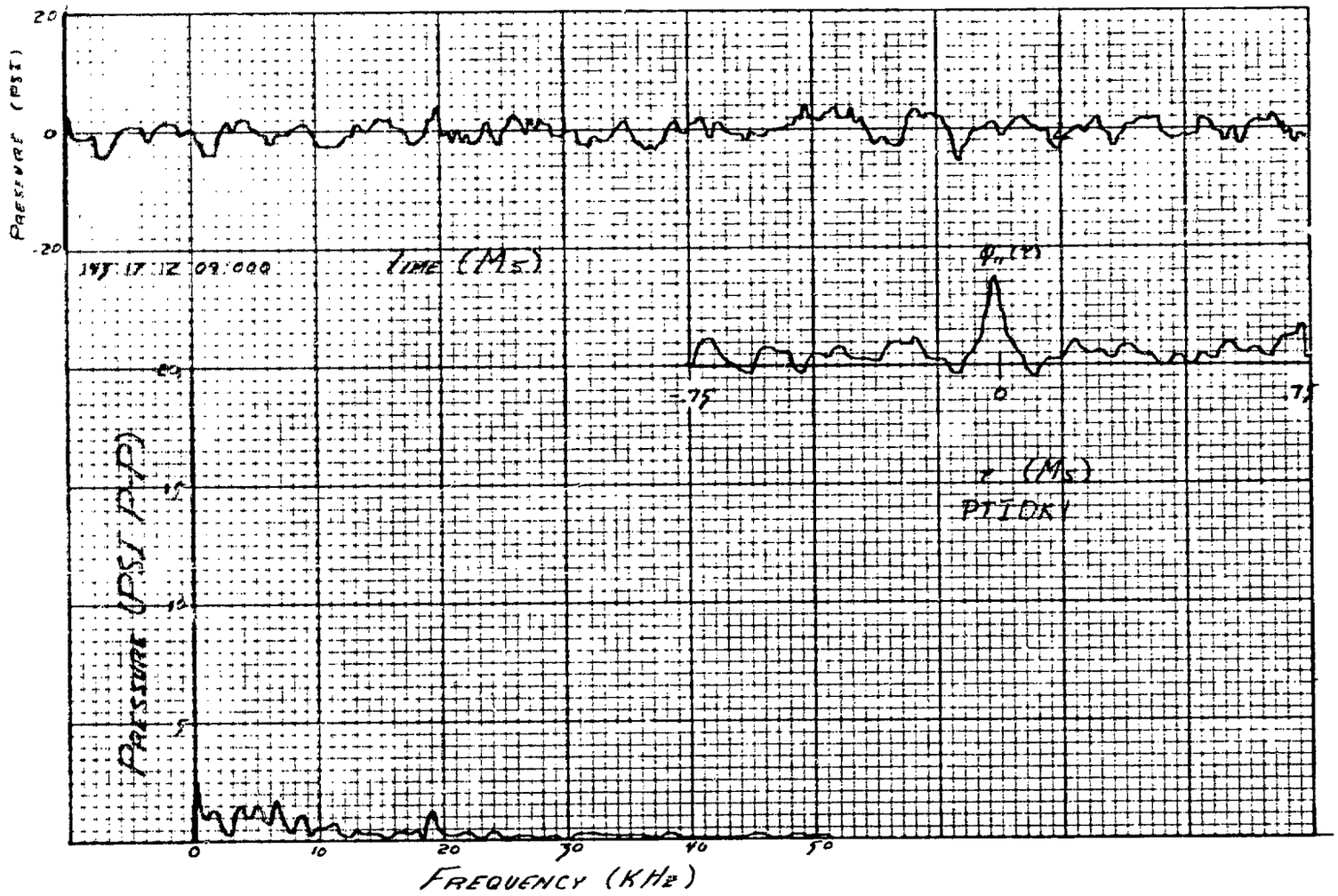

Figure 242. High-Frequency Response Data, 70% Speed, Steady-State, PTIDK1.

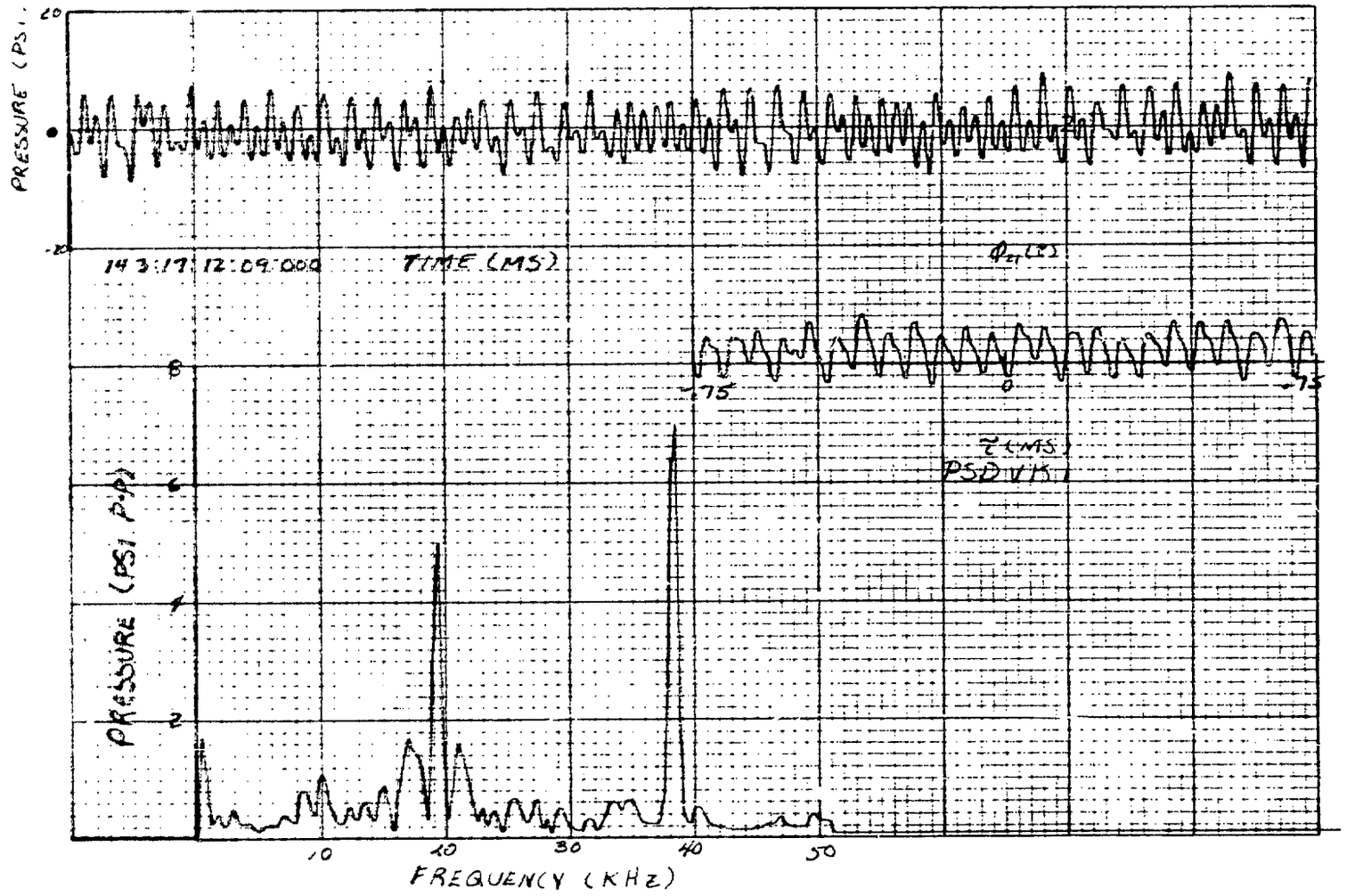

Figure 243. High-Frequency Response Data, 70% Speed, Steady-State, PSDVK1.

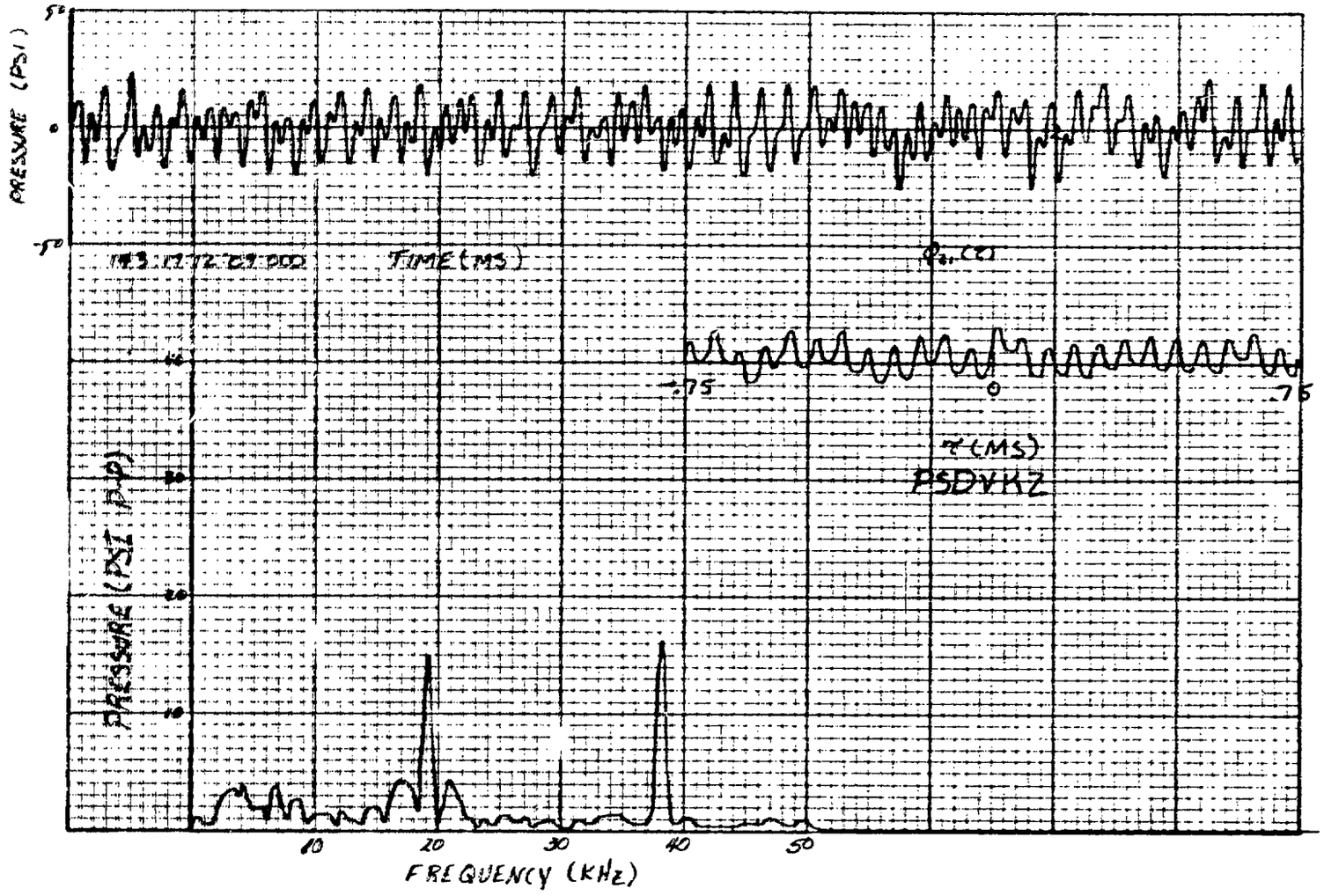

Figure 244. High-Frequency Response Data, 70° Speed, Steady-State, PSDVK2.

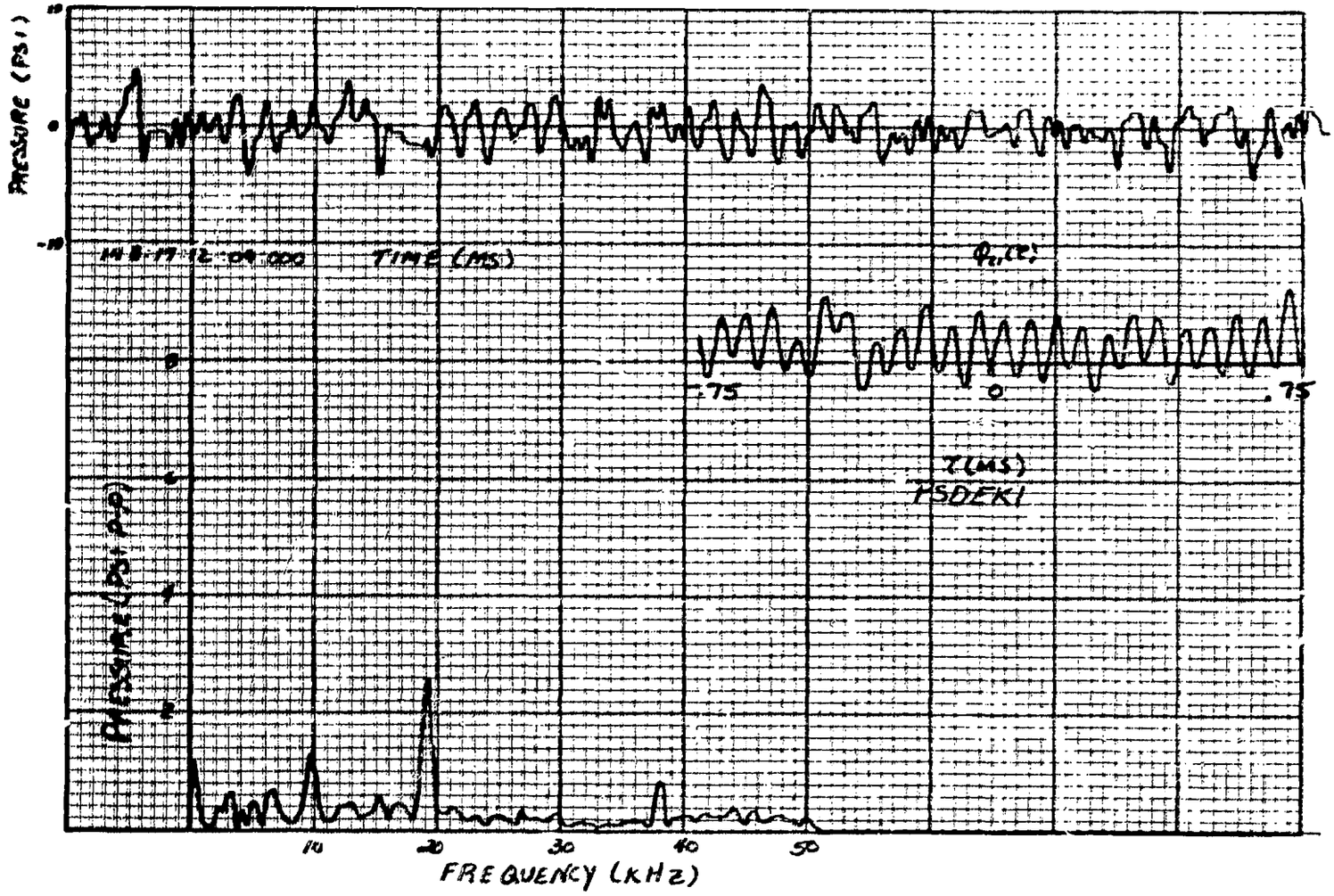

Figure 245. High-Frequency Response Data, 70% Speed, Steady-State, PSDEK1.

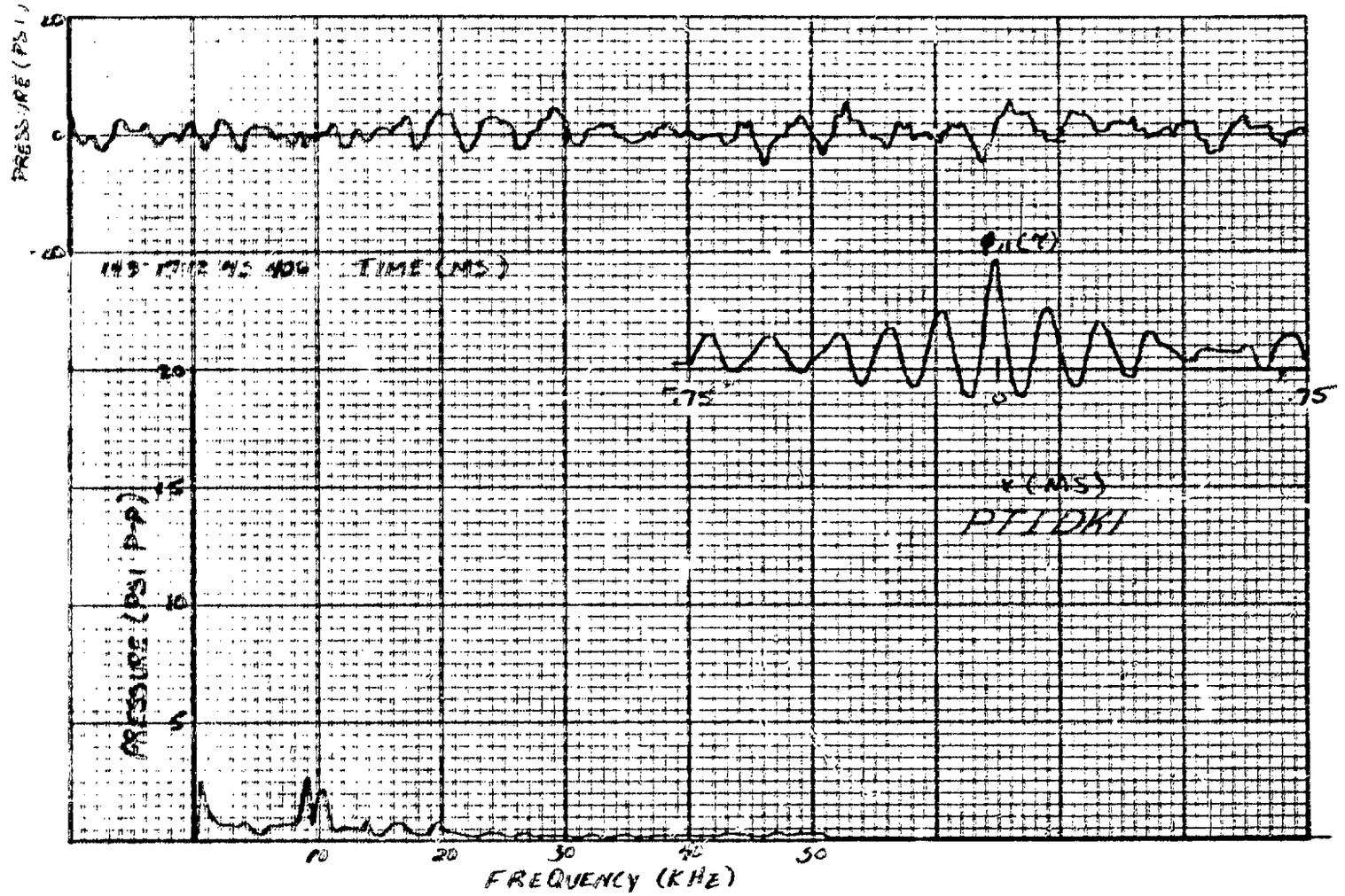

Figure 246. High-Frequency Response Data, 70% Speed, Stall Transient, Time 406, PTIDK1.

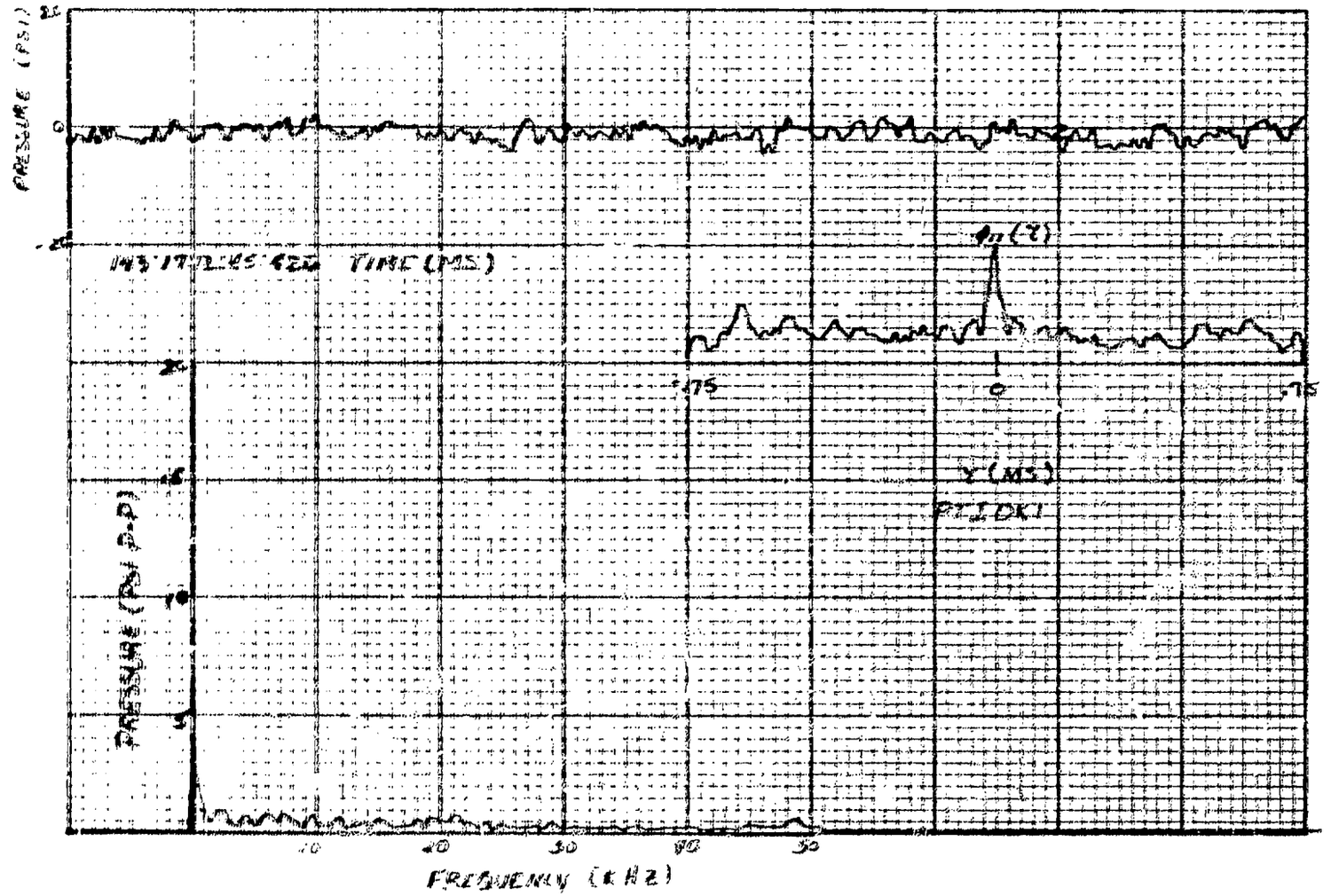

Figure 247. High-Frequency Response Data, 70% Speed, Stall Transient, Time 126, PT1DK1.

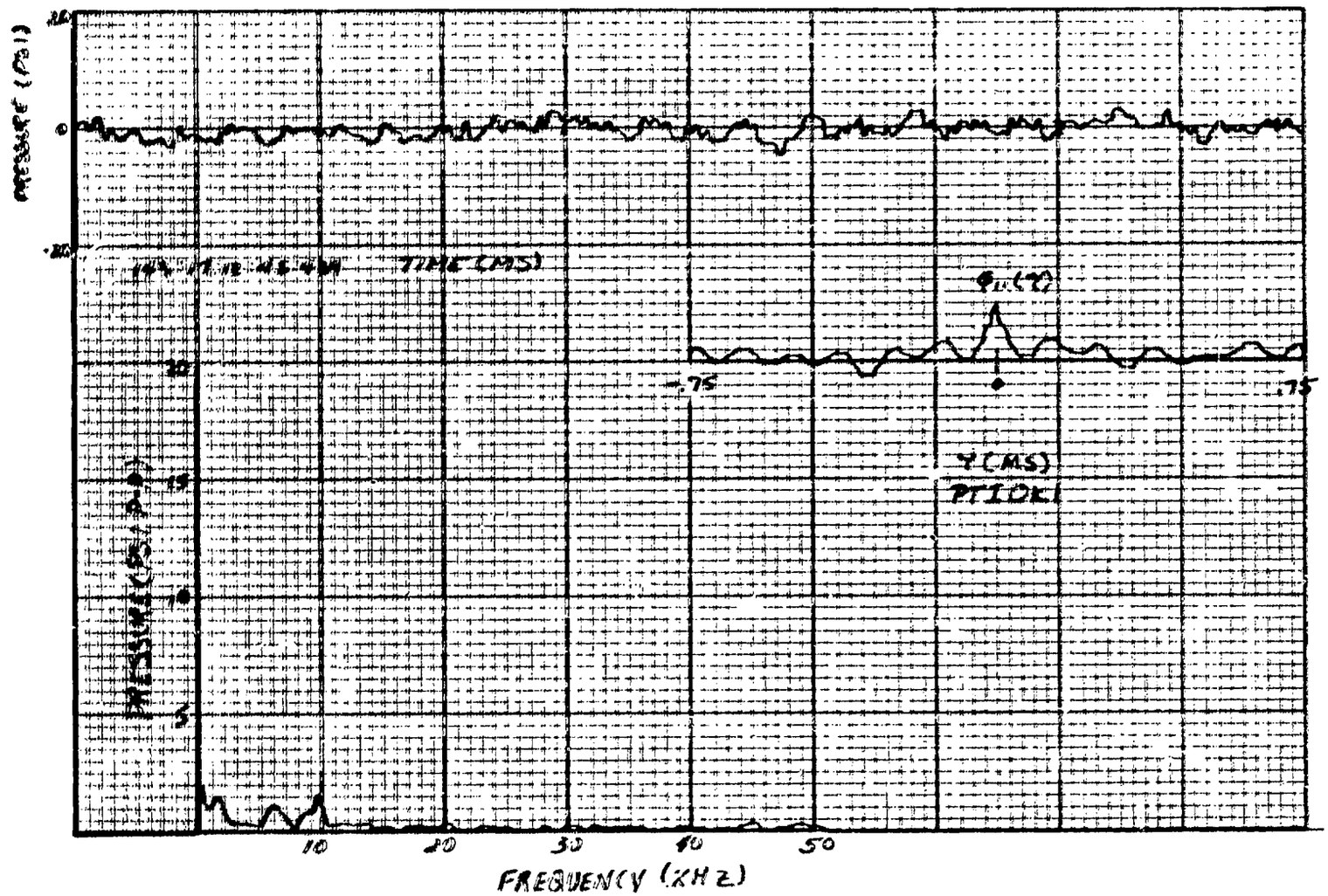

Figure 248. High-Frequency Response Data, 70% Speed, Stall Transient, Time 434 PTIDK1.

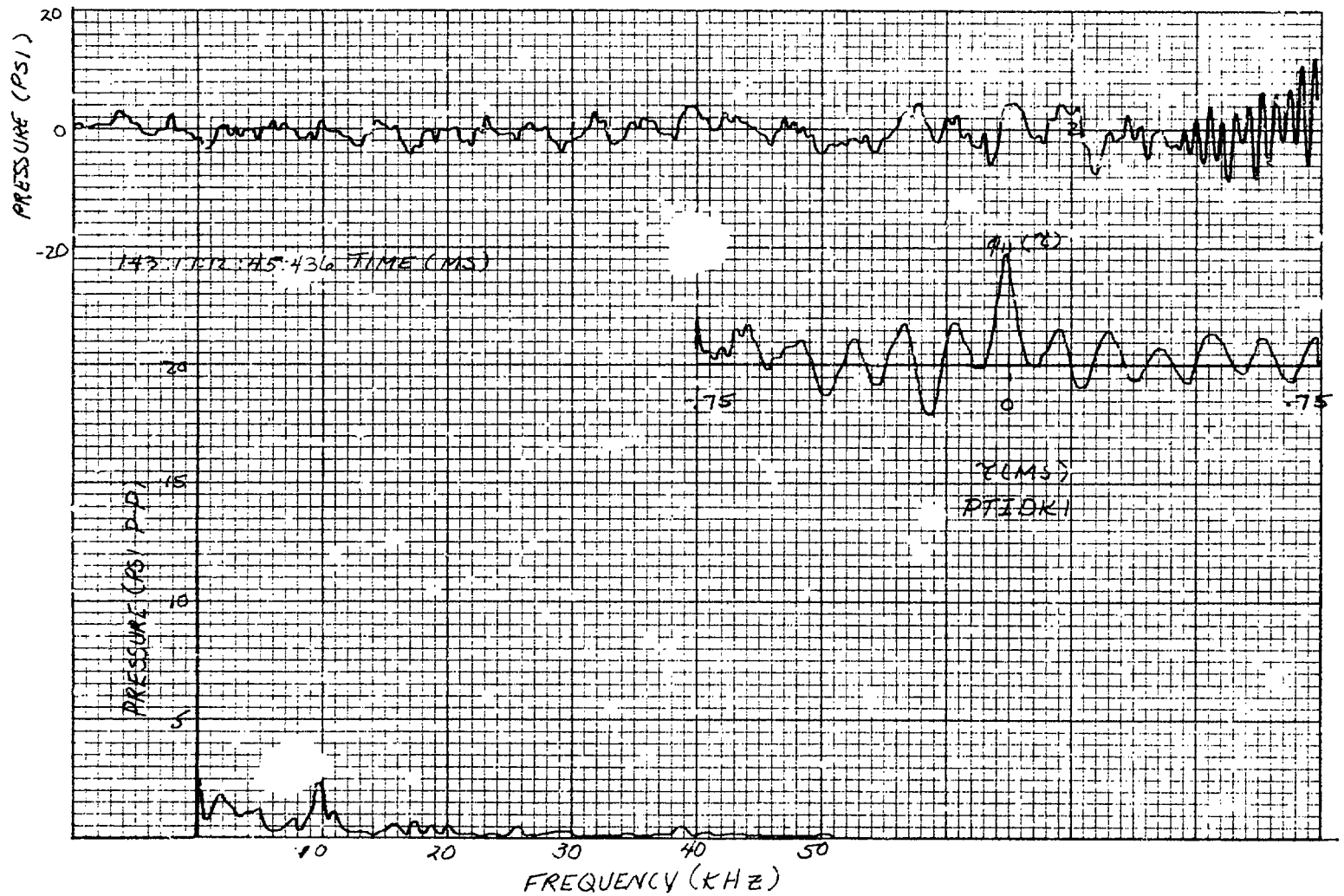

Figure 249. High-Frequency Response Data, 70% Speed, Stall Transient, Time 436, PTIDK1.

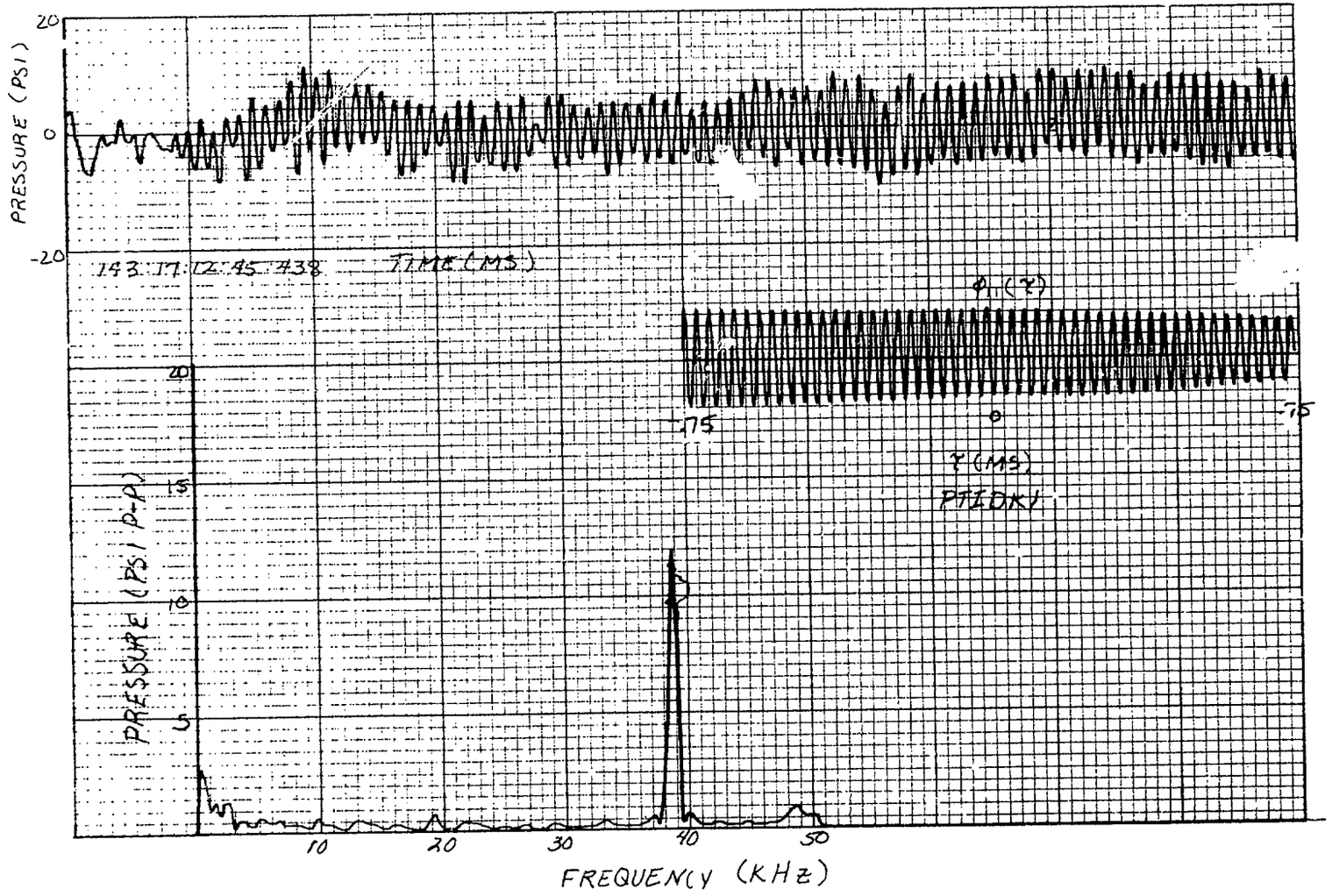

Figure 250. High-Frequency Response Data, 70% Speed, Stalled, Time 438, PTIDK1.

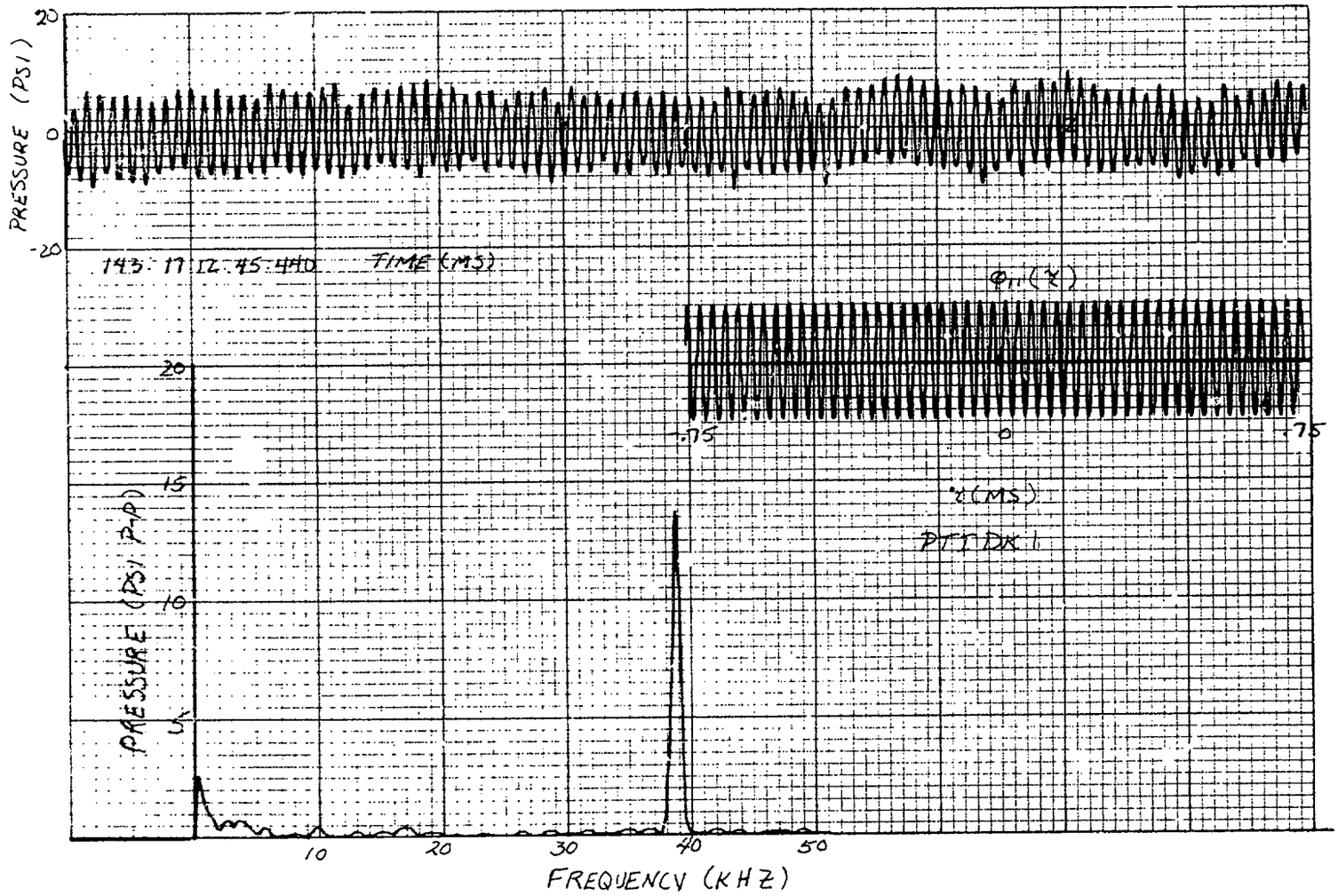

Figure 251. High-Frequency Response Data, 70% Speed, Stalled, Time 440, PTIDK1.

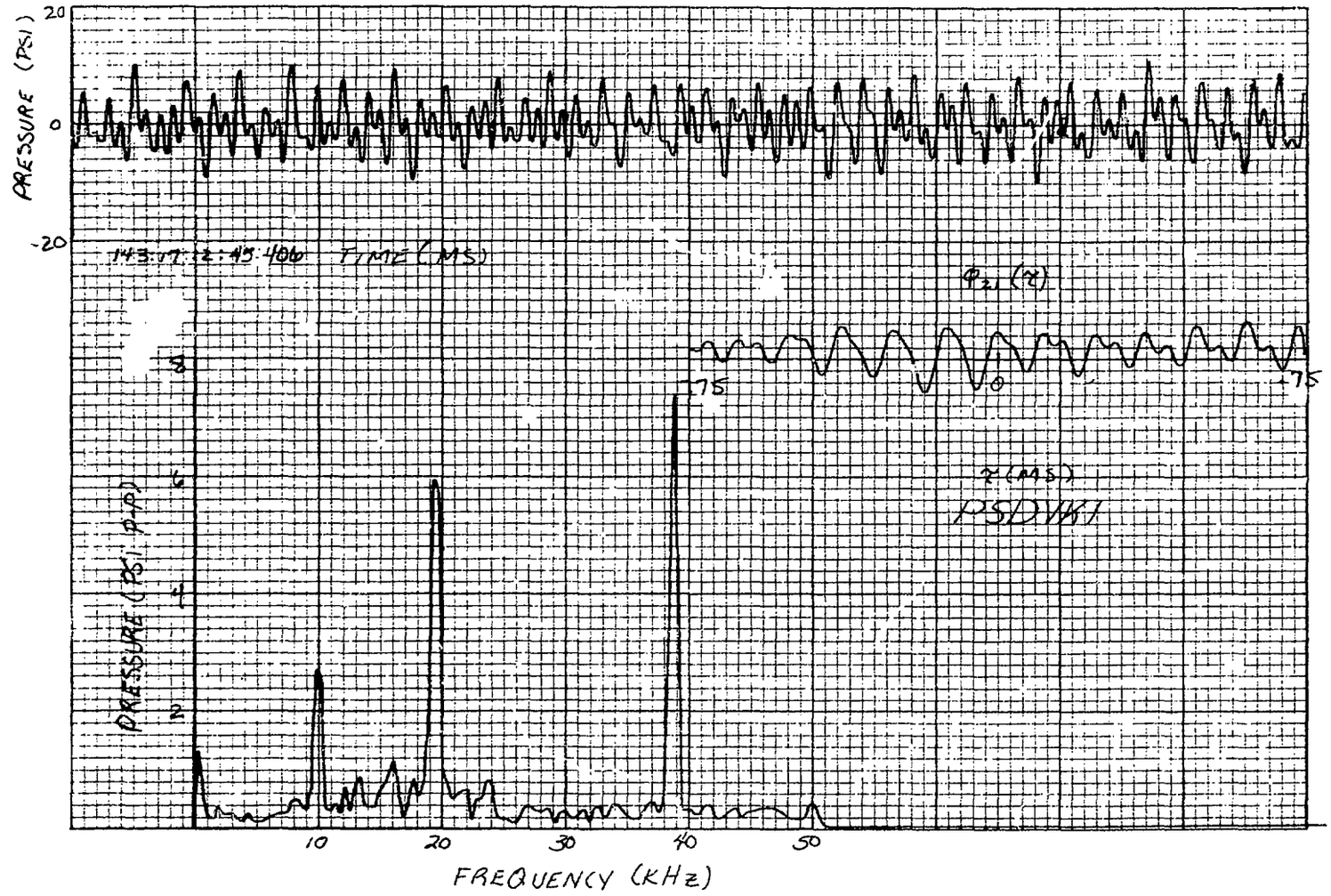

Figure 252. High-Frequency Response Data, 70% Speed, Stall Transient, Time 406, PSDVK1.

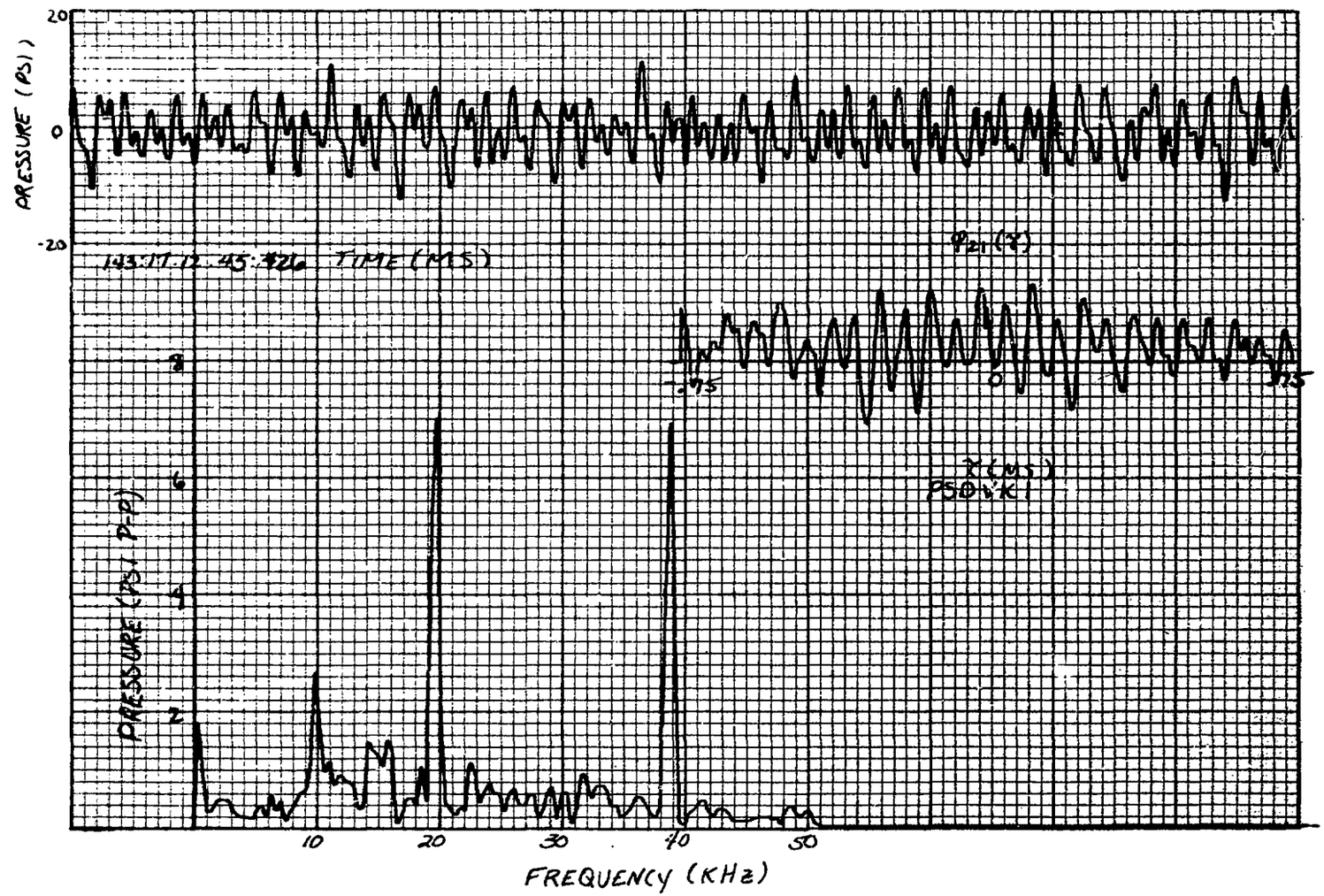

Figure 253. High-Frequency Response Data, 70% Speed, Stall Transient, Time 426, PSDVK1.

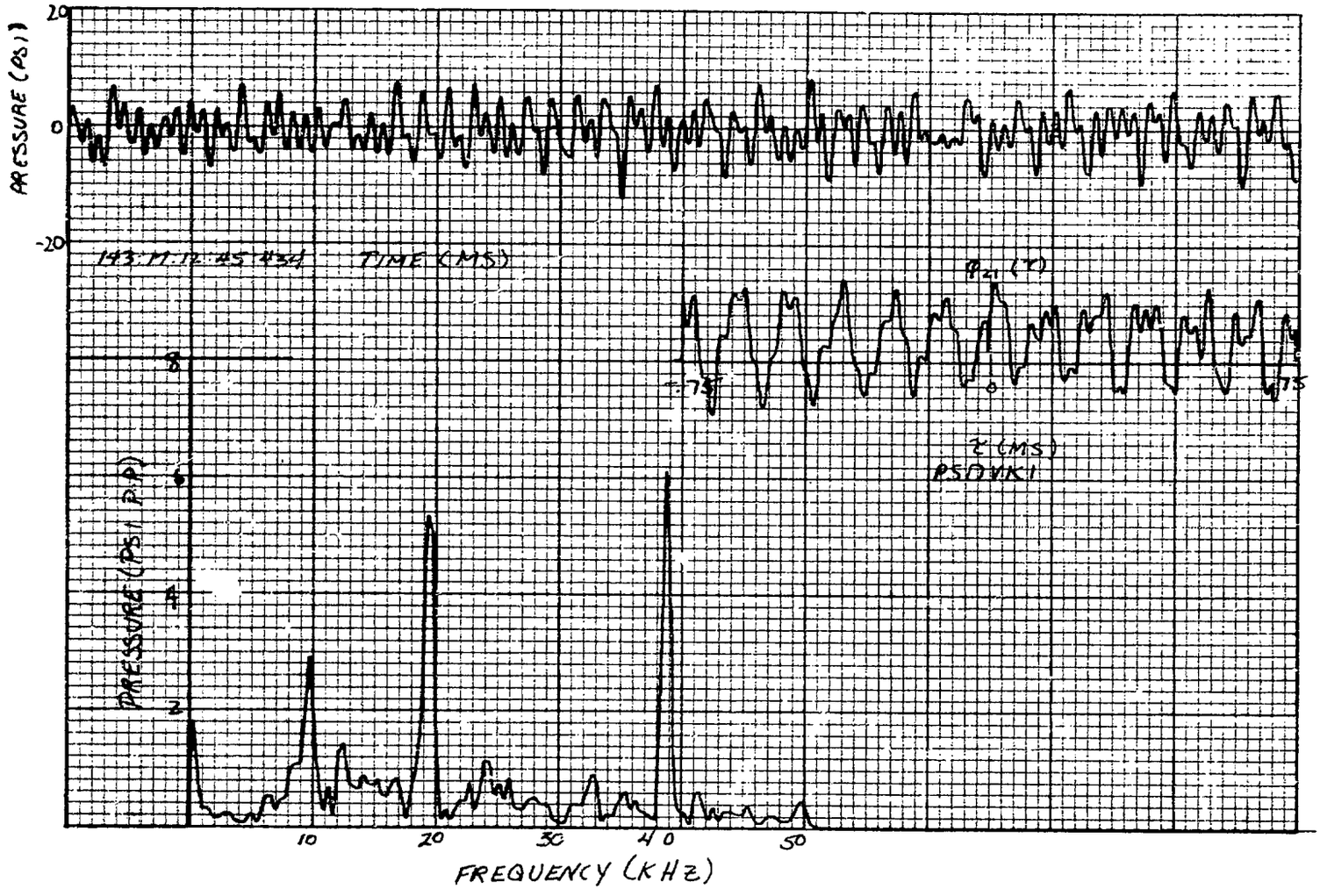

Figure 254. High-Frequency Response Data, 70% Speed, Stall Transient, Time 434, PSDVK1.

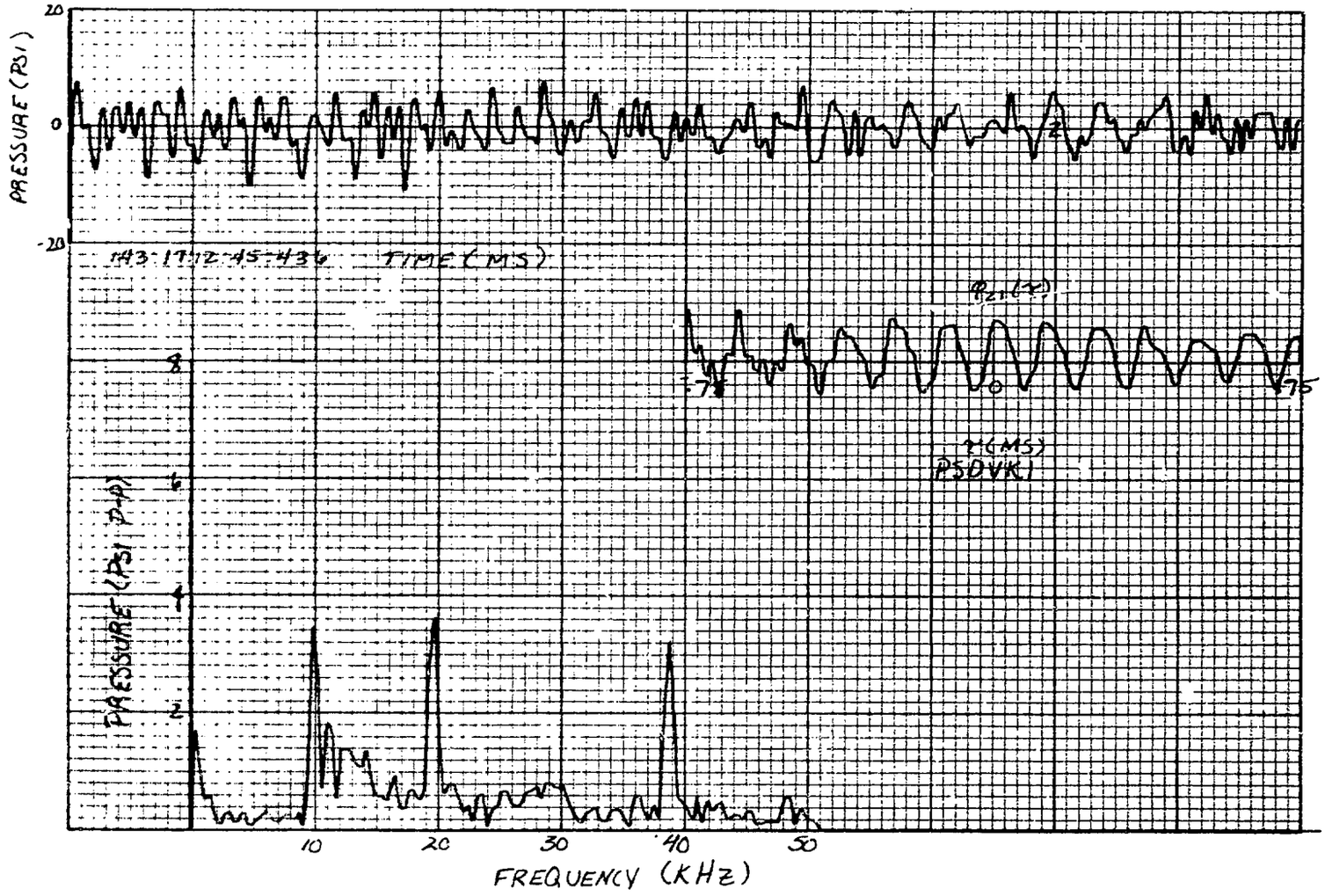

Figure 255. High-Frequency Response Data, 70% Speed, Stall Transient, Time 43[6] PSDVK1.

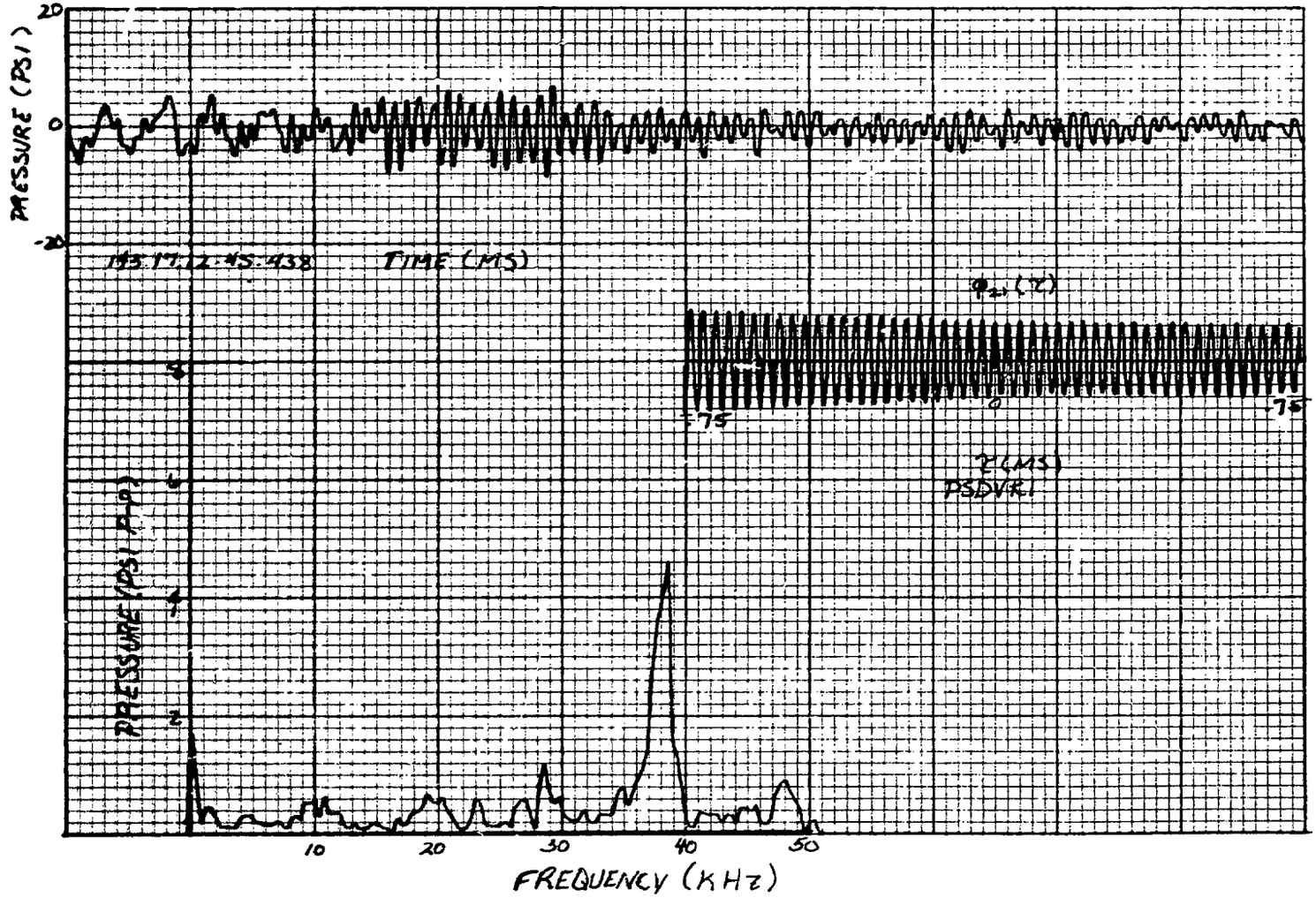

Figure 256. High-Frequency Response Data, 70% Speed, Stalled, Time 438, PSDVK1.

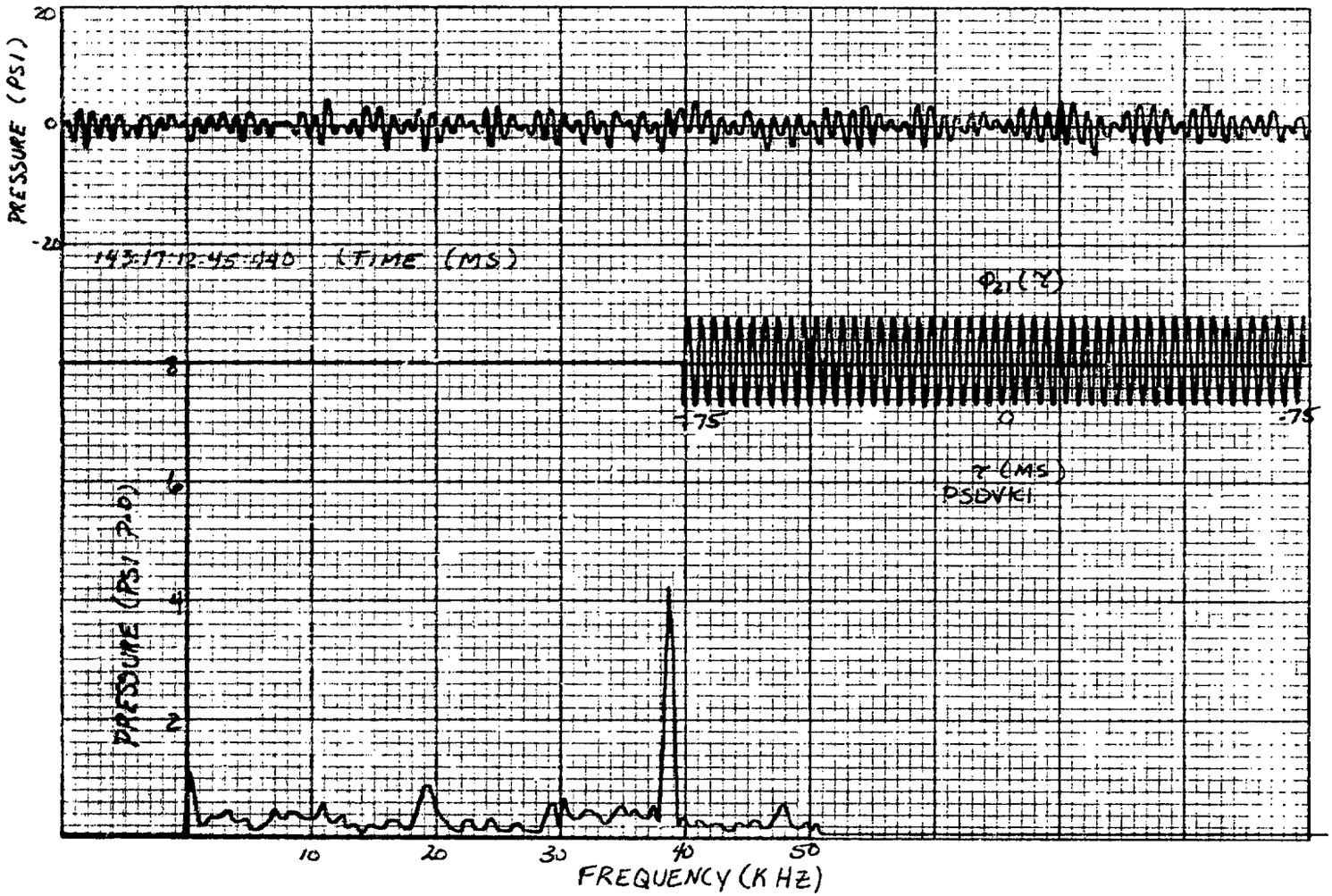

Figure 257. High-Frequency Response Data, 70% Speed, Stalled, Time 440, PSDVK1.

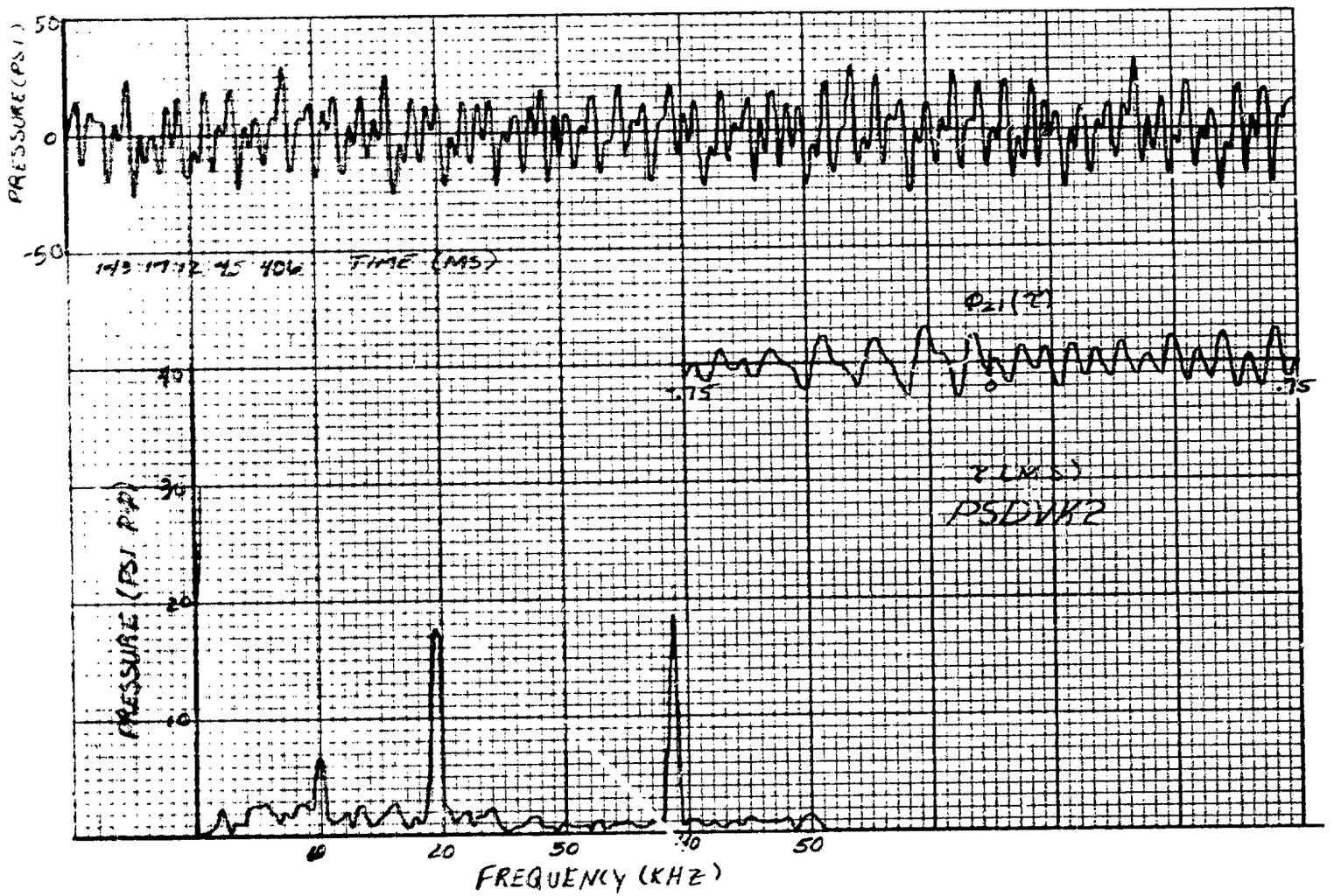

Figure 258. High-Frequency Response Data, 70% Speed, Stall Transient, Time 406, PSDVK2.

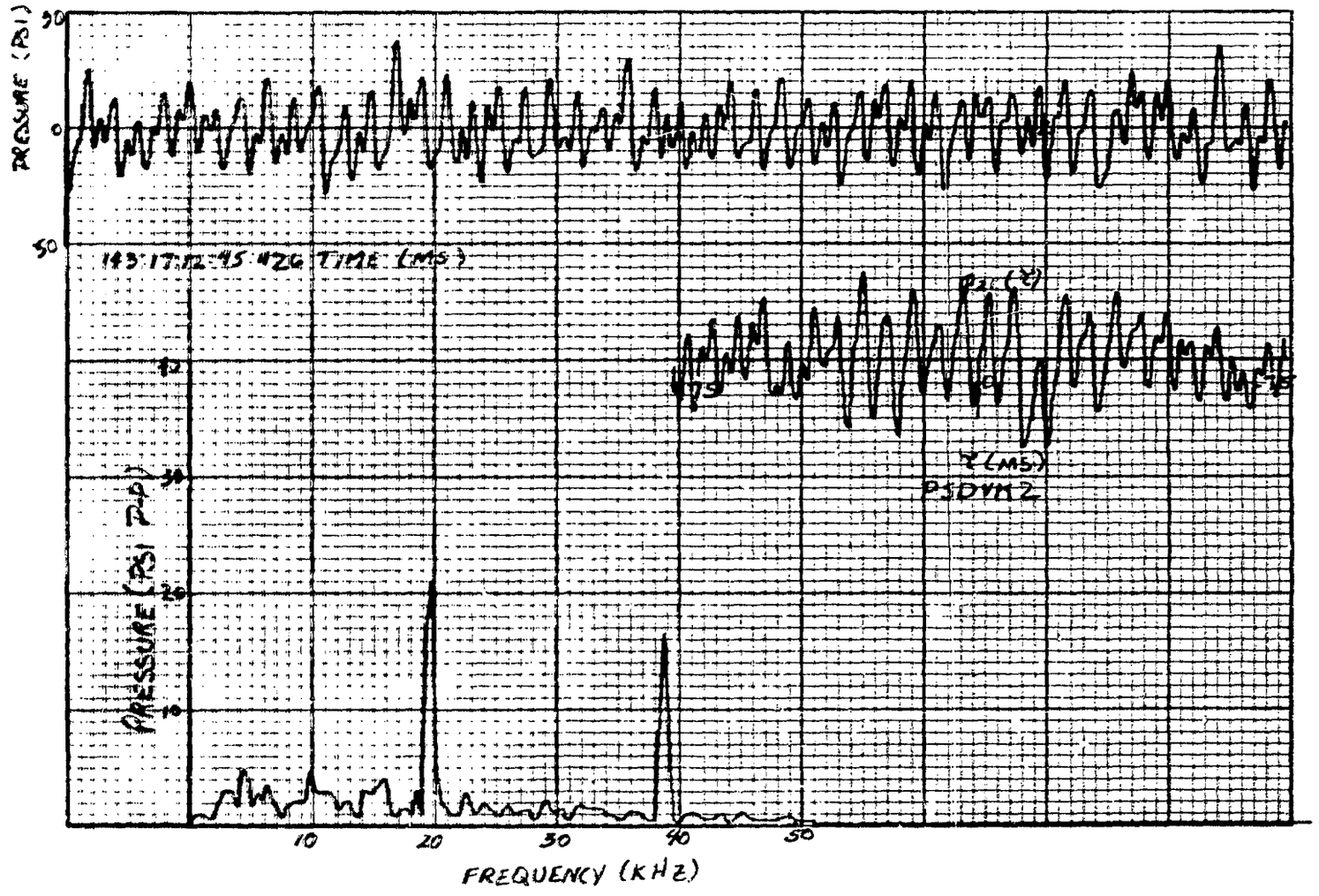

Figure 259. High-Frequency Response Data, 70% Speed, Stall Transient, Time 426, PSDVK2.

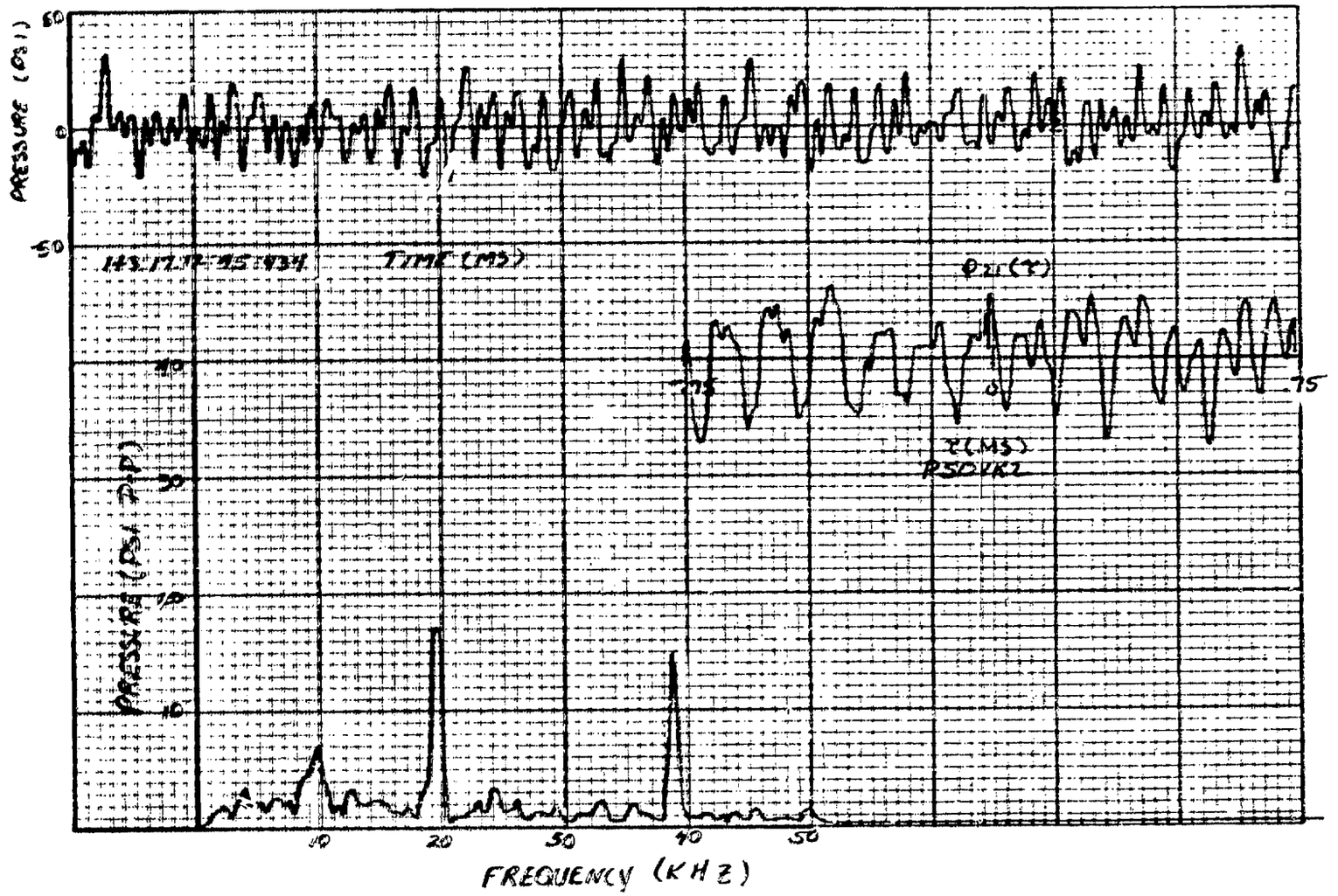

Figure 260. High-Frequency Response Data, 70% Speed, Stall Transient, Time 434, PSDVK2.

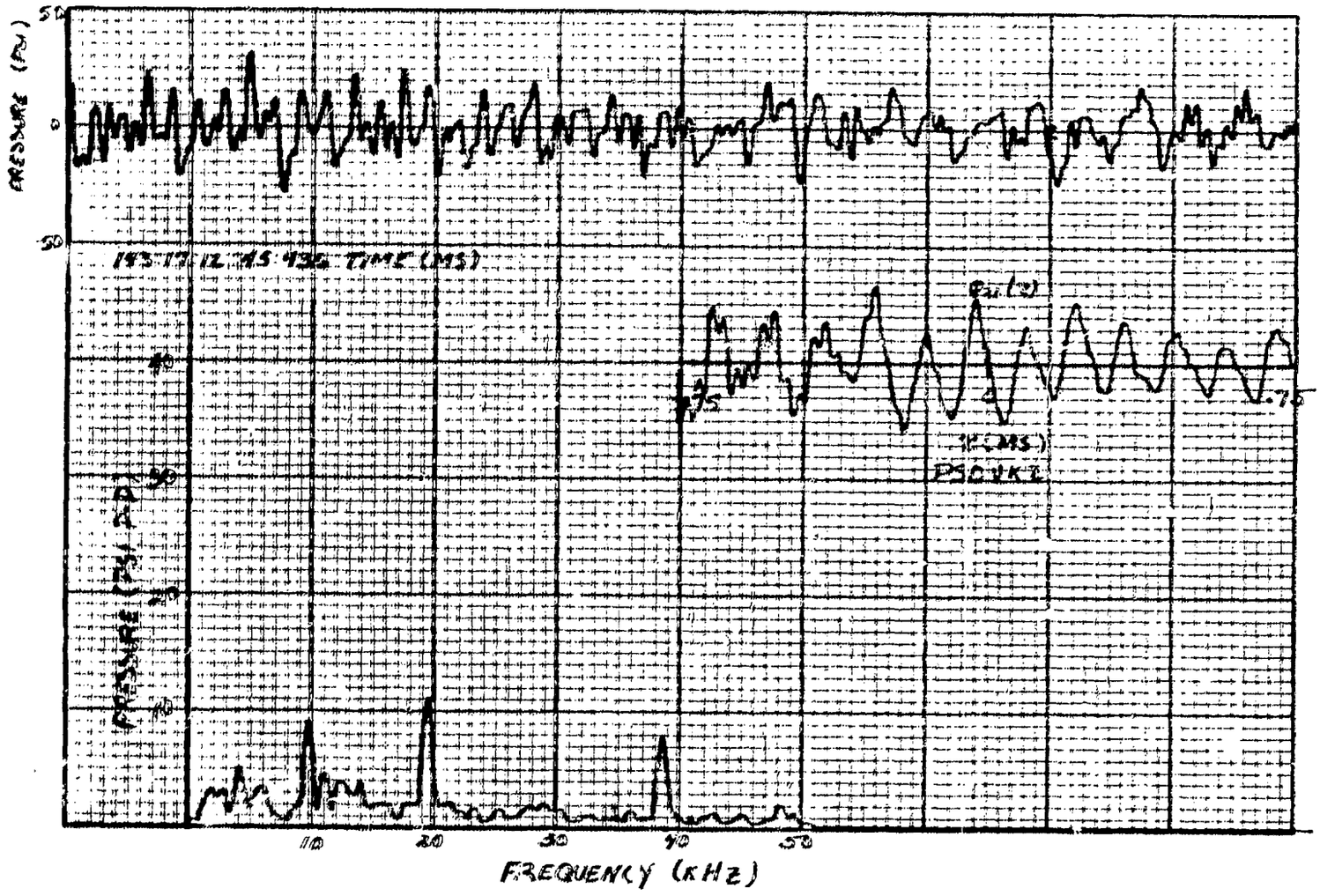

Figure 261. High-Frequency Response Data, 70% Speed, Stall Transient, Time 436, PSDVK2.

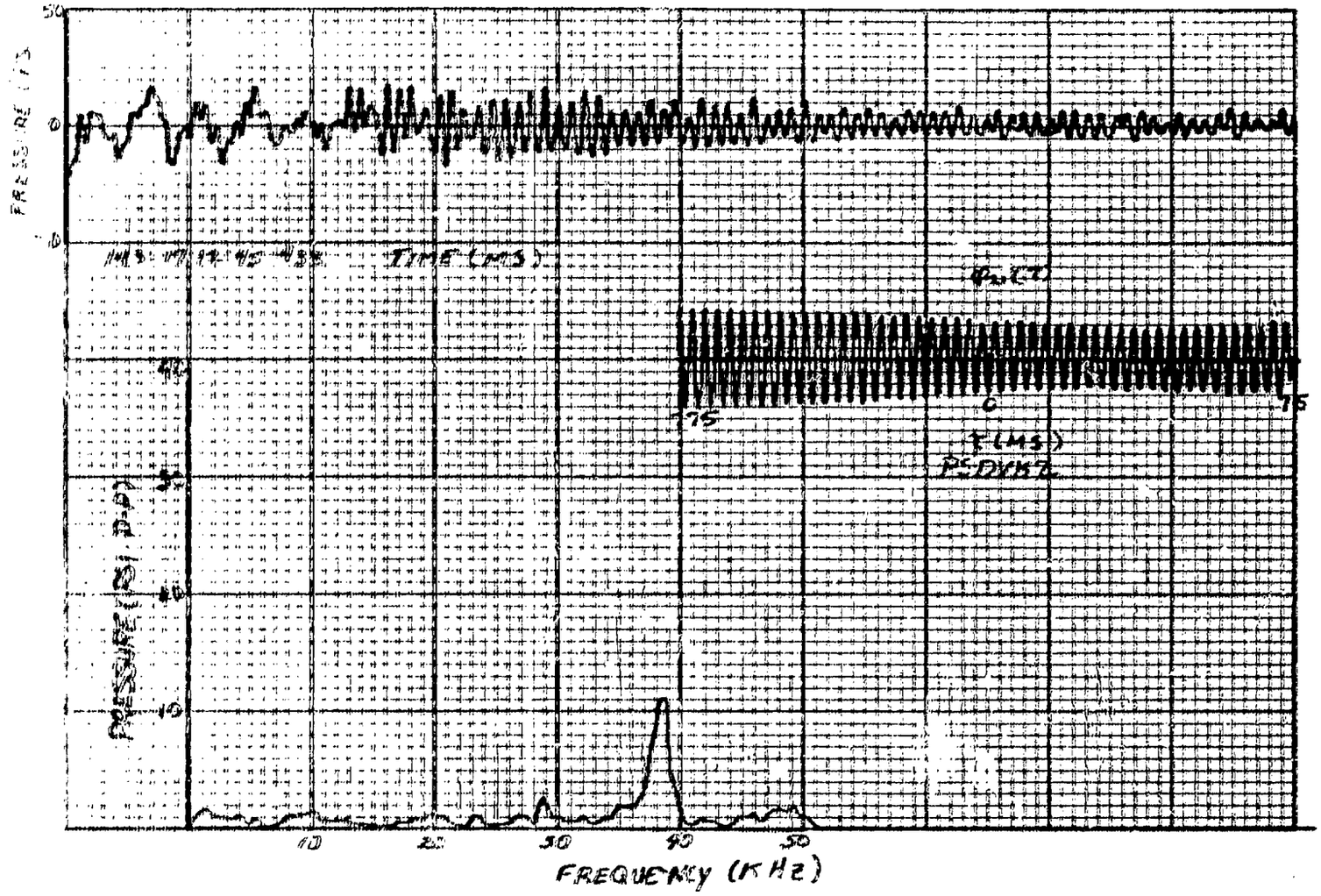

Figure 262. High-Frequency Response Data, 70% Speed, Stalled, Time 438, PSDVK2.

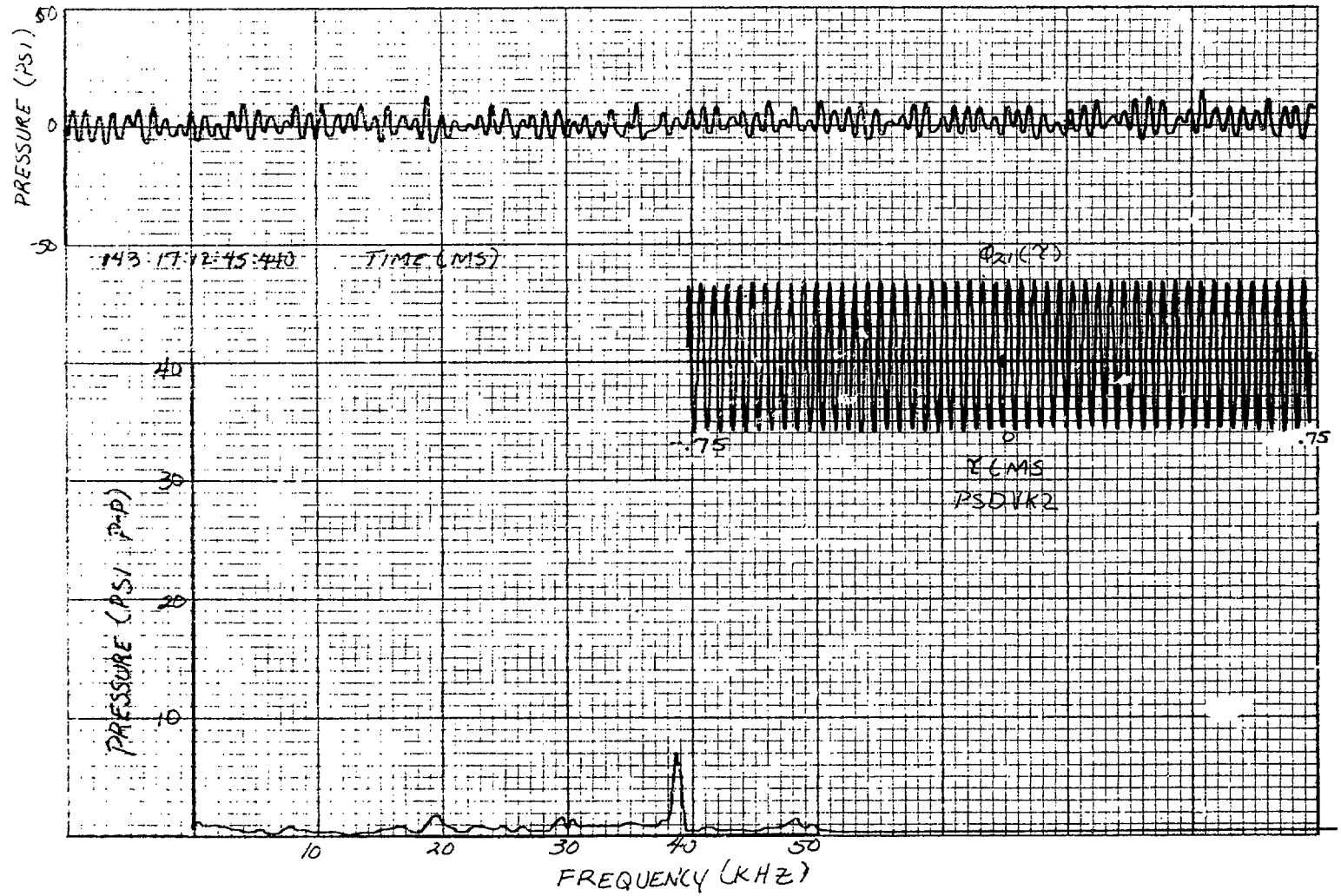

Figure 263. High-Frequency Response Data, 70% Speed, Stalled, Time 440, PSDVK2.

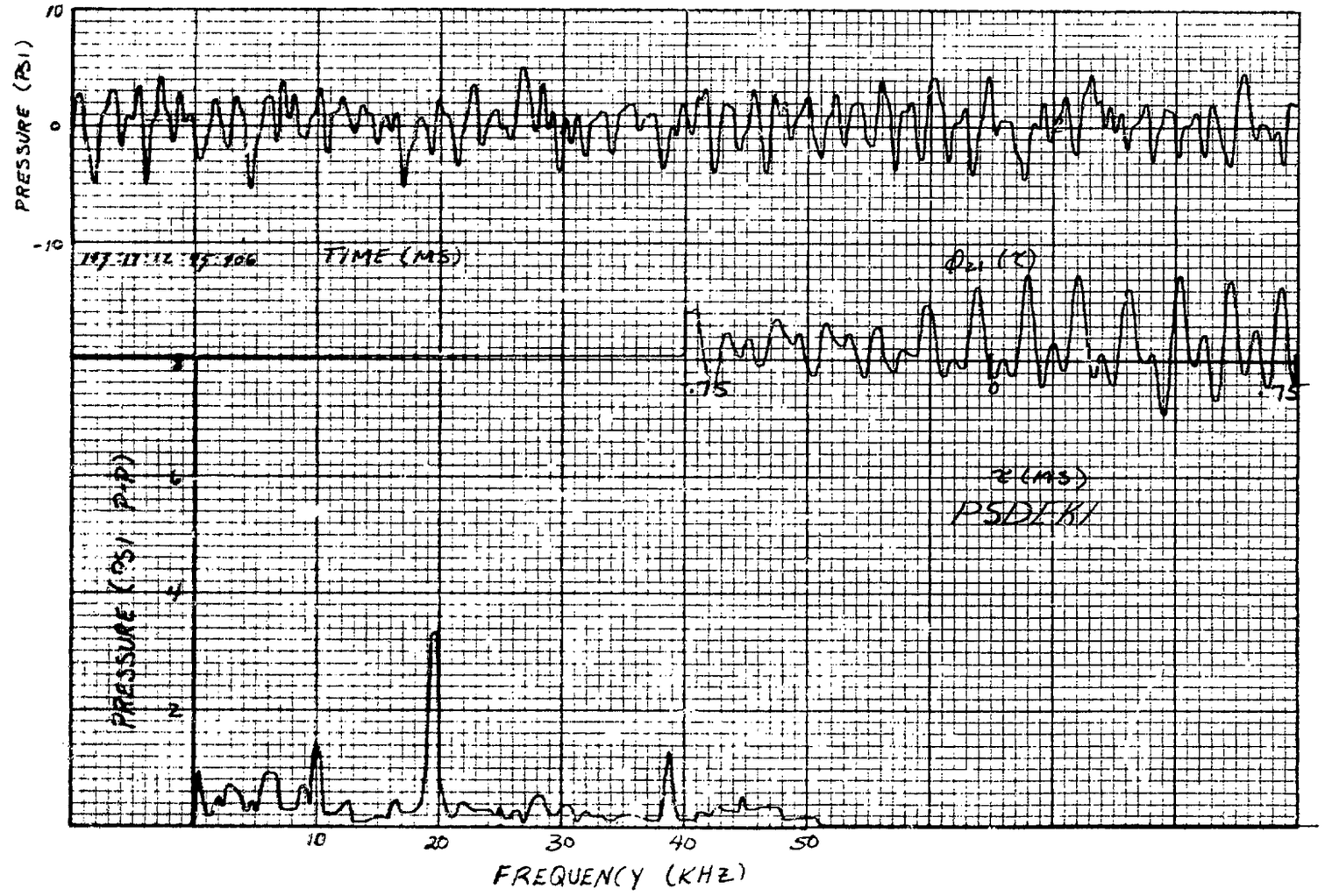

Figure 264. High-Frequency Response Data, 70% Speed, Stall Transient, Time 406, PSDEK1.

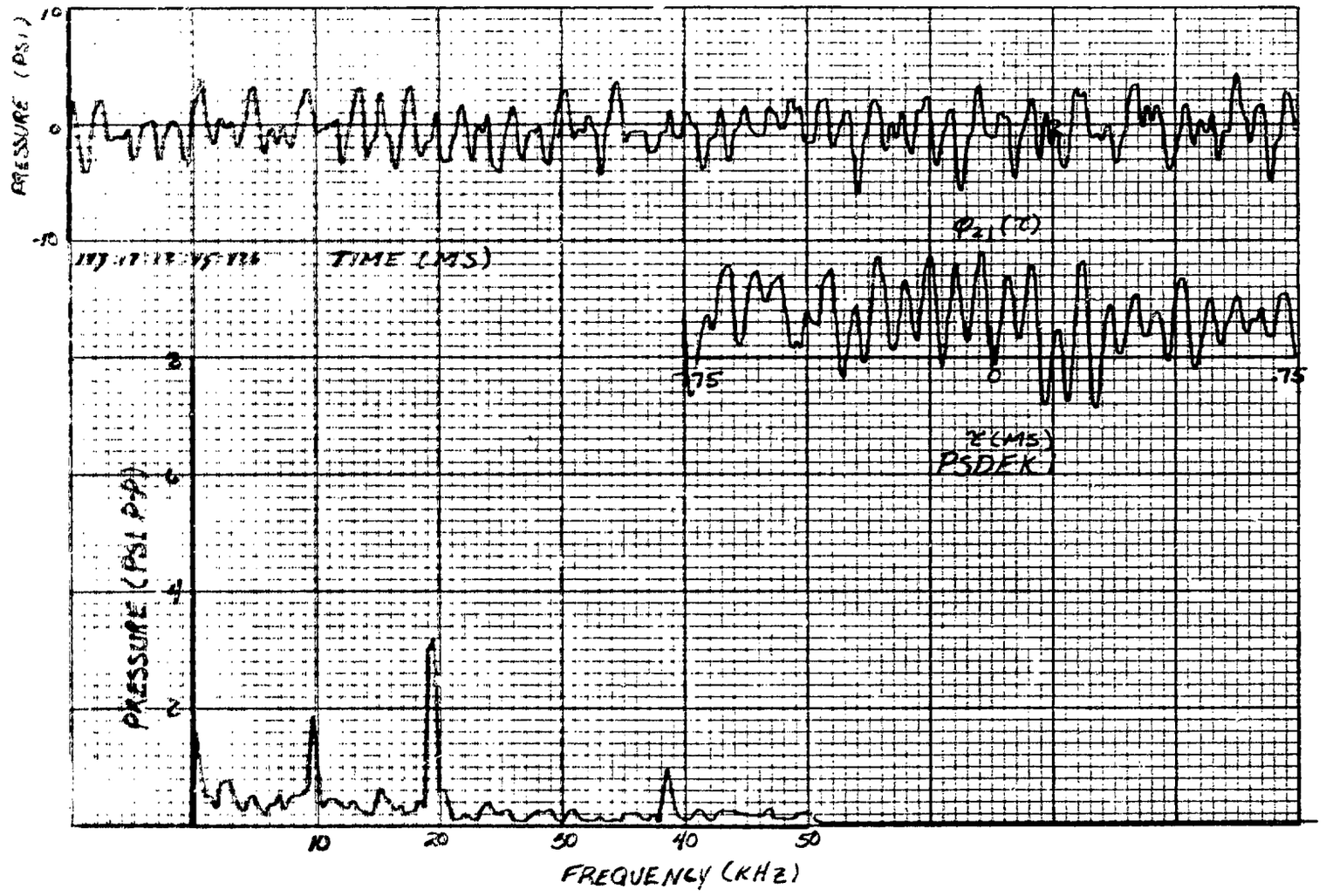

Figure 265. High-Frequency Response Data, 70% Speed, Stall Transient, Time 426, PSDEK1.

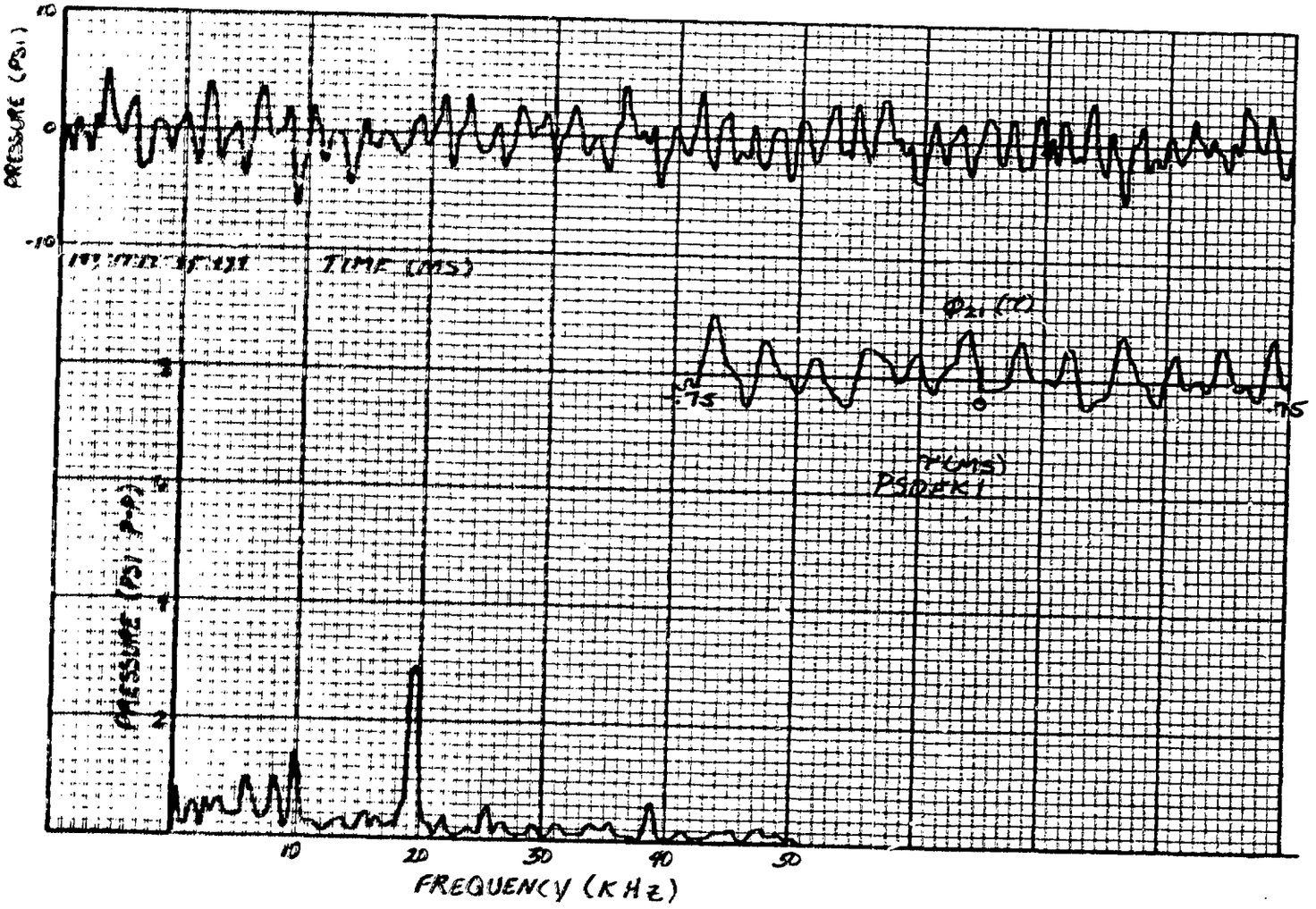

Figure 266. High-Frequency Response Data, 70% Speed, Stall Transient, Time 434, PSDEK1.

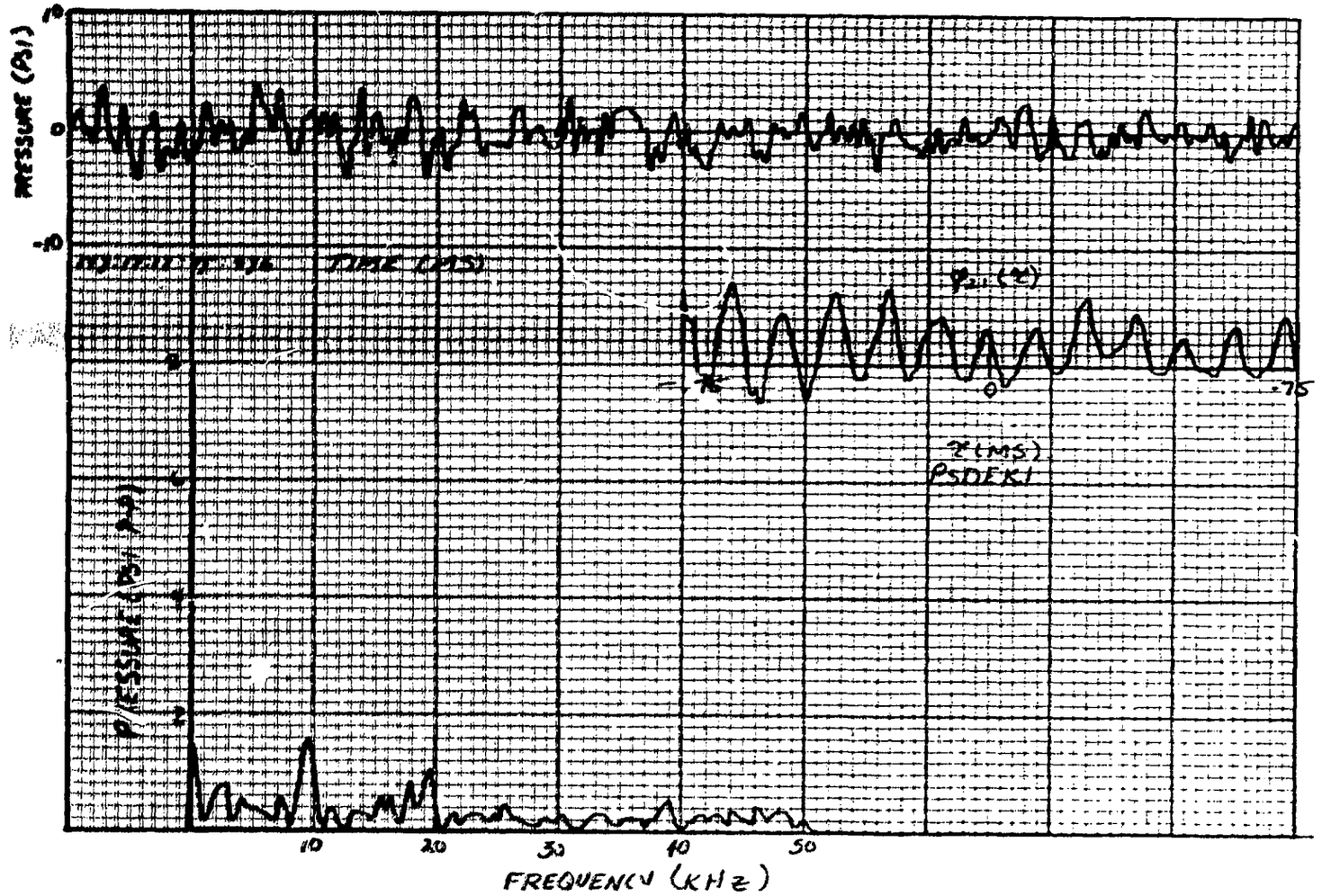

Figure 267. High-Frequency Response Data, 70% Speed, Stall Transient, Time 436, PSDEK1.

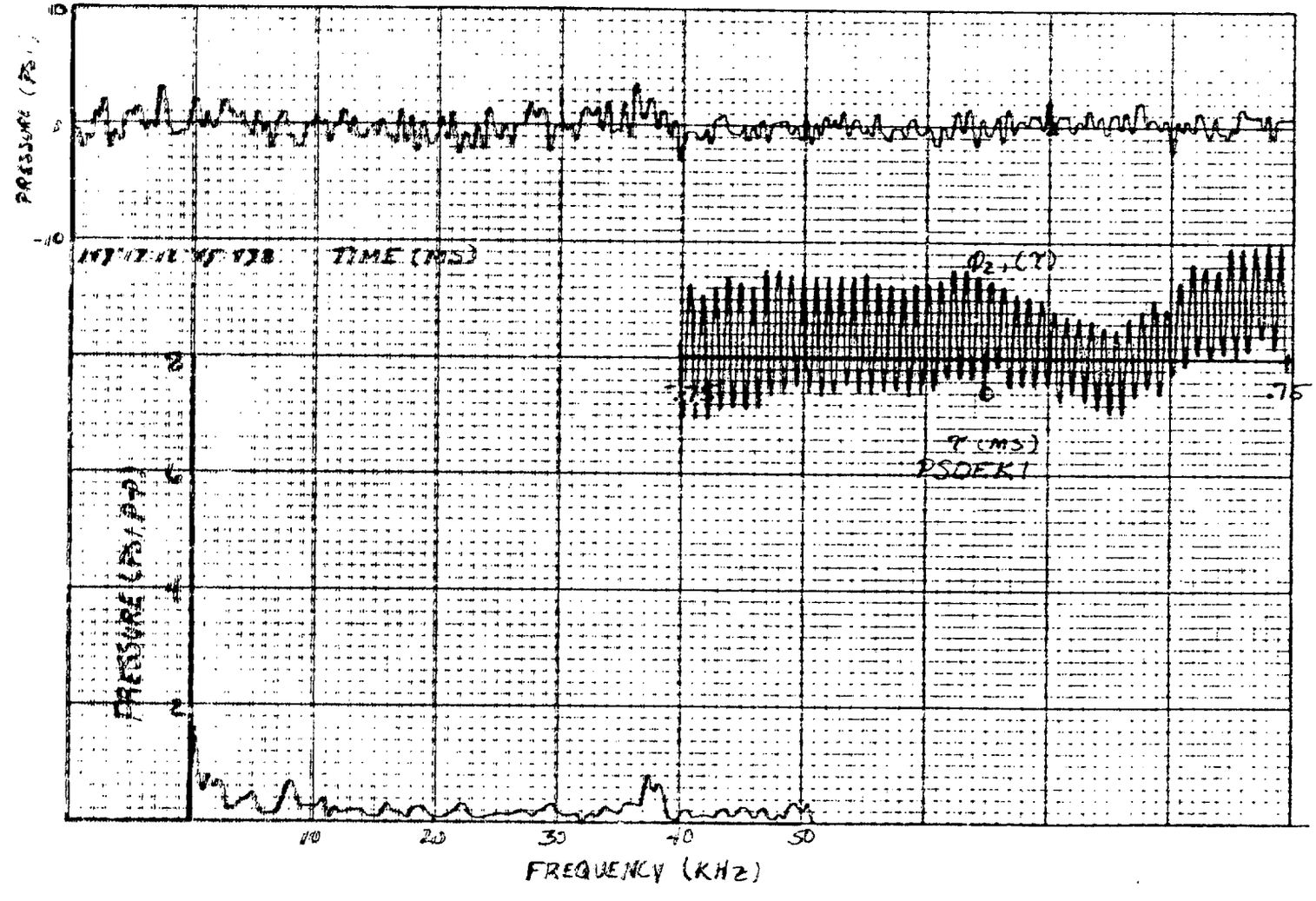

Figure 268. High-Frequency Response Data, 70% Speed, Stalled, Time 438, PSDEK1.

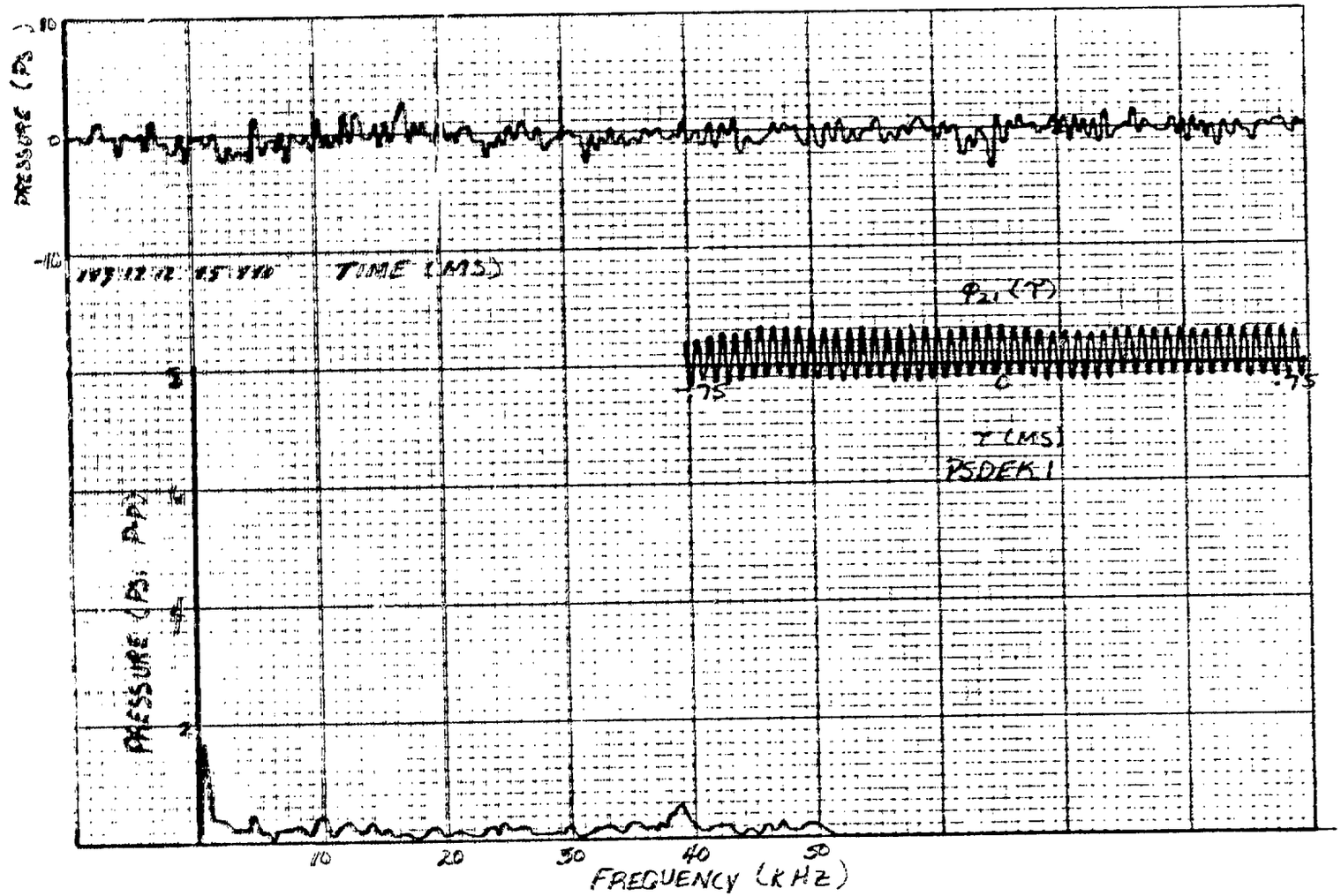

Figure 269. High-Frequency Response Data, 70% Speed, Stalled, Time 440, PSDEK1.

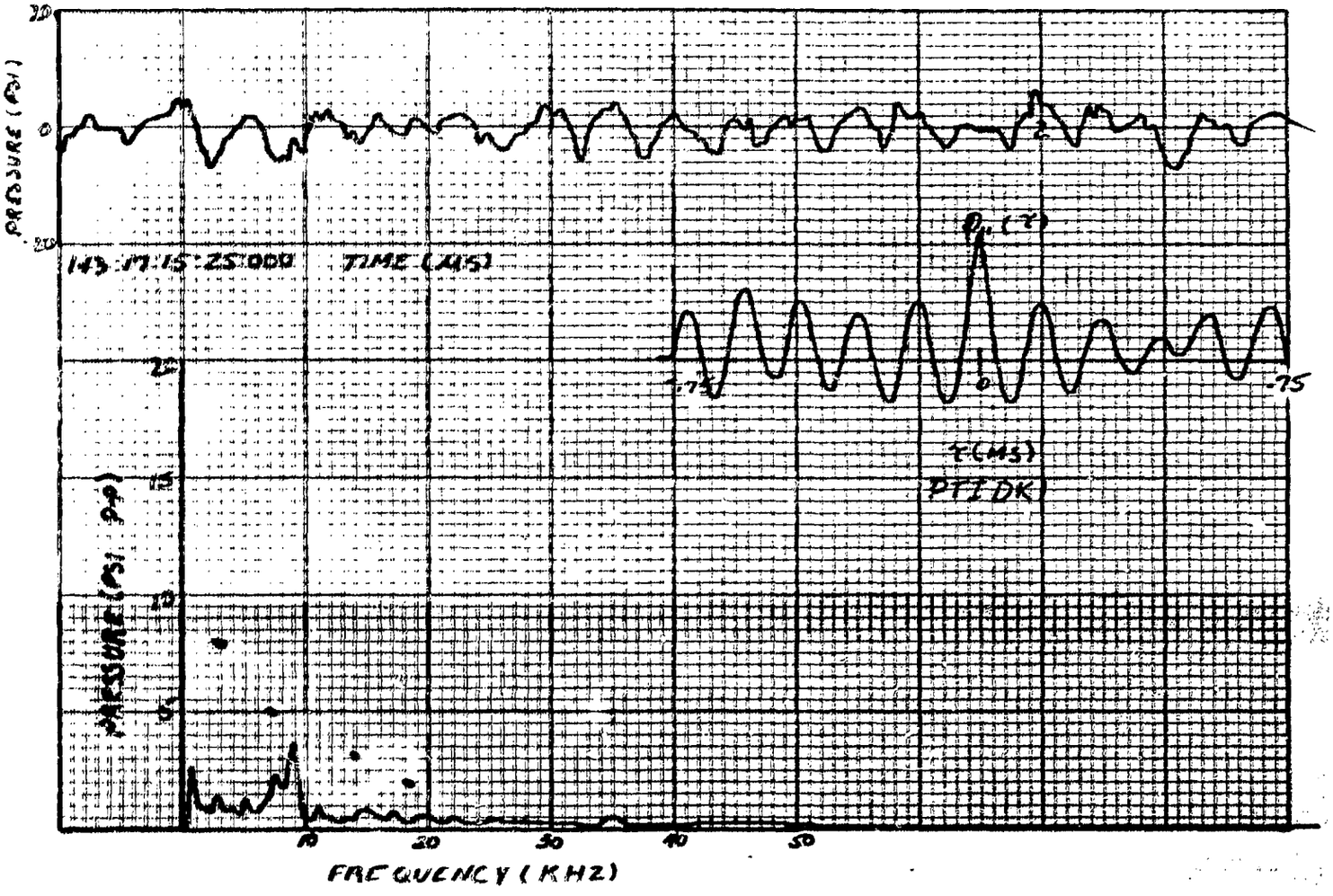

Figure 270. High-Frequency Response Data, 78% Speed, Steady-State, PTIDK1.

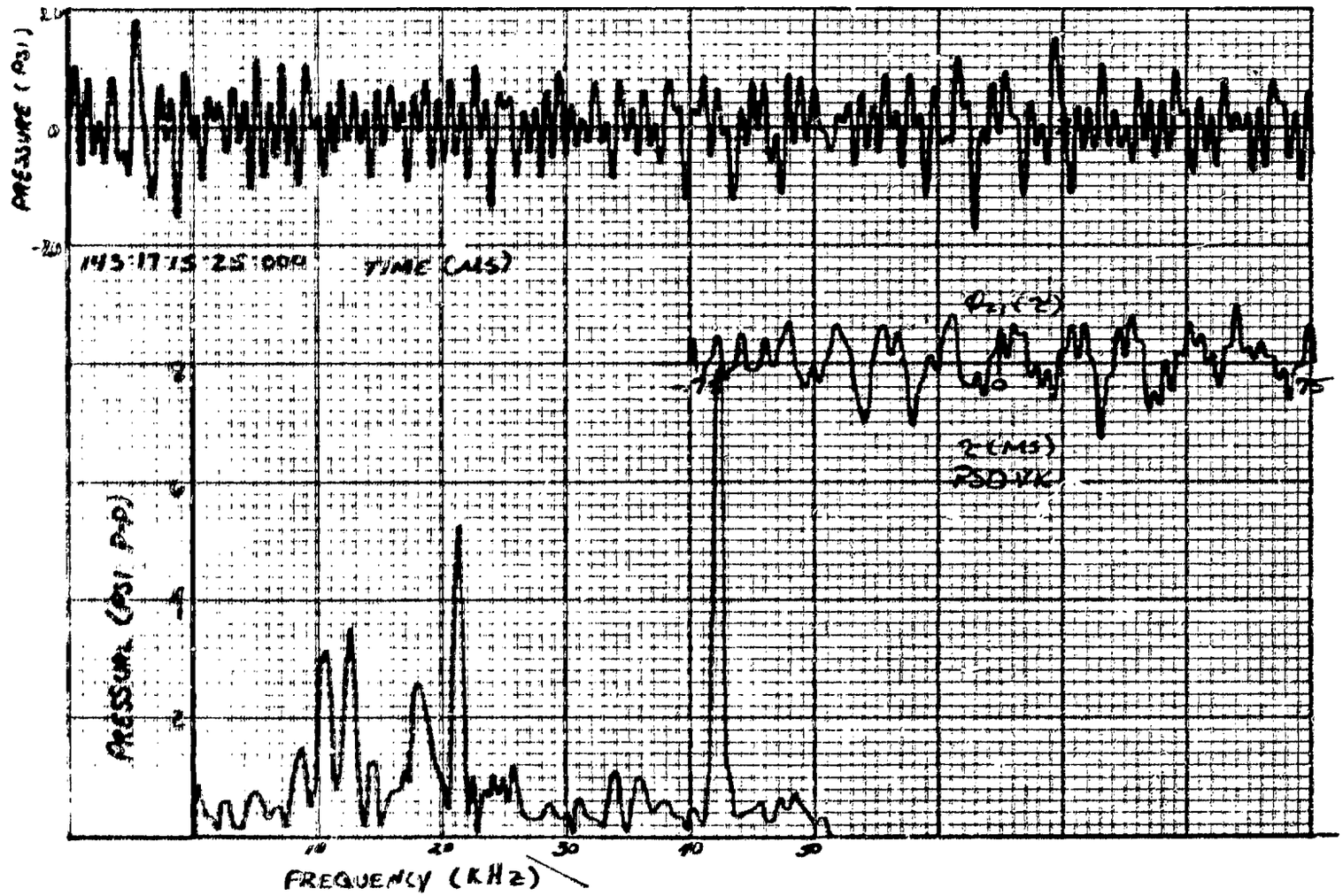

Figure 271. High-Frequency Response Data, 78% Speed, Steady-State, PSDVK1.

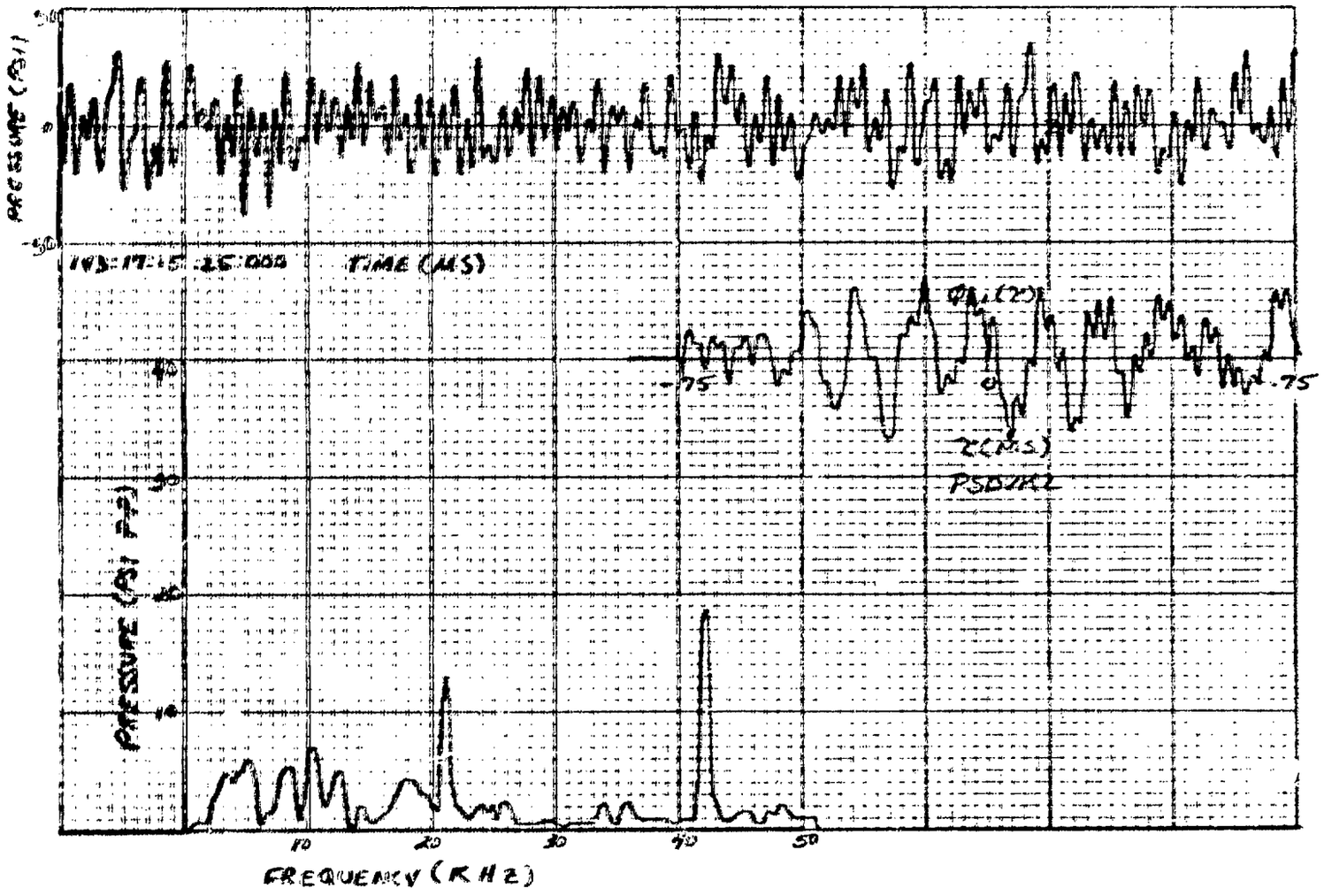

Figure 272. High-Frequency Response Data, 78% Speed, Steady-State, PSDVK2.

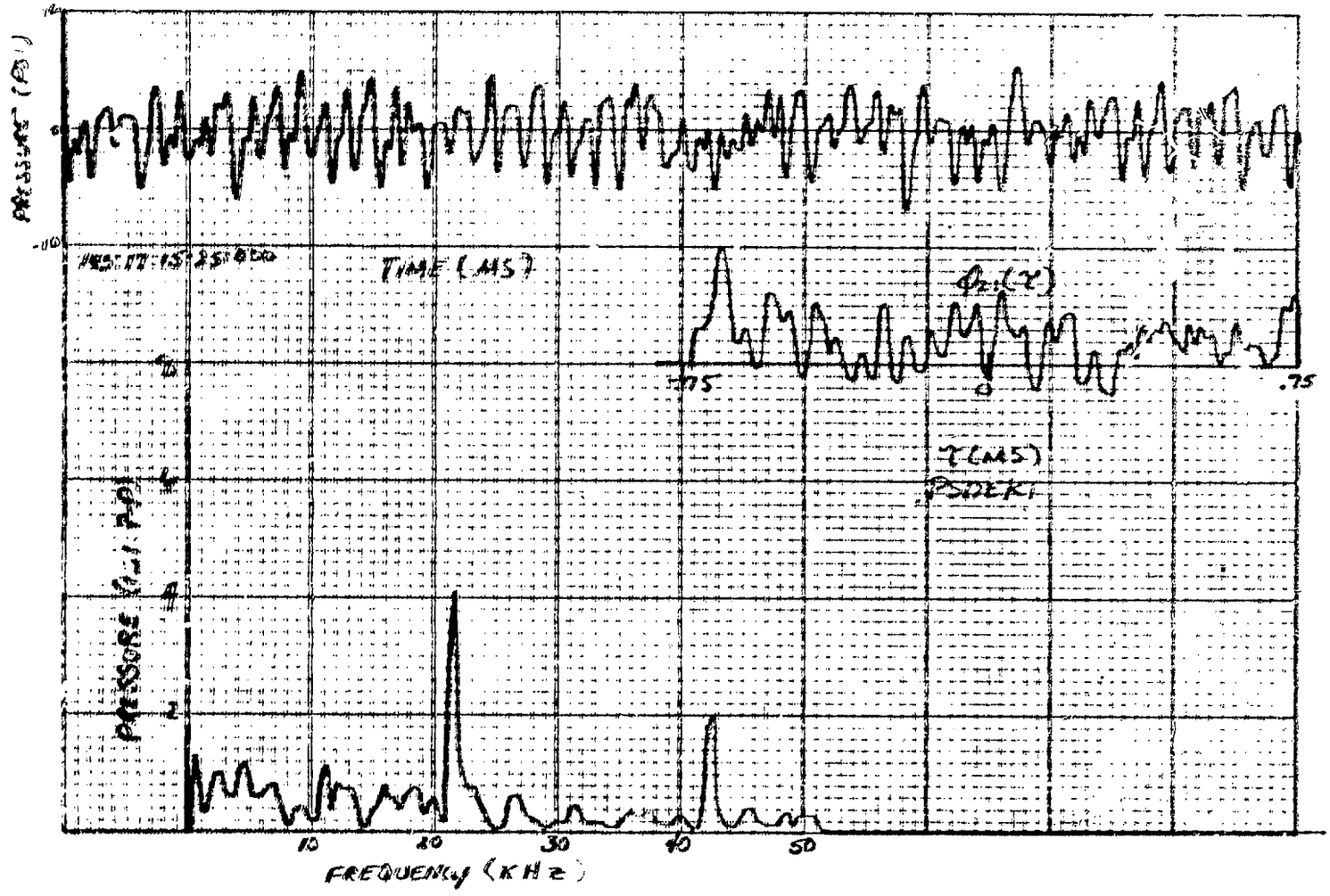

Figure 273. High-Frequency Response Data, 78% Speed, Steady-State, PSDEK1.

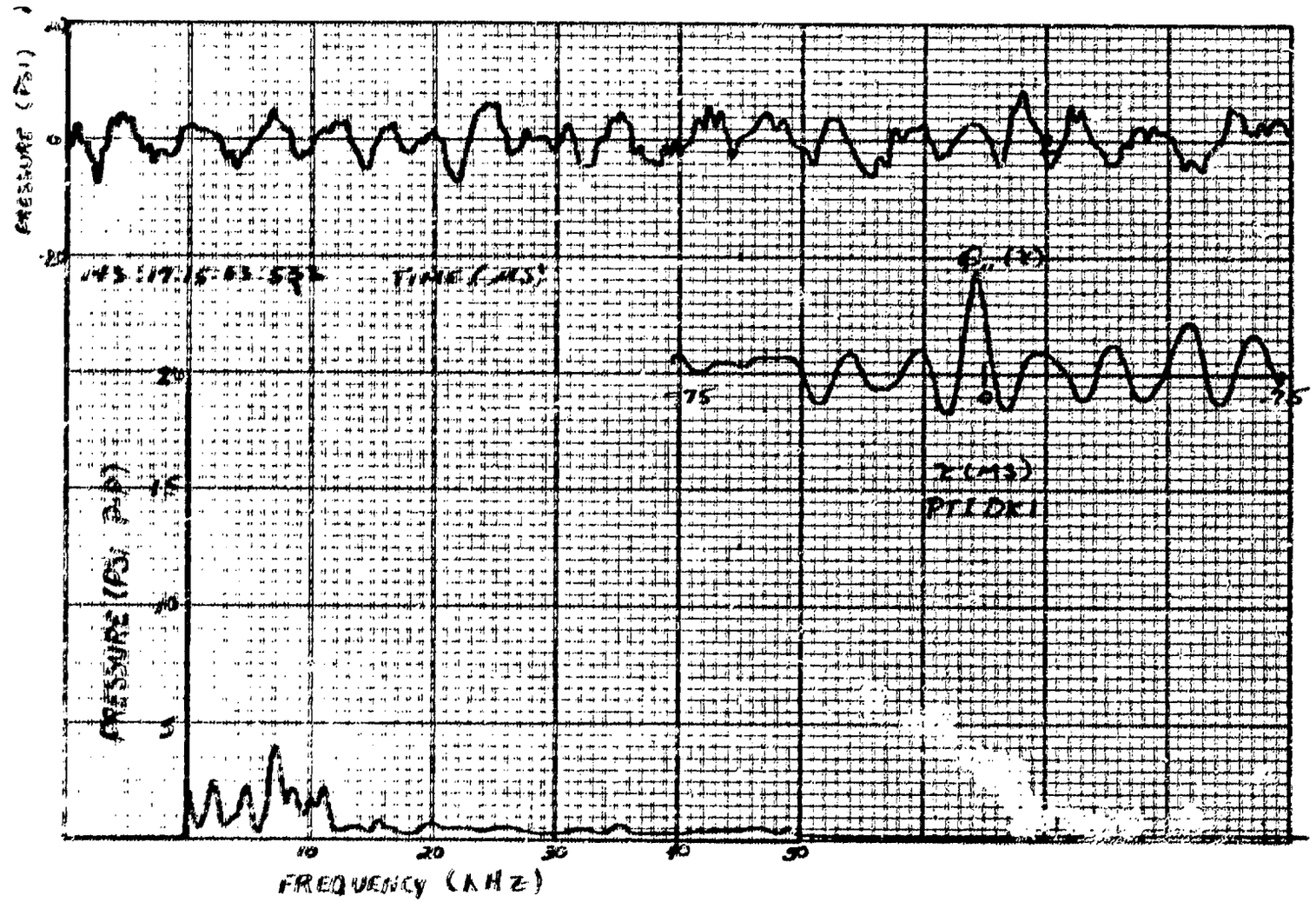

Figure 274. High-Frequency Response Data, 78% Speed, Stall Transient, Time 533, PT1DK1.

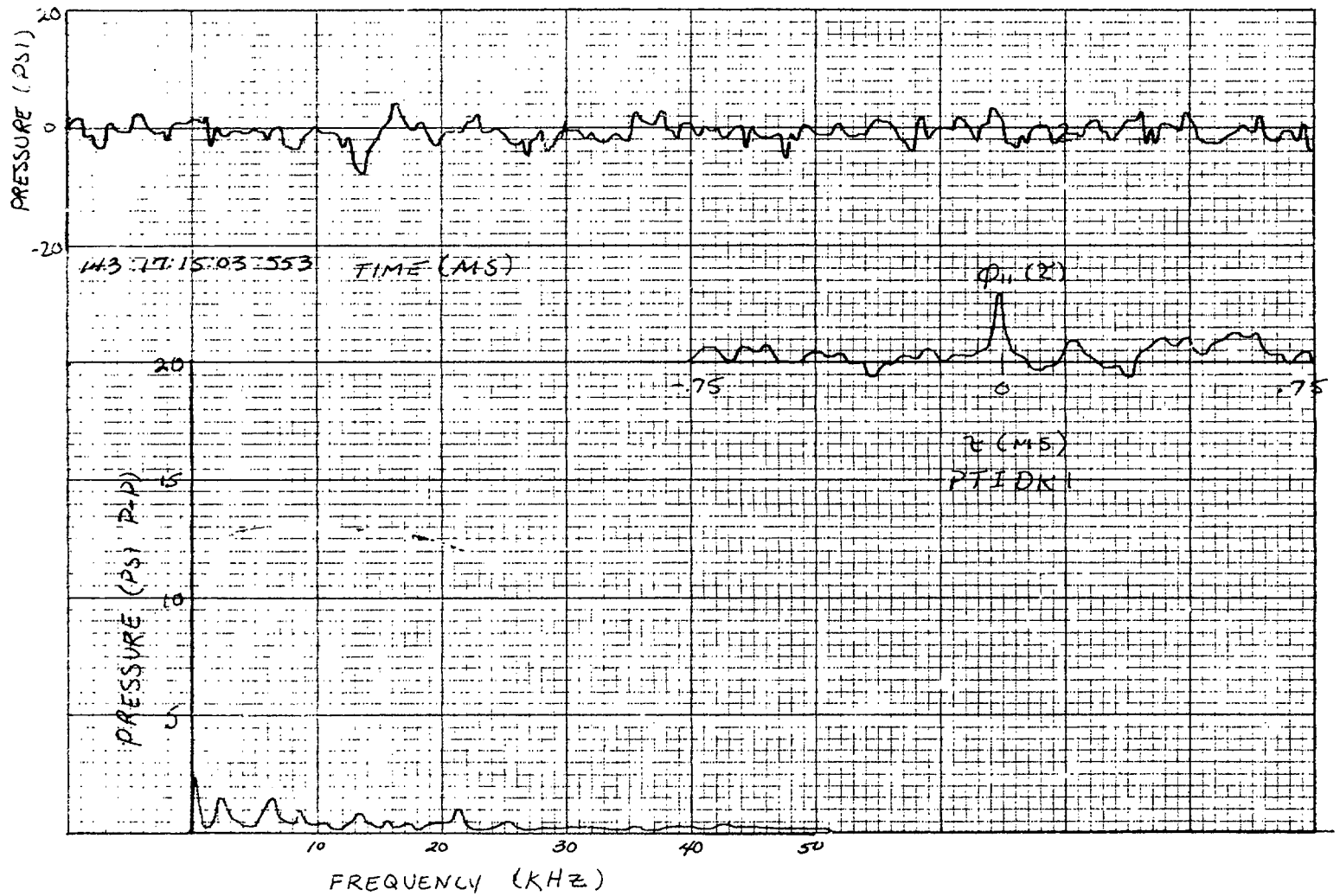

Figure 275. High-Frequency Response Data, 78% Speed, Stall Transient, Time 553, PTIDK1.

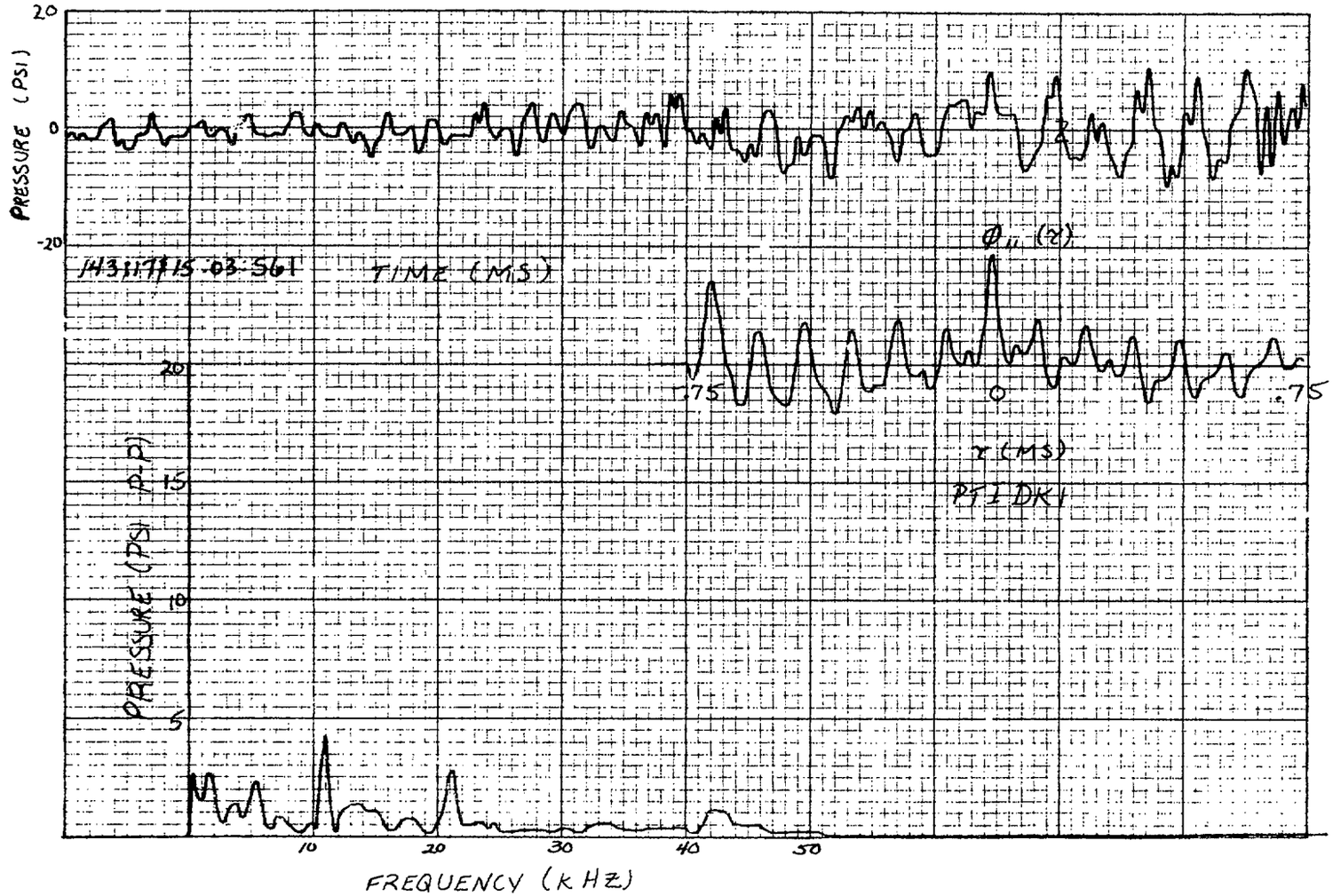

Figure 276. High-Frequency Response Data, 78% Speed, Stall Transient, Time 561, PTIDK1.

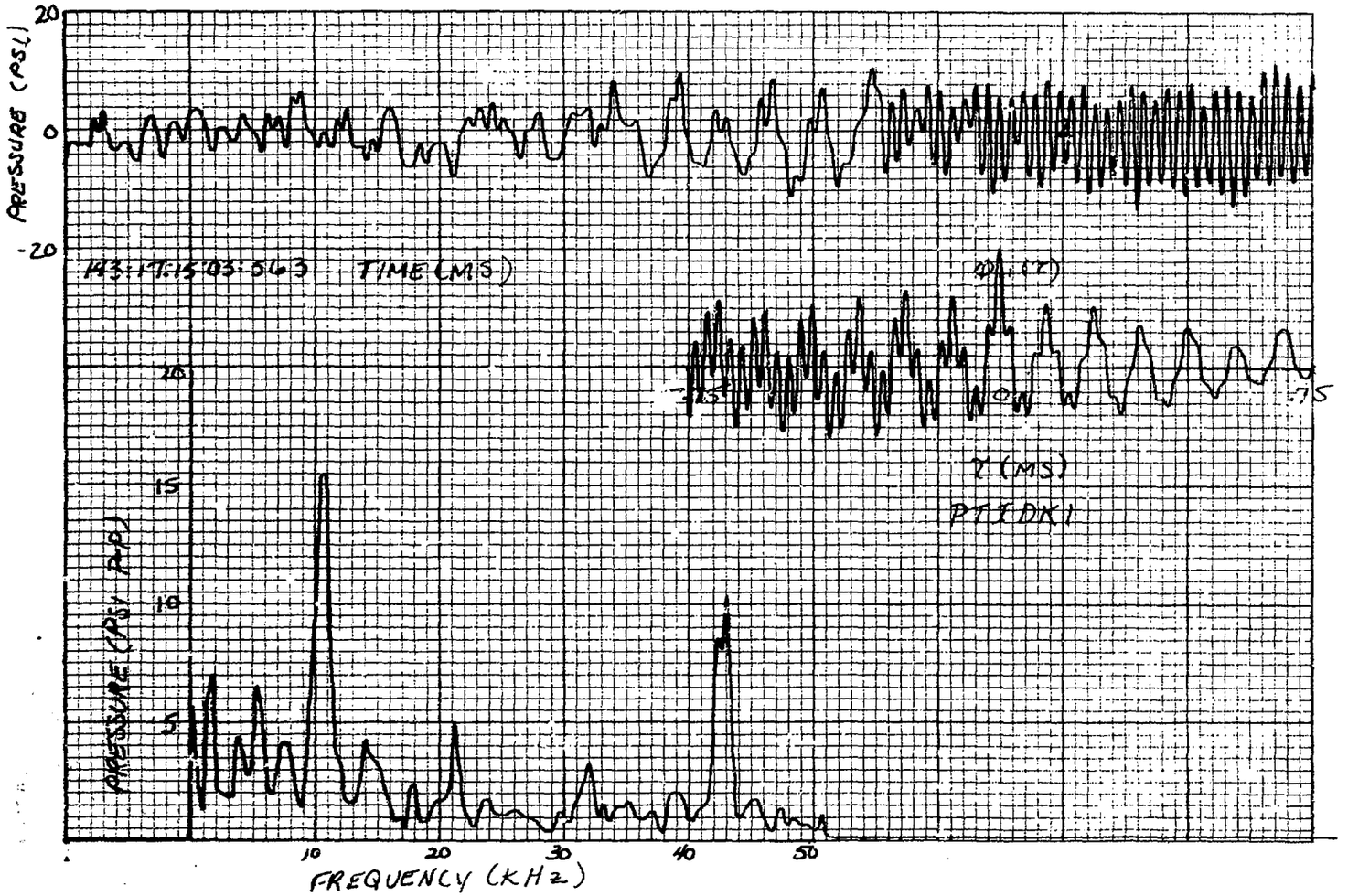

Figure 277. High-Frequency Response Data, 78% Speed, Stall Transient, Time 563, PTIDK1.

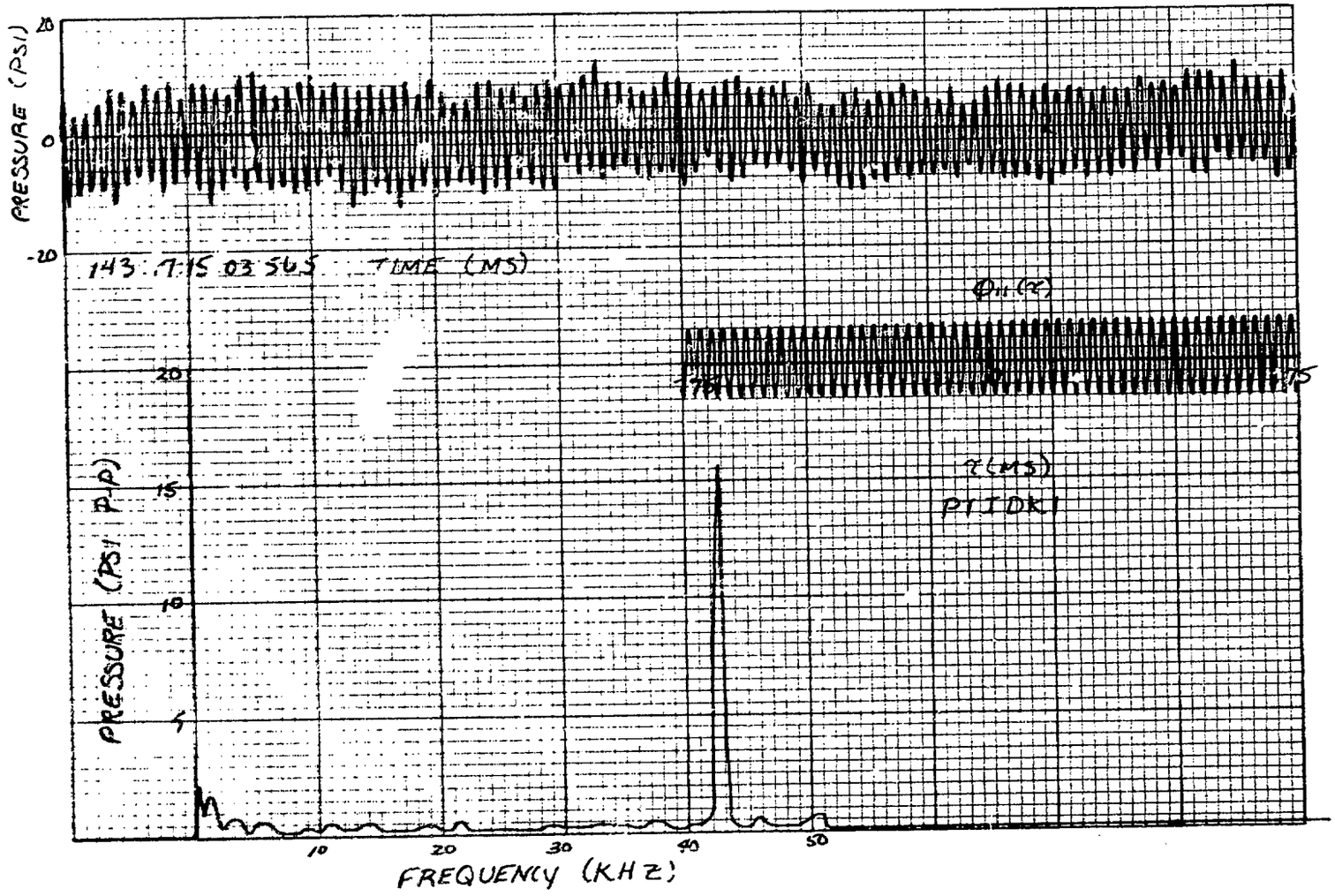

Figure 278. High-Frequency Response Data, 78% Speed, Stalled, Time 565, PTIDK1.

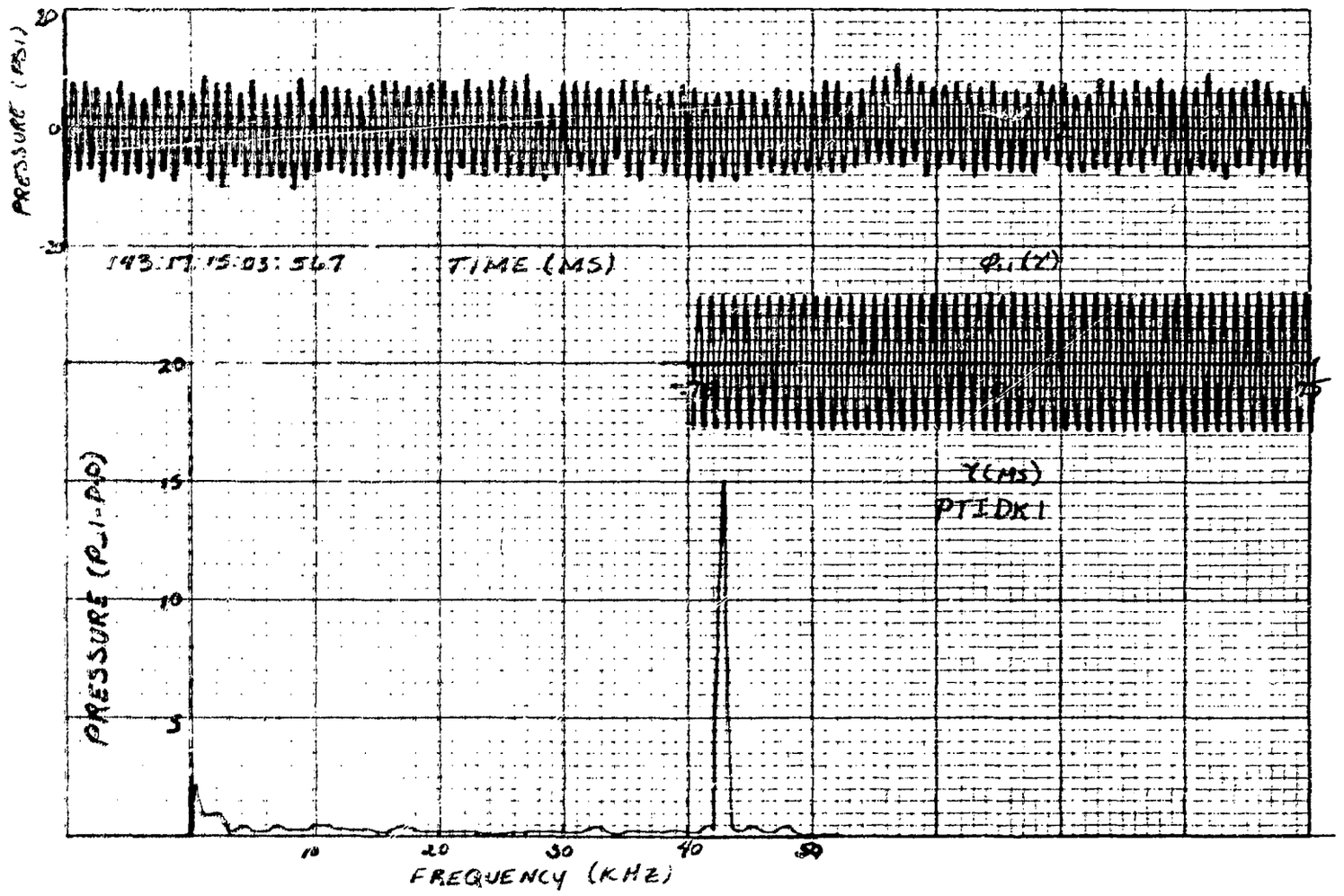

Figure 279. High-Frequency Response Data, 78% Speed, Stalled, Time 567, PTIDK1.

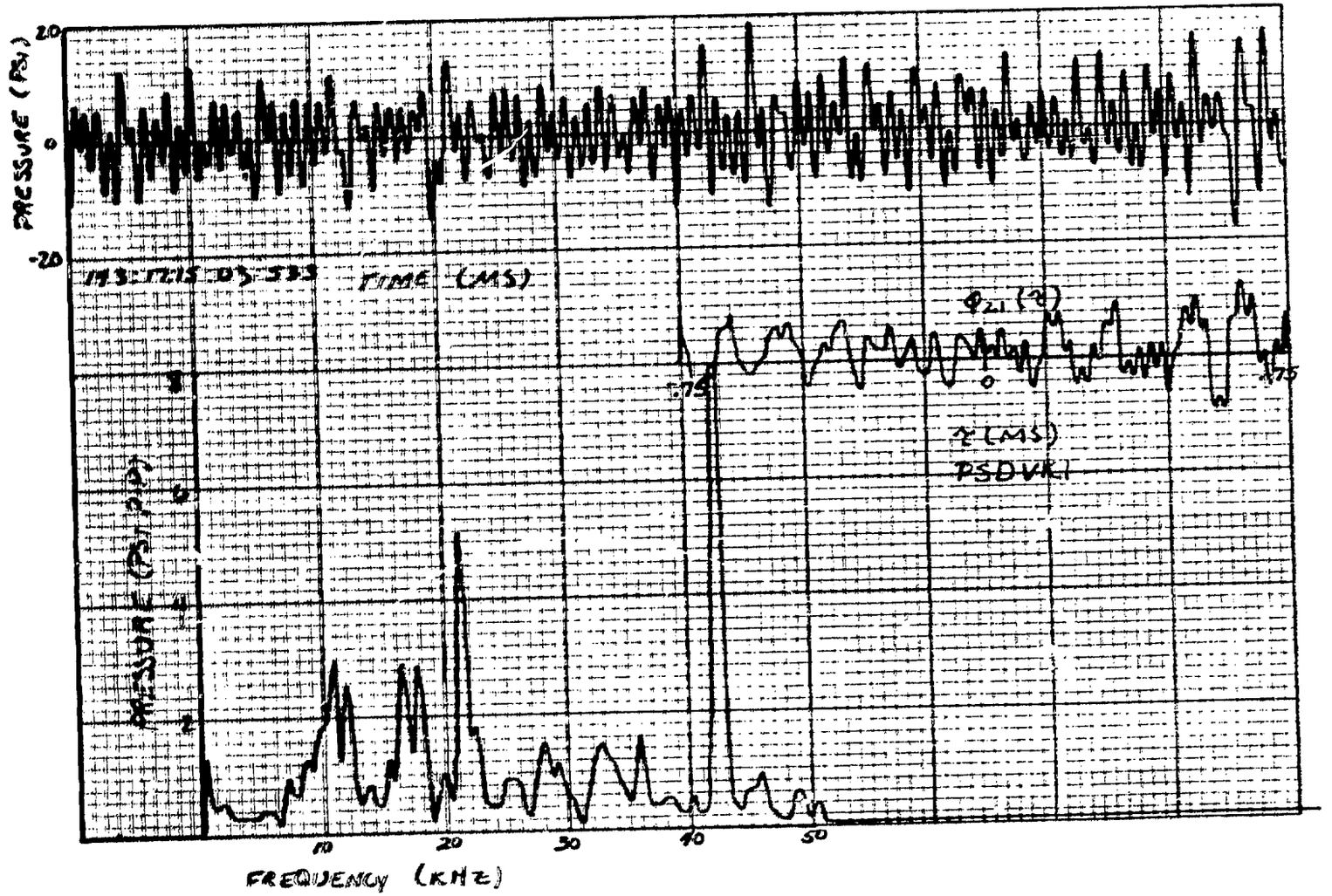

Figure 260. High-Frequency Response Data, 78% Speed, Stall Transient, Time 533, PSDVK1.

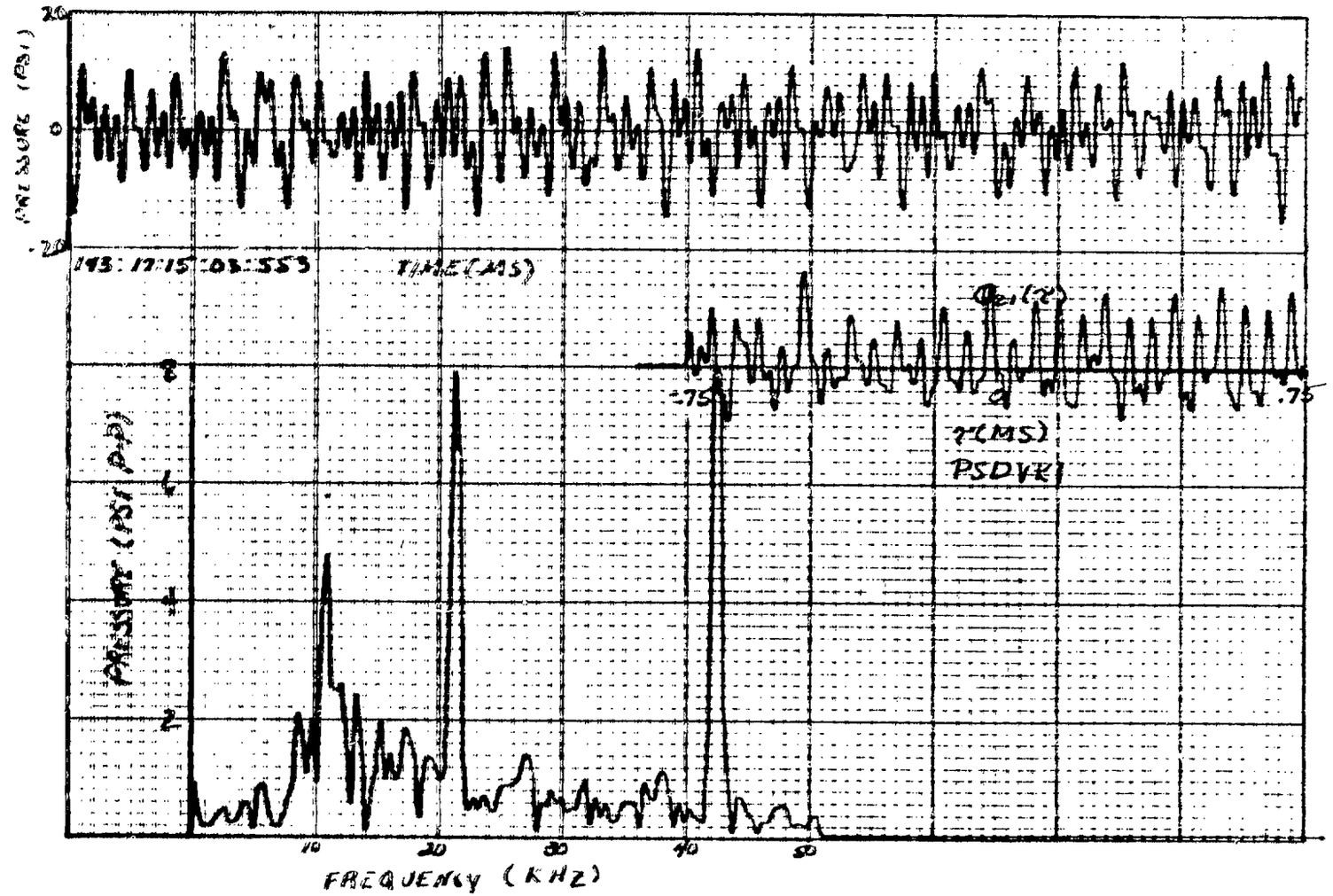

Figure 281. High-Frequency Response Data, 78% Speed, Stall Transient, Time 553, PSDVK1.

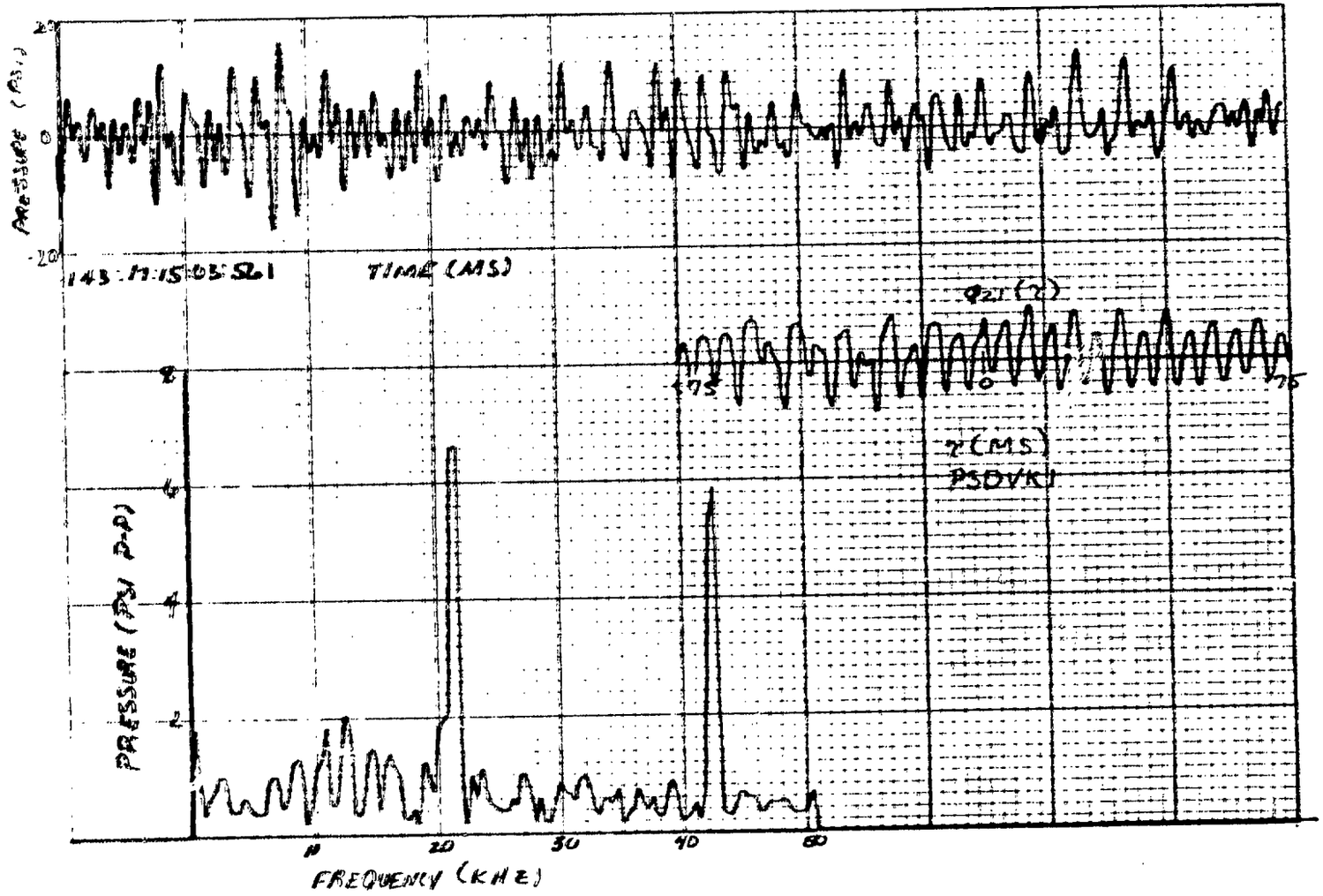

Figure 282. High-Frequency Response Data, 78% Speed, Stall Transient, Time 561, PSDVK1.

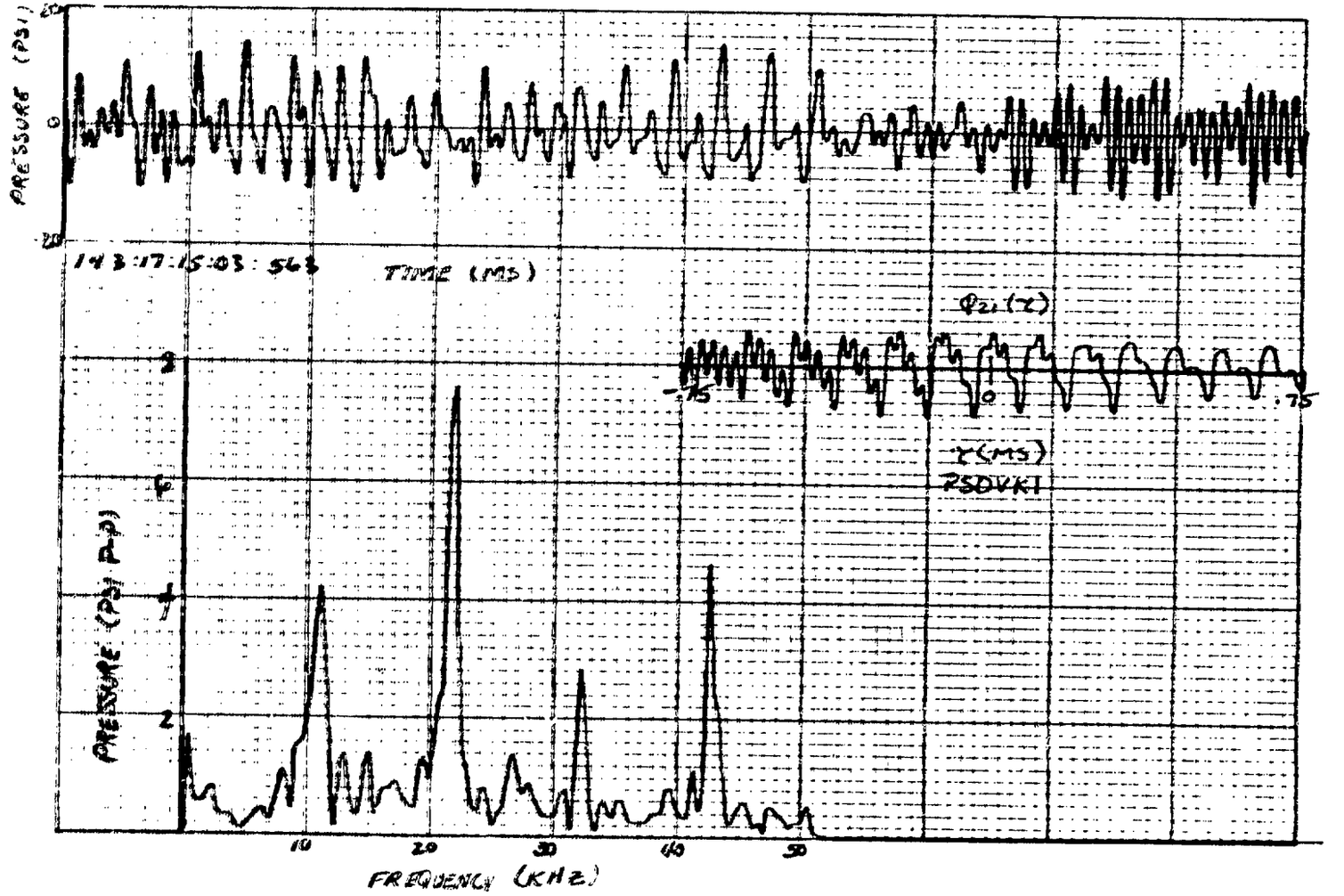

Figure 283. High-Frequency Response Data, 78% Speed, Stall Transient, Time 563, PSDVK1.

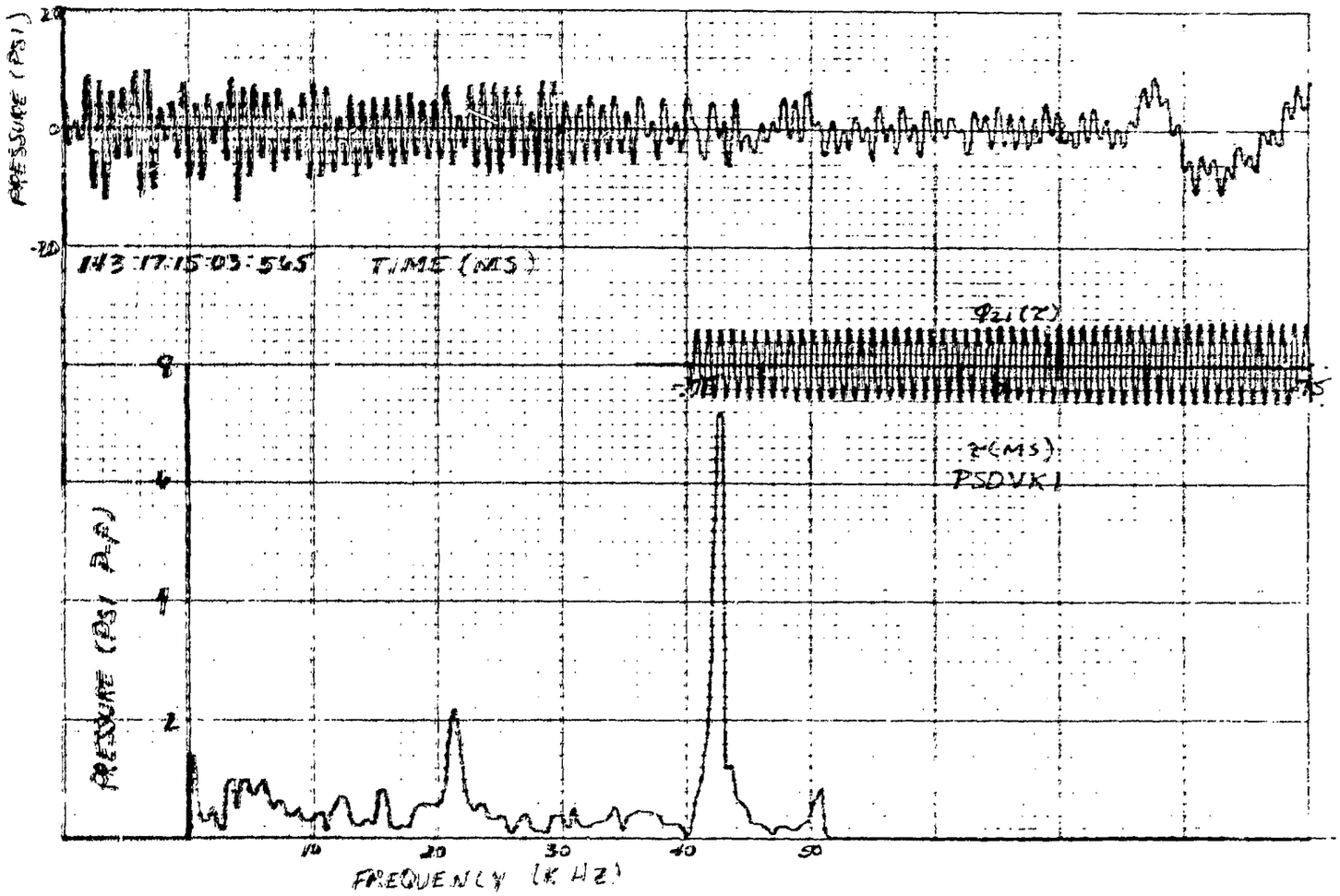

Figure 284. High-Frequ... ...sponse Data, 78% Speed, Stalled, Time 565, PSDVK1.

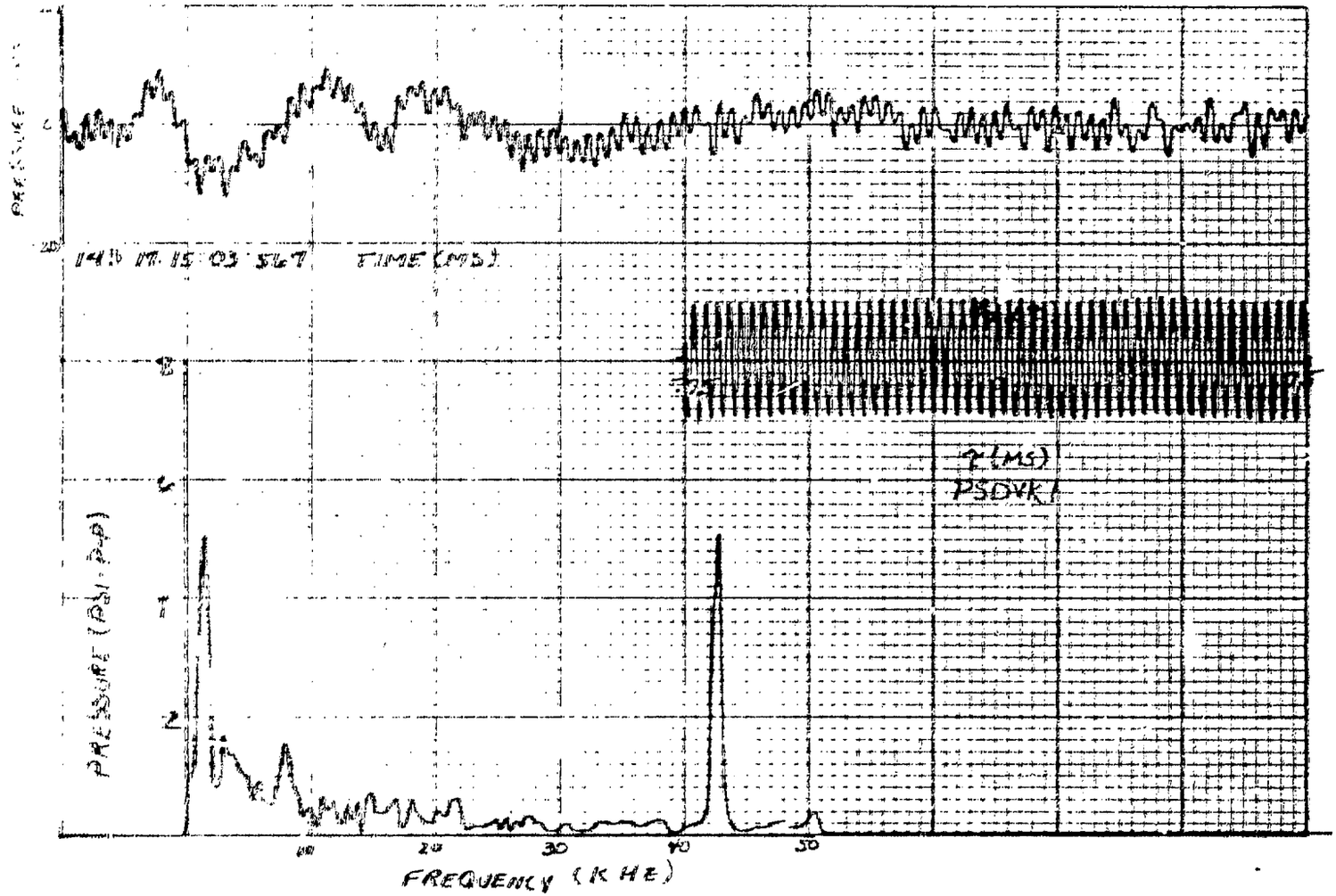

Figure 285. High-Frequency Response Data, 78% Speed, Stalled, Time 567, PSDVK1.

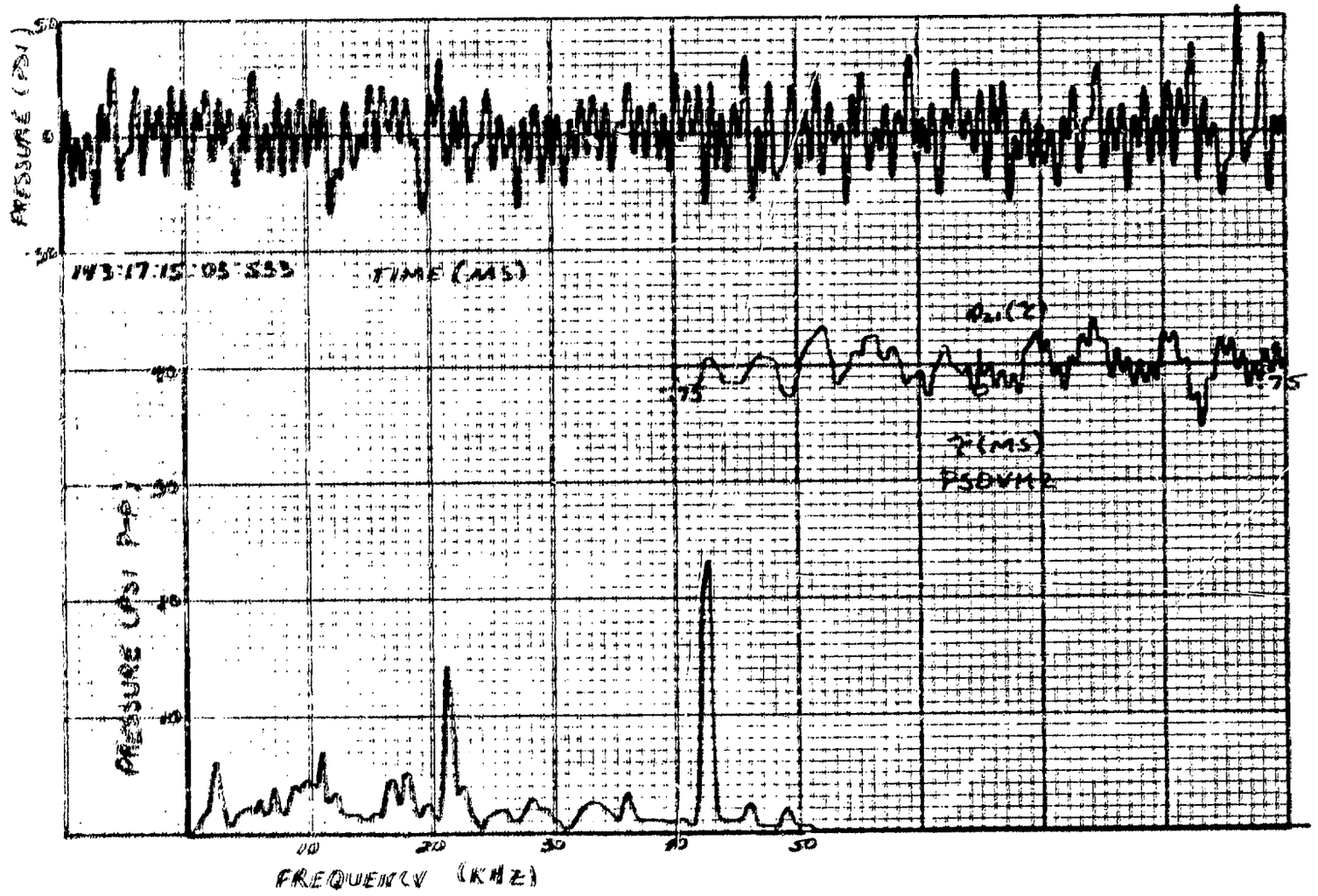

Figure 286. High-Frequency Response Data, 78% Speed, Stall Transient, Time 533, PSDVK2.

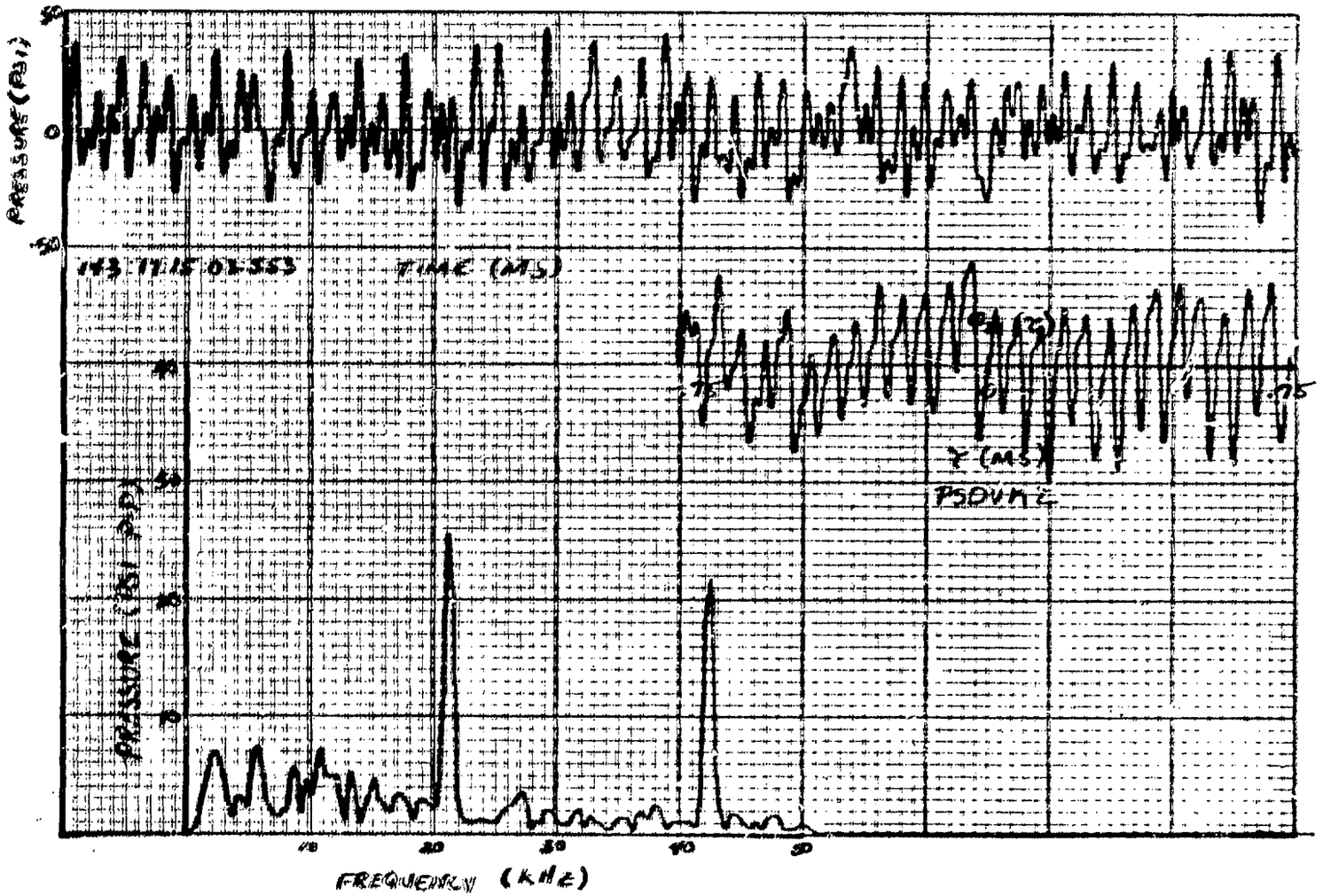

Figure 289. High-Frequency Response Data, 78% Speed, Stall Transient, Time 553, PSDVK2.

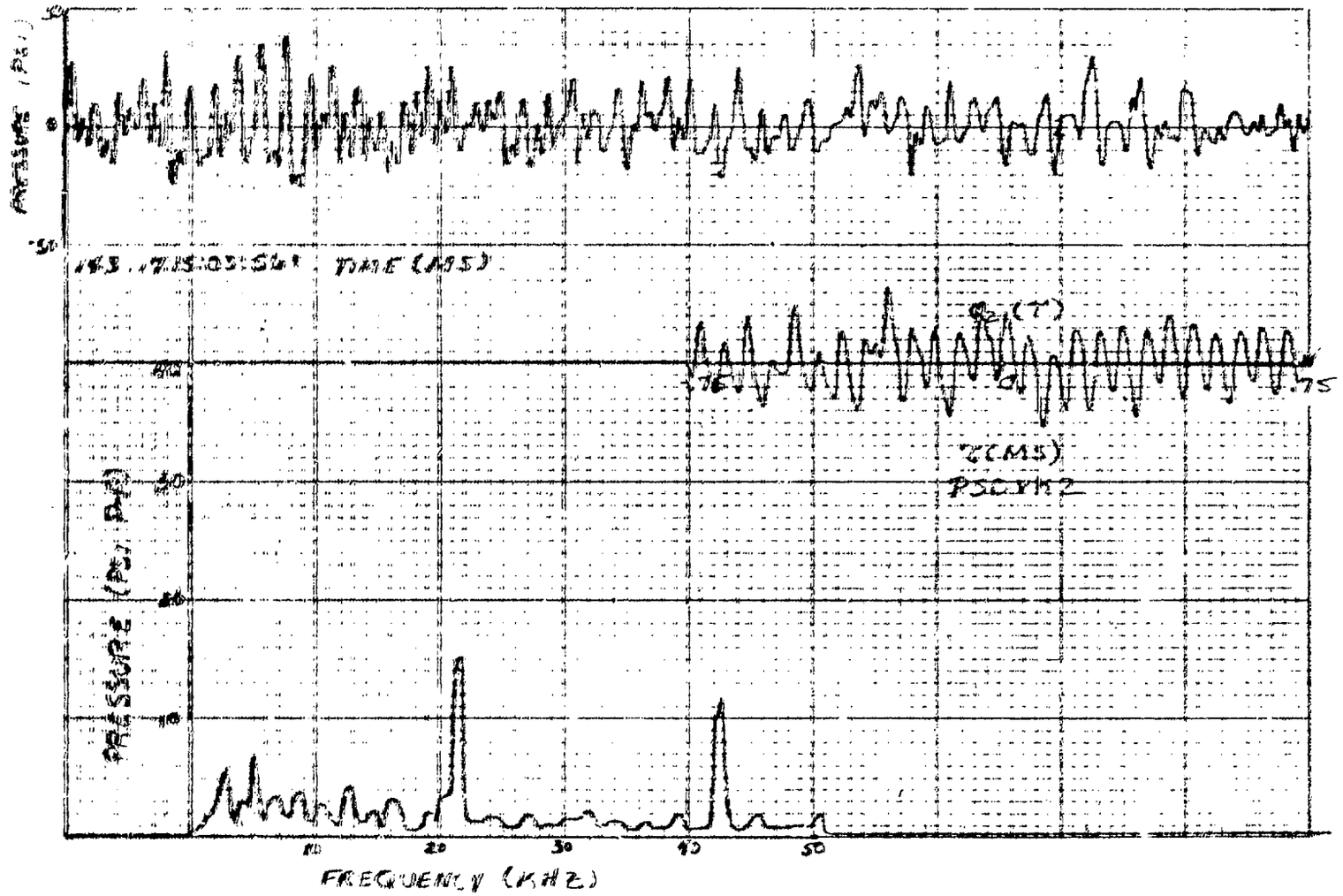

Figure 268. High-Frequency Response Data, 78% Speed, Stall Transient, Time 561, PSDVK2.

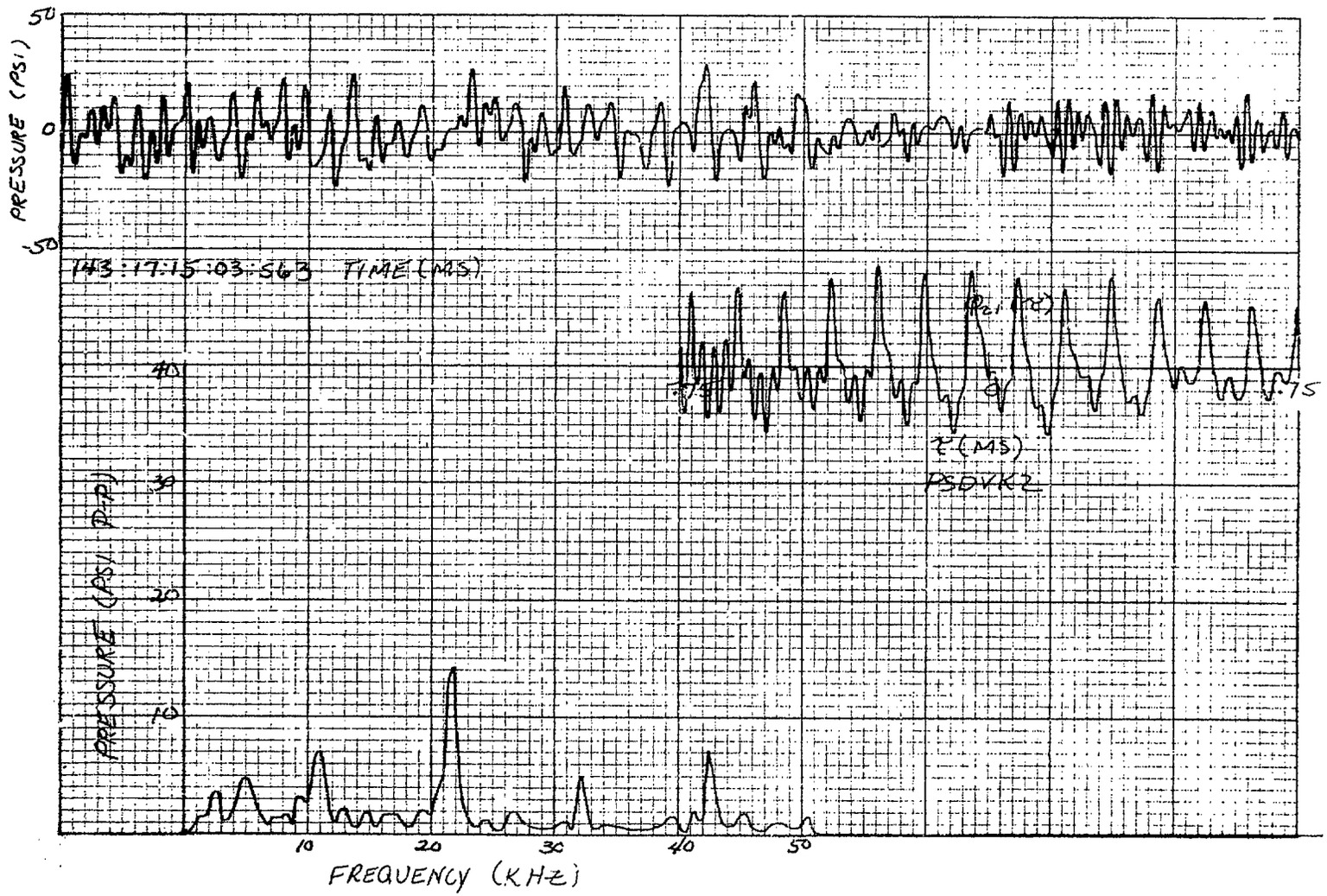

Figure 289. High-Frequency Response Data, 78% Speed, Stall Transient, Time 563, PSDVK2.

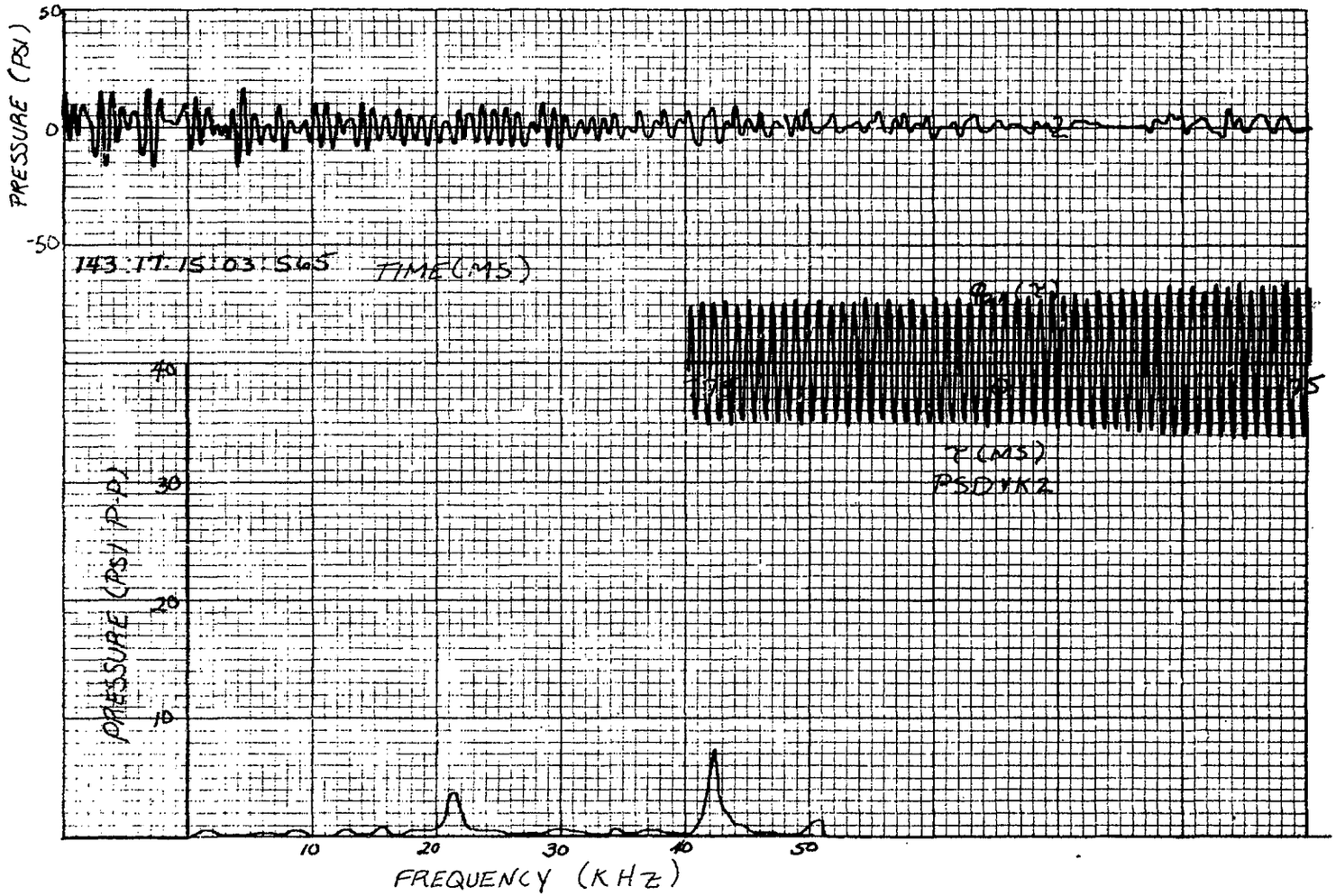

Figure 290. High-Frequency Response Data, 78% Speed, Stalled, Time 565, PSDVK2.

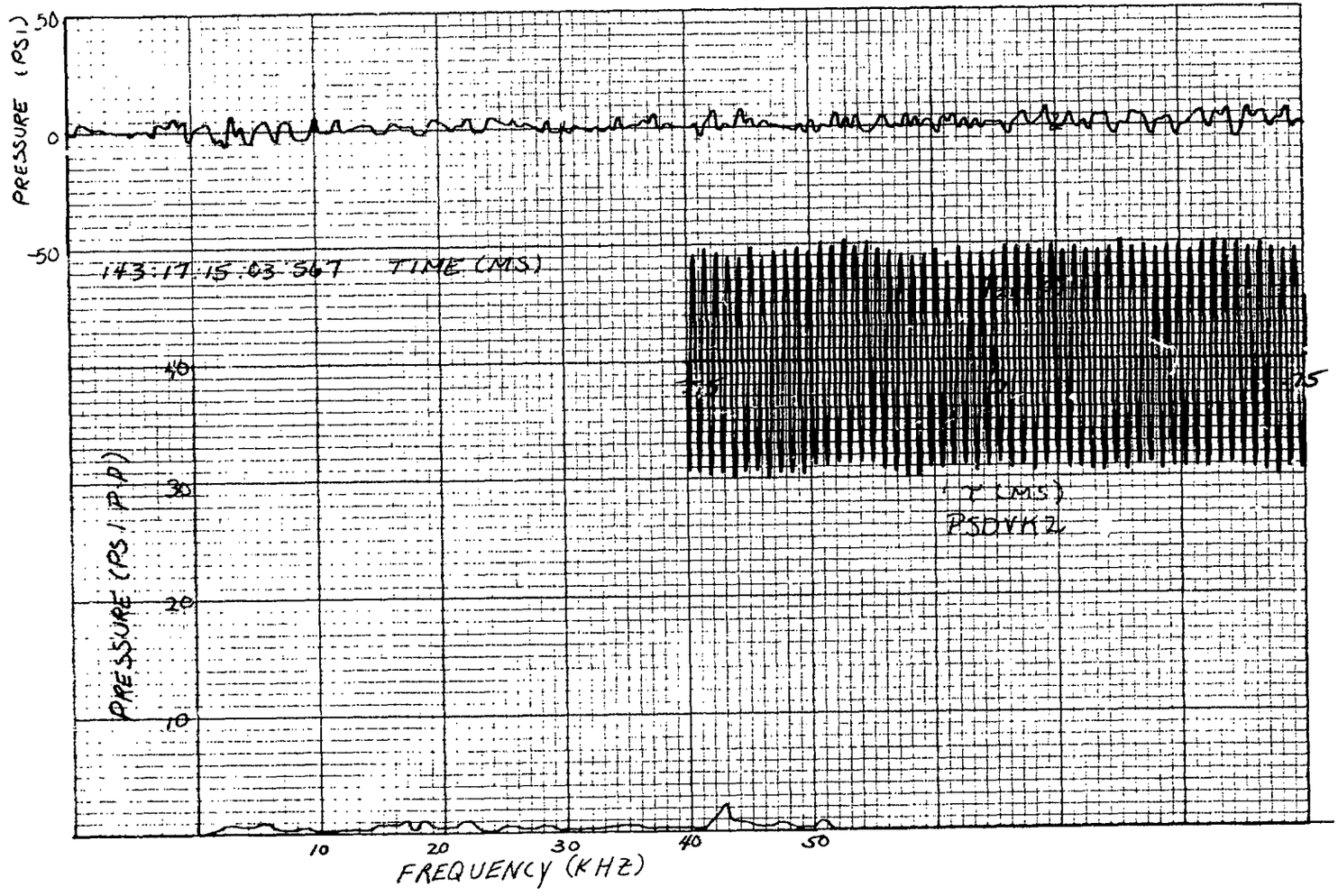

Figure 291. High-Frequency Response Data, 78% Speed, Stalled, Time 567, PSDVK2.

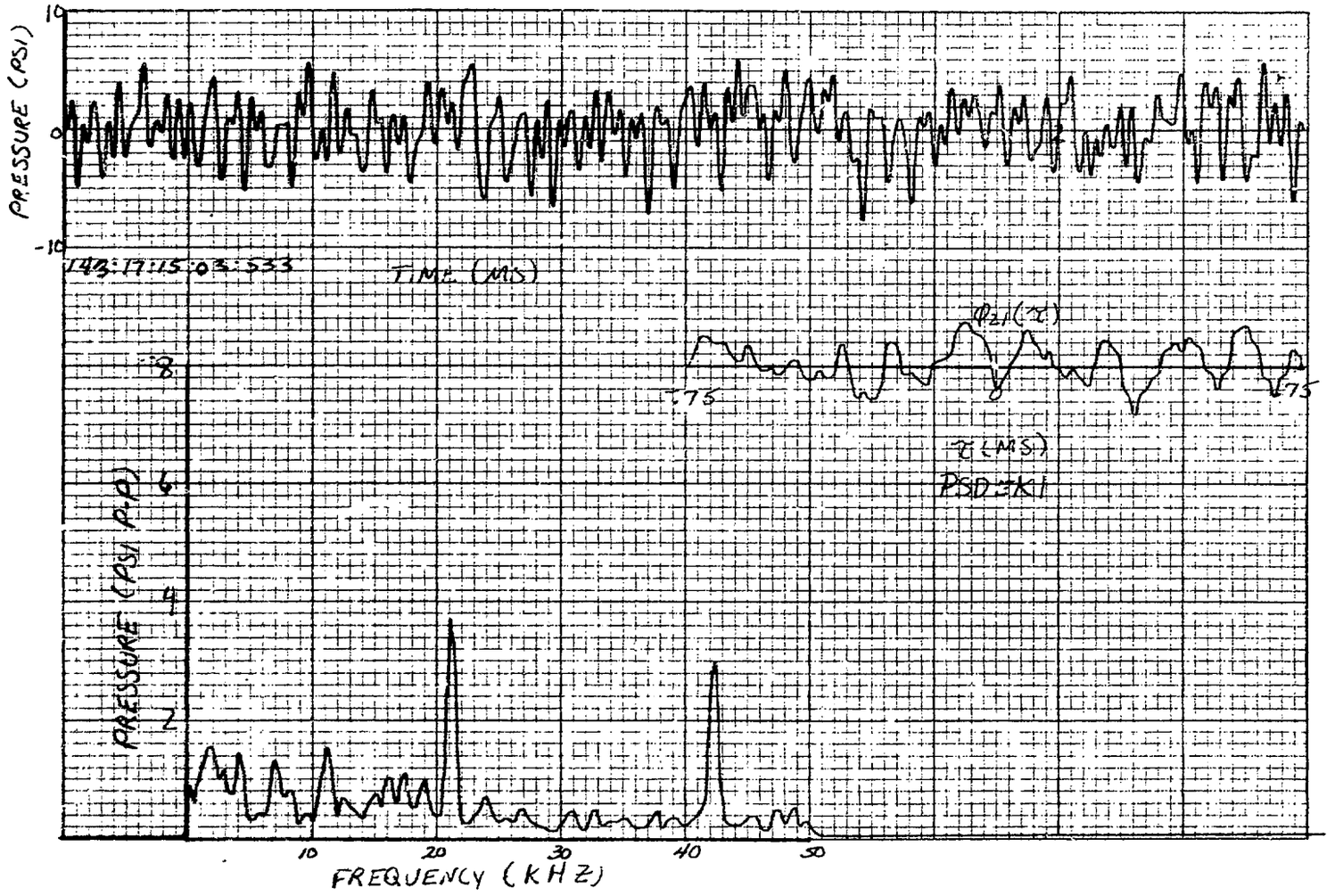

Figure 292. High-Frequency Response Data, 78% Speed, Stall Transient, Time 533, PSDEK1.

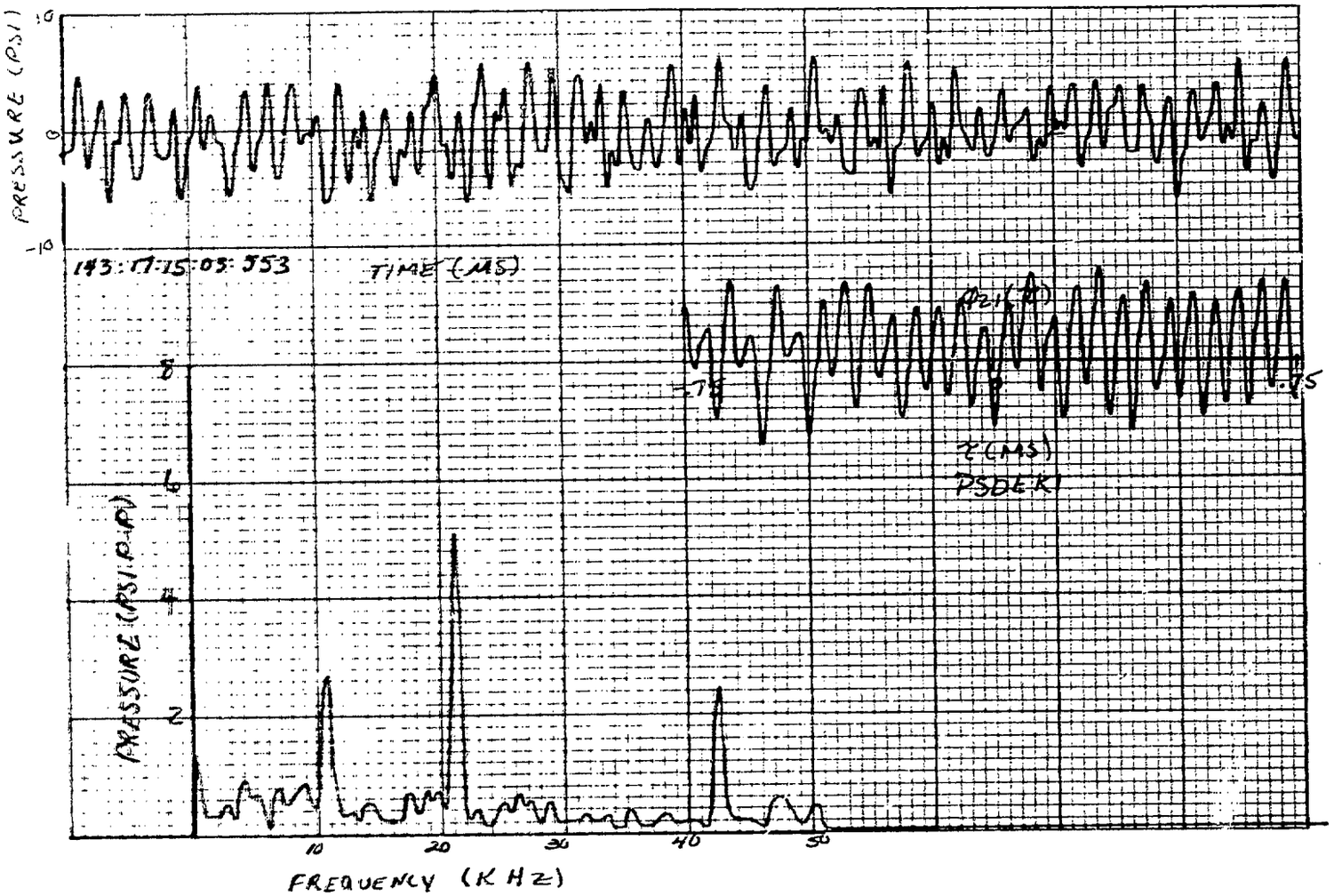

Figure 293. High-Frequency Response Data, 78% Speed, Stall Transient, Time 553, PSDEK1.

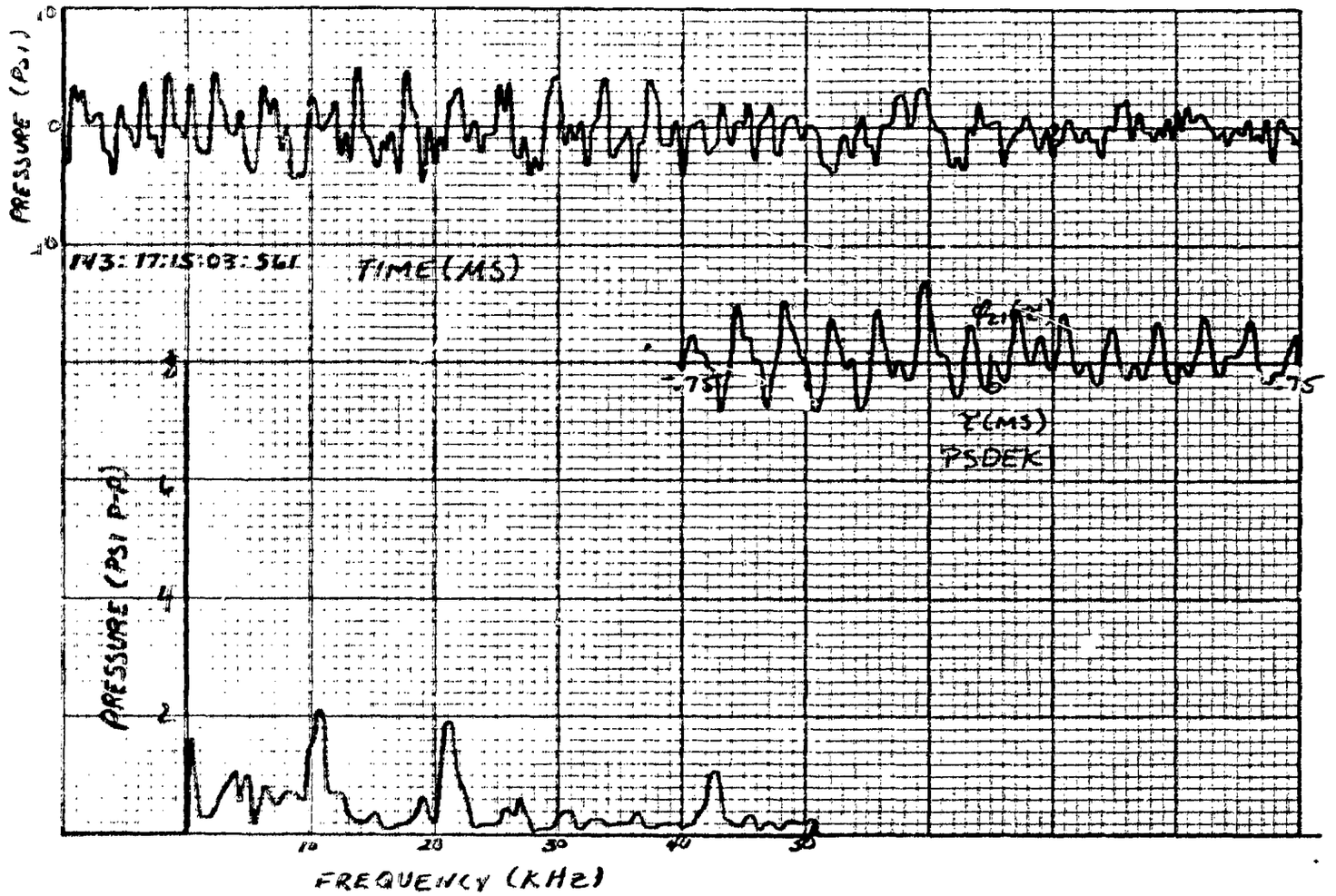

Figure 294. High-Frequency Response Data, 78% Speed, Stall Transient, Time 561, PSDEK1.

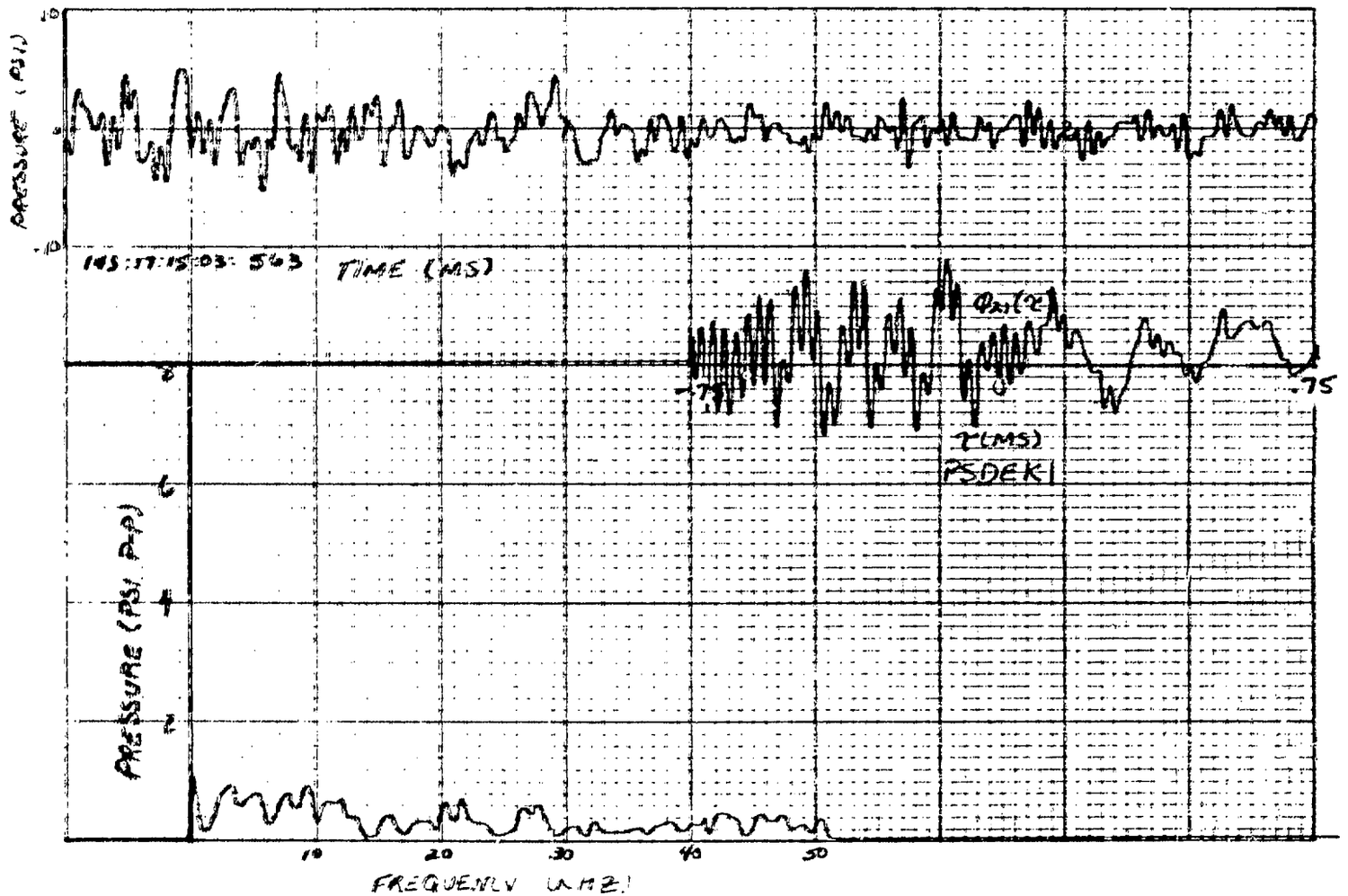

Figure 295. High-Frequency Response Data, 78% Speed, Stall Transient, Time 563, PSDEK1.

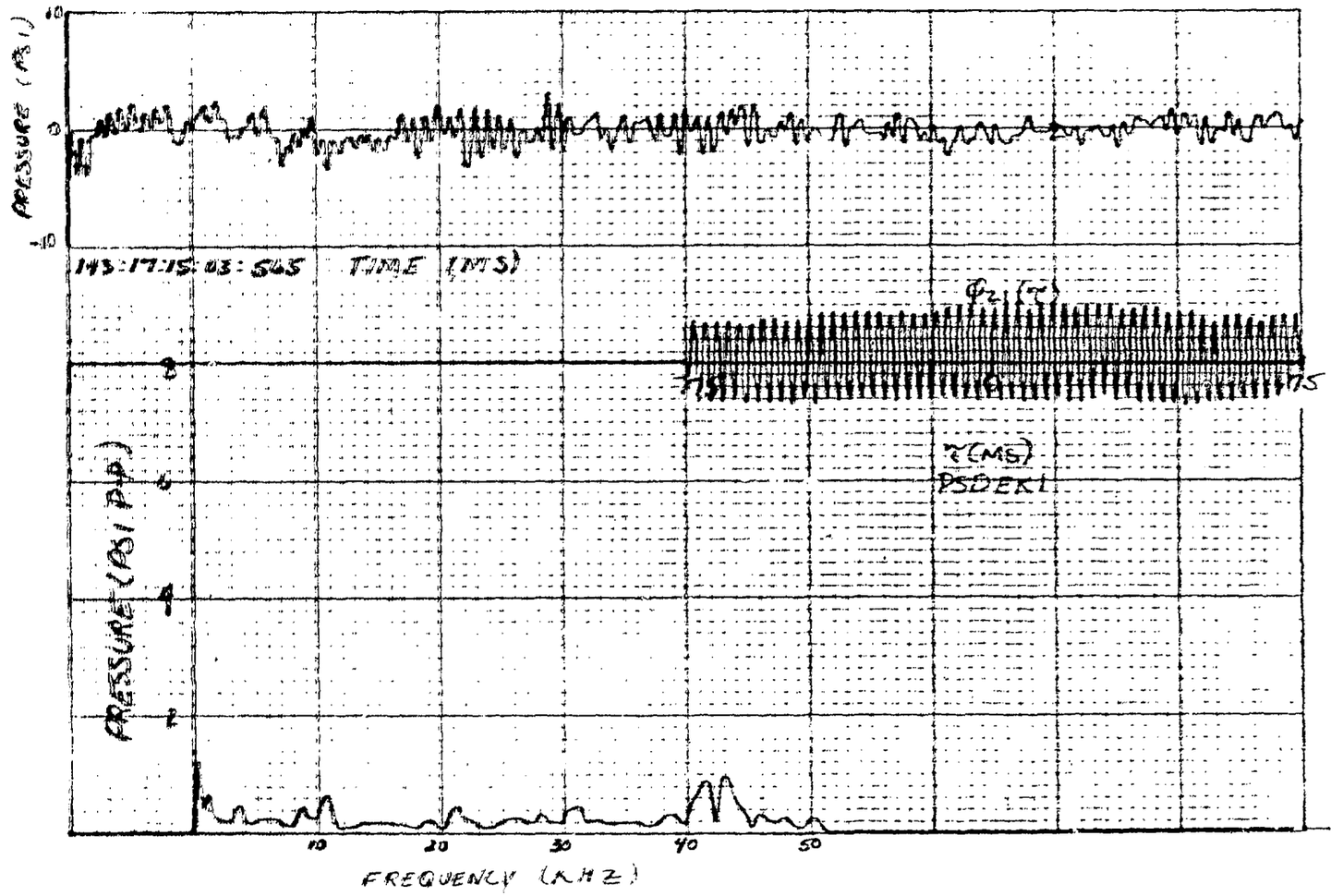

Figure 296. High-Frequency Response Data, 78% Speed, Stall Transient, Time 565, PSDEK1.

Figure 297. High-Frequency Response Data, 78% Speed, Stalled, Time 567, PSDEK1.

IMPELLER EXIT 17% STALL TRANSIENT DATA

This section contains stall transient data obtained with the impeller exit (Station 2) cobra probe sensor positioned 17% of the flow path width from the shroud wall. The cobra probe and recording equipment were identical to that used in regular traverses. Frequency response of this system should be considered poor for transient characteristics. Impeller exit air angle and total pressure and collector static pressure are presented vs time. The pressures were ratioed to standard day conditions. The key denotes the proper symbol to the scales from right to left in ascending order. Each condition was recorded at two scanning rates, one scan/sec and maximum (approximately 6 scans/sec). Conditions for Figures 298 and 299 were 101% speed, 5-deg IGV; Figures 300 and 301 were 101% speed, 0-deg IGV; Figures 302 and 303 were 101% speed, -4-deg IGV; Figures 304 and 305 were 94.5% speed, 15-deg IGV; and Figures 306 and 307 were 95% speed and 10-deg IGV.

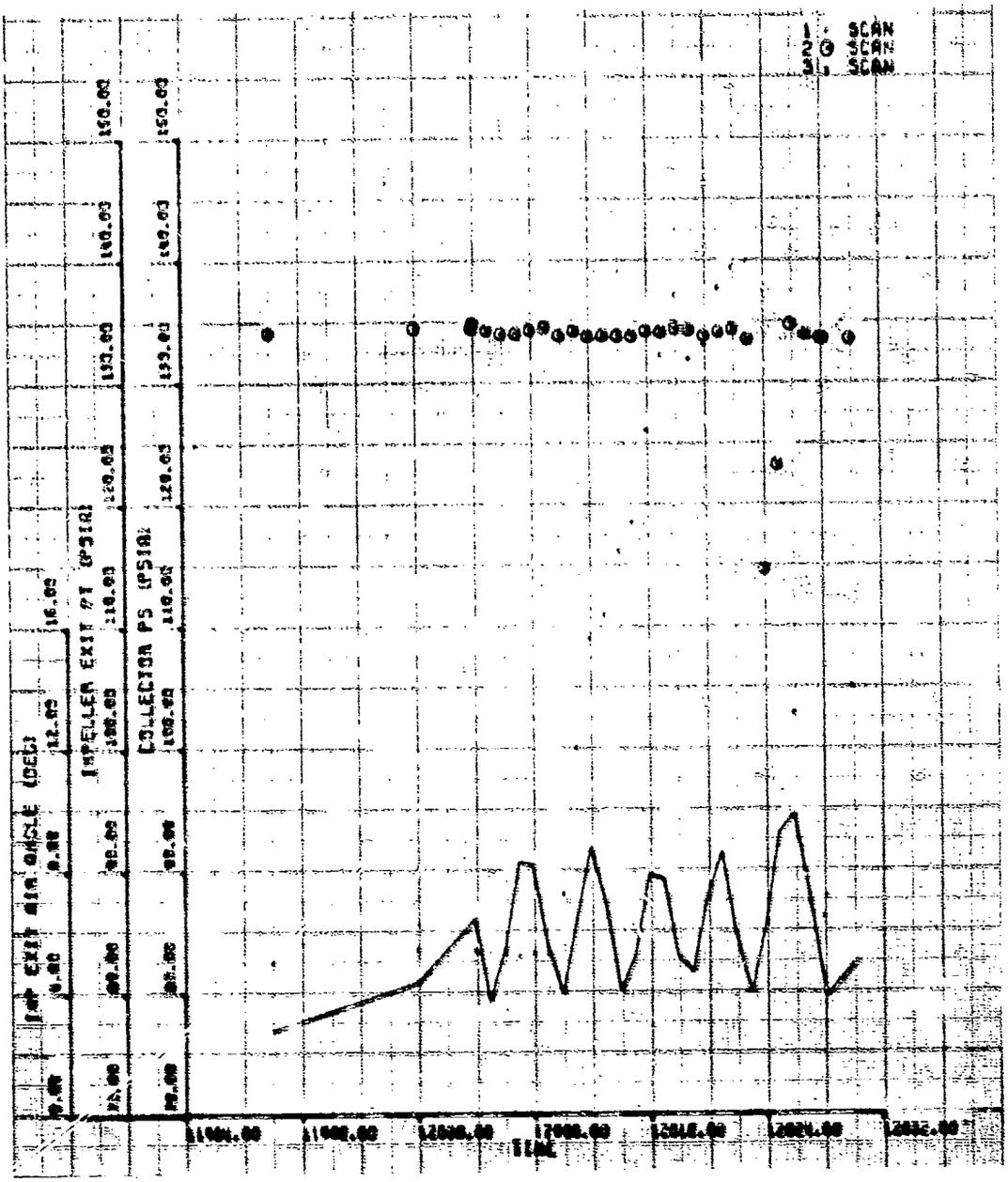

Figure 298. Stall Transient Data, 101% Speed, 5-deg IGV, ISPS Rate.

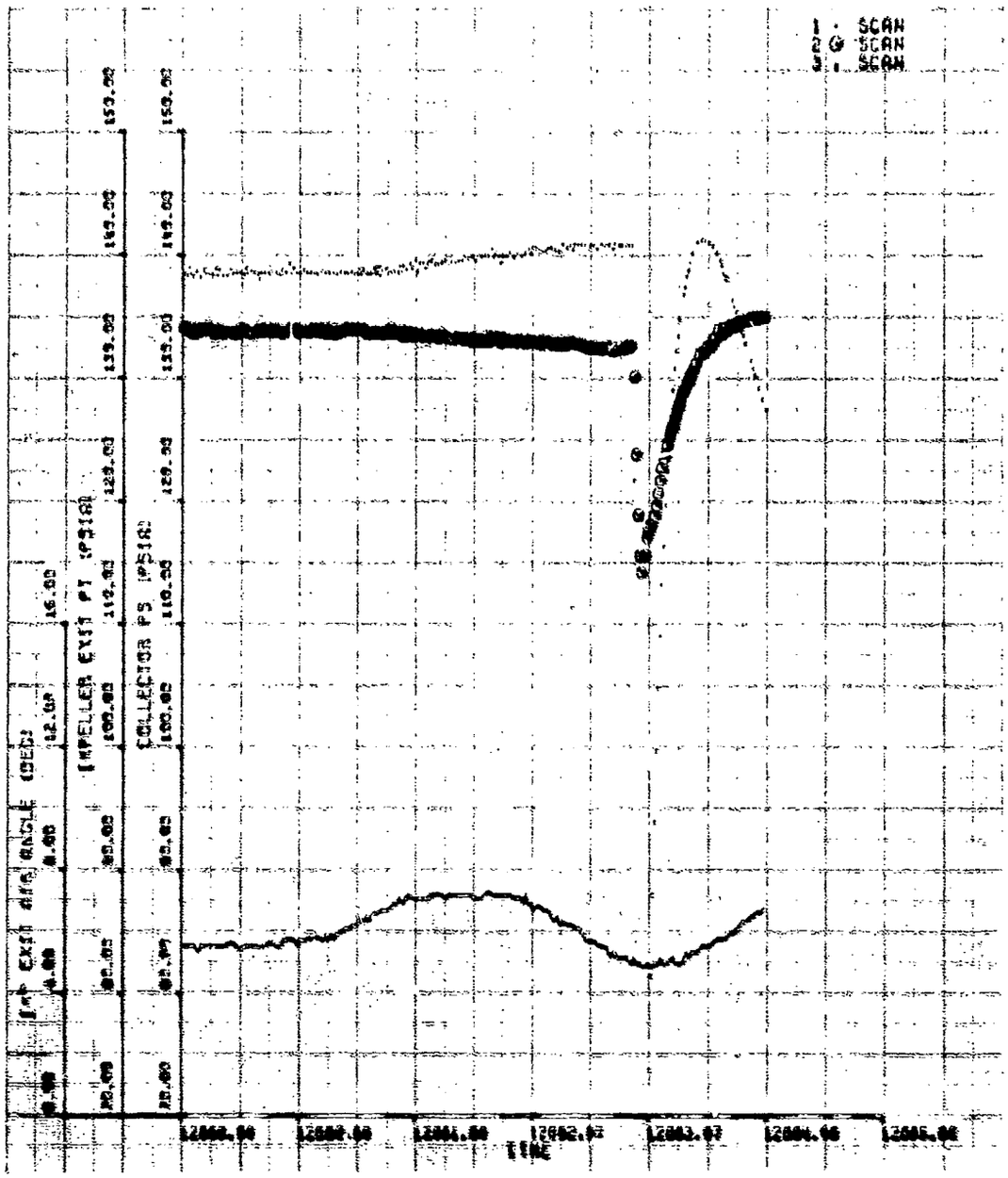

Figure 299. Stall Transient Data, 101% Speed, 3-deg IGV, Maximum Rate.

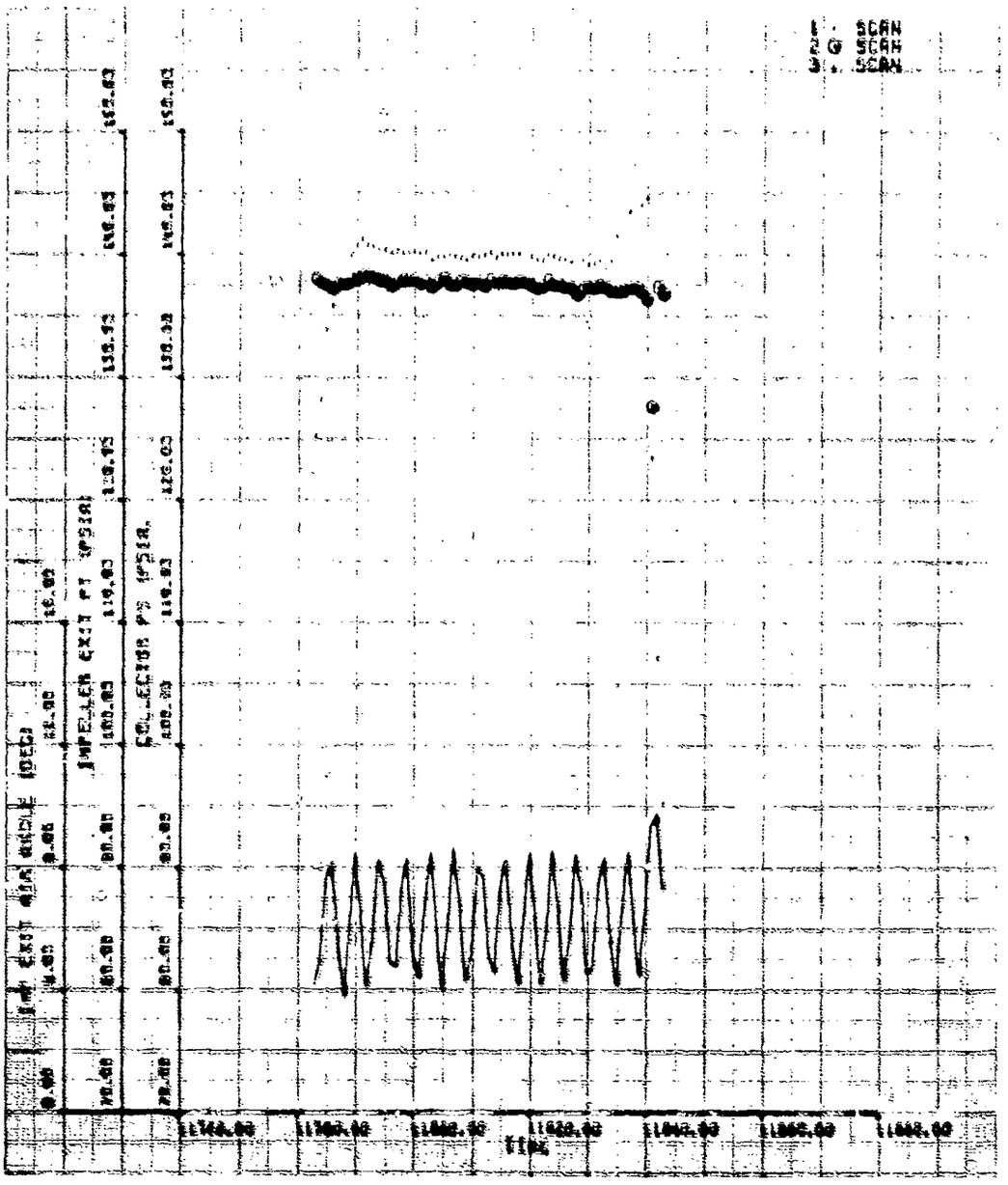

Figure 306. Stall Transient Data, 101% Speed, 0-deg IGV, 15PS Rate.

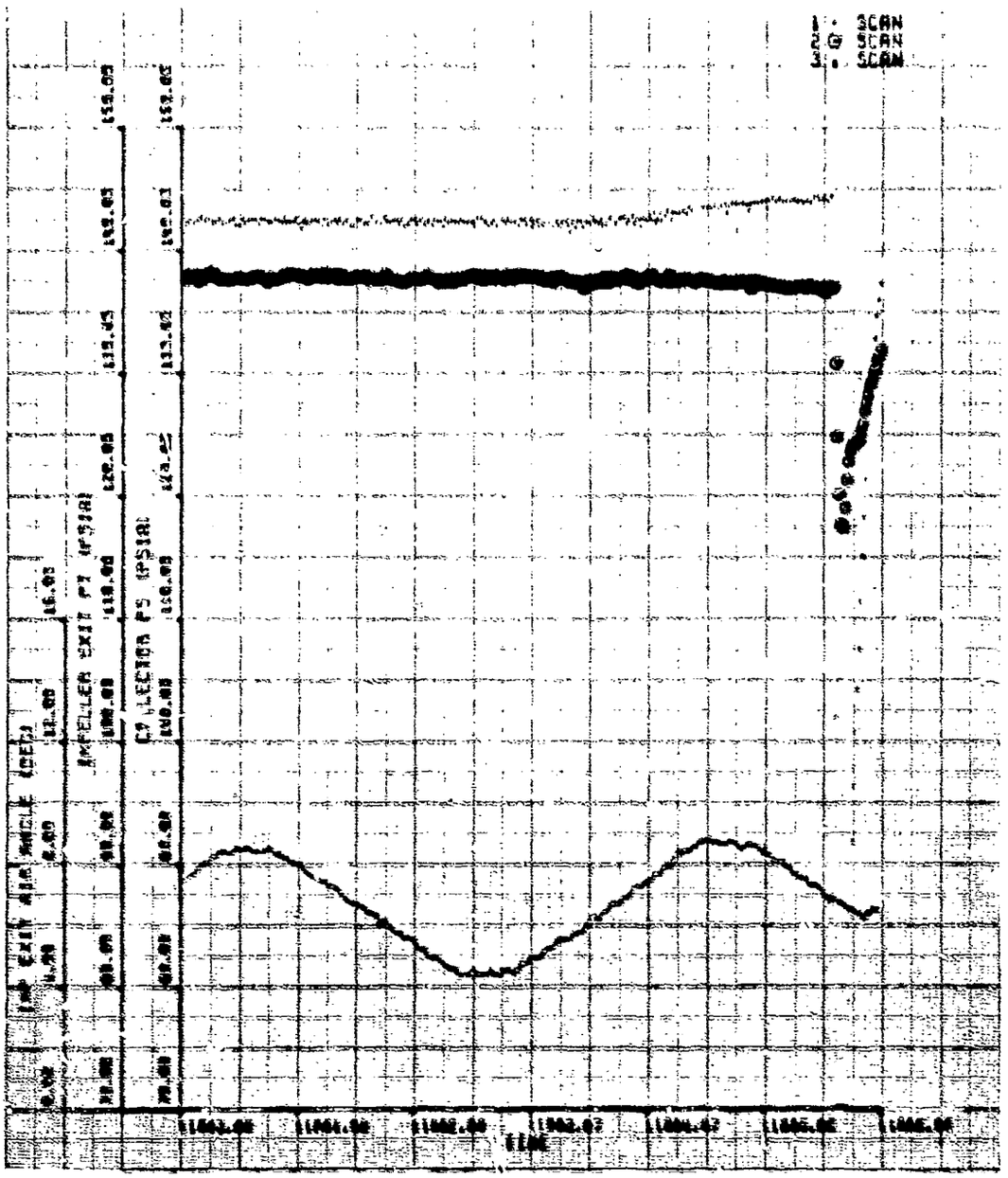

Figure 301. Stall Transient Data, 101% Speed, 0-deg IGV Maximum Rate.

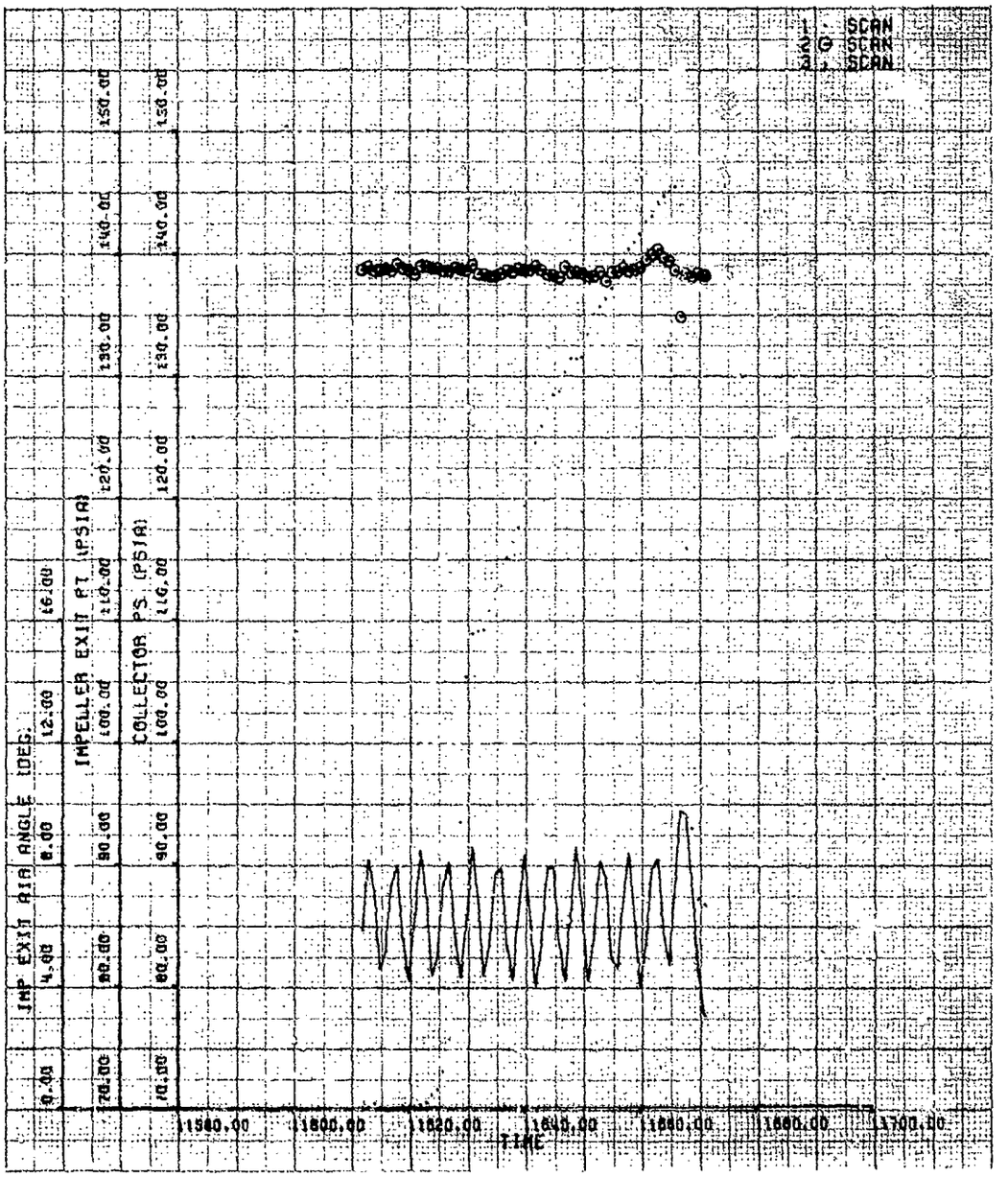

Figure 302. Stall Transient Data, 101% Speed, -4-deg IGV, ISPS Rate.

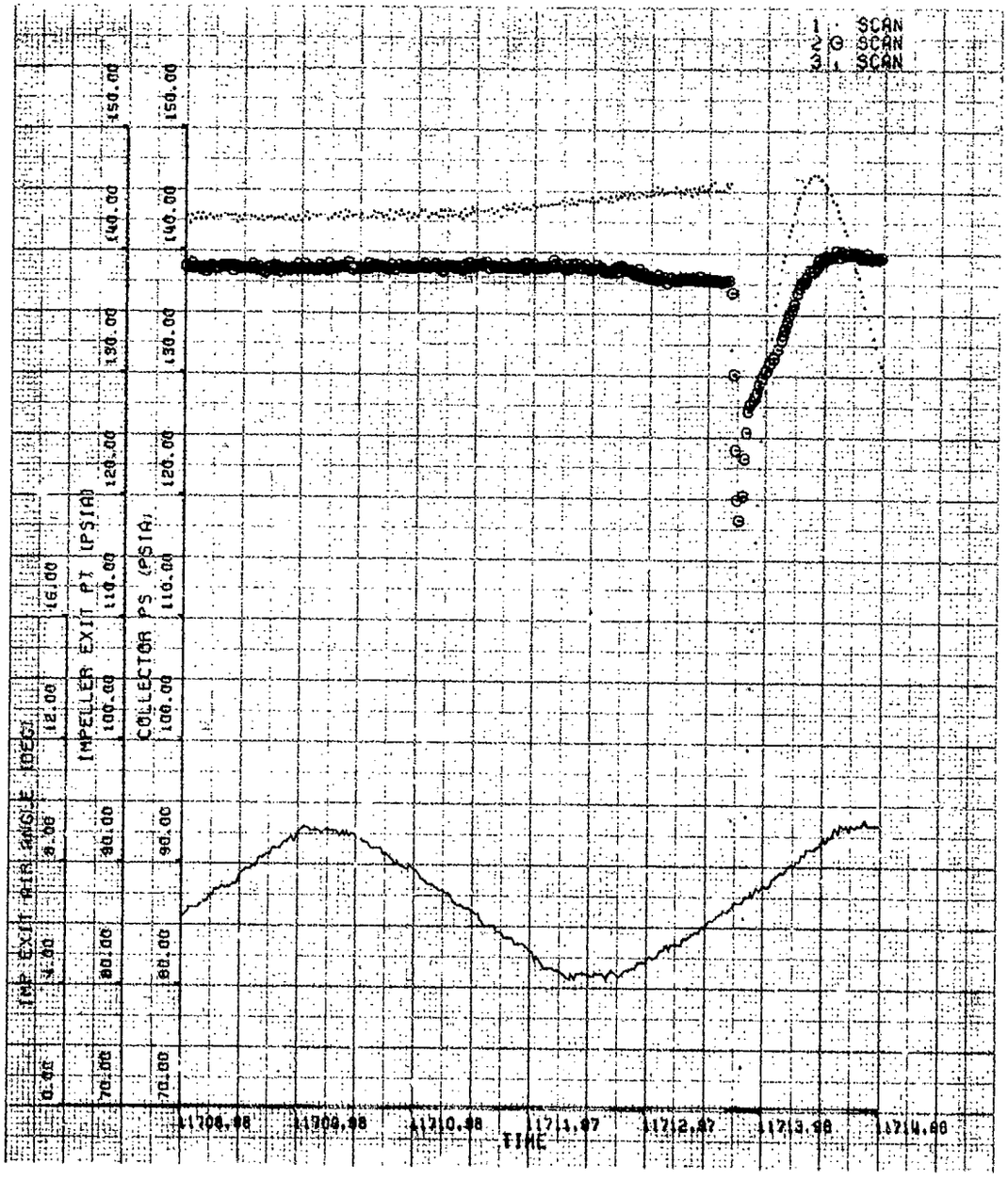

Figure 303. Stall Transient Data, 101% Speed, -4-deg IGV, Maximum Rate.

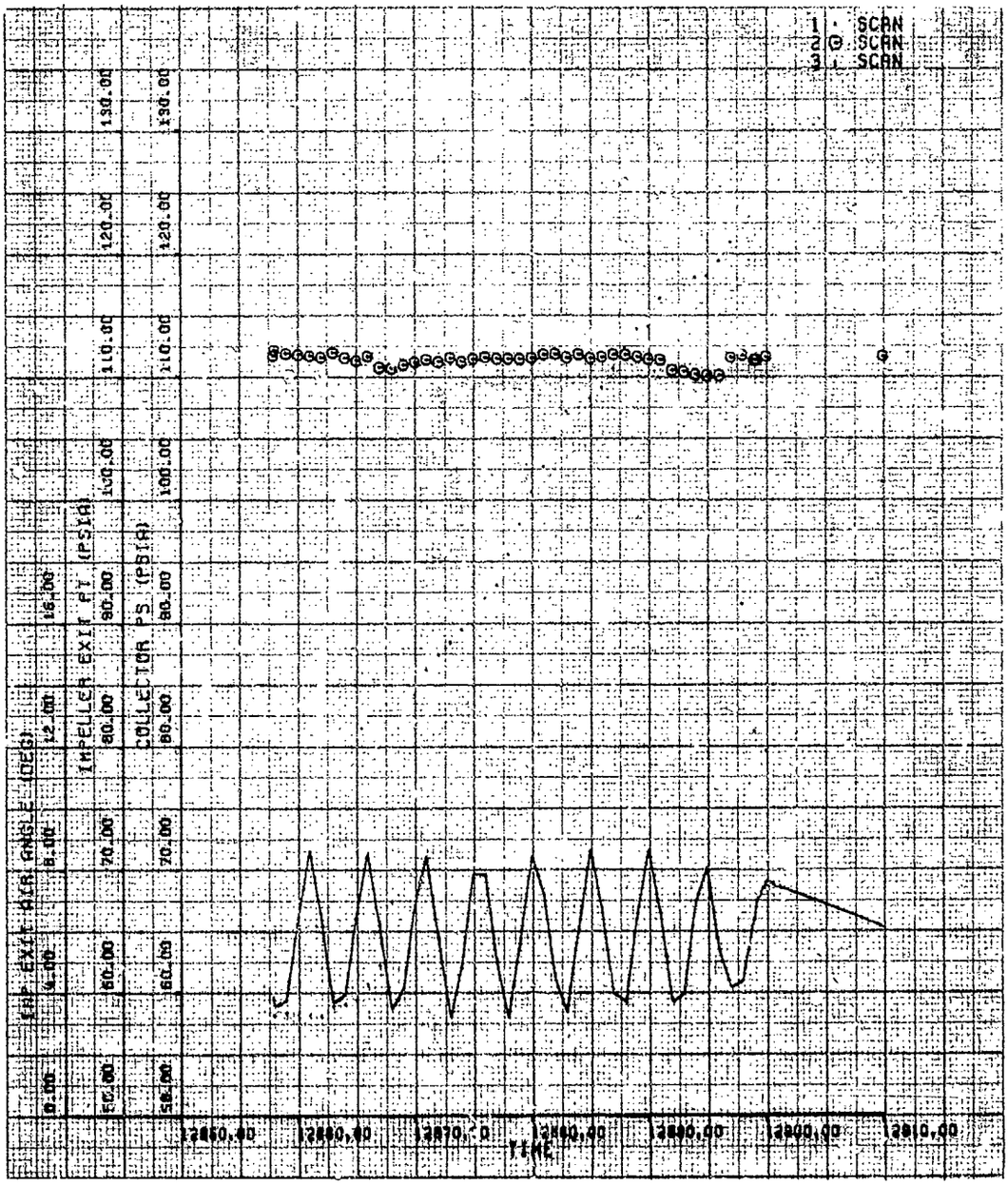

Figure 304. Stall Transient Data, 94.5% Speed, 15-deg IGV, 1SPS Rate.

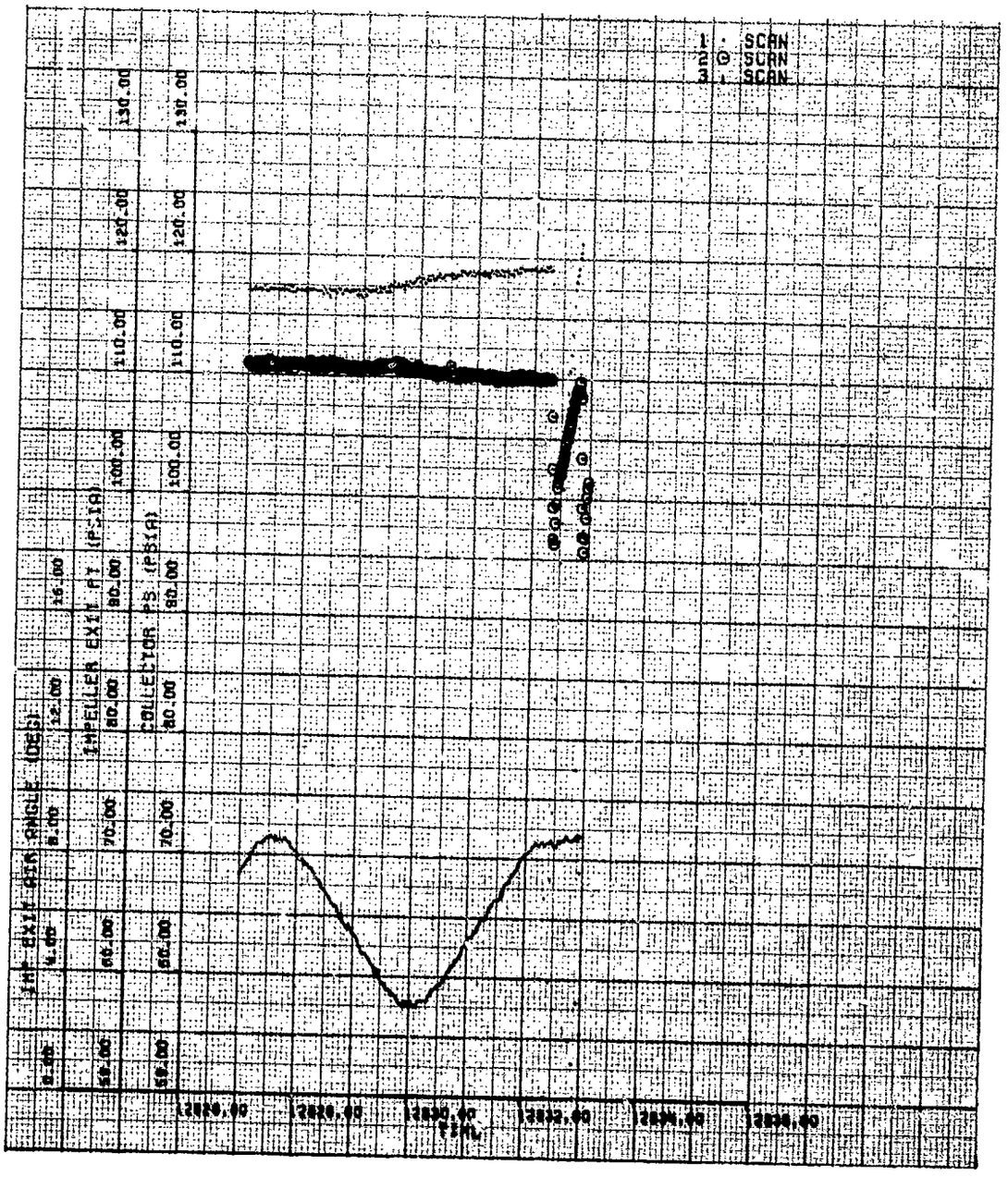

Figure 305. Stall Transient Data, 94.5% Speed, 15-deg IGV, Maximum Rate.

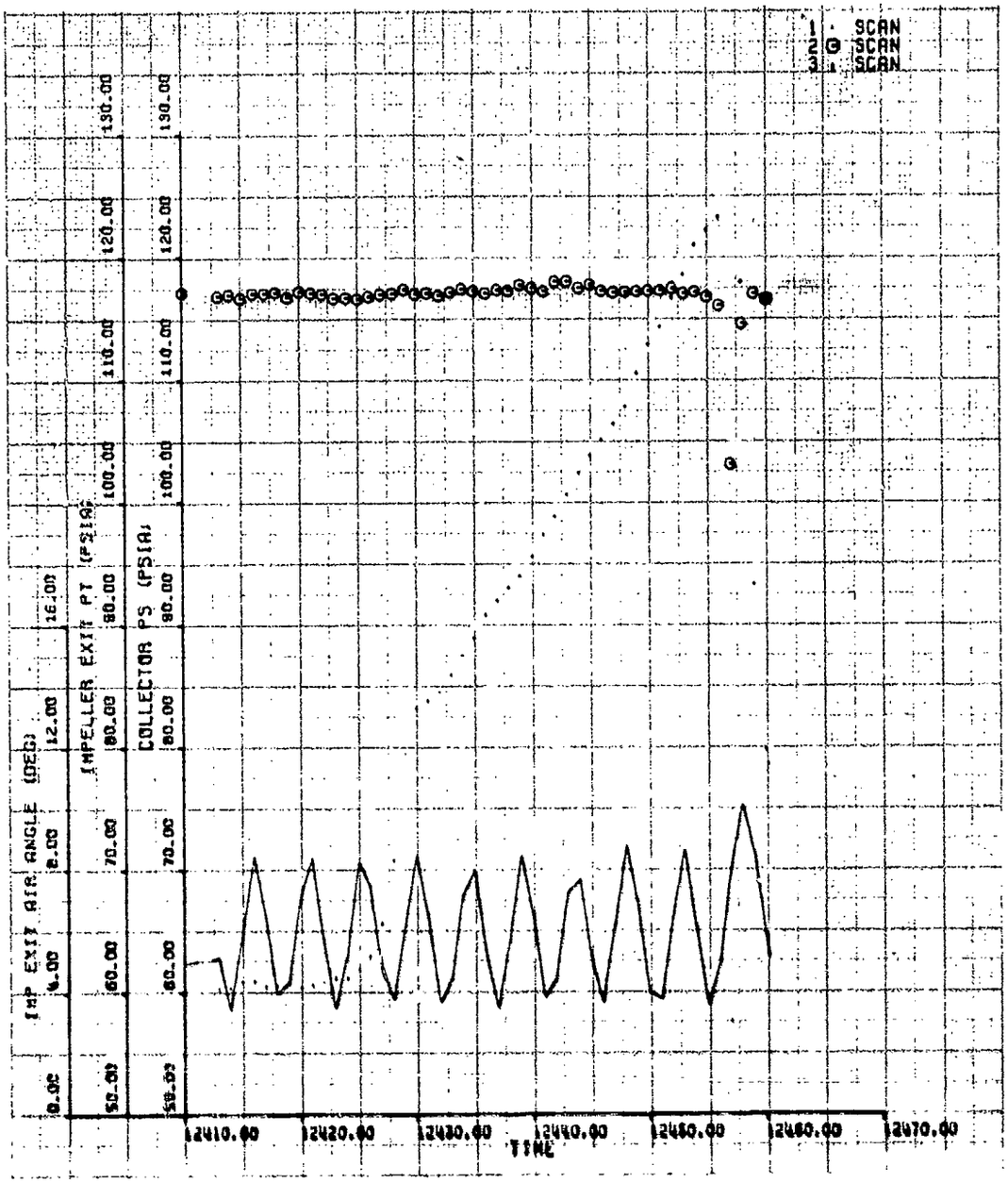

Figure 306. Stall Transient Data, 95% Speed, 10-deg IGV, ISPS Rate.

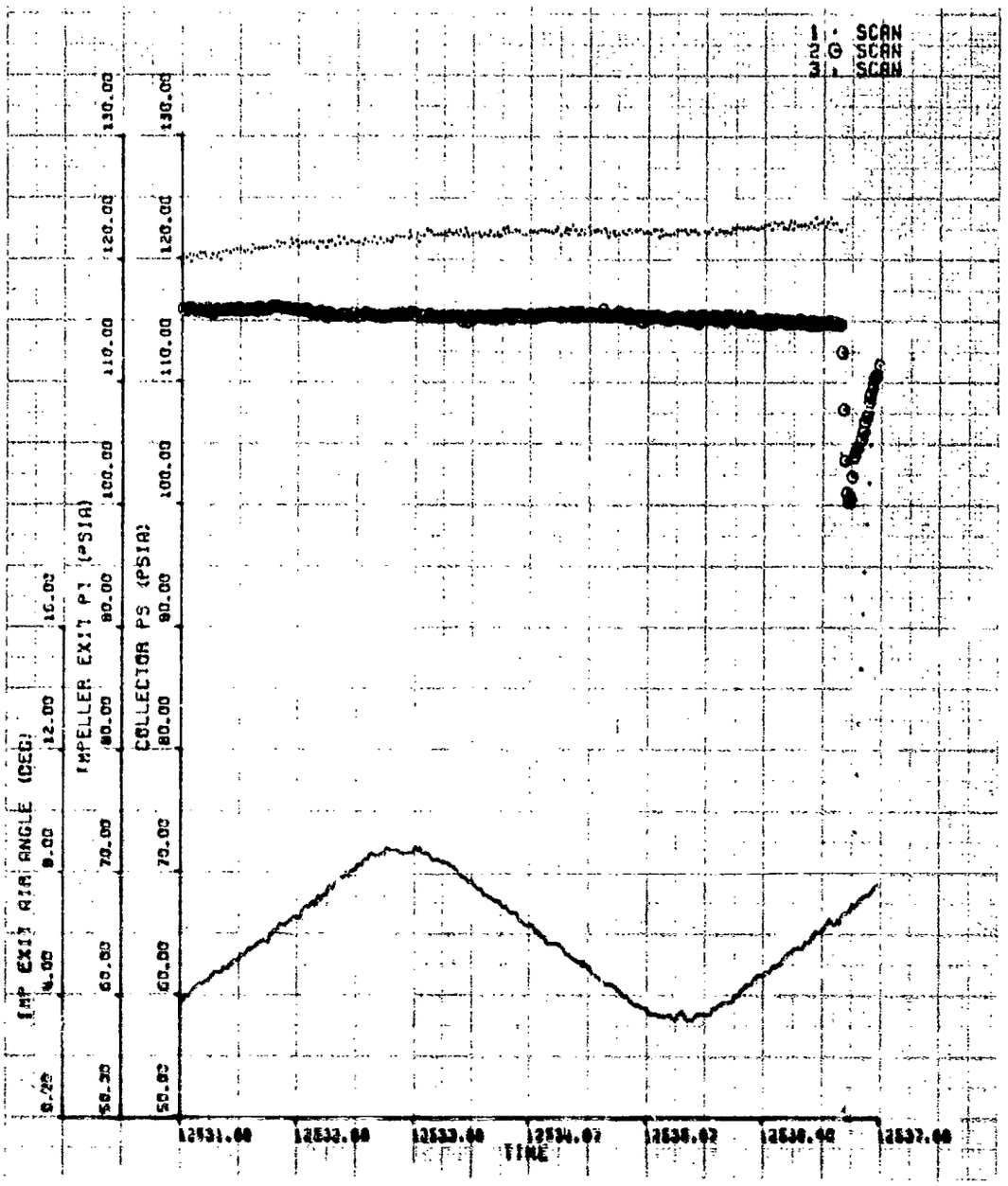

Figure 307. Stall Transient Data, 95% Speed, 10-deg IGV, Maximum Rate.

DISTRIBUTION

Director of Defense Research & Engineering	2
Assistant Secretary of the Army (R&D)	1
Deputy Chief of Staff for Logistics, DA	1
Chief of R&D, DA	1
Army Materiel Command	3
Army Aviation Systems Command	2
Hq, Army Air Mobility R&D Laboratory	2
Systems Research Integration Office, AMRDL	1
Ames Directorate, Army Air Mobility R&D Laboratory	1
Eustis Directorate, Army Air Mobility R&D Laboratory	20
Langley Directorate, Army Air Mobility R&D Laboratory	2
Lewis Directorate, Army Air Mobility R&D Laboratory	2
Army Aviation Systems Test Activity	2
Army R&D Group (Europe)	2
Army STINFO Team (Europe)	1
Army Aeromedical Research Laboratory	1
Army Coating & Chemical Laboratory	1
Harry Diamond Laboratories	1
Army Ballistic Research Laboratories	1
Army Research Office	1
Army Materials & Mechanics Research Center	5
Army Test & Evaluation Command	1
Army Materiel Systems Analysis Agency	1
Army Missile Command	1
USACDC Aviation Agency	3
Army Transportation School	1
Army Arctic Test Center	1
Army Field Office, AFSC	1
Air Force Aero Propulsion Laboratory	2
Air Force Flight Dynamics Laboratory	2
Aeronautical Systems Division, AFSC	2
Naval Air Systems Command	9
Chief of Naval Research	2
Naval Air Development Center	1
Naval Air Propulsion Test Center	2
Naval Ship R&D Center	3
Marine Corps Liaison Officer, Army Transportation School	1
Ames Research Center, NASA	4
Langley Research Center, NASA	2
Lewis Research Center, NASA	1
Goddard Space Flight Center, NASA	1
STINFO Facility, NASA	2
National Aviation Facilities Experimental Center, FAA	1
Department of Transportation Library	1
Eastern Region Library, FAA	1
Federal Aviation Administration, Washington	2
Government Printing Office	1
Defense Documentation Center	2

Unclassified

Security Classification

DOCUMENT CONTROL DATA - R & D

(Security classification of title, body of abstract and indexing annotation must be entered when the overall report is classified)

1. ORIGINATING ACTIVITY (Corporate author) Pratt & Whitney Aircraft Division United Aircraft Corporation Florida Research and Development Center West Palm Beach, Florida	2a. REPORT SECURITY CLASSIFICATION Unclassified 2b. GROUP

3. REPORT TITLE

10:1 PRESSURE RATIO SINGLE-STAGE CENTRIFUGAL COMPRESSOR PROGRAM

4. DESCRIPTIVE NOTES (Type of report and inclusive dates)

Final Report

5. AUTHOR(S) (First name, middle initial, last name)

William J. McAnally, III

6. REPORT DATE	7a. TOTAL NO. OF PAGES	7b. NO. OF REFS
April 1974	429	

8a. CONTRACT OR GRANT NO.	9a. ORIGINATOR'S REPORT NUMBER(S)
DAAJ02-70-C-0006 b. PROJECT NO. c. Task 1G162203D14413 d.	USAAMRDL Technical Report 74-15 9b. OTHER REPORT NO(S) (Any other numbers that may be assigned this report) FR-6086

10. DISTRIBUTION STATEMENT

Distribution limited to U. S. Government agencies only; test and evaluation; April 1974. Other requests for this document must be referred to the Eustis Directorate, U. S. Army Air Mobility Research and Development Laboratory, Fort Eustis, Virginia 23604.

11. SUPPLEMENTARY NOTES	12. SPONSORING MILITARY ACTIVITY
	Eustis Directorate, U. S. Army Air Mobility Research and Development Laboratory Fort Eustis, Virginia

13. ABSTRACT

The objective of this program was to design, fabricate and test a 3.1-lb/sec airflow single-stage centrifugal compressor that could be incorporated in a future Army advanced technology gas turbine engine. The design performance goals were to exceed 75% efficiency at 10:1 pressure ratio. Since gas turbine engines for Army aircraft applications operate under part-power conditions a majority of the time, an off-design performance goal of 80% efficiency at 8:1 pressure ratio was established.

In the design of the compressor, parametric studies were conducted to select an overall design consistent with optimum compressor performance at both performance goals. These studies defined the compressor inlet corrected flow rate, impeller inlet hub and tip radii, corrected impeller rotational speed, and inlet prewhirl. Airflow selection and the selection of the hub radius were influenced by the decision to design a compressor that could be used in a small turboshaft engine with a concentric shaft front drive.

The tip radius was selected after determining the effect on axial Mach number, inducer tip relative Mach number, and inlet choke flow margin. The effect of inlet guide vane losses, inlet shock losses, diffuser losses, and shroud friction heating were parametrically evaluated before selecting an IGV prewhirl and rotor speed to provide optimum overall compressor performance. A remote inducer design was selected over an integral inducer-impeller configuration so that the inducer could be designed using transonic axial-flow compressor technology. The work split between the inducer and impeller was selected so that the relative Mach number into the impeller would be subsonic. A pipe diffuser was selected over vane island and cascade diffusers, because it has the lowest demonstrated losses over the largest range of Mach number and because P&WA had substantial experience in designing and fabricating this type of diffuser.

Demonstrated total-to-static performance was as high as 79.6% efficiency at 8.192:1 pressure ratio and 73.8% efficiency at 10.03:1 pressure ratio. Performance adjusted for increased losses from a damaged diffuser (10.15:1 pressure ratio and 75.9% efficiency) indicates that the basic compressor design would surpass the 10:1 pressure ratio program goal. Evaluation of component performance data revealed that excessive losses occurred in the inducer above 95% of design speed and that a redesign of this component could produce an additional performance improvement at 10:1 pressure ratio.

DD FORM 1 NOV 68 1473 REPLACES DD FORM 1473, 1 JAN 64, WHICH IS OBSOLETE FOR ARMY USE.

Unclassified

Security Classification

14. KEY WORDS	LINK A		LINK B		LINK C	
	ROLE	WT	ROLE	WT	ROLE	WT
Compressors Fabrication Pressure Ratio Engines Turbines Performance (Engineering)						